Innovative Model Based Systems Engineering approach for the design of hypersonic transportation systems

Doctoral Dissertation

Doctoral Program in Aerospace Engineering (32nd Cycle)

Innovative Model Based Systems Engineering approach for the design of hypersonic transportation systems

By

Davide Ferretto

Supervisor(s):
Prof. Nicole Viola, PhD, Supervisor
Prof. Eugenio Brusa, PhD, Co-Supervisor

Doctoral Examination Board:

Dr. Guillermo Ortega, PhD, Referee, European Space Agency
Dr. Marco Marini, PhD, Referee, Centro Italiano Ricerche Aerospaziali
Dr. Bayindir Saracoglu, PhD, Board Member, Von Karman Institute for Fluid Dynamics
Dr. Victor Fernandez Villace, PhD, Board Member, European Space Agency
Prof. Paolo Maggiore, PhD, Board Member, Politecnico di Torino

Politecnico di Torino

2020

Declaration

I hereby declare that, the contents and organization of this Dissertation* constitute my own original work and do not compromise in any way the rights of third parties, including those relating to the security of personal data.

Davide Ferretto

2020

* This Dissertation is presented in partial fulfilment of the requirements for **Ph.D. degree** in the Doctoral School of Politecnico di Torino (ScuDo). This Dissertation has been carried out in the framework of the Stratospheric Flying Opportunities for High-Speed Propulsion Concepts (STRATOFLY) Project, funded by the European Union's Horizon 2020 research and innovation programme under grant agreement No 769246. All data and results reported in the manuscript are updated to the submission date.

"Stepping out into the universe, (...) we must confront the realities of interstellar travel" (Interstellar, 2014).

Acknowledgment

PhD career is an exciting and challenging endeavour which cannot be run solo. I would like to take this opportunity to first thank my family, which always supported me in my graduate and post-graduate student career. I would like to heartfelt thank my loving wife for her patience, irreplaceable help and true love, which always allowed me moving forward through the everyday work.

I would also like to acknowledge my supervisors for their invaluable suggestions provided and for the opportunities offered during these three years, always encouraging me to invest the best of my capabilities within the research described in this Dissertation.

Ultimately, I would like to thank a lot all the colleagues and friends that I have met during my PhD career, which made this experience special and left nice memories in my mind, some of which I will never forget.

Abstract

The Dissertation proposes a new methodology for conceptual and preliminary design of hypersonic transportation systems. Particularly, after a short introduction on historical studies on hypersonic regimes and projects, the Dissertation presents the overall design methodology, formalized through the Systems and Software Engineering Meta-model (SPEM). Notably, the analysis is focused on the conceptual design and validation of the STRATOFLY MR3 concept, a commercial civil hypersonic cruiser capable to reach Mach 8 along antipodal routes. In details, the presented methodology has been designed to support both the conceptual as well as the preliminary design phases. As far as the conceptual design is concerned, the process starts from the derivation of the mission statement, conceived to mirror the high-level mission objectives, and continues with functional and interface analyses to end up in the vehicle matching analysis and feasibility analysis. In particular, these studies include the definition of mission objectives and requirements, the identification of proper high-level performance indexes, such as required Thrust-to-Weight ratio (T/W) and wing loading, for the different flight phases, as well as a vehicle size assessment in terms of wing surface and internal available volume. For this purposes, an innovative Multiple Matching Chart approach is proposed. Complementary, the preliminary design process for on-board subsystems is described, and specifically applied to the design of the Thermal and Energy Management Subsystem (TEMS) allocated on STRATOFLY MR3 vehicle. Preliminary design methodology includes functional and interface analyses up to component level, performance

and physical characterization of the subsystem and constituent components, with special attention to safety and reliability considerations as well as to design margin policies. Ultimately, the preliminary analysis is completed with a Life Cycle Cost (LCC) assessment including new cost estimation models specifically developed to support the estimation of development, production and operating costs for high-speed vehicles.

Contents

List of Figures

List of Tables

A	
AD	Activity Diagram
AEP	Aircraft Estimated Price
AI	Artificial Intelligence
AIAA	American Institute of Aeronautics and Astronautics
ALD	Available Landing Distance
ANSI	American National Standards Institute
AOTV	Aero-assisted Orbital Transfer Vehicle
APU	Auxiliary Power Unit
AR	Acceptance Review
ARP	Aerospace Recommended Practice
ARV	Ascent and Re-entry Vehicle
ASF	Assembly level Function
ASK	Available Seat Kilometre
ASSET	Aero-thermodynamic Elastic Structural Systems Environmental Tests
ATA	Air Transport Association
ATLLAS	Aerodynamic and Thermal Load interactions with Lightweight Advanced materials for high Speed flight
ATM	Air Traffic Management
ATR	Air Turbo Rocket
ATS	Access To Space
B	
BDD	Block Definition Diagram
BoC	Bottom of Climb
C	
CAD	Computer Aided Design
CAV	Cruise and Acceleration Vehicle
CCA	Common Cause Analysis
CDR	Critical Design Review
CEF	Cost Escalation Factor
CER	Cost Estimation Relationship
CFD	Computational Fluid Dynamics
CMC	Ceramic Matrix Composite
CNS	Communication, Navigation and Surveillance
ConOps	Concept of Operations
COTS	Commercial Off-The Shelf
CPI	Consumer Price Index
CR	Configuration Requirement
CRV	Crew Return Vehicle
D	
DLR	Deutsche Zentrum fur Luft und raumfahrt
DMR	Dual Mode Ramjet
DOC	Direct Operating Cost
DoDAF	Department of Defence Architecture Framework
E	
EASA	European Aviation Safety Agency
EC	European Commission
ECLSS	Environmental Control and Life Support Subsystem
ECS	Environmental Control System
ECSS	European Cooperation for Space Standardization
ECTV	Experimental Captive-carry Test Vehicle
EEAB	External Expert Advisory Board
EFTV	Experimental Free-flight Test Vehicle
EFTV-A	Experimental Free-flight Test Vehicle – Air launched
EFTV-G	Experimental Free-flight Test Vehicle – Ground launched
EIA	Electronic Industries Alliance
EIP	Entry Interface Point

ELR	End-of-Life Review
ELTV	Experimental LEA mounted Test Vehicle
EPS	Electrical Power System
EQF	Equipment level Function
ER	Equivalent Ratio
ESA	European Space Agency
ESM	Experimental Service Module
EU	European Union
F	
FAA	Federal Aviation Administration
FBSE	Functions-Based Systems Engineering
FCS	Flight Control System
FCU	Fuel Control Unit
FEM	Finite Element Analysis
FESTIP	Future European Space Transportation Investigations Programme
FFBD	Functional Flow Block Diagram
FHA	Failure Hazard Analysis
FRR	Flight Readiness Review
FMEA	Failure Modes and Effects Analysis
FMECA	Failure Modes and Effects and Criticality Analysis
FMI	Functional Mock-up Interface
FP	Framework Programme
FQR	Flight Qualification Review
FR	Functional Requirement
FTA	Fault Tree Analysis
G	
GOP	General Operating Parameter
GPU	Ground Power Unit
GTO	Geostationary Transfer Orbit
H	
HEXAFLY	High-Speed Experimental Fly vehicle
HIKARI	HIgh speed Key technologies for future Air transport - Research & Innovation cooperation scheme
HOPE - X	H-2 Orbiting Plane Experimental
HOTOL	HOrizontal Take Off and Landing
HPT	High-Pressure Turbine
HST	High Speed Transportation
I	
IBD	Internal Block Diagram
ICAO	International Civil Aviation Organization
IEC	International Electro technical Commission
IEEE	Institute of Electrical and Electronics Engineers
INCOSE	International Council on Systems Engineering
INEA	Innovation and Networks Executive Agency
IOC	Indirect Operating Cost
IR	Interface Requirement
ISO	International Organization for Standardization
IT	Information Technology
IXV	Intermediate eXperimental Vehicle
L	
LAPCAT	Long-Term Advanced Propulsion Concepts and Technologies
LCC	Life Cycle Cost
LDE	Logical Development Environment
LEA	Lyotnii Experimentalnii Apparat
LEO	Low Earth Orbit
LFL	Landing Field Length
LOX	Liquid Oxygen
LPC	Low Pressure Compressor
LPT	Low-Pressure Turbine
LR	Launch Rate
LRE	Liquid Rocket Engine

LRR	Launch Readiness Review
M	
MAKS	Multipurpose aerospace system
MBSE	Model Based Systems Engineering
MCR	Mission Close-out Review
MDO	Multidisciplinary Design Optimization
MDR	Mission Definition Review
MGA	Mass Growth Allowance
ML	Mission Level
MLW	Maximum Landing Weight
MODAF	Ministry of Defence Architecture Framework
MMC	Multiple-Matching Chart
MR	Mission Requirement
MTOV	Maximum Take-Off Volume
MTOW	Maximum Take-Off Weight
N	
NASA	National Aeronautics and Space Administration
NASP	National Aero-Space Plane
NCOSE	National Council on Systems Engineering
O	
OEI	One Engine Inoperative
OEV	Operating Empty Volume
OEW	Operating Empty Weight
OMG	Object Management Group
OP	Operational Requirement
ORR	Operational Readiness Review
OSLC	Open Services for Lifecycle Collaboration
P	
PASA	Preliminary Aircraft Safety Assessment
PD	Package Diagram
PDE	Physical Development Environment
PDR	Preliminary Design Review
Per_HL	Performance High Level Requirement
Per_LL	Performance Low Level Requirement
PO	Primary Objective
PRD	Parametric Diagram
PRIME	Precision Re-entry Including Manoeuvring re-Entry
ProgR	Programmatic Requirement
PRR	Preliminary Requirements Review
PSM	Process Safety Management System
PSSA	Preliminary System Safety Assessment
Q	
QFD	Quality Functional Deployment tool
QR	Qualification Review
R	
RAMS	Reliability Availability Maintainability and Safety
RBCC	Rocket Based Combined Cycle
RD	Requirements Diagram
RDB	Requirements Database
RDTE	Research Development Test and Evaluation cost
REL	Reaction Engines Ltd.
RLV	Reusable Launch Vehicle
RRAsy	Assembly Level Reliability Requirement
RREq	Equipment Level Reliability Requirement
RRSub	Subsystem Level Reliability Requirement
RTA	Revolutionary Turbine Accelerator
RV-NW	Non-Winged Re-entry

	Vehicle
RV-W	Winged Re-entry Vehicle
	S
SAAsy	Assembly Level Safety Requirement
SABRE	Synergistic Air-Breathing Rocket Engine
SAE	Society for Automotive Engineering
SAEq	Equipment Level Safety Requirement
SASub	Subsystem Level Safety Requirement
SCS	Space Cruiser System
SD	Sequence Diagram
SE	Systems Engineering
SEE	Systems Engineering Environment
SEF	Segment Level Function
SegL	Segment Level
SEP	System Engineering Process
SEV	Structural Empty Volume
SFC	Specific Fuel Consumption
SHO	StakeHolders Objectives
SMD	State Machine Diagram
SMV	Space Maneuver Vehicle
SO	Secondary Objective
SoI	System of Interest
SOP	Specific Operating Parameter
SoS	System of Systems
SoSL	System of Systems Level
SoW	Statement of Work
SP	Secondary Parameter
SPEM	Software & Systems Process Engineering Metamodel
SRR	System Requirements Review
SSA	Systems Safety Assessment
SSTO	Single Stage To Orbit
STRATOFLY	Stratospheric Flying Opportunities for High-Speed Propulsion Concepts
SUB	Suborbital flight
SubSysL	Subsystem Level
SysL	System Level
SysML	Systems Modelling Language
	T
TAV	Trans Atmospheric Vehicle
TBCC	Turbine Based Combined Cycle
TCS	Thermal Control Subsystem
TEMS	Thermal and Energy Management System
TFU	Theoretical First Unit
TLF	Top Level Function
ToC	Top of Climb
TOC	Total Operating Cost
TP	Technology Parameter
TPS	Thermal Protection Subsystem
TRL	Technology Readiness Level
TSTO	Two Stage To Orbit
	U
UCD	Use Case Diagram
UML	Unified Modelling Language
	V
VCE	Variable Cycle Engine
	Z
ZEHST	Zero Emissions High-Speed Technologies

Introduction

A century of innovation and beyond

The Twentieth century can be considered as the beginning of aviation era, from the very early stages to the global airlines market. The evolution of the aviation sector in that period was characterized by a very fast development, especially due to political and economic boosts, such as the two World Wars and the Cold War. Through those years, depending on the political, economic and technological context, several milestones have been reached, pursuing different objectives thanks to a wide and heterogeneous spectrum of basic research activities and technology development programmes. However, while moving towards the new millennium, the need to renovate civil passengers air-vehicles and mission concepts started urging the scientific and engineering community. The focus on climate impact reduction of the aviation sector, a more integrated and autonomous air traffic management and a more responsible air transportation brought out a new set of challenging issues to be faced by the designers. Specifically, pollutant and noise emission reductions, together with overall costs reduction started driving the design of current and future commercial aircraft. At the same time, after several decades of subsonic commercial flight, supersonic and even hypersonic regimes are becoming again very attractive to conceive the transport of the far future towards the horizon 2050. Complementary, suborbital commercial flight is now a reality and different initiatives related to the enhancement of technology for high speed flight are spreading all over the world. This era may be potentially characterized by a new considerable effort in the field of high speed transportation, which is attractive for both, private companies,

public research institutions and military application. Actually, hypersonic flight has been a leitmotif in aeronautics since the 1950's, when some of the most valuable engineering concepts, currently used as reference, where defined for the first time. However, differently to what happened in the past, today the final purpose of the technology development is not an exclusive military feature, but it is extensively considered also for civil purposes. Many analogies with past studies can be in any case found since the engineering problem, far from being completely understood, always brings a high level of complexity in the design process of such kind of vehicle prototypes. Nowadays, the efforts to improve the knowledge on the topic are justified by the renewed interest in hypersonic flight, which is seen as peculiar test bed for the development of several high-speed enabling technologies. In fact, hypersonic flight represents, on one side, the natural evolution of the commercial aviation but, on the other hand, it is a mandatory step to exploit a fully reusable access to space architecture based on Single Stage To Orbit (SSTO) technologies for Low Earth Orbit (LEO) payload delivery. Neglecting the research in military fields, which are most of the time classified, several initiatives started years ago, in and outside Europe, to investigate the feasibility of the concept for civil applications, to establish a roadmap towards the enhancement of the Technology Readiness Level (TRL) of main critical areas and to demonstrate how hypersonic flight can represent a valuable solution to improve the quality of commercial aviation, basically stable in its paradigm since the entry into service of the Boeing 707 in 1959. Particularly, the work presented in this Dissertation[1] has been performed within the frame of European initiative related to collaborative research on high speed flight, funded by European Commission and started in 2006, reaching now its latest step with the Horizon 2020 STRATOFLY Project (Viola, et al., 2019) and dealing with Stratospheric Flying Opportunities for High Speed Propulsion Concepts. Since 2006, almost 10 Projects were funded by the European Commission on the topic, with the aim of increasing the TRL of enabling technologies for hypersonic flight, and with the final goal of demonstrating the feasibility of the roadmap conceived to reach TRL 6 by 2035. The number of past and present initiatives in this domain is an evidence of the complexity related to the field. Notably, this complexity is mainly due to the high degree of integration of different disciplines. In fact, far from being a simple and mere sum of different ingredients, the System of Interest (SoI) shall be designed looking at multiple

[1] The results described in this Dissertation are original work from the Author as part of the PhD activities performed within the framework of STRATOFLY Project.

aspects. The success of the system will strictly depend on its compliancy with a large set of requirements that, starting from the conceptual design up to operation and end-of-life, shall be managed and traced. It is then necessary to adopt a "systems thinking" approach to set up a proper design platform able to support the design process and related methodology. The Systems Engineering, especially in its Model-Based approach, is a typical example of "systems thinking" attitudes giving a high priority to requirements management and trace during product lifecycle. This work will analyse several aspects of the design of a hypersonic vehicle, at conceptual and preliminary stages, always aiming at keeping trace of the big picture, providing a consistent and as much as possible complete view over the entire design process. The main aim and innovation point of the work consists in proposing a fully integrated Model-Based aircraft design approach for High Speed Transportation (HST), applying a Systems Engineering approach to the design process, with particular focus on requirements coverage analysis. Functional and performance aspects are studied in detail and presented in the different chapters of the Dissertation, trying to provide a reusable approach for the development of hypersonic aircraft and related technologies, making benefit of existing standards, languages and frameworks in the field of Model-Based Engineering. Current bottlenecks for Model-Based design, such as interoperability of tools, will be also discussed during the design process, where classical tools and engineering software shall be applied in a seamless way to assure the complete traceability of requirements. Each chapter specifically deals with a particular topic related to aircraft and systems design, starting from high level requirements definition through stakeholders needs identification, as well as mission analysis and functional design, up to aircraft concept definition and systems characterization, taking into account also reliability, safety and cost. The rationale behind the work presented in this Dissertation aims at emphasizing the importance of jointly considering the aforementioned aspects in a holistic approach, with the final goal of defining a feasible and sustainable new paradigm of high-speed vehicle concept. For this reason, aspects related to vehicle size, volume allocation, subsystems configuration and performance, as well as design to reliability are assessed, specially looking at their mutual interactions. To enhance the reusability of the approach and to provide the reader with a clear overview of the proposed approach, each chapter is introduced by a description of the related process, implemented through a SPEM metamodel to provide a common formalization example. Particularly:

- Chapter 1 introduces to the hypersonic domain, starting from an historical perspective, and depicting an overview concerning the main features characterizing the high speed flight with respect to traditional one;
- Chapter 2 presents the challenge for a completely integrated aircraft design method, starting from the evolution of typical best practices used in aeronautics since previous century, to enhance the way products are designed, produced and operated. In this context, the adoption of a Model-Based Systems Engineering approach is described from early definitions up to methodology development and application;
- Chapter 3 introduces the case study analysed within the Dissertation. It is the MR3 vehicle concept developed during the STRATOFLY Project, dealing with the design of a Mach 8 hypersonic cruiser for passengers transportation. The main characteristics of the aircraft are discussed, together with the incremental path which led to the definition of this vehicle platform starting from previous projects and experiences;
- Chapter 4 describes the core of the work presented in the Dissertation. It presents the methodology for HST systems conceptual design with particular focus on MR3 vehicle case study. Notably, the design of the reference case study is re-analysed starting from stakeholders analysis in conceptual design, and the definition of both functional capabilities and performance of the aircraft is totally re-assessed. The final aim consists in the derivation of the high level requirements specification for the aircraft, as well as in the validation of the configuration with respect to the previous version, in terms of propulsion plant design point, aircraft size and volume;
- Chapter 5 introduces a lower level of design methodology, moving from aircraft to on-board systems analysis. Notably, the focus is dedicated to the Thermal and Energy Management Subsystem (TEMS), which may affect considerably the configuration at aircraft level and whose architecture is particularly critical to assess because of the multi-functional nature that characterizes it. Particular attention is devoted to system budgets (mass, volume and power), with reference to the design point derived at aircraft level, taking into account also design margins as well as safety and reliability issues;
- Chapter 6 introduces the importance of cost estimation within the design process of a hypersonic vehicle as mean to predict development, production and operating costs and to assess the economic viability of the concept;

- Chapter 7 draws major conclusions and proposes future works for the enhancement of the provided design methods for hypersonic aircraft, suggesting next steps and discussing strong points and weaknesses still present;
- Chapter 8 lists the different appendixes and annexes used as references within the core text.

Looking at the origins of aviation and considering the current research topics briefly introduced in this section, it is clear how amazingly technologies grew over the last century. Only one hundred years were sufficient to bring more than two billion passengers up in the air starting from scratch, with the trend currently breaking the threshold of four billion. It is also surprisingly evident how some research topics in aeronautics are cyclically tackled, depending on the socio-economic and political context, such as the theme of hypersonic flight. There is now a favourable momentum to face very challenging and promising elements related to the aviation of the future, since it is widely agreed that a boost towards more efficient, environmental friendly and fast vehicles shall be introduced to improve the current aviation segment, being frozen for too much time. So, why hypersonic? The answer is simple: because it's time to look forward to the future, it's time for new challenges concerning technology evolution, which may be useful also for other kinds of domains, out of the aerospace scope. It's time to move forward to imagine the aviation of tomorrow, reaching new frontiers, reducing the gap between aeronautics and space, and extending our world. It's time to re-join the incremental path established by our predecessors. It's time for innovation: one century and counting.

1

The challenges of hypersonic flight

This chapter aims at introducing the challenges of hypersonic flight related, on one side, to the understanding of the basic physical phenomena of this peculiar flight regime and, on the other side, to the preliminary design of vehicles and related subsystems conceived to fly hypersonic. In particular, the chapter starts with an historical overview of the major milestones achieved in the field of high-speed transportation (Section 1.1), presenting the main aircraft and mission concepts developed during the past decades, as well as foreseeing plausible way forward. It is important to notice that one of the main historical achievement in this context has been the definition of the main characteristics of high-speed flow together with the identification of the main challenges (Section 1.2). Consequently, a classification of the main types of hypersonic vehicles is provided together with a discussion about their main peculiarities. This allows the author highlighting the heterogeneity of the phenomena occurring at different speeds. The general trends towards 2050 are then presented, in terms of initiatives related to current and future research, as well as of interest of the aerospace community towards the development of the aforementioned vehicles types. Ultimately, Section 1.3 provides a final description of the challenges associated to the design of such kinds of vehicles, and, particularly, of hypersonic cruisers. This gives an overview of the entire design process, the so-called “big picture”, highlighting typical aspects like airframe-propulsion integration, available volume analysis, thermal management, environmental impact and cost.

1.1 An historical perspective

1.1.1 From the challenge of sound barrier to the new millennium

The dream of flying at hypersonic speed is not a peculiar desire of the Twenty-first century, but it has been pursued for a long time. The concept of hypersonic flight was already tackled in 1950's and even before. In fact, in 1949, the first attempt of reaching high speed at high cruise altitude was performed within the American WAC Corporal program with the Bumper rocket (Laney, 2015), a multistage sounding rocket incorporating part of the concept derived by the German V2 rocket (Kennedy, 1984) used in World War II. The Bumper 5 (Fig. 1) was able to reach Mach numbers higher than 5 coming back to Earth atmosphere after reaching the altitude of 393 km.

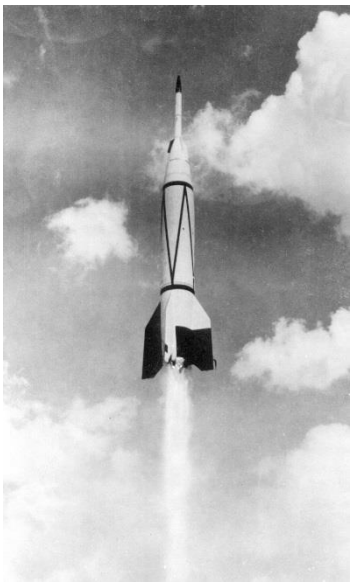

Fig. 1: The Bumper 5

In the following years, the "Space Race" contributes to increase the rate of technical development in the field of high speed flight and, particularly, the study of re-entry environment. It is then possible to affirm that the origins of hypersonic flight were related to space applications, because of the attempt of reaching Low Earth Orbit (LEO) before coming back on ground. In 1961, the Soviet Vostok I (Fig. 2) was launched on orbit and the cosmonaut Yuri Gagarin experienced, for the first time, the space environment (Hall & Shayler, 2001). Moreover, he was

the first man surviving the re-entry phase of its capsule and also the first one to fly hypersonic, reaching Mach numbers higher than 25 during the descent.

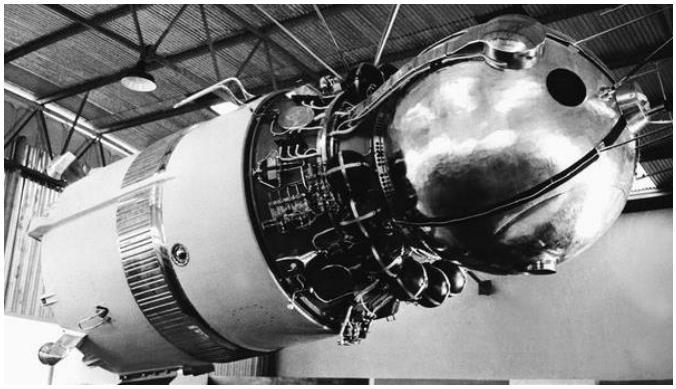

Fig. 2: The Vostok I

Only one month later than Vostok I, Alan Shepard, on board the Freedom 7 spacecraft (Fig. 3) of the US Mercury 3 mission, reached 187 km over a suborbital trajectory characterized by Mach numbers higher than 5 during the descent. It was the first, but not last, manned flight for the US Mercury program (Alexander, et al., 1966).

Fig. 3: The Freedom 7 capsule

In order to train the astronauts for high speed and space environment, the X-15 program (NASA, 1968), based on a rocket powered aircraft, was ongoing in the

same years. The aircraft (Fig. 4) was set to break several records of altitude and speed for winged vehicle flight, reaching for the first time Mach 5.3 in 1961 and Mach 6.7 in 1967.

Fig. 4. The X-15-3 hypersonic aircraft

The success of the X-15 paved the way for the development of new concepts to assess challenges and opportunities of hypersonic flight regimes. The X-15 itself constituted a fundamental test bed for most of the technologies related to the understanding of the main phenomena of re-entry from LEO. An additional example is the X-20 Dyna-Soar (Fig. 5), originally conceived as test aircraft to verify manoeuvrability at high speed, which was then designed in order to support different missions like bombing, space rescue, satellite maintenance etc… Moreover, as the name suggests, the possibility of performing dynamic soaring was also another key aspect of the design of the vehicle. The idea was aiming at demonstrating the concept of atmospheric skipping and hypersonic glide at high altitudes. The program (Bilstein, 2003) was however cancelled by the American government right before the production of the vehicle.

Fig. 5: Concept for the X-20 Dyna-Soar

While the X-20 program was closed, between the 1960 and 1970 the need for further development of enabling technologies related to this kind of application was growing within the scientific community. In particular, the attention moved to

lifting body configurations for aerodynamic characterization of the flight regime. Some examples include ASSET and PRIME (Jenkins, et al., 2003). Moreover, M2-F2, HL-10, X-23 as well as X-24A (Fig. 6), X-24B and X-24C were developed to perform several tests, some of which related to re-entry from LEO.

Fig. 6: The lifting body family: X-24A, M2-F3 and HL-10

Notably, X-23 was a lifting body conceived to acquire data related to manoeuvrability during this flight phase, while X-24s (in different versions) were designed to assess the whole set of flying conditions from hypersonic to low-speed. X-24 was also designed to integrate scramjet engine for Mach 8 conditions. In the same years, Eugen Sänger started the development of its Sänger I for hypersonic passengers transportation and Two Stages To Orbit (TSTO) option, conceived to deploy payloads on orbit. Another important progress occurred between 1970 and 1980 when the experience acquired with X-vehicles in USA was used to begin the design of the Space Shuttle (Fig. 7) (Williamson, 1999) that reached the orbit in 1981 and was able to successfully remain in service up to 2011.

Fig. 7: Space Shuttle Orbiter Enterprise during test campaign (upper) and Atlantis during landing (lower)

Unfortunately, during phase B of the project, serious problems arose with the concept of full reusability of the vehicle and major issues related to cryogenic propellant storage, as well as Thermal Protection System (TPS), caused a unexpected increase of program cost. For this reason, the American Air Force started investigating the concept of the Trans-Atmospheric Vehicle Program (TAV), later replaced by the NASP program (Schweikart, 1998). The National Aero-Space Plane (NASP) (Fig. 8) received the official governmental approval in 1986, constituting one of the most important milestone for Point-to-Point transportation system and Single Stage to Orbit (SSTO).

Fig. 8: The concept for X-30 SSTO vehicle of the NASP program

In fact, the goal of demonstrating feasibility of sustained hypersonic cruise, introducing a vehicle able of flying directly to low Earth Orbit, moved completely the focus of the technological challenge. Indeed, this opened a new period in hypersonic vehicles design, when the need of developing transportation systems, characterized by features typical of both aircraft and spacecraft, influenced a lot the research in this particular field. The experimental vehicle coming out from the NASP program was designated as X-30. Even if the program was cancelled at the beginning of 1990's, the NASP program accelerated the technology related to the development of the so-called spaceplanes. Other initiatives were started in the same years also outside the USA, such as the HOrizontal Take Off and Landing (HOTOL) from United Kingdom, which took an inspiration from the problem associated to the overwhelming costs of Space Shuttle program, trying to propose an affordable solution to reduce access to space economic efforts (Parkinson, 1990). This was an important endeavour, since it helped focus the attention on the cost-effectiveness of space programs, especially in Europe. The German Sänger II (Weiland, 2014) and the ESA Future European Space Transportation Investigation Program (FESTIP) (Dujarric, 1999) were the indirect results of this policy. As happened to X-20 and X-30, the HOTOL program was aiming at delivering an operational launch system and, thus, it was not intended as a purely research

project. Unfortunately, the program did not succeed in its goal. In parallel, the Hypersonic Technology Program was approved by the German government and the Sänger II (Fig. 9) concept was conceived.

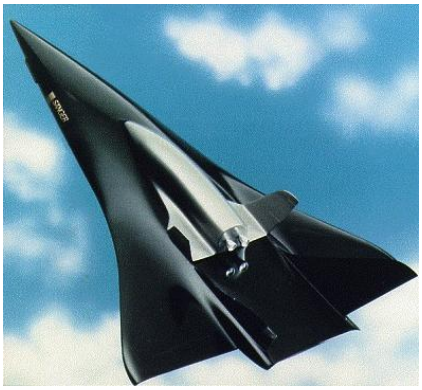

Fig. 9: The concept of the Sänger II

The basic idea was to create a space transportation system, following what already investigated with Sänger I. "*The vehicle was supposed to take off exploiting its own landing gear from a dedicated runway and to accelerate using turbojet engines up to 10 km of altitude*" (Fusaro, 2016). Several phases were then envisaged depending on the mode of operation of the power plant. Particularly, after Mach 3.5, the propulsion system was conceived to move from turbojet to ramjet, up to 35 km of altitude and Mach 6.8. This is the condition were stage separation was expected, after a proper manoeuvre. While the second stage was designed in order to perform orbital manoeuvres and payload commissioning, the manned first stage could fly back to the launch site for servicing. The second stage was designed with a modular approach, in order to possibly either fly as unmanned or to host crew members. The overall mission duration was expected around 50 hours from take-off to the landing of the second stage (following a glide and unpowered but controlled approach). Even if the attention to costs was one of the most important aspects considered by the project, producing important studies still valid today for the assessment of life cycle cost of hypersonic vehicles (Koelle, 2012), the need of developing two different stages deeply impacted on the outcomes of the program. On the other side of Europe, France was also interested in high-speed air-breathing flight. Having successfully designed and operated the Mach 2 Concorde, *"the most interesting hypersonic initiatives were related to the PREPHA program* (Falempin, et al., 1998)*, focused on 5 main research areas: propulsion system, CFD numerical techniques, materials, vehicle subsystems"* (Fusaro, 2016) as well as improvements to test facilities. At the same

time, while Soviet Union, was focusing on the re-use of their Antonov AN-225 as carrier for the MAKS program (Zagainov & Plokhikh, 1991), "*also in Japan, many activities related to hypersonic transportation systems have been carried out. In particular, the Japan National Aerospace Laboratory put lot of efforts in the definition of a SSTO aimed at providing crewed launch to an hypothetical space station orbiting at LEO, defining a purely experimental version of HOPE vehicle"* (Fusaro, 2016). Several other vehicles all over the world were conceived, such as the Hermes spaceplane in Europe (Van den Abeelen, 2016) and the Hope-X (Yanagihara, et al., 2001) experimental vehicle in Japan. In 1988 Russian Buran (Hendrickx & Vis, 2007) was capable of performing its first (and, unfortunately, last) flight. The progressively growing attention to costs of access to space pushes American Government to keep investing in the X-Aircraft program. In particular, X-33, X-34, X-37, X-38 Crew Return Vehicle and X-40A were conceived for different purposes. X-33 (Fig. 10) *"was designed to demonstrate unique aerospike engines, composite liquid hydrogen tanks, a metallic thermal protection system"* (Jenkins, et al., 2003).

Fig. 10. Concept for the X-33 vehicle

Instead, the X-34 project focused on low-cost technologies for access to space, having as major goal the development of a prototype able to reach Mach 8 and 80 km of altitude. Its development was then moved within the X-37 Pathfinder program in 1999. "*A completely different idea led the design of the X-38. This was a demonstrator for a crew return vehicle (CRV) from the International Space Station (on orbit since 1998). Differently to the previous ones, the X-40* (Fig. 11) *was a scaled version of the X-37, conceived as a Space Manoeuvre Vehicle (SMV) carried to hypersonic speeds by a sub-orbital reusable first stage*" (Fusaro, 2016).

Fig. 11: The X-40 during a flight test

In 2001, *"the X-43A Hyper X program seeks to overcome one of the greatest aeronautical research challenges – air-breathing hypersonic flight"* (Jenkins, et al., 2003). The aim was related to the validation of propulsive air-breathing technologies for high speed flight (Mach 7 to 10). The vehicle (Fig. 12) was designed to be hosted on top of a Pegasus booster, launched itself from a NB-52B carrier. Even if the first attempt failed because of the loss of control of the booster, several other attempts provided the desired results, setting speed records and allowing the collections of data for the high-speed propulsion and combustion dynamics, with scramjets operating for at least 10s after the ignition.

Fig. 12: Concept for the X-43 vehicle

Coming to the last two decades, honourable mentions can be devoted to the business of commercial spaceflight. Among the various initiatives, the X PRIZE Foundation offered a very important occasion for the acceleration of sub-orbital flight development, from a commercial point of view. The X PRIZE (Byko, 2004) was again focused on high efficiency access to space solutions, capable of reducing cost. In 2004, the X PRIZE was won by the Space Ship One concept, which has been improved by Virgin Galactic, and it's currently in operation as Space Ship Two (Fig. 13) for commercial suborbital flight in USA (Virgin Galactic, 2016).

Fig. 13: Space Ship One (upper) and Space Ship Two (lower) attached to the White Knight I and II carriers

At the beginning of 2000 USA continued also to develop commercial programs. "*Among the most famous American commercial programs, Astroliner* (Mihara, 2003)*, Rocketplane* (Raymer & Burnside Clapp, 2012)*, Space Access-1 and Space Cruiser System* (Gopalaswami, 2010) *could be remembered. In particular, Astroliner* (Fig. 14) *was conceived to be towed into the air by a modified Boeing 747 aircraft to an altitude of 6 km so to proceed on a sub- orbital trajectory under its own power. However, Astroliner was based on expendable upper stages for the delivery of payload into orbit at an altitude of 125 km and a speed of Mach 6.5*" (Fusaro, 2016). The concept designed by Pioneer Rocketplane (Fig. 14), named Pathfinder, was a candidate for the X-34 program. Even if not selected, the development was continued by the company which originally proposed the solution. The pathfinder is a crewed spaceplane powered by both air-breathing jet engines and LOX/kerosene rocket engines.

Fig. 14: Concepts for Astroliner (left) and Rocketplane (right)

The vehicle is supposed to take off horizontally using turbofan jet engines, to reach an altitude of 6 km for air-to-air LOX refuelling operations, and subsequently to ignite its rocket engine for a climb up to an altitude of 112 km at Mach 15. A conventional liquid rocket upper stage can then carry the payload into orbit as the spaceplane re-enters the atmosphere. After deceleration to subsonic speeds, the vehicle should be able to switch on its jet engines and perform a powered horizontal landing. The Space Assess SA-1 has been proposed to conduct satellite launches by Space Access LLC. It consists of an unpiloted spaceplane that uses a hybrid propulsion system and rocket-powered upper stages to deliver payloads to LEO or Geostationary Transfer Orbit (GTO). The Space Cruiser System (SCS) vehicle was designed to carry six passengers on a sub-orbital flight reaching an altitude of just over 100 km. SCS is a two-stage horizontal-take-off and landing concept that employs both air-breathing and rocket engines. The first stage booster will be piloted by a two-member crew and will be powered by two jet engines. The second stage spaceplane (hosting two crew members and six passengers) will be carried underneath the first stage. The two stages will climb together to about 15 km where the second stage separates aiming at reaching 100 km using its three rocket engines. During re-entry into the atmosphere, the second stage will fire retro-rockets to slow the vehicle descent and to activate two turbo-jet engines to return to a landing site.

More recently, in Europe, different initiatives were successfully providing encouraging results. Among them, the successful mission performed by Intermediate eXperimental Vehicle (IXV) (Tumino & Yves, 2006) has been a real demonstration of the European capabilities of designing, developing and also operating vehicles for access to LEO. In particular, IXV (Fig. 15) consolidated the knowledge and expertise necessary for the development of future European re-entry systems.

Fig. 15: Concept of the IXV

1.1.2 The future trends towards 2050

Nowadays, hypersonic flight is still a hot topic and the interest among the worldwide community appears to be in a growing trend. On one side, there are both an evolution towards innovative civil aviation concepts, bringing out new configuration of aircraft and missions as well as continuous efforts to develop reusable access to space technology. On the other hand, military research projects are progressing, especially outside Europe, in the attempt to conceive new kinds of weapons, for which, however, information and data are highly restricted. The experience acquired during the previous century has provided engineers with a lot of concepts and examples to be used as reference for the development of new vehicles, specifically targeting the needs urging the new millennium. Even if the pace is less persistent with reference to the period described in Section 1.1.1, important initiatives have been funded to investigate hypersonic flight and related technologies. It is interesting to see that, in many cases, the new initiatives are not starting from scratch but they are somehow re-using data, concepts or facilities coming from last century, in order to make benefit of the research previously performed. There is in fact a "re-discovering process" of some concepts designed in 1960's, which is highly relevant from the point of view of the engineering practice. In particular, it is possible to recognize a set of initiatives that in early 2000's paved the way for the instantiation of specific research branches that are used to associate the different programs within a specific roadmap for technology development. Concisely, the hypersonic research domain is then now dominated by a strong re-use of past experience in the field, and by a more categorized focus on incremental path towards the 2050 horizon. Europe had a very important role in this context, in the last years, becoming one of the most important key player of the research.

For example, one the most interesting initiative is the one carried out by Reaction Engines Ltd. that is currently continuing the design and development of the SKYLON (Fig. 16) (Varvill & Bond, 2004), whose project roots date back to the HOTOL concept (Parkinson, 1990). This vehicle is an unmanned, reusable spaceplane intended to provide SSTO services. It will be capable of transporting 15 tonnes of cargo into space, exploiting the Synergistic Air-Breathing Rocket Engine (SABRE), which combines air-breathing and rocket cycles in order to enable the take-off from conventional runway, to fly direct to earth orbit and to land, just like an aircraft.

Fig. 16: Concept for the Skylon SSTO

For what concerns high speed transportation, LAPCAT II (Long-Term Advanced Propulsion Concepts and Technologies) (Steelant, et al., 2015) is a follow-up of the previous European Community (EC) co-funded project LAPCAT (Steelant, 2008). The primary objective of the first project was to develop different vehicle concepts enabling the potential reduction of antipodal flight times to about 4 hours, investigating main enabling technologies. Among the several vehicle configurations analysed during the project, only two concepts for Mach 5 and Mach 8 (Fig. 17) flight, were selected for further evaluations in LAPCAT II.

Fig. 17: Concepts for Mach 5 (left, A2) and Mach 8 (right, MR2.4) hypersonic cruisers designed in LAPCAT project series

At the same time, in Germany, DLR is proposing a concept for a vehicle which aims to fill-in the gap between aeronautics and space domains. Indeed, he Spaceliner (Fig. 18) is a two stage Reusable Launch Vehicle (RLV) aimed at performing ultra-long-haul routes, like Europe – Australia in 90 minutes, promising, in general, to reach intercontinental destinations in slightly more than one hour (Sippel, et al., 2015). Moreover, in the last years, a new mission concept is under investigation, allowing the exploitation of the two-stage vehicle to deliver payload delivery in LEO, fostering reusability (Sippel, et al., 2018). In USA, the Boeing X51-A (Fig. 19) (Hank, et al., 2012), a hypersonic waverider demonstrator based on the heritage of X-Aircraft program, was successfully tested, after some failed attempts, flying at Mach 5 after being launched from a B-52 carrier aircraft.

Fig. 18. Concept for Spaceliner system

This was a test bed for free-flight of a hypersonic vehicle conceived to assess the validation of waverider concept, as well as to acquire data from a real flight test campaign.

Fig. 19: X-51 attached to B-52 wing pylon

Based on the experience of Tu-144 and Tu-360 concepts, also Russia is looking again with interest to hypersonic regime, proposing new aircraft configurations and actively taking part to European projects like HEXAFLY and HEXAFLY International (Favaloro, et al., 2015). From 2018, the European project STRATOFLY (Viola, et al., 2019) is making benefit of the experience acquired within the LAPCAT and HEXAFLY project series, as well as of the heritage of technology studies performed in ATLLAS (Steelant, 2009) and HIKARI (Blanvillain & Gallic, 2015) projects, proposing a Mach 8 hypersonic cruiser for passengers transportation (Fig. 20). This interesting case study, which encapsulates most of the experience gained in European context in the last 20 years, is described in detail in Chapter 3 and it is used throughout this Dissertation as the reference case study.

Fig. 20: Concept for the STRATOFLY MR3 vehicle

It is particularly interesting to evaluate the trend related to hypersonic flight research, looking at the main investigated areas, to understand the change of focus during the years. This helps understanding the origin of the study and contributes in the comprehension of future evolution of the technology. A summary of the main programs briefly described in Sections 1.1.1 and 1.1.2 is provided in Table 1, starting from the X-15 (studies about re-entry capsules are here neglected).

Table 1: Summary of main research programs and vehicles related to hypersonic flight

Program/Vehicle	**Developer's Country**	**Program/Vehicle development progress**	**Research area**	**M**	**Year**
X-15	USA	Retired 1968	SUB, ATS	6.7	1959
X-20	USA	Concept	HST, SUB, ATS	18	1963
ASSET	USA	Retired 1965	Re-entry	25*	1963
Sänger I	DE	Concept	ATS	N/A	1965
PRIME, X-23	USA	Retired 1967	Re-entry	25*	1966
M2-F2	USA	Retired 1967	Re-entry	0.7	1966
X-24 series	USA	Retired 1971	Re-entry	1.6	1969
HL-10	USA	Retired 1970	Re-entry	1.8	1970
Space Shuttle	USA	Retired 2011	ATS	25*	1977
HOTOL	UK	Concept	ATS	N/A	1985
Sänger II	DE	Concept	ATS	6.8	1985
HOPE-X	JP	Concept	ATS	N/A	1985
NASP X-30	USA	Concept	ATS	11	1986
PREPHA	FR	Concept	ATS	N/A	1986
HERMES	EU	Concept	ATS	N/A	1987
MAKS	RU	Concept	ATS	N/A	1988
X-33	USA	Concept	SUB, ATS	13	1990

Astroliner	USA	Concept	ATS	N/A	1990
X-34	USA	Concept	SUB, ATS	8	1995
X-38	USA	Concept	Re-entry	N/A	1995
X-40A	USA	Retired 2001	ATS	1.5	1998
X-43	USA	Retired 2004	HST	7	2001
Space Ship One	USA	Retired 2004	SUB	3.5	2003
Rocketplane	USA	Concept	SUB	15	2005
Space Access - 1	USA	Concept	ATS	N/A	2005
Space Cruiser System	USA	Concept	SUB	N/A	2005
Spaceliner	DE	Concept	HST, ATS	20	2005
SKYLON	UK	Concept	ATS	28*	2006
LAPCAT MR2	EU	Concept	HST	8	2008
X-37	USA	In Service	ATS	6	2010
X51-A	USA	In Service	HST	5	2010
HEXAFLY	EU	Concept	HST	7	2012
HEXAFLY Int.	EU - RU	Concept	HST	8	2014
IXV	EU	Retired 2015	ATS, Re-entry	28*	2015
STRATOFLY MR3	EU	Concept	HST	9	2018

Table 1 reports the different research programs and related vehicle depending on the year of first flight or, in case of concepts, of contract award. Research areas include Access To Space (ATS), Suborbital flight (SUB), High Speed Transportation (HST) and Re-entry. Mach number refers to maximum Mach reached during test or flight campaigns, where available. Mach numbers marked with a star refers to re-entry conditions at available reference point of the trajectory (actual or predicted). It is worth performing a post-processing of the data reported in Table 1 in order to better see the evolution of research within the hypersonic field, as previously described.

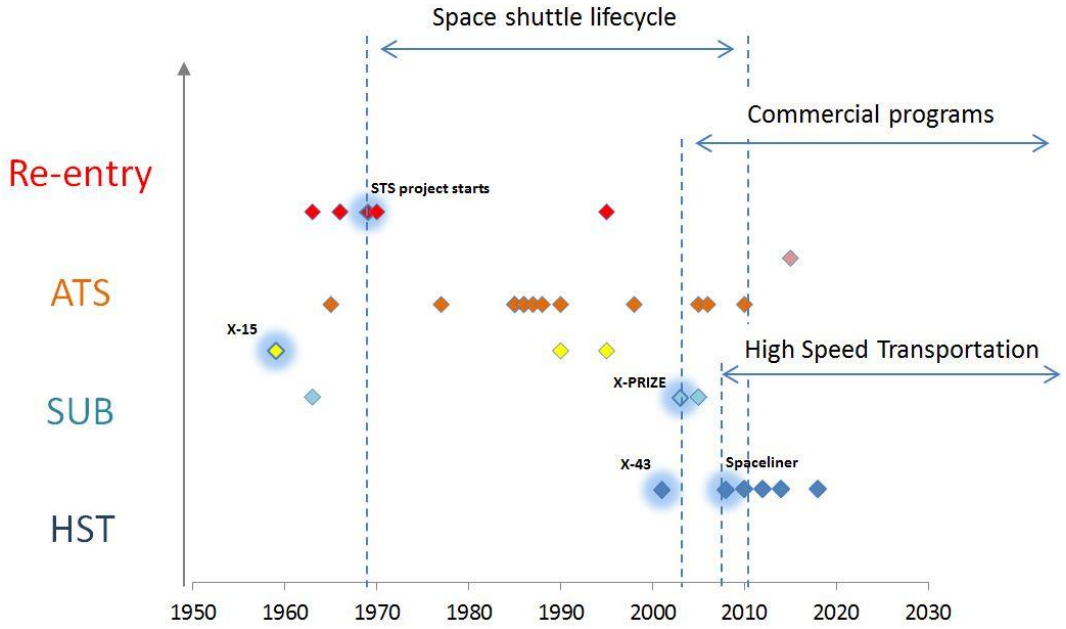

Fig. 21: Summary of research in hypersonic field

Actually, from Fig. 21 it is possible to distinguish three main periods and several milestones that drove the main research activities. On the left of the chart an early development region, characterized by ten years of understanding of basic phenomena (no vehicles developed) and by a subsequent decade of records, starting with the entry into service of X-15, can be identified. Being in between suborbital and ATS domains, the X-15 was the most important milestone for the early hypersonic flight, since it was extensively used as test bed for both development of the enabling technology and for multi-purpose astronauts training. At the end of 1960's, the Space Shuttle Program was ready to start, with its entry into service scheduled for 1980's. Particularly, Fig. 21 indicates the period 1969 – 2011 as the Space Shuttle Lifecycle, from program start to retirement. This period was characterized by a high focus on re-entry and ATS topics, especially when the cost associated to the operation of the Shuttle rapidly grew. The worldwide community was then triggered to think about innovative solution to allow a more cost efficient ATS through new configurations of vehicles. While the way to fully reusable ATS is still not completely understood, the millennium brought an important change in hypersonic research field. The first flight of an air-breathing hypersonic propulsion plant paved the way towards the concept of HST with the X-43 and, almost at the same time, the X-PRIZE provided a considerable acceleration on suborbital vehicles development. The era of commercial programs started, and keeps running still today. Moreover, the progress related to high

speed initiatives, led to the design of different concepts for passengers' transportation, especially in Europe. On the other hand, the successful test of the X-51 in 2010, as evolution of the X-43, contributed to the development of innovative propulsion concepts. In general, a progressive reduction of altitude can be noticed in the field of hypersonic flight research, with the HST used also as main platform to develop efficient ATS vehicles. This is a new trend if compared to past decades, where the rush for finding a solution related to the high cost associated to not fully reusable vehicles for space applications was driving the research to focus mainly on ATS topics. Suborbital flights are also increasing in these years and the commercial flight related to space tourism surely constitutes a radical change with respect to past years. In 2016, Boeing (The Boeing Company, 2016) declared that hypersonic cruiser for passengers transportation can be potentially developed by 2040 – 2050 and, with a similar timeline, also European Commission is including the development of high-speed clean enabling technologies in its Flightpath 2050 (Krein & Williams, 2012). The time is now then, and several exciting years are yet to come for hypersonic.

1.1.3 A general classification to be used as starting point

From Sections 1.1.1 and 1.1.2 it is clear that the need to investigate the hypersonic regime was historically driven by the progress in space domains, especially concerning re-entry. The focus then changes over the years, moving to the analysis of more efficient access to space possibilities and, only recently, to the opportunities related to high speed commercial flight for passengers transportation, in case of point-to-point missions. The two latest topics still constitute the main current research areas for hypersonic vehicles related to Earth environment. Because of the heterogeneity of vehicles types and purposes, as well as of the physical phenomena characterizing the hypersonic flow in different conditions, in 2005 (Hirschel, 2005) proposed a classification for hypersonic vehicles that can be summarized as follows:

- Cruise and Acceleration Vehicles (CAV) – Aircraft-like, slender vehicles, typically exploiting air-breathing engines for flight at high altitude in atmosphere and low hypersonic regime, performing a point-to-point mission similar to those of commercial airliners. They are conceived to maximize lift-over-drag ratio in cruise to cover long distances;
- Ascent and Re-entry Vehicles (ARV) – SSTO vehicles conceived for ATS and space transportation purposes. They are usually designed to reach LEO, so they need to host rocket propulsion in parallel to air-breathing

engines (if present). They cover different flight regimes, from orbit to subsonic flight, thus requiring a challenging compromise between spacecraft and aircraft characteristics;

- Winged Re-entry Vehicles (RV-W) – vehicles capable of performing a controlled re-entry within Earth (or planet) atmosphere, generally adopting a gliding trajectory. They are properly designed to withstand the re-entry thermal environment but they shall be able to fly like a conventional aircraft while in atmosphere. They are not responsible for ascent, typically carried by first stage(s) or booster. The Space Shuttle Orbiter is the most evident example of the category;
- Non-Winged Re-entry Vehicles (RV-NW) – vehicles able of performing a ballistic re-entry within planet atmosphere depending on the Entry Interface Point (EIP). They include capsules or lifting bodies with limited controllability. The design is highly influenced by the need of maximizing drag capability for deceleration, within structural and thermal limits, thus usually proposing blunt shaped objects. As RV-W, they are delivered on orbit thanks to multiple ascent stages;
- Aero-assisted Orbital Transfer Vehicles (AOTV) – this is a very peculiar vehicles class, including spacecraft able to make benefit of planet atmosphere to control their trajectory. They are typically equipped with fixed, deployable or inflatable heat shields to be used in high altitude atmosphere to decelerate the vehicle for multiple purposes. Typical applications are related to spacecraft deceleration through multiple atmosphere transfers for planet orbital insertion (aero-capture), as well as progressive deceleration (aero-braking) prior to lander release for re-entry. The spacecraft is then designed first for high altitude high speed hypersonic regime, with progressive reduction of Mach number and height.

The list of vehicle classes here provided includes the complete set of flight conditions characterizing the hypersonic regime, from high supersonic to orbit. It is clear that the typical environment of CAV is quite different from the operating conditions characterizing AOTV, thus requiring a detailed analysis of hypersonic sub-regimes. Moreover, it is crucial to first provide a definition of hypersonic before moving to the description of its main phenomena. This would allow not only for a clarification of the boundaries of the analysis, easing the comprehension of main physical aspects, but also for the understanding of the main challenges to be considered within the design of the aforementioned vehicles

classes. For these reasons, Section 1.2 provides an introduction to the main characteristics of hypersonic environment, starting from its basic definitions and qualitatively analysing the main phenomena occurring in previously-cited conditions.

1.2 Hypersonic flight regime at a glance

Following the definition available in literature, *"there is a conventional rule of thumb that defines hypersonic aerodynamics as those flows where the Mach number is greater than 5"* (Anderson, 2006). In fact, there is not a real barrier or discontinuity, as it happens when moving from subsonic to supersonic, and, depending on the physical condition as well as on the phenomena involved, it is possible to consider a different threshold to speak about hypersonic. The reason for selecting Mach 5 is rather related to the change in characteristics of the flow when accelerating above this speed. The hypersonic regime is actually a supersonic one, with additional phenomena, starting to occur at Mach 5, which characterize the peculiarity of this flow. The reason for the difficulty of establishing a universal threshold is mainly associated to the behaviour of the flow itself and to the presence of these phenomena. As a matter of fact, the transition from pure supersonic to hypersonic is generally smooth and some physical events, typical of the hypersonic regime, already occur at Mach 3, whilst others appear only at Mach 7 or higher. In general, the hypothetical threshold of Mach 5 is selected because that's the stage at which the importance associated to new gas dynamics phenomena becomes relevant, if compared to supersonic flow. In order to understand the nature of hypersonic flow, this paragraph briefly describes the main characteristics of the regime, pointing out those issues that shall be considered as the most important aspects for the design of RV-W/NW, ARV and CAV. The main characteristics of hypersonic flow are listed hereafter:

- thin shock layer;
- additional presence of an entropy layer;
- viscous interaction effects are present;
- high-temperature effects are present;
- generally, low density effects are present for high altitude flight.

Hypersonic regime is, as it happens for supersonic, dominated by shock waves. Compressions and expansions at these high speeds usually lead to discontinuities within the flow, characterized by regions having very different pressure,

temperature and density levels. Following the principles of the oblique shock theory (Anderson, 2007), the angle between the shock wave and the undisturbed flow field tends to assume the value of the angle of the object which generates the shock itself. This means that the flow field between the shock wave and the body, namely the shock layer, is particularly thin. This effect is even more evident in presence of chemically reacting gas, as usually happens when dealing with high temperature flow. The position of the shock wave, which lies close to the body, brings a series of problems related to the design of its leading edges, since the flow has not the time to reduce is temperature, transferring most of its energy as heat and producing high heat fluxes through the object. Moreover, in front of leading edge, the shock may experience a bow-shaped surface (in this case it is referred to as bow-shock) which can be treated as a nearly normal shock. Also in this case, the distance between the bow-shock (stand-off distance) and the body is very limited, with critical heating problems. Additionally, boundary layer is highly affected by strong entropy gradient, since the stand-off distance is smaller than the shock layer distance downstream. The gradient is a direct consequence of the presence of the shock, which increases the entropy level of the flow, and it is not so strong, so that a specific entropy layer can be identified in the mathematical models when dealing with boundary layer interactions. The shock layer close to the normal shock is in fact characterized by a higher level of entropy if compared to shock layers located downstream, creating a sort of additional zone all along the body leading edge, which is characterized by a high vorticity, generally thicker than the boundary layer itself. This is a general problem of such kind of regime, considering also that, in hypersonic, the boundary layer is itself thicker with respect to a more conventional one. This is due to the relevant increase of temperature within the layer because of the transformation of kinetic energy into internal energy at walls. This effect produces, on one side, an increase of gas viscosity and, on the other hand, a local decrease of density (the pressure in the normal direction of the layer is constant). Both phenomena contribute to substantially increase the thickness of the layer. As result, from the point of view of the far flow field, the object appears bigger than it actually is, since the thick boundary layer may interfere with the inviscid flow incoming. This one can then be subjected to strong deviations, influencing pressure distribution, lift and drag. The phenomenon is known as viscous interaction and may have non negligible effect on the aerodynamic efficiency of the vehicle and on the heat transfer at the wall. Viscous dissipation due to friction is in fact one of the most critical aspects of hypersonic flow, together with the presence of high temperature shock layer very close to the body, as already mentioned. Depending on flight regime and

type of mission, temperature may rise from hundreds of degrees Kelvin up to 11000 K (Apollo re-entry) and even more. This means that high temperature effects on hypersonic flow are very different depending on the Mach number. In general, high temperature or real gas effects are related to the characteristics of the flow within the boundary layer, which is constituted by a chemically reacting gas, completely modifying the mathematical models able to predict its behaviour. Phenomena like dissociation and even ionization can create new chemical species within the gas mixture, influencing aerodynamic characteristics of the vehicles and chemically interacting with the material of body exposed to the flow. Again, there is not a universal threshold at which these phenomena occur, since high temperature effects depend on pressure ratio and chemical composition of the gas. For air at sea level pressure conditions, dissociation starts to be important at temperature higher than 800 K and, notably, O_2 as well as N_2 starts dissociating at 2000 K and 4000 K respectively. Molecular oxygen and nitrogen even disappear at 4000 K and 9000 K respectively, when nitric oxide is created by the combination of the two atomic species. Ionization occurs instead at higher temperatures, being a typical phenomenon of the re-entry phase, where this effect causes also the well-known problems related to communication black out (high number of ions and electrons are present within the plasma around the vehicle). It is then clear how the design problem related to hypersonic vehicles sizing shall be carefully investigated, focusing on the definition of the mission first, so to identify proper aerothermodynamic issues to be solved for the proper environment. However, in general, hypersonic flight is characterized by low density flows, because of the intrinsically high altitude at which the vehicles fly. In fact, at low altitudes, the gas can be treated according to the continuum hypothesis, thus considering the mixture to be a single gas even if composed by different molecules. This hypothesis is based on the value of mean free path among molecules, i.e. the average distance between successive collisions among the molecules of the mixture. In order to formulate the continuum hypothesis, the Knudsen number (1) is usually adopted so to compare the mean free path λ and the reference length to be used within the analysis L

$$Kn = \frac{\lambda}{L} \qquad (1)$$

A flow is considered continuum if $Kn < 0.01$. While decreasing flow density, the mathematical model shall change so to represent slip flow ($0.01 < Kn < 0.1$) or even free molecular flow ($0.1 < Kn < 10$). The way in which flow is modelled can be radically different depending on the conditions since, for example, in free

molecular regime gas particles collisions among each other is such rare that only the collision with the vehicle can be considered. On the other hand, in transitional and continuum flow regimes, proper models, such those based on Navier-Stokes equations of fluid dynamics, shall be applied with related hypotheses. For intermediate regimes, a statistical approach can even be used, such as Direct Simulation Monte-Carlo, to represent particle flow. In general, the situation can be qualitatively represented by Fig. 22 (Anderson, 2006), which can also be used as summary for this brief discussion on the typical phenomena characterizing the hypersonic regime.

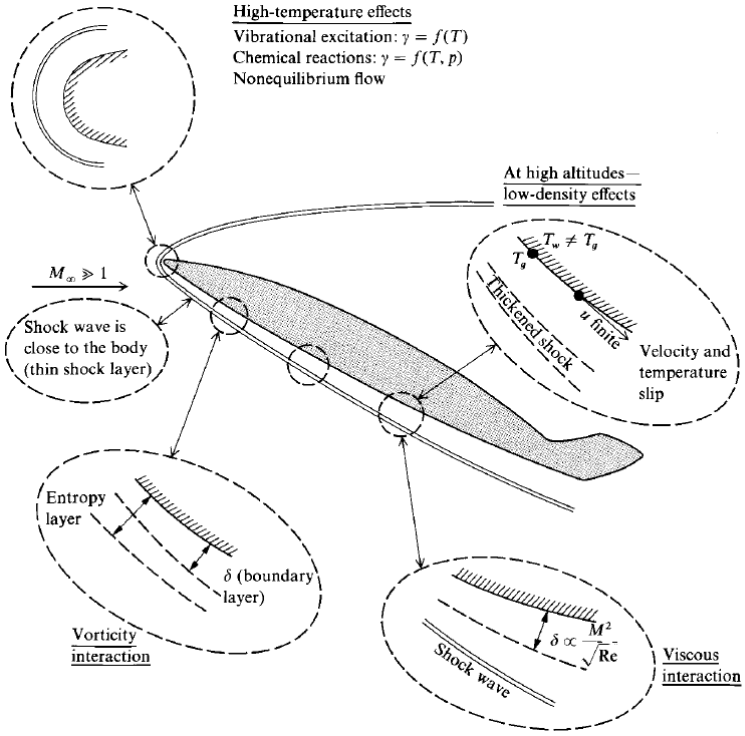

Fig. 22: Summary of hypersonic flow characteristics (Anderson, 2006)

These kinds of topics would require more extensive analyses. However, the aim of this section is not to provide a detailed description of these phenomena, being out of the scope for this Dissertation, but rather to introduce the problems associated to high speed flight, so to anticipate those issues typically affecting hypersonic vehicles design. Starting from the basic description of the phenomena provided in this section, subsequent Sections 1.2.1 to 1.2.3 provide additional details about the main phenomena to be considered for the design of RV-W/NW, ARV and CAV.

1.2.1 Re-entry vehicles

Re-entry vehicles (both winged and non-winged) are conceived to perform the last part of a space mission, from Entry Interface Point (EIP) in atmosphere to actual landing. Depending on the application, they can be characterized by different features, materials and shapes but, in general, they have a common point: during re-entry phase they experience a wide range of Mach number, from high hypersonic ($M = 30$) to subsonic regime ($M \approx 0$). This means that, during the flight, they encounter most of the conditions and the phenomena briefly described in Section 1.2, in very short time. The design is thus quite complex since different aspects shall be taken into account. Traditionally, re-entry vehicles are configured to maximize deceleration capabilities, being thus characterized by a blunt shape, which is also beneficial for heat fluxes alleviation. Curvature radii of the leading edges are in fact high to mitigate fluxes peaks in critical regions, especially considering that the vehicles are flying at high angle of attack. Aerodynamic efficiency is also low, since drag is high and lift generation capability is not very effective (even for winged vehicles). Thermal loads are high, requiring a dedicated Thermal Protection System (TPS) with different characteristics depending on the location on the vehicle and phenomena related to thermo-chemical surface effects. In fact, re-entry vehicles fly through both ionized plasma and dissociated flow while decelerating, being affected by alteration of chemical composition of the material on external surface. Moreover, they experience a wide range of atmospheric conditions, from free molecular environment up to continuum flow. RV-NW sub-category usually comprehends re-entry capsules, which are designed to perform a ballistic re-entry within planet atmosphere, with limited control capabilities. Depending on the mission, they may have different characteristics related to shape, deceleration strategies and heat shields. Planetary re-entry capsules, for example, experience higher re-entry speeds if compared to manned re-entry vehicles from LEO, thus requiring a different configuration. In general, the main aim of the capsule is to protect its payload during the descent and to maintain internal environmental conditions suitable for payload survivability also when on ground, up to recover. Since they are performing a ballistic re-entry, they usually conclude the descent with a parachute-assisted ground landing or splash-down. Re-usability of the vehicle is limited, especially considering that most of the TPS reaches surface temperatures that can be affordable for single use only. Volume capacity is also small. RV-W and lifting bodies are instead conceived for a glide controlled re-entry through planet atmosphere. They are always designed to produce a relevant deceleration

capability but they are also capable of generating a reduced amount of lift for final descent. Most of the characteristics are similar to RV-NW even if they can offer a higher payload volume, a less steep trajectory and a variable attitude during descent. One of the most critical aspects for RV-W is the design of control surfaces, which shall be able to operate in very different conditions and, generally, in a hostile environment. The most successful example of RV-W is the Space Shuttle Orbiter, which is also capable of landing on a prepared runway, exploiting its own landing gear. Most parts of these vehicles can be re-used, even if a re-conditioning of some components, especially belonging to the TPS, may be required.

1.2.2 Ascent and re-entry vehicles

Ascent and re-entry vehicles are probably the most complex vehicles category to be designed, since they are conceived to fly in the same regime of RV-W ($0 < M < 30$) but they have also conflicting design and performance requirements, especially in terms of slenderness. In fact, aerodynamic efficiency shall be determined through a trade-off to guarantee the required deceleration capabilities, as well as to ensure flight performance during climb and low-speed phases. At the same time, angle of attack during the mission changes a lot, thus producing a non-negligible effect on both lift and drag. Both thermo-chemical and viscous effects are present during the mission profile on the surface and the evaluation of thermal loads, which can be high during re-entry phase such as for RV-W, shall be carefully assessed since the flight time is usually higher than simple re-entry vehicles. In order to be able to perform ascent, the ARV shall be equipped with a propulsion plant suitable to provide thrust at different altitudes and flight regimes. The selection of the type of engines (air-breathing, rocket, combined cycle etc…) is thus fundamental for vehicle configuration, especially concerning airframe – propulsion integration. In case of air-breathing engines, the design of air-intake for atmosphere flight, as well as nozzle definition, are particularly critical. Selection of propellant type both in case of air-breathing and rocket engines is also important not only for power plant performance but also for mass and volume efficiency evaluation. Propulsion plant design itself is quite complex, since the optimum solution related to modes of operation and overall architecture shall be determined. Moreover, the need of performing a fully controlled flight brings additional challenges considering control surfaces design, as for RV-W. Currently, there are no examples of ARV in operation, but some concepts for SSTO vehicles, such as the SKYLON (Section 1.1.2) are being developed. Main

challenges hampering the development of this kind of vehicles are related to propulsion technologies, design to reusability, payload capacity in LEO and operating cost management.

1.2.3 Cruise and acceleration vehicles

Cruise and acceleration vehicles are radically different from RV and ARV since they are conceived to fly within atmosphere only. Typical examples of CAV concepts (Section 1.1) are designed to perform either military or civil mission with very high range (15000 – 20000 km), flying in cruise at an altitude of around 20 – 40 km at Mach 5 – 10. They shall thus maximize aerodynamic efficiency, reducing drag and adopting a slender configuration. Due to the reduced temperature that are reached with respect to the vehicles categories mentioned in the previous sections, thermo-chemical effects are less important and viscous interactions are instead dominating. Heat fluxes are lower if compared to RV but the need for a slender configuration, i.e. for sharper leading edges, may anyway induce thermal management problems. Actually, thermal management is one of the key aspects of the design, since the long flight time may produce high heat loads accumulation. Innovative solutions for heat dissipation shall then be considered to guarantee suitable environmental parameters on board and also to maintain TPS and structure materials within their operational temperature ranges. Another crucial aspect to be properly taken into account is the integration of power plant within the airframe. Many concepts exploit air-breathing engines and, similarly to ARV, the design of intake and nozzle is fundamental for the derivation of a proper aircraft configuration. Also in this case, the definition of the sequence of operation for the propulsion plant is important to select its architecture, considering the need for flying both at subsonic, supersonic and hypersonic regimes. Volumetric efficiency of the vehicle is another interesting parameter to validate the viability of the concept, since aircraft design is heavily payload-driven. This is even more critical when evaluating cryogenic propellants, typically characterized by a higher energy per unit mass, but a considerable lower energy per unit volume. Controllability of the aircraft is an important aspect to be investigated as well, since control surfaces shall be designed to guarantee proper manoeuvrability both in hypersonic and at low speed. Additional constraints related to operational characteristics of the aircraft shall be carefully assessed too. In case of civil applications, aspects associated to environmental impact, both in terms of pollutant and noise emissions, shall be considered while sketching the overall aircraft and mission configuration. Moreover, Air Traffic Management

(ATM) integration and safety aspects shall be included within the design to meet current regulations. As for the ARV, there are not existing examples of CAV, but many concepts are currently under design. The interest of global scientific communities on this category is very high since most of the enabling technologies related to sustained hypersonic flight, associated typically to scramjet propulsion and thermal management, are under development in this field, with the aim of providing flying prototypes in the next years. CAV are in fact seen both as a natural evolution of current civil aviation, but they might also represent an intermediate step towards reusable access to space.

1.3 Challenges of hypersonic aircraft design

Independently from the considered category, hypersonic vehicles design is characterized by a high level of complexity, mainly due to the different aspects to be considered within a multidisciplinary environment. As already described in previous sections, from a purely technical point of view, the main challenges are related to propulsion technology development, thermal management, airframe-propulsion integration (especially for CAV and ARV), vehicle controllability, aerodynamic design and on-board subsystems architecture definition. Depending on vehicle category, these aspects can be more or less relevant, even if generally present. Fig. 23 provides a schematic overview of the importance of the different topics within the design of RV, ARV and CAV, also referring to (Hirschel, 2005). A hypothetical scoring between 1 (low relevance) and 5 (high relevance) is proposed to allow the visualization of the impact of the different topics on vehicle design. As it can be seen, propulsion-related topics play a crucial role for CAV and ARV.

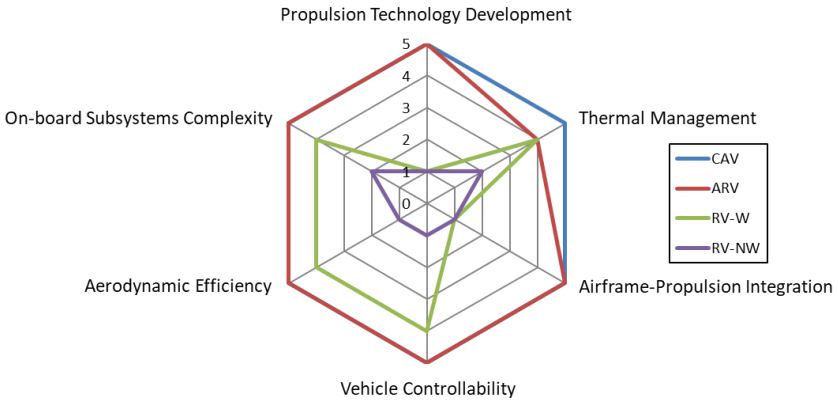

Fig. 23: Summary of main design aspects

This is due to the fact that these vehicles need to fly exploiting their own propulsion plant in atmospheric environment, usually making benefit of air-breathing engines, which are quite difficult to tune and to integrate inside the vehicle. Technology readiness for high speed air-breathing propulsion is also lower with respect to rocket propulsion, providing an even more challenging problem. For ARV and CAV, aerodynamic design might also be quite complex, because of the need to trade between conflicting requirements. For example, the definition of vehicle shape for CAV is driven by the need of reaching the highest possible aerodynamic efficiency, as explained in Chapter 4. On the other hand, the allocation of a suitable amount of volume is necessary to make the aircraft able to carry its payload and to host the other subsystems, thus constituting a set of opposing design requirements (the higher the vehicle volume, the lower the efficiency (Kuchemann, 2012)). For ARV, the need of balancing the requirements related to ascent and those associated to re-entry is even stronger, having a crucial impact on the final design. Vehicle controllability is again a typical problem when dealing with CAV and ARV, but also with RV-W, even if with different priorities. The need to provide control during different mission profile phases influences a lot the control surfaces architecture of the vehicle, particularly while flying in in atmospheric conditions. Thermal management is also directly associated to the time spent in critical environment, such as the atmospheric one. In fact, even if RV and ARV experience the most hostile environment in terms of temperature and heat fluxes, the exposure time is usually very limited for them. CAV are instead supposed to fly for hours within a condition of aerodynamic heating, at an altitude where the effect of drag is relevant. Moreover, they usually exploit air-breathing engines which are subjected to high internal temperatures to be managed, especially close to the combustion chambers. These aspects make thermal management a more critical issue for CAV than for ARV. On the contrary, RV are designed for very specific conditions, limited in time, and usually faced with less complex TPS and Thermal Control Systems (TCS). In fact, systems complexity gives an idea of the overall vehicle configuration, which is simpler for RV-NW if compared to CAV and ARV. Indeed, usually, (Fig. 23) re-entry capsules have simple TPS and on-board subsystems architectures, as well as for aerodynamic characteristics. Moreover, RV-NW have very limited controllability and they usually do not host a proper propulsion plant (excluding landing/deceleration systems like retro-rockets). Conversely, RV-W are more complex than RV-NW for what concerns on-board subsystems, control and aerodynamics and thermal management whilst, also in this case, a propulsion

plant might not be necessary. Conversely, controllability requirements can be softened with respect to ARV, since RV-W are not responsible for ascent.

The outcomes of this short analysis may appear counterintuitive, since CAV result to be the most complex category of vehicles. This is however true because the complexity is mainly associated to the number of parameters and aspects which are strictly interrelated, rather than to the intrinsic difficulties of the topics to be studied. One shall also consider that, looking at the application for which vehicles are designed, CAV result to be bigger in terms of dimensions and mass if compared to others. Particularly, the trade-off between required aerodynamic efficiency and available volume is actually one of the most crucial topics to be faced in conceptual design, at early definition stages (Chapter 4). Moreover, CAV shall be designed in such a way that they can be operated for a longer lifecycle without replacement, in order to be competitive. Far from being a "one-shot" solution, they are configured as hypersonic airliners, and this imposes additional constraints related to safety, operations, cost and environmental impact. Operational challenges are then also quite demanding if compared to other vehicles categories. The worldwide effort related to technology development in the field of CAV, as already mentioned in Section 1.1, is in fact tightly coupled with the research on operational challenges related to the support of the vehicle in service. The integration between technical and operational aspects is fundamental for the development of hypersonic cruisers, since the feasibility of the solution will require a high level of competitiveness in operation to survive and thrive. These are also the objectives of the already mentioned STRATOFLY Project (Viola, et al., 2019), framework within which this work is performed.

The management of vehicle design phases, from conceptual and preliminary design up to subsequent stages shall then be carried out following a formalized approach, specifically conceived to deal with highly integrated and complex systems. Before moving to the presentation of the case study and of the issues related to its design (Chapter 3), it is then worth introducing the Model-Based Systems Engineering (MBSE) methodology that supports this work, both from the point of view requirements management and development, as well as of process formalization. For this reason, after this introduction related to the description of hypersonic flight characteristics and challenges, Chapter 2 introduces to the concepts of Systems Engineering (SE) and to the methodology applied within the work described in this Dissertation.

2

Model-Based aircraft design

This chapter aims at introducing the basics of modern aircraft design, providing an overview of the main trends characterizing the evolution of methodologies, specifically looking at the way in which they have changed to cope with increasing level of innovation and complexity of the products. In particular, the Systems Engineering methodology is presented, and, specifically, the Model-Based approach is introduced with focus on the aerospace domain. The goal is to provide the readers with an overview of the elements of the Model-Based aircraft design approach that are exploited throughout this Dissertation. In details, Section 2.1 provides an historical perspective on aircraft design methodologies, underlying the main reasons that brought to the adoption of Systems Engineering approaches and to the main paradigm shift: from Document Based to the Model Based approaches. Thus, Section 2.2 discusses the main elements and pillars of the Systems Engineering approach, while Section 2.3 introduces the basic concepts of model-based aircraft design, with reference to peculiar innovations.

2.1 A century of aircraft design

Aircraft design *"is a discipline of aeronautical engineering, different from the analytical disciplines such as aerodynamics, structures, controls and propulsion"* (Raymer, 2012), defining the engineering process through which flying vehicles are developed. In particular, closely looking at the aircraft design methodologies from an historical perspective, it is clear that they evolved following the need for *"radical technological change which characterized aviation in the last century, being triggered by innovation"* (Young, 2007), moving from 1930's up to the new millennium. Particularly, specific needs and design philosophies can be allocated on different historical periods, starting from the so called "Faster, Higher, Farther" concept, prevailing during Second World War, up to the "Better, Faster, Cheaper" leitmotif characterizing the second half of twentieth century, because of economic considerations (Young, 2007). In particular, the trends reported in Fig. 24 can be noticed. After Second World War, the amount of new design configurations for aircraft started to drop, both because of the identification of dominant architectures and of the consistently changed philosophy, for which design drivers progressively moved from performance to cost and environmental friendly characteristics. At the same time, the complexity characterizing the design increased substantially with a monotonic trend, not because new products are intrinsically complicated, but since they shall be designed looking at an increased number of requirements and constraints, being highly integrated with the operational context in which they shall behave.

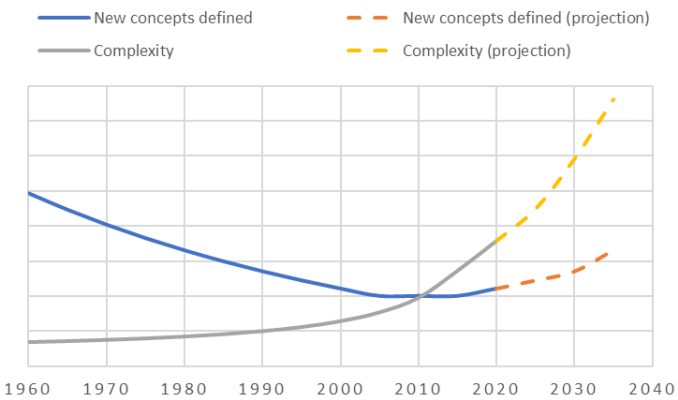

Fig. 24: Qualitative trends concerning aircraft concepts design and complexity from 1960

However, as introduced in Chapter 1, new concepts and ideas concerning aircraft configuration were pointed out in the last decade. In fact, top aviation players and

institutions (The Boeing Company, 2016), (European Commission - High Level Group on Aviation Research, 2011) recently agreed that aviation needs a sort of renovation, being stuck from 1960 for what concerns airliners and general aviation (the basic concept developed within Boeing 707 program (Lombardi, 2007) is, actually, still in use, while for general aviation a relevant evolution has still to be found). For what concerns airliner concepts, new configurations and missions are evaluated in the field of high-speed and environmental friendly transportation, as more effective solution to solve the problem of growing traffic. At the same time, the evolution of the so-called urban mobility is becoming a reality in general aviation world. These aspects contribute inverting the trend related to the definition of new aircraft concepts, also pushing the limits of complexity associate to their development. These new development trends lead also to the definition of more advanced methodologies and tools to support the aircraft design process. Moreover, together with the introduction of new topics within the design process, raising the complexity related to the identification of the optimal solution for the aircraft configuration under study, between 1980's and 1990's, several well-known best practices and guidelines to aircraft design were published (Torenbeek, 1976), (Roskam, 1985), (Raymer, 1995), (Jenkinson, et al., 1999) with the aim of sharing the experience gained within the topic during the years. More recently, a shift from a document-based approach, usually funded on waterfall and report-oriented milestones process, to model-based aircraft design methodologies, relying on proper representations of the system of interest and on the related implementation, generally referred to as simulation, was a clear need emerging from the intrinsically innovative nature of new systems. The increasing complexity, i.e. the higher level of integration of the different aspects of design, was a crucial trigger to move towards a model-based world for two main reasons: first of all, *"models and simulations confirm the need for the systems and the anticipated system behaviours before proceeding with the development. Moreover, models and simulations present a clear, coherent design to those who will develop, test, deploy and evolve the system, thereby maximizing productivity and minimizing error"* (Walden, et al., 2015). This allows thus representing the different elements of the design in a single consistent environment, able to integrate the design disciplines. Also, new engineering activities were defined with the aim of evaluating different design aspects at once, such as the Multidisciplinary Design Optimization (MDO) method. Current trends are progressively embracing Agile methods to face aircraft systems engineering processes.

Considering the importance of understanding the main concepts related to the world of the so-called model-based aircraft design, it is worth defining the main elements of the general approach to the design of complex systems, known as Systems Engineering, as reported in Section 2.2. Then, Section 2.3 presents the model-based aircraft design approach, with reference to existing processes from aeronautics and space domains, highlighting the strong points and the weaknesses of the methods, to introduce the way in which the methodology presented in this Dissertation is defined and implemented.

2.2 The Systems Engineering

2.2.1 Historical notes

As for aircraft design, the Systems Engineering (SE) process has been formalized in early 1990's, following the publication of several theories, standards and methodologies, even if its origins shall be found definitely before this period. For this reason, even if, along the years, different definitions of Systems Engineering have been proposed, the most complete is currently reported in the Handbook of the International Council on Systems Engineering (INCOSE), the highest institution for the formalization of the topic: *"Systems engineering is an interdisciplinary approach and means to enable the realization of successful systems. It focuses on defining customer needs and required functionality early in the development cycle, documenting requirements, and then proceeding with design synthesis and system validation while considering the complete problem: operations, cost and schedule, performance, training and support, test, manufacturing and disposal. Systems engineering integrates all the disciplines and specialty groups into a team effort forming a structured development process that proceeds from concept to production to operation. Systems engineering considers both the business and the technical needs of all customers with the goal of providing a quality product that meets the user needs"* (INCOSE, 2015). Looking back at the origins of the SE approach, it might be noticed that the definition and production of complex military systems during World War II generated, for the first time, the need of studying and operating the system as a whole, requesting for an holistic view of product development and operations. Moreover, the "Space Race" in 1950's was one of the most important periods for the development of the Systems Engineering. In that period, *"some preliminary references appeared and were applied to space programs and intercontinental ballistic weapons, thus promoting some methodologies to develop the systems*

(Systems Engineering) and to assure the full accomplishment of the goals of technical projects (Project Management), together with an effective prediction of risk (Risk Analysis and Management)" (Brusa, et al., 2018). Another example belonging to the same historical time frame was related to the design of telecommunication and power distribution plants, which were seen for the first time as complex systems, i.e. characterized by a high level of interfaces with existing infrastructure. In the following years, the publication of "A Methodology for Systems Engineering" (Hall, 1962) and of the so-called "General Theory of Systems" (Bertalanffy, 1972) are universally recognized as two crucial steps towards the complete formalization of Systems Engineering in the second half of Twentieth Century. In 1990, the National Council on Systems Engineering (NCOSE) was born in USA and the importance of having a unique institution as reference for the definition of Systems Engineering processes and principles was so widely accepted that in 1995 the international council was funded (INCOSE). In the following years, the main standards related to Systems Engineering were released. Particularly, the EIA 632 (ANSI/EIA, 1998) was published by Electronic Industries Alliance and adopted by American National Standards Institute with the aim of defining the processes related to the engineering activities. In parallel, the IEEE 1220 (IEEE, 1998) was more focused on project management and relationships with Systems Engineering approach. In 2002 the most important standard, i.e. the ISO/IEC 15288, defining process, activities, tasks and main concepts of Systems and Software Engineering, was released and adopted by IEEE in 2003. In 2008, ISO, IEC, IEEE and INCOSE among the most important institutions, decided to fully harmonize the Systems Engineering concepts in the ISO/IEC/IEEE 15288:2008 (ISO, 2015). The high acceleration of the end of the century can be fully understood looking at the needs of the designers of agreeing on a unique definition of the main concepts around Systems Engineering. Particularly, the use of proper system views over the product led to the implementation of architecture framework to be used as a sort of dictionary between designers and customers, to really understand system architecture and characteristics. These architecture frameworks were proposed by public institutions and communities, generally belonging to a specific engineering field, and are still in use nowadays. Some of the most famous are the DoDAF (US Department of Defence Architecture Framework) and MODAF (UK Ministry of Defence Architecture Framework), but several others exist (Brusa, et al., 2018). Current trends are establishing robust Model-Based Systems Engineering (MBSE) approaches to manage the data and information generated and collected within product lifecycle, guaranteeing full traceability with requirements and customer

needs throughout the operational life of the system. This approach relies undoubtedly on proper IT architectures where models of the systems are stored, not only as alternative way of representation, with reference to Document-Based approaches, but also as proper databases capable of interface each other to retrieve information and to navigate the data through proper query-based approaches. Moreover, linked data concepts (Vagliano, et al., 2017) and Digital Twin and Threads architectures (Bachelor, et al., 2019) are used to make available the information related to the system, in terms of representation (Twins) under different point of views (such as functional, logical, physical etc…), and of associated relationships (Threads). In the last years, Agile methodologies (Dove, 2012) able to effectively face requirements evolution during design, with particular focus on risk management and cost scheduling, are emerging as new ways of managing complexity in projects. Ultimately, the development of AI, of expert systems and of knowledge-based approaches, currently representing the most innovative research areas in Systems Engineering topics, are expected to provide a considerable improvement to the domain in the next years.

2.2.2 Definitions, concepts and pillars

2.2.2.1 System

System can be defined as *"an integrated set of elements, subsystems or assemblies that accomplish a defined objective. These elements include products (hardware, software, firmware), processes, people, information, technique, facilities, services and other support elements"* (INCOSE, 2015), or, simply as *"a combination of interacting elements organized to achieve one or more stated purposes"* (ISO, 2015). From this definition, the following characteristics can be derived :

- a system is made of a set of elements, thus it can be decomposed following a proper breakdown, organized in subsystems, assemblies, components etc… which follow a hierarchical structure;
- the elements of a systems are interacting each other, i.e. several interfaces among the elements of a system can be defined internally through the instantiation of a proper network. The combination of system breakdown and interfaces network produces the system architecture;
- the different elements of a system work together to reach a common goal or purpose. Therefore, a system is usually defined as an integrated entity, which cannot be represented only as a sum of its own parts.

It is important to specify that the concept of system can be very different depending on the technical context. For example, for an aircraft manufacturer point of view, the system is the actual aircraft, while for a power plant company the system can be the engine (which is actually a subsystem or an assembly from the point of view of former manufacturer).

2.2.2.2 SE Process

From the INCOSE specification, the SE process is focused on the definition of customer needs in order to identify proper requirements and to shape system related functionalities early in the design. Moreover, the SE process shall include the validation of the design synthesis of the system, in an integrated and interdisciplinary method. The main features of a SE process can then be summarized as follows:

- the focus of the process is the collection and definition of customer needs, which are the core of the SE approach. The system shall be designed to produce tangible and successful solutions to guarantee the satisfaction of the customer (i.e. the system shall meet customer needs);
- the whole design is based on requirements, which are identified starting from the customer needs (elicitation). Requirements are specific, measurable, assignable, realistic and time-related statements that are used to characterize several aspects of the system of interest;
- several kinds of requirements exist, and their classification depends on the engineering domain and practice, but one of the main requirements "family" is related to functionalities. Functional requirements are established early in the design process to identify the functions that the system shall be able to perform. In fact, before moving to the performance and numerical characterization, it is necessary to clearly state which are the capabilities strictly required for the system to meet the needs, so to avoid adding useless behaviours to the final product;
- the process shall include means to verify that requirements are satisfied by the system or system elements, to validate the final concept. Actually, verification and validation are not synonymous and, even if often confused, they cannot be used in the same context. Particularly, verification is the *"confirmation [...] that specified requirements have been fulfilled"* (ISO, 2015), since the verification process can be defined as *"a set of activities that compares a system or system element against the required characteristics"* (INCOSE, 2015). On the contrary, validation is

the *"confirmation [...] that the requirements for a specific intended use or application have been fulfilled"* (ISO, 2015) or, in other words, the validation process *"is a set of activities ensuring that a system is able to accomplish its intended use, goals and objectives in the intended operational environment"* (INCOSE, 2015). Validation is thus at higher level, aiming at assessing that the system concept meets stakeholders expectations, while the verification process refers specifically to requirements, at different levels, aiming at comparing the system specification with the actual behaviour;

- the design is performed specifically looking at operation (and, eventually, disposal) of the system, being not limited to the mere development phase for what concerns traceability. The product lifecycle is in fact the time frame, going from conceptual design up to product disposal, which identifies the chronological time for the system to exist, both as abstract and/or real entity, within an engineering program;
- ultimately, SE process is highly interdisciplinary. This means that it encompasses a design which is not focused on a single aspect or engineering domain, but it is enlarged to include different point of views and topics.

2.2.2.3 The pillars

Even if the SE approaches may be different when moving from an engineering domain to another one, as explained in Section 2.2.1, the aforementioned aspects can be considered as the common points of different methodologies and processes. Looking at the core characteristics of SE, one can identify four pillars (Brusa, et al., 2018) which can be considered as the foundation of the method, i.e.:

- methodology
- language
- tools
- data management

First of all, it is clear that the different elements of SE shall be organized within a formalized methodology to be consistently implemented through a real process. Moreover, the formalization of the methodology and the implementation of the process both require a proper language, to define the different elements of the methods involved and to be universally shared among designers (this is also an

important element to guarantee the repeatability of the approach). Within the SE analyses, several tools are also used to obtain results and to perform dedicated assessments. Ultimately, since the SE process deals with data, independently from the use of either a document-based or a model-based approach, data management is crucial to guarantee traceability of the elements within product lifecycle.

Methodology. The methodology is the most important pillar of the SE and the reason for its relevance can be understood looking at the associated definition: *"a methodology can be defined as the collection of related processes, methods and tools used to support a specific discipline"* (Martin, 1996). It is thus not a synonymous of method, which is, on the contrary, *"a systematic procedure, technique or mode of inquiry employed by or proper to a particular discipline or art"* (Merriam Webster, 2002). It is thus clear that the methodology includes both aspects related to methods, belonging to the specific domain of the engineering, and elements associated to their integration in a process, which is the expression of the implementation of the methodology itself. For this reason, this pillar includes aspects coming from technical domain as well as from project management and formalization. Different methodologies exist within the world of SE, being characterized by dedicated processes, typically influenced by the engineering domain and related practices. However, one of the most common structure used to build tailored methodologies is the so-called V-diagram concept (Forsberg, et al., 2005), especially for what concerns design phases, requirements definition and management, verification and validation plans (Fig. 25).

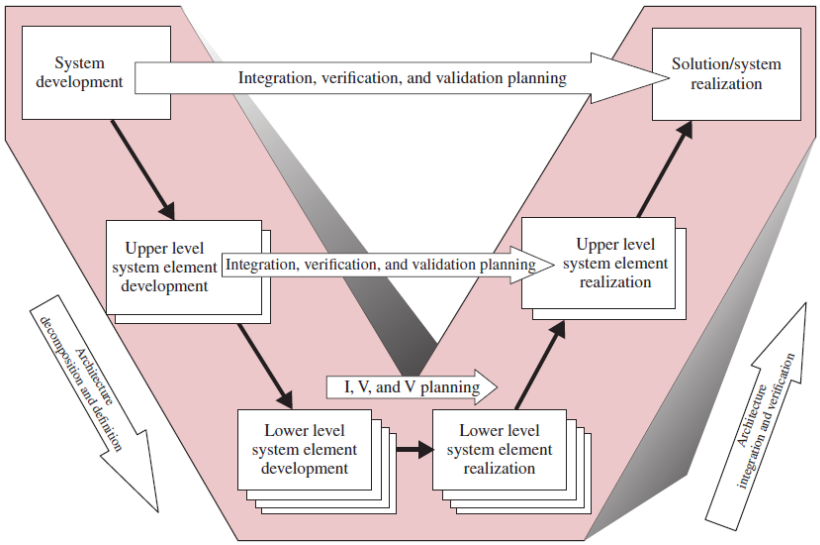

Fig. 25: The V-diagram of a typical SE approach (Forsberg, et al., 2005)

The diagram presents two main branches which are depicted on the symmetrical parts of the "V". The left branch represents the actual design process, descending from high level conceptual estimations, up to low level detailed design. In this part of the diagram, the architecture of the system is defined through the decomposition principle. The right part of the diagram represents instead the realization of the system, which is usually implemented starting from low level components up to high level assemblies. In this branch, the architecture of the system is integrated and verified with respect to requirements. Verification and validation activities are in fact represented by horizontal paths connecting the two branches of the diagram, at common level of hierarchy (i.e. level of detail of the analysis). For each stage, it is necessary to verify that the considered elements meet the requirements (verification) and that system to be built is still in the "right direction" for what concerns its final goal (validation). The V-diagram, as shown in Fig. 25, is the representation of the first part of the product lifecycle, since it basically includes conceptual, preliminary and detailed design, as well as the related verification campaigns. However, some theories based on the same paradigm propose an extension towards pre-feasibility studies in very early design stages (Nichele, 2016), whilst other approaches recommend a multidimensional process for the verification campaigns, to be executed in parallel during the development branch in a sort of "multi-V" process (Stesina, 2014). Other paradigms are instead focusing on the recursive nature of the SE approach, introducing the concept of the "spiral diagram" shown in Fig. 26 (Brusa, et al., 2018), that can be in any case led back to the original concept when considering a sector of the spiral.

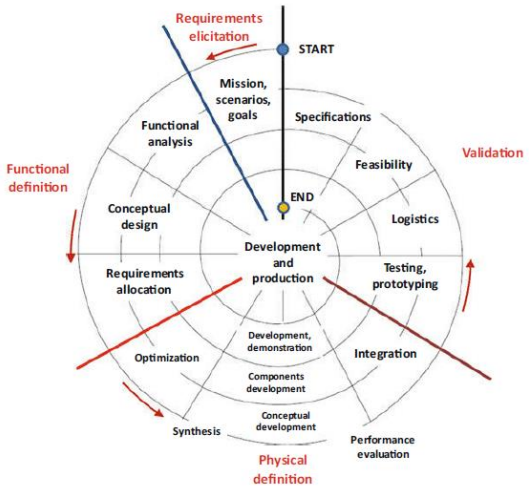

Fig. 26: Example of a spiral diagram for SE approach (Brusa, et al., 2018)

The selection of the methodology is not just a formal step when applying a SE approach. It actually influences a lot the design, since it identifies a specific process that can be more or less suitable for the considered case study. Moreover, when dealing with MBSE, the implementation of the design in model-based environment is highly affected by the high-level process selected. Additionally, the tailoring of general-purpose methodology paradigms, as those presented in this section, to domain-specific environment, is a widely used technique to adapt effective approaches to specific engineering fields. Aircraft design, for instance, is one of these fields and detailed discussions on available methodologies for aircraft and spacecraft design are provided in Section 2.3, particularly for what concerns model-based approaches. Moreover, the definition and formalization of methodologies in SE makes benefit of two main elements to describe in a standard way the process and related tasks, i.e. language and tools. The first one represents a reference language to be commonly understood by designers belonging to a specific domain, or even to different domains. The second one is the list of the tools to be used within the different activities to perform the related analyses. Following sections specifically deals with these two pillars to provide the reader with a full understanding of SE design process, with an outlook on MBSE.

Language. A proper language for SE activities is a clear need to establish common patterns, not only among different technical fields, but even within the same engineering domain. In fact, usually, a design process is carried out by different specialists, which may require a common vocabulary to be able to understand each other within a project. Particularly, one of the most important language defined in the context of MBSE is the so-called Systems Modelling Language (SysML), proposed by (Object Management Group - OMG, 2007). This language benefits from the paradigm and concepts already defined within the Unified Modelling Language (UML) framework, from which it actually derives. SysML was then defined by adapting the previous language to the needs of Systems Engineering, introducing new concepts and modifying existing views and schemes. SysML is in fact based on a set of nine diagrams (Fig. 27), each one representing specific properties for the system under design through a combination of model objects and related links.

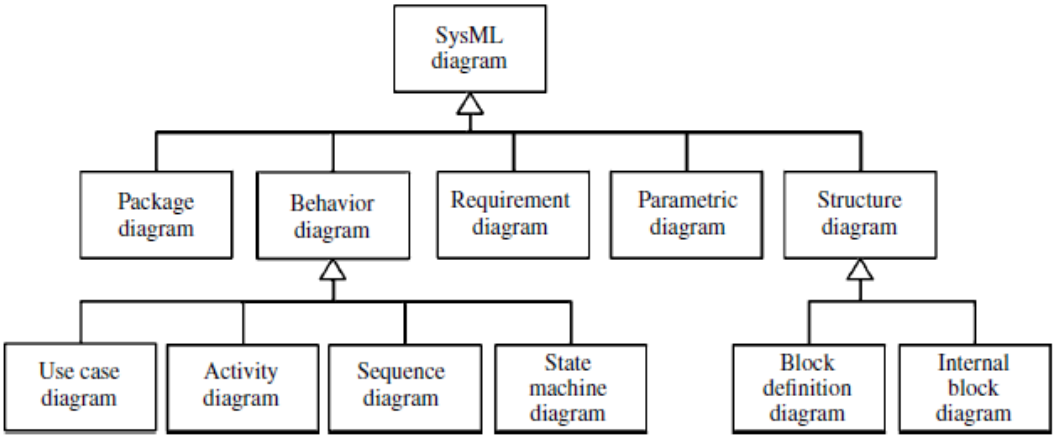

Fig. 27: SysML diagram types (Friedenthal, et al., 2012)

All the diagrams can be grouped in two families: the behaviour diagrams and the structure diagrams. The behaviour diagrams, namely, are used to model the behaviour of the system, and, notably:

- *"the Use Case Diagram (UCD) provides a high-level description of the system functionality in terms of how users and external systems use the system to achieve their goals;*
- *the Activity Diagram (AD) represents the transformation of inputs to outputs through a controlled sequence of actions;*
- *the Sequence Diagram (SD) represents interaction in terms of the time-ordered exchange of messages between collaborating parts of a system;*
- *the State Machine Diagram (SMD) describes the states of a system or its parts; the transitions between the states; the actions that occur within states or upon transition, entry or exit; and the events that trigger transitions"* (INCOSE, 2015).

Complementary, structure diagrams are instead conceived to provide views concerning system breakdown and internal interfaces, providing the actual system architecture together with the behaviour diagrams previously described. Notably:

- *"the Block Definition Diagram (BDD) describes the system hierarchy and classification of system elements;*
- *the Internal Block Diagram (IBD) depicts the internal structure of a system in terms of how its parts are interconnected [...]"* (INCOSE, 2015).

Additionally, three "service diagrams" are proposed as independent instances of the diagrams tree. They are used as connection within the model-based approach to integrate the SysML elements in the design process, being crucial for model organization, interoperability and effectiveness of the MBSE environment:

- *"the Package Diagram (PD) is used to organize the model into packages that contain other model elements. This facilitates model navigation and reuse, as well as access and change control;*
- *the Requirement Diagram (RD) captures text-based requirements. Having requirements within the model enables fine-grained traceability from requirements to requirements* (internal traceability) *and between requirements and design, analysis and verification elements in the model* external traceability);
- *the Parametric Diagram (PRD) represents constraints on system property values as necessary to support detailed engineering analysis. These constraints may include performance, reliability, and mass properties among others. SysML can be integrated with other engineering analysis models and tools to execute the analysis"* (INCOSE, 2015).

The effectiveness of the language can be directly understood from the description of its diagrams, as provided by INCOSE. In fact, most of the concepts introduced previously in Chapter 2 are captured by SysML, and, among others: the connection between system functionalities and actors goals (UCD), system hierarchy (BDD), interfaces among system parts (IBD), exchange of data and messages among them (SD), traceability of requirements (RD), change control (PD), interoperability between engineering analyses (PRD), and so on. The detailed description of the diagrams, and of their main elements, is provided within Chapter 4, where SysML is applied to support the methodology developed to face the design of HST and specifically used to characterize the case study.

Before moving to next section, it is worth mentioning also those languages that are used to describe processes. In fact, apart from the need for a specific language to formalize the design activities, a unified way to describe processes at higher level emerged earlier in the Software Engineering domain. This is also applicable to SE approach and, especially, to MBSE design methods. An interesting specification for process modelling, based on UML, is the Software & Systems Process Engineering Meta-Model (SPEM) (Object Management Group, 2002). This is actually a meta-model used as an industry standard for modelling processes and process families within software and systems engineering. SPEM

allows defining roles and tasks to be executed within a workflow of activities, similar to what specified by the AD in SysML and UML, with particular focus on work product produced (outputs) and required input for each activity and category. All these elements, which are part of the "body of knowledge" of the methodology adopted, are known as "method content" in the framework of SPEM. All aspects related to schedule and plan of work product usage, tasks allocation and role involvement within the process are instead referred to as "process" in SPEM. Proper guidance material can then be provided as support to run the process. This allows understanding that the SPEM notation (Fig. 28) is fairly simple, since it is based on a modelling language for graphical representation and on the concepts of method definition (the method content, where the knowledge related to the activities to be performed within the domain specific process is stored) and method allocation (the process, where the knowledge is used in a specific sequence). As for the SysML, a detailed description of the elements of SPEM used to describe the activities performed within the frame of model-based aircraft design, applied to the case study, is provided in Chapter 4.

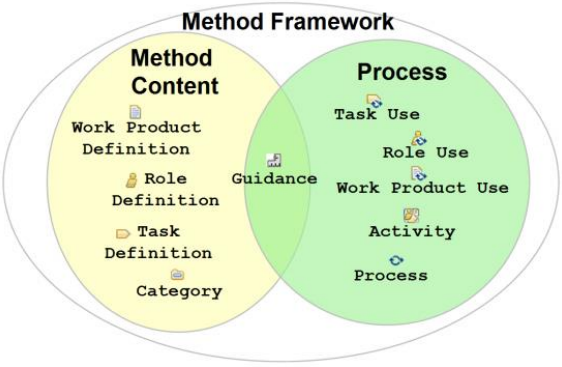

Fig. 28: Main concepts of SPEM method framework (Object Management Group, 2002)

Tools. Methodologies supporting SE processes make use of a wide set of tools in order to be able to perform several analyses in different phases. Since processes may vary a lot depending on the engineering domain and even technical sub-areas, the tools used within SE may be quite heterogeneous and a clear definition of tool shall be established in order to identify what actually a tool is, and which are its functions. In the widest expression, the tool is a mean through which information and/or data are managed, generated and produced. This means that the scope of tool definition is quite extended and may include a graphical representation, a diagram, a table, a process and even a phase of the design, like

the functional analysis (in fact, the functional analysis is a tool through which systems functions are defined and managed, starting from the goals specified by the customers through their needs). However, for the sake of clarity, tools are generally referred to as real or virtual representations or even models, characterized by certain construction rules and semantics, which can be used to compute or define a specific system feature. For example, all the above mentioned SysML diagrams are tools (virtual graphical representations), generally showing structure, behaviour or other characteristics of the system. However, even before the introduction of MBSE techniques, systems engineers were already comfortable in using tools that are still adopted for many kinds of design processes, even if originally conceived for a document-based approach. It is the case, for example, of the common functional tree, used to derive systems functions, the well-known Quality Functional Deployment tool (QFD) or "house of quality" as well as the Functional Flow Block Diagram (FFBD), extensively used in the field of spacecraft and space missions design (NASA, 2007). It is actually important to distinguish between tool and software. For sure, a software is a tool, but a tool is not always a software. However, the power of MBSE process is not actually the use of software and models. Instead, the crucial aspect of MBSE is the enhanced traceability that the model-environments provided by software offer for the management of the data generated during the design process. The connection of software environments, the capability of data exchange and the so-called interoperability are some of the most important innovation within MBSE, being also a crucial aspect to consider when developing the process and its implementation through an IT infrastructure. The well-known interoperability standards and software connectors or adapters are solutions conceived to allow the communication among software trying to overcome the concept of stand-alone applications and pushing towards the suite or platform concept. For example, one of the most important standards for data exchange based on linked-data concept is the Open Services for Lifecycle Collaboration (OSLC) (Bachelor, et al., 2019), while the Functional Mock-up Interface (FMI) (Blochwitz, et al., 2011) is widely used to connect in a standard way several domain specific software, with the aim of constituting a seamless MBSE approach for the management of early product lifecycle phases. The model-based aircraft design process presented in Chapter 4 makes use of some of the aforementioned tools and software, as well as some of the cited standards for interoperability, as solutions for the implementation of the IT infrastructure. It is thus clear how data management can be considered as a fourth pillar of the SE approach, especially considering model-based processes, as described in following section.

Data management. The way in which data are generated, stored and managed within a SE design process is not an exclusive issue of MBSE approach. In the early era of SE, designers needed to face this problem through the document-based approach, usually relying on proper reports and databases. The problem of data management for sure grew since the development of dedicated software and models able to shift data from paper to computers for two main reasons. The first one is related to the need of designing proper import/export facilities to make software able to communicate (i.e. the interoperability issue). The second is related to the security of the data that shall be protected against abuse (i.e. the data protection problem). For what concerns the first problem, three main solutions can be generally identified:

- the first solution relies on point-to-point connectors, based on proprietary data formats, which can be used to integrate software coming from the same vendors or associated. This solution is generally effective and reliable for what concerns the capability of transferring data, but it is very limited and specific, usually based on the synchronization concept to update data;
- the second solution is always based on point-to-point connectors but it exploits interoperability standards rather than proprietary formats. This allows reaching a wider range of software, since the open-source nature of the standards allows multiple vendors to implement the specification. It is thus more effective for what concerns the applicability but it is still lacking data navigation capability (it is still based on synchronization);
- the third solution, currently adopted by most advanced MBSE platform, is based on linked-data concept. The linked-data "*is a structured data which is interlinked with other data so that become more useful through semantic queries"* (Bizer, et al., 2009). The data is thus not stored within the software which is requesting the data, as for happens for point-to-point connectors, but it resides in the environment which has generated it. The data is thus accessed via html, read and used, but it does not move from one environment to the other. This implementation requires a more advanced programming process, even if it is still based, usually, on open source paradigms, but it is really effective since it can reach different tools live, allowing the navigation of data without the need of synchronization.

For the purpose of the analysis performed in Chapter 4, the adopted model-based environment is quite simple and usually based on interoperability standard as well

as on stand-alone applications, since the aim of the study is not to investigate the feasibility of the model-based approach from an IT perspective, but to show the benefit of the methodology from the point of view of aircraft design.

2.3 Definitions and principles of Model-Based aircraft design

Definitions provided in Section 2.2 are general purpose principles and concepts of SE, generally independent from the engineering domain being considered. It is then necessary to re-define those concepts for usage within the model-based aircraft design process. Considering the field of application of this Dissertation, both aeronautical and space related concepts are here investigated. As already described in Section 2.2, the success of an aerospace system and its competitiveness in operation depends on the quality of the process and of the methodology, especially during conceptual and preliminary design. These are, in fact, the phases in which most of the added value of the product is allocated (Fig. 29). It is thus necessary to guarantee that the amount of data produced within the lifecycle, starting from concept definition, are *"captured, analysed, shared and managed […] to improve communication among the development stakeholders, to increase the ability to manage system complexity, by enabling a system model to be viewed from multiple perspectives, to analyse the impact of changes, to improve product quality by providing an unambiguous and precise model of the system that can be evaluated for consistency, correctness and completeness, to enhance knowledge capture and reuse of the information and, ultimately, to improve the ability to teach and learn SE fundamentals by providing a clear and unambiguous representation of the concepts"* (INCOSE, 2015). MBSE enhances these capabilities making benefit of models, being defined as *"the formalized application of modelling to support system requirements, design, analysis, verification and validation activities beginning in the conceptual design phase and continuing throughout development and later life cycle phases"* (INCOSE, 2007). The model-based aircraft design is thus the process exploiting MBSE for this kind of engineering activity, being specifically tuned to match its needs. It is thus not necessary to "re-invent the wheel" but it is actually crucial to adapt the model-based to the domain of interest, combining the technical requests with the formalisms of this type of approach.

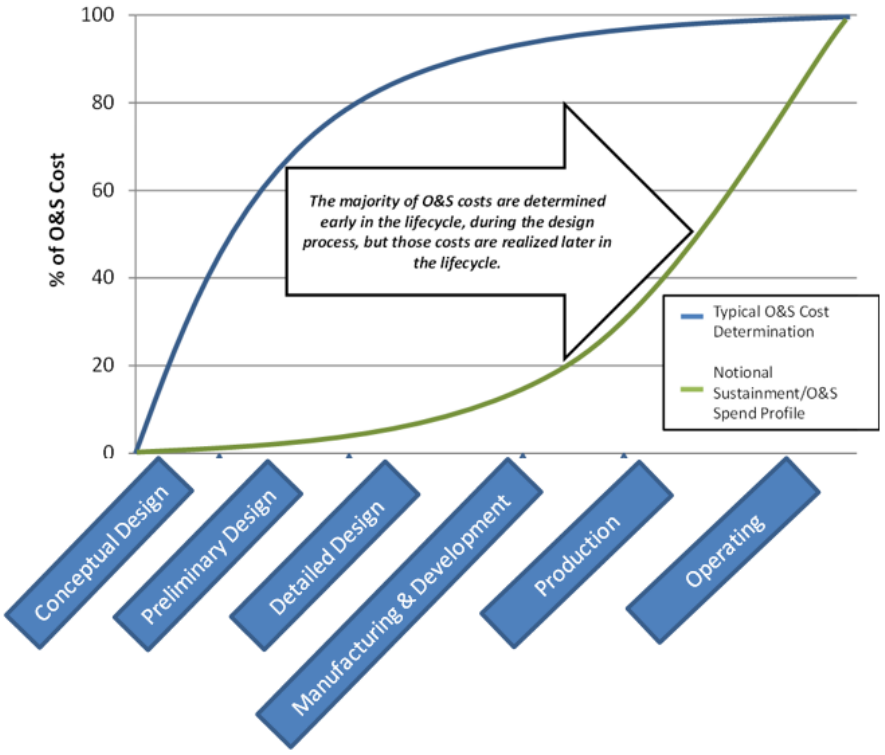

Fig. 29: Cost allocation and spending profiles over time (Berteau, 2016)

For what concern conventional aircraft design, a very well-known guideline for the development of civil aircraft and related systems is reported within the Aerospace Recommended Practice (ARP) 4754 (SAE, 2010), typically adopted by aerospace companies as example to define their own internal workflow. Since the kind of products designed in the field of aeronautical engineering are highly safety-critical, the ARP 4754 suggests a design process which is mainly focused on the identification and development of safety requirements, consistently to what specified by applicable regulations (EASA, 2019) (FAA, 2019). The schematic of the design process is shown in Fig. 30. As it can be seen, the graph recalls the V-diagram described in Section 2.2.2.3. It is also very clear how the design is hierarchically organized, moving from high-level aircraft requirements up to items design. On the other hand, the verification campaign is specular, starting with item verification up to aircraft-level validation. For each phase, several analyses coming from Reliability, Availability, Maintainability and Safety (RAMS) domain are introduced (white boxes). The overall design is, in fact, a Functions-Based Systems Engineering method (FBSE), i.e. *"an approach to SE that focuses on the functional architecture of the system"* (INCOSE, 2015). This means that, in parallel with classical aircraft design approach, based on definition of

configuration and basic performance, the design of functional architecture is performed with the aim, in this case, of assessing safety and reliability aspects. Functional breakdowns are defined, with related interfaces and internal networks, so to build the architecture of the product at aircraft, system and items levels. Together with the development of functional architecture, safety assessments are performed, such as the Functional Hazard Analysis (FHA), identifying potential sources of hazards and classifying failure events affecting the defined functionalities, so to specify safety requirements in terms of probability for the events to occur, and Preliminary Aircraft Safety Assessment (PASA), which includes several activities to face the design-to-safety approach. These analyses are performed for different hierarchical level, together with other activities, and tools like the Fault Tree Analysis (FTA), able to decompose the previously defined failures to identify basic faults generating the main event, and Common Cause Analysis (CCA), which is instead focusing on critical events affecting several failures on different functionalities at once, are included in the design loop.

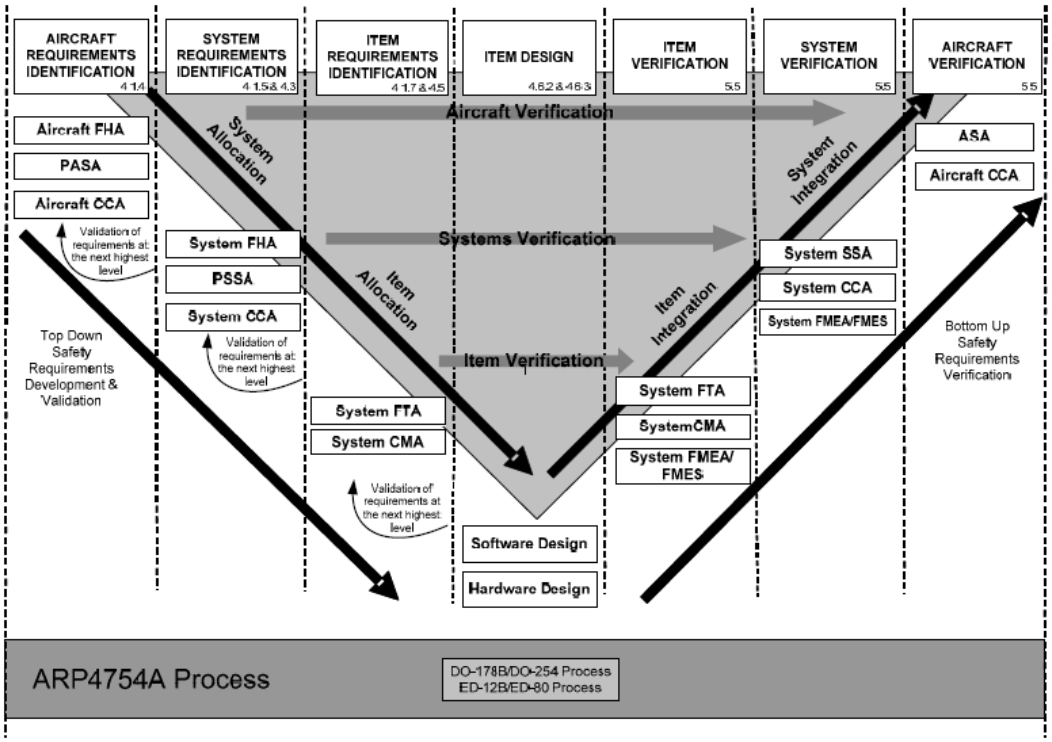

Fig. 30: ARP 4754 reference process (SAE, 2010)

Another important concept is the allocation process of functions to products, which is ruling the descending branch of the V-diagram embedded within Fig. 30. A function is, in fact, *"a characteristic task, action, or activity that must be performed to achieve a desired outcome"* (INCOSE, 2015). As consequence, during early design processes, functionalities are allocated on "logical" products (i.e. product concepts which have no direct reference on the market of real components and systems) defining a preliminary architecture for the system of interest. The real physical breakdown made up of Commercial Off The Shelf elements (COTS) or specifically designed components, will be defined in a subsequent phase, where physical elements will be associated to logical ones to complete the process. This is a very effective way to proceed within the design, allowing easy traceability of requirements, functions and logical/physical elements, linking functional breakdown to RAMS aspects for highly safety-critical systems. The allocation process has in fact an interesting impact on RAMS design. Particularly, during PASA and Preliminary System Safety Assessment (PSSA) processes, reliability is allocated on logical breakdown, i.e. several reliability values are defined and established for each logical component in order to identify reliability requirements that the associated physical elements shall be able to satisfy. Afterwards, the verification of reliability requirements is performed on physical elements in order to predict real values to be compared with those allocated previously. This is, again, a very well-organized approach which completely meets the idea of the SE methodology, being easy to implement within a model-based environment aiming at enhancing traceability.

However, comparing the typical reference life-cycles processes from aeronautical and space domains, it is evident that a preliminary evaluation of stakeholders needs and mission analysis is missing in (SAE, 2010), on the aeronautical side. This can be clearly understood by the fact that the approach proposed by SAE is more focused on safety issues rather than on customer expectations (actually, it is focused on end-users, which will be flying on the final aircraft, by assuring a proper safety level of the product). However, within a complete MBSE approach, the need of including this preliminary phase to the process is unquestionable. For this reason, methodologies proposed by space agencies like NASA and ESA (Fig. 31) can be very helpful to identify standard approaches for the very preliminary phases of the process.

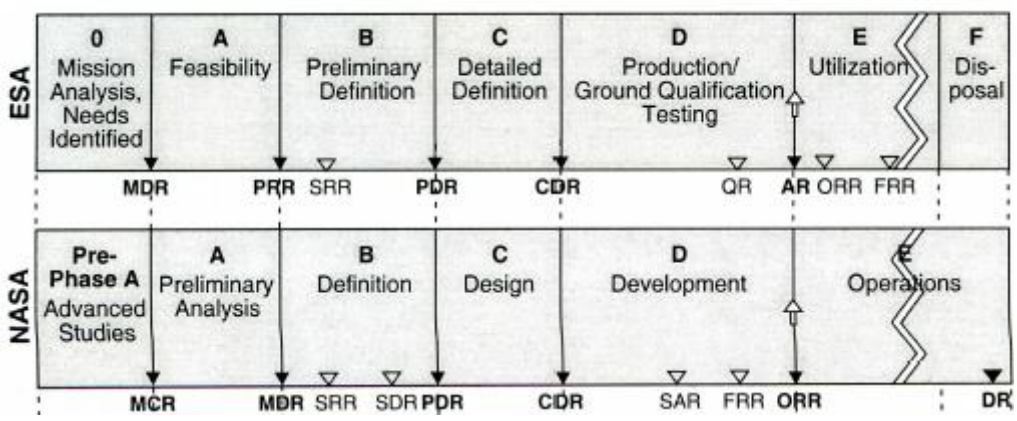

Fig. 31: Comparison of ESA and NASA product lifecycles (Messerschmid & Bertrand, 1999)

A clear overview of the connections between stakeholders analysis, mission analysis, functional analysis as well as performance assessment in early design stages is provided by Fig. 32 (NASA, 2007). The left side of Fig. 32 is an evidence of the activities to be performed before moving to the definition of functional architecture of the system of interest, i.e. mission objectives and constraints definitions, operational environment characterization as well as mission statement analysis.

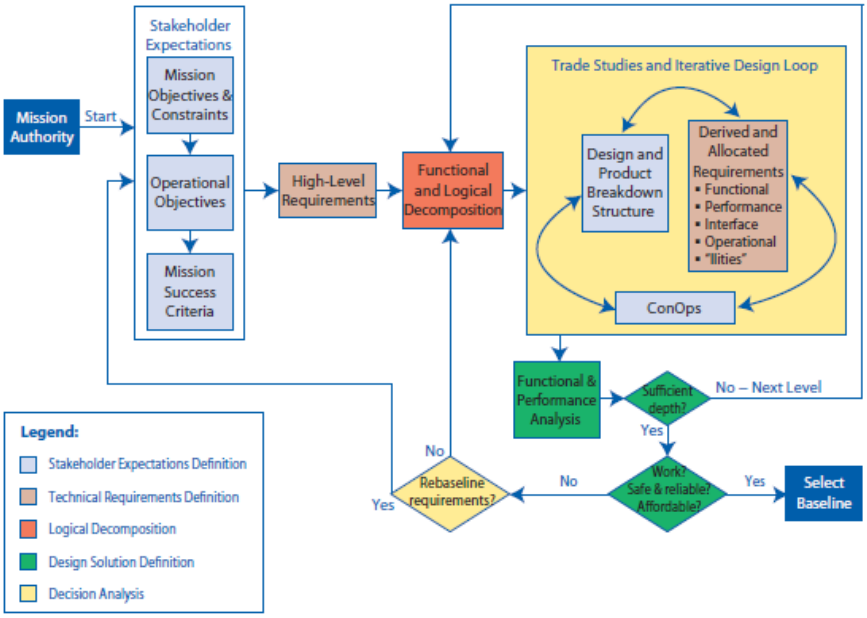

Fig. 32: Space systems design process workflow (NASA, 2007)

For the sake of clarity, it is necessary to say that this kind of approach to MBSE in aerospace domain is already in use as demonstrated by (Bachelor, et al., 2019) and in (Gregory, et al., 2019). However, a dedicated model-based aircraft design approach, including FBSE characteristics for the conceptual and preliminary design of hypersonic vehicles represents a clear element of innovation and it is currently a crucial research topic in aeronautics. The overall structure of the MBSE approach described in this work represents the current deployment of the methodology. However, as already mentioned in Section 2.1, advancements concerning MBSE approaches are available in literature, especially for what concerns flexibility and ability to face requirements updates and modification in short time. Dealing with uncertainty and change may be difficult even adopting MBSE approach, which may be driven by a non-negligible complexity of organization structure and IT platform. New Lean (Oppenheim, 2011) and Agile (Dove, 2012) approaches are then growing in SE world as alternative to the current MBSE methodologies. Thus, this Dissertation does not pretend to provide a “golden rule” for a universal approach to aircraft design, but actually aims at proposing a model-based view on the early definition process of a highly complex product, showing which can be the benefits of the approach when dealing with disruptive innovation and breakthrough technologies in the field of aeronautics.

3

Case study for a hypersonic cruiser concept

Considering the European context already depicted in Chapter 1, that is currently urging the aeronautical and aerospace sectors to enhance the maturity level of key enabling technologies in the field of high-speed transportation, the STRATOFLY project ("Stratospheric Flying Opportunities for High Speed Propulsion Concepts") has been funded by the European Commission, under the framework of Horizon 2020 plan. STRATOFLY project aims at assessing the potential of this type of high-speed transportation to reach TRL6 by 2035, with respect to key technological, societal and economical aspects. Main issues dealt within the project are related to thermal and structural integrity, low-emissions combined propulsion cycles, subsystems design and integration, including smart energy management, environmental aspects impacting climate change, noise emissions and social acceptance, as well as economic viability accounting for safety and human factors. The following sections aims at providing an overview of the STRATOFLY Project starting from a summary of the last fifteen years of European research activities in the field of High-Speed Transportation (Section 3.1), looking also at the Long-Term Advanced Propulsion Concepts and Technologies (LAPCAT) project and its resulting MR2.4 concept, which the STRATOFLY MR3 vehicle configuration (Section 3.2) is stemming from.

3.1 A fifteen-years path towards the development of a hypersonic aircraft

3.1.1 Long-term Advanced Propulsion Concepts And Technologies (LAPCAT – 2005-2008)

As discussed in Chapter 1, hypersonic flight has been already investigated in the past by different institutions and agencies all over the world. Researches were at the beginning mainly driven by military needs and sponsorships, while moving towards civil applications and reusable access to space at the end of the last century. In Europe, besides a set of heterogeneous and independent national initiatives carried out in the 90s, a clearer development trend can be noticed since the beginning of the years 2000, when aerospace community decided to focus on high-speed air-breathing propulsion. It is in this context that, in 2005, The LAPCAT project (Steelant, 2008), has been funded by the European Commission under the sixth European Framework Programme (FP6), constituting for the first time a joint multidisciplinary working group in Europe on innovative high-speed aircraft design, specifically tackling the analysis of breakthrough enabling technologies as well as the study of brand-new propulsion systems. In fact, being focused on the development of high-speed propulsion concepts, the project had the objectives of evaluating both Turbine-Based Combined Cycles (TBCC) and Rocket-Based Combined Cycles (RBCC) engines for Mach 4 to Mach 8 flight, as well as to assess critical technologies related to integrated engine/aircraft performance, to engine components (turbines, heat exchangers etc…) and to high-speed combustion. During the three years of the project (2005 – 2008) several aircraft concepts were defined in order to assess the feasibility of propulsion technologies. Particularly, a Mach 5 hydrogen fuelled cruiser, a Mach 4.5 kerosene fuelled cruiser and a Mach 8 hydrogen fuelled cruiser were considered.

One of the outcomes was the LAPCAT A2 (Fig. 33) concept of a hydrogen fuelled vehicle flying at Mach 5 in cruise.

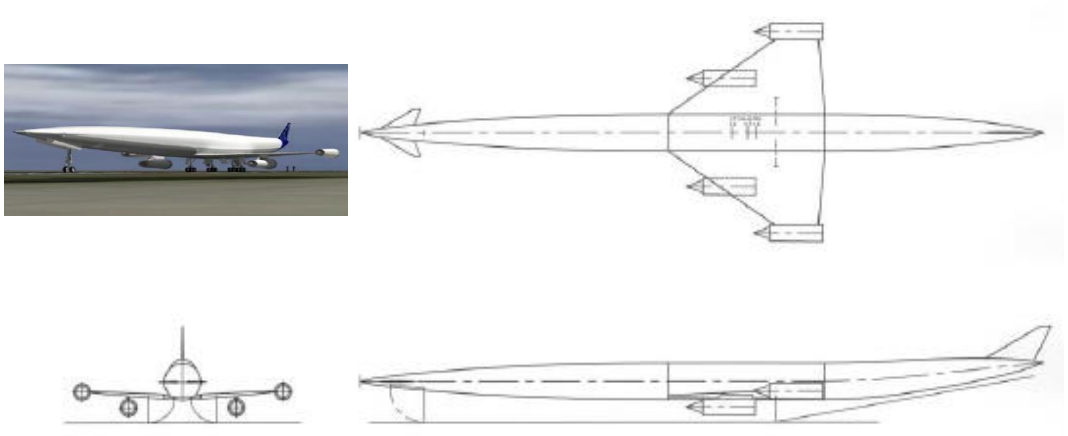

Fig. 33: Three-views and artist's impression of LAPCAT A2 (Steelant, 2008)

Characterized by a wing-body configuration, the LAPCAT A2 concept is capable of carrying 300 passengers on routes ranging up to 18700 km, exploiting a 139 meters long fuselage, with a diameter of 7.5 meters, a delta wing, with a wingspan of 41 meters, a canard and a traditional vertical tail. The overall wing surface is about 900 m^2 while the Maximum Take Off Weight (MTOW) is around 400 tons. The aircraft hosts 4 Scimitar (Jivraj, et al., 2007) pre-cooled engines (Fig. 34) designed by Reaction Engines Ltd. (REL), as the overall concept.

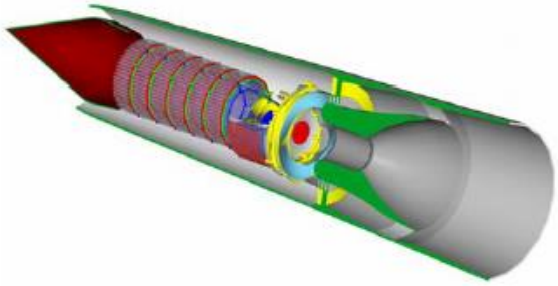

Fig. 34: Schematic of the Scimitar pre-cooled engine by REL (Jivraj, et al., 2007)

This kind of engine allows covering the whole set of flight conditions characterizing the selected mission through a single air breathing propulsive solution, exploiting liquid hydrogen as fuel. The reference mission was conceived to represent an example of vehicle for a set of antipodal routes to be covered in 2 to 5 hours (e.g. Brussels – Sydney in 3.8 hours, Brussels – Los Angeles in 2.5 hours, Los Angeles – Tokyo in 2.0 hours, Los Angeles – Singapore in 3.0 hours etc…) (Bond, 2007).

The Mach 5 concepts proved higher maturity with respect to all the other competing alternatives during the conceptual design. However, the need for defining a viable set of concepts able to fly at Mach 8 pushed the designers to focus mainly on the propulsive subsystem, switching from RBCC to TBCC, as it will be studied within LAPCAT II project (Section 3.1.3) (Fig. 35).

Fig. 35: The LAPCAT MR1 concept for Mach 8 flight (Steelant, 2010)

3.1.2 Aerodynamic and Thermal Load interactions with Lightweight Advanced materials for high-Speed flight (ATLLAS – 2006-2009)

The ATLLAS project (Steelant, 2008), funded in 2006 under the sixth European Framework Programme (FP6), was conceived to explore the material technologies suitable for low hypersonic flight. Starting from two main reference platforms able to fly at Mach 3 and at Mach 6, this project focused mainly on materials, aero-thermodynamics, sonic boom and general aircraft performance. The Mach 3 vehicle was selected by looking at the well-known examples of the Valkyrie XB-70 and the Blackbird SR-71, whilst the Mach 6 concept was derived from the HYCAT vehicle (Longo, et al., 2009), sketched in Fig. 36.

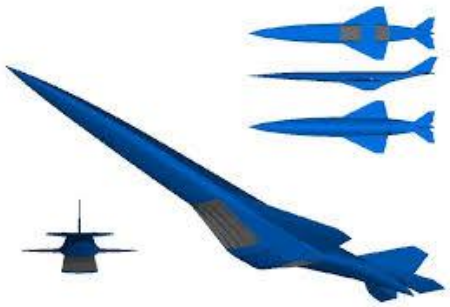

Fig. 36: Views of the HYCAT aircraft (Longo, et al., 2009)

The synthesis of the different studies produced a new kerosene fuelled Mach 3.5 vehicle named M3T, characterized by a MTOW of 300 tons and capable of hosting 200 passengers for long haul flights with a range of 10000 km. On the other hand, a Mach 6 hydrogen fuelled vehicle similar to HYCAT, characterized by a MTOW of 278 tons, and by a similar payload, was still considered a feasible option to cover routes of about 7400 km.

3.1.3 Long-term Advanced Propulsion Concepts And Technologies II (LAPCAT II – 2008-2013)

LAPCAT II is the follow-up of LAPCAT project, funded under the seventh European Research Framework Programme (FP7) in 2008. It started from the outcomes of the previous LAPCAT project, with the aim of further developing the Mach 5 and Mach 8 concepts. Notably, the concept from REL was selected as reference for the Mach 5 vehicle, whilst different studies were conducted for the Mach 8 aircraft since the design loop did not converge in LAPCAT project. Four configurations were assessed: a rocket-propelled vehicle based on PREPHA project (Section 1.1) proposed by ONERA (Falempin, et al., 1998), a more conventional concept for hypersonic vehicle based on ventral TBCC power plant from University of Rome (Ingenito, et al., 2009), an axisymmetric concept suggested by MBDA (Falempin, et al., 2009) and a waverider with dorsal engines designed by ESA (Langener, et al., 2014). Concepts from ONERA and University of Rome were subsequently merged to constitute an aircraft based on air breathing propulsion, since RBCC could not match the long-range requirement.

The Mach 5 concept represents an evolution of the vehicle designed during LAPCAT project, which has been refined for what concerns aerodynamics and propulsion plant. Particularly, even if the main concept for the pre-cooled SCIMITAR engine was retained, the intake and position of the different elements were redesigned in detail, as shown in Fig. 37 (Steelant, et al., 2015). Moreover, different integration options were assessed.

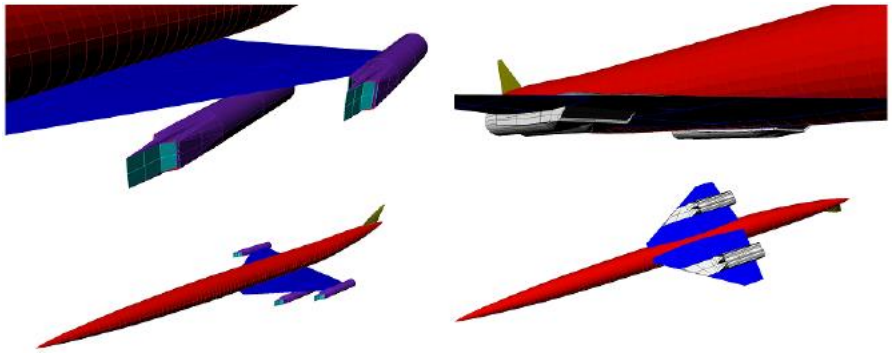

Fig. 37: Power plant integration options and intake refinement for LAPCAT A2 concept (Steelant, et al., 2015)

Combustor and nozzle performance for this kind of engine were studied as well in detail. Ultimately, a structural analysis of the entire vehicle was established.

Complementary, among the Mach 8 vehicle configurations assessed, the concept proposed by ESA (Langener, et al., 2014) was selected. The MR2.4 aircraft (Fig. 38) is a waverider-based hydrogen fuelled vehicle equipped with a dual air breathing propulsion plant placed on the leeward side of the fuselage.

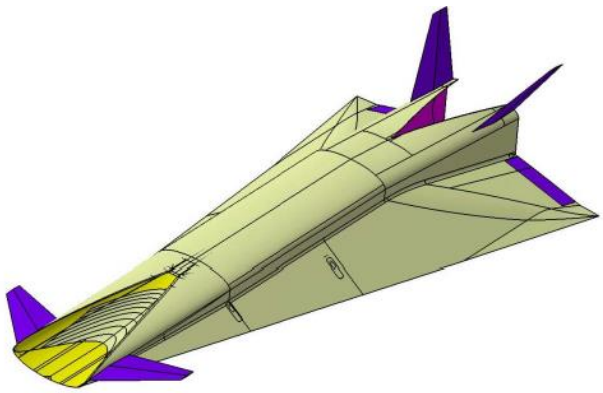

Fig. 38: The MR2.4 concept from ESA (Steelant, et al., 2015)

The configuration is a sort of blended wing-body characterized by an elliptical air intake, placed directly on the fuselage leading edge, where the canard is also installed, and by twin vertical tails. The vehicle is 94 meters long and has a wingspan of 41 meters. The planform area is about 2491 m^2 hiding an internal volume of 9956 m^3. The powerplant occupies most of the dorsal part of the vehicle, where intake, combustor and nozzle are placed. Actually, the main intake is characterized by movable ramps able to feed the low-speed propulsion plant,

made of six Air Turbo Ramjet (ATR), working from take-off up to Mach 4.5, and of the main DMR for flight from Mach 5 to Mach 8 (in closed configuration). The vehicle is able to reach an altitude of 33 km in cruise, with a total range of 18700 km carrying 300 passengers. The MTOW of the aircraft is around 400 tons. For this concept, several analyses have been carried out during the project, including mission analysis, nose-to-tail CFD, combustor modelling, emissions evaluation, aerodynamic characterization, heat flux evaluation in different conditions, stability analysis, preliminary mass estimation as well as thermal control and protection subsystems sizing. Several tests were also conducted on a small scale combustion chamber and on a scaled version of the vehicle itself.

3.1.4 Aerodynamic and Thermal Load interactions with Lightweight Advanced materials for high-Speed flight II (ATLLAS II – 2011-2015)

ATLLAS II is the follow-up of ATLLAS project, funded under the seventh European Research Framework Programme (FP7) in 2011 and running in parallel to LAPCAT II for a certain period of time. The project focused on the analysis of material and cooling techniques for airframe and propulsion concepts for low hypersonic speed flight, making benefit of the results of ATLLAS. Moreover, special attention was devoted to sonic boom alleviation and emissions in cruise. The reference aircraft, differently from what was applicable to ATLLAS, was selected following a Mach 5 vehicle conceptual design trade-off. The selected aircraft *"features a wide body fuselage sheltered behind a nose-mounted variable geometry intake for the main engine together with nacelle-mounted engines on each wing behind smaller intakes"* (Steelant, et al., 2017), as shown in Fig. 39.

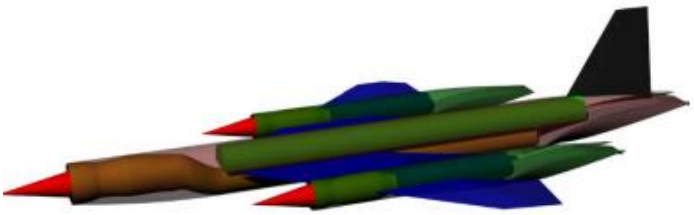

Fig. 39: Baseline vehicle for ATLLAS II project (Steelant, et al., 2017)

Analyses performed within the project include conceptual structural and thermal design, vehicle optimization through MDO approach, integration of aerodynamics and airframe, thermal analysis as well as materials investigation for outer skin, tail and combustor chamber.

3.1.5 High-speed EXperimentAl FLY vehicles (HEXAFLY – 2012-2014)

HEXAFLY was funded under the seventh European Research Framework Programme (FP7) in 2012. It aimed at designing an experimental powered high-speed vehicle to increase the TRL of critical technologies developed during ATLLAS and LAPCAT projects series. The acronym comes from the identification of six main areas of interest concerning high-speed: vehicle concept design, aerodynamics, propulsion, high-temperature materials and structure, flight control as well as environmental impact. The project defined three different vehicle architectures (Steelant, 2014) for flight test, to propose a proof-of-concept capable of demonstrating the feasibility of the preliminary design focused on the aforementioned topics, the identification of most promising configurations as well as the integration of airframe and propulsion integration aimed at guaranteeing a positive propulsive balance at Mach 8 (Fig. 40).

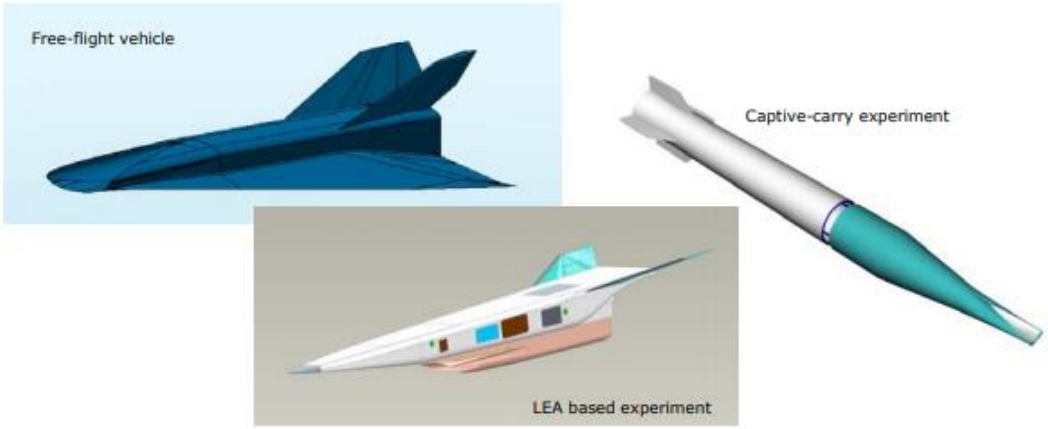

Fig. 40: HEXAFLY test vehicles (Steelant, 2014)

The first one, consisting in a free-flight experiment test vehicle (EFTV), is shown in Fig. 41 (final version). Additional configurations included an experimental LEA mounted test vehicle (ELTV), constrained to the Lyotnii Experimentalnii Apparat (LEA) (Serre & Falempin, 2013) and an experimental captive-carry test vehicle (ECTV) based on the SHEFEX II delivery module (Weihs, et al., 2008). The EFTV had two versions, one air-launched (EFTV-A) and another ground-launched (EFTV-G).

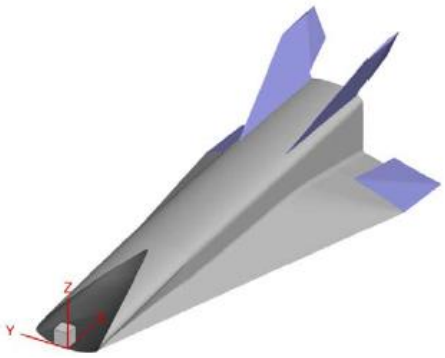

Fig. 41: The HEXAFLY EFTV vehicle (Steelant, 2014)

The 3 meters long EFTV appears as a scaled version of MR2 vehicle from LAPCAT II, even if vertical tail and elevons were re-designed. Canard was eliminated. Main body was refined, especially for what concerns lower trailing edge of the fuselage and nozzle upper part. Internal structure and volume were re-allocated depending on specific needs of subsystems integration and test execution. The original trajectory included a target flight Mach of 7.4 and a ceiling of 31.9 km.

3.1.6 HIgh speed Key technologies for future Air transport - Research & Innovation cooperation scheme (HIKARI – 2013-2015)

HIKARI (Chavagnac, 2014) was funded under the seventh European Research Framework Programme (FP7) in 2013. The main goal of the project was to promote the generation of a roadmap for technology development and demonstration related to high-speed flight, putting together different research efforts in the field and fostering international cooperation, as well as making benefit of previous initiatives such as the Zero Emission High Speed Technologies (ZEHST) project (Blanvillain, 2014), whose vehicle is shown in Fig. 42. Moreover, special attention was devoted to the analysis of the economic sustainability of the concept as well as to its future commercial market. In terms of technologies, three main areas have been investigated: fuel consumption and environment-related technologies, thermal and energy management and propulsion.

Fig. 42: Artist impression of ZEHST vehicle (Blanvillain, 2014)

Results showed that the most promising aircraft configuration shall be characterized by a Mach 5 cruise on routes up to 14000 km of range, exploiting liquid hydrogen as fuel and carrying 100 passengers per flight.

3.1.7 High-speed EXperimentAl FLY vehicles – International (HEXAFLY-International – 2014-2019)

HEXAFLY-International (HEXAFLY Int, 2017) is the follow-up of HEXAFLY project, funded under the seventh European Research Framework Programme (FP7) in 2014. Thanks to the analyses and the results obtained HEXAFLY, this new research project aimed at performing the final vehicle design, manufacturing, assembly and verification as well as the tuning of the mission to be executed within the test campaigns, designed within the project (Steelant, et al., 2018). The evolution of the design led to the development of a glider version of the EFTV (Fig. 43), supported by an Experimental Service Module (ESM) and ground-launched by a sounding rocket.

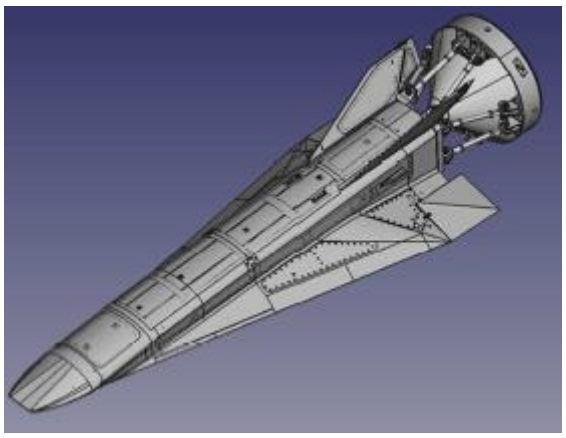

Fig. 43: HEXAFLY International flight test vehicle (Andro, et al., 2018)

The overall mission was based on the exploitation of a S-43 rocket able to reach an altitude of 90 km, where the test vehicle, equipped with the ESM, was supposed to be ejected from the carrier. The ESM was conceived to allow a pull-out manoeuvre to ultimately start the gliding phase in which the test could be conducted. The test was then set to have two main phases: the first one, after the pull-out, was scheduled to be characterized by a Mach 7.4 flight, where aerodynamic balance could be evaluated; subsequently a second phase, where Mach number was supposed to decrease from 7.4 to 5, characterized the real gliding phase. The level flight was set at 31.9 km of altitude. The real test was not performed within the project and it is currently expected to be part of future initiatives on the topic, with the aim of validating the aerothermodynamic models, the load and the trajectory analyses performed numerically.

3.1.8 STRATOspheric FLYing opportunities for high-speed propulsion concepts (STRATOFLY – 2018-2020)

STRATOFLY was funded under the Horizon 2020 Research Programme in 2018. Making benefits of the whole set of European projects on high-speed transportation, it is the last joint research effort in this field for European funded projects. The project is in line with the technology roadmap established within HIKARI and aims at raising the TRL for critical high-speed technologies up to level 6 by 2035. Its main goals are: multi-functional integration of propulsion plant, airframe and on-board subsystems design as well as harmonization of different disciplines, aiming at defining and detailing a high-speed aircraft configuration enabling long-haul travels starting from the MR2.4 platform, established within the LAPCAT II Project. Moreover, the project aims at assessing the sustainability of the vehicle and its mission concept from several perspectives: pollutant and noise emissions, environmental impact, human factors, social acceptance as well as market analysis. From the external layout perspective, the STRATOFLY MR3 vehicle, shown in Fig. 44, is very similar to the MR2.4, being characterized by the same propulsion plant and external configuration, but slightly modified for what concerns mobile surfaces, rounding of all the leading edges and refinements of the nozzles area.

Fig. 44: STRATOFLY MR3 vehicle

Conversely, the internal vehicle architecture has been subjected to several updates and changes, some of which comes from the results of part of the work described in this Dissertation, as preliminary described in Section 3.2, and discussed in detail in Chapters 4 and 5. Particularly, the new configuration was re-designed starting from a review of conceptual design phase, where the waverider shape was derived and updated keeping in mind subsystems and internal compartments integration, with the aim of reaching a higher level of volumetric efficiency with respect to MR2.4. Cabin compartment, tanks architecture and thermal management subsystems were completely re-analysed, together with some of the main on-board subsystems, keeping trace of the evolution of mass and volume breakdowns with reference to external configuration and mission. Actually, the vehicle is always supposed to have a MTOW of about 400 tons, maintaining the external dimensions of the MR2.4. The design process for the theoretical determination of reference surface and volume was completely reconsidered to validate these characteristics with reference to its predecessor. The vehicle is still supposed to host 300 passengers over long-haul flights, performing a mission similar to the one sketched for MR2.4, even if the possibility of performing a powered descent in the final phase is under evaluation. Apart from the pure design, additional numerical investigations concerning CFD, combustion modelling, emission evaluation, noise suppression, trajectory analysis and structural analysis were scheduled, some of which are currently ongoing. Moreover, additional test campaigns on plasma-assisted combustion and on the validation of emissions model are scheduled. The final objective of the project consists in suggesting a refined roadmap following the example of HIKARI, providing an evidence of the feasibility of this kind of transportation concepts and supporting the European Flightpath 2050 on the vision for future aviation (European Commission - High Level Group on Aviation Research, 2011).

3.2 The STRATOFLY MR3 hypersonic cruiser

As it has already been clarified, the STRATOFLY project aims at making benefit of all the advancements and achievements of the last 15 years of research activities in the field of high-speed carried out in Europe. Thus, the most promising vehicle configuration has been selected among all those investigated during the past projects, i.e. LAPCAT MR2.4. In particular, it is worth noticing that the European projects described in Section 3.1 mainly focused on vehicle layout optimization, looking closely at aerothermodynamics and propulsive issues. Conversely, apart from some preliminary studies specifically tackling the propulsive subsystem and the Thermal and Energy Management Subsystem (TEMS) (Balland, et al., 2015), very few analyses were addressing the other on-board subsystems and their integration. It is mainly for this reason that the H2020 STRATOFLY project has been funded to face the design, sizing and integration of all the main subsystems to be installed on-board. The present section aims at reporting the current status of the STRATOFLY MR3 vehicle configuration, both from the point of view of the external layout as well as from the internal subsystems integration, underlying the major steps forward with respect to the LAPCAT MR2.4.

3.2.1 STRATOFLY MR3 external layout

3.2.1.1 The waverider concept

Considering the high-level of confidence of the outcomes of the previous research activities focusing on aero-thermo-propulsive integration, the STRATOFLY MR3 vehicle maintains the same optimized outer shape resulting from the LAPCAT MR2.4 configuration (Fig. 45). Thus, STRATOFLY MR3 is a waverider aircraft conceived to host 300 passengers and to fly at a cruise altitude of about 33 km for a range of 18700 km. The vehicle is 94 meters long and has a wingspan of 41 meters, with an overall planform surface of about 2491 m^2 and a wing planform area of 1296 m^2. Specifically, a waverider *"is any vehicle designed such that the bow shock generated by the shape is perfectly attached or nearly attached along the outer leading edge at the design flight condition"* (Cockrell, et al., 1996). This kind of configuration offers several advantages concerning aircraft performance, and particularly high lift/drag ratio, if compared to conventional non-waverider architectures.

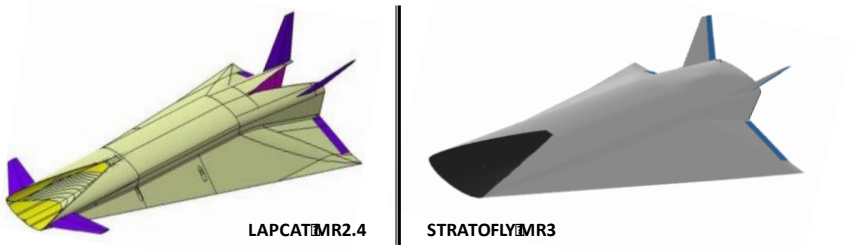

Fig. 45: Comparison between MR2.4 and MR3 vehicles configurations

Several theories and techniques are available in literature to generate the shock-based shape of the vehicle, thus highlighting a sort of "inverse" design process trend (Viola & Fusaro, 2019), where aircraft configuration is derived from a flow field analysis. The flow field characterization is performed defining the reference object flying in the desired conditions, to model the shock wave and to set its shape. Depending on the characteristics of this object (2D wedge, 3D cone etc…), different shock surfaces can be generated leading to several aircraft configurations (wedge-derived, wedge-cone based, osculating cone-derived etc…). Particularly, osculating cone-derived theory was considered as enabling methodology to properly sketch and refine the external vehicle layout for this specific case study. In fact, the MR2.4 was based on an iterative design process, starting from the application of the osculating cone theory (Ding, et al., 2015) and moving to an hybrid approach based on an elliptical flare flow field stream-tracing technique proposed by (Murray, 2011) to provide an easier integration of the propulsion system. Morevoer, one of the most attractive characteristics of waverider for what concerns airframe-propulsion integration is the availability of an ideal pre-compression surface that can be used to feed the power plant (Ding, et al., 2018). Particularly, for the MR2.4 and MR3 vehicles, the intake has been completely integrated within the fuselage leading edge, matching the front leap and providing a very high mass capture (if compared, for example, to other configurations studied within previous projects, as described in Section 3.1). The waverider shape has been foreseen to maximize the lift–to-drag ratio (L/D) during cruise, guaranteeing a maximum value of 6.5.

3.2.1.2 Aero-thermo-propulsive improvements

Looking at the external layout, the main improvements with respect to LAPCAT MR2.4 are related to the new empennages design and sizing, as well to the definition of proper radius of curvature to be used as rounding for the various leading edges. Indeed, an increment in leading edge radius (moving from a pure

wedge shape to a rounded contour) is necessary for manufacturing process as well as for the integration of subsystems and thermal protection technologies, such as the heat pipes. Even if the introduction of a proper curvature is positive because of the reduction of the heat flux on the leading edges, the introduction of a rounding on the lips of the air-intake (lower, lateral and cowl) might have a detrimental effect on the propulsive characteristics. Thus, as a first attempt, the semi-empirical model presented in (Curran & Murthy, 2001) has been used to evaluate the mass flow rate capture efficiency, obtaining a suggested radius of 11.3 mm (Fig. 46). Currently, detailed CFD simulations are being performed to evaluate and compare the impact of a specific radius on the overall propulsive performance.

Fig. 46: STRATOFLY MR3 air intake leading edge design and analysis

In terms of external layout optimization, one for the most interesting results stemming from the LAPCAT II project has been the AEroDataBase (AEDB), describing the trends of the vehicle aerodynamic coefficients in the different flight regimes, from subsonic up to hypersonic. However, the characterization of lift and drag coefficients for low speed has been entirely revised at the beginning of the STRATOFLY project, substituting the already available evaluations with the Nose-to-Tail analysis results coming from (Krempus, 2017). Fig. 47 and Fig. 48 report the new lift and drag variations with angle of attack as function of Mach number. Complementary, the high-speed AEDB has been checked, but only minor improvements have been necessary.

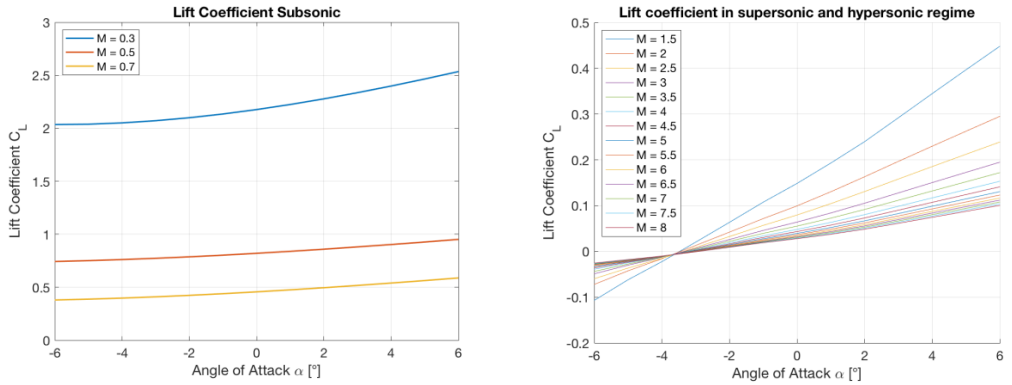

Fig. 47: STRATOFLY MR3 Lift coefficients (Bader, 2019)

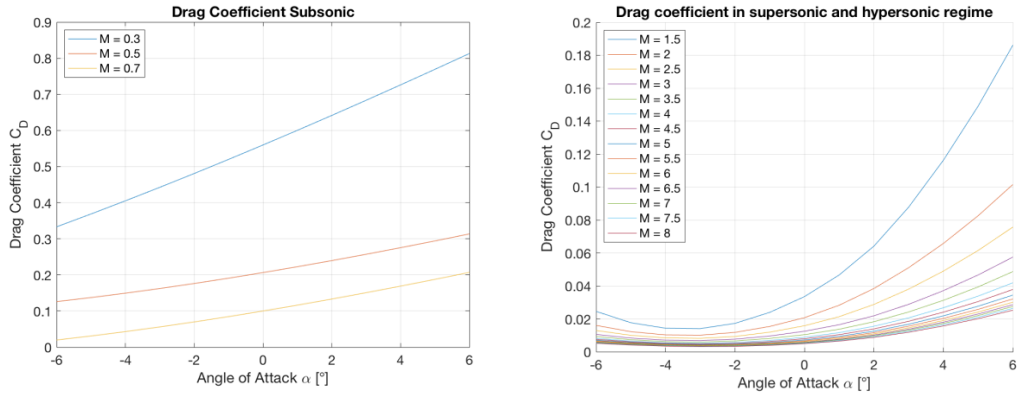

Fig. 48: STRATOFLY MR3 Drag coefficients (Bader, 2019)

3.2.1.3 Propulsive Subsystems integration improvements

It is worth noting that the subsystem with the highest impact onto both the external and internal vehicle layout is the propulsive subsystem (Fig. 49). Indeed, consistently with the results obtained during the LAPCAT II project, the power plant is made up of two engine types and occupies the whole dorsal section of the aircraft. Six ATRs are designed to bring the aircraft from ground up to Mach 4.5, performing a similar turbojet cycle. Moreover, a switch from ATR to DMR at around Mach 4.5 occurs, functioning first in ramjet-mode and then in scramjet mode, accelerating the aircraft up to Mach 8.

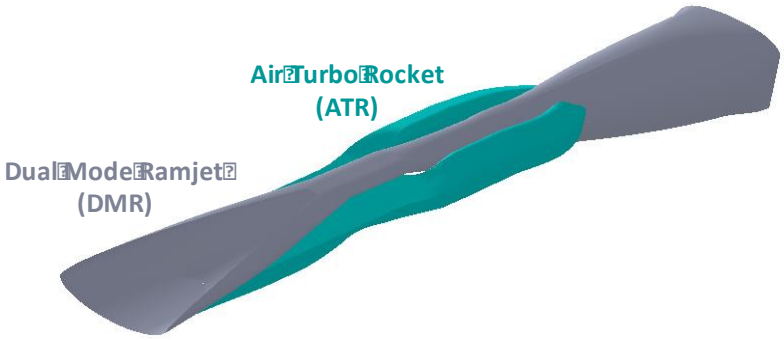

Fig. 49: STRATOFLY MR3 propulsive plant

The intake feeds both low-speed (cyan) and high-speed (grey) engines by actuating several sliding doors on the bottom of the ramp. When the doors are retracted, the ATR engines are fed. These engines are located in the constant section of the lateral ducts (cyan) of the Fig. 49 schematic, three on the left and three on the right. The exhaust converges directly within the main 3D nozzle, where other sliding doors are responsible to open the paths. The high-speed configuration is instead characterized by a closed ramp, where all airflow is diverted to the central DMR combustor (grey path), where hydrogen is injected through longitudinal struts, and where a Plasma Assisted Combustion (PAC) module is located to guarantee flame stability in different conditions. Between the combustor and the 3D nozzle, a 2D constant section nozzle is present. When working in high-speed mode, the doors between ATR ducts and the 3D nozzle are closed. The expected performance of the two engines types are shown in Fig. 50. Both ATR and DMR performance is shown with an Equivalent Ratio (ER) for fuel-to-air mixture equal to one.

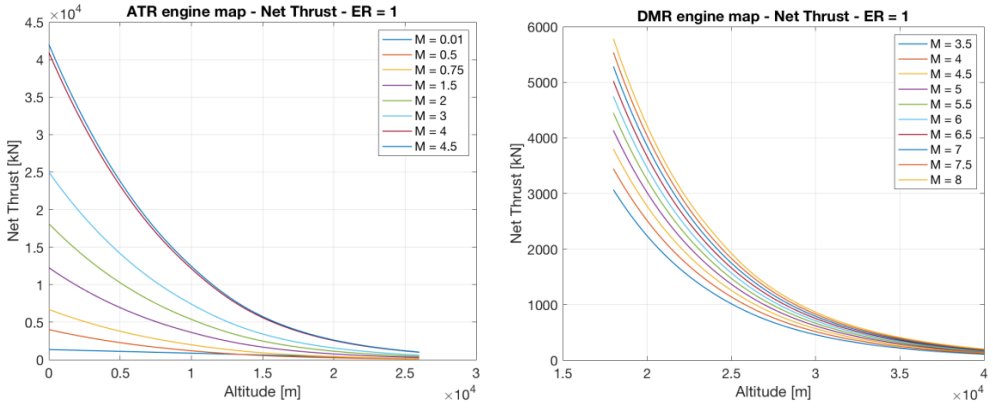

Fig. 50: ATR (a) and DMR (b) computed thrust as function of altitude and Mach number (Langener, et al., 2014)

From the Propulsive subsystem standpoint, the main upgrades with respect to the original LAPCAT MR2.4 configuration can be summarized as follows:

- the impact of the introduction of air-intake rounding onto the low-speed and high-speed working modes has been considered;
- re-design of the rear nozzle shape, moving from a V-cutted bell to a more traditional configuration has been performed. Aerothermodynamic, propulsive and aeroacustic investigations of the impact of this change onto the main vehicle performances are on-going;
- re-design of the integration of the ATR nozzle duct with the DMR duct to improve the flow characteristics downstream, thus reducing jet noise, (Nista, 2019) has been performed;
- the analysis of the best location of DMR injector struts to reduce the NOx emissions, especially during the high-speed phase, has been conducted. This analysis shall be coupled with the analysis of the impact of the new combustor arrangement onto the low hypersonic regime (Vellaramkalayil, et al., 2013).

3.2.1.4 Empennages and Control Surfaces

The last upgrade of the vehicle external layout is related to the empennages and flight control surfaces. Indeed, starting from the original vehicle layout, they have been completely redesigned, following a MBSE approach. The current configuration is depicted in Fig. 51. Following this modification, a new set of aerodynamic investigations, based on an engineering method, have been carried out in order to update the AEDB with the aerodynamic contributions of the movable surface, throughout the mission. Preliminary results are currently available for supersonic and hypersonic speed (Marini & Roncioni, 2019), whilst work is still on-going for the subsonic flight regime. The MR3 vehicle is provided with four elevons, on the trailing edge of the wing (two on each side), in order to reduce the actuation loads on the Flight Control Subsystem (FCS). The configuration of vertical tails has been maintained in terms of movable surfaces, even if the dimensions of both stabilizers and rudders have been reviewed. The canard wings have been preliminarily eliminated.

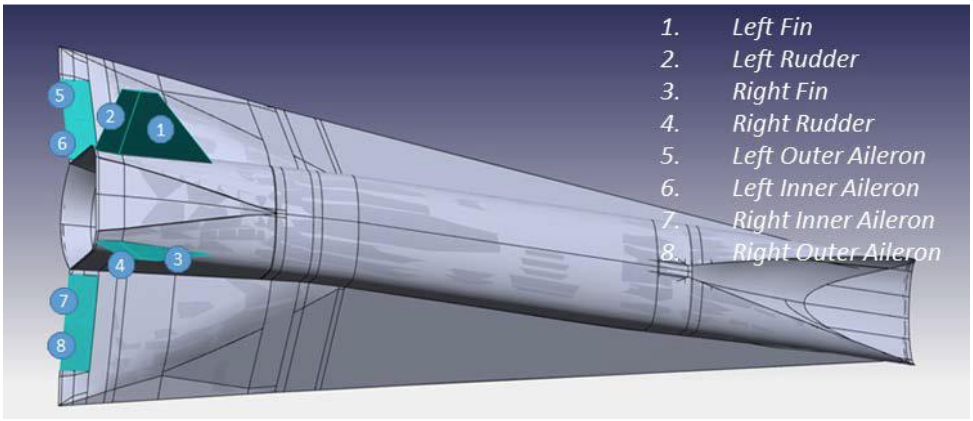

Fig. 51: Empennages and Flight Control Surfaces Definition

3.2.2 STRATOFLY MR3 internal layout

Even though aero-thermal-propulsive and airframe integration is a crucial aspect driving the external configuration, the vehicle and mission concepts feasibility can be validated only if the layout can host the payload, the propellant and all other subsystems. In this case, the STRATOFLY MR3 internal vehicle configuration has been entirely reconsidered, starting from the revised external vehicle layout (defining an internal volume of 9956 m^3) and maintaining the same geometry of the propulsive system (taking up to 3327 m^3, i.e. more than 30% of the internal volume). Then, a cabin compartment of about 1200 m^3 has been designed and sized to host 300 passengers with a proper level of comfort. This means that, in the remaining 5429 m^3, the propellant tanks shall be fitted, also remembering that a percentage of about 30-32% of this residual volume shall be accounted for the integration of all other subsystems.

3.2.2.1 The cabin

The design of the cabin compartment of the MR3 vehicle has been sketched from scratch referring only to the high-level requirements list elicited at the beginning of the design process. Indeed, the layout envisaged for the MR2.4 was highly unconventional and resulting from the optimization of the contact surface of the cabin with respect to the tanks. Conversely, a more conventional approach for cabin definition has been used in STRATOFLY. Fig. 52 reports a comparison of the two cabin concepts.

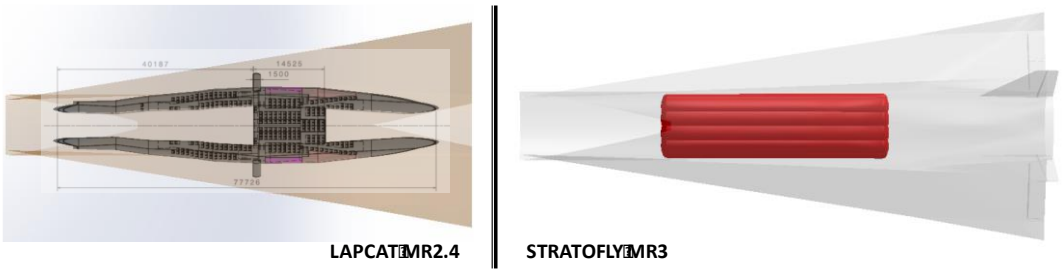

Fig. 52: STRATOFLY MR3 Cabin Compartment design and sizing

The new cabin has been designed looking at (EASA, 2019) regulation for what concerns dimensions of aisles, seats configurations, access doors and cabin attendants location. As for MR2.4, the cabin has no windows.

3.2.2.2 The Propellant Subsystem

Together with the propulsive subsystem and the cabin compartment, the propellant subsystem (Fig. 53) has a deep impact onto both mass and volume budgets at vehicle level. Indeed, in order to cover antipodal routes, about 200 tons of LH2 shall be stored on board. However, considering the LH_2 low volumetric efficiency, this subsystem is expected to occupy 30-35% of the overall vehicle internal volume (around 2825 m^3 considering uniquely fluid volume).

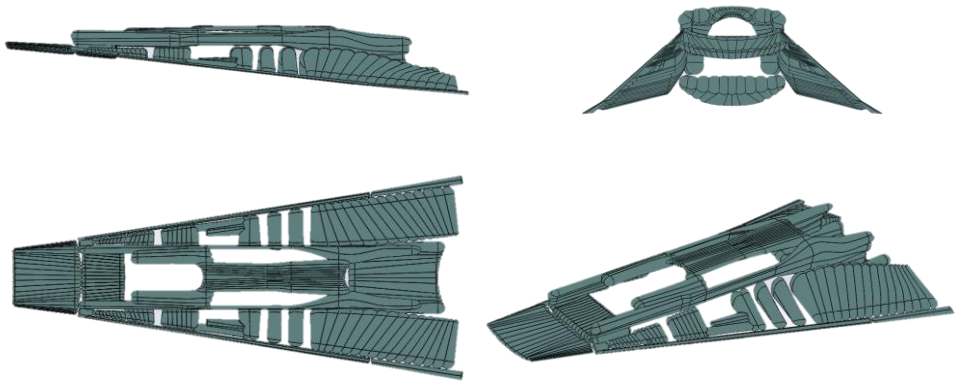

Fig. 53: STRATOFLY MR3 vehicle: propellant subsystem

Several compartments have been envisaged and a new architecture, relying on a high number of compartments, has been selected if compared to MR2.4 (Fig. 55). This was done mainly considering the need of interfacing the Thermal Protection Subsystem (TPS) and the TEMS with tanks in different sections of the aircraft.

Moreover, this allowed increasing the overall volumetric efficiency of the vehicle, taking into account the need of hosting the other on-board subsystems, and, especially, the landing gear as well as the TEMS itself (Section 3.2.2.3).

3.2.2.3 The Thermal and Energy Management Subsystem

Considering the noticeable heat loads penetrating the aeroshell throughout the mission, a Thermal and Energy Managements Subsystem (TEMS), assuring a proper internal environment for passengers and the different subsystems, has been envisaged since the LAPCAT project designed, as shown in Fig. 54.

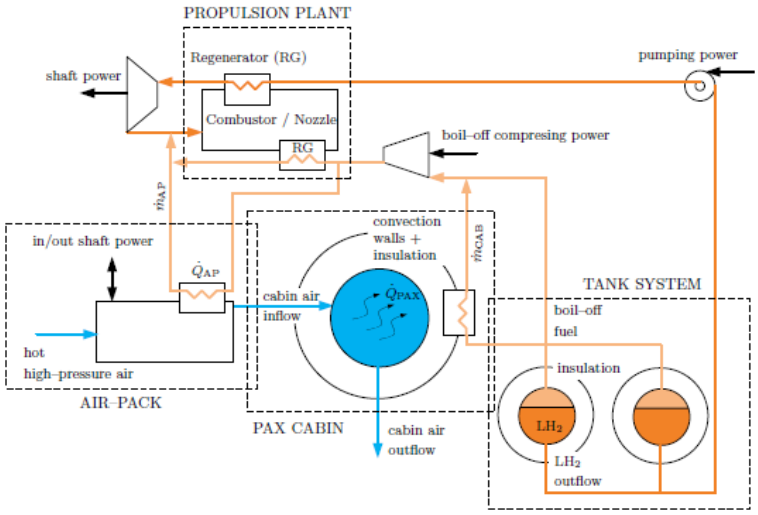

Fig. 54: The TEMS schematic of the MR2.4 (Fernandez Villace & Steelant, 2015)

The TEMS integrates propellant subsystem, Environmental Control Subsystem (ECS), Thermal Control Subsystem (TCS) and Electrical Power Subsystem (EPS) functionalities in a single assembly, capable of assuring cooling of structure, power plant and cabin, exploiting both boiled-off and liquid hydrogen. The subsystem is also capable of generating secondary electrical power on-board at high-speed, when engines cannot be used since rotating parts are absent or by-passed depending on the flight phase and trajectory. A thermal analysis allowed hypothesizing an external average distribution for the pressure side temperature of the vehicle of about 1000 K, whilst higher peaks are expected on leading edges and intake leaps.

3.2.2.4 *On-board Subsystems Integration issues*

For the sake of clarity, Fig. 55 allow comparing the original LAPCAT MR2.4 and the current STRATOFLY MR3 vehicle configuration in terms of main on-board subsystems design and integration.

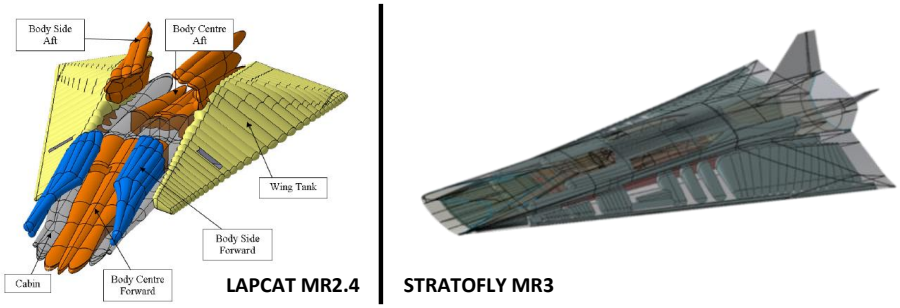

Fig. 55: Comparison between MR2.4 and MR3 vehicles internal layouts

As it can be seen, special attention was devoted to the integration of landing gear, FCS, TPS, TEMS and cabin. Particularly, compartments for landing gear retraction have been re-designed, also considering structural elements. A proper definition of elevons scheme was performed and integration with structure was analysed. Dedicated LH2 tanks have been positioned close to the leading edges, to provide heat rejection capabilities and to interface with passive TPS. Moreover, TEMS interfaces in critical areas, such as intakes, cabin and propulsion plant have been designed. Cabin integration was carefully assessed and passengers access have been relocated considering the interface with propellant tanks.

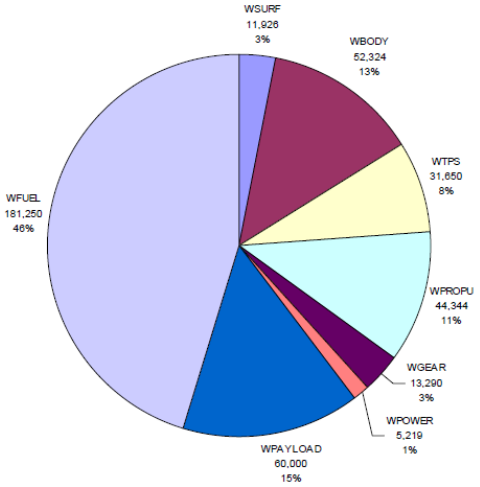

Fig. 56: Mass breakdown for MR2.4 at take-off (Steelant, et al., 2015)

A reference mass distribution similar to MR2.4 was considered for conceptual design. However, only 30 tons were dedicated to the passengers, even if additional mass was originally accounted for provisions (Steelant, et al., 2015). The MTOW is about 400 tons.

3.2.3 STRATOFLY MR3 reference mission concept

The reference mission is shown in Fig. 57 for the Brussels-Sydney route.

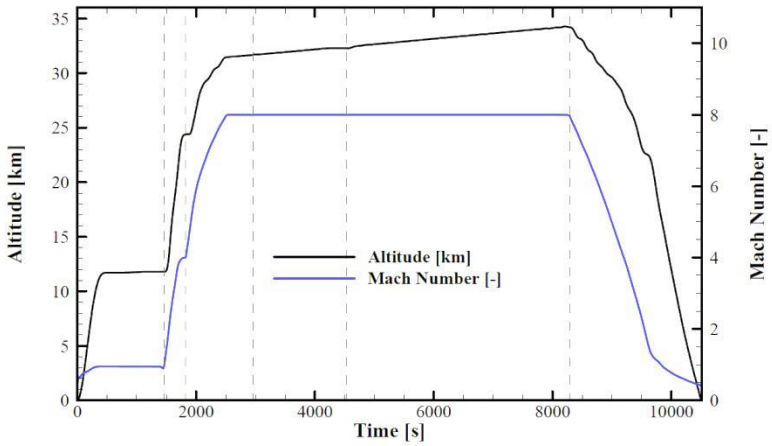

Fig. 57: Reference mission for the MR2.4 concept (Langener, et al., 2014)

It is made of several phases including, after the take-off, a subsonic climb up to 12000 m, a subsonic cruise leg to reach unpopulated area, a supersonic climb, a short supersonic cruise where ATR are shut-off and DMR is ignited (around 24000 m), a hypersonic climb up to 32000 m and a final hypersonic cruise between 32000 and 35000 m. The descent is here supposed unpowered and it is performed in a single segment. The total flight time is about 2h 47m. In order to be able to reach the aforementioned range, 180 tons of liquid hydrogen shall be stored within the vehicle tanks.

4

Model-Based Systems Engineering approach to the conceptual design of hypersonic vehicles

This chapter aims at introducing the methodology conceived for the MBSE approach to the design of hypersonic transportation systems, which is here specifically applied to the STRATOFLY MR3 case study. Starting from the analysis of the typical aerospace product lifecycle discussed in Chapter 2, an integrated methodology has been developed, together with its implementation process. Specifically, in this chapter, an overview of the methodology envisaged to support the conceptual and preliminary design phases is proposed, together with the *description* of high-level activities (Section 4.2). Notably, after a short introduction (Section 4.1) the use of SPEM notation (Chapter 2), to formalize and *discuss* the aforementioned process, aims at providing a homogenous and consistent view on the engineering activities involved. The chapter moves on with the first stage of the methodology, i.e. the conceptual design. This is *described* in Section 4.3 and related mission statement, functional and interface analyses are *discussed* and implemented on MR3 study, as well as aircraft performance matching and feasibility assessments, in Section 4.5. Section 4.4 proposes the System Engineering Environment (SEE) adopted for the proposed approach. Ultimately, Section 4.6 proposes a mapping between the proposed methodology and the ECSS reference process (Chapter 2).

4.1 Introduction

The need for a dedicated methodology to face high-speed transportation systems design appears clear when looking at the complexity of the product and at its level of innovation with reference to conventional aircraft. Moreover, the absence of a proper guideline able to lead designers towards the development of a vehicle in between aeronautics and space domains is a clear aspect which often hampers the positive outcome of the effort. As discussed in Section 2.3, several methodologies for aircraft and space systems design are available in literature, encouraging the possibility of generating a tailored process, dedicated to high-speed transportation systems development. For the purpose of the case study described within this Dissertation, considering the always growing need for standardization of processes, and taking into account the marked European profile of the STRATOFLY Project, the systems engineering practices specified by the European Cooperation for Space Standardization (ECSS) are used as main reference for process and activities definition (ECSS, 2004). This applies not only to nomenclature and technical semantics but also to product lifecycle phases. Notably, the methodology described within Section 4.2 aims at integrating its activities and tasks within the process described in Fig. 58, introducing a tailored approach to high-speed transportation systems design and replacing the existing workflows for Phases 0 and A of ECSS. The overall approach refers to the so-called *"three-levels lifecycle"* (ECSS, 2004). This is a typical implementation of systems engineering practices where the analysis *"is repeated, with various degree of tailoring, in all lower level elements of the system decomposition"* (ECSS, 2004). This means that Phase 0, dealing with *"Mission analysis and needs identification"* (ECSS, 2004), is performed only once, at high-level, while a progressively increasing detail is devoted to product design, from system up to subsystems and components (N+1, N+2 levels).

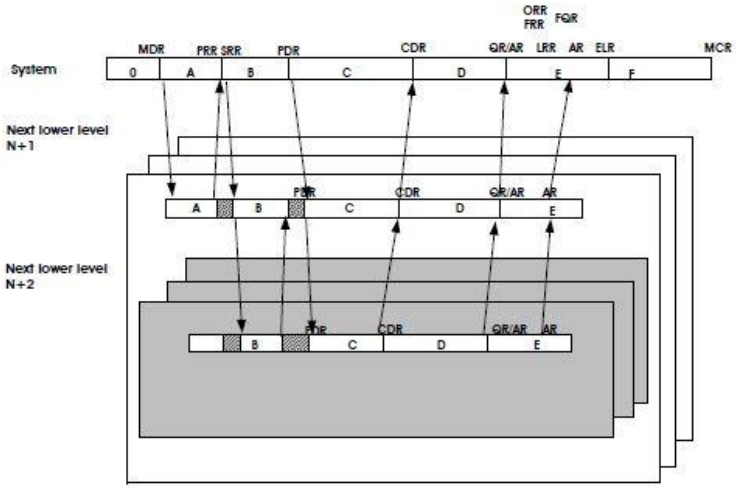

Fig. 58: The "Three-levels lifecycle" from ECSS (ECSS, 2004)

The ECSS workflows for Phases 0 and A are shown in Fig. 59 and in Fig. 60. Phase 0 is mainly dedicated to the set-up of the SE plan, together with the identification of stakeholders, needs, constraints and the so-called mission statement analysis. The identification of primary and secondary objectives leads to the definition of programmatic and mission requirements, through which a very high-level characterization of possible concepts can be hypothesized.

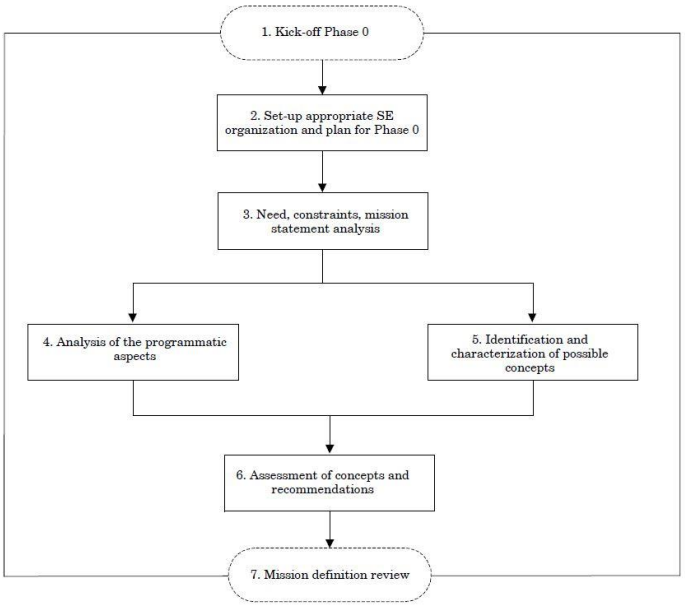

Fig. 59. Workflow for Phase 0 (ECSS, 2004)

Phase A, *"Feasibility"* (ECSS, 2004), starts instead from the configuration of the Systems Engineering Environment (SEE) for a lower level of analysis, producing, first, the functional specification of the system of interest as well as proposing the consolidation of programmatic aspects. Functional analysis is performed at the desired level and technologies are investigated in order to establish a set of possible concepts alternatives, and related trade-off, to identify the best solution. Once the baseline is selected, proper requirements allocation and verification approaches shall be established to provide a valuable system technical specification.

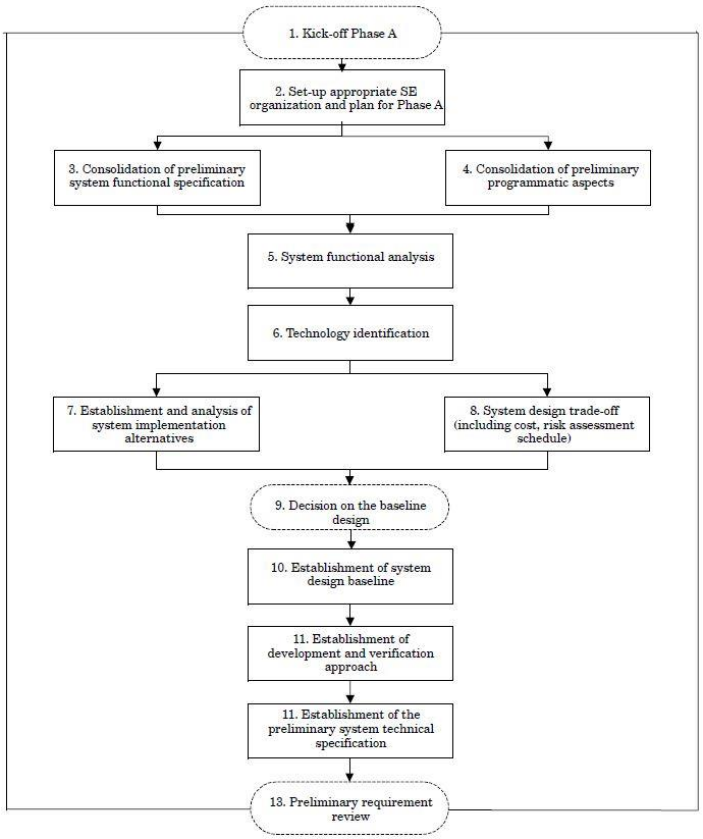

Fig. 60: Workflow for Phase A (ECSS, 2004)

In this context, the proposed Conceptual Design Phase, *described* in Section 4.3, aims at introducing a new workflow for Phases 0 allowing a seamless integration with subsequent Phase A of ECSS, with dedicated updates and modifications, through the exploitation of a model-based environment. Preliminary Subsystems Design Phase, introduced in Chapter 5, refers instead to the application of Phase

A at N+1 and N+2 levels. Moreover, LCC estimation, defined in Chapters 6, is an example of additional *"specialty engineering activities"* (INCOSE, 2015) included within the process, but for which a dedicated discussion appears appropriate.

4.2 Design methodology and main reference process

This section aims at presenting the overall design methodology and the related System Engineering Process (SEP). In particular, the process is described and implemented adopting the already mentioned SPEM notation (Section 2.2.2.3). The structure of the Dissertation itself is organized mirroring the process formalized through SPEM, describing the activities and related tasks in the following sections and paragraphs.

Following the SPEM specification (Object Management Group - OMG, 2008), the activity is defined as *"a grouping of nested Breakdown Elements such as other Activity instances, Task Uses, Role Uses, Milestones, etc…"* (Object Management Group - OMG, 2008). This means that the activity represents a group of tasks, to be performed within a determined workflow, which can be further decomposed at lower levels. In fact, the proposed approach follows a recursive method to describe the different processes, from high-level standpoint up to lowest possible implementation steps. The different activities *described* in this section are then *discussed* in details within the dedicated chapters and paragraphs dealing with conceptual design process. For this purpose, the *description* focuses on the tasks required to accomplish the aforementioned activities, being defined as *"elements defining the work being performed by role instances within a specific activity and associating input as well as output work products to the process"* (Object Management Group - OMG, 2008), whilst the *discussion* deals with detailed topics of the different engineering activities. Each task is characterized by detailed steps required to transform a set of input into output, both represented by work products and by an instance which is in charge for the work. At the end of each section *discussing* the detailed process, a mapping between ECSS and proposed methodology is provided, in terms of input and output of each phase, to demonstrate the possibility of integrating it within the overall workflow proposed by ESA. The overall design process supporting the proposed methodology is shown in Fig. 61.

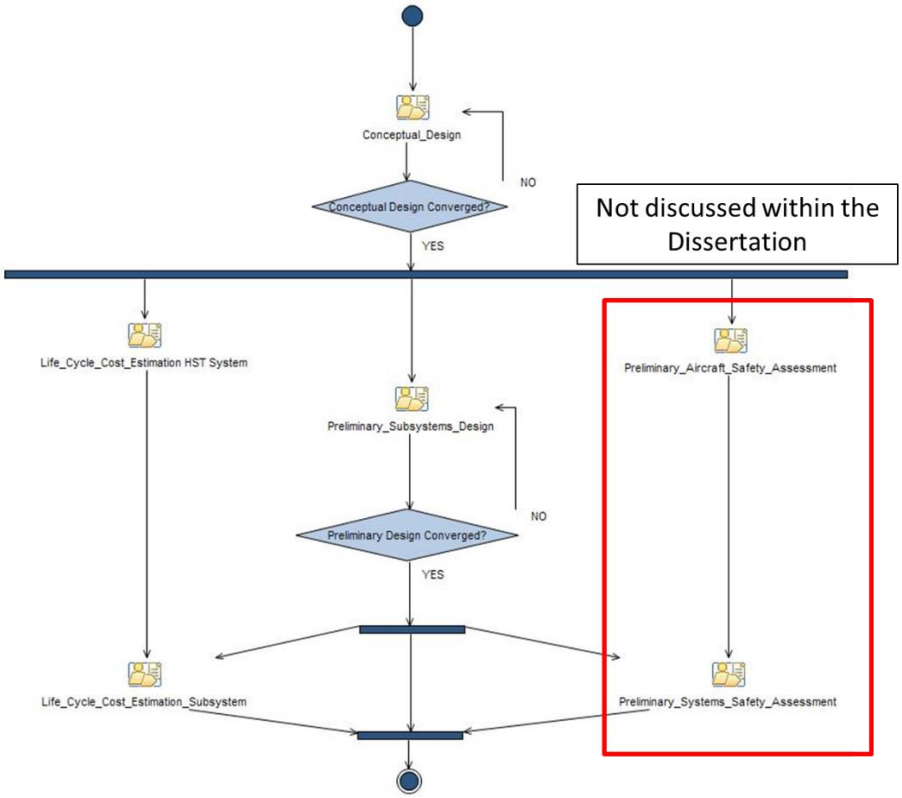

Fig. 61: High-level reference process

The process is made up of six major activities:

- conceptual design;
- preliminary subsystems design;
- Life Cycle Cost (LCC) estimation at aircraft (High-Speed Transportation System) level;
- Life Cycle Cost (LCC) estimation at subsystem level;
- Preliminary Aircraft Safety Assessment (PASA), (not discussed within the Dissertation);
- Preliminary System Safety Assessment (PSSA), (not discussed within the Dissertation).

The process starts with the conceptual design activity, where a vehicle concept is defined both in terms of functional architecture and of high-level performance as well as configuration requirements. When the concept converged to a stable configuration, it is possible to move forward, considering LCC estimation and

PASA at high level, as well as preliminary subsystems design. Both LCC and PASA focus on aspects concerning cost and safety estimations at aircraft levels, while the preliminary subsystem design activity aims at characterizing the lower levels of the product breakdown (notably subsystems and related assemblies). Considerations about low-level LCC and PASA can be usually hypothesized right after the formalization of high-level evaluations, even when the preliminary design is not concluded yet. However, to move towards the end of the process the convergence of subsystems design activity is required. This can also provide refinements to LCC and PSSA activities during following iteration cycles. It is worth saying that the presented process diagrams, and following ones, aim at identifying only the main iterations. Most of the activities are in fact characterized by intrinsic design loops even if not explicitly represented in the diagrams, in order to reduce their complexity for visualization reasons.

The Dissertation describes the different activities of the high-level process in a formalized way. Each of the major activities reported in Fig. 61 is in fact characterized by a set of low-level activities. Complementary, activities of low-level processes are furthermore characterized through proper tasks. After a brief *description* of the high-level processes, following sections deal with a detailed *discussion* of the low-level tasks. The *discussion* is moreover focused on the STRATOFLY MR3 case study (Chapter 3). The meta-model for the proposed approach to *description and discussion* of the methodology is shown in Fig. 62.

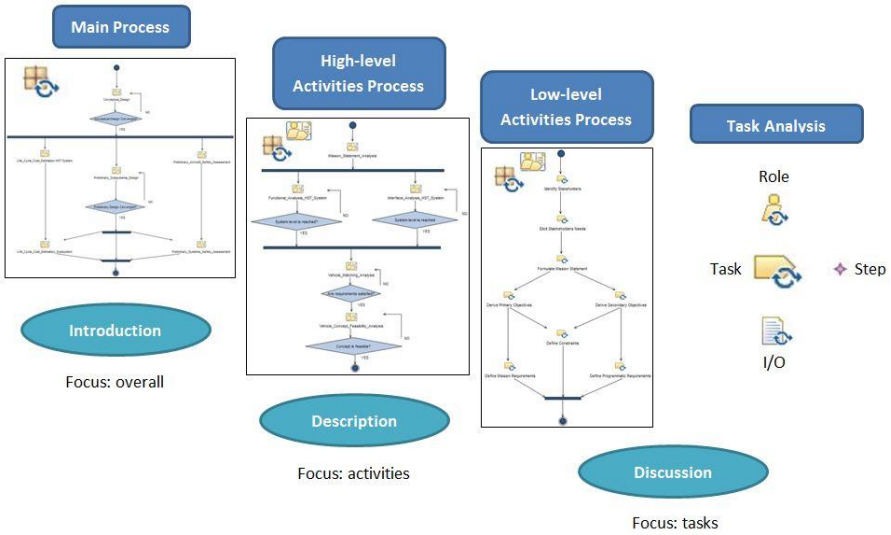

Fig. 62: Process elements convention for *descriptions* and *discussions* in the Dissertation

4.3 Description of high-level Conceptual Design process

The conceptual design process represents the workflow of the first activity of Fig. 61. Within this high-level process, the mission statement is derived and mission objectives, constraints, as well as requirements are identified together with stakeholders (Wertz & Larson, 2005). Moreover, the main functional architecture of the aircraft, is sketched and a conceptual interface analysis is performed. Additionally, traditional activities related to performance determination are exploited, with particular focus on aircraft matching (Loftin, 1980) and on other feasibility studies (Ingenito, et al., 2009). The reference process for (Model-Based) conceptual design is shown in Fig. 63. The overall workflow starts from the mission statement analysis (ECSS, 2004), where stakeholders are identified, together with their needs, and a so-called mission statement, representing *"a concise definition of high-level objectives of a mission"* (Wertz & Larson, 2005), is derived as short description of the purpose of the object to be designed. From the mission statement, primary mission objectives are derived, whilst secondary objectives are mainly detected looking at additional stakeholders needs. Furthermore, the derivation of the primary objectives paves the way towards the definition of the first set of mission requirements, whilst secondary objectives are crucial to determine programmatic requirements. This activity helps defining the mission concept as well as the Top Level Function (TLF) of the High-speed Transportation System (HST), to be determined as first step of the subsequent activity. The functional analysis aims at defining the functional breakdown of the vehicle, generating functional requirements and identifying possible products on which functions can be allocated. This is a recursive process starting from the TLF and moving forward up to the required level of detail. In this case, the conceptual design process is supposed to end when reaching the subsystem level, i.e. when high-level, segment level, system and subsystems levels are defined in a preliminary way. The functional breakdown, together with the allocation process, allows defining a corresponding product breakdown that can be used as basis to start the interface analysis. Actually, functional and interface analyses are performed jointly for each level treated within conceptual (and also preliminary) design phase.

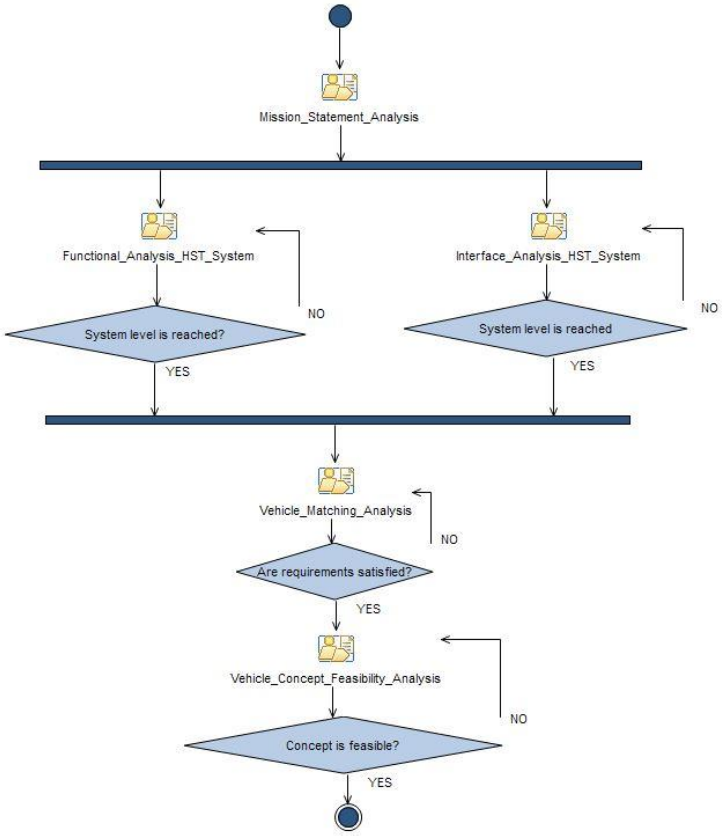

Fig. 63: Reference process for conceptual design activity

The combination of the two activities is usually referred to as functional or logical architecture in literature (Brusa, et al., 2018). Interface analysis allows deriving also the related interface requirements, which, together with functional requirements associated to products, constitute the conceptual functional specification for the vehicle. Moreover, a concept of operation is determined within the last stages of functional analysis, so to conceptually characterize the mission. From the initial functional specification, it is also possible to derive high-level performance requirements, able to specify quantitative assumptions related to qualitatively-driven functional aspects. A typical example can be the definition of the product responsible to generate lift (i.e. the wing, at system level), whose efficiency (i.e. lift/drag ratio) is specified by dedicated performance requirements for the different phases, whilst its presence in vehicle architecture depends on the allocation of the related function on a logical product, through the generation of a proper functional requirement. An usual sketch of the links instantiated between

requirements and functional/interface analysis is reported in Fig. 64 through a non-formalized notation.

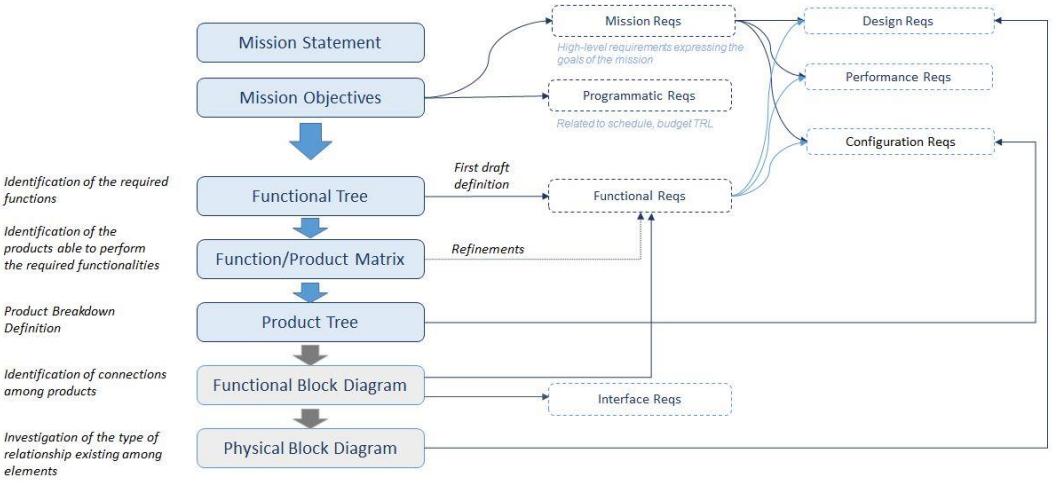

Fig. 64: Sketch of logical requirements specification derivation

As soon as this functional/logical set of activities is completed, characterizing the main elements of the vehicle, the focus can move to performance analysis in terms of matching as well as, ultimately, feasibility. The matching analysis (Loftin, 1980) consists in the verification of vehicle concept by computing thrust-to-weight ratio requirements as function of wing loading in different flight conditions. This activity is performed to identify the design point (or space) for the vehicle under study, basing on some preliminary characteristics or assumptions on weight and balance, aerodynamic performance, propulsion plant characteristics etc… . When the performance design point (or space) is identified, the feasibility study associated to configuration can start. For HST systems this is mainly related to the verification of the compatibility of mission requirements with vehicle architecture in terms of available volume on-board (Ingenito, et al., 2009). This is performed by relating the wing surface (or reference planform surface) of the concept, as derived from performance requirements and verified within matching analysis, to its theoretical available volume. The definition of product breakdown, up to subsystems level, allows furthermore to account for required volume by means of statistical and semi-empirical relationships for the different elements of the breakdown itself (Chudoba, et al., 2012). An additional design space can be then identified, looking at physical dimensions of the concept, with reference to mission requirements such as range, cruise Mach and maximum aerodynamic efficiency. The conceptual design is considered completed as soon

as the concept is validated in terms of logical architecture, matching and feasibility, i.e. when the configuration can be frozen and when requirements specification is fully characterized for the desired level. Detailed discussions on tasks, steps, roles and work products for each activity of the conceptual design process for HST systems are reported in Section 4.5, together with the mapping with ECSS phase 0 (ECSS, 2004) in Section 4.6.

4.4 The Systems Engineering Environment (SEE)

The proposed methodology makes use of a process which is conceived to provide means of implementation of the different tasks within a dedicated model-based Systems Engineering Environment (SEE). This is a context made up of commercial tools, enabling the whole set of MBSE approach peculiarities, enhancing the effectiveness of the design process and demonstrating the possibility of exploiting seamless toolchains to support the design of complex and highly integrated systems. The environment is mainly organized upon:

- a Logical Development Environment (LDE), where mission statement, functional and interface analyses are implemented adopting SysML language and exploiting fully traceable links with requirements stored within an external database;
- a Requirements DataBase (RDB), where the requirements specification is defined, managed and updated;
- a Physical Development Environment (PDE), where numerical modelling is performed and classical aircraft design techniques are exploited to characterize the high-level configuration of the vehicle. This environment can be linked to the RDB and also to CAD.

The reference SEE is qualitatively shown in Fig. 65. The Requirements hub (RDB) is used to collect the specification and to keep trace of updates and synchronization among different tools. Mission and programmatic requirements as well as functional and interface ones are in fact derived within the LDE and linked to the RDB. Performance and physical requirements are instead connected to simulation platform of PDE. CAD environment can be also connected to both PDE and RDB (Fusaro, et al., 2016).

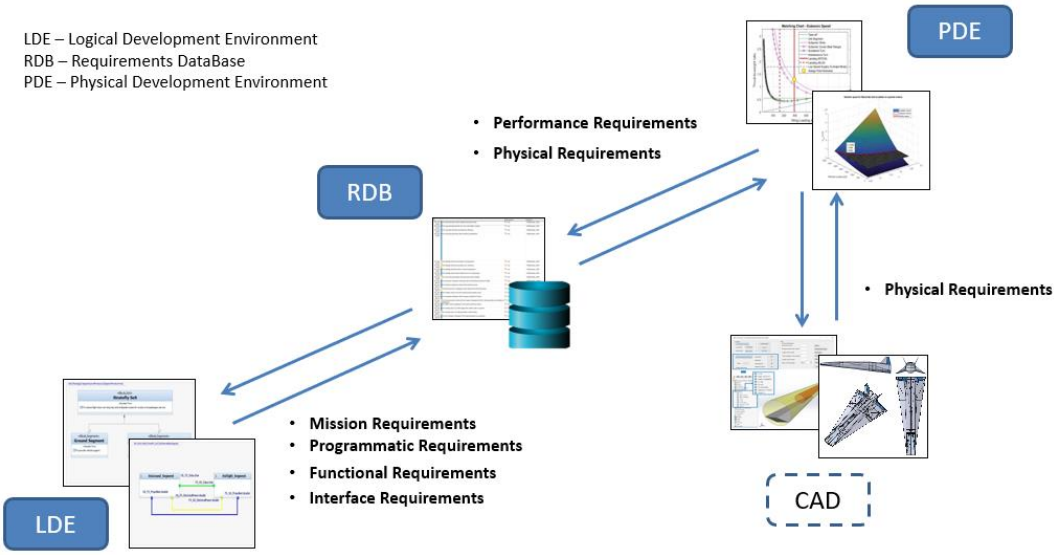

Fig. 65: Qualitative representation of the SEE and internal data exchange

The seamless connection with requirements hub allows effective change management and complete configuration control. The connection of different tools is implemented through point-to-point adapters or export facilities already available out of the box. Existing platforms have been selected and exploited since the main aim of the work is not related to the development of the SEE and of the interoperability specification, but it is actually focused on the design methodology and implementation.

4.5 Discussion on low-level Conceptual Design processes for STRATOFLY MR3

4.5.1 Mission Statement Analysis

4.5.1.1 Mission Statement Analysis workflow

The first activity of conceptual design process reported in Fig. 63 is the Mission Statement Analysis. Considering the crucial role of this first activity, a low-level workflow consisting of tasks (Fig. 66) has been derived to be here analysed and discussed more in details.

As already anticipated in Section 4.3, the first step of the analysis consists in the *identification of stakeholders and of the related needs*. Subsequently, when

designers and stakeholders agreed upon a common Statement of Work (SoW), a global mission statement can be derived to describe the mission very synthetically. Then, from mission statement, primary objectives are derived and information contained within the statement can be used also to enrich the secondary objectives, usually obtained from stakeholders expectations and needs directly. When objectives are known and formalized, high-level requirements concerning mission and programmatic aspects can be defined as well as constraints (representing non-tradable requirements). The process is thus very simple in its formalization, even if, usually, the definition of mission requirements is made of some loops of iteration, being the most critical design phase in terms of characteristics allocation on final product (Section 2.3). This phase can be considered completed when requirements and constraints are both available.

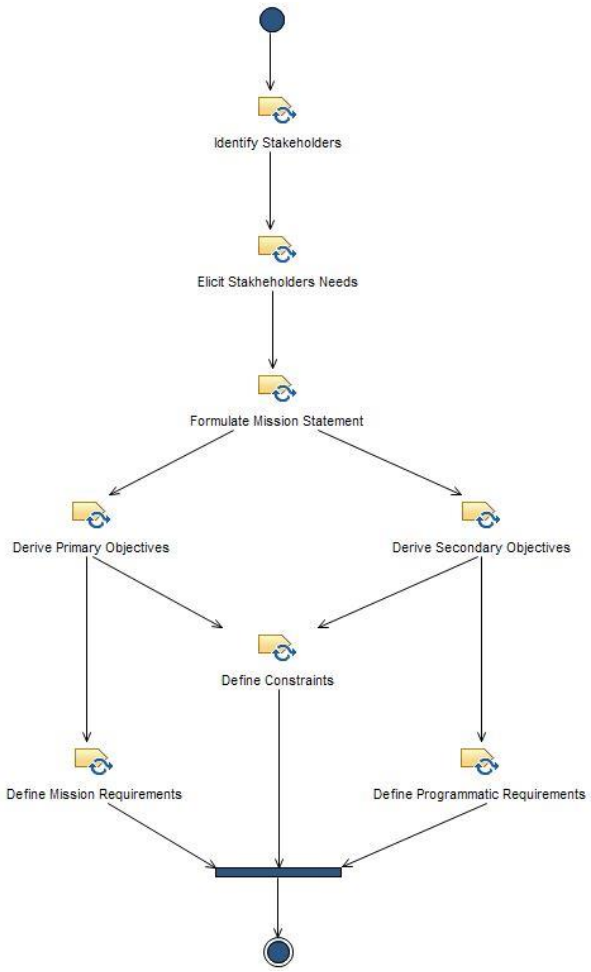

Fig. 66: Mission Statement Analysis workflow

4.5.1.2 Identify stakeholders

The identification of stakeholders is the first task of the Mission Statement Analysis workflow (Fig. 66). At the same time, this task also represents the first step of the so-called stakeholders analysis, which include, as second step, the elicitation of their needs (Section 4.5.1.3). The identification task is necessary as preparatory duty not only to capture the crucial entities expressing interests towards the system, but also to propose a classification that can be helpful to better characterize the needs in the subsequent task. Particularly, the stakeholders identification task aims at pointing out external actors which might be interested in supporting, buying, using and/or operating the systems. They are usually defined as sponsors, customers, end users and operators respectively. For the sake of clarity, Fig. 67 shows the stakeholders and related families identified within STRATOFLY case study, as listed hereafter:

- Sponsors – European Commission (through Innovation and Networks Executive Agency - INEA);
- Customers – Passengers;
- End users – STRATOFLY consortium;
- End users – Scientific Community;
- End users – External Experts Advisory Board (EEAB);
- Operators – External Experts Advisory Board (EEAB).

In this graphical representation, stakeholders are represented as SysML actors, instantiated through generalization dependencies to identify the different families in a Use Case Diagram (UCD).

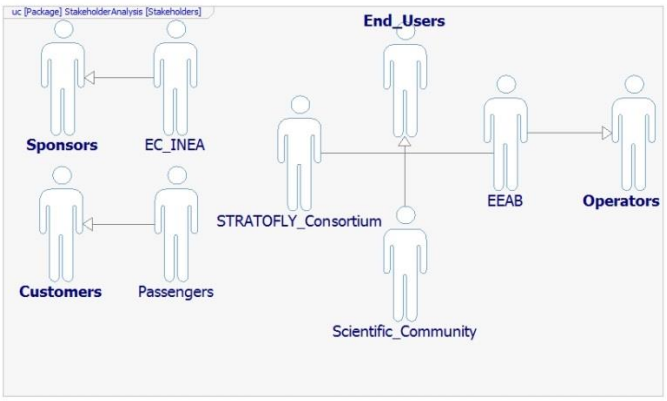

Fig. 67: Stakeholders identified within the STRATOFLY Project

Generalization is a type of SysML association specifying subtypes for a certain element and, thus, it can be used to relate diagram elements belonging to the same group. Looking at the STRATOFLY specific case study, the only sponsor is the EC, funding the project through its executive agency. Final customers are the passengers themselves, whose interests shall be safeguarded during the project. The end-users, i.e. those who will benefit from the development of the technology, belongs to the internal project consortium, to the scientific community in general and to the project advisory board, selected for specific interests within the topic. Notably, since an airline can also be included within the EEAB, this group of stakeholders can be identified also as operator. It is interesting to consider that, depending on the viewpoint through which the stakeholder is classified, the role of each actor can change, as the related needs (Section 4.5.1.3).

4.5.1.3 Elicit stakeholders' needs

Once the role of stakeholders has been qualified, it is possible to elicit needs that will be used to identify stakeholders goals, to be included within the SEE. In fact, use cases are usually the main diagram elements populating the UCD and they can be interpreted as goals of the stakeholders (Brusa, et al., 2018). It is thus necessary to perform a pre-processing step to translate needs into goals. Needs can be actually derived by looking at the SoW, which usually describes these kinds of aspects. For the purpose of STRATOFLY project, the following situation can be summarized for what concern needs:

- Sponsors – European Commission (through INEA agency), expresses the need of extending the industrial European leadership and the knowledge about technologies associated to hypersonic flight (like propulsion, innovative configurations, on-board systems architecture etc…). Moreover, it aims at raising the technologies which are currently at readiness level (TRL) lower than 3. The final goal will be to sketch a sustainable path to guarantee that all the enabling technologies could reach TRL 6 in the next decade. Furthermore, the EC provides time and budget constraints;
- Customers – Passengers, are the final travellers that will use the system and that will pay for this service. They ask for a safe, shorter in time and higher in speed flight. Moreover, they search for a cost-effective product, being able to meet their expectations related to comfort on-board. They

also care about environmental issues related to pollution, expecting an environmental friendly and clean product.

- End users – STRATOFLY consortium, benefits from the case study to increase the knowledge in hypersonic vehicles design and promoting the research in the field.
- End users – Scientific Community, as the consortium, may benefit from the advancement in worldwide understanding of hypersonic vehicles technologies also for different applications.
- End users – External Experts Advisory Board (EEAB), is interested in hypersonic vehicles topic for both research and industrial reasons. EEAB is made of companies and research institutions that might have different interests towards the project, but they are all related to technology development or commercialization of the final product.
- Operators – External Experts Advisory Board (EEAB), is also constituted by possible operators that will be responsible for product entry into service and support during its lifecycle. They are thus interested in reducing the cost during operation and they are searching for a product easy to maintain and, in general, easy to operate.

It shall be also pointed out how stakeholders' needs are usually represented as qualitatively statements, difficult to be formalized and managed within a model-based environment, being described by natural language. This is also the reason why goals and, subsequently, requirements, will constitute the main model and specification elements, so to be able to trace this first qualitative but crucial information for subsequent phases. A summary of stakeholders objectives (SHO), derived from the aforementioned needs, is reported in Table 2.

Table 2: List of stakeholders objectives

Objective ID	Objective description	Objective owner
SHO1	To extend the European industrial leadership	EC
SHO2	To extend knowledge related to propulsion, configuration and innovative subsystems for HST vehicles	EC, Consortium, Scientific Community, EEAB
SHO3	To raise technologies characterized by low TRL up to TRL 6	EC
SHO4	To reduce flight time	Passengers

SHO5	To fly safely	Passengers
SHO6	To fly comfortably	Passengers
SHO7	To fly cost-effectively	Passengers
SHO8	To fly responsibly	Passengers
SHO9	To promote research in the field of HST systems	Consortium
SHO10	To reduce lifecycle cost	EEAB
SHO11	To ease maintainability and operation procedures	EEAB

It is also important to highlight that these objectives are direct expression of stakeholders and shall not be confused with primary or secondary objectives related to HST mission or system, described within Sections 4.5.1.5 and 4.5.1.6.

4.5.1.4 Formulate mission statement

Considering the SoW, the context of the project and the main problems related to the research topic, it is possible to formulate the STRATOFLY mission statement as:

To shorten the flight time of one order of magnitude (with respect to the state of the art of civil aviation) of at least 300 civil passengers along long haul and antipodal routes, through the preliminary design of LAPCAT MR2.4 (Mach 8 waverider vehicle) flying at stratospheric altitudes within a future CNS/ ATM scenario, reducing the impact on existing on ground infrastructure, in compliance with environmental compatibility and safety issues, assessing the overall economic feasibility of the solution.

The formulation of the mission statement is usually performed looking at the root problem for which the system of interests shall be defined. The statement shall include a very high-level reference to how the problem can be solved, including additional top level objectives for the scenario. Of course, it shall benefit from the analysis of stakeholders and of their needs, especially looking at customers' and end-users' expectations. Mission statement can be included within the UCD, as fully traceable element, as top level use case from which primary and secondary objectives can be derived.

4.5.1.5 Derive primary objectives

Primary mission objectives are directly derived from the mission statement. Using the SysML notation, both statement and objectives can be represented within a dedicated UCD highlighting the links among them Fig. 68.

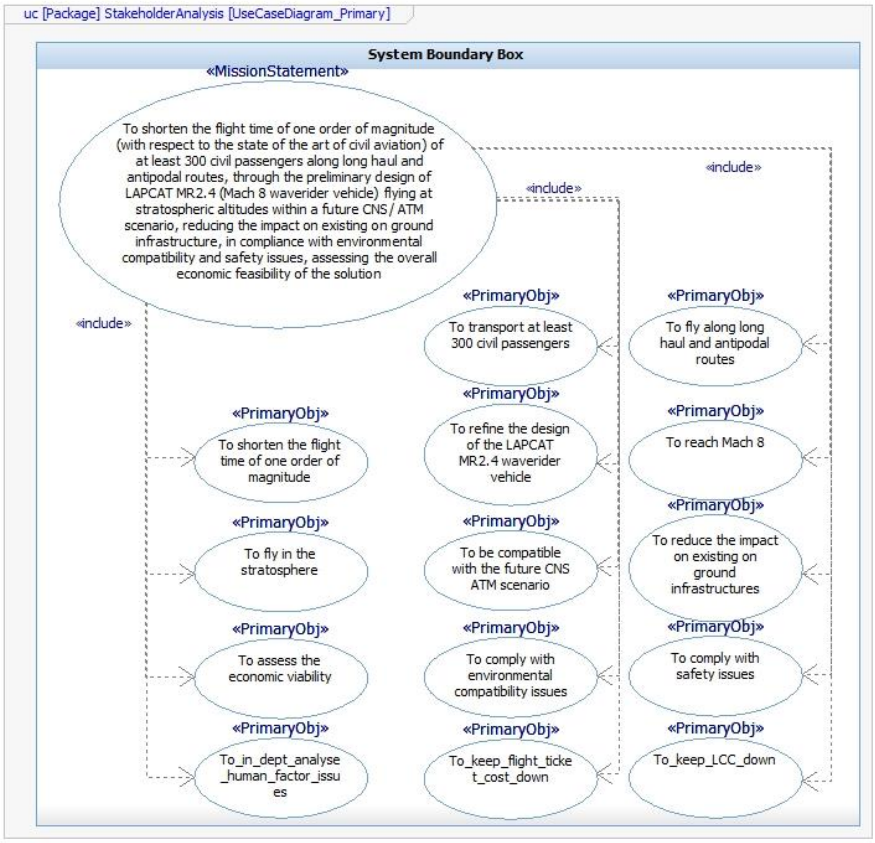

Fig. 68: Use Case Diagram with primary mission objectives

Dependencies are instantiated between the main use case (mission statement) and mission objectives to guarantee traceability within the derivation process. Dependencies are general purpose relationships expressing a directional influence between two or more elements. The type of relationship is specified by a stereotype, which is a property of SysML object identifying a set of characteristics. Stereotypes can be tailored and customized. Particularly, use cases stereotypes are clearly visible within Fig. 68. The list of derived objectives is also reported in Table 3.

Table 3: List of primary mission objectives

ID	Objective definition
PO1	To shorten the flight time of one order of magnitude
PO2	To transport at least 300 civil passengers
PO3	To fly along long haul and antipodal routes
PO4	To refine the design of LAPCAT MR2.4 waverider vehicle
PO5	To reach Mach 8
PO6	To fly in the stratosphere
PO7	To be compatible with the future CNS-ATM scenario
PO8	To reduce the impact on existing on-ground infrastructure
PO9	To assess the economic viability
PO10	To comply with environmental compatibility issues
PO11	To comply with safety issues
PO12	To in depth analyse human factor issues
PO13	To keep flight ticket cost down
PO14	To keep LCC down

4.5.1.6 Derive secondary objectives

Complementary to the elicitation of primary mission objectives, stakeholders' needs are used to derive secondary objectives as well. A dedicated UCD for secondary objectives can be implemented showing the relationships between actors and use cases to represent this link (Fig. 69). Simple associations are used to relate use cases and stakeholders (actors), while dedicated anchor connectors are exploited to link use cases to eventual constraints elements. In fact, secondary objectives identify programmatic aspects and can be also linked to proper constraints, as visible in Fig. 69 and explained in Section 4.5.1.9.

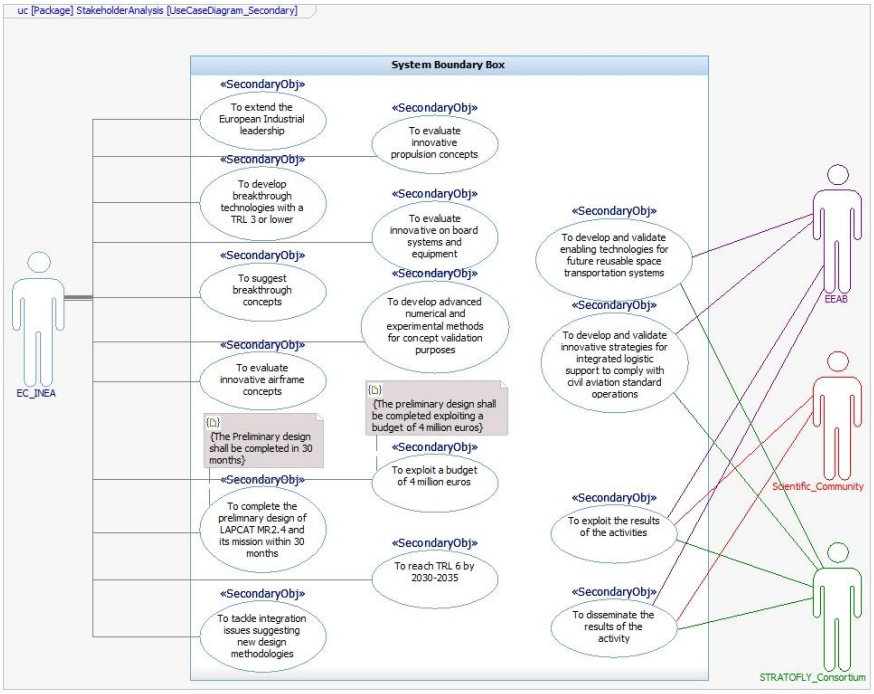

Fig. 69: Use Case Diagram with secondary mission objectives

Passengers are not here represented as an actor since their needs mainly coincide with most of the Primary Objectives. Thus, dedicated Secondary Objectives have not been derived as they would have resulted redundant. The definition of the different secondary objectives and the relations with the stakeholders is summarized in Table 4.

Table 4: List of secondary objectives

ID	Objective definition	Stakeholder involved
SO1	To extend the European industrial leadership	European Commission (INEA)
SO2	To develop breakthrough technologies with a TRL 3 or lower	European Commission (INEA)
SO3	To reach TRL 6 by 2030-2035	European Commission (INEA)
SO4	To suggest breakthrough concepts	European Commission (INEA)
SO5	To evaluate innovative airframe concepts	European Commission (INEA)
SO6	To evaluate innovative propulsion concepts	European Commission

		(INEA)
SO7	To evaluate innovative on board systems and equipment	European Commission (INEA)
SO8	To tackle integration issues suggesting new design methodologies	European Commission (INEA)
SO9	To develop advanced numerical and experimental methods for concept validation purposes	European Commission (INEA)
SO10	To exploit a budget of 4 million euros	European Commission (INEA)
SO11	To disseminate the results of the activity	Scientific Community, EEAB, STRATOFLY Consortium
SO12	To exploit the results of the activities	Scientific Community, EEAB, STRATOFLY Consortium
SO13	To develop and validate enabling technologies for future reusable space transportation systems	EEAB, STRATOFLY Consortium
SO14	To develop and validate innovative strategies for integrated logistic support to comply with civil aviation standard operations	EEAB, STRATOFLY Consortium

4.5.1.7 Define mission requirements

Once the objectives are defined, it is possible to derive mission requirements from primary objectives. Requirements are defined and stored in the main database hub and are accessible within the main SEE as SysML elements (thus they can be used within diagrams to guarantee traceability). Mission requirements are the basis for the development of functional and logical architectures (Section 4.5.2) and are used to derive other types of requirements. Derivation is implemented within the database through proper internal traceability tools, included within the specification structure, whilst external traceability (i.e. the set of links relating requirements and elements of the SEE) is managed directly in the model environment (Brusa, et al., 2018). Even if some aspects are here anticipated, a dedicated discussion on traceability types and tools is reported in Section 4.5.2, since it becomes quite critical during functional analysis. Mission requirements are collected in Section 8.1.1.

Requirements are linked to primary mission objectives, represented as use cases through SysML trace dependencies to implement external traceability. The overview of these links is shown in Fig. 70, where a matrix view is provided as visualization tool (Section 4.5.2).

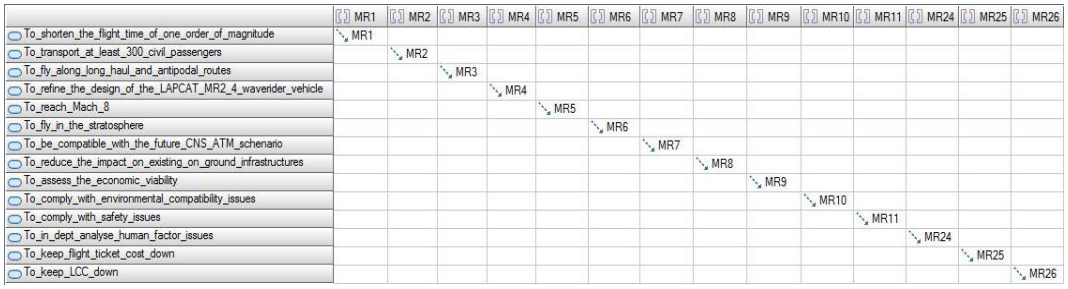

Fig. 70: External traceability between mission requirements and primary objectives

4.5.1.8 Define programmatic requirements

Similarly, programmatic requirements (Section 8.1.2) can be derived looking at secondary objectives, defined following the analysis of stakeholders needs. A matrix view summarizing the links with Secondary Objectives can be implemented as well, as shown in Fig. 71. Moreover, the Model-Based environment allows associating directly requirements to the stakeholders, since these are ultimately derived from the objectives identified looking at the related needs. The traceability is then completely available and links can be navigated live within the environment.

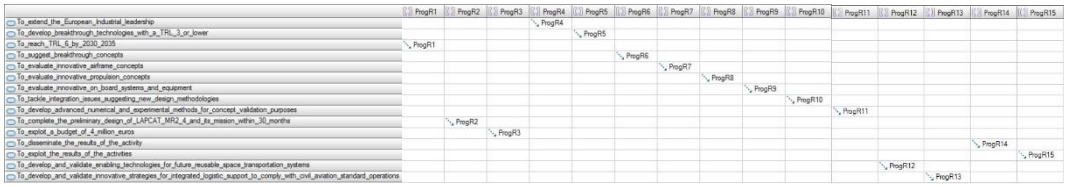

Fig. 71: External traceability between programmatic requirements and secondary objectives

4.5.1.9 Define constraints

Requirements and constraints are *"quantitative expressions of how well we achieve our objectives"* (Wertz & Larson, 2005) but, as requirements express the main characteristics of the system of interest and can be subjected to change during the project, constraints are non-tradable. This is also a reason why they

mainly deal with programmatic aspects derived from secondary objectives. However, they might be also related to design aspects, such as interface, regulation or standards that shall be respected. In this case, the identification of constraints, at least at high-level, is fairly simple, since only programmatic aspects emerge (there are no regulations or standards currently available for this kind of systems and the vehicle is designed completely within the same project, limiting interfaces with external entities). From Fig. 69, it is clear that two main aspects are constraining the project: budget and time (as it often happens). These constraints are specified by the main sponsor, since the funding is dedicated to a certain period and is limited. For this reason, the constraints reported in Table 5 can be identified.

Table 5: High-level constraints list

Derived from	ID	Constraints definition
SO10	C1	The preliminary design of the STRATOFLY vehicle, based on LAPCAT MR2.4, shall be completed in no more than 30 months
SO10	C2	The preliminary design of STRATOFLY vehicle, based on LAPCAT MR2.4, shall be completed exploiting a budget of no more than 4 million euros

Constraints are defined in SysML through the dedicated elements and associated to use cases which have generated them exploiting anchor connectors.

4.5.2 Functional Analysis

4.5.2.1 Functional Analysis workflow

Functional analysis is one of the most important phases of the conceptual design process, since it defines the main system capabilities to be included within the logical architecture. The process (Fig. 72) takes advantage of the mission objectives derived within the mission statement analysis (and of the statement itself) to define the Top Level Function (TLF) for the system under design. This is the starting point for the definition of functional breakdown. Particularly, the breakdown is conceived to derive the functions related to system elements progressively at lower levels (i.e. recursively).

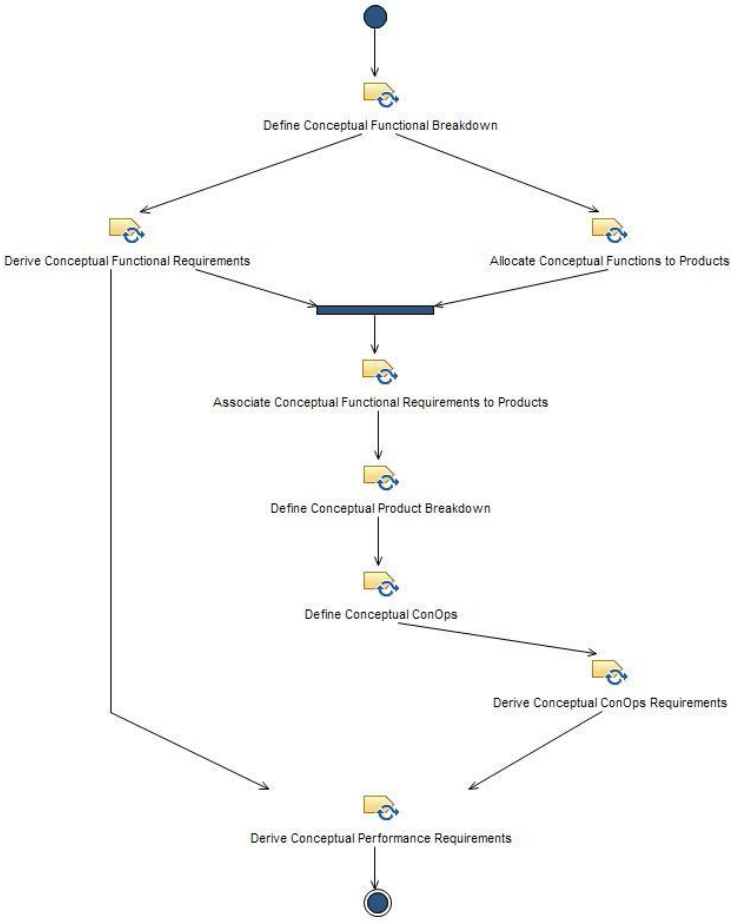

Fig. 72: Functional analysis workflow

Conceptual breakdown includes, in this case, all the hierarchical levels up to subsystems, since this is the minimum set of capabilities able to represent the overall configuration for the vehicle. In fact, in order to proceed with performance and feasibility analyses, data concerning the type of subsystems on board are required (even if these are not detailed). For each level, functional requirements are derived and a proper allocation process is implemented to derive the products responsible for the selected capabilities. Once products are identified, dedicated product breakdown, depicting the logical hierarchy of system elements, is also built. Requirements are also associated to products in order to guarantee traceability. Starting from functional breakdown and high-level mission statement, the ConOps analysis can be instantiated in terms of mission characterization, functional flow and phase analysis. Details related to the mission and to physical models will be refined and updated when matching and feasibility analyses will be

completed (Section 4.5.4 – 4.5.5). Functional analysis offers also the basis for the derivation of conceptual requirements related to performance. Even if this aspect may appear contradictory, the procedure to derive performance requirements starts from early mission characterization and, also, from functional aspects. Performance requirements aims in fact at specifying quantitative values which characterize the qualitative capabilities described by functional requirements (and, ultimately, by functions themselves). The overall process is considered completed when functional breakdown and corresponding product breakdown are defined, together with the relations with requirements (both functional and performance ones). Additionally, the ConOps at conceptual level, with related requirements, shall be completed.

4.5.2.2 Define conceptual functional breakdown

The definition of functional breakdown is the main task of the functional analysis process. Functions derivation is traditionally performed defining a suitable functional tree able to represent the functional breakdown of the system of interest in a hierarchical way. Starting from a TLF, which is conceived to represent the very high level purpose of the system, low level functions are derived within consecutive levels to detail more and more the functionalities. The TLF for STRATOFLY system (i.e. the overall service which includes ground and flight segments) is reported hereafter:

To reduce flight time over long haul and antipodal routes for routine civil passengers' service.

This function represents the top of the tree. Two segment level functions (SEF) can then be derived as represented in Fig. 73 and listed in Table 6. The functional tree is represented as a Block Definition Diagram (BDD) in SysML, where blocks (i.e. functions) are connected each other through directed composition links. Compositions are peculiar types of association relationships which can specify hierarchy (producing parts instances for the target blocks that are included within the source block structure). For example, the two derived functions of Fig. 73 (target blocks for the composition links) are parts of source block (the TLF).

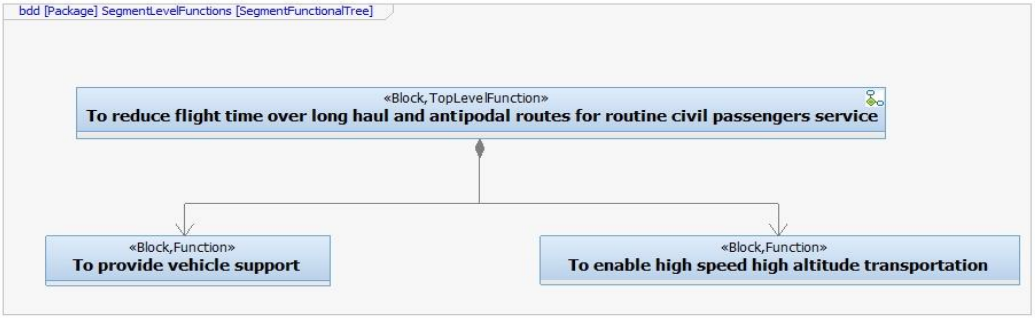

Fig. 73: Functional tree (BDD) up to segment level

Top level functional breakdown is summarized in Table 6.

Table 6: Top and segment level functions list

ID	Function @ Top Level
TLF1000	To reduce flight time over long haul and antipodal routes for routine civil passengers service.
ID	**Function @ Segment Level**
SEF1000	To provide vehicle support.
SEF2000	To enable high speed high altitude transportation.

Starting from the leaves of the tree, defined in the previous level, it is possible to further decompose segment level functions. The updated tree, developed up to system level is shown in Fig. 74.

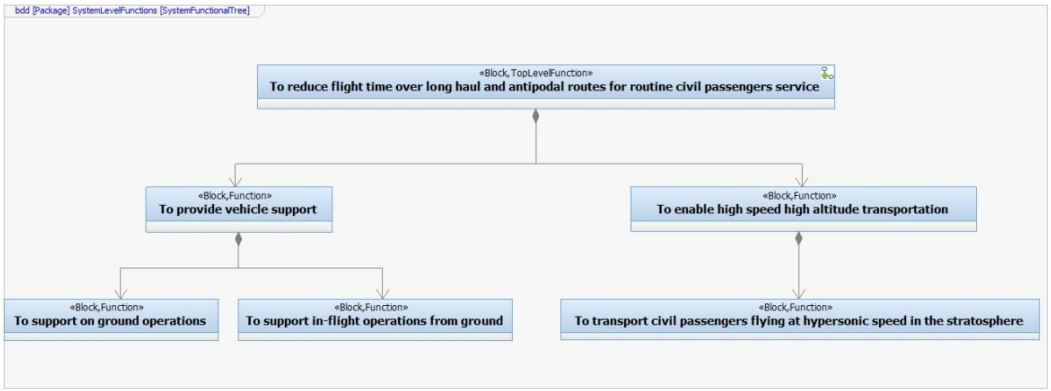

Fig. 74: Functional tree (BDD) up to system level

Following this stage of derivation, the functions reported in Table 7 can be defined.

Table 7: Functions list at system level

ID	Functions @ System Level
SYF1000	To support on-ground operations.
SYF2000	To support in-flight operations from ground.
SYF3000	To transport civil passengers flying at hypersonic speed in the stratosphere.

Functional tree can be further updated starting from system level in order to analyse sub-system level. For the purpose of this analysis only vehicle system is detailed and, for clarity, only SYF3000 is developed in Fig. 75. The list of functions at subsystem level is provided in Table 8.

Table 8: Functions list at subsystem level

ID	Functions@ Subsystem Level
SUF1000	To withstand structural loads.
SUF 2000	To generate lift over the whole flight envelope.
SUF 3000	To maximize aerodynamic efficiency.
SUF 4000	To guarantee safe emergency splashdown.
SUF 5000	To accommodate civil passengers.
SUF 6000	To accommodate crew members.
SUF 7000	To host other on-board subsystems.
SUF 8000	To provide sufficient arm for empennages.
SUF 9000	To guarantee static stability.
SUF 10000	To generate thrust allowing hypersonic flight.
SUF 11000	To provide hydraulic power.
SUF 12000	To provide electrical power.
SUF 13000	To provide auxiliary power.
SUF 14000	To manage propellant on board.
SUF 15000	To guarantee survivability of passengers.
SUF 16000	To control the vehicle.
SUF 17000	To support the vehicle when on ground.
SUF 17500	To guarantee a safe landing.
SUF 19000	To guarantee fire protection.
SUF 20000	To guarantee thermal protection.
SUF 21000	To guarantee vehicle management capabilities.
SUF 22000	To provide thermal control.

The need for providing hydraulic power shall be carefully assessed during further studies, even if it cannot be excluded a priory at this stage. This is the bottom level for conceptual breakdown for what concerns functions. However, the analysis is just at the beginning, since functional requirements shall be derived

and associated to products responsible to perform functions, as reported in the following sections.

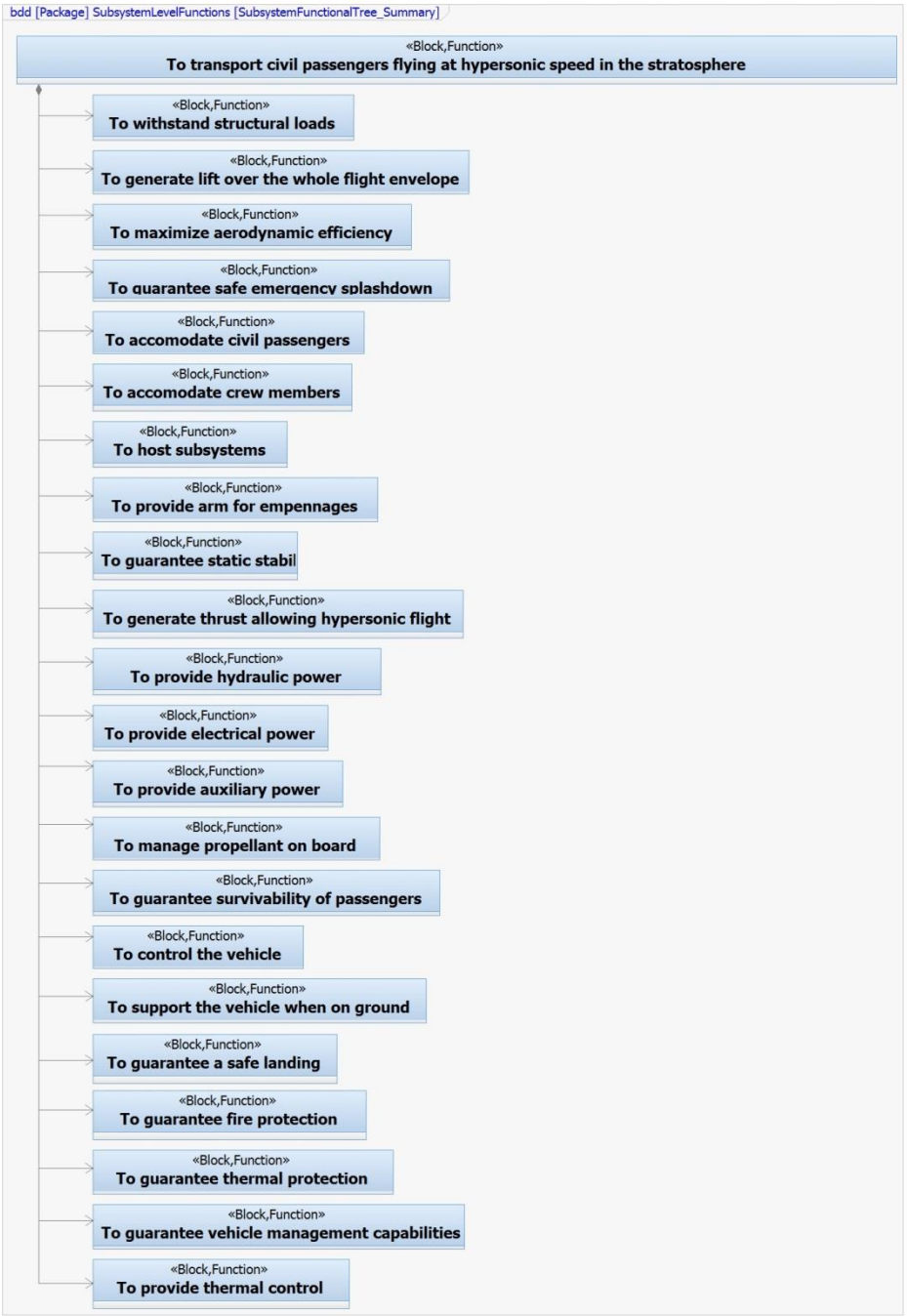

Fig. 75: Functional tree (BDD) at subsystem level starting from SYF3000

4.5.2.3 Allocate conceptual functions to products

Allocation process consists in deriving a suitable logical product able to perform the predicted functions. However, in order to take into account the need of maintaining consistency with LAPCAT MR2.4 configuration (see requirement MR4000), a set of high-level configuration requirements shall be explicated before moving to product allocation, since some parts of the product breakdown can be directly specified. Particularly, Section 8.1.3 shows the conceptual configuration requirements specification, where system and subsystems elements are already stated. In the SEE, matrix views can be created to implement and summarize the allocation process between functions and products, as shown in Fig. 76 for segment level (TLF is obviously allocated on STRATOFLY service). The links instantiated between function and product blocks are dependencies with dedicated stereotypes (allocation).

	Ground_Segment	Flight_Segment
To_provide_vehicle_support	Ground_Segment	
To_enable_high_speed_high_altitude_transportation		Flight_Segment

Fig. 76: Matrix view of the allocation of functions on products at segment level

Product breakdown is developed in the same way of functional one, thus the related allocation matrix is shown in Fig. 77.

	Airport	Ground_Station	Vehicle
To_support_on_ground_operations	Airport		
To_support_in_flight_operations_from_ground		Ground_Station	
To_transport_civil_passengers_flying_at_hypersonic_speed_in_the_stratosphere			Vehicle

Fig. 77: Matrix view of the allocation of functions on products at system level

Ultimately, the allocation shown in Fig. 78 has been performed to match functions and products at subsystem level.

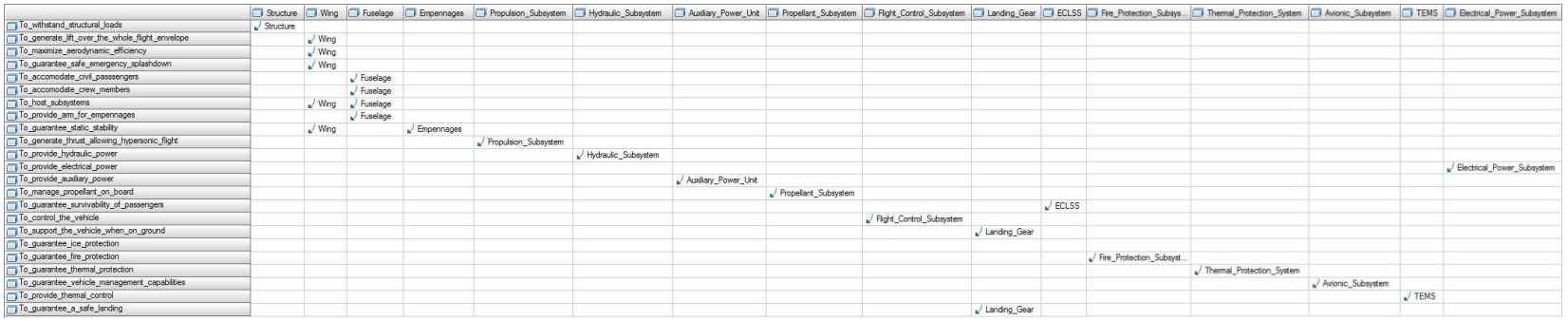

Fig. 78: Matrix view of the allocation of functions on products at subsystem level

4.5.2.4 Derive conceptual functional requirements

Once that the trees are established, it is possible to derive functional requirements associated to current functional breakdown. In general, the subject of the requirements can be indicated only after the conclusion of the allocation process (requirements can be associated to a product only when the functions are allocated). Requirements list are shown in their final version within the tables of Section 8.1.4. The traceability process from functions to products for what concerns requirements dependencies is guarantee by the SEE as already shown previously. Matrix views can be generated to show relations between requirements and functions (trace). These links are dedicated dependencies with specific stereotypes, as for allocation. The matrix view is shown in Fig. 79, being quite simple at this stage of the analysis.

Fig. 79: Matrix view of the requirements derivation from functions (trace)

Functional requirements for system level can be derived similarly to what already described at segment level. The functional requirements at system level are shown in Section 8.1.4. Requirements have been connected to functions and products through trace and satisfaction links respectively (Fig. 80 and Fig. 82).

Fig. 80: Matrix view of the requirements derivation from functions at system level

Functional requirements can be derived from previous considerations at subsystem level (Section 8.1.4). Related matrix view for functions trace is difficult to be shown within the document due to their size. Trace links have been in any case instantiated as already done for other levels. This approach towards traceability within the SEE aims at relating the requirements contained within the database with other model elements and, especially, with the functional breakdown of the system. This can be referred to as external traceability, since links are established outside the specification. In parallel, an additional traceability level can be defined within the specification itself, highlighting the aspect of requirements inter-derivation or influence, usually referred to as internal traceability. In general, it is true that the requirements are derived from analysis of

different aspects, such as the functional ones, thus being justified by model elements. However, a helpful way to evaluate whether the specification is actually considering the whole set of topics for a determined study consists in running the derivation check internally to the specification, creating proper matrices within the requirements database to associate one-another the different statements. It is thus easy to verify if a requirement has no low-level statements associated with it, identifying blank spots of the analysis. This approach can also be followed to simply couple requirements for other reasons, such as similarity of topics and data as well as for refinement. It is a very powerful tool for requirements engineering and brainstorming in high-level analyses (Brusa, et al., 2018).

4.5.2.5 Associate conceptual functional requirements to products

Once that allocation process is completed, requirements can be associated to product similarly to what already done with functional blocks. Matrix views can be generated to show relations between requirements and products (satisfaction). These views are shown in Fig. 81 and in Fig. 82 for segment and system levels respectively. Subsystem level view is difficult to show in the document because of its dimensions, even if the same approach has been applied within the SEE.

	FR_SegL1	FR_SegL2
Ground_Segment	FR_SegL1	
Flight_Segment		FR_SegL2

Fig. 81: Matrix view of the requirements association to products (satisfaction)

	FR_SysL1	FR_SysL2	FR_SysL3
Airport	FR_SysL1		
Ground_Station		FR_SysL2	
Vehicle			FR_SysL3

Fig. 82: Matrix view of requirements association to products at system level

4.5.2.6 Define conceptual product breakdown

The product tree associated to the highest level of functional breakdown is reported in Fig. 83. Product trees are represented similarly to what already done for functional trees, exploiting BDD. In this case, the directed composition links are enriched with multiplicity properties, to highlight the number of elements with same characteristics present within the breakdown. In this way it is possible to

better express interfaces, as described in Section 4.5.3. Multiplicity is a property of directed composition associations in SysML.

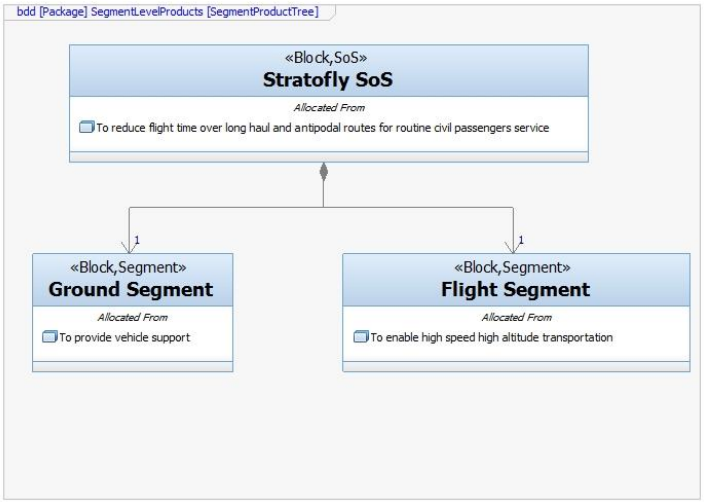

Fig. 83: Product tree (BDD) up to segment level

Product breakdown is detailed in the same way of functional one, thus the product tree at system level can be represented as in Fig. 84.

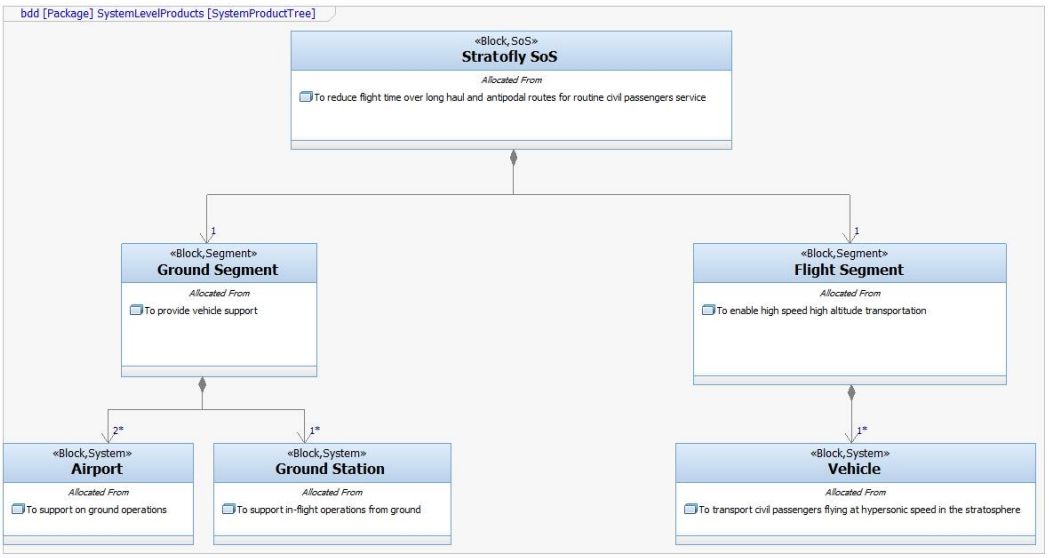

Fig. 84: Product tree (BDD) up to system level

It is interesting to discuss the role of Flight Segment and Vehicle, respectively father and child blocks. A functional or product tree is usually built defining more

than one child block for each father block, every time a new level is defined. This is generally done because, otherwise (i.e. if a father block had only one child), father and child block would actually represent the same element. However, the case represented in Fig. 84, is conceived to consider also multiple stages configuration for the modelled service. In case of STRATOFLY, it is thus true that the vehicle coincides with the flight segment, but this may be not applicable for other types of transportation system architectures. It is also interesting to note the role of multiplicity within the diagram. The number reported close to the composition arrow indicates the number of possible instances of the same block. For example, at least two, or more, airports (2*) shall be taken into account for a typical point-to-point mission. At the same way, since the diagram was conceived to include also multiple stages configurations, one or more (1*) vehicles may constitute the flight segment related systems.

Once system level is defined, it is possible to develop the product tree at subsystem level, which actually reflects the functional tree provided in Section 4.5.2.2. It shall be noticed that, as high level objective of the overall project, STRATOFLY is aimed at detailing the design of LAPCAT MR2.4 vehicle (Langener, et al., 2014). The architecture of subsystems thus reflects also this aspect. For clarity, product tree is shown starting from vehicle block only in Fig. 85.

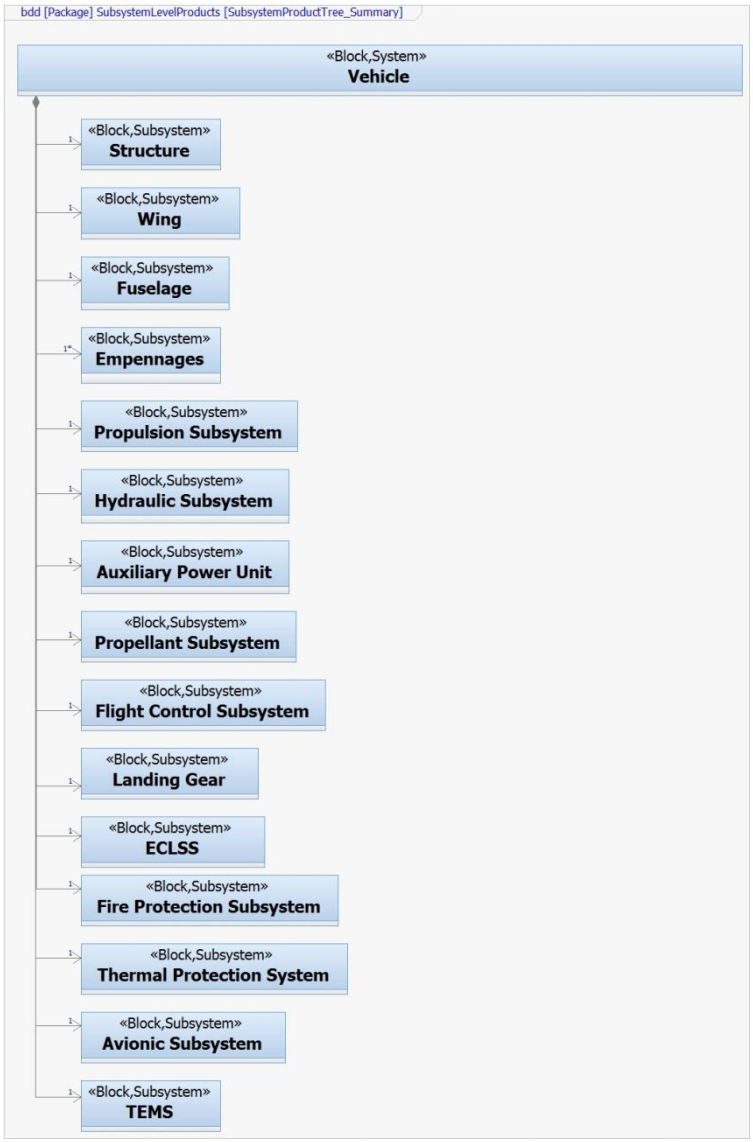

Fig. 85: Product tree (BDD) at subsystem level

4.5.2.7 Define mission concept

A crucial step for the definition of high-level logical and mission architecture of a HST system is the identification of the reference mission concept. This is *"a broad statement of how the mission will work in practice consisting of four main elements: data delivery, communications architecture, tasking, scheduling and control, mission timeline"* (Wertz & Larson, 2005). The first two elements are mainly associated to data generation management and collection as well as to

communication architecture inside the system. The third and fourth elements are instead more focused on system modes and on mission phasing. Starting from the vehicle configuration derived in functional analysis, it is possible to exploit MBSE approach and SysML language to integrate mission concept analysis within the Logical Development Environment (LDE) guaranteeing traceability. The proposed approach is based on the definition of a high-level mission architecture, which starts from the mission requirements derived during mission statement analysis (Section 4.5.1). This method aims at identifying and characterizing the main phases and the main modes of operations of the system, where the capabilities defined within functional analysis are used in a determined functional flow. This task of the conceptual analysis process is a fundamental phase of the design, since it allows connecting functional and physical aspects, enriching the system specification and setting the bases for the definition of the performance required for the system while in operation. It is thus a mandatory task for future matching and feasibility analyses (Sections 4.5.4 and 4.5.5).

Considering the semantics of the LDE, the high-level mission definition can start from the analysis of product lifecycle, where mission and, in general, operations constitute the most important phase. Lifecycle can be represented as an additional UCD, where use cases represent the main phases starting from conceptual design up to disposal. In this way, it is possible to link the highest level of the lifecycle with the stakeholders defined in Section 4.5.1, preparing at the same time the basis for a deeper characterization of operational behaviour of the system. Fig. 86 shows the UCD representing product lifecycle at high-level for STRATOFLY MR3. In the context of mission concept definition, the operation use case is detailed to identify phases in line with the hierarchical levels of the breakdown for products. This means that the mission is detailed more and more in details, starting from top and segment levels, up to lower levels. A very important point within this process consists in moving the attention onto the HST system itself, while entering the operation use case. In fact, the mission is fully within the boundaries of the system, thus the interfaces and the data network, derived from the analysis, shall be instantiated among system elements, rather than considering external actors as the high-level context of Fig. 86 still shows.

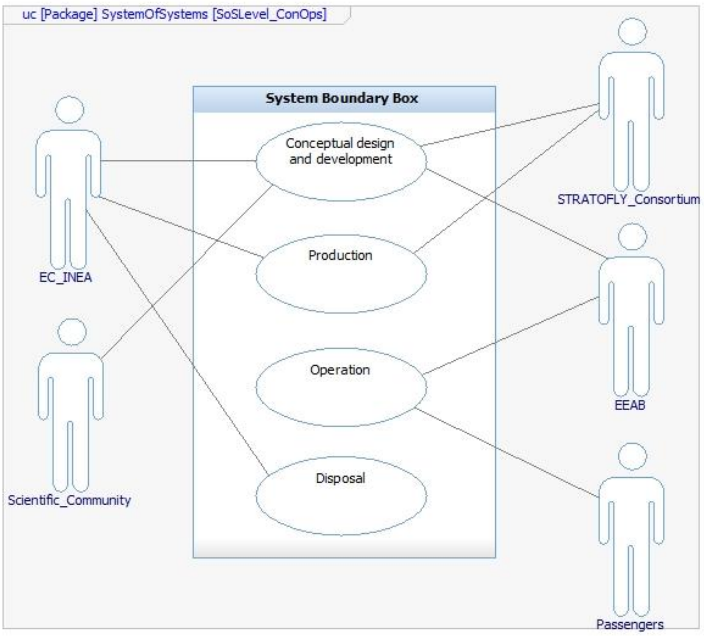

Fig. 86: High-level lifecycle representation for STRATOFLY MR3

As evidence of this process, the segment level mission concept is depicted in Fig. 87.

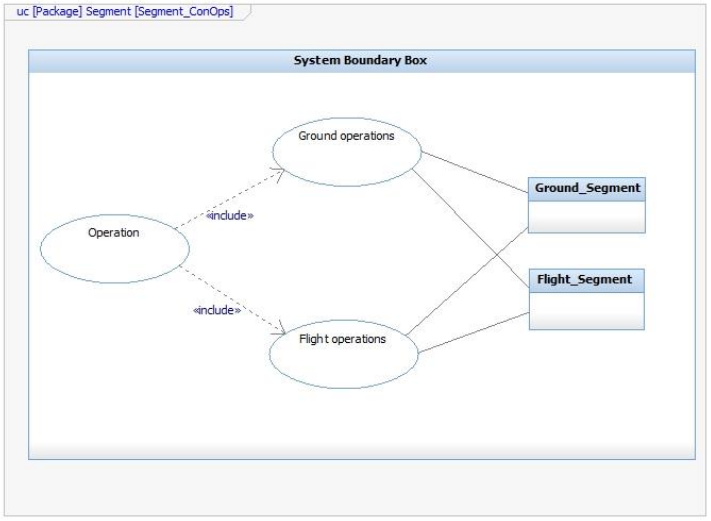

Fig. 87: Segment level mission concept

Operation phase is here characterized by a ground and a flight phase, where both ground and flight segment are involved. Particularly, the two phases benefit from

the capabilities described within the functional breakdown at segment level, allocated, in turn, on the aforementioned products. Particularly, in order to understand the relationships between the different functions within a determined phase, Functional Flow Block Diagrams (FFBD) can be implemented exploiting a dedicated format of Activity Diagram (AD). Notably, top level FFBD is shown in Fig. 88, where the instances executed in parallel recall the segment level functions defined within the breakdown (Fig. 73). From the diagram it is possible to see that the two functions are performed together during operation.

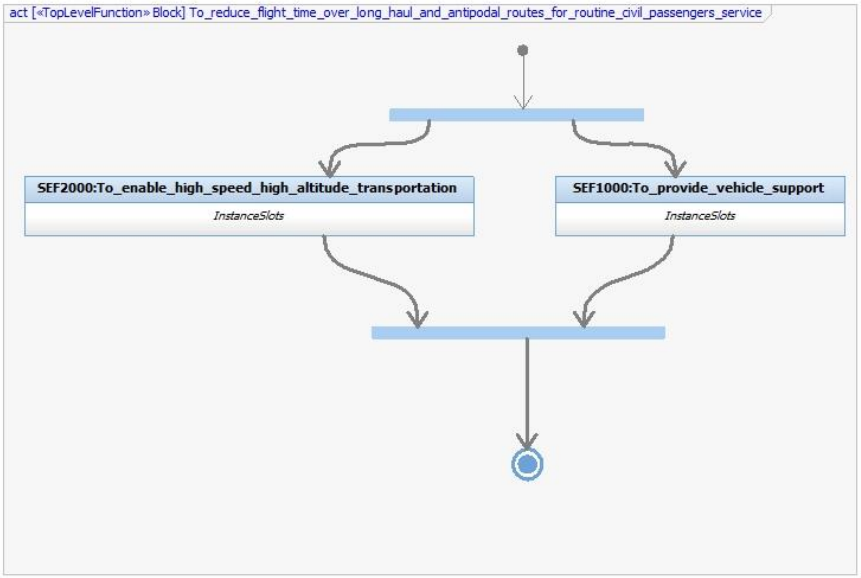

Fig. 88: Example of high-level FFBD for MR3 mission

The analysis acquires more relevance while moving to lower levels of details, as it happens for system level mission concept definition. Firstly, the different mission phases are derived from the low-level UCD (Fig. 89), where corresponding products of the breakdown are related to the different use cases (the vehicle is associated to all the use cases so it is neglected in Fig. 89 for picture clarity). FFBD associated to ground operation is shown in Fig. 90, where the functions derived at system level are shown. The FFBD related to flight operation is quite simple since the majority of functions associated to the vehicle are performed in parallel during the mission. The diagram is thus omitted for conciseness.

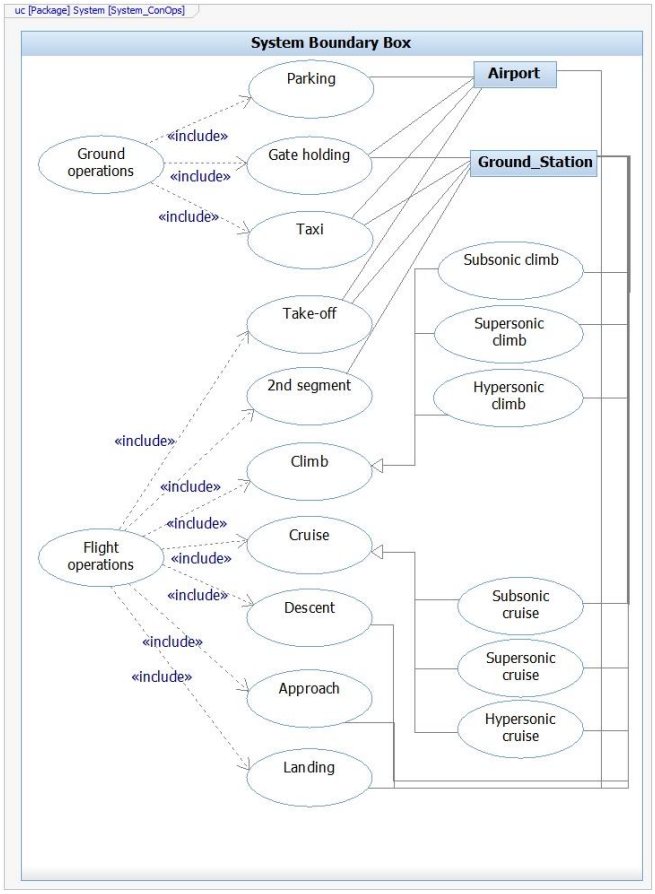

Fig. 89: System level mission concept

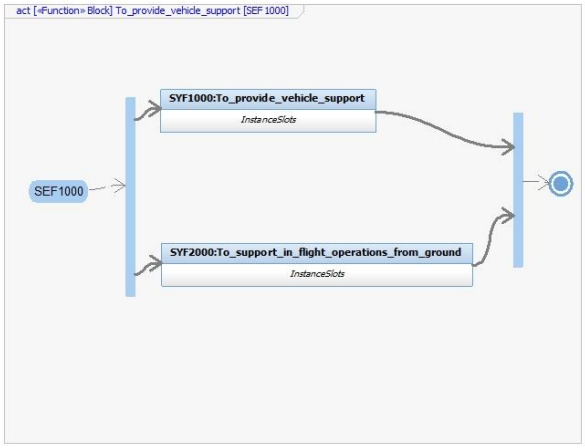

Fig. 90: Example of the FFBD related to ground operation for MR3 mission at system level

At this point, the phases can be characterized in terms of sequence of tasks to be performed, and of system states in which they are included. This is the direct representation of tasking and timeline in a single environment. The timeline can be represented exploiting the Sequence Diagram (SD), where the main products responsible to accomplish the tasks are shown, together with the vehicle operating in different phases (Fig. 91). For the sake of clarity, only nominal scenarios are reported.

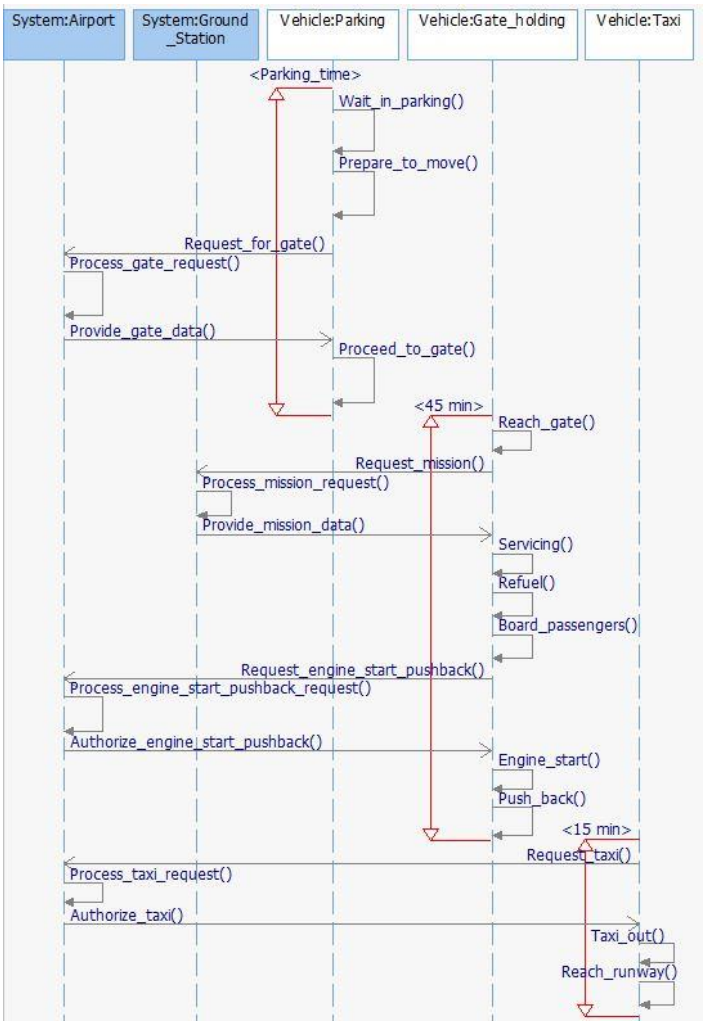

Fig. 91: Ground operations timeline (nominal scenario)

In this case, airport and ground station infrastructures are communicating with the vehicle in different phases to accomplish a set of tasks. Tasks are grouped vertically through time intervals (red) identifying possible duration for the

different phases. Phases are implemented through vertical lines. As it can be seen, the sketch of mission operations is, at this level, very qualitative, since it is conceived to provide a very preliminary information about phases, conceptual communication network and timing. On the other hand, a preliminary identification of system states in which the tasks are performed is necessary for further studies related to control allocation (autonomy). A State Machine Diagram (SMD) summarizing the data shown in the SD can be built as in Fig. 92.

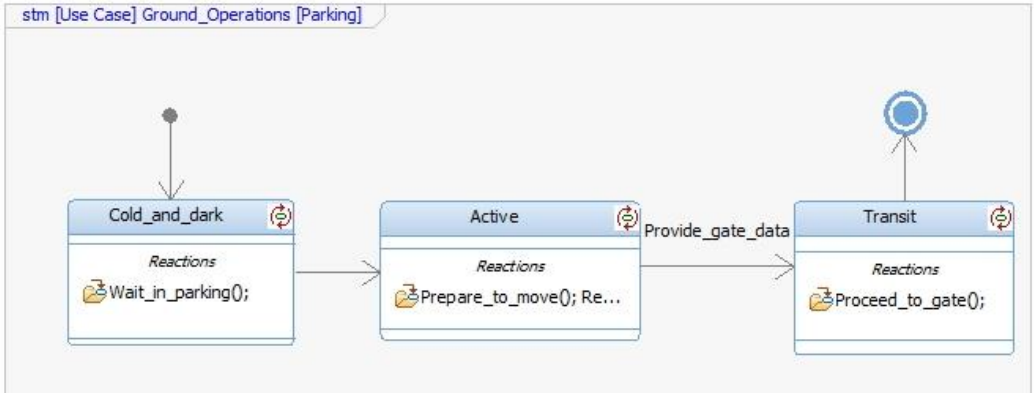

Fig. 92: Example of a SMD for system states identification (ground phases)

As it can be seen, the vehicle moves from a “cold and dark” state, where nothing is operational, to an active state, where it is prepared to start moving and where it requests authorization to proceed to the gate. As soon as gate data are provided (by airport infrastructure, as shown in Fig. 91), the vehicle is allowed to proceed to the gate, entering within the transit state. Again, this is a preliminary representation of the mission concept data, but it is sufficient to sketch a high-level architecture. Flight phases can be described in similar way to what already done for ground phases, as in Fig. 93.

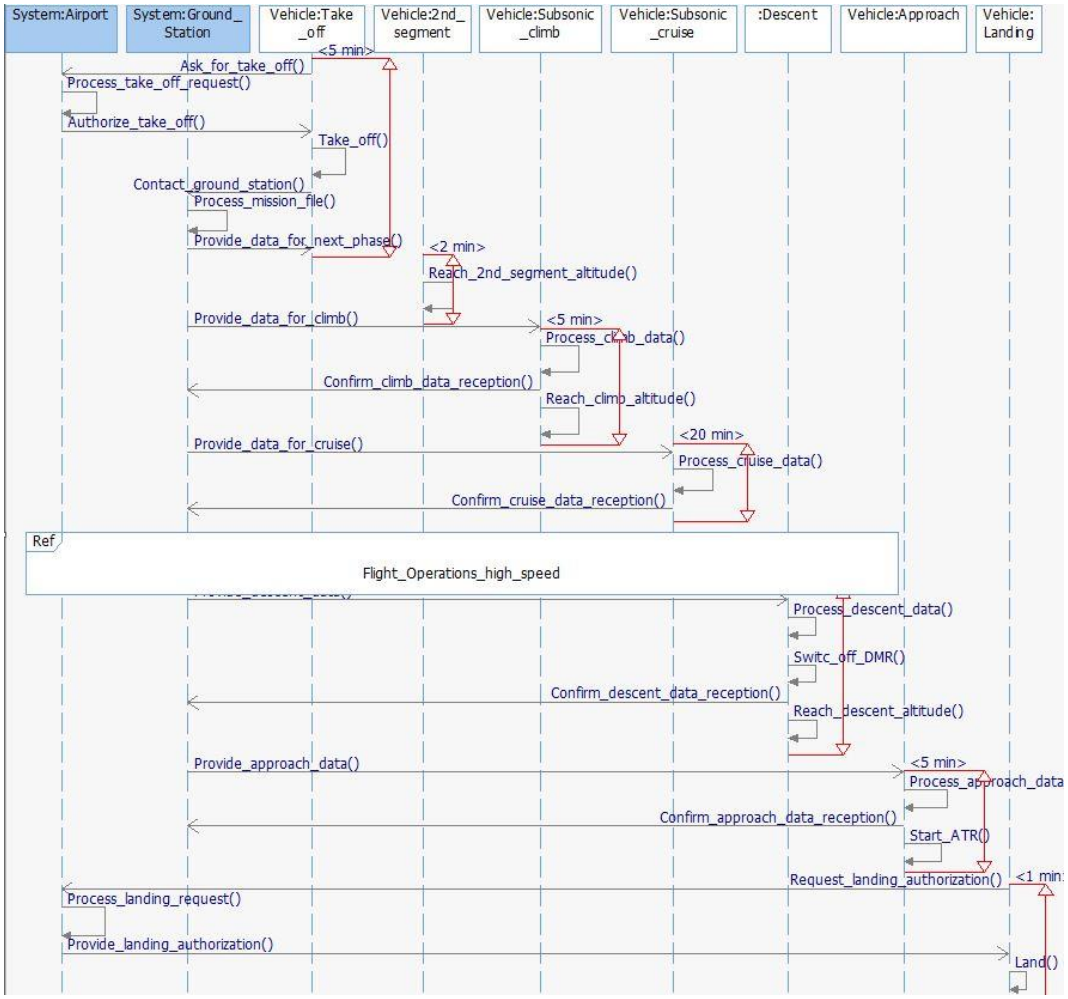

Fig. 93: Flight operations timeline (nominal scenario)

High-speed phases have been summarized within a referenced element, whose content is shown in Fig. 94. In general, each phase includes a communication with the ground station where authorization to move to next phase is provided together with required data. Several main activities of the phases can be also seen, such as the take-off and landing manoeuvres as well as engine ignition and switch-off.

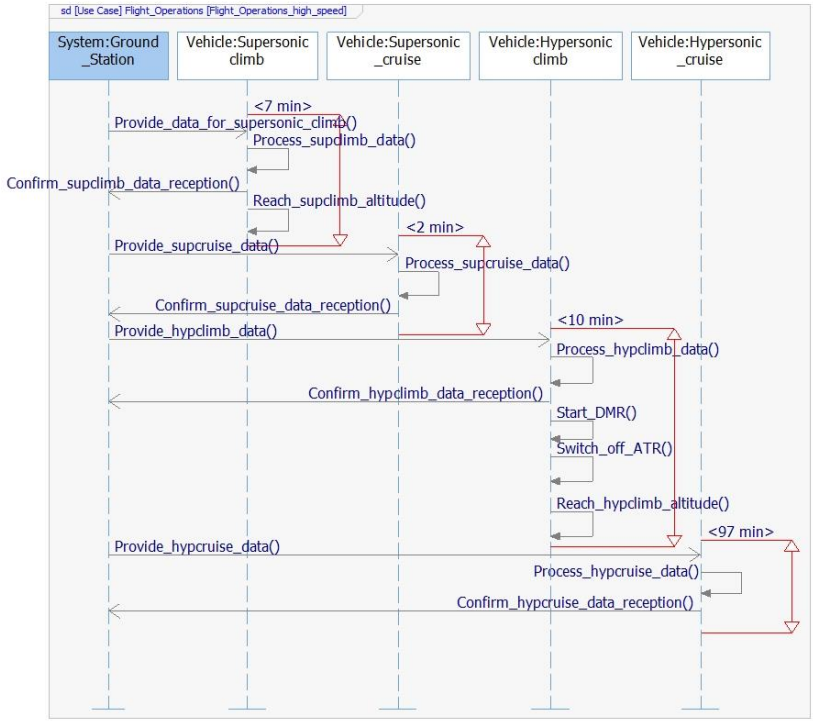

Fig. 94: Flight operations timeline (nominal scenario), detail of high-speed phases

Also in this case, a preliminary modes of operation analysis can be performed through a dedicated SMD (Fig. 95).

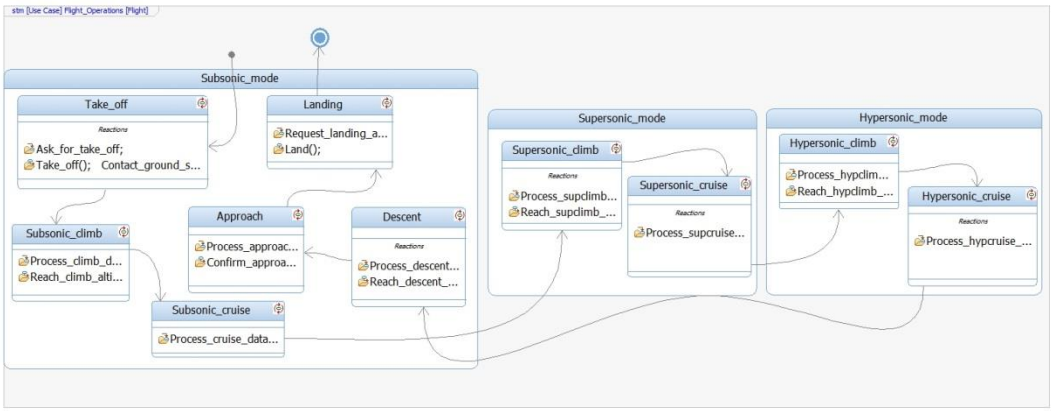

Fig. 95: Example of a SMD for system states identification (flight phases)

Three main states can be identified, depending on the flight regime. Moreover, the vehicle is characterized by several sub-states depending on the specific flight phase. The structure follows the timing analysis performed within the related SD.

The approach here briefly summarized for the higher levels of the breakdown is applied throughout the hierarchy of the HST system to characterize the mission, the states and the tasks that the different elements shall perform. Several requirements are obtained (Section 8.1.5) and traceability is implemented by linking the different objects together. Particularly, phases are associated to the functions used, which are furthermore characterized by the sub-level tasks described within the SD. Products, on which functions are allocated, are also responsible to perform the tasks within a specific sequence of events (timeline). Requirements are finally collected within the LDE and reported in the RDB for enhanced accessibility. The data included within the mission concept analysis are used to characterize not only the operational requirements themselves, but also to enrich the specification with updated mission and performance requirements. Moreover, the set of data related to mission phases is used to initialize matching and feasibility studies (Sections 4.5.4 and 4.5.5) to physically characterize the vehicle and to evaluate its effectiveness in operation.

4.5.2.8 Derive mission concept requirements

Following the mission concept analysis, many requirements can be derived for what concerns mission phases, timing and system modes of operation. Following the structure of the analysis described above, requirements can be organized hierarchically and allocated on products defined within functional assessment. Information concerning the mission are crucial for subsequent studies, like matching and feasibility analyses (Sections 4.5.4 and 4.5.5), since, for example, flight altitude, speed and time can be used to physically characterize the phases. An example of the most important requirements derived within the mission concept analysis is provided in Section 8.1.5. Mission concept requirements, together with functional and configuration requirement, previously specified, lead to the definition of proper performance requirements, as described in Section 4.5.2.9.

4.5.2.9 Define conceptual performance requirements

Complementary, performance requirements are used to specify physical characteristics of the HST system, detailing information implicitly or explicitly included within the functional specification. They provide a mean to quantify different aspects of the vehicle, making them verifiable in subsequent phases of the design. Section 8.1.6 includes the high-level performance requirements,

derived directly from mission and/or functional statements, reporting the identifier of the object which has contributed to the generation of the requirements themselves. Please notice that the current version of the specification reported in Section 8.1.6 includes results coming from the matching analysis, discussed in Section 4.5.4. Subsystems level is instead explored within Chapter 5 for what concerns performance. Particularly, it has to be noticed that, many requirements, such as those related to range, payload, flight time as well as, in general, high level data on mission-related performance, are coming from the need of refining LAPCAT MR2.4 configuration (Section 4.5.1), being the reference starting point. Most of these requirements are verified when looking at matching and feasibility analyses according to the validation process of STRATOFLY MR3 and are included in configuration requirements (Section 8.1.3).

4.5.3 Interface Analysis

4.5.3.1 Interface Analysis workflow

Interface analysis is strongly coupled to functional analysis since, together with functional breakdown, it aims at finalizing the logical architecture of the system by defining the internal interface network. It is mainly focused on products, since it defines logical interfaces, specifying types and direction of the links, associating different model elements. Notably, it focuses on the several levels of the breakdown, to produce views of internal context of the blocks defined within functional analysis, studying the internal arrangement of parts within a specific block. This is a direct consequence of the use of a model-based approach exploiting a dedicated semantics to specify hierarchy (Section 4.5.2.6). In fact, the directed composition used to relate blocks within the BDD is a very powerful tool to identify the context in which instantiate the interfaces at different levels. Particularly, the first task consists in defining the context in which implement the interfaces, by means of Internal Block Diagrams (IBD).

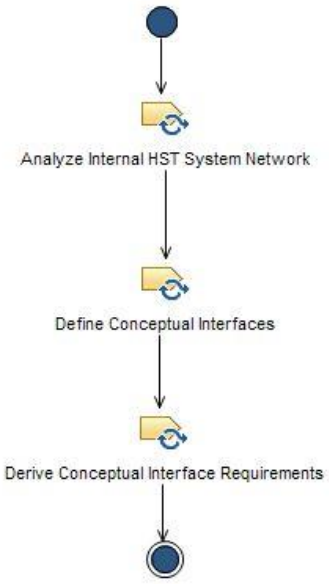

Fig. 96: Interface analysis workflow

Subsequently, interfaces are characterized and associated requirements, specifying the type and the direction of the interface, are generated. The process (Fig. 96) is fairly simple, since it is performed jointly to functional analysis, level by level. Of course, even if not shown within Fig. 96, iterations may be necessary to modify the interfaces depending on design needs. The process is completed when all interfaces are characterized for each level, and associated requirements are derived.

4.5.3.2 Analyse internal HST system network

In this task, IBD are created for each hierarchical level of product breakdown to identify the context of the interface analysis. Moreover, general interfaces are identified on the elements of the diagram (parts), even if without specifying a type or a direction. It is simply decided whether two or more system elements shall have (or require) an interface. SysML semantic is quite powerful within this scope, since it is based on parts concept. The part is an instantiation of a block within a specific context. Moreover, since the BDD were defined using compositions, the part is also hierarchically at lower level with respect to the context itself (it is actually contained in it). The boundaries of the context (and of the diagram) represent the limits of the block in which the designer is looking. This means that a low-level block is actually a part of a wider context, at higher

level, such as a subsystem is a part of a system. Interfaces are instead defined through directional flow-ports (Object Management Group - OMG, 2018). The aim of this task is to catch this kind of network, instantiating embryonal interfaces where needed. In order to provide an example of this approach, a simple IBD at segment level is shown in Fig. 97. In fact, all diagrams are detailed within the following section and are here neglected for conciseness. Fig. 97 shows that, within the HST system, a ground segment and a flight segment exist and shall be interfaced. At the moment, a single interface is shown (since the number of connections and type are not available yet). However, it is necessary for them to be interfaced to make the system operational. The direction of the link is, at the same way, very general (bi-directional) since this information is not yet available. This representation is typical for all levels and interfaces, being performed consistently for other elements within the SEE prior to move to next task (characterization), described in Section 4.5.3.3.

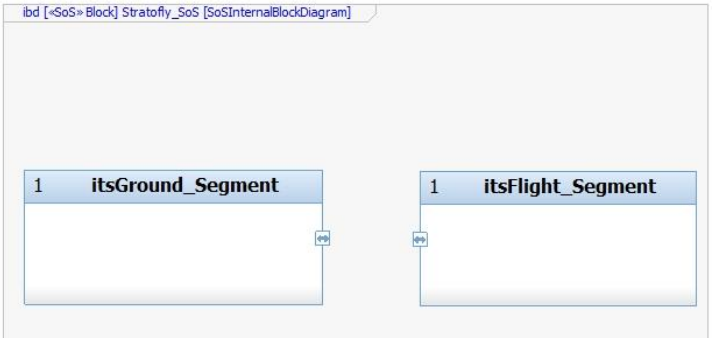

Fig. 97: Internal network of STRATOFLY HST system with provisional interfaces

4.5.3.3 Define conceptual interfaces

Once that the internal system network has been hypothesized, it is possible to analyse the interfaces among different products belonging to the same level, starting from segment level. In fact, the top level block (i.e. the STRATOFLY HST system) is not actually part of an IBD, being the highest hierarchical instance of the product tree. Actually, top level block is the context itself of segment level interface analysis, since the IBD representing segment parts show the context within the top level environment. At the same way, segment level blocks will be the context of system level interface analysis and so on. The fully characterized IBD for segment level interfaces (evolution of the one reported in Fig. 97) is shown in Fig. 98. As it can be seen, three kinds of interfaces are now instantiated,

and, notably, a bi-directional data interface (green), a one directional electrical interface (yellow) and a bi-directional fluidic (propellant) interface (blue), between ground and flight segment. Data interface is required for mission planning and handling on ground, requiring flight and ground segment to communicate in both ways. Electrical interface is present to guarantee the possibility of providing power to the flight segment when on ground, but this is only provided from ground segment and cannot be instantiated backwards. Ultimately, propellant interface is required for fuelling and de-fuelling operations, being defined as bi-directional.

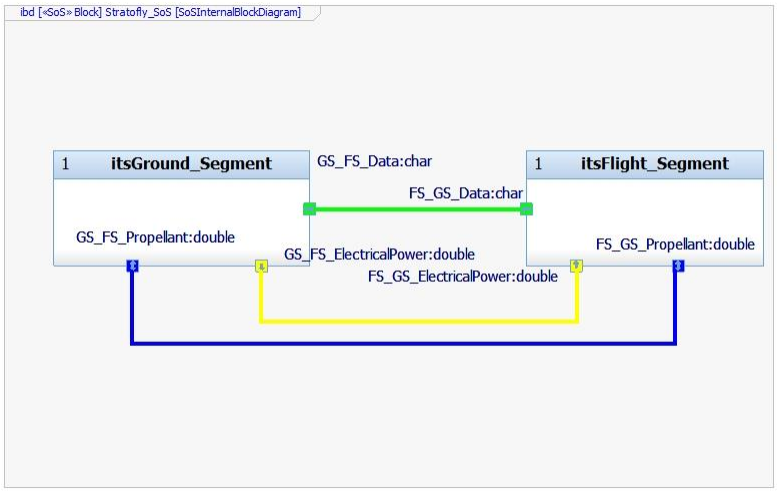

Fig. 98: Segment level interfaces diagram (IBD)

Subsequent level focuses on ground and flight segment respectively for the selected configuration of HST system (single-stage), as explained in Section 4.5.2.6. Ground segment interfaces are shown in Fig. 99.

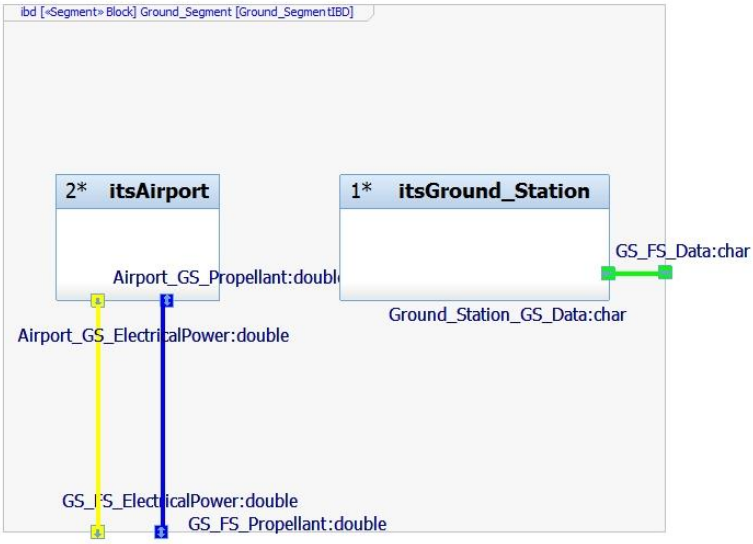

Fig. 99: Interfaces definition for ground segment related systems

As it can be seen, the ground segment is now populated with its low-level systems (i.e. the airport and the ground station system). They are, generally, represented as separated instances, even if they can be embedded in a single infrastructure eventually. Particularly, the airport is responsible for logistic support, including electrical and propellant interfaces with same directions specified at segment level. The ground station is instead only responsible for data, as previously specified. In fact, the function of the airport is to provide handling services to the flight segment, while, even if conventional airports provide also mission planning and data interfaces, this service is peculiar of a ground station profile. It is thus possible to say that, a typical airport infrastructure includes both systems, with different roles (they actually do not have a direct interface between each other). Information about block multiplicity, reported in the product tree, is here still visible on parts label, as it can also be seen within the IBD for flight segment specification (Fig. 100). In this case, a single part, representing the vehicle is present, including the interfaces previously defined.

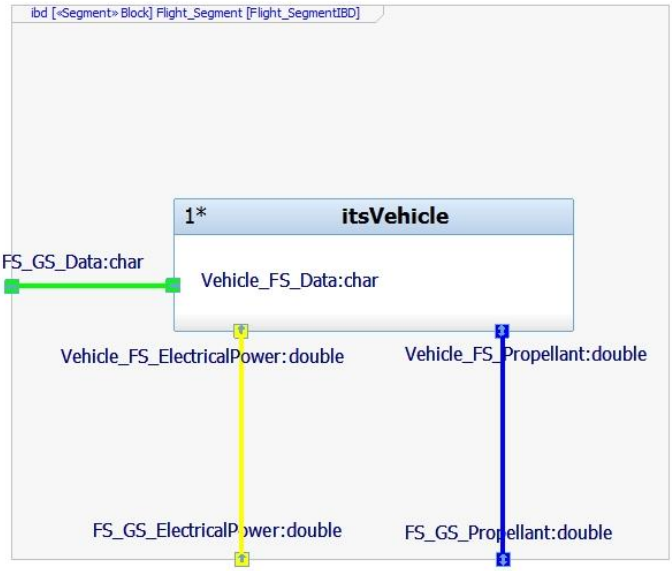

Fig. 100: Interfaces definition for flight segment related system

The internal network for the vehicle, i.e. the MR3 aircraft, it is instead way more complex, since the different subsystems are defined and many interfaces can be identified. A single diagram is thus not the most convenient way of representing the whole set of interfaces, as it can be seen in Fig. 101.

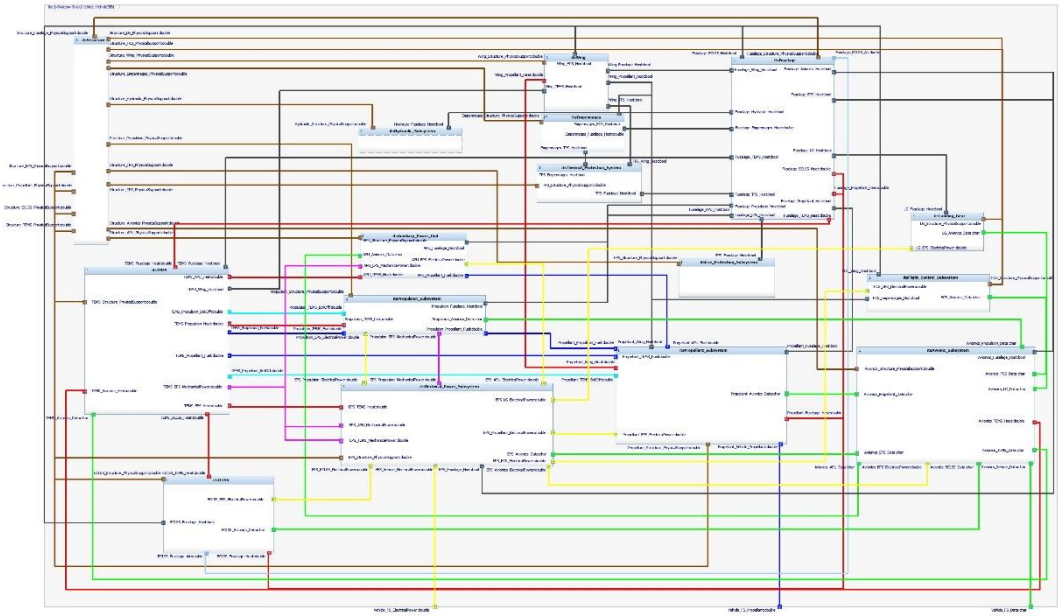

Fig. 101: Derivation of interfaces at subsystems level through IBD

It is thus worth analysing the different kinds of interfaces instantiated in the main diagram looking at simplified IBD. Fig. 102 shows the structural interfaces. Basically, the main vehicle structure supports all other subsystems.

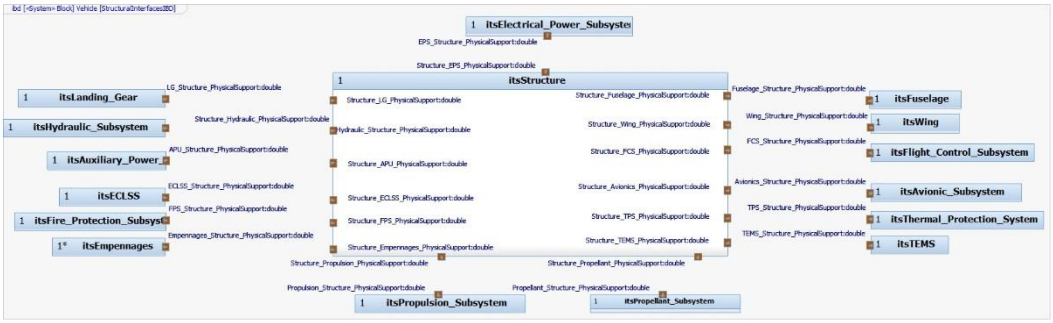

Fig. 102: Structural interfaces at subsystem level

Fig. 103 shows the interfaces associated to actual hosting of the different elements on board.

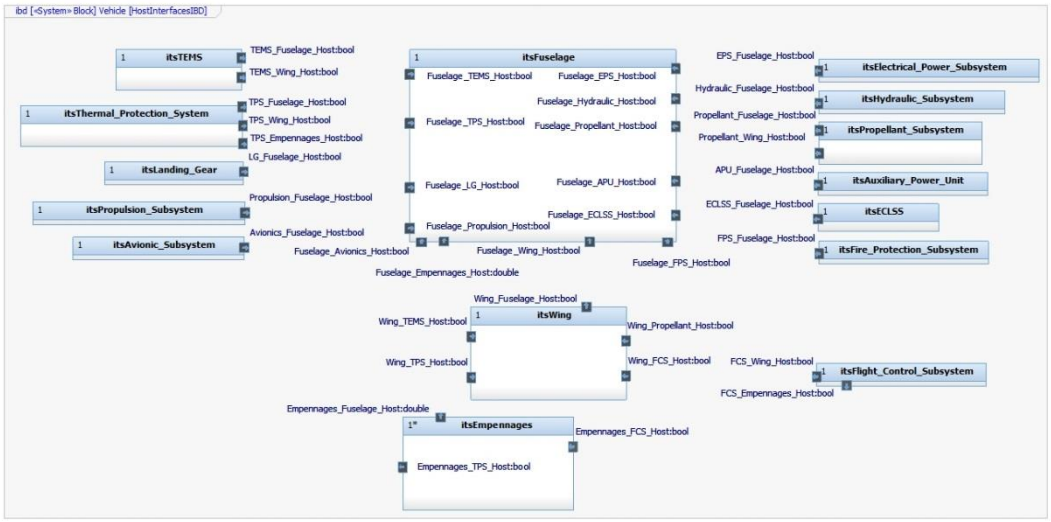

Fig. 103: Host interfaces at subsystem level

The majority of the subsystems are hosted within the fuselage of the vehicle, even if some of them, like TPS and FCS, are allocated on wing and empennages also because of their function. Data interfaces are shown in Fig. 104.

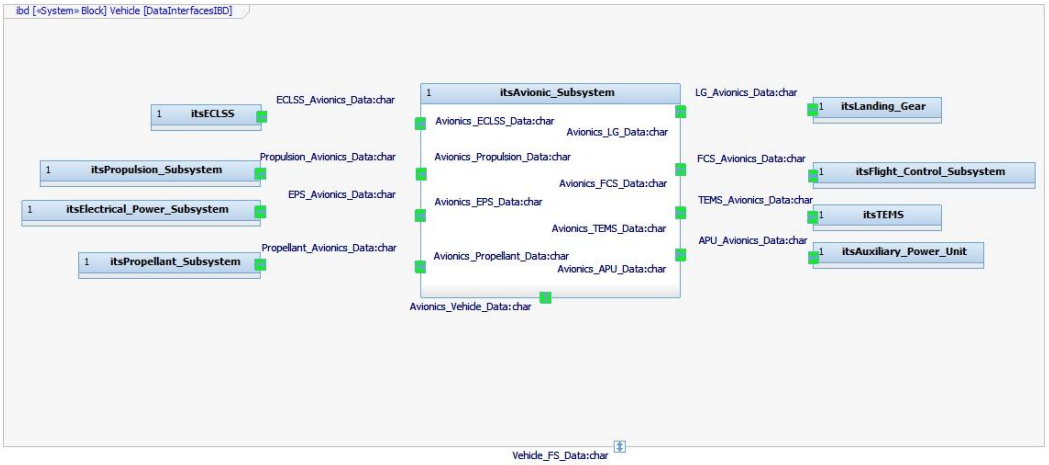

Fig. 104: Data interfaces at subsystem level

The avionic subsystem is the main responsible to send and receive data to the main subsystems on-board the vehicle. Connection has been hypothesized as bi-directional in all cases. Electrical interfaces are shown in Fig. 105.

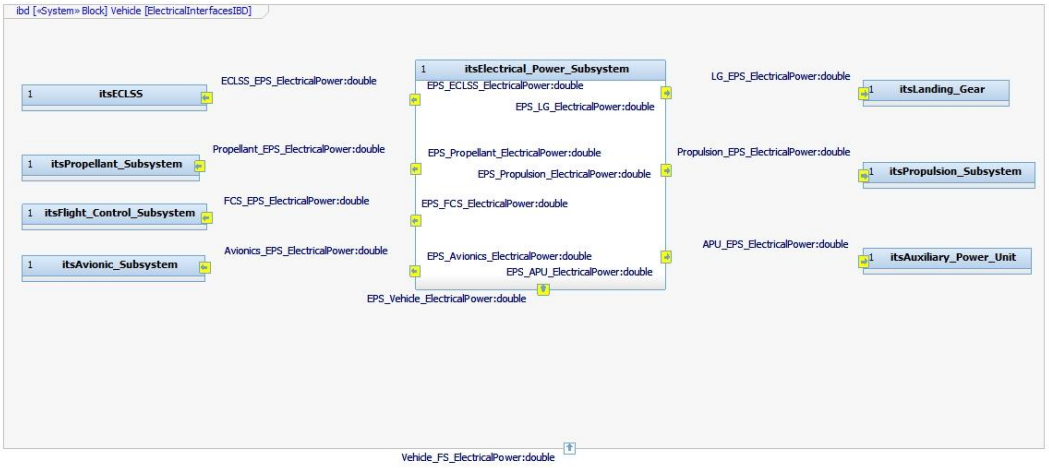

Fig. 105: Electrical interfaces at subsystem level

The Electrical Power System (EPS) provides power to the main subsystems through its equipment which are allocated on engines and TEMS. These items, even if physically located on federated areas are considered to be part of the EPS. Mechanical interfaces are shown in Fig. 106.

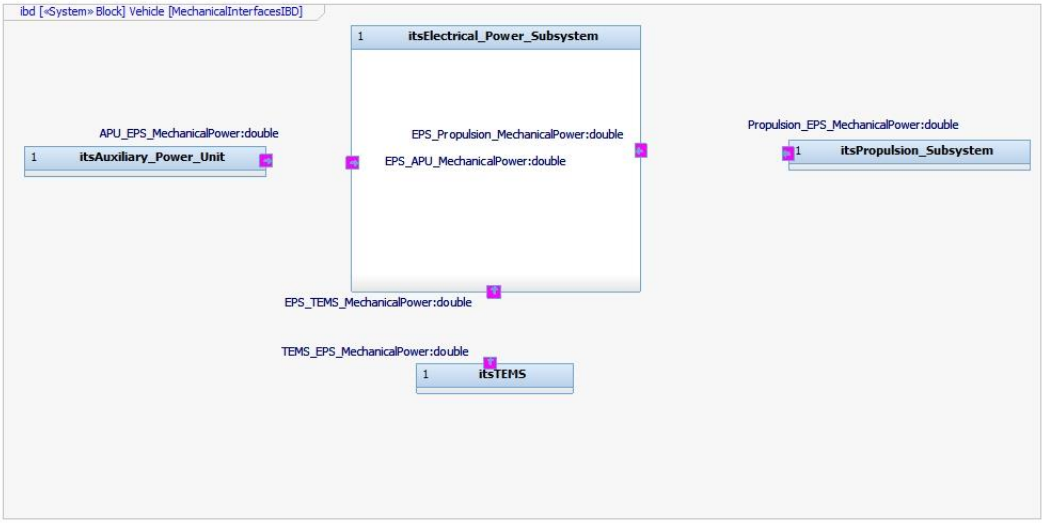

Fig. 106: Mechanical interfaces at subsystem level

These interfaces are mainly associated to the transmission of mechanical power. In this case, the main sources for mechanical power has been identified within APU, propulsion plant and TEMS. They would be responsible to provide mechanical power to EPS equipment for the generation of electrical power. Thermal interfaces are shown in Fig. 107.

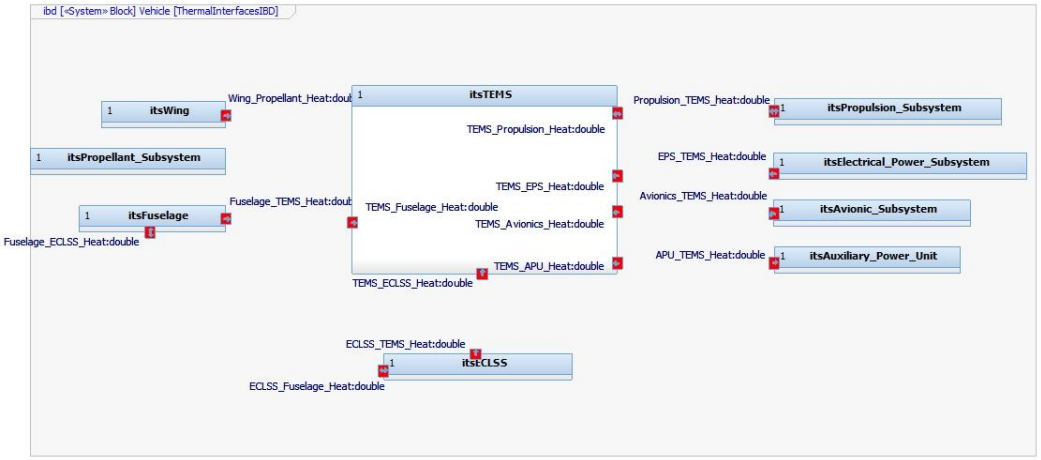

Fig. 107: Thermal interfaces at subsystem level

The TEMS is responsible to receive, transport and reject the heat coming from different sources. It is thus the main hub receiving heat flow from the other subsystems. Propellant interfaces are shown in Fig. 108.

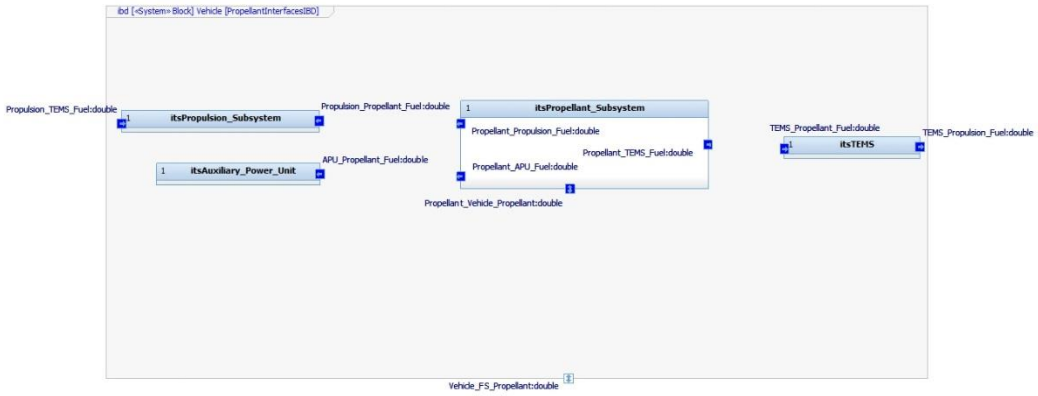

Fig. 108: Propellant interfaces at subsystem level

Propellant subsystem is responsible to provide LH2 to propulsion plant, APU and TEMS. Boil-off is managed by TEMS and rejected within propulsion plant as indicated within Fig. 109, where main gas (boil-off) interfaces are shown.

Fig. 109: Boil-off interfaces at subsystem level

Ultimately, another type of gas interfaces, related to airflow to be managed in cabin, can be defined as indicated in Fig. 110.

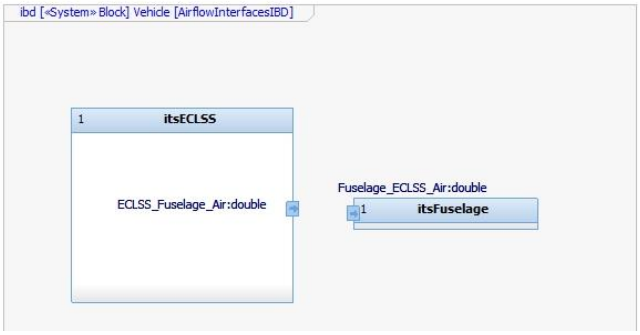

Fig. 110: Airflow interfaces at subsystem level

4.5.3.4 Define conceptual interface requirements

For each of the interfaces instantiated within the previous task, it is now possible to define one or more requirements depending on the number of the directions of the link (one-way, two ways). This is done for each level, consistently with functional analysis approach. Requirements shall specify the target and source of interface, its type and the direction of the link. Requirements are linked to interfaces (ports) via verification dependencies, so to create other matrix views to assess the complete coverage. Interface requirements at segment level are listed in Section 8.1.7 and the traceability view is provided in Fig. 111.

	IR_SegL1	IR_SegL2	IR_SegL3	IR_SegL4	IR_SegL5	IR_SegL6	IR_SegL7	IR_SegL8	IR_SegL9	IR_SegL10
GS_FS_Data	IR_SegL1			IR_SegL4						
GS_FS_ElectricalPower		IR_SegL2								
GS_FS_Propellant			IR_SegL3		IR_SegL5					
FS_GS_Data						IR_SegL6			IR_SegL9	
FS_GS_ElectricalPower							IR_SegL7			
FS_GS_Propellant								IR_SegL8		IR_SegL10

Fig. 111: Matrix view of interface requirements association at segment level

System level interface requirements can be derived similarly to what already described at segment level, as shown in Fig. 112.

Table 9: Interface requirements list at system level

	IR_SysL1	IR_SysL2	IR_SysL3	IR_SysL4	IR_SysL5	IR_SysL6	IR_SysL7	IR_SysL8	IR_SysL9	IR_SysL10
Airport_GS_ElectricalPower	IR_SysL1									
Airport_GS_Propellant		IR_SysL2	IR_SysL3							
Ground_Station_GS_Data				IR_SysL4	IR_SysL5					
Vehicle_FS_Data						IR_SysL6		IR_SysL8		
Vehicle_FS_ElectricalPower									IR_SysL9	
Vehicle_FS_Propellant							IR_SysL7			IR_SysL10

Fig. 112: Matrix view of interface requirements association at system level

Ultimately, subsystem level interface requirements are defined as in Section 8.1.7. Due to the number of relations, it is not possible to represent in the report the summary of links through matrix views for verification. The same approach used for segment and system level analyses has been adopted.

4.5.4 Vehicle matching analysis

4.5.4.1 Vehicle matching analysis workflow

The conceptual design process (Section 4.3) aims at sketching the general layout of the aircraft, providing preliminary mass breakdown as well as the indication of the aircraft general performance. The final goal of the conceptual design phase is the assessment of the feasibility of both the vehicle and the mission concept from the technical and operational standpoints. Many best practices and guidelines for aircraft conceptual design are available in literature (Roskam, 1985) (Jenkinson, et al., 1999) (Raymer, 1995), suggesting typical workflows to draft a vehicle configuration and to evaluate the impact of requirements on the vehicle architecture and performance. In these processes, special attention is devoted to the identification or development of tools able to depict the design space at a glance, meeting stakeholders' expectations with design feasibility criteria (Fusaro, et al., 2017). For high-speed vehicles, the proper definition of the basic performance (e.g. mass, thrust and lifting surface) is crucial for the selection of a plausible design point to be considered as the baseline for the next development phases. In the '80s NASA introduced a simple way to match the propulsion plant requirements with vehicle configuration within the so-called Matching Chart (Loftin, 1980). This is a graphical representation which relates Thrust-to-Weight ratio (T/W) to the Wing Loading (W/S) of the aircraft on a 2D chart (Fig. 113). This chart allows the identification of a feasible design space and the definition of a design point describing the optimal vehicle configuration in terms of Maximum Thrust, Maximum Take-Off Mass and Wing Surface, meeting all the high-level requirements.

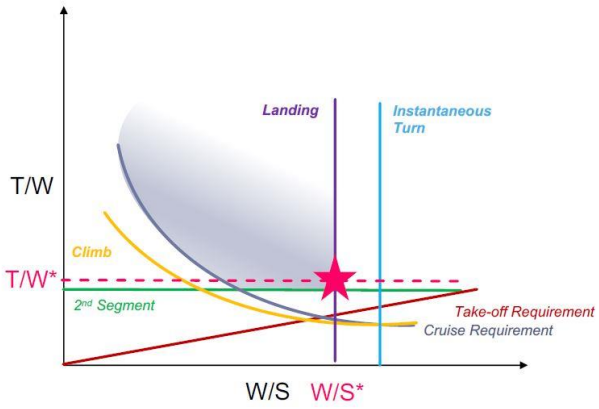

Fig. 113: Sketch of a typical Matching Chart

In the Matching Chart, the different curves are mathematical equations that express requirements for each mission phase in terms of T/W as function of the W/S. Practically speaking, the diagram identifies a spectrum of feasible solutions, in terms of required thrust, to counteracts the drag generated during the flight, with a direct correlation to the lift generation capability of the aircraft. The selection of this approach, which provides a global overview of aircraft performance as preliminary assessment, has been exploited, in the past, for a wide range of case studies, encompassing conventional and innovative configurations, as well. At this purpose, updates and upgrades of the tool have been suggested to cope with a wider number of mission concepts and vehicle configurations (Fioriti, 2014). Furthermore, in order to extend the applicability of the tool towards the more complex high-speed vehicle design, multi-dimensional or parametric analyses have been included into additional methodologies available in literature (Chudoba, et al., 2012) (Ingenito, et al., 2009).

The overall process (Fig. 114) is simply represented considering four main tasks. The characterization of mission phases is the first one, taking advantages from the phases definition within ConOps and using proper models to derive thrust-to-weight ratio requirements as function of wing loading for each part of the mission (physical characterization of the phases). Subsequently, the vehicle concept is characterized from the point of view of its high-level configuration (MTOW, wing area and general dimensions) and performance (especially for what concerns aerodynamic efficiency and propulsion plant). Within this task, a deep iterative approach is adopted to evaluate vehicle configuration, starting from assumptions and statistics, and to propose a sustainable concept from the point of

view of the consistency between MTOW and wing surface (Section 4.5.4.3), in the whole set of operating regimes.

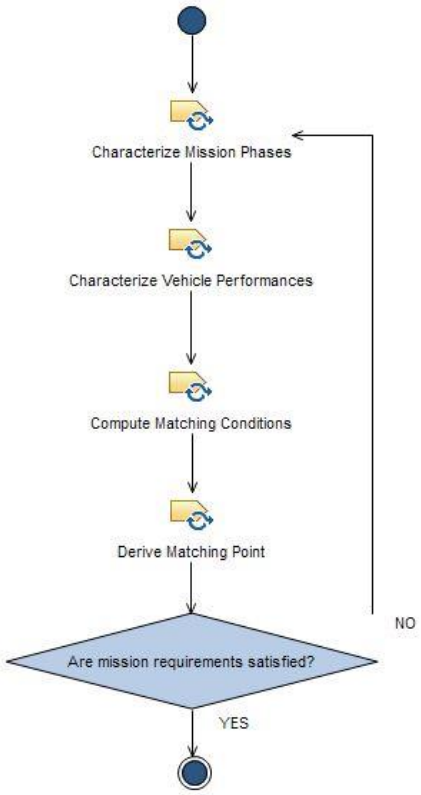

Fig. 114: Vehicle matching analysis workflow

A verification loop on performance and mission requirements is present to assess whether the result of the analysis is in line with the expectation or, on the contrary, whether the mission or the vehicle concept itself shall be modified accordingly. As soon as both environment and vehicle concepts are sufficiently characterized, it is possible to compute the matching conditions and, as consequence, to identify a proper design point in terms of wing loading and thrust-to-weight ratio for the different phases. The phase is concluded when a reference mission and a consistent vehicle configuration design point are identified.

4.5.4.2 Characterize mission phases

On the basis of the ConOps analysis (Section 4.5.2.7), it is possible to develop a mathematical model for the derivation of each of the curves of the chart. In general, three families of relationships can be defined in the Matching Charts:

- equations in which $^{T}/_{W} = f(^{W}/_{S})$, such as take-off, climb, cruise and sustained turn requirements;
- equations which are characterized by $^{T}/_{W} = const$, such as second segment requirement;
- equations which are characterized by $^{W}/_{S} = const$, such as landing and instantaneous turn requirements.

As a final remark, it is important to highlight that, for subsonic phases, sea-level density is always used as reference value for the normalization of the different requirements, whilst, for higher speed phases, different and more appropriate references shall be considered (Section 4.5.4.4).

Take-off distance requirement. The take-off phase is usually defined as the sequence of run, rotation or manoeuvre and climb segments which brings the aircraft from ground up to 35 ft (around 11 m) of altitude with reference to ground elevation. The overall horizontal distance travelled during the whole phase is known as take-off field length, while the distance required for the aircraft to leave the ground is called lift-off distance (corresponding basically to run segment). In general, Matching Chart requirements are usually referring to this specific parameter, even if usually addressed as take-off distance. To maintain consistency with literature, the same concept is here adopted. The simplified derivation of the lift-off distance requirements is proposed, making the hypothesis that the aerodynamic drag on ground can be neglected as well as the rolling friction between the wheels and the runway. The following constitutive equations are then applied: (2) defines the run to lift-off l_{LO}, (3) represents the equilibrium condition and (4) identifies the lift-off speed V_{LO}.

$$l_{LO} = \frac{V_{LO}^2}{2a_{LO}} \quad (2)$$

$$\frac{T_{LO}}{W_{LO}} = \frac{a_{LO}}{g} \quad (3)$$

$$V_{LO} = \sqrt{\frac{W_{LO_{kg}} g}{\frac{S C_{L_{LO}} \rho}{2}}} \quad (4)$$

Where:

a_{LO} is the acceleration at lift-off in $\left[\frac{m}{s^2}\right]$
g is the gravity acceleration in $\left[\frac{m}{s^2}\right]$
T_{LO} is the thrust generated by the propulsion plant at lift-off in $[N]$
W_{LO} is the aircraft weight at lift-off in $[N]$
$W_{LO_{kg}}$ is the aircraft mass at lift-off in $[kg]$
S is the wing surface of the aircraft in $[m^2]$
ρ is reference air density in $\left[\frac{kg}{m^3}\right]$
$C_{L_{LO}}$ is the lift coefficient at lift-off

By combining the constitutive equations, it is possible to express the lift-off distance, i.e. take-off run (5), in terms of Wing Loading and Thrust to Weight Ratio.

$$l_{LO} = \frac{W_{LO_{kg}}/S}{T_{LO}/W_{LO} \, C_{L_{LO}} \rho_0 \sigma} \quad (5)$$

Where:

$\sigma = \rho/\rho_0$ is the density ratio between reference air density and sea level density

Ultimately, the lift-off distance requirements can then be defined as in (6), simply re-arranging (5).

$$\left(\frac{T}{W}\right)_{LO} = \frac{W_{LO_{kg}}/S}{\rho_0 \sigma l_{LO} C_{L_{LO}}} \quad (6)$$

Second segment requirement. The second segment is the portion of flight path during take-off starting from gear-up altitude (after the 35 ft obstacle) and ending at 400 ft minimum. Applicable regulations for conventional aircraft (EASA, 2019) define the phase and provide some details regarding reference speed and climb gradient to be guaranteed in case of engine failure as follows:

- flight speed is constant and equal to V_2;
- minimum climb gradient G_{2nd} to be guaranteed in case of multiple engines configuration is equal to
  - 2.4% in case of two engines;
  - 2.7% in case of three engines;
  - 3.0% in case of four engines.

Since there is neither a specification for more than four engines, nor even suggestions for high speed transportation systems, the strictest requirement coming from (EASA, 2019) is adopted. The following constitutive equation (7) can be used:

$$\left(\frac{T}{W}\right)_{2nd} = \left(\frac{D}{W}\right)_{2nd} + G_{2nd} \qquad (7)$$

where

$\left(\frac{T}{W}\right)_{2nd}$ is the Thrust-to-Weight ratio in second segment

$\left(\frac{D}{W}\right)_{2nd}$ is Drag-to-Weight ratio in second segment

Considering that, as preliminary assumption, lift shall compensate the weight in all conditions and that the climb gradient G_{2nd} shall be guaranteed also in case of One Engine Inoperative (OEI) scenario, second segment requirement (8) can be derived starting from (7):

$$\left(\frac{T}{W}\right)_{2nd} = \frac{N_{engines}}{N_{engines} - 1}\left(\frac{1}{E_{2nd}} + G_{2nd}\right)\left(\frac{1}{\sigma}\right) \qquad (8)$$

where

E_{2nd} is the aerodynamic efficiency in second segment

As it can be seen from (8), this requirement is not a function of wing loading.

Subsonic climb requirement. The subsonic climb requirement can be simply derived following the traditional approach that consists in using the equation of the quadratic polar theory to define drag as in (9):

$$D = C_{D_0} + kC_L^2 \quad (9)$$

where

C_{D_0} is the drag coefficient at zero lift
C_L is the lift coefficient
$k = \frac{1}{\pi Ae}$ where A is the aspect ratio and e is the Oswald factor

Moreover, the contribution of the second term of (9), representing the induced drag, is usually neglected as preliminary assumption. Drag can then be computed as in (10)

$$D \approx q_\infty S C_{D_0} \quad (10)$$

where

q_∞ is the dynamic pressure of the incoming flow in $[Pa]$

For this specific flight regime, the computation of C_{D_0} is performed using subsonic drag component build up (Raymer, 2012), as specified in (11), neglecting the contribution of miscellaneous as well as leakages and protuberances drag

$$\left(C_{D_0}\right)_{subsonic} \approx \frac{\sum C_f F_F Q S_{wet}}{S_{ref}} \quad (11)$$

where

C_f is the skin-friction drag coefficient
F_F is the form factor of selected component (fuselage, wing, tail etc…) that estimates pressure losses due to viscous separation
Q is the interface factor for the selected component
S_{wet} and S_{ref} are the wetted surface for the selected component and the reference wing surface respectively expressed in $[m^2]$

In (11), the contributions for miscellaneous as well as leakages and protuberances drag, which are typically included in the build-up process, are neglected. Considering that the Thrust-to-Weight ratio can be expressed in a similar way with respect to (7), the subsonic climb requirement can be derived as in (12):

$$\left(\frac{T}{W}\right)_{subclimb} = \left(\frac{q_\infty C_{D_0}}{W_{kg}/_S g} + G_{subclimb}\right)\frac{1}{\pi\sigma} \quad (12)$$

where

$G_{subclimb}$ is the subsonic climb gradient
π is the throttle

This requirement is usually corrected using density ratio σ in order to be consistent with sea-level conditions. Moreover, throttle is used to evaluate the required Thrust-to-Weight ratio increase in case of flight at throttle level less than 100%, for fuel saving purposes.

Subsonic cruise requirement. The model for subsonic cruise is similar to the one proposed for the subsonic climb. However, in this case, the climb gradient is neglected since the aircraft shall maintain its altitude. Preliminary assumptions used in (9) and (11) still apply, even if additional details shall be included in order to take into account the type of cruise considered. In fact, even if for hypersonic vehicles the subsonic cruise is supposed to be just an intermediate phase in the mission profile, it is still possible to distinguish between best range (13) and best endurance (14) (Raymer, 2012) for the computation of the drag coefficient.

$$C_{D_{BR}} = \frac{4}{3}C_{D_0} \quad (13)$$

$$C_{D_{BE}} = 2C_{D_0} \quad (14)$$

This leads to the definition of subsonic cruise requirements to be used within the Matching Chart as in (15) and (16).

$$\left(\frac{T}{W}\right)_{subcruise_{BR}} = \left(\frac{q_\infty S\frac{4}{3}C_{D_0}}{W_{kg}/_S g}\right)\frac{1}{\pi\sigma} \quad (15)$$

$$\left(\frac{T}{W}\right)_{subcruise_{BE}} = \left(\frac{q_\infty S 2 C_{D_0}}{W_{kg}/_S g}\right)\frac{1}{\pi\sigma} \quad (16)$$

Supersonic climb requirement. The model for supersonic climb is again very similar to the one used for subsonic climb, even if the drag coefficient is computed in different way. The climb equilibrium equation is the same of (7), even if with a different climb gradient $G_{superclimb}$, but the drag coefficient for zero lift can be computed as in (17).

$$\left(C_{D_{0_{supersonic}}}\right) \approx \frac{\sum C_f S_{wet}}{S_{ref}} + C_{D_{wave}} \quad (17)$$

As it can be seen from (17), the contributions of form and interface factors are not included in the supersonic formulation. Moreover, as for (11), contributions for miscellaneous as well as leakages and protuberances drag, which are typically included in the build-up process, are here neglected. The contribution of wave drag is instead included referring to the equivalent Sears-Haack body characterized by the same length and total volume (Raymer, 2012).

Being out of boundaries for the application of quadratic polar theory, the $C_{D_{supersonic}}$ is simply computed as in (17) and $C_{L_{supersonic}}$ is derived using Ackeret rule (Raymer, 2012).

Ultimately, the supersonic climb requirement can be derived as in (18).

$$\left(\frac{T}{W}\right)_{superclimb} = \left(\frac{q_\infty C_{D_{supersonic}}}{W_{kg}/_S g} + G_{superclimb}\right)\frac{1}{\pi\sigma^*} \quad (18)$$

The correction with reference density in this case can be different, depending on the configuration of the propulsion plant. σ^* can then be adapted looking at Top of Climb (ToC), Bottom of Climb (BoC) or other reference altitude.

Supersonic cruise requirement. The supersonic cruise requirement can be derived as already done for supersonic climb requirement neglecting climb gradient. It is then straightforward to derive the equation for the requirement reported in (19).

$$\left(\frac{T}{W}\right)_{supercruise} = \left(\frac{q_\infty C_{D\,supersonic}}{W_{kg}/_S\, g}\right)\frac{1}{\pi\sigma^*} \quad (19)$$

Similar considerations concerning σ^* applies also for supersonic cruise.

Hypersonic climb requirement. The derivation of proper requirements for the hypersonic phases are quite different from those of the other flight regimes, since the physical models representing these conditions are no more applicable. After a review of the available models describing the behaviour of the vehicle in hypersonic flight regime, the Newton theory has been selected (Hirschel, 2005). This approach allows evaluating the aerodynamic characteristics for simplified geometrical shapes by relating pressure coefficients to the vehicle flight attitude that determines the external flow conditions. In particular, the scenario can be described by means of the angle of attack α, angle of the oblique shock β and angle characteristic of the body θ (such as leading edges angle etc…). In this case, the drag coefficient can be defined as in (20).

$$C_{D\,hypersonic} = C_{p_{Newton}} \sin\alpha \quad (20)$$

Where pressure coefficient can be computed as in (21)

$$C_{p_{Newton}} = 2(\sin\theta)^2 \quad (21)$$

Apart from the format of drag coefficient equation, the hypersonic climb requirement is similar to the one specified for previous climb segments. The Thrust-to-Weight ratio equation is hypersonic climb is then reported in (22).

$$\left(\frac{T}{W}\right)_{hyperclimb} = \left(\frac{q_\infty C_{D\,hypersonic}}{W_{kg}/_S\, g} + G_{hyperclimb}\right)\frac{1}{\pi\sigma^*} \quad (22)$$

Hypersonic cruise requirement. Similar assumptions apply also to hypersonic cruise requirement that can be derived looking at the model used for hypersonic climb, neglecting climb gradient term. The result is reported in (23).

$$\left(\frac{T}{W}\right)_{hypercruise} = \left(\frac{q_\infty C_{D\,hypersonic}}{W_{kg}/_S\, g}\right)\frac{1}{\pi\sigma^*} \quad (23)$$

Instantaneous turn requirement. Instantaneous turn is a typical specification for military aircraft, such as fighters and trainers. It is a high performance feature allowing the evaluation of the manoeuvrability. However, this requirement can also be included in the Matching Chart for other types of flight vehicles, since the maximum load factor during the turn can be an index for structural integrity, identifying a proper level of wing loading associated to the manoeuvre. In fact, the turn rate can be determined as in (24)

$$\dot{\psi} = \frac{g\sqrt{n^2 - 1}}{V} \quad (24)$$

where

n is the load factor of the maneuver

Equation (24) has a simple physical interpretation, provided that n equal to one is required to sustain the aircraft, while the remaining load can be used to accelerate the vehicle on the horizontal plane on a circular trajectory. With this in mind, it is possible to express the load factor as in (25).

$$n = \frac{q_\infty C_L}{{W_{kg}}/{S}\, g} \quad (25)$$

Subsequently, the instantaneous turn requirement can be derived in terms of wing loading as in (26). Thus, this is not a requirement impacting on Thrust-to-Weight ratio, being represented as a vertical line on the Matching Chart.

$$\left(\frac{W_{kg}}{S}\right)_{IT} = \left(\frac{q_\infty C_{L_{MAX}}}{ng}\right)\frac{1}{\sigma} \quad (26)$$

The instantaneous turn requirement uses the maximum lift coefficient in order to represent the maximum manoeuvre condition, consistent with maximum structural capability. Moreover, the density correction can be usually referred to sea level conditions, since the most of high load manoeuvres are performed at low speed, in subsonic conditions. For other flight regimes, if this is the case, σ can be substituted with σ^*, if a different reference altitude is used.

Sustained turn requirement. Sustained turn is defined as a turn performed at constant altitude and speed. This is, similarly to the case of the instantaneous turn,

a typical requirement for fighter aircraft, for which it may be important to perform high performance manoeuvre during dogfight without losing speed. This requirement is here included as additional way to consider manoeuvres close to minimum speed for hypersonic aircraft when flying at subsonic speed. The lift coefficient for the turn can be derived making equation (25) explicit. Moreover, since in the equilibrium during the turn the thrust shall compensate the drag, equation (27) can be derived.

$$T = q_\infty S C_{D_0} + q_\infty S k C_L^2 = q_\infty S C_{D_0} + \frac{n^2 W_{kg}^2}{q_\infty S k} \quad (27)$$

The sustained turn requirement can then be derived by making explicit equation (27), as shown in (28).

$$\left(\frac{T}{W}\right)_{ST} = \left(\frac{q_\infty C_{D_0}}{W_{kg}/_S g}\right)\frac{1}{\sigma} + \left(\frac{W_{kg}}{S} g \left(\frac{n^2}{q_\infty \pi A e}\right)\right)\sigma \quad (28)$$

As for instantaneous turn, density ratio σ refers to sea level conditions.

Landing requirement. Landing requirement is important for commercial aircraft since it generally determines wing surface extension and related wing loading. The requirement is in fact a simple threshold for the wing loading in landing conditions, being as for the instantaneous turn, a vertical line on the Matching Chart. The landing model used for this work comes from the Loftin statistics (Loftin, 1980), which is based on the evaluation of some semi-empirical parameters for jet-engine landing phase. Moreover, prescriptions from regulation (EASA, 2019) are applied to compute reference landing speed in non-icing conditions. In general, starting from the available landing distance s_{ALD} it is possible to compute the landing field length s_{LFL} as specified by (29).

$$s_{LFL} = 1.6 s_{ALD} \quad (29)$$

Where $s_{ALD} = \frac{V_{app}^2}{k_{app}^2}$ is the available landing distance obtained by dividing the approach speed by the approach parameter specified as $k_{app} = 1.7\sqrt{\frac{m}{s^2}}$ in Loftin model.

Looking at landing equilibrium, it is possible to derive equation (30).

$$\frac{W_{kg}}{S} = \frac{\rho V_{ldg}^2}{2g} C_{L_{MAX}} = \frac{1.23 \rho_0 \sigma C_{L_{MAX}} k_{app}^2 s_{LFL}}{2g} \quad (30)$$

Equation (31) can be re-arranged to obtain a simple format as shown in (31).

$$\frac{W_{kg}}{S} = k_L \sigma C_{L_{MAX}} s_{LFL} \quad (31)$$

Where

k_L is the Loftin parameter in $\left[\frac{kg}{m^3}\right]$

The shape of landing requirement can then be different depending on the actual configuration of the aircraft. In fact, it is possible to express wing loading at landing with both typical landing mass or higher. The selection of landing mass has in fact a considerable impact on the size of the wing and it is also influenced by regulatory aspect in case landing is required right after take-off, in case of non-nominal conditions. Generally, it is possible to indicate two different landing requirements, as indicated in (32) and (33).

$$\left(\frac{W_{MLW_{kg}}}{S}\right)_{LDG1} = k_L \sigma C_{L_{MAX}} s_{LFL} \quad (32)$$

$$\left(\frac{W_{MTOW_{kg}}}{S}\right)_{LDG2} = \frac{k_L \sigma C_{L_{MAX}} s_{LFL}}{W_{MLW_{kg}} / W_{MTOW_{kg}}} \quad (33)$$

The first requirement is derived for Maximum Landing Weight (MLW) for which a specific landing mass is selected. The second requirement is instead referred to Maximum Take-Off Weight (MTOW) as main design mass. This second condition can be used to specify additional requirements on structural capability. Also other reference mass can be specified, depending on the amount of fuel on board during landing. Both wing loadings use the same reference surface.

4.5.4.3 Characterize vehicle performance

Conventional aircraft are typically designed to meet high-level requirements generally related to payload, range, cruise specifications (i.e. Mach number and ceiling) as well as to airport performance, such as the take-off field length or

balance field length, landing distance or missed approach and second segment climb gradient. These performance requirements have a direct impact onto many physical characteristics of the aircraft, and thus on the vehicle size and mass breakdown. Fig. 115 summarizes the activity flow leading to the generation of the Matching Chart, as reported in (Loftin, 1980). The analysis starts from the definition of proper requirements concerning airport performance and cruise parameters to determine Thrust-to-Weight ratio and Wing Loading in the different flight conditions. In addition, looking at the parameters used to describe each of the mission phases (Section 4.5.4.2), at least a first set of guess data for the aerodynamic characteristics of the aircraft, shall be available at the beginning of the process. They can also serve as a starting point for further parametric analyses to assess the impact of the hypothesized aerodynamic configuration of the aircraft onto the design space. The block called simultaneous solution (step 6 of the flow in Fig. 115) is the Matching Chart itself, which collects the different requirements expressed in terms of T/W and W/S and defines a performance-oriented design space. Through the Matching Chart, it is possible to select specific values of Thrust-to-Weight ratio and Wing Loading (step 7 of the flow-chart in Fig. 115) and thus, to select a single configuration to be used as a baseline for additional investigations. In particular, for each design point, it is possible to define a proper mass breakdown, as well as to verify the consistency with the range requirement. Indeed, at this level, the mass breakdown encompasses payload mass, fuel and main subsystems mass, i.e. ultimately, the maximum take-off mass. Complementary, the range equation, typically computed following the Breguet model (Raymer, 2012) in conceptual design, allows relating the performance of the propulsion plant, such as thrust and specific fuel consumption, with cruise data and fuel mass.

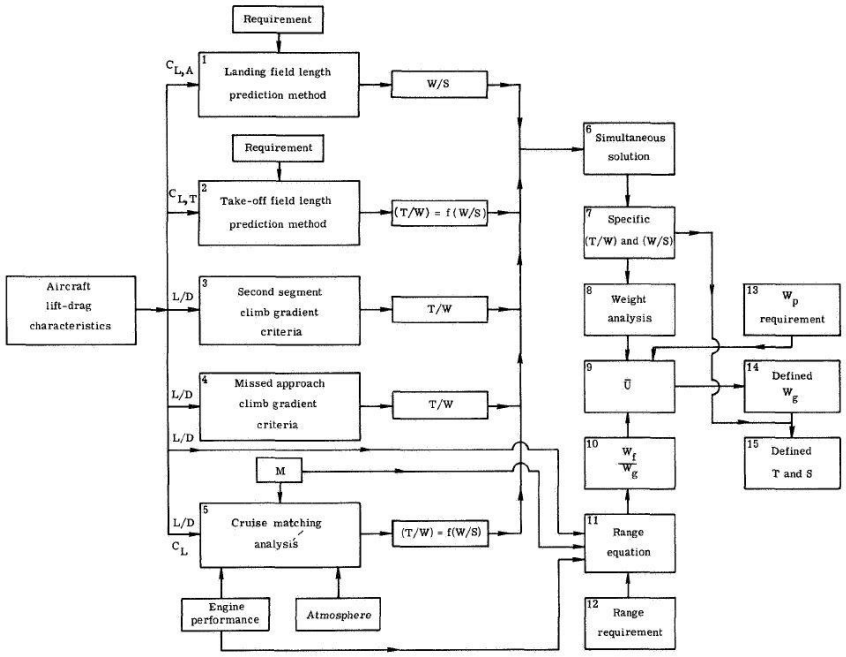

Fig. 115: Subsonic aircraft conceptual design process (Loftin, 1980)

This aircraft sizing process allows evaluating the different flight conditions and propulsion subsystem performance in one-shot, since the engine can be described in terms of the performance that shall be achieved in all mission phases, working as a typical turbojet or turbofan. At the same time, the aerodynamics of the aircraft can be characterized by looking at the most demanding flight regime. This is one of the main benefits of exploiting the Matching Chart tool during the conceptual design for conventional aircraft, which allows a self-contained process providing a single and consistent configuration as result. Fig. 116 shows a typical example of Matching Chart for a jet aircraft as reported in (Loftin, 1980). The different requirements are depicted as curves on the graph, representing the required Thrust-to-Weight ratio as function of Wing Loading for the flight phases. In particular, the requirements for take-off and landing, missed approach, second segment and cruise are reported. In order to be comparable, the different equations are corrected to represent equivalent trends at sea level. The design space can be identified as the part of the graph characterized by T/W higher than the most stringent requirement (in this case, the cruise) and with Wing Loading lower than the most stringent requirement (in this case, the landing). In particular, the match point is located where the minimum Thrust-to-Weight ratio is reached, coupled with consistent Wing Loading value. Usually, maximum Wing Loading (i.e. minimum required wing surface) is selected, taking into account landing

requirement for civil aircraft. On the contrary, in the case reported in Fig. 116, the take-off requirement is considered as the most critical, since a higher wing surface (i.e. a lower Wing Loading) is selected, thus giving priority to a lower Thrust-to-Weight ratio. The landing requirement would have led to the selection of a higher Wing Loading with a higher Thrust-to-Weight ratio, more demanding for the propulsion plant. This may be caused by additional constraints on power plant or specific needs of the stakeholders.

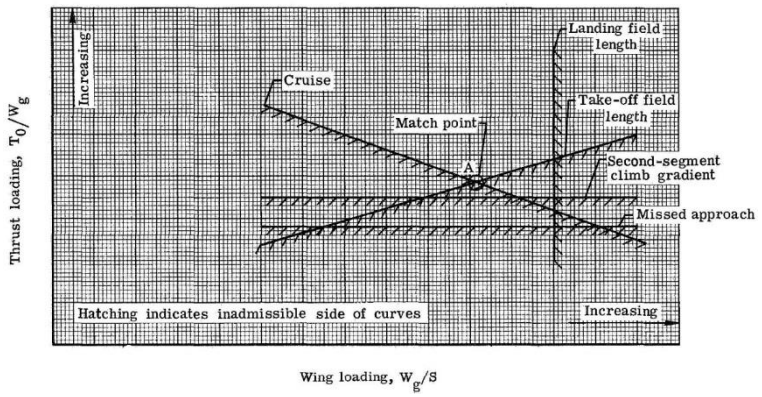

Fig. 116: Example of a typical matching chart for jet-powered aircraft (Loftin, 1980)

From this simple but complete example, it is possible to understand the powerfulness of this tool: it allows defining the design space and the selection of a feasible baseline since the very beginning of the design process, providing a direct link between vehicle configuration and high-level requirements.

Even if the Matching Chart provides the designer with a complete understanding of the design space for conventional and non-conventional aircraft during conceptual activities, it cannot be applied in its classical formulation for the analysis of high-speed transportation systems for several reasons:

- the limits of application of the mathematical formulations for the already existing curves shall be extended to cover supersonic and hypersonic flight regimes;
- the higher level of complexity, innovation and integration of the high-speed vehicles shall also be considered to develop a tool able to provide results with an acceptable confidence level;
- high-speed vehicles are often equipped with different propulsive subsystems to cover the wide spectrum of flight regimes and operative

environments. The same considerations are applicable in case of the most recent combined cycle propulsive subsystems.

Taking all these considerations into account, it appears clear that a single Matching Chart cannot be anymore sufficient to represent the whole set of requirements and that a single design point can only describe a specific mode of operation of the propulsive subsystem. Reporting all the requirements coming from different speed regimes on the same design space, within a unique diagram, may lead to wrong results and unfeasible solutions. For example, traditionally, the T/W requirements are normalized using a specific altitude (e.g. sea level), to allow comparisons among the whole set of phases, but this is no more applicable for high-speed transportation, especially considering that subsonic engine may not be operative in high-speed flight and vice-versa. Indeed, in the case of hypersonic transportation, the attempt to create a single Matching Chart representing several propulsive subsystems, operating at different altitudes, may lead to an overestimation of the T/W requirement (black star in Fig. 117).

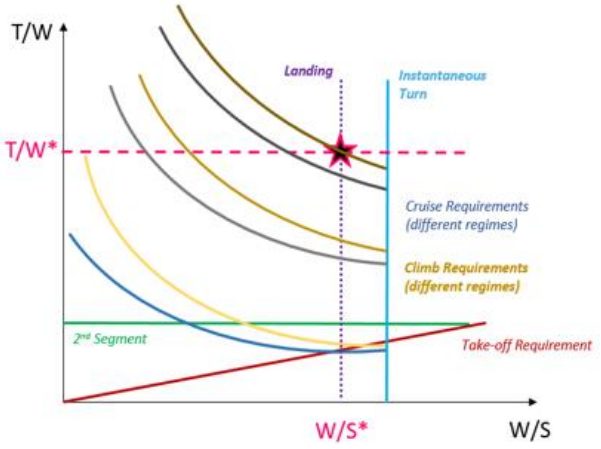

Fig. 117: Multi-regime, single Matching Chart approach

Moreover, as far as high-speed transportation is concerned, the comparison between subsonic and hypersonic cruises requirements is not meaningful anymore. Indeed, the two cruise legs are performed by different engines or even by the same engine but working in completely different operating conditions. Complementary, the normalization of the hypersonic cruise requirement using sea-level as reference atmospheric condition, would results in an extremely high required thrust. Therefore, a Multiple Matching Charts (MMC) approach is

suggested to tackle the conceptual design of hypersonic vehicles, for which preliminary requirements and performance assessment shall be carried out for each speed regimes separately. However, even if the MMC approach can be pursed for several T/W requirements, i.e. different scales can be considered to draw T/W requirements for the various flight regimes, this is not applicable for the W/S requirements. Indeed, even if different T/W requirements may change all along the mission, the wing surface cannot. Thus, after the derivation of T/W requirements using the MMC approach, iterations shall be carried out to identify a unique value of wing surface able to generate a sufficient amount of lift to fulfil the requirements of the various flight regimes. The subsonic condition, and in particular the landing requirement, is expected to drive the selection of a unique design point, being the most demanding requirement (i.e. the widest wing surface). Of course, landing requirement curves are not present in the Matching Charts for supersonic or hypersonic regimes and the manoeuvres requirements in high speed flight are limited by passenger comfort and maximum structural loads, thus requiring a lower wing surface. Local design points for subsonic, supersonic and hypersonic regimes would then be probably different in terms of required surface. Moreover, the selection of a suitable wing loading at high speed is influenced by a lower vehicle mass, if compared to subsonic regimes (the propellant required to reach hypersonic cruise altitude has already been used during the acceleration phases). This means that, for example, it is not realistic to define the requirement for hypersonic cruise considering the Maximum Take-Off Weight (MTOW). These different aspects contribute to define local design points for each regime (i.e. for each Matching Chart), identified by specific values of wing loading and Thrust-to-Weight ratio. The consistency of the final solution shall be guaranteed, iterating the process up until all selected design points are characterized by the same wing surface (determined within the most critical flight regime) as well as by the reference mass of the considered phase. This means that an additional requirement is implicitly present in the chart, imposing the consistency among the different flight regimes in terms of wing surface. Local (purple star) and global (green star) design points shall then be identified within the Multiple Matching Charts depending on the number of flight regimes (Fig. 118), where the global solution identifies the point characterized by the Wing Loading computed with the maximum required wing surface as well as by the highest Thrust-to-Weight ratio. The target value of thrust to be used for the sizing of the propulsion plant will then be the one corresponding to the value of Wing Loading specified by the consistency requirement (most demanding condition).

The exploitation of the Multiple Matching Charts approach allows preventing the underestimation of thrust requirements in high-speed, which might result from very small wing surface usually evaluated locally for the high-speed regime. Global design point allows instead selecting the correct value of thrust, taking into account the consistency of the geometrical configuration, considering all flight regimes. At the same time, the value of thrust obtained using the MMC approach, is way more reasonable than the one computed with the traditional single chart methodology, affected by several errors related to wrong requirements normalization, to misleading propulsion plant operation and not consistent aircraft mass (black star in Fig. 118).

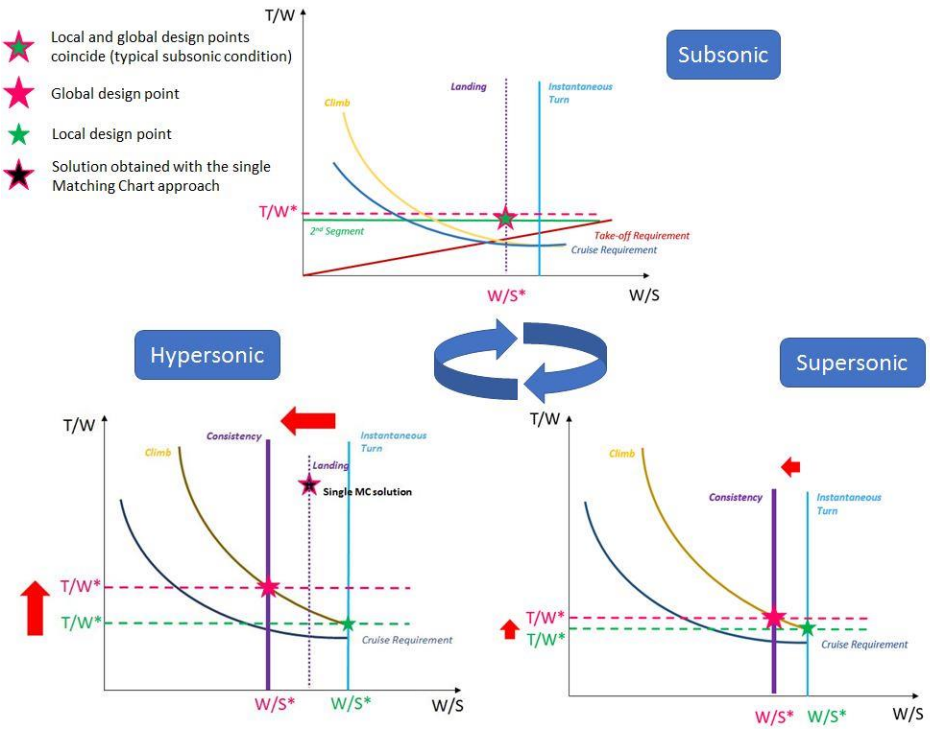

Fig. 118: Multi-regimes, multiple Matching Chart approach

From the sketch reported in Fig. 118 it is possible to notice the progress towards the identification of the design points. In the subsonic case, global and local solutions usually coincide, since this is the most critical condition for the determination of wing surface. In supersonic regime, a smaller number of requirements is present, but two possible solutions exist. In fact, the requirements for the pure supersonic regime provide a local design point determined by the combination of climb and manoeuvres. However, the consistency requirement

determined by the configuration obtained in subsonic shall be satisfied, allowing the selection of a global design point characterized by a higher Thrust-to-Weight ratio and a lower Wing Loading. Ultimately, the progressive reduction of reference mass (from subsonic to hypersonic flight regime) produces a global design point in hypersonic which is even further from the local one if compared to the supersonic phase for similar reasons. Moreover, while focusing on the hypersonic Matching Chart, it is possible to see that the difference between this global design point and the one that would have been produced by the single Matching Chart approach (black star, typically located on the trace of subsonic landing requirement for that specific methodology) is usually non-negligible, in terms of both Wing Loading and Thrust-to-Weight ratio. This is also due to the fact that the density correction (thrust normalization) with respect to sea level conditions can be considered no more meaningful, as in the original Matching Chart methodology, whilst different reference altitudes thresholds shall be identified per each flight phase. This leads to the selection of proper bottom-of-climb altitudes for supersonic and hypersonic flight phases as reference to normalize the requirements (Section 4.5.4.2). The core of the multi-matching analysis is thus the iterative computation of charts for the different regimes, taking into account the considerations previously discussed.

The first two tasks described by the matching analysis process (Fig. 114) are crucial for this activity and it is thus necessary to look into the details of their related steps. The steps for mission phases characterization task are reported in Fig. 119, as formalized using SPEM. First step consists in the derivation of mission phases and of the associated data from ConOps analysis (Section 4.5.2.7). Subsequently, main flight regimes are identified and characterized following the theoretical equations described in Section 4.5.4.2. Several flight conditions are then characterized for each regime and associated requirements curves can be derived. As expected, subsonic regime is characterized by a higher number of requirements whilst supersonic and hypersonic regimes account only for climb, cruise and manoeuvre.

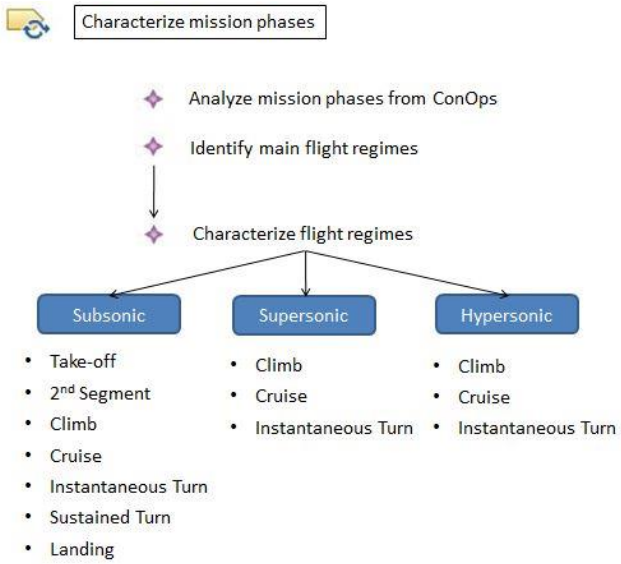

Fig. 119: Mission phases characterization task overview

Once applicable requirements are identified, it is possible to move on with the vehicle performance characterization task (Fig. 120). This is an iterative procedure that, starting from data initialization related to vehicle configuration, obtained from statistical estimation on existing vehicles available from past HST projects, is based on the computation of wing surface and reference vehicle mass. The second aspect concerns the estimation of the characteristics of the atmosphere within which the vehicle is flying. This allows the evaluation of the aerodynamic coefficients, essential to estimate the performance of the vehicle in relation with the operational environment. The third step consists in the estimation of the Wing Loading variable, necessary for the evaluation of wing surface and of the vehicle mass.

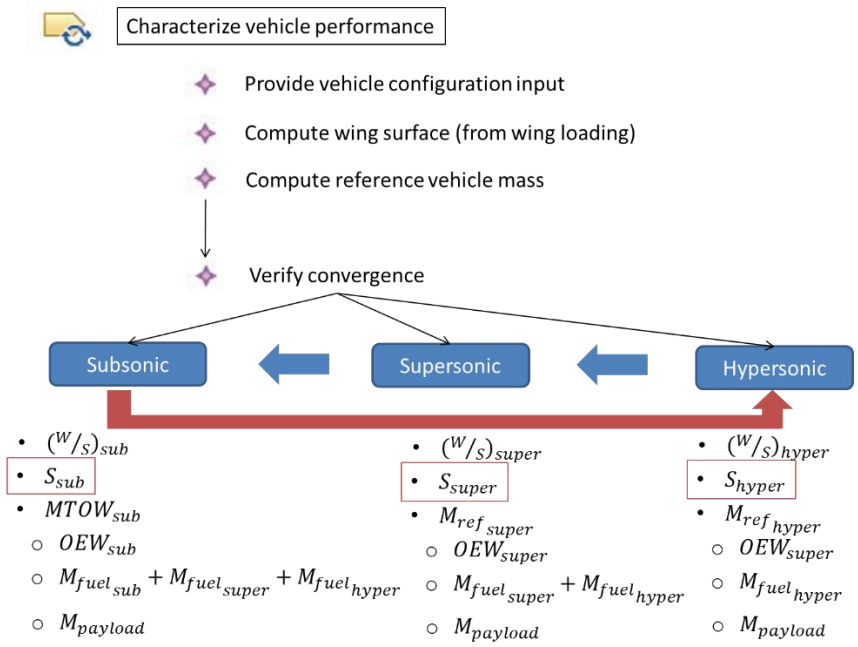

Fig. 120: Overview of the Conceptual Design section of the tool with related output.

The aerodynamic characterization of the vehicle is performed consistently with the derivation of matching requirements, and classical theories described in Section 4.5.4.2 are used to compute lift and drag coefficients (Raymer, 2012). Subsequently, vehicle characterization is performed for each regime, starting from the hypersonic one. In fact, this is the only flight phase which, at the beginning of the analysis, can be fully characterized (it is not generally known, when studying subsonic phase, which will be the propellant required for supersonic and hypersonic segments, thus it is not possible to determine MTOW through closed mathematical formulation). For this purpose, a reference mass is hypothesized, a proper range requirement is allocated on hypersonic phase, together with the aerodynamic characterization previously performed, and, as result, new values of wing loading, wing surface and vehicle mass are obtained. The core of the process is the estimation of reference vehicle mass and wing surface, which are correlated. In fact, a reference wing loading provided by the hypersonic manoeuvre requirement (turn) drives the definition of the surface, based also on the hypothesized mass. The mass itself, however, is function of wing dimensions, since propellant fraction depends on vehicle size through the drag coefficient. Breguet model (Raymer, 2012) is used to compute the required propellant for the

different phases, as reported in (34 – 36), where α and β coefficients are used to adapt the model for the case of HST vehicle, including contribution of other phases (such as descent for each regime, take-off and landing) directly within the main ones, i.e. cruise and climb segments.

$$M_{fuel_{cruise_i}} = \alpha * M_{ref_{i-1}} \left(1 - e^{\frac{-Range*SFC}{\frac{L}{D}*V\infty}} \right) \qquad (34)$$

$$M_{fuel_{climb_i}} = \beta * M_{ref_{i-1}} \qquad (35)$$

$$M_{fuel_{TOT_i}} = M_{fuel_{cruise_i}} + M_{fuel_{climb_i}} \qquad (36)$$

An iterative process is thus required to reach convergence. Actually, hypersonic requirements concerning wing surface are quite low if compared to other regimes, since manoeuvres are very limited and, even if the climb and cruise requirements may be critical because of the altitude, the speed is so high that a small wing is enough to generate the required lift. The wing loading is thus large, also considering that most of the propellant is consumed within this phase, heavily contributing to the overall reference mass. The process moves on with the analysis of supersonic regime, where the same approach is re-applied considering that the propellant calculated for hypersonic flight shall be accounted within the reference mass. This produces a higher estimation of final vehicle mass, requiring also a higher wing surface. At the same time, analysis of subsonic phase shall take into account the propellant mass required for other phases, determining a final MTOW. Actually, subsonic phase include landing analysis for what concerns the determination of wing surface, usually resulting in the most critical condition (sizing condition) for the wing dimensions (also considering the poor aerodynamic characteristics of this kind of vehicle at low speed). The process is iterated also globally, to adjust wing surface depending on the highest value, producing updated vehicle configurations for the different regimes. The overall process is qualitatively summarized in Fig. 121.

After the first iteration cycle, the wing surface is fixed at the most critical value (approximately assessed during subsonic phases) for all regimes. This aspect is essential in order to determine the impact of the size of the vehicle on the

aerodynamic performance. In fact, the wing surface is a significant driver for propellant mass computation, since it firmly influences the consumption. Of course, while iteration moves on, the most critical value of wing surface is updated to take into account additional mass contributions coming from hypersonic and supersonic phases, where a larger wing is imposed, if compared to local design point, thus producing higher propellant consumption and an intrinsically bigger OEW (wing size influences also airframe mass). As soon as a vehicle concept configuration converges globally, matching conditions can be computed, as explained in Section 4.5.4.4.

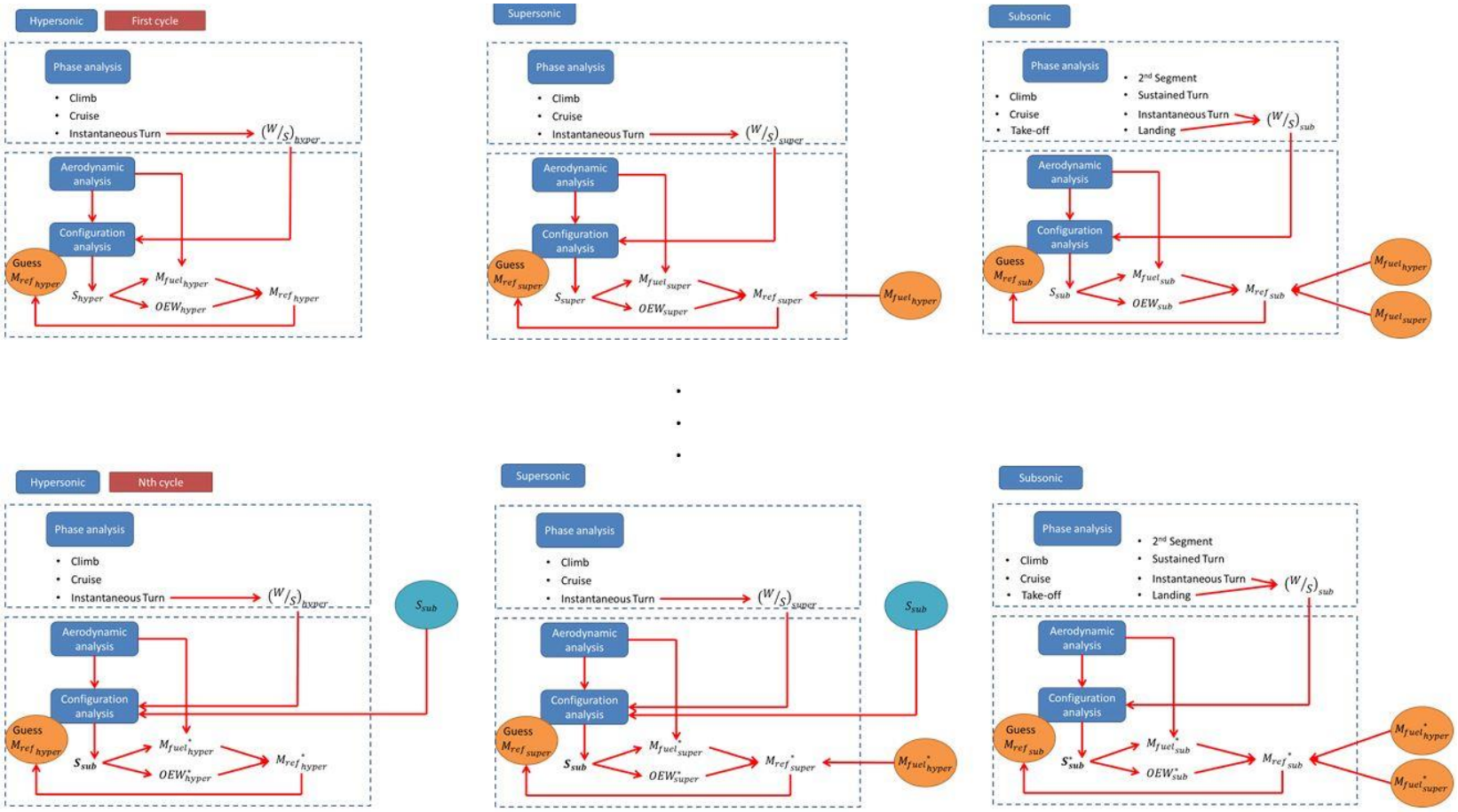

Fig. 121: Multiple Matching Chart iteration process

4.5.4.4 Compute matching conditions & derive matching point

This task aims at computing the matching chart curves and at building the diagram itself. The process is here used to show the results of the validation procedure for the final version of STRATOFLY MR3 configuration. Particularly, considering the characteristic of the vehicle concept which allows the process to converge, reported in Table 10, as well as the overall approach to hypersonic vehicles design reported in the previous sections, the analysis here proposed is based on the evaluation of aircraft matching on three different conditions, corresponding to the subsonic, supersonic and hypersonic flight regimes. As comparison, the multi-regimes single Matching Chart approach is also provided at the end of this section (Fig. 125) to show the magnitude of the error related to the estimation of Thrust-to-Weight ratio in case of simultaneous matching of all conditions in a single chart. The Matching Chart for subsonic flight regime is shown in Fig. 122. The requirements are corrected referring to the conditions specified by sea level. The landing requirement determines the wing loading (considering MTOW, solid red line), whilst the maximum Thrust-to-Weight ratio is obtained for subsonic climb condition. With the low-speed configuration of the ATR engines, the propulsion plant is able to provide the required thrust in all conditions.

Table 10: STRATOFLY MR3 aircraft specifications

Parameter	**Value**	**Unit of Measure**	**Specified by**
Length	94	m	CR_SysL6000
Wingspan	41	m	CR_SysL5000
Aspect ratio	~1	-	(implicit)
MTOW	400000	kg	CR_SysL7000
Reference Mass @ ToC subsonic	375000	kg	Hypothesis from LAPCAT II
Reference Mass @ ToC supersonic	350000	kg	Hypothesis from LAPCAT II
N° of passengers	300	-	MR2000
Subsonic Cruise Mach	0.8	-	OP_SysL28000
Supersonic Cruise Mach	4	-	OP_SysL32000
Hypersonic Cruise Mach	8	-	MR5000
Subsonic Cruise Altitude	12000	m	OP_SysL27000
Supersonic Cruise Altitude	24000	m	OP_SysL31000

Service Ceiling	33000	m	Per_HL6000
Range	18700	km	Per_HL4000
ATR engines thrust @ sea level (total)	3000	kN	Hypothesis from LAPCAT II
ATR engine thrust @ ToC subsonic (total)	2800	kN	Hypothesis from LAPCAT II
DMR engine thrust @ ToC supersonic	500	kN	Hypothesis from LAPCAT II
DMR engine thrust @ hypersonic cruise level	1033	kN	Hypothesis from LAPCAT II

Additionally, the aerodynamic coefficients reported in Table 11 have been considered for the MR3 vehicle. Please, notice that, these aerodynamic coefficients are first guess values coming from the currently under development AEDB.

Table 11: Aerodynamic coefficients used for the validation of MR3 matching

Coefficient	Mach	Value
$C_{L_{TO}}$	0.4	0.2
$C_{D_{TO}}$	0.4	0.09
$C_{L_{LDG}}$	0.4	0.35
$C_{D_{LDG}}$	0.4	0.09
$C_{L_{subclimb}}$	0.8	0.19
$C_{D_{subclimb}}$	0.8	0.065
$C_{L_{subcruise}}$	0.8	0.14
$C_{D_{subcruise}}$	0.8	0.06
$C_{L_{superclimb}}$	0.8	0.06
$C_{D_{superclimb}}$	4	0.01
$C_{L_{supercruise}}$	4	0.05
$C_{D_{supercruise}}$	4	0.009
$C_{L_{hyperclimb}}$	8	0.037
$C_{D_{hyperclimb}}$	8	0.0065
$C_{L_{hypercruise}}$	8	0.028
$C_{D_{hypercruise}}$	8	0.005

Supersonic and hypersonic manoeuvres consider the aerodynamic coefficients of related cruise phase, whilst subsonic turns are derived using the highest lift coefficients for subsonic regime. Table 12 summarizes the design point for

subsonic regime. The minimum planform surface required for the subsonic design point is 1117 m^2 (which satisfy the requirement CR_SysL9000 concerning minimum wing surface). This surface will be used as reference to consider the consistency requirements in other flight regimes.

Table 12: Design point for subsonic regime

Parameter	Value	Unit of measure
Wing loading (subsonic)	358	$\frac{kg}{m^2}$
Thrust-to-Weight ratio (subsonic)	0.732	-

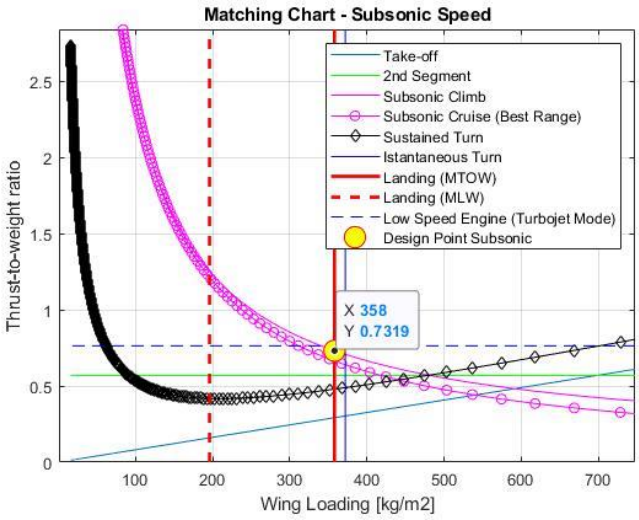

Fig. 122: STRATOFLY MR3 matching in subsonic flight

The Matching Chart for the supersonic regime is reported in Fig. 123. Please, notice that the diagram is corrected to show all trends with reference to the supersonic BoC, at 12000 m.

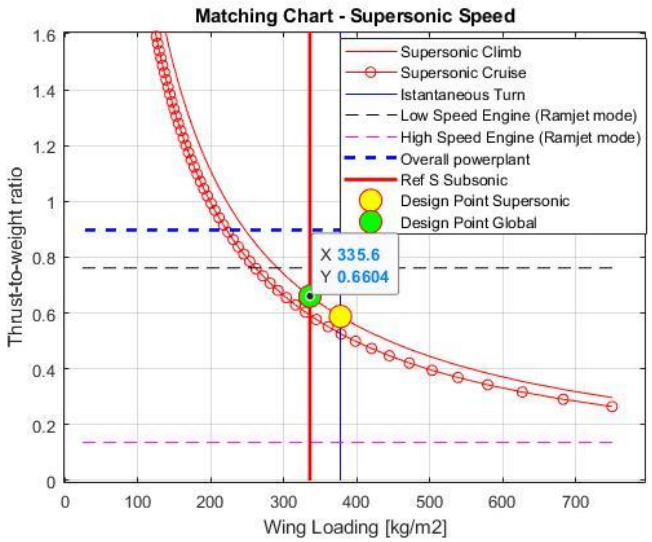

Fig. 123: STRATOFLY MR3 matching in supersonic regime

For the supersonic flight regime, only climb and cruise requirements are included. Instantaneous turn is used to evaluate a possible wing loading to be used as reference for local design point (yellow). The turn is here hypothesized to generate a maximum acceleration load on passenger cabin of about 0.3g (relative acceleration). The additional vertical red line (consistency requirement) reports the Wing Loading derived using the surface determined for subsonic condition with the aircraft mass consistent with supersonic regime (Table 10). This allows representing a more realistic situation for the global design point (green) in supersonic conditions, assuring a good estimation for the required Thrust-to-Weight ratio with respect to the local solution. In any case, the ATR engines in ramjet configuration are able to assure aero-propulsive balance of the vehicle. Moreover, an additional contribution to the overall thrust, provided by the DMR, can be also taken into account as demonstrated by (Ispir, et al., 2019). The summary of global design point coordinates in supersonic regime is provided in Table 13.

Table 13: Global design point for supersonic regime

Parameter	Value	Unit of measure
Wing loading (supersonic)	335.6	$\frac{kg}{m^2}$
Thrust-to-Weight ratio (supersonic)	0.66	-

The Matching Chart for hypersonic regime is shown in Fig. 124. The diagram is corrected to show all trends with reference to the hypersonic BoC, at 24000 m.

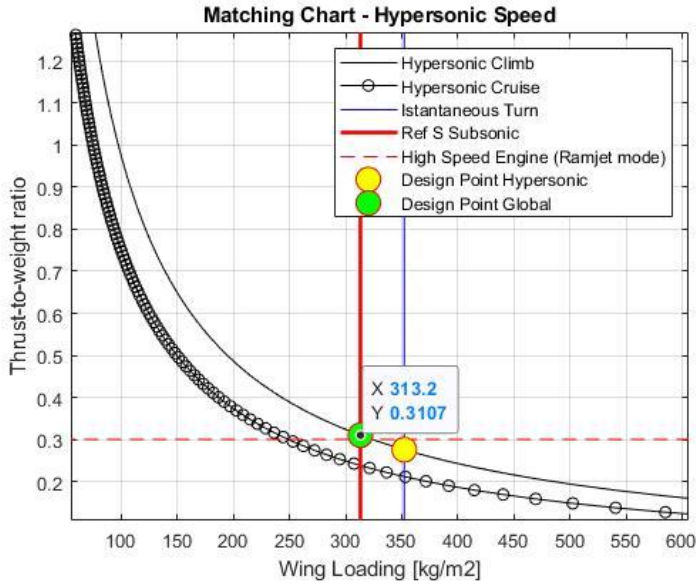

Fig. 124: STRATOFLY MR3 matching in hypersonic regime

As for the supersonic regime, only hypersonic climb and cruise are included. The instantaneous turn requirement is conceived in similar way to what already applied for the supersonic case. Moreover, the additional consistency requirements (red line in Fig. 124), positioned further on the left side and derived using subsonic wing surface and aircraft mass in hypersonic regime, suggests the need for a higher required thrust. In fact, the required Thrust-to-Weight ratio is not totally sufficient to support the aircraft in hypersonic cruise, even if the difference with DMR thrust line is marginal. Table 14 summarizes the coordinates for global design point in hypersonic conditions.

Table 14: Global design point for hypersonic flight regime

Parameter	Value	Unit of measure
Wing loading (hypersonic)	313.2	$\frac{kg}{m^2}$
Thrust-to-Weight ratio (hypersonic)	0.311	-

In order to provide a mean of comparison between the results obtained with the proposed approach and those derived with the single Matching Chart methodology, Fig. 125 shows the equivalent design point for the MR3 vehicle in the single design space.

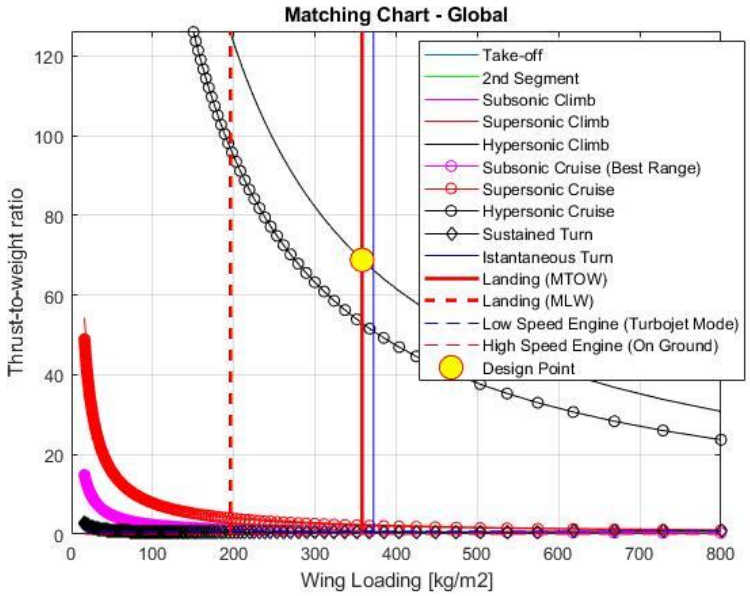

Fig. 125: Design point (unrealistic) obtained through the single Matching Chart approach for the MR3 vehicle

As it can be seen, the hypersonic climb requirement is setting a design point in terms of Thrust-to-Weight ratio which is unrealistic and out of bounds for any air-breathing propulsion plant. This is due to the use of a reference MTOW mass for all flight phase and, notably, to the normalization at sea level atmospheric conditions (i.e. it is not a physical condition, rather a problem of chart setting). Even neglecting the climb requirement, the hypersonic cruise is also quite high in terms of Thrust-to-Weight ratio, with a value around 55 for the selected Wing Loading. Similar conditions affect also supersonic requirements (around 5). On the contrary, since the landing requirement is computed in the same way, the value of Wing Loading is consistent with the multiple Matching Chart approach (the subsonic condition is the most demanding one for the determination of wing surface). Configuration and performance requirements (Sections 8.1.3 and 8.1.6) can thus be updated according to the matching analysis by including information

about propulsion plant and vehicle data, together with the results coming from the feasibility analysis discussed in Section 4.5.5.

4.5.5 Vehicle concept feasibility analysis

4.5.5.1 Vehicle concept feasibility analysis workflow

The vehicle concept feasibility analysis aims at exploiting the results coming from matching and performance analysis to verify if the configuration of the vehicle, in terms of major dimensions, is consistent with mission requirements (such as required fuel volume, range etc…). In fact, hypersonic aircraft shape and volume breakdown are deeply related to performance aspects, such as aerothermodynamics, achievable range and aerodynamic efficiency. In particular, the actual possibility of hosting payload, subsystems and propellant on board shall be assessed carefully for the determined concept, especially in case of waveriders, since, usually, the required volume is considerably high, and available volume tends to be reduced by designers to maximize aerodynamic efficiency. In fact, a big vehicle, in terms of volume, experiences a reduction of aerodynamic efficiency, increasing fuel consumption and, subsequently, reducing the achievable range. On the other hand, a smaller aircraft might be very good from the aerodynamic performance standpoint, but it may be not capable of hosting the required payload. Since the capability of flying over long haul routes, reducing cruise time, is the crucial advantage of this kind of vehicle category, range requirement is a priority within conceptual design study, to assure competitiveness of the product in operation. Additionally, economic sustainability may require to design the aircraft on a significant payload mass, to face operating costs which may be substantially higher than those associated to conventional aircraft (Chapter 6). These contradictory needs can be used to identify a design space where a trade-off on vehicle configuration can be performed. Feasibility analysis thus combines results coming from matching analysis, in terms of reference surface, wing loading and thrust-to-weight ratio, to determine the required volume on board, making benefit also of some semi-empirical relations to estimate the volume allocation on the different elements of its breakdown. Additionally, this analysis allows performing a preliminary validation of the concept, verifying if mission, operational and performance requirements, defined within previous activities of the conceptual design process, can be truly achieved. The process (Fig. 126) starts from the computation of available and required volumes, which is based on input and assumptions coming from the results of

previous analyses. Following the comparisons of the obtained values, a design space can be identified. If the concept appears feasible, both from the point of view of physical breakdown and of performance, the vehicle configuration is validated and related requirements can be defined and/or refined.

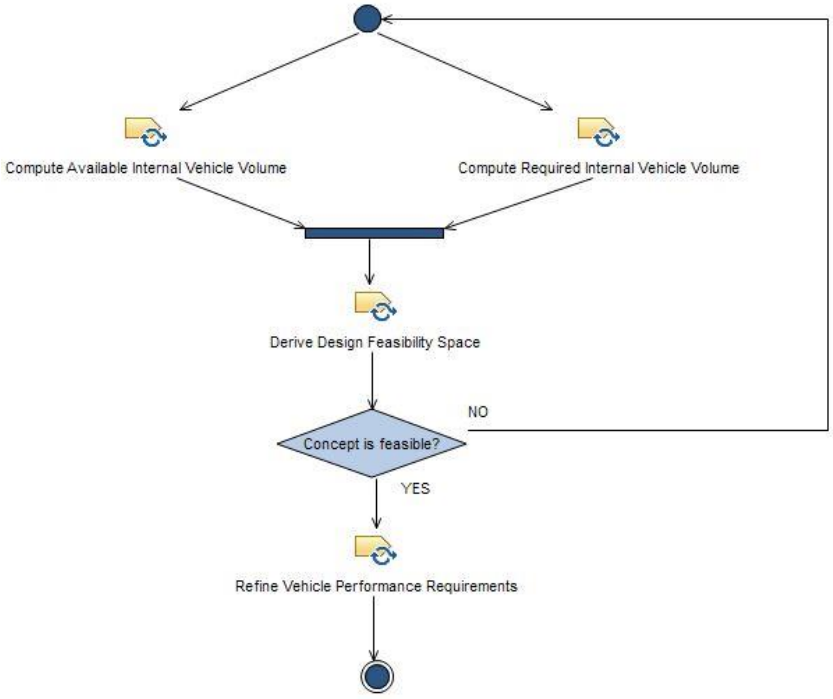

Fig. 126: Vehicle concept feasibility analysis workflow

4.5.5.2 Compute available internal vehicle volume

The derivation of total vehicle volume starting from the identified planform surface is the first step towards the physical characterization of the configuration. Notably, a very simple model conceived to produce a relationship between planform surface and total volume, able to pursue maximum aerodynamic efficiency for different architectures, has been proposed by (Kuchemann, 2012). A driving parameter was then conceived to set a proper ratio between these characteristics, as indicated in (37).

$$\tau = \frac{V_{tot}}{S_{plan}^{1.5}} \quad (37)$$

It is thus quite easy to derive the vehicle volume, once planform surface, which is related to wing surface for a specific configuration, is known and a value for τ is selected. Typically, τ parameter ranges from 0.01 up to 0.3, even if higher values can be considered for very blunt configurations (Fig. 127).

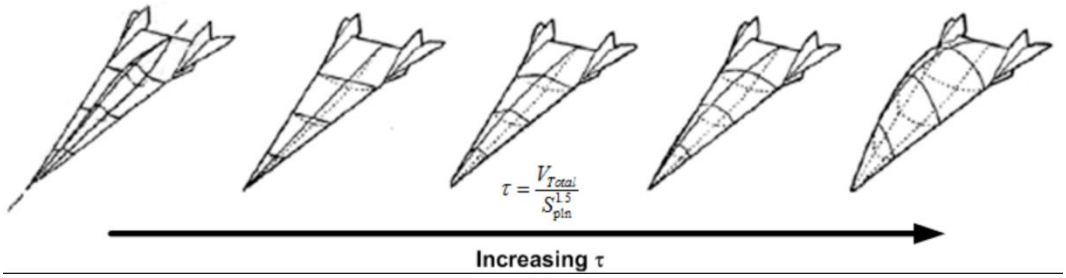

Fig. 127: Qualitative impact of τ on aircraft configuration (Chudoba, et al., 2012)

The selection of this parameter is driven by the computation of aerodynamic efficiency of the aircraft as function of the τ itself. The process can thus be iteratively performed to reach the desired level of lift-over-drag ratio prescribed by performance requirements and it can be ultimately traded to obtain a blunter or sharper configuration, depending on volume allocation needs. Particularly, different theories available in literature (Corda & Anderson, 1988) (Bowcutt, 2001) allow defining a typical equation for the computation of aerodynamic efficiency as indicated in (38), (39) respectively.

$$\left(\frac{L}{D}\right)_{Max_{Corda}} = \frac{6(M_\infty + 2)}{M_\infty} \quad (38)$$

$$\left(\frac{L}{D}\right)_{Max_{Bowcutt}} = \frac{4(M_\infty + 3)}{M_\infty} \quad (39)$$

However, these are general purpose relations that show a dependency between lift-over-drag ratio and cruise Mach number, without considering directly the τ parameter. During LAPCAT II project (Steelant, et al., 2015), a more advanced version of the equation has been applied following wind tunnel tests to include the dependency from τ, as shown in (40) (Ingenito, et al., 2009).

$$\left(\frac{L}{D}\right)_{Max} = \frac{4(M_\infty + 3)}{M_\infty}\left(\frac{1.0128 - 0.2797 \cdot \ln\left(\frac{\tau}{0.03}\right)}{1 - \frac{M_\infty^2}{673}}\right) \quad (40)$$

Since this is based on LAPCAT II studies, it makes sense to keep the relation also for feasibility analysis in STRATOFLY, provided that the two projects are strongly connected. Equation (40) can be in any case updated according to the considered configuration, as already done for the basic versions proposed in (38) and (39). Additionally, Breguet model can be re-applied to verify if the selected aerodynamic efficiency (i.e., ultimately, the selected τ) can be compliant with the range specified by requirements, as shown in (41).

$$Range = -\Delta V \cdot I_{sp} \cdot \frac{L}{D} \ln\left(1 - \frac{M_{fuel}}{MTOM}\right) \quad (41)$$

Proper loops on τ may be necessary to obtain the required results, even if the process remains quite simple. However, looking at the approach proposed in Section 4.5.4 for matching analysis, it is necessary to look at local and global results also within feasibility analysis. In fact, feasibility analysis shall be performed jointly with matching analysis to assure consistency within the design process and to evaluate together performance as well as physical characteristics within the trade-off. In the methodology here proposed, the planform surface, as well as the data related to speed and engine performance are associated to a specific regime computed within the matching analysis. Particularly, the surface is the one corresponding to subsonic, supersonic or even hypersonic regime, range is referred to the cruise leg of each mission phase (i.e. not to the global one) and specific impulse of power plant is indicated for a specific flight condition. Global and local design points can be thus located on the design space, as it is discussed in Section 4.5.5.4. However, before moving to the analysis of the space, it is necessary to compute the required volume, as indicated in Section 4.5.5.3

4.5.5.3 Compute required internal vehicle volume

The computation of required vehicle volume is based on the subdivision of volume breakdown in different items, which are assessed separately using semi-empirical or statistical relationships. Notably, (Chudoba, et al., 2012) proposes a promising model for the evaluation of volume budget of HST systems, which *"works well for any configuration"* (Chudoba, et al., 2012). The approach deals

with the identification of Structural Empty Volume (SEV), systems and propulsion plant volumes. Payload volume and propellant volume can be derived separately to ultimately obtain the final Maximum Take-Off Volume (MTOV). In this context, the (Chudoba, et al., 2012) method is coupled to the proposed MMC approach (Section 4.5.4) to define the feasibility design space, described within Section 4.5.5.4).

The first task consists in the estimation of different volume contributions. Payload volume can be easily computed as in (42)

$$V_{pay} = \frac{M_{pay}}{\rho_{pay}} \quad (42)$$

where

M_{pay} is the payload mass in $[kg]$
$48.0 \leq \rho_{pay} \leq 130$ is the payload density in $\left[\frac{kg}{m^3}\right]$
Power plant volume can be computed as in (43)

$$V_{eng} = k_{ve} \cdot \frac{T}{W} \cdot WR \cdot OEW \quad (43)$$

where:

$WR = \frac{MTOW}{OEW}$ is the weight ratio;
$0.25 \leq k_{ve} \leq 0.75$ is the specific volume (empirical) for propulsion plant in $\left[\frac{m^3}{ton}\right]$
The volume associated to other subsystems can be computed through a two-steps approach that considers separately cockpit-hosted assemblies and other on-board plants. Cockpit assembly is computed as shown in (44)

$$V_{cockpit} = V_{un} + f_{crew} N_{crew} \quad (44)$$

where

$5.0 \leq V_{un} \leq 7.0$ is the volume allocated to unmanned elements in $[m^3]$
$11.0 \leq f_{crew} \leq 12.0$ is the volume accounted for each pilot (statistical) in $\left[\frac{m^3}{person}\right]$
N_{crew} is the number of pilots

Volume associated to cabin attendants' provisions and seating is computed in similar way as in (45)

$$V_{cabinCrew} = N_{cabinCrew}\left(V_{pcrv} + k_{cabinCrew}\right) \quad (45)$$

where

$N_{cabinCrew}$ is the number of cabin attendants
$5.0 \leq V_{pcrv} \leq 6.0$ is the volume associated to crew provisions in $[m^3]$
$0.9 \leq k_{cabinCrew} \leq 2.0$ is the volume accounted for each cabin crew seat in $\left[\frac{m^3}{person}\right]$

Main subsystems (not included within the cockpit) are computed directly exploiting a percentage on SEV, which can be in any case derived straightforward, using the aforementioned contributions, as in (46)

$$SEV = \frac{\tau S_{plan}^{1.5}(1 - k_{vv} - k_{vs}) - V_{pay} - V_{fix} - V_{crew}}{\frac{WR - 1}{\rho_{fuel}} + k_{ve}\left(\frac{T}{W}\right)WR} \quad (46)$$

where

$0.10 \leq k_{vv} \leq 0.20$ is the void volume fraction
$0.02 \leq k_{vs} \leq 0.04$ is the main subsystems volume percentage

Total volume of subsystems can be thus computed starting from (46) as in (47).

$$V_{sys} = V_{cockpit} + k_{vs}SEV \quad (47)$$

Void volume can be also computed as function of SEV, as in (48).

$$V_{void} = k_{vv}SEV \quad (48)$$

MTOV can be subsequently computed summing all the contributions as in (49)

$$MTOV = SEV + V_{pay} + V_{fuel} + V_{void} + V_{sys} \quad (49)$$

where

$V_{fuel} = \frac{M_{fuel}}{\rho_{fuel}}$ is the volume allocated to propellant in $[m^3]$

4.5.5.4 Derive design feasibility space

Once the available and required volumes are known for the different flight regimes and reference surfaces are identified, starting from the analysis of wing loading within the matching chart, it is possible to analyse the feasibility design space. Usually, this is reported on a 3D carpet plot relating Volume (both available and requirement values), Surface and τ. The different plots shown in this section aim at maintaining consistency with the matching charts shown in Section 4.5.4, thus they are represented separately for the different regimes.

Subsonic regime. As a starting point, the subsonic feasibility space for STRATOFLY MR3 is shown in Fig. 128. The surfaces representing available (cyan) and required (orange) volumes are mathematically represented by (37) and (49) respectively. The feasibility threshold (red line) is obtained overlapping available and required surfaces in the same carpet plot like in Fig. 128. From the mathematical standpoint, this line represents the intersection of the two surfaces, while, from the physical point of view, it allows identifying the minimum required volume, under which the configuration cannot be considered feasible. Particularly, the diagram shows that configurations characterized by τ lower than 0.07 may be subjected to lack of internal volume because of excessive slender characteristic. Of course, this depends on the planform surface used as reference. However, considering that the subsonic leg is reduced in time, volume requirement is quite low and most of the carpet identifies feasible solutions. Particularly, the local design point for subsonic conditions identifies an available volume of about 10000 m^3, considerably higher than the minimum required. In fact, subsonic regime is critical for what concerns wing surface definition (Section 4.5.4) thus identifying the biggest required extension for the wing if compared to other regimes. This justifies the really big available volume. For the sake of comparison, the LAPCAT MR2.4 was characterized by a τ of about 0.08, thus, also considering the need of maintaining consistency with configuration requirements (Section 8.1.3) the same value is assumed for MR3 to fix the design point. Particularly, looking at the possible subsonic range obtainable with the considered propellant mass fraction and τ (Fig. 129), it is possible to see that the results are in line with the expectations (around 700 km), and the concept of MR3 is feasible.

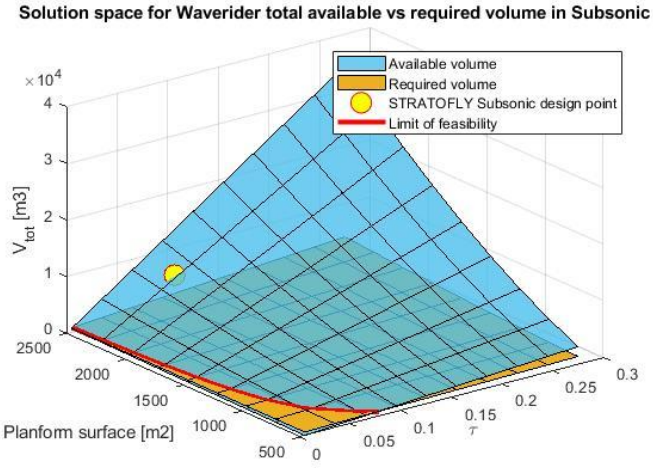

Fig. 128: Feasibility solution space for subsonic regime

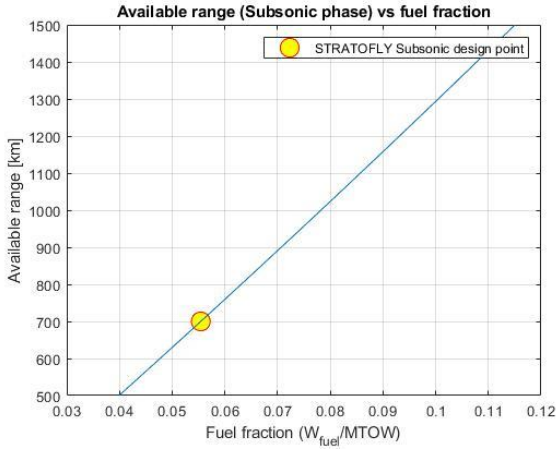

Fig. 129: Available range vs propellant mass fraction for subsonic leg

Supersonic Regime. Similarly, the feasibility space can be identified for supersonic regime (Fig. 130), where, even if the available volume is lower (required wing surface is lower than subsonic one), keeping the same τ, the minimum volume required is still quite far from the design point.

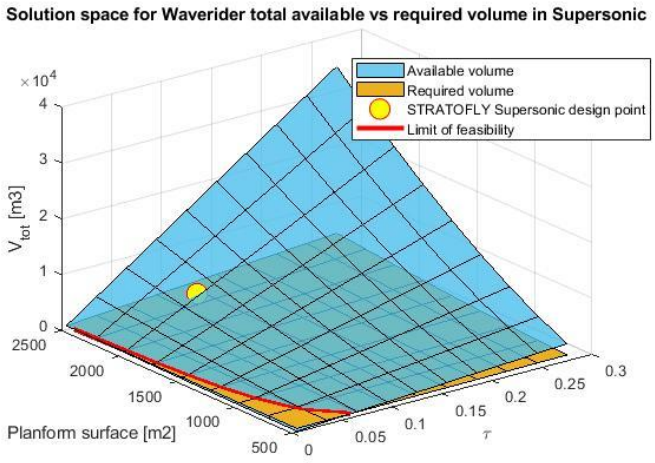

Fig. 130: Feasibility solution space for supersonic regime

Particularly, it can be also seen that the volume requirement has lowered. In fact, looking at the plot, the minimum τ for which volumetric problems occur is around 0.05. Considerations on the achievable range in supersonic conditions are also in line with requirements with the available vehicle data (Fig. 131).

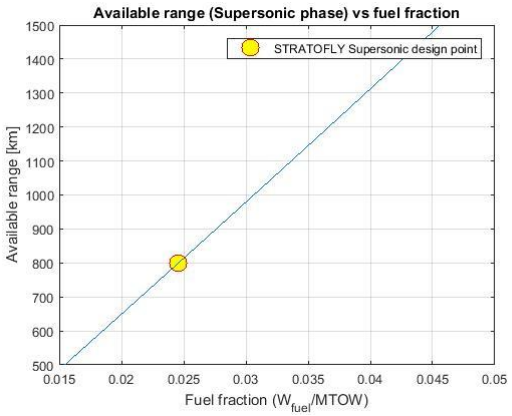

Fig. 131: Available range vs propellant mass fraction for supersonic leg

Moreover, in supersonic and hypersonic regimes it can be worth verifying whether the required aerodynamic efficiency (L/D) can be achieved as well. Fig. 132 shows the trend for different values of τ. Required value of 6.5 for LAPCAT MR2.4 is still achievable by the updated MR3 configuration with τ equal to 0.08.

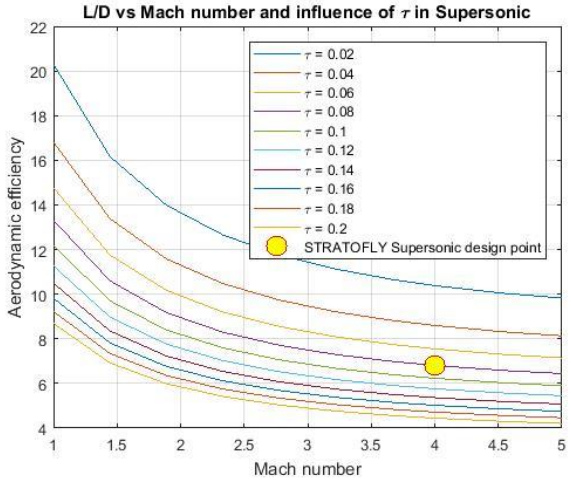

Fig. 132: Aerodynamic efficiency as function of Mach and τ in supersonic regime

Hypersonic regime. Ultimately, hypersonic regime associated feasibility space can be evaluated as in (Fig. 133). In this case, volume requirement is stringent and closer to the local design point. In fact, the required wing surface is low in hypersonic, whilst the propellant volume is highly impacting the configuration. However, the design evaluated locally is still feasible.

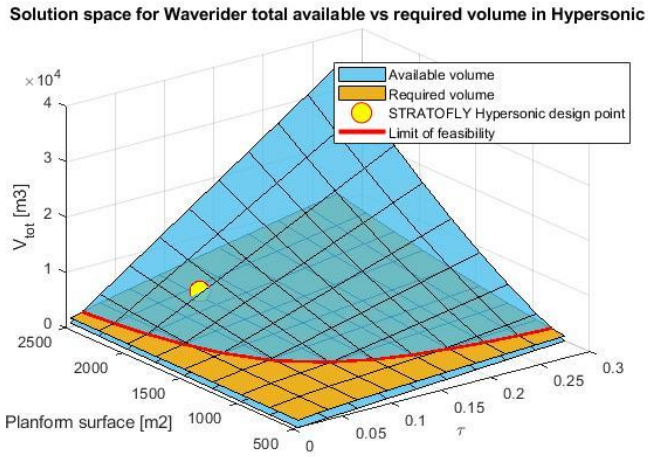

Fig. 133. Feasibility solution space for hypersonic regime

The range requirement in hypersonic regime (representing most of the mission) is met with the considered τ, as shown in Fig. 134.

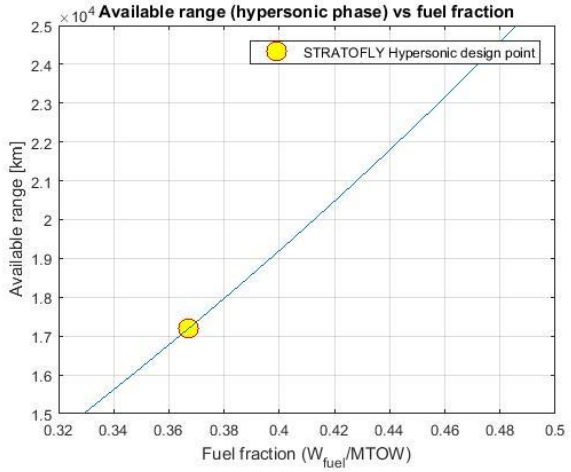

Fig. 134: Available range vs propellant mass fraction for hypersonic leg

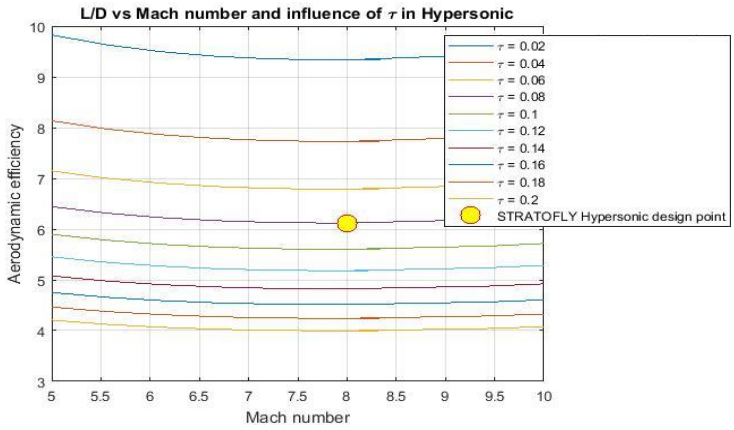

Fig. 135. Aerodynamic efficiency as function of Mach and τ in hypersonic regime

For what concerns the evaluation of aerodynamic efficiency for the local design point in hypersonic, the chart reported in Fig. 135 shows that the required level of aerodynamic efficiency (L/D) cannot be met at Mach 8 with the considered τ. This means that the MR3 concept shall be arranged to trade available volume with aerodynamic performance, for example reducing the margin from the feasibility line to enhance the efficiency at high speed. This aspect may result even more critical when looking at the global solution, obtained through the selection of the widest wing surface, as explained in Section 4.5.4. The feasibility space for the global solution is shown in Fig. 136.

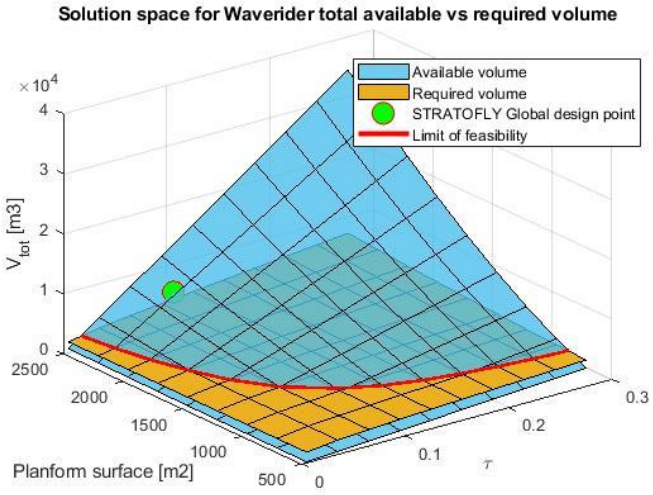

Fig. 136: Global feasibility solution space

As it is possible to expect, volume requirement remains high, since the overall mission is considered in terms of range. However, the selection of the widest surface as reference guarantees a sufficient volume to host the different contributions specified within Section 4.5.4.3. The overall range is still achievable with a lower propellant mass fraction if compared to the associated requirements. However, the global solution may be affected by underestimation of propellant consumption, especially in descent phase, thus further analyses shall be envisaged.

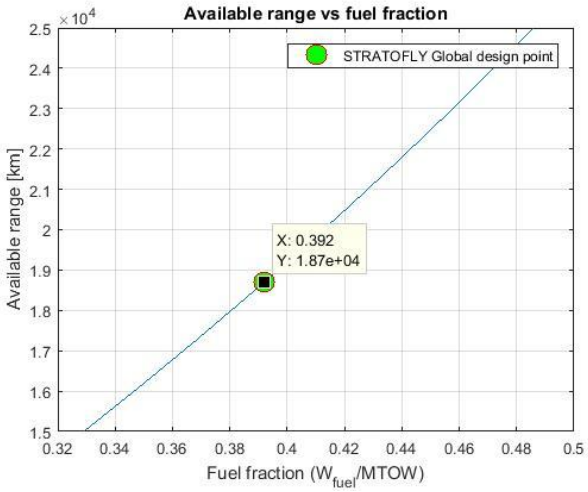

Fig. 137: Available range vs propellant mass fraction for global solution

Problems associated to aerodynamic efficiency are even more critical, since the hypersonic regime is characterized by a lower lift-over-drag ratio if compared to requirements, even if the effect of a larger wing does not have a heavy impact on the final value of efficiency (Fig. 138).

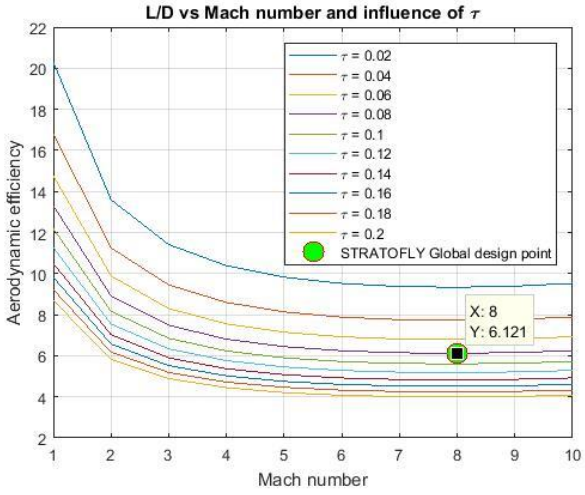

Fig. 138: Aerodynamic efficiency as function of Mach and τ for global solution

Section 4.5.5.5 ultimately summarize performance and configuration requirements collected within the conceptual design phase, showing the derivation strategy and traceability means implemented within the SEE.

4.5.5.5 Refine vehicle performance and configuration requirements

Following the analysis performed in Sections 4.5.4 and 4.5.5 it is possible to update the performance requirements specification with system-level statements, mainly addressing vehicle characteristics. Particularly, requirements associated to aerodynamic efficiency, power plant performance as well as vehicle configuration can be generated, looking at the results of matching and feasibility analyses. At the same time, requirements concerning vehicle configuration can be generated to detail the information concerning size and mass. Apart from τ requirement, all specifications are met by STRATOFLY MR3 configuration. Particularly, requirements generated by feasibility study and included within the configuration requirements specification are linked together through the design space surface, which can be used to identify the minimum volume required to host the subsystems, specified within the LAPCAT MR2.4 derived architecture. Actually, the design point is higher for what concerns volume even if the aerodynamic

efficiency value is not met. It may be required to slightly reduce the size of the vehicle in order to reach a lift-over-drag ratio of about 6.5 in hypersonic cruise, simply moving towards a Kuchemann parameter of about 0.09. This can be done by reducing volume only, since wing surface is constrained by matching analysis. Requirements can be easily linked to existing performance specification within the RDB as well as within the PDE through a direct link with the database. They can also be implemented in LDE to be allocated on target components, guaranteeing cross-platform traceability. Requirements list associated to matching and feasibility analyses results are included in Sections 8.1.3 and 8.1.6, whilst additional subsystems requirements are assessed within Chapter 5.

4.6 Mapping of proposed methodology on ECSS Phase 0 workflow

The proposed conceptual design methodology is supported by a process conceived to be compatible with ECSS systems engineering practices (ECSS, 2004). In this section, a short comparison between tasks and work products included within the two processes is provided. Particularly, the list of tasks of ECSS phase 0 and associated input/output is reported in Table 15.

Table 15: ECSS Phase 0 tasks and associated input/output (ECSS, 2004)

ID	ECSS Task	Input	Output
1	*Kick-off Phase 0*	-	Agreed Technical Assumptions
2	*Set-up appropriate SE organization and plan for Phase 0*	Mission Statement Systems Engineering Process	Systems Engineering Process for Phase 0
3	*Need, constraints, mission statement analysis*	Mission Statement SOW	First issue of system functional specification
4	*Analysis of the programmatic aspects*	Mission Statement SOW Management instructions	Synthesis of programmatic aspects
5	*Identification and characterization of possible concepts*	First issue of system functional specification	Set of possible concepts including associated risk assessment
6	*Assessment of concepts*	First issue of system	Preliminary system

ID	ECSS Task	Input	Output
	and recommendations	functional specification	functional specification
		Synthesis of programmatic aspects	System concept report
		Set of possible concepts	Requirements justification file
			Preliminary mission description document
			Systems Engineering Process for next phases
			Project phasing and planning requirement document for next phases
			Trade-off report
7	*Mission Definition Review (MDR)*	MDR plan	Preliminary system functional specification
		MDR data package	Preliminary mission description document
			Requirement justification file
			System concept report

As it can be seen, most of the work products involved within the tasks are compliant with the proposed methodology and, notably, the output associated to the main milestone of Phase 0, i.e. the Mission Definition Review (MDR), where preliminary system functional specification, preliminary mission description, requirements justification file and system concept report shall be provided. Actually, functional specification is provided by the joint exploitation of mission statement analysis, functional analysis and interface analysis of the proposed methodology, while the system concept is the analogous result of matching and feasibility analyses. Additional outputs, like the requirements justification file and the mission description document are provided by the SEE itself, through the instantiation of traceability links within the different activities, and by the ConOps analysis performed within the functional one. Intermediate outputs are mainly managed within the LDE of the proposed SEE, such as programmatic aspects, needs, objectives and constraints, whilst the instantiation of the SEP for Phase 0 and A is provided by the process formalized through the SPEM notation.

5

On-board subsystems design for hypersonic vehicles: the case of a multi-functional system

This chapter aims at describing the process associated to on-board subsystems design for high-speed vehicles. This process represents the continuation of the conceptual design phase, since, starting from the results obtained in Chapter 4, it provides an insight of on board subsystems characterization from both functional and physical points of view. The adopted methodology is conceived to be applicable to different kinds of on-board subsystems, even if the Dissertation focuses on the Thermal and Energy Management Subsystem (TEMS) of the MR3 vehicle, presented in Section 3.2. The TEMS is configured as a multi-functional subsystem, contributing to different duties, such as thermal control, engines feed, power generation etc…, typically distributed on several plants on-board. Moreover, the need of extending its boundaries in terms of capabilities is translated in a considerable number of interfaces with other plants, to be carefully assessed. At the same time, the required performance shall be verified in a demanding operational environment and the impact on vehicle breakdown is crucial to guarantee concept feasibility. As for Chapter 4, the overall process is described in Section 5.1, while the detailed discussion of the activities and associated tasks is reported in Section 5.2. Ultimately, Section 5.3 propose a mapping between the proposed approach and the Phase A of ECSS.

5.1 Description of high-level Preliminary subsystems design process

Preliminary subsystem design process is devoted to the characterization of functional, performance and physical aspects of on-boards plants, starting from the requirements and constraints derived within conceptual design, at vehicle level (Chapter 4). The proposed methodology, and the related process, can be associated to the Phase A of ECSS (ECSS, 2004), as already anticipated in Section 4.1. The analysis is performed from subsystem level up to equipment and components, so to investigate the low-level product breakdown. The process supporting the methodology discussed within Section 5.2 is depicted in Fig. 139.

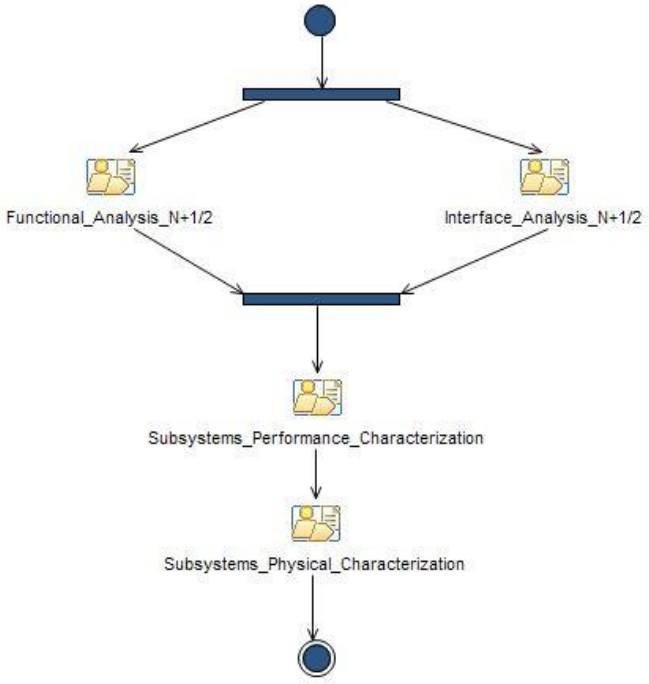

Fig. 139: Reference high-level process for preliminary subsystem design

As for the conceptual design, it is necessary to identify the different functions to be performed by subsystems elements before moving to the pure performance analysis. In fact, the main link between conceptual and preliminary design phases for the proposed MBSE approach, is the functional architecture, represented within the LDE. Notably, the identification of proper capabilities necessary to perform subsystem level functions allows the definition of the updated functional

specification, with the associated requirements. Functional breakdown can be then allocated on a suitable product breakdown, representing the hierarchical structure of the subsystems. The logical architecture of the different subsystems is furthermore completed through the characterization of the associated interfaces. Particularly, the communication network among assemblies, equipment and components (i.e. among elements with lower hierarchical levels if compared to subsystems) becomes more and more detailed while deepening the characterization, moving closer to the final implementation of the plant. Low-level interface requirements are thus crucial for further determination of performance and physical characteristics of the equipment, since they have a considerable impact on final subsystem layout. As for the conceptual design, the logical architecture can be completely defined only when functional and interface analyses are completed. Those analyses are in fact performed jointly, level by level, since, once the functional breakdown is identified and allocated on products, interfaces can be defined and characterized accordingly. For the purpose of this analysis, the logical architecture is considered completed as soon as the component level is reached, after having analysed assembly and equipment levels. Depending on the engineering practices adopted and on the standards used as reference, however, this breakdown can be subjected to modifications. Actually, the subsystem design process is heavily impacted by the usual policies adopted for specific engineering domains. Sizing processes, constituting the next step towards a full subsystems definition, are in fact peculiar of each technical area, and tasks associated to the mathematical modelling can be characterized by non-negligible differences when moving from one field to another. The process here described aims at proposing a general approach to identify the main activities related to subsystems design and to point out the main differences, as well as the common points, between performance and physical design, provided that a fundamental preparatory step to these studies is the development of logical architecture, already described. In fact, performance characterization represents the task aiming at defining a preliminary operating envelope for the subsystem and its components. More properly, the sizing process is related to the determination of the minimum set of performance and operating parameters of a certain equipment, or pieces of equipment constituting the subsystem, that can be used to describe the behaviour of the plant for a specific design point, without identifying a physical implementation (i.e. selection of commercial or ad hoc design product from real world). Physical analysis is instead conceived to characterize the different elements of the subsystems, as well as the subsystem itself, in terms of

breakdowns, including dimensions, volume and mass estimations. This allows attributing real characteristics to the different elements, contributing to the selection of the final product to be put in place for the correct operation of the plant. The difference between the two types of studies may appear not so important, but it is actually fundamental to understand the engineering process depicted in Fig. 139. In fact, the physical analysis makes use of the results of performance analysis to characterize the subsystem, previously studied only from the point of view of its behaviour. The two activities are thus not reversible, since they follow a determined workflow and they share specific work products following a rational order. Thus, the main focus for the sizing of a subsystem is first, generally, related to the determination of operating environment and on its critical operating points, to actually rate the technical problem by understanding the required level of performance. Afterwards, it is possible to detail the analysis, by using information coming both from the breakdown sketched during logical architecture definition and the performance data coming from the sizing process, to characterize the different elements of the subsystems in terms of physical features, such as mass, dimensions and volume. Both performance and physical analyses provide very useful requirements that can be used also to validate the high-level vehicle architecture proposed during conceptual design, thus constituting a valuable mean to provide traceability between high and low-level design choices. The overall process is put in place within this Dissertation focusing on the case study of TEMS in Section 5.2. Notably, Section 5.2.1 and 5.2.2 describes the functional and interface analyses in similar way to what already done at higher-level. Section 5.2.3 focuses on the typical process for the characterization of performance for an aerospace on-board subsystem, particularly conceived to be hosted on high-speed vehicles. A dedicated process for the identification of physical breakdown starting from operating parameters evaluation is provided in Section 5.2.4. Ultimately, Section 5.2.5 gives some insights about reliability aspects associated to subsystems design as well as about the need for a proper margin policy to be instantiated in early definition process.

5.2 Discussion on low-level preliminary subsystems design processes for STRATOFLY MR3

5.2.1 Functional analysis at subsystem level

5.2.1.1 Functional analysis workflow (subsystem level)

The functional analysis for preliminary subsystem design (Fig. 140) is very similar to the analogous process adopted at conceptual level (Section 4.5.2). It starts from the identification of a suitable functional breakdown, from subsystem level up to components. This allows a seamless connection with the conceptual design, since the functional analysis at high level.

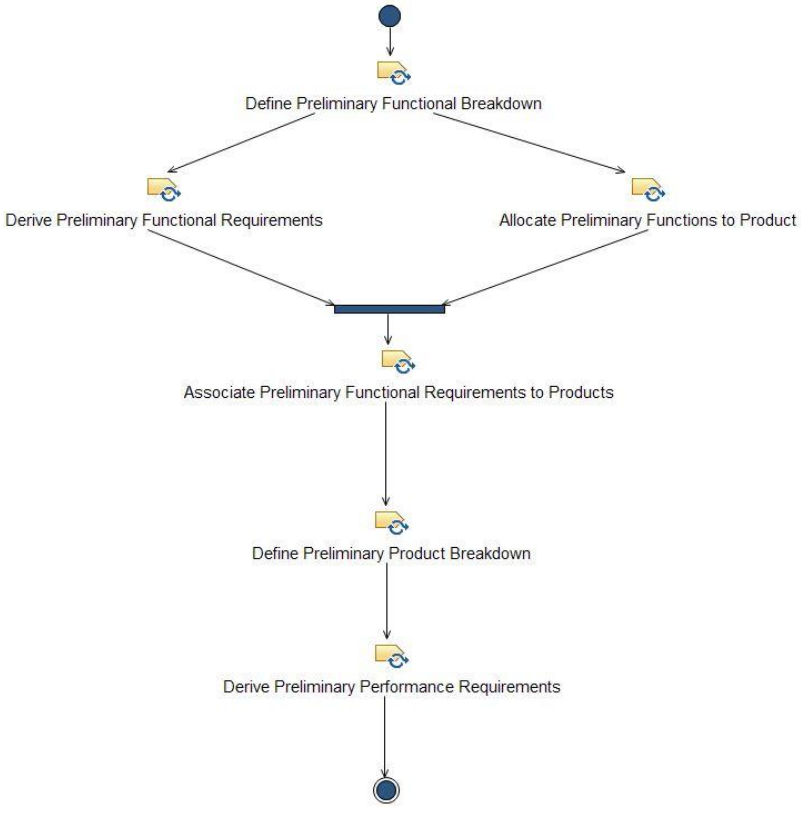

Fig. 140: Functional analysis workflow at subsystem level

In fact, the functional analysis workflow is continuous within the LDE, collecting the data for the different levels as a unique process. Once the breakdown is defined, functional requirements can be formulated and functions can be, in

parallel, allocated on products. Moreover, low-level functional requirements are associated to the products themselves and a consistent product breakdown can be defined as well. Ultimately, performance requirements can be derived to specify quantitative characteristics for the capabilities defined within the low-level functional architecture.

5.2.1.2 Define preliminary functional breakdown

The low-level functional breakdown starts from the subsystem functions derived during the last step of previous analysis. This means that, for each subsystem level function, it is possible to build the breakdown for assemblies, equipment and components. In order to focus on TEMS preliminary design, functional breakdown is here developed only for the thermal control capability, as shown in Fig. 141.

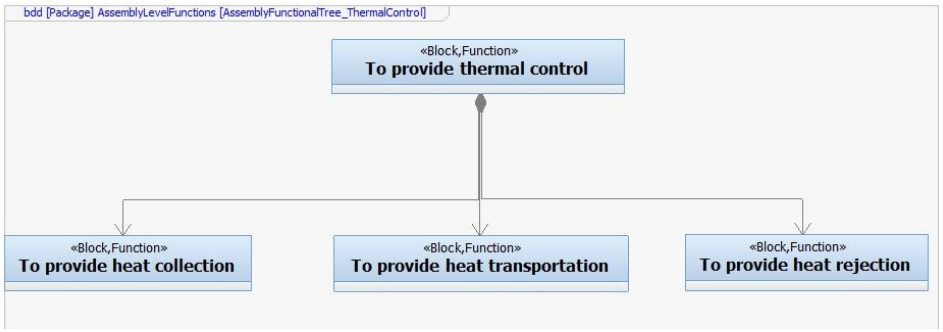

Fig. 141: Functional breakdown at assembly level for thermal control capability

The list of derived functions at assembly level is collected in Table 16.

Table 16: Functions list at assembly level for TEMS

ID	Functions @ Assembly Level
ASF1000	To provide heat collection capabilities.
ASF2000	To provide heat transport capabilities.
ASF3000	To provide heat rejection capabilities.

Following the breakdown, the thermal control capability is performed by collecting the heat produced, by internal and external sources, by transporting it and by rejecting it. For each assembly level function, equipment level tree can be derived. Fig. 142 shows the details of the heat collection tree, where the need of

collecting heat from external skin, from the cabin, as well as from the propulsion plant and the ECS is highlighted.

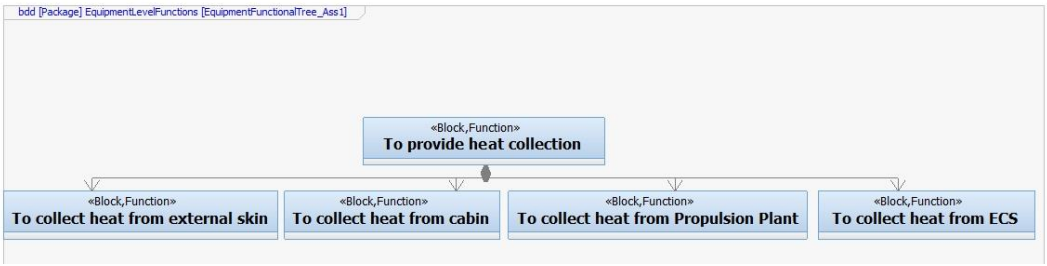

Fig. 142: Functional breakdown at equipment level for heat collection capability

The list of associated equipment level functions is shown in Table 17.

Table 17: Functions list at equipment level for first TEMS assembly

ID	Functions @ Equipment Level
EQF1000	To collect heat coming from external skin.
EQF2000	To collect heat coming from passenger cabin.
EQF3000	To collect heat from propulsion plant.
EQF4000	To collect heat from the Air Pack.

Together with heat collection capabilities, heat transport functions can be defined. These are related to the need of transporting heat among the different subsystems and TEMS equipment, as defined within the product breakdown (Section 5.2.1.6). The analysis of heat transport capabilities is also very useful when studying the interface network (Section 5.2.2). The list of associated equipment level functions is shown in Table 18.

Table 18: Functions list at equipment level for second TEMS assembly

ID	Functions @ Equipment Level
EQF5000	To transport heat from tanks to cabin collection equipment.
EQF6000	To transport heat from tanks to high pressure transport equipment.
EQF7000	To transport heat from high pressure transport equipment to propulsion heat collection equipment.
EQF8000	To transport heat from cabin to high pressure transport equipment.
EQF9000	To transport heat from Propulsion plant to boil-off collection equipment.
EQF10000	To transport heat from ECS to boil-off collection equipment.

ID	Functions @ Equipment Level
EQF11000	To transport heat from the compressor to the ECS.
EQF12000	To assure an adequate pressure level in heat transportation assembly.

Fig. 143 shows the tree associated to heat rejection capability. In this case, the aim is to use the boil-off to reject the heat collected from different sources, so to prepare the fluid for the injection within the Fuel Control Unit (FCU) of the propulsion plant. The tree is, thus, quite simple.

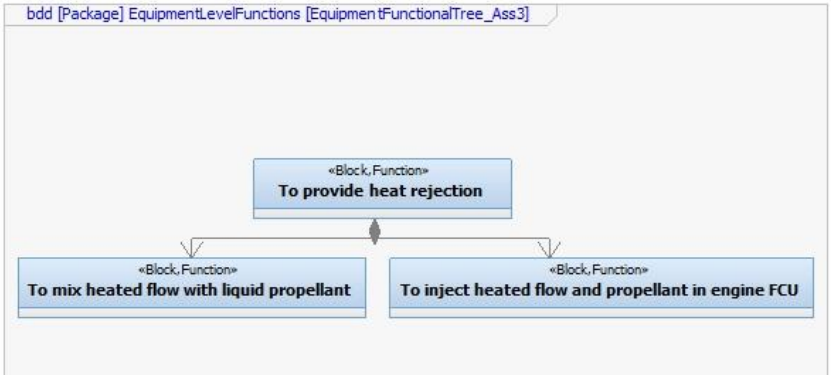

Fig. 143: Functional breakdown at equipment level for heat rejection capability

The list of the associated equipment level functions is shown in Table 19.

Table 19: Functions list at equipment level for third TEMS assembly

ID	Functions @ Equipment Level
EQF13000	To mix heated flow with liquid propellant.
EQF14000	To inject heated flow and propellant in engine FCU.

The preliminary design of TEMS has not reached the components level. For this reason, no functional tree is available for the lowest level of the analysis.

5.2.1.3 Derive preliminary functional requirements

Functional requirements can be derived for the aforementioned functions. As for conceptual level, a hypothesis on the product responsible to accomplish the function is made and the different requirements already include the subject on

which the function is allocated, even if the formalization of the process is reported in Section 5.2.1.4. Requirements derivation from functions is traced using proper matrix views in the LDE, as shown in Fig. 144 for assembly level.

	FR_AL1	FR_AL2	FR_AL3
To_provide_heat_collection	FR_AL1		
To_provide_heat_transportation		FR_AL2	
To_provide_heat_rejection			FR_AL3

Fig. 144: Requirements derivation at assembly level for thermal control capability

Requirements for assembly level are listed in Section 8.1.4. The same approach can be used for equipment level requirements, where traceability matrix is shown in Fig. 145, and requirements list is reported in Section 8.1.4.

Fig. 145: Requirements derivation at equipment level for thermal control capability

5.2.1.4 Allocate preliminary functions to product

Proper functions-products matrices can be defined looking at the functional breakdown just analysed. The matrix is reported in Fig. 146 for assembly level.

	Heat_collection_assembly	Heat_transport_assembly	Heat_rejection_assembly
To_provide_heat_collection	Heat_collection_assembly		
To_provide_heat_transportation		Heat_transport_assembly	
To_provide_heat_rejection			Heat_rejection_assembly

Fig. 146: Allocation of functions to products at assembly level for TEMS

Equipment level matrix is too big to be reported in the Dissertation, even if the same approach has been followed. Information related to the allocation process can be found directly within the property compartment of SysML blocks represented through the product trees (BDD).

5.2.1.5 Associate preliminary functional requirements to products

Once the functions-products matrices are instantiated, it is possible to formalize the connection between functional requirements and products through

proper traceability links. Views reported in Fig. 147 for assembly level and in Fig. 148 for equipment level summarize the process.

	FR_AL1	FR_AL2	FR_AL3
Heat_collection_assembly	FR_AL1		
Heat_transport_assembly		FR_AL2	
Heat_rejection_assembly			FR_AL3

Fig. 147: Requirements association to products at assembly level for TEMS

	FR_EL1	FR_EL2	FR_EL3	FR_EL4	FR_EL5	FR_EL6	FR_EL7	FR_EL8	FR_EL9	FR_EL10	FR_EL11	FR_EL12	FR_EL13	FR_EL14
LH2_tanks	FR_EL1													
Cabin_exchanger		FR_EL2												
Propulsion_plant_exchangerL			FR_EL3											
Air_pack_exchanger				FR_EL4										
Tank_pipe					FR_EL5								FR_EL13	
Cabin_pipe						FR_EL6								
Propulsion_Plant_pipe							FR_EL7							
Air_pack_pipe								FR_EL8						
TEMS_compressor									FR_EL9					
Boil_off_Expander										FR_EL10				
Boil_off_fuel_collector											FR_EL11			
Compressor_pipe												FR_EL12		FR_EL14
Propulsion_plant_exchangerG			FR_EL3											

Fig. 148: Requirements association to products at equipment level for TEMS

5.2.1.6 Define preliminary product breakdown

Ultimately, a consolidated product breakdown can be defined for both assembly and equipment level (the component level is not yet available for TEMS). Fig. 149 shows the assembly level product breakdown.

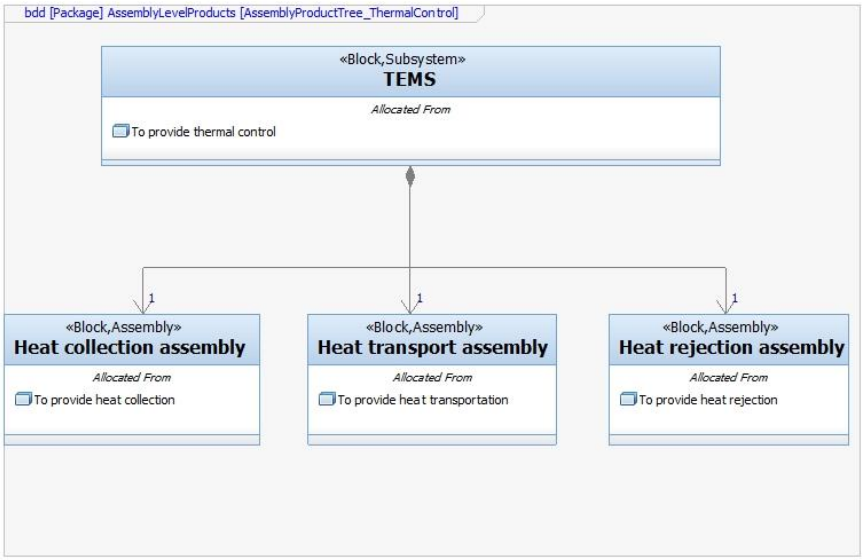

Fig. 149: Product breakdown at assembly level for TEMS

The assembly breakdown is quite simple, and it follows the functional breakdown presented in Fig. 141. In particular, three main assemblies are identified, looking at the definition of the capabilities performed during functional breakdown identification. The product tree for equipment level is a bit more complex, so it is reasonable to look into the breakdown for each assembly separately. The breakdown for heat collection assembly is shown in Fig. 150.

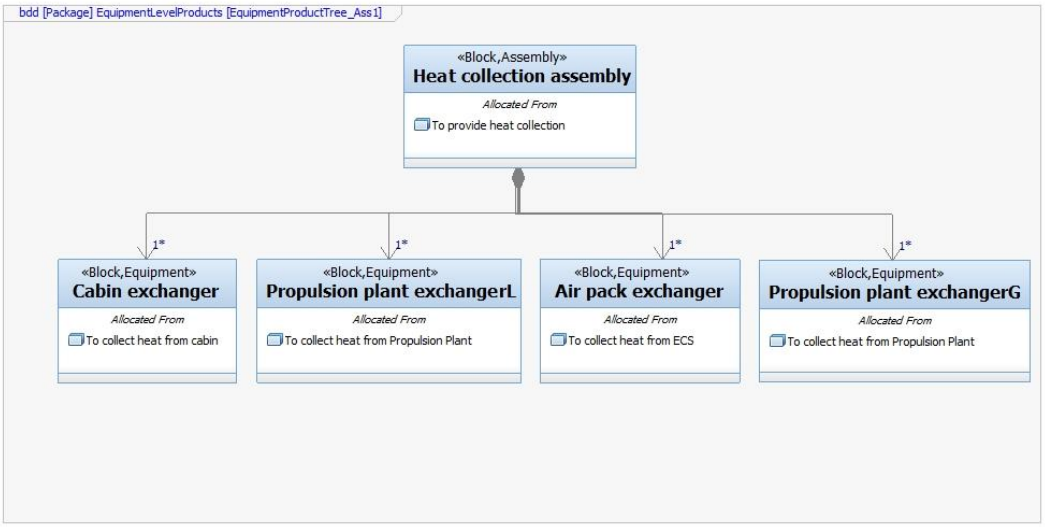

Fig. 150: Product breakdown at equipment level for heat collection assembly of TEMS

The heat collection is provided through different exchangers, located, for example, within the cabin, the propulsion plant and the ECS. Particularly, one or more exchangers need to be envisaged for the different compartments of the vehicle and both liquid and gas exchangers are considered to cool down the propulsion plant using LH2 and its boil-off respectively. This allows making benefit of a regenerative engine cycle for the feeding line where LH2 is provided, while using also the remaining amount of boil-off to increase the cooling capability of the subsystem. The heat transport assembly breakdown in shown in Fig. 151.

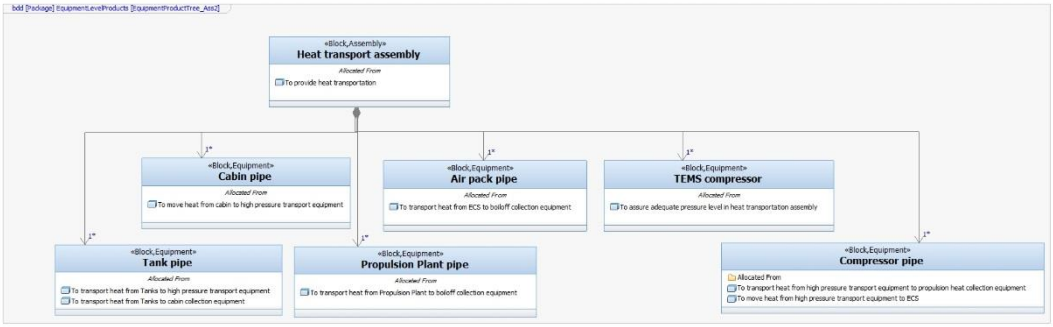

Fig. 151: Product breakdown at equipment level for heat transport assembly of TEMS

This assembly mainly consists of a pipes network responsible to move the fluid through the different elements of TEMS. Moreover, a dedicated compressor is present to guarantee a suitable level of pressure within the lines and to move the gas towards the rejection assembly where the boil-off is injected in the propulsion plant. The heat rejection assembly (Fig. 152) is in fact made of an expander (turbine) which decreases the temperature of the fluid and reduces its temperature before injecting it into the fuel collector of the propulsion plant. Both liquid and boiled-off hydrogen are injected in engines combustors, following a specific ratio, to produce thrust.

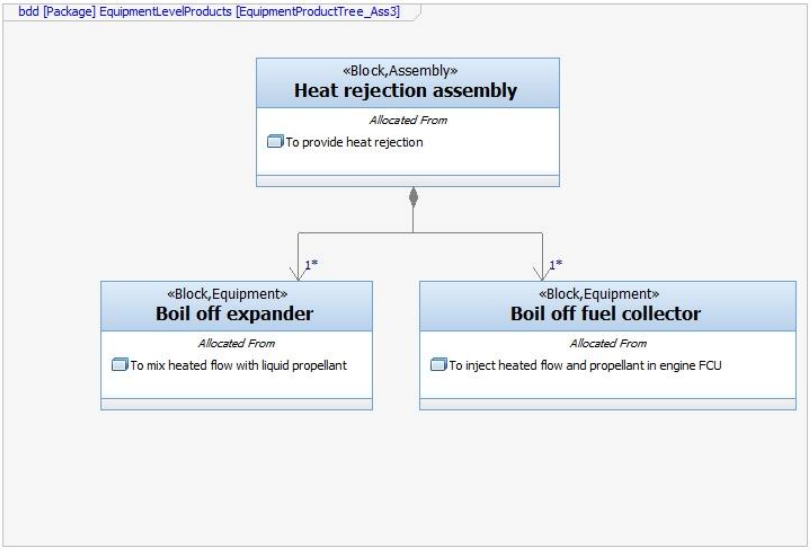

Fig. 152: Product breakdown at equipment level for heat rejection assembly of TEMS

5.2.1.7 Define preliminary performance requirements

Following the analysis of functional aspects at subsystems and elements level, the requirements specification is updated with preliminary performance data. Subsystems performance requirements are derived also considering the results of low-level performance analysis, described in detail for the TEMS in Section 5.2.3. The derivation of performance requirements is always driven by the need of quantifying the functional capabilities just defined, but, often, the study of subsystems elements, such as assemblies and equipment, is crucial to populate the specification and to point out performance characteristics. This activity includes, even if it is not limited to, operational environment analysis, static sizing as well as dynamic analysis (not discussed within the Dissertation). Derived requirements belong to several engineering domains, since subsystems can be quite different from each other. For this reasons, different kinds of requirements can be defined, from structural aspects up to thermal issues. The list of preliminary performance requirements is reported in Section 8.1.6.

5.2.2 Interface analysis at subsystem level

5.2.2.1 Interface analysis workflow (subsystem level)

The interface analysis at subsystem level is, as already mentioned for functional analysis, similar to what already performed at conceptual level. The main difference is in fact related to the level at which the study is conducted, since, in this case, the analysed interfaces are related to subsystems and low-level elements (assemblies, equipment etc…). The process is shown in Fig. 153.

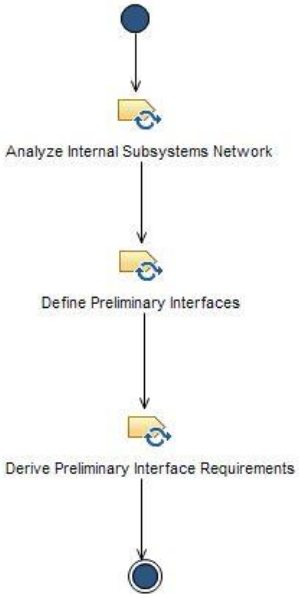

Fig. 153: Interface analysis workflow at subsystem level

The analysis of subsystems network is the first step towards the definition of a low-level network of interfaces. This is performed in tight cooperation with the analysis of functional assemblies, as mentioned in Section 5.2.1, especially when dealing with thermal control subsystems or, in general, hydraulic plants. In fact, "transport" assemblies are crucial to define interfaces and network responsible to move fluids within a specific path. Preliminary interfaces can then be defined for the different elements of the breakdown ad associated requirements can be formulated. The interface analysis at low-level is crucial to design on-board plants, since the network defined within the study are more and more close to the final implementation of the subsystem. The traceability of the different elements is then really important to understand the issues associated to the final allocation of the subsystem on the vehicle concept.

5.2.2.2 Analyse internal subsystems network

The analysis of internal subsystems network follows the method adopted for the analogous step at conceptual design level, where interfaces for the different elements of the breakdown are identified in a preliminary way, without specifying a type or direction. The analysis of low-level interfaces is a bit more complex than the one performed during conceptual design, since the higher level of components makes difficult to describe the interface network without specifying the data

related to the interfaces themselves. The complete description is thus provided within the following section (Section 5.2.2.3) to provide the reader with a clear overview of the designed network within the TEMS, up to equipment level (component level is not yet defined for this subsystem).

5.2.2.3 Define preliminary interfaces

Preliminary interfaces definition starts at assembly level. The TEMS is a highly integrated subsystem within the vehicle architecture, thus embedding a high number of interfaces, characterized by different types. In fact, it shall include thermal and fluid interfaces to manage the cooling process (with liquid and gas), as well as mechanical connections to actuation and power generation equipment. Additionally, data connection is required to control the plant, while structural interfaces with the airframe is crucial to support the different assemblies. The interface network for heat collection assembly is shown in Fig. 154. Thermal and fluid interfaces are highlighted, even if structural interfaces can still be seen (they are not connected to improve diagram readability). Thermal interfaces are used to receive heat from different sources, as specified within product breakdown (Section 5.2.1.6), while a main thermal line goes from collection assembly to transport assembly (red output, top right in Fig. 154). There is also a direct thermal connection between collection and rejection assemblies. Heat collection makes use of both liquid and boiled-off hydrogen to perform cooling, thus requiring both gas and liquid interfaces. The interface concerning the boil-off (cyan) is conceived as bi-directional since this is continuously exchanged between collection and transport equipment (e.g. the exchanger receives fluid from a pipe and then send it to another pipe while going out to another TEMS element). Liquid line (blue) is instead one-directional since the LH2, which comes from the propellant subsystem, is used to cool down only the power plant and it is sent directly to the heat rejection assembly. In addition, a mechanical line (magenta) connects the expander to a gearbox to produce and transfer mechanical power. Heat transport assembly receives boil-off from the propellant subsystem and send it to the rejection assembly (as well as to the collection assembly as already mentioned). A thermal line to rejection assembly is also included. Ultimately, a data interface (green) is required to control and monitor the active equipment of the different assemblies (not shown for picture clarity).

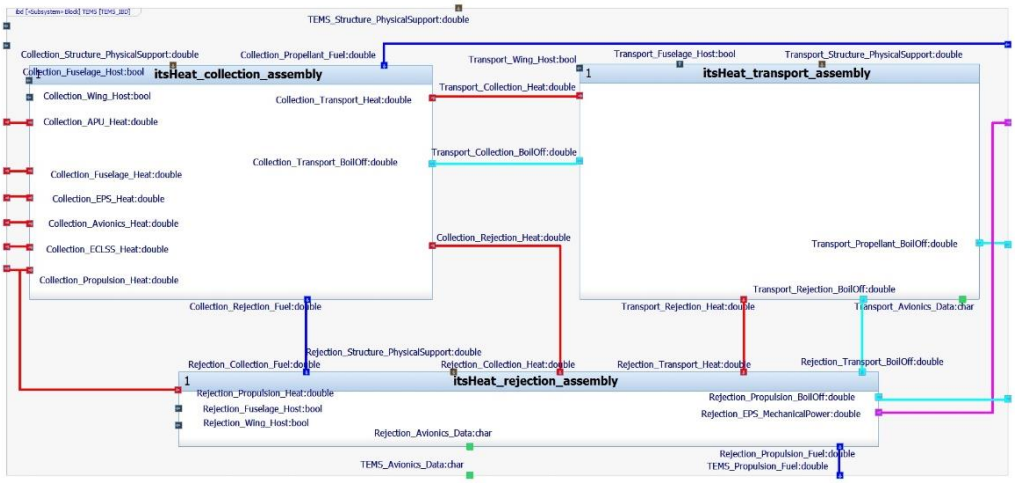

Fig. 154: Interfaces definition at assembly level for TEMS

The details of the different interfaces become clearer when looking at equipment level. Fig. 155 shows the detail related to heat collection assembly. Indeed, the different exchangers receive heat from several sources and use the boil-off coming in to collect the heat and send it back to the transport assembly, together with the fluid itself. Propulsion plant exchanger is also connected to the LH2 line, since it uses liquid hydrogen to cool down the engines assembly. Each exchanger is thus characterized by an input and output scheme for the driving fluid (gas or liquid) as well as for the thermal flow. Additionally, structural interfaces (not shown) are present.

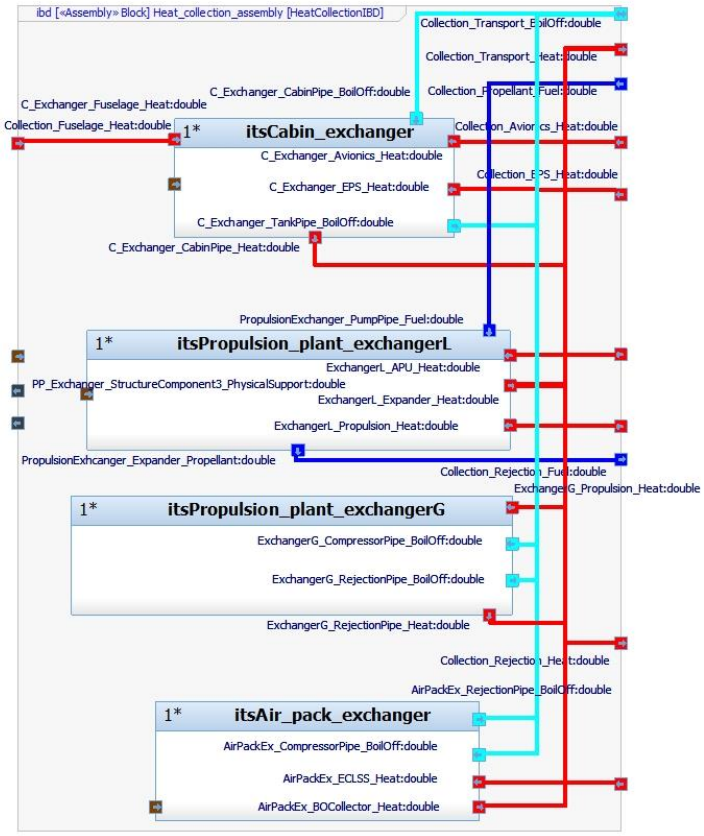

Fig. 155: Interfaces definition at equipment level for heat collection assembly of TEMS

Heat transport assembly interfaces are shown in Fig. 156. Depending on how the TEMS scheme is hypothesized, the different equipment exchange heat and gas to collection assembly or among each other. This is due to the fact that the pipes network is made of different parts communicating either to each other or with elements of the collection assembly directly. It is moreover interesting to notice that there is not LH2 interface within this assembly, since the delivery line of LH2, which shall be interfaced with the liquid exchanger of the propulsion plant, is included within the propellant subsystem (i.e. the delivery line is part of the propellant subsystem not of the TEMS). A single gas output (bottom right) sends the heated boil-off to the heat rejection assembly, together with its thermal energy.

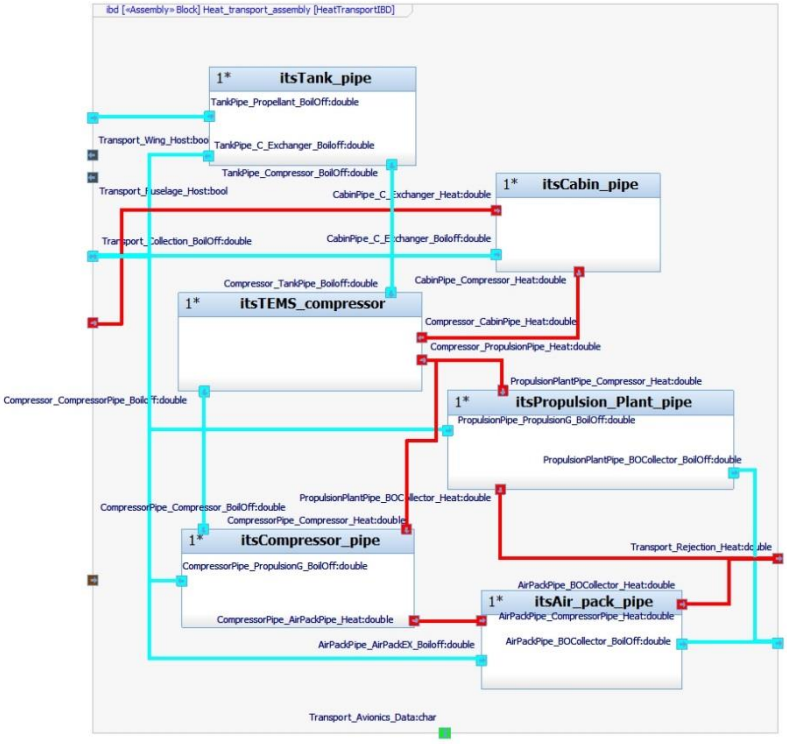

Fig. 156: Interfaces definition at equipment level for heat transport assembly of TEMS

The heat rejection assembly is shown in Fig. 157.

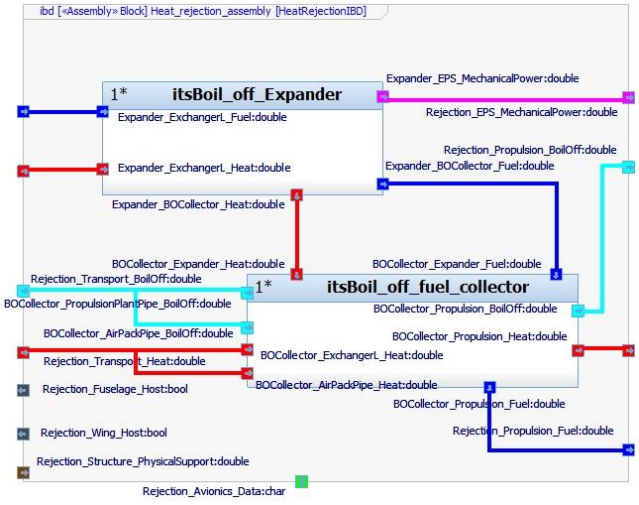

Fig. 157: Interfaces definition at equipment level for heat rejection assembly of TEMS

The boil-off expander receives liquid hydrogen from the regenerative cycle of the power plant, together with its thermal energy. It provides mechanical power to TEMS active equipment and to other elements on board the vehicle (to produce secondary power). Moreover, it sends heat and cooled LH2 to the fuel collector, which mix it with the boil-off received from other assemblies. Ultimately, the two fluids and the heat are transferred to the combustor of the different engines, to produce thrust. As always, data and structural interfaces are always needed to monitor the working cycle of the different elements and to provide airframe connection.

5.2.2.4 Derive preliminary interface requirements

Dedicated interface requirements can be derived from the interface analysis performed at assembly and equipment levels. Assembly and equipment levels interface requirements are included within Section 8.1.7.

5.2.3 Subsystem performance characterization

5.2.3.1 Subsystem performance characterization workflow

The subsystem characterization process represents one of the most common workflow of tasks belonging to the preliminary design phase. It is the core of engineering activities around the sizing of on-board subsystems for a reference vehicle. The process aims at deriving subsystem performance requirements by analysing the related operational environment. This allows deriving the required performance for the subsystem of interest, through the sizing process, and to ultimately analyse the dynamic behaviour of the plant and its components (not shown within the Dissertation). The process is shown in Fig. 158. The workflow starts with the definition of a proper mathematical model for the operational environment of the subsystem, starting from high-level mission analysis. This allows understanding the impact of mission phases on the boundary conditions in which the subsystem is supposed to operate. The characterization of the environment is a mandatory step to analyse subsystem required performance, and, ultimately, to perform a proper sizing of its elements.

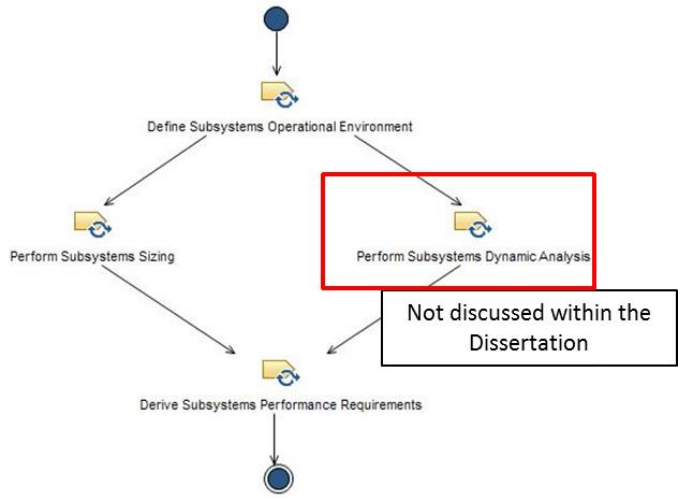

Fig. 158: Subsystem performance characterization workflow

This is the typical situation in which subsystem is sized in its expected most critical conditions. In parallel, it is possible to look at the time or frequency domain to analyse which is the subsystem behaviour as function of mission time. This allows understanding the global trend of operational variables and the impact on performance during a proper simulation. This task is not focused exclusively on most critical operating point, rather looking to nominal conditions during the mission. Both studies can be ultimately used to derive performance requirements related to the subsystem and to its elements, contributing to update the specification. The overall process is reported in the following sections for the case study of TEMS.

5.2.3.2 Define subsystem operational environment

As example of environment identification, the characterization of TEMS operating condition is mainly constituted by the definition of thermal equilibrium considering both external and internal heat sources. External equilibrium shall consider the heat coming from atmosphere drag (convection), while internal contributions come mainly from propulsion plant, payload and subsystems. In order to compute the different thermal loads, a proper software application has been developed. For what concerns the external equilibrium, the code is based on literature studies concerning *"a zero-dimensional steady-state analysis based upon a convective-radiative-conductive heat transfer balance whereby the external geometry of the vehicle is represented by flat plates"* (Steelant , et al., 2015). Moreover, the model has been updated with new algorithms for the

computation of friction coefficient, for the evaluation of internal equilibrium within the different compartments and for the estimation of hydrogen boil-off fraction. In order to provide an overall computation of thermal state for the vehicle surfaces, consisting in *"the temperature of the gas at the wall surface (or directly the temperature of the wall if low-density effects are not present), the temperature gradient at the wall as well as the heat flux acting on the surface"* (Hirschel, 2005), a proper parametrization of four main zones of the aircraft is proposed (Fig. 159):

- Forward Fuselage (Area 1), from the intake leading edge up to the crotch region, including propellant tanks and subsystems compartments;
- Central Fuselage (Area 2), from crotch region up to the end of 2D nozzle, including power plant, cabin compartment, propellant tanks and other subsystems;
- Aft Fuselage (Area 3), from the end of 2D nozzle up to the trailing edge of the vehicle, including mainly propellant tanks and subsystems;
- Wing (Area 4 and 5), including propellant tanks and subsystems.

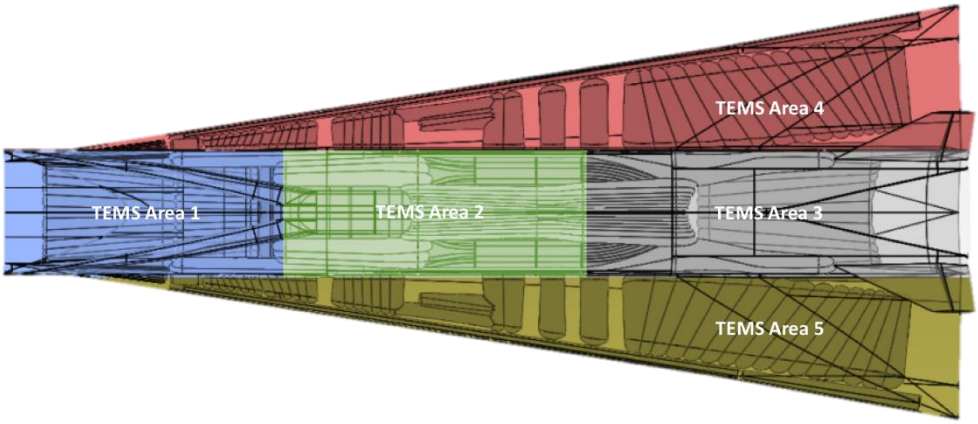

Fig. 159: Area parametrization for thermal properties evaluation on MR3 vehicle

The application can be set-up to adapt to different vehicle configurations. A simplified mission profile is taken as reference to perform the computation. The different zones are characterized starting from the data associated to mission phases environment. In fact, the different aircraft sections represent the on-board operating environment for the TEMS, being affected by the vehicle operational scenario described within the high-level mission concept (Section 4.5.2.7). The

hypersonic cruise has been selected as most critical phase and as basis for subsequent sizing of the subsystem. The external heat balance for each zone is computed as in (50).

$$h_{conv}(T_{rec} - T_w) = \epsilon\sigma T_w^4 + \frac{k}{t}(T_w - T_{LH2}) \quad (50)$$

This equation represents the equilibrium between the incoming heat flux caused by the aerodynamic heating, as well as the outgoing heat rejected through radiation (radiation cooling of the surface) and transferred to the hydrogen tanks through conduction, where:

T_w is the external wall temperature in $[k]$
ϵ is the emissivity of the surface material
σ is the Boltzmann constant, equal to $1{,}38 \cdot 10^{-23}\left[\frac{J}{K}\right]$
k is the global conductivity of the layers of materials between the surface and the tank in $\left[\frac{W}{mK}\right]$
t is the thickness of the layers of materials between the surface and the tank in $[m]$
T_{LH2} is the temperature of liquid hydrogen inside the tanks (equal to $20\ K$)

Recovery temperature can be computed as in (51).

$$T_{rec} = T_\infty\left(1 + \frac{R(\gamma - 1)}{2}M_\infty^2\right) \quad (51)$$

Where:

T_∞ is the static air temperature of the incoming flow in $[K]$
$R = Pr^{1/3}$ is the recovery factor (for turbulent flow) based on Prandtl number

The convective heat transfer coefficient can be computed as in (52).

$$h_{conv} = St \cdot \rho_\infty \cdot V_\infty \cdot c_p \quad (52)$$

Where:

ρ_∞ is airflow density in $\left[\frac{kg}{m3}\right]$
V_∞ is incoming flow speed in $\left[\frac{m}{s}\right]$

c_P is the specific heat at constant pressure for the considered airflow in $\left[\frac{J}{kgK}\right]$

and

$$St = \frac{0.074}{Re^{\frac{1}{5}}} \cdot \frac{1}{2 \cdot 0.95} \qquad (53)$$

Is the Stanton number derived following the expression for the skin friction coefficient of turbulent flow through the Reynolds number.

Additionally, in order to consider internal heat balance contributions, 6500 $\frac{W}{m^2}$ are added in those zones where powerplant is present nearby, whilst 200 W are considered to account for the thermal power produced by a single human body. Ultimately, an operating temperature of 323 K for subsystems compartment is considered to account for electrical and electronic heating. The internal thermal balance is thus defined as in (54) for each zone.

$$q_{engines} + q_{pax\&crew} + q_{sys} = \frac{k_{int}}{t_{int}}\left(T_{w_{int}} - T_{LH2}\right) \qquad (54)$$

Where thermal power coming from the different sources is distributed over compartments reference (interface) areas. Following the computation of thermal loads, using the parametrization specified above, the trend reported in Fig. 160 has been obtained for what concerns average external skin temperature.

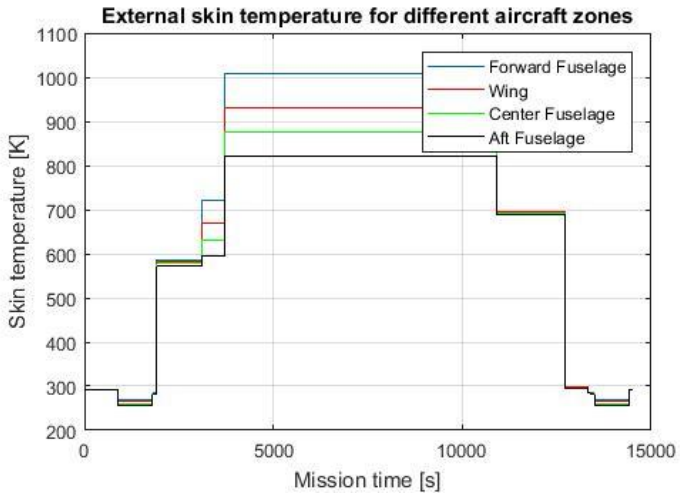

Fig. 160: External skin temperature trend during the mission

The forward fuselage reaches the highest value, together with the wing, around 900 – 1000 K in cruise (average). This temperature trend corresponds to the average heat flux reported in Fig. 161.

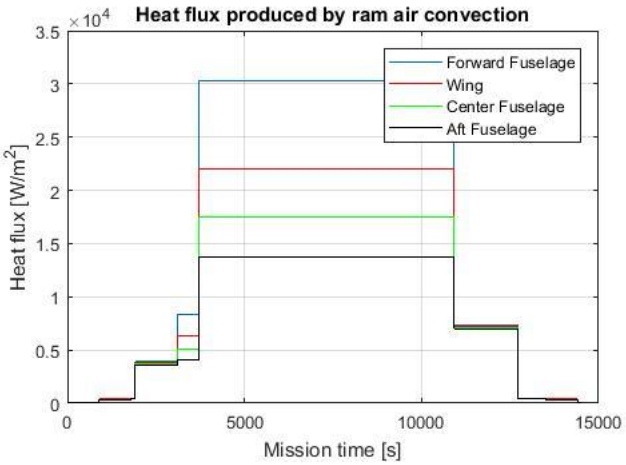

Fig. 161: Heat flux acting on different aircraft zones because of aerodynamic heating

As for temperature, the highest value of heat flux is reached in cruise, with an average of about $30\frac{kW}{m^2}$ for forward fuselage. The overall heat load accumulated during the mission can be computed by integrating the heat flux over mission time, as reported in Fig. 162. Globally, the vehicle accumulates a heat load of around 22 GJ throughout the reference mission.

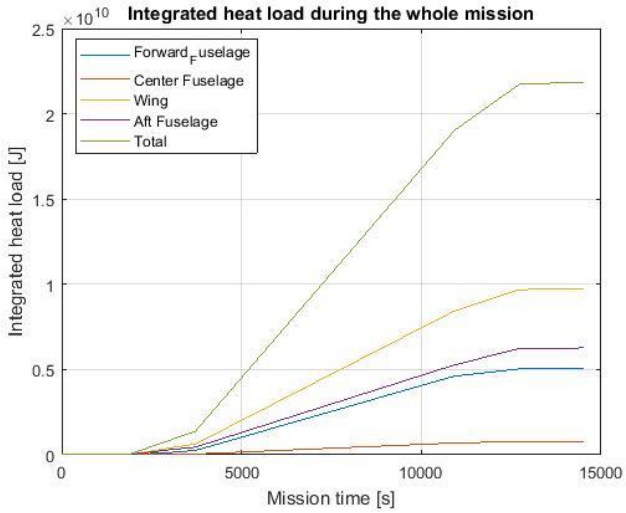

Fig. 162: Total heat load accumulated during the reference mission

Looking at the temperature values in each compartments, the results of the preliminary assessment show that the conduction-based heat exchange is not enough to guarantee proper comfort level for passengers and survivability limit for subsystems. For this reason, an additional cooling equipment shall be introduced within the system architecture. This new element shall make benefit of the boil-off fraction produced by the different heating sources. The produced boil-off can be computed as in (55).

$$\dot{m}_{BO_p} = \frac{S_{ref}\frac{k}{t}(T_w - T_{LH2})}{H_{vap}} + \frac{S_{ref_{int}}\frac{k_{int}}{t_{int}}\left(T_{w_{int}} - T_{LH2}\right)}{H_{vap}} \quad (55)$$

Where

H_{vap} is the enthalpy of vaporization for the hydrogen $\left[\frac{J}{kg}\right]$

In parallel, the required boil-off to cool down the air within passengers and subsystems compartments can be computed using, as preliminary estimation, the basic heat exchanger model proposed in (56).

$$\dot{m}_{BO_r} = \frac{S_{ref}h_{conv_{forced}}(T_{compartment} - T_{BO})}{c_{p_{BO}}(T_{BO_{out}} - T_{BO_{in}})} \quad (56)$$

Where

$h_{conv_{forced}}$ is forced convection heat coefficient, set to $100\left[\frac{W}{m^2K}\right]$
$T_{compartment}$ is air temperature within the compartments, set respectively to 309 and 323 $[K]$ in case of manned or unmanned zones
$T_{BO_{in}}$ and $T_{BO_{out}}$ are boil-off temperature in the range of 150 – 240 $[K]$
$c_{p_{BO}}$ is the specific heat at constant pressure for the H2 gas

Following the comparisons of the results it is possible to identify a proper boil-off rate as indicated in Fig. 163.

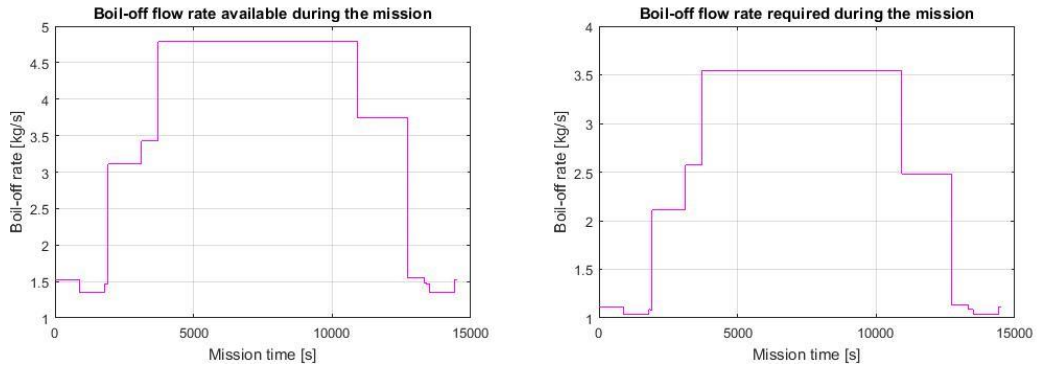

Fig. 163: Comparison between produced (available) and required boil-off rates

Results show that a value of about 3.5 kg/s of hydrogen boil-off is enough to keep compartments temperature within the limits. The resulting boil-off mass produced during the mission can be computed by integrating the boil-off rate throughout the trajectory, as indicated in Fig. 164.

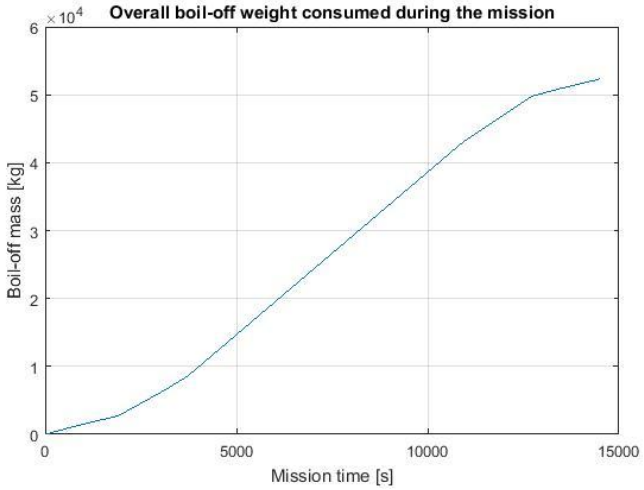

Fig. 164: Total mass of hydrogen boiled-off during reference mission

Approximately, 52 tons of hydrogen evaporate, producing boil-off. Results have been validated with those obtained for LAPCAT MR2 configuration, reported in (Steelant & Fernandez Villace, 2015), where a few differences can be highlighted, even the analyses appear to be in line. While temperature estimation matches the MR2 results (Fig. 165), total heat load appears to be lower than for LAPCAT case study (Fig. 166). This is mainly due to the exploitation of a simplified model

based on the adoption of average values for temperature and heat fluxes (which induce an underestimation of loads in critical regions such as leading edges).

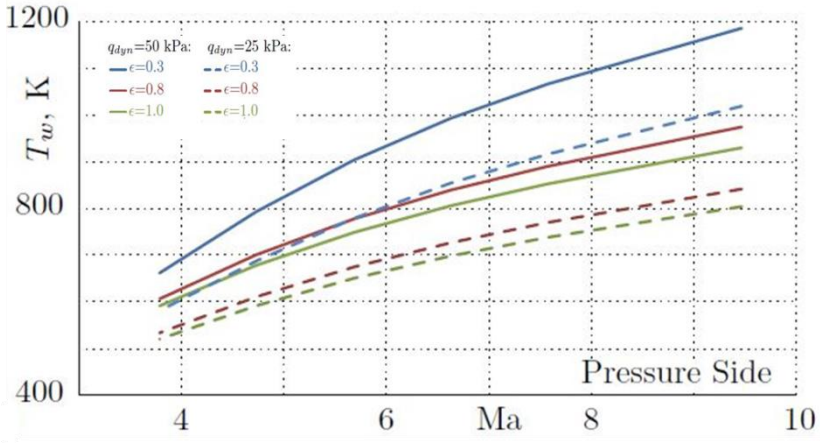

Fig. 165: Conductive-Radiative equilibrium solution for LAPCAT MR2.4 (Steelant & Fernandez Villace, 2015)

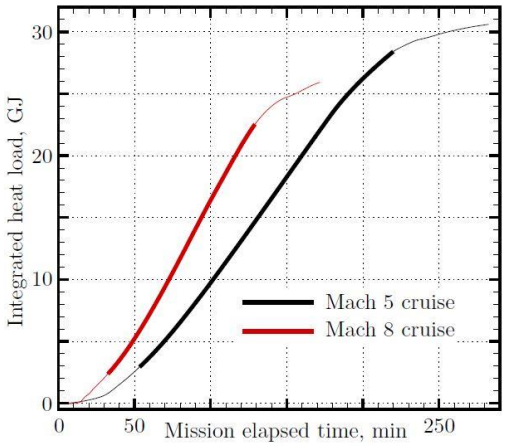

Fig. 166: Predicted heat load for LAPCAT MR2.4 vehicle configuration (Steelant & Fernandez Villace, 2015)

This produces a required boil-off rate which is half the one predicted for LAPCAT. Moreover, the overall boil-off is lower as well (around 20 tons less than what expected for MR2), as shown in (Fig. 167).

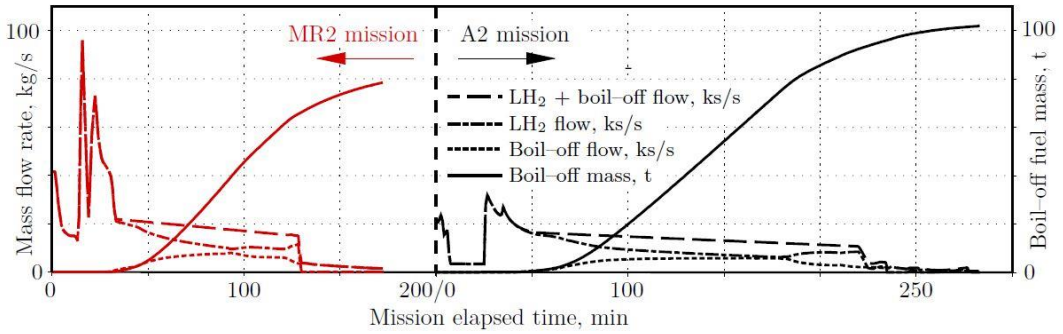

Fig. 167: Boil-off rate and total mass for LAPCAT MR2.4 case study (Steelant & Fernandez Villace, 2015)

The model applied is anyway characterized by a set of simplified equations and the mission itself is re-arranged for a steady-state analysis (mission phases have instantaneous transition, speed is considered constant during a phase etc…). For this reason, even considering a slightly different vehicle configuration, results may be underestimated. However, heat flux computation appears in line with similar aircraft concepts, like the one associated to the X-34 (Section 1.1), provided by (Mahulikar, 2005). Results of this analysis are taken into account when formulating performance requirements, in Section 5.2.3.4.

5.2.3.3 Perform subsystem sizing

Sizing of performance for the elements of a thermal control subsystem usually aims at evaluating the mechanical and thermal power managed by active and passive equipment. Three main active components can be identified within the TEMS: the boil-off compressor, the expander and the feeding pump. The turbine is particularly critical for the power budget of the subsystem, since it is in charge of producing the power needed for the TEMS elements, while guaranteeing a certain amount of extra power for other on-board subsystems. TEMS sizing can then start from the evaluation of the power associated to the working cycle of turbomachinery. Particularly, it is possible to derive the power required by the compressor as in (57).

$$P_{compressor} = \frac{1}{\eta_C} c_{p_{BO}} \dot{m}_{BO} \left(T_2^\circ - T_1^\circ\right) \quad (57)$$

Where

η_C is the adiabatic efficiency of the compressor
T_2° is the total temperature at compressor outlet $[K]$
T_1° is the total temperature at compressor inlet in $[K]$

Furthermore, it is possible to consider that

$$T_1^\circ = T_{BO}\left(1 + \frac{\gamma_{BO} - 1}{2} M_{BO}^2\right) \quad (58)$$

$$T_2^\circ = T_1^\circ\left(1 + \frac{1}{\eta_C}\left(\beta_C^{\frac{\gamma_{BO}-1}{\gamma_{BO}}} - 1\right)\right) \quad (59)$$

and

$$M_{BO} = \frac{\dot{m}_{BO}}{\rho_{BO} A_{ref} c_{BO}} \quad (60)$$

Where

M_{BO} is the Mach number of boil-off flow within the pipes
c_{BO} is the speed of sound of the flow within the pipes in $\left[\frac{m}{s}\right]$
A_{ref} is the collector pipe reference cross-section area in $[m^2]$
β_C is the compressor pressure ratio

Moreover, the power produced by the expander can be computed as in (61).

$$P_{expander} = \eta_T c_{P_{LH2}} \dot{m}_{LH2}\left(T_3^\circ - T_4^\circ\right) \quad (61)$$

Where

η_T is the adiabatic efficiency of the turbine
$C_{P_{LH2}}$ is the specific heat at constant pressure for the liquid hydrogen $\left[\frac{J}{kgK}\right]$
$\dot{m}_{LH2}$ is the mass flow of liquid hydrogen required by the powerplant in $\left[\frac{kg}{s}\right]$
T_4° is the total temperature of the flow at turbine outlet in $[K]$
T_3° is the total temperature of the flow at turbine inlet in $[K]$

The expander exploits in fact the liquid hydrogen of the feeding line to produce power. Temperatures at expander outlet and inlet are determined depending on the variables of the regenerative cycle of the power plant (Balland, et al., 2015).

In order to evaluate the power remaining for the different on-board subsystem, it is possible to estimate the pumping power required during the mission, since all required data are already available. The power required to the pump is determined by evaluating the pressure losses within the delivery pipes and considering the pressure level required at the Fuel Control Unit (FCU) of the engines as well as the expected mass flow. The friction coefficient inside the pipes, used to evaluate the distributed pressure losses can be computed as in (62), where an explicit version of Colebrook – White formulation is used, known as approximated Haaland model (Keady, 1998)

$$\frac{1}{\sqrt{\lambda}} = -1{,}8 \log\left(\left(\frac{\varepsilon_D}{3{,}7}\right)^{1{,}11} + \left(\frac{6{,}9}{Re_{LH2}}\right)\right) \qquad (62)$$

where

ε_D is the relative roughness of the pipe
λ is the friction coefficient

Distributed pressure losses can then be computed as in (63)

$$p_{loss_{distributed}} = \frac{1}{2}\rho_{LH2} v_{LH2}^2 \lambda \left(\frac{l}{d}\right) \qquad (63)$$

where

l is the length of delivery line in $[m]$
d is the pipe diameter in $[m]$

Additional losses can be considered, such as concentrated losses due to circuit elements (not know a priori at this stage of analysis) and due to manoeuvres, or differences in height within the delivery lines. With the data specified in (Balland, et al., 2015) the trend (Fig. 168) of the required delivery pressure as function of volumetric flow can be obtained. Depending on the required amount of propellant, delivery pressure may vary from 61 to 75 bar.

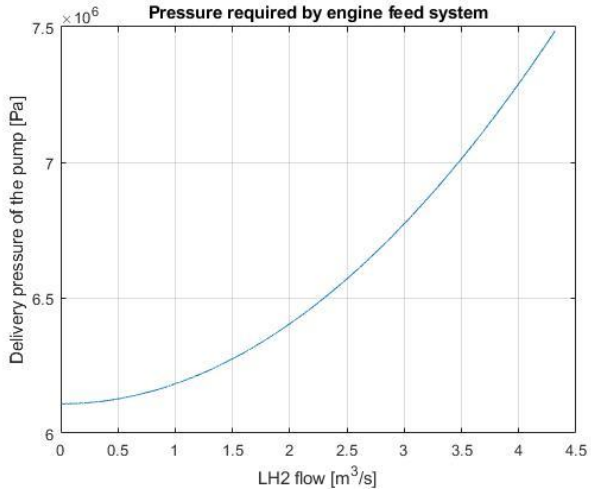

Fig. 168: Delivery pressure required for engine pumps

The overall power budget is shown in Fig. 169. As it can be seen the expander is capable of generating a very high of power, even if the amount that can be used for subsystems, because of losses and efficiencies, is around 50 MW. This is the extra power that can be used to feed other on-board utilities. A similar value is consumed by boil-off compressor (40 MW), while pumps require around 5-10 MW. Values are in line with the estimation of (Balland, et al., 2015). The TEMS is then a very important source of power on-board and, even if it can work only with engines active, it can be efficiently used during ramjet and scramjet operations.

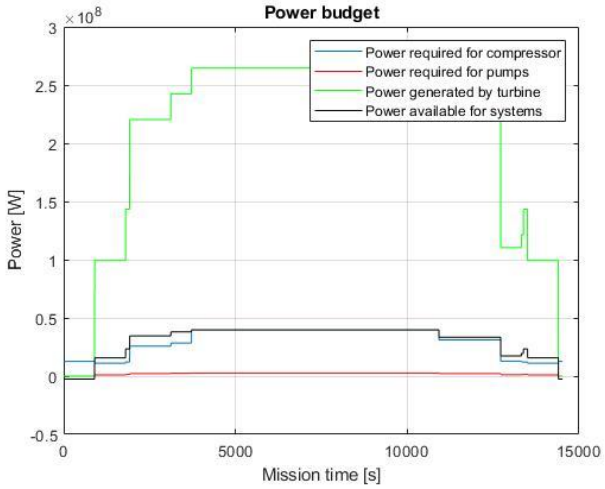

Fig. 169: Power budget for TEMS

The analysis allows understanding that the power levels are quite far from the results related to conventional aircraft, where power peaks are around 1 MW for the entire vehicle. The study is, however, simplified, and aims at providing a preliminary result concerning power sizing for the elements of the subsystem, looking at an approximated mission profile. Results are already plotted as function of mission time, even if most of the phases are considered as steady conditions and transitions are not considered.

5.2.3.4 Derive subsystem performance requirements

The results coming from the subsystems sizing can be used to enrich the low-level requirements specification, since they can be directly translated in performance requirements for the characterization of the related subsystems and components. Derived requirements can be used to quantify functional capabilities derived in Section 5.2.1. For what concerns the TEMS case study, requirements reported in Section 8.1.7 can be derived, summarizing the main results provided in Section 5.2.3.3.

5.2.4 Subsystem physical characterization

5.2.4.1 Subsystem physical characterization workflow

Both sizing and dynamic analysis processes are focused on the determination of either static or dynamic results for operating parameters of subsystems elements. Typical examples of operating parameters are physical variables like speed of fluid or mass flow, pressure, temperature, power or even characteristics of specific equipment like rotating speed, pressure ratios etc…

Usually, the identification of proper physical characteristics of the sized equipment is not part of the sizing process during conceptual and preliminary design, being rather the main goal of the physical characterization process, here described (Fig. 170). In fact, *"it has to be noticed that performance and physical modelling techniques are quite different one to each other because mainly because of their different final aim: performance analysis targets the identification of the performance behaviour in a quantitative way, while physical analysis is usually based on statistical approaches with a very different fidelity level"* (Fusaro, et al., 2019). As consequence, the process starts with the analysis of reference subsystems and related physical models that can be used to derive a suitable set of algorithms to perform the identification of characteristics, through

tailored approach. Subsequently, the operating parameters to be used for the development of physical models are identified in a general-purpose way. This allows focusing on those parameters that can be used within a certain engineering domain to characterize the behaviour of a specific machine or component. Once the model is ready to be exploited, the analysis moves to the case study, for which it is necessary to select a subset of operating parameters to perform the tailoring process. In fact, even if the definition of so-called estimation relationships can be hypothesized already at higher level, when looking at typical domain-oriented operating parameters, a dedicated low-level analysis is necessary to adapt the model to the selected case study. The identification of suitable and applicable relationships is thus performed in parallel to the identification of case study-related operating parameters. This allows overcoming the problem of lack of statistical data, in case of highly innovative products, since proper semi-empirical models can be formulated by enriching existing literature models with proper factors and coefficients related to technology type and level. Typical results of this process are so-called subsystem breakdowns, usually consisting of mass and volume budgets for the different elements, as well as of estimation of components dimensions. Even if this approach is theoretically different from performance analysis, physical characterization makes benefit of the data obtained during sizing and even dynamic analysis for the selected subsystem, since the understanding of operating parameters and behaviour of the plant is a crucial step to move towards physical characterization. The rating of the subsystems elements is in fact fundamental to tune the relationships and to obtain a reliable estimation of physical characteristics.

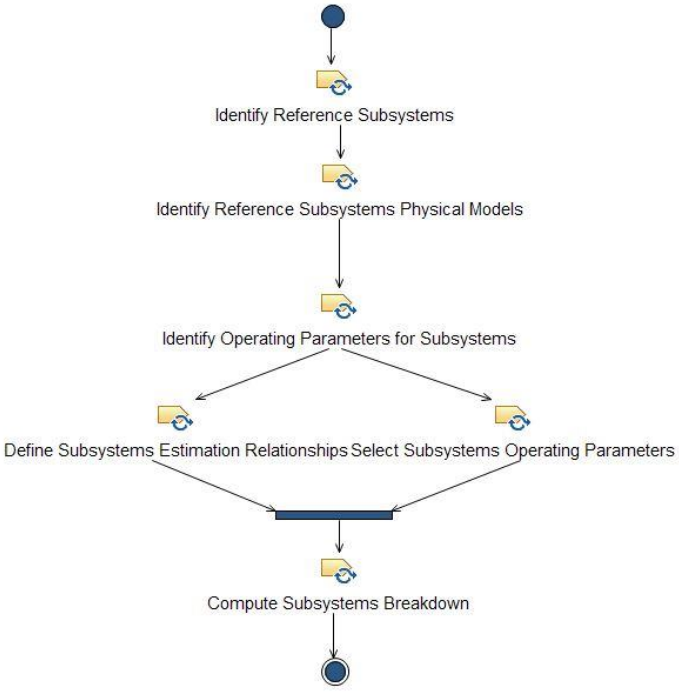

Fig. 170: Subsystem physical characterization workflow

5.2.4.2 Identify reference subsystems

The identification of reference subsystems and related elements is a preparatory step towards the development of the physical models. This task is conceived to select similar plants to the one investigated within the case study, so to set the boundaries of the analysis and to properly identify the elements of subsystems breakdown that shall be characterized. For what concerns the TEMS, it is clear that suitable reference subsystems belong to the thermal control domain, even if the multi-functional features, embedded within the plant, brings also characteristics typical of environmental control and propellant subsystems on the foreground. Available references in literature (Balland, et al., 2015) provide information related to its sizing, which, together with the results of the process described in Section 5.2.3, allows preparing the physical analysis. From the product breakdown of the TEMS (Section 5.2.1) and its qualitative scheme (Section 3.2), it is possible to identify several active and passive pieces of equipment. The main active components of the TEMS (compressor, turbine and pump) have already been preliminary sized providing power budget in specific working conditions (design point) as reported in Section 5.2.3. Additional considerations have been performed on passive components, such as tanks

dimensions and pipes diameters (Fig. 171) (Balland, et al., 2015), as well as on elements from other subsystems which, still, have important interfaces with the TEMS itself (e.g. delivery pump).

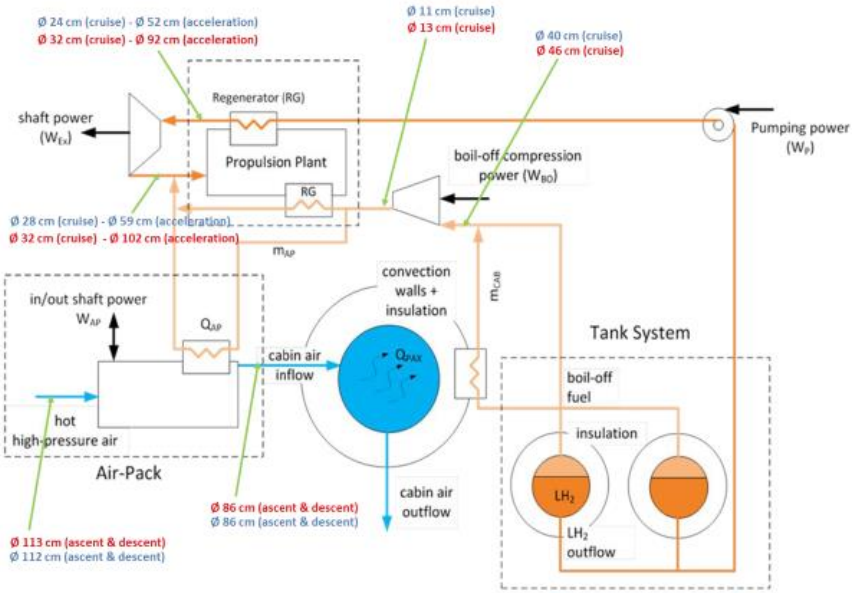

Fig. 171: Preliminary evaluation of TEMS pipes diameter (Balland, et al., 2015)

Moreover, different types of heat exchangers have been hypothesized for the different portions of the scheme of the systems (gas-gas, liquid-gas), for which a preliminary evaluation of thermal energy exchanged can be made depending on the operating conditions. The following sections thus suggest a new approach to estimate the mass, dimensions and volumes of the components listed in Table 20, allowing the physical characterization of the components of the TEMS.

Table 20: List of TEMS elements to be characterized through physical analysis

Active Components	**Passive Components**
Turbopumps[2]	Tanks
Turbine	Pipes
Compressor	Heat Exchangers

[2] The physical analysis for TEMS turbopumps is taken from R. Fusaro, D. Ferretto, N.Viola, V. Fernandez Villace, J. Steelant *"A methodology for preliminary sizing of a Thermal and Energy Management System for a hypersonic vehicle"*, The Aeronautical Journal, 123 (1267), Cambridge University Press, doi 10.1017/aer.2019.109, 2019, (Fusaro, et al., 2019). The summary of the process reported in Sections 5.2.4.3 to 5.2.4.7 is original part of Author research.

5.2.4.3 Identify reference subsystems physical models

Different design and sizing models dealing with the components listed in Table 20 are available in literature. "*However, in general, these sizing approaches are almost exclusively related to the definition of the components performance of machine and devices, with small contributions upon the correlation of these performance to physical characteristics of the components. This is a typical issue of active components that during the conceptual design phase are mainly characterized by focusing on the operating parameters and conditions. Conversely, passive components are mainly characterized on the basis of their physical features (e.g. weight and thickness for tanks and pipes, etc…)"* (Fusaro, et al., 2019). Performance characteristics mainly differ from physical ones because, generally, the former can be computed by means of exact and closed mathematical formulations, which rely on well-established models (Rangwala, 2005) (Larson, et al., 1995), whilst physical aspects can only be hypothesized following best practices or general high-level requirements (usually depending on integration issues) acting as guidelines (Saunders, 1979). "*Thus, it is quite common for active components, to compute performance directly, whilst physical characteristics are derived through statistical approaches or legacy data coming from literature analysis and/or reports resulting from test campaigns. The so-called Weight Estimation Relationships (WERs) are, in fact, equations which aim at proposing mass derivation strategies based upon specific drivers coming from the operational parameters of the components collected as statistical population* (Sagerser, et al., 1971)" (Fusaro, et al., 2019). This approach shows some weaknesses, typically related to the quality of the components database upon which the statistical analysis is based, and, even if it represents a good starting point to partially bridge the gap between physical and performance derivation, it still remains far from an exact derivation (actually it is an approximated result). On the other hand, passive components can be easily characterized from a physical standpoint, since the main requirements associated to their design come from the necessity to withstand operating conditions from a structural point of view (Larson & Pranke, 1999). In general, it is thus possible to point out that:

- *"Performance and physical analyses are characterized by a different level of accuracy of the results, coming from exact / closed mathematical formulations and approximated estimations / qualitative hypotheses respectively.*

- *Physical estimations for active components available in literature are generally based upon statistical derivation, which is highly dependent on the technological characteristics of the historical period in which the population was built.*
- *Physical estimations for passive components are instead more reliable, since they are referring to structural resistance and strength required to operate within the limits prescribed by the environmental conditions (and by regulations / standards)"* (Fusaro, et al., 2019).

Many references propose semi-empirical formulation for the derivation of physical characteristics of the main components starting from assumptions and models related to their performance. The approach described hereafter aims at overcoming the limits of the statistical derivation, suggesting the development of proper semi-empirical models to increase the accuracy of formulations leading to the estimations of physical characteristics mass, dimensions and volumes, based directly upon operational parameters. The main difference with respect to the currently available methods is that, instead of using a database of components to build an Estimation Relationships (ERs), physical data are derived directly from operating parameters (using those performance relationships, characterized by being exact, in a convenient way) and then compared to available values for validation purposes only. The introduction of coefficients and corrective parameters is adopted only for those configuration and fabrication characteristics that cannot be included in other ways.

5.2.4.4 Identify operating parameters for subsystems

The derivation of correlations allowing the estimation of physical characteristics as function of a set of operational parameters and performance is a challenging and demanding issue to be solved. The proposed approach "*aims at deriving a common integrated methodology that can be applied to a wide range of active and passive components in order to provide reliable model for the prediction of their physical characteristics. Moreover, each estimation model shall be conceived to have an easy integration within the overall design approach, exploiting, the output of performance analysis as main parameters of the mathematical equations to predict mass, volume and dimensions of the devices"* (Fusaro, et al., 2019). An overview of the overall derivation process is qualitatively reported in Fig. 172

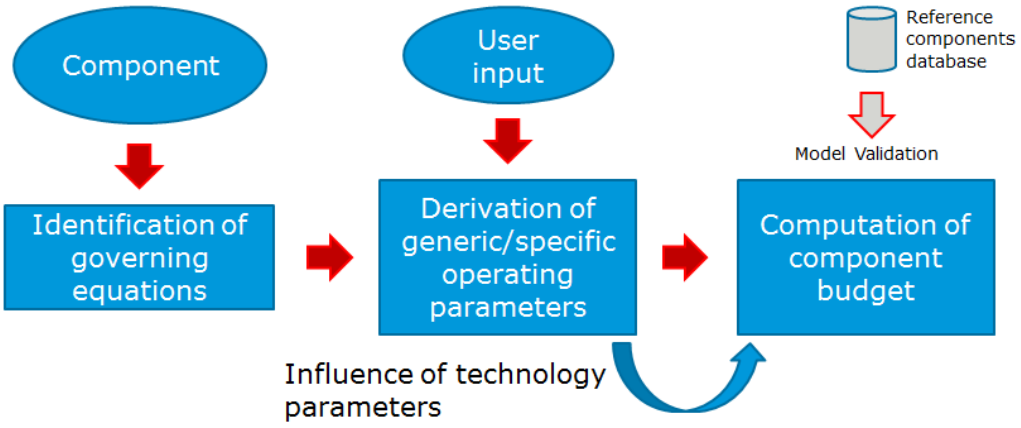

Fig. 172: Operating parameters identification for physical breakdowns computation (Fusaro, et al., 2019)

The methodology leading to the formalization of proper sizing parametric equations can be split into three different steps. "*The first one is related to the identification of the set of governing equations for the under-analysis component. This can be done by referring to the applicable scientific literature describing the behaviour of specific devices, looking for the constituting relationships bringing together the main operating parameters. These parameters are the core of the whole method since they are the basis for the derivation of the relationships that allow the computation of power budget. A proper classification of these parameters is performed within the second phase of the method, with the objective of analysing their impact on the governing equations. The identification of the relationships, occurring among parameters and between variables and parameters, allows to express each variable (e.g. mass, diameter, etc…) as a function of this set of parameters. Then, in the third phase, thanks to the exploitation of results coming from empirical estimations, simulations or literature, it is possible to find out the proper mathematical formulations to express those relationships occurring between each variable and its subset of parameters"* (Fusaro, et al., 2019). In this context different kind of parameters or "drivers" can be identified depending on the variables they represent. For the purpose of this study, four different categorizes have been identified:

- Generic Operating Parameters (GOP);
- Specific Operating Parameters (SOP);
- Secondary Parameters (SP);
- Technology Parameters (TP).

A brief overview of meanings and characteristics of these parameters is provided in Table 21.

Table 21: Classification of estimation drivers

Type of parameter	**Acronym**	**Description**	**Example of parameters**
Generic Operating Parameter	GOP	Variables related to operating conditions of a general component (performance). They are not specific for a kind of machine but they can be used for different components.	n rotational speed D diameter Q volumetric flow (and mass flow) H head rise (and p pressure rise)
Specific Operating Parameter	SOP	Variables related to operating conditions of a specific component. They may be expressed in non-dimensional format.	σ speed number (and Ns - Specific speed) δ diameter number (and Ds - Specific diameter)
Secondary Parameter	SP	Variables related to operating conditions of a specific component. They are usually functions of SOP since they represent very detailed aspects of the component.	u, c, w peripheral, absolute and radial velocities
Technology Parameter	TP	Coefficients that depend upon the kind of component and usually refer to architecture and technology level	Ñ number of stages Ũ presence of specific components (inducers for cavitation problems etc…)

Ultimately, "*when dealing with the construction of an estimation model, an important aspect to be considered, is the limited availability of data that imposed a pruning of the parameters to be used in conceptual design phases. In fact, since the model is conceived to host some determined variables in its expressions, it is important that the user may have access to these kinds of information in order to*

be able of performing the computation (e.g. it could be difficult to ask the user for a specific value of the tangential speed of the flow over an impeller blade, being easier to ask for general performance like the mass flow and then implementing a proper equation to derive it where it is necessary in the model). In other words, it is necessary to decide which drivers among the GOP, the SOP and the SP shall be used to make the model applicable at the proper design level" (Fusaro, et al., 2019). Looking at the formal representation of typical equations adopted for physical characterization it is possible to say that, since the governing equations $\mathcal{G}$ can be usually represented as in (64)

$$\mathcal{G} = g(GOP, SOP) \quad (64)$$

The final estimation relationship $\mathcal{F}$ will be assembled (65) as a function of the aforementioned drivers

$$\mathcal{F} = f(\mathcal{G}, SP, TP) \quad (65)$$

where

$$SP = \tilde{f}(SOP) \quad (66)$$

5.2.4.5 Define subsystem estimation relationships

The definition of estimation relationships for the elements of the subsystem (Table 20) is provided in this section. Both active and passive components are described hereafter.

Turbopumps[3]. *"Turbopumps are widely used devices for different aerospace applications, from engine feed (typically for rockets), to thermodynamics cycles that require moderate to high power. Different models for performance estimations are present in literature, starting from theoretical derivation of the operational parameters* (Sobin, 1974). *Moreover, some legacy data, referring to some specific design points, are available and can be used to statistically derive mass and sizing models* (Campbell & Farquhar, 1974) (Saunders, 1979)*"* (Fusaro,

[3] The physical analysis for TEMS turbopumps is taken from R. Fusaro, D. Ferretto, N.Viola, V. Fernandez Villace, J. Steelant *"A methodology for preliminary sizing of a Thermal and Energy Management System for a hypersonic vehicle"*, The Aeronautical Journal, 123 (1267), Cambridge University Press, doi 10.1017/aer.2019.109, 2019, (Fusaro, et al., 2019). A summary is reported in this section.

et al., 2019). Typical domain best practices use to represent this kind of machines through dimensionless or specific parameters like the specific speed N_S and diameter D_s

$$N_s = \frac{NQ^{1/2}}{H^{3/4}} \quad (67) \qquad D_s = \frac{DH^{1/4}}{Q^{1/2}} \quad (68)$$

where

N is the rotating speed [rpm]
Q is the volumetric flow rate (usually expressed in imperial units as [gpm])
H is the head rise [ft] (as far as imperial units are concerned)
D is the diameter of the machine [ft] (as far as imperial units are concerned)

These numbers can be used to compare and rate different turbopumps by representing their operating maps on a single diagram, known as Balje diagram (Dick, 2015). Aforementioned variables can be also used to derive other constitutive parameters. Simplifications of the design problem are proposed in literature (Epple, et al., 2010), for preliminary sizing and characterization purposes, by hypothesizing a working point for a specific machine located at optimum efficiency. This approach allows defining an optimum value for volumetric flow rate, head rise and rotating speed of the equipment to be considered for the analysis. In this context, specific speed and diameters are substituted by speed σ (Dick, 2015) and diameter δ numbers

$$\sigma = 0{,}355\Omega_s \quad (69) \qquad \delta = \frac{\sqrt{\pi}}{2^{3}/_{4}} D_s \quad (70)$$

with

$$\Omega_s = \frac{\Omega Q^{1/2}}{Y^{3/4}} \qquad (71)$$

where

Ω_s is the specific speed with reference to Ω
Ω is the rotating speed [rad/s]
Q is the volumetric flow rate [m^3/s]
$Y = gH$ is the specific head [J/kg]

Speed and diameter numbers can thus be effectively used to represent a simplified working condition for the machine, representing, ultimately, the governing equation from which it is possible to obtain physical breakdowns, in the optimal situation, as function of the variables reported in (72).

$$\mathcal{G} = g(GOP) = \ g(\sigma, \delta) = g(N, Q, H, D) \quad (72)$$

The derivation process of the governing equation can be represented as in Fig. 173.

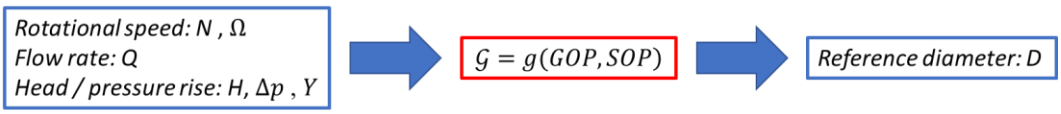

Fig. 173: "*Variables flowchart for input/output of governing equation of turbopumps*" (Fusaro, et al., 2019)

From the analysis of optimum efficiency, it is possible to derive directly the diameter number, re-arranging the equation of speed number, defining the system of equations reported in (73).

$$\begin{cases} \sigma = \dfrac{1}{\sqrt{\pi}} \dfrac{\Omega Q^{1/2}}{(2Y)^{3/4}} \\ \eta_{opt} = 1 - \dfrac{1}{4\delta^2}\left(\dfrac{4}{\delta^2} + \dfrac{1}{\sigma^2}\right) \end{cases} \quad (73)$$

Once the diameter number is derived, it is straightforward to obtain the specific diameter (70) as well as the reference diameter for the turbopump (68). Governing equations are thus made of the following operating parameters (Table 22).

Table 22: *"List of operating parameters for turbopump governing equations"* (Fusaro, et al., 2019)

Parameter	**Type of parameter**
Volumetric mass flow Q	GOP - Input
Head rise (and related variables) H	GOP - Input
Rotational speed N	GOP - Input
Efficiency η	GOP - Input
Specific speed Ω_s	SOP

Specific diameter D_s	SOP
Speed number σ	SOP
Diameter number δ	SOP
Flow coefficient φ	SOP
Head coefficient ψ	SOP
Impeller blade angle β	SP
Absolute, relative and radial velocities c, u, w	SP

The reference diameter, usually representing the impeller one, is the core physical parameter through which it is possible to define the whole set of estimation relationships for turbopumps. In fact, through the analysis of boundary conditions, operating point and through the identification of proper constructional parameters, it is possible to compute the diameter of the machine, the length and, in general, its dimensions, as well as volume and mass. The pump diameter D_P is derived from (74), where the reference impeller diameter is still provided by (68).

$$D_P = D_{P_{imp}} \left(1 + k_{P_{D_{other}}}\right) \quad (74)$$

An additional coefficient $K_{P_{D_{other}}}$ are used to characterize the diameter of other elements of the pumps, such as diffuser, inducer as well as inlet/outlet configuration. Detailed descriptions of these values are reported in (Fusaro, et al., 2019). As the diameter is characterized through the combination of different contributions, the length of the turbopump can be computed by exploiting a similar approach. In general, the overall length (in meters) can be defined as in (75)

$$l_{TP} = l_{imp}(1 + k_{L_{ind}} + k_{L_{Pb}} + k_{L_{out}} + k_{L_{other}}) + l_b + l_t \quad (75)$$

where

l_{imp} is the impeller length at the hub in $[m]$;
l_b is the length of the bearings in $[m]$;
l_t is the length of the turbine in $[m]$;
$k_{L_{pb}}$ is the contribution of pre-burner (if present)
$k_{L_{ind}}$ is the contribution of the inducer;
$k_{L_{out}}$ is the contribution of the outlet channel/volute;
$k_{L_{other}}$is the contribution of other additional elements.

Length of impeller, bearings and turbine are evaluated directly, by looking at specific width/length ratio of similar machines and considering simple fluid

dynamics parameters. Contributions of pre-burner, inducer, inlet/outlet and other components are instead evaluated through empirical coefficients (Fusaro, et al., 2019). The final volume can then be easily approximated as in (76)

$$V_{Tp} = \frac{l_{TP}\pi D^2}{4} \qquad (76)$$

Mass budget computation makes benefit of data related to turbopump material characteristics. The overall mass of the turbopump can be computes as in (77).

$$M_{TP} = I(M_{P_{casing}} + M_{P_{impeller}} + M_{T_{rotor}} + M_{T_{shaft}} + M_B) \qquad (77)$$

Where

$$M_{P_{casing}} = \rho_{cP}(\pi R_{TP}^2) l_{TP} \qquad (78)$$

$$M_{P_{impeller}} = \rho_P R_{impeller}^2 l_{imp} \qquad (79)$$

$$M_{T_{rotor}} = l_T R_T^2 \rho_r \qquad (80)$$

and

ρ_{c_P} is the density of pump casing material in $\left[\frac{kg}{m^3}\right]$
ρ_P is the density of the pump impeller material in $\left[\frac{kg}{m^3}\right]$
ρ_r is the density of turbine rotor material in $\left[\frac{kg}{m^3}\right]$

An additional coefficient I defined in (81) is provided to introduce a proper tuning in mass computation depending on pump rotational speed and processed mass flow.

$$I = I_N \cdot I_{\dot{m}} \quad (81)$$

Values of these coefficients are reported in Table 23 and Table 24.

Table 23: *"Values of I_N coefficients"* (Fusaro, et al., 2019)

Rotational Speed [rpm]	**I_N value**
$N \leq 8{,}000$ rpm	0.17
$8{,}000 < N \leq 10{,}000$ rpm	0.25
$10{,}000 < N \leq 20{,}000$ rpm	0.5
$20{,}000 < N \leq 30{,}000$ rpm	0.55
$30{,}000 < N \leq 80{,}000$ rpm	0.6
$80{,}000$ rpm $< N$	0.75

Table 24: "*Values of $I_{\dot{m}}$ coefficient*" (Fusaro, et al., 2019)

Mass Flow rate [kg/s]	**$I_{\dot{m}}$ value**
$\dot{m} \leq 100$ kg/s	1
$100 < \dot{m} \leq 300$ kg/s	1.5 – 2 *
$\dot{m} > 300$ kg/s	5
*this range of values is due to the impact of pressure rise. Lower $I_{\dot{m}}$ values are suggested for low values of Δp.	

Compressor and turbines. Gas turbines are one of the most used category of turbomachines, through which it is possible to transfer energy from a driving fluid to a rotor or a shaft in order to produce mechanical and/or electrical power. In aeronautics, gas generators based on Joule-Brayton cycle are the core of air breathing engines, like turbojets, turbofans and turboprops, which usually adopt them as internal stage constituted by a compressor, a combustor and a turbine. Other several applications include turboshafts with wide ranges of power and dimensions, for example in case of helicopter propulsion and secondary power generation through Auxiliary Power Units (APU). However, gas generators cycles are also selected for specific on board subsystems to provide a dedicated source of power in operation, to feed some other devices to which they are mechanically connected, or to exploit particular types of thermodynamic cycles like the Rankine as well as vapour cycles for thermal management systems. The architecture of a Joule-Brayton gas generator is typically characterized by the presence of a compressor, which consumes power to increase the pressure of a fluid flow, a combustor, which provides chemical energy through the introduction of the fuel, and a turbine, which provides power by expanding the exhaust gas coming from

the combustion process. In other applications, the combustor is replaced by dedicated heat exchangers which provide thermal energy without the presence of a real combustion (as in closed loop cycles). This strategy is also adopted for turbopump feed systems where compressor is substituted by a pump that is mechanically connected to a turbine, receiving the driving fluid without a combustion (even if in some cases dedicated pre-burners can be added to the turbine feeding line). All of these machines have in common the working principle, which is based on a set of operating variables determining some families of input and output parameters. Looking at the gas generator it is possible to represent a general scheme of the machine and of its working parameters as in Fig. 174.

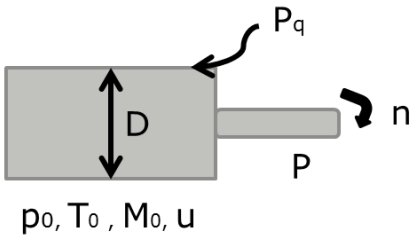

Fig. 174: General schematic of a gas generator

The machine uses a driving fluid with specific initial conditions (pressure p_0 and temperature T_0) that allow characterizing its density ρ_0, Mach number M_0 and mass flow $\dot{m}$. The machine, which has a reference dimension usually represented by the diameter D, produces power P, transferred by a shaft rotating at a certain speed n, by transforming the thermal or chemical power P_q received from an external source. During performance determination, especially when considering on-design conditions, it is a common procedure to refer to specific performance, in order to be independent from the dimensions of the machine. However, when looking at off-design conditions it is better to refer to non-dimensional variables and, in case of a fixed fluid and machine size, to the so-called corrected performance. Actually, for the purposes of this study, specific and corrected performance are not so suitable to identify the physical characteristics of the assembly, since they do not include them in the formulation. On the other hand dimensionless variables can represent in a better way the phenomena affecting the behaviour of the component as well as its physical parameters. For this reason, in order to identify a proper "shape" of the governing equation, dimensional analysis is performed. The classical approach, also described in literature (Rangwala,

2005), makes benefit of the Buckingham π Theorem, stating that, if there is a physically meaningful equation involving a certain number n of physical variables, then the original equation can be rewritten in terms of a set of $\pi = n - m$ dimensionless parameters, where m is the number of physical dimensions involved. In this case it is possible to say that the governing equation of the phenomenon can be written as (82).

$$\mathcal{G} = g\left(P^{\alpha}, D^{\beta}, p_0^{\gamma}, (RT_0)^{\delta}, u^{\varepsilon}, N^{\eta}, P_q^{\vartheta}\right) \quad (82)$$

Where

R is the individual gas constant in $\left[\frac{J}{kgK}\right]$
$P_q = \dot{m}_b H_i$ for a general arrangement where the combustor is included, having
$\dot{m}_b$ fuel mass flow in $\left[\frac{kg}{s}\right]$
H_i lower heat of combustion of the selected fuel in $\left[\frac{J}{kg}\right]$
and other variables are as indicated above in Fig. 174.

In this case, seven physical variables are included in the formulation but, looking at the basic physical dimensions, it is possible to conclude that all variables are composed functions of length, mass and time (83). Thus,

$$\mathcal{G} = g(GOP, SOP) = g(\pi_1, \pi_2, \pi_3, \pi_4) \quad (83)$$

The selection of the π parameters can be made in different ways, accordingly to the focus of the study. Typical strategies refer to the selection of dimensionless power and flowrate as main entity to derive the parameters but, since in this case the flowrate is in some ways more related to the dimensions of the machine (84), the choice of dimensionless power as main parameter is made. The process of deriving the shape of π parameters is based on the identification of the proper relationships with the basic physical dimensions to which they depend. When considering dimensionless power as function of other parameters, it is possible to derive the governing equation as expressed in (84)

$$\frac{P}{D^2 p_0 \sqrt{RT_0}} = g\left(\frac{u}{\sqrt{RT_0}}, \frac{ND}{\sqrt{RT_0}}, \frac{Pq}{D^2 p_0 \sqrt{RT_0}}\right) \quad (84)$$

The function contains a dimensionless speed (of the fluid), a dimensionless rotational speed (of the machine) and a dimensionless power (which is referred to the thermal power provided to the machine). Particularly, it is worth noticing that $\frac{u}{\sqrt{RT_0}} = M_0\sqrt{\gamma}$. In fact, since the ratio of specific heat is dimensionless, the aforementioned analysis does not capture it, in the original formulation. In the same way, function g should be also dependent on Reynolds and Prandtl numbers that are neglected. This is usually adopted also in classical formulation because of the reduced effect of fluid viscosity and thermal conductivity on the general phenomenon. This approach leads to the identification of proper operating performance map for the turbomachinery components that, however, are usually expressed through the adoption of corrected performance in literature. Fig. 175 shows a typical map for an axial Low Pressure Compressor (LPC) of a jet engine, where compression ratio is reported as function of corrected mass flow with dimensionless rotational speed as parameter, considering the alternative correlation reported in (85).

$$\frac{\dot{m}\sqrt{RT_0}}{p_0 D^2} = g'\left(M_0, \frac{ND}{\sqrt{RT_0}}, \frac{\dot{m}_b H_i}{D^2 p_o \sqrt{RT_0}}\right) \rightarrow \dot{m}_c = g'_c\left(M_0, \frac{N}{\sqrt{T_2^o}}, \frac{T_4^o}{T_2^o}\right) \quad (85)$$

Where

$\dot{m}_c$ is the corrected flow rate
g'_c is the function g' expressed for fixed machine dimension and constant fluid properties
T_i^o are total temperatures of specific fluid stations of the machine

As mentioned before, this study is in any case referring to the non-dimensional performance, rather than to the corrected one. So, the obtained trends will assume different shapes, even if the approach is still based on the evaluation of proper maps for the turbomachinery components. Starting from these assumptions, it is possible to try deriving an explicit version of equation (85).

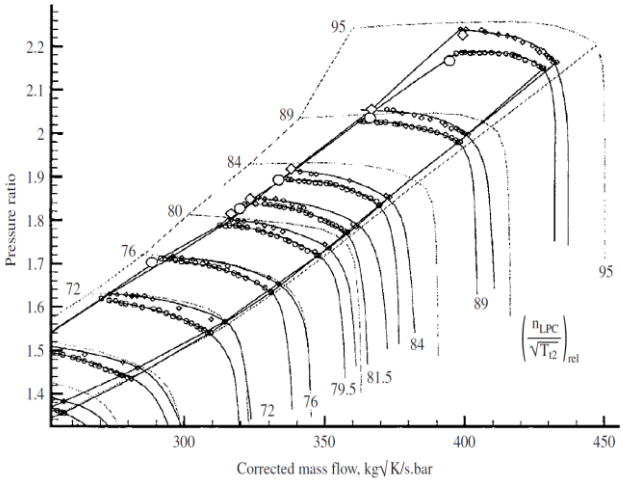

Fig. 175: Typical compressor map based on corrected performance (Rangwala, 2005)

Since the main variable which is unknown a-priori is the diameter D, equation g can be expressed as (86)

$$\frac{P}{D^2 p_0 \sqrt{RT_0}} = \frac{u/\sqrt{RT_0}}{\sqrt{RT_0}/_{ND}} \left(\frac{Pq}{D^2 p_0 \sqrt{RT_0}} \right) \qquad (86)$$

and reducing the different contributions

$$D = \frac{uPq}{NP} \qquad (87)$$

where Pq may have a general expression.

This simple formulation can be used at preliminary design level to evaluate, as first attempt, the diameter of the turbomachinery under study, with the hypothesis of considering a direct drive architecture (turbine and compressors are rotating at the same speed). In order to derive the reference diameter, the initial conditions are referred to the compressor inlet, whilst the reference power is the one generated by the machine. Thermal power is an additional input and depends on the kind of thermal energy provided and on the transfer process. In this way, the result is mostly related to the compressor, which is however not the largest element of the machine in terms of diameter. In fact, the turbine disk is usually larger because of the need of expanding the fluid through the exhaust. The result

shall then be taken as preliminary attempt, to be further extended by conservative coefficients when looking at the real dimension of the turbomachinery upon installation. However, the difference is not so high comparing compressor inlet and turbine outlet (Rangwala, 2005) (Sagerser, et al., 1971), so the obtained values can be still considered as representative. The assumptions made to implement equation (87) are valid for a turbomachinery which uses the same working fluid for both compressor and turbine. When dealing with decoupled fluid flows it is instead necessary to perform dedicated computations for both components. In this case, the operating parameters which are populating the equation shall be referred to compressor and turbine in a separate way, as indicated in (88).

$$D_C = \frac{u_C Pq}{NP_C} \quad ; \quad D_T = \frac{u_T Pq}{NP_T} \qquad (88)$$

The thermal power provide is instead the same, since it is specific for the considered machine. Apart from this difference, since the shape of the equations remain fixed, it is possible to identify the diameter as the main output of the governing equation, to be further used for computation of budgets. This follows the approach already used for turbopumps. Main operating parameters (listed in Table 25) are then the rotational speed and the power of the machine as well as the initial conditions of the flow and the thermal power provided. The situation is clarified in Fig. 176.

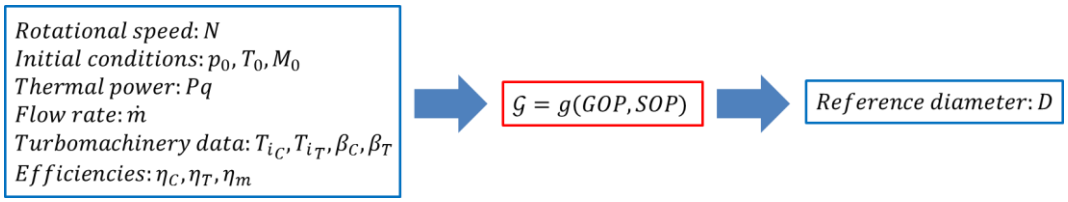

Fig. 176: Variables flowchart for input / output of governing equation of turbomachinery

Static pressure and temperature can be used to compute the speed of sound of the flow and, together with the hypothesized Mach number, the real speed of the fluid at the inlet. Moreover, since the dimension of the machine is unknown at this stage, the flow rate is required as input. In order to evaluate the power processed by the turbomachinery and related components, some other data are required,

since power consumed by compressor and power produced by the turbine can be written as in (89) and (90) respectively.

$$P_C = \frac{1}{\eta_C}\dot{m}c_P T_{i_C}\left(\beta_C^{\frac{\gamma-1}{\gamma}} - 1\right) \quad (89)$$

$$P_T = \eta_m \eta_T \dot{m} c_P T_{i_T}\left(1 - \frac{1}{\beta_T^{\frac{\gamma-1}{\gamma}}}\right) \quad (90)$$

Where

η_C, η_T, η_m are compressor adiabatic efficiency, turbine adiabatic efficiency and mechanical efficiency
T_{i_C}, T_{i_T} are the temperatures at the inlet of compressor and turbine
β_C, β_T are the compressor pressure ratio and turbine expansion ratio

Table 25: List of operating parameters for turbomachinery governing equations

Parameter	**Type of parameter**
Rotational speed N	GOP – Input
Initial static pressure p_0	GOP – Input
Initial static temperature T_0	GOP – Input
Mach number at inlet M_0	GOP – Input
Mass flow rate $\dot{m}$	GOP – Input
Compressor inlet temperature T_{i_C}	GOP – Input
Turbine inlet temperature T_{i_T}	GOP – Input
Mechanical efficiency η_m	GOP – Input
Thermal power Pq	GOP – Input
Fluid speed u	GOP
Fluid density ρ_0	GOP
Power consumed by compressor P_C	GOP
Power produced by turbine P_T	GOP
Compressor pressure ratio β_C	SOP – Input
Turbine expansion ratio β_T	SOP – Input
Compressor adiabatic efficiency η_C	SOP – Input
Turbine adiabatic efficiency η_T	SOP – Input

Once that the reference diameter of the machine is derived, the identification of the dimensions and of the mass is possible. Particularly, (Sagerser, et al., 1971) includes some semi-empirical models for the estimation of gas generator components of turbojets and turboshafts for aeronautical applications, providing mass estimations for the different sub-parts of the engines. For this reason, as far as the performance envelope remains within the ranges prescribed by (Sagerser, et al., 1971) and summarized in Table 26, it is reasonable to apply the methodology also for simple gas generators (i.e. not necessarily implemented within an engine cycle) by neglecting the terms related to inlet, fan stage and combustor (when this is not required).

Table 26: Range of validity for main parameters described in the semi-empirical model (Sagerser, et al., 1971)

Component	**Variable**	**Range**
Compressor	Number of stages	2 - 14
	Inlet hub-tip diameter ratio	0.38 – 0.83
	Pressure ratio	1.5 - 15
	Average stage pressure ratio	1.15 – 1.46
	Mean diameter	0.34 – 0.98 m
	Length to inlet mean diameter ratio	0.29 – 1.4
Turbine	Hub-tip diameter ratio	0.52 - 0.89
	Mean diameter	0.43 – 1.2 m
	Number of stages	1 – 6
	Mean blade tangential velocity	120 – 510 m/s

The mass of the compressor is computed in (Sagerser, et al., 1971) as function of the reference diameter D, of the number of stages $\mathcal{N}$ and on the length to inlet mean diameter ratio L_C/D. The diameter is provided as input in (Sagerser, et al., 1971) within a range that is the consequence of a statistical analysis on existing machines. In the proposed model, it is the result of the computation of the governing equation, based on operating parameters. The number of stages and the L_C/D ratio can be instead derived from the equations proposed in (Sagerser, et al., 1971). Particularly, the number of stages can be computed looking at (91) for which

$$\mathcal{N} = \frac{\ln(\beta_C)}{\ln(\beta_{stage_C})} \qquad (91)$$

since

$$\beta_{stage_C} = (\beta_C)^{\frac{1}{\mathcal{N}}} \quad (92)$$

where

β_{stage_C} is the compression ratio of a single stage.

With this assumptions, the number of stages can be hypothesized, allocating a certain β_{stage_C} to each stage or, on the contrary, β_{stage_C} can be computed making benefit of the statistical correlation proposed in (Sagerser, et al., 1971), which is function of corrected speed (i.e. relying on operating maps of compressors having performance within the ranges specified by Table 26). The equation is provided in (93).

$$\beta_{stage_C} = 1 + \left[\frac{\left(\frac{U}{\sqrt{\vartheta}}\right)}{A} - C(\beta_C)^{1.8} + B - 1\right] \quad (93)$$

Where

U is the mean tangential blade velocity in $\left[\frac{m}{s}\right]$
ϑ is the total to static temperature ratio at inlet
A is the reference tangential blade speed in $\left[\frac{m}{s}\right]$
B,C are dimensionless numbers to take into account loading levels and statistical diameter correlations

With the derivation of the number of stages, it is possible to compute the length to inlet mean diameter ratio as indicated in (94).

$$\frac{L_C}{D} = 0.2 + \left[0.234 - 0.218\left(D_{ht_C}\right)\right]\mathcal{N} \quad (94)$$

Where

D_{ht_C} is the hub-tip diameter ratio that shall be provided as input (in the range of 0.38 – 0.83 to be consistent with the model in (Sagerser, et al., 1971)).

It is clear that, once the diameter in known, equation (94) can be also used to derive L_C and, consequently, the volume of the compressor as indicated in (95).

$$V_C = \frac{L_C \pi D^2}{4} \qquad (95)$$

The computation of compressor mass (96) can then be performed with the results coming from (91) and (94)

$$M_C = K_C D^{2.2} \mathcal{N}^{1.2} \left[1 + \frac{{}^{L_C}/_{D}}{\left({}^{L_C}/_{D}\right)_{ref}} \right] \qquad (96)$$

where

$$\left({}^{L_C}/_{D}\right)_{ref} = 0.2 + 0.081\mathcal{N} \qquad (97)$$

is a reference ratio assuming $D_{ht_C} = 0.7$

and

$K_C = 24.2$ for cruise engines (taken as reference also for turboshaft) which is a sort of mass per unit (transversal) surface obtained as statistical regression in $\left[\frac{kg}{m^{2.2}}\right]$

The length and mass of the turbine are again function of reference diameter, number of stages and rotating speed, as for the compressor. The first step proposed in (Sagerser, et al., 1971) concerns the computation of turbine length L_T as indicated in (98).

$$L_T = \mathcal{N}_T\left(C_{x_r} + C_{x_s}\right) + (2\mathcal{N}_T - 1)S_T \qquad (98)$$

Where

$\mathcal{N}_T$ is the number of turbine stages, which can be hypothesized as free parameter in the range specified by Table 18
C_{x_r}, C_{x_s} are axial length of rotor blade and stator gaps $[m]$

S_T is the additional clearance between rotor stages and stator stages $[m]$ as defined in (95).

Particularly,

$$C_x = \frac{D_{t_T} - D_{h_T}}{2AR_x} \qquad (99)$$

Where

C_x has been considered as standard axial chord length value for both rotor blade and stator gap $[m]$
D_{t_T}, D_{h_T} are the tip and hub diameter respectively (the tip diameter is computed from performance analysis whilst a hub-tip diameter ratio shall be hypothesized also for the turbine) in $[m]$

AR_x is the blade axial aspect ratio defined as (100)

$$AR_x = A' + B' \frac{D_{h_T}}{D_{t_T}} \qquad (100)$$

With

$\frac{D_{h_T}}{D_{t_T}}$ as the aforementioned turbine hub-tip diameter ratio
A', B' are dimensionless coefficients to take into account spool pressure

Moreover,

$$S_T = a_T C_x \qquad (101)$$

With

a_T proportionality constant for gaps computation depending on axial chord length (varying from 0.2 to 1.0 in the selected range)

The mass of the component can then be expressed as in (102).

$$M_T = K_T D^{2.5} \mathcal{N}_T U_T^{0.6} \qquad (102)$$

Where

$K_T = 7.9$ for cruise engines (taken as reference also for turboshaft) which represents again a specific mass as for K_C in (96) expressed in $\left[kg\frac{s^{0.6}}{m^{3.1}}\right]$ which is very similar to a mass per unit volumetric flow rate.

The overall volume for the turbine can be computed as in (103).

$$V_T = \frac{L_T \pi D^2}{4} \qquad (103)$$

Additional contributions to the overall mass of the machine coming from controls, accessories and, notably, support structure can be added to have a more clear view over the real mass of the component. Particularly, (Sagerser, et al., 1971) provides a general function to compute the mass of controls and accessories as function of engine thrust and Specific Fuel Consumption (SFC), as reported in (104).

$$M_{CA} = K_{CA} F[1 + a_{CA}(SFC)] \qquad (104)$$

Where

F is the installed thrust $[N]$

SFC specific fuel consumption in $\left[\frac{\frac{kg}{hr}}{N}\right]$

K_{CA}, a_{CA} are coefficients

The results provided in (Sagerser, et al., 1971) showed that the mass of controls and accessories is between 9 – 30% of total mass of the engine. However, jet engine is equipped with many devices and interface connectors with different on-board systems, being far from the selected case study. A reference value in the range of 10 - 20% (k_{CA}) is then selected for the proposed model, as reported in (105), also because it is not possible to use the original formulation where thrust and SFC are used as drivers.

$$M'_{CA} = k_{CA}(M_C + M_T) \qquad (105)$$

Moreover, this kind of approach can be adopted to compute the mass of structural components. The work performed in (Sagerser, et al., 1971) suggest to use a reference additional percentage to the total mass which is around 10 – 18 %. Since the lower value is indicated as representative for lift engines only, the upper one was selected for the proposed study, so that:

$$M_S = 1.18(M_C + M_T + M'_{CA}) \quad (106)$$

The total mass of the selected machine can be then derived as in (107).

$$M_{TOT} = M_C + M_T + M'_{CA} + M_S \quad (107)$$

Tanks. Tanks are one of the most common element of a hydraulic system, having the main function of collecting the fluid necessary for the operations and of maintaining the environmental conditions necessary to guarantee its characteristics within the specific ranges of application. The design of tanks and the selection of their type depend largely on the kind of fluid which they host and on vehicle integration aspects. In many applications, tanks are obtained directly from integral parts of vehicle structure, in order to reduce mass and increase the usable volume. In other cases, where it is not possible to use structural compartments, rigid tanks are exploited. These usually allows the adoption of simpler shapes, even if the overall mass of the vehicle increases because of the presence of the additional vessels. For the purpose of this study, in order to evaluate the mass of the components, non-integral tanks are considered to develop the physical model. This allows estimating the main characteristics of the vessels with a general approach, without restrictions related to specific shape or volume requirements. The proposed methodology is focused on the evaluation of the main structural aspects which determine the final mass and volume of the tank. Thus, the focus is mainly concentrated on the identification of pressure levels and induced stresses on the materials. Moreover, the analysis applied to STRATOFLY MR3 (which adopts integral tanks) is mainly related to the selection of equivalent rigid tanks capable of hosting the same amount of LH2. The expected outcome is a fictional value of mass allocated on rigid tanks that can be used to understand the mass saving produced by the adoption of integral tanks. For this reason, a reduced mass contribution due to tanks is included in the overall breakdown, while considerations on volumes and dimensions are discussed in a conventional way. Independently from the type of the tank, the design shall start from the analysis of the required fluid volume. A general expression for the propellant tank design volume (Huzel & Huang, 1967) is reported in (108).

$$V_t = V + T + B + U \quad (108)$$

Where

V_t is the tank design volume $[m^3]$

V is the actual volume of fluid required by the system $[m^3]$
T is the volume of fluid trapped within the system (not usable) $[m^3]$
B is the volume of fluid subjected to boil-off (only in case of cryogenic fluids) $[m^3]$
U is the ullage volume $[m^3]$

Together with volume, the assumptions related to wall thickness, material and shape are fundamental to complete the evaluation of dimensions and mass. The selection of material and thickness are actually related to the working loads, whilst the shape can be traded depending on the configuration. Thus, the other fundamental aspect, in parallel with the computation of required volume, is the determination of working loads, as herein proposed. In general, the maximum allowable working stress is defined as a reference strength of the material (typically the yield strength or the ultimate strength) divided by a safety factor. In (Huzel & Huang, 1967) the criteria reported in (109) and (110) are proposed.

$$S_{w_1} = \frac{F_y}{1.33} \quad (109)$$

$$S_{w_2} = \frac{F_u}{1.65} \quad (110)$$

Where

S_{w_1} and S_{w_2} are the maximum allowable stresses [Pa] (tests may require higher requirements in terms of pressure than the one computed for operating environment).
F_y and F_u are the yield and ultimate strengths respectively [Pa]. In case yield is not present for a determined material $F_{0.2}$ is used as reference, being the strength at which a plastic deformation of the material of about 0.2% arises

The lower between S_{w_1} and S_{w_2} shall be used as conservative value (reported simply as S_w in the following). It is important to notice also that, in case of tanks, it may be difficult to distinguish between governing equation and estimation relationships. It is possible to say that the main drivers are V_t and S_w, with proper hypothesis concerning material and shape, thus making the estimation problem quite straightforward to be solved. In particular, two kinds of rigid tanks are considered:

- Spherical tanks
- Cylindrical tanks (with both ellipsoidal and spherical tank ends)

As the sensitivity analysis shows in Section 5.2.4.6, the effect of tank and tank ends shape is not negligible for the determination of component mass. For the sake of clarity, following sections refer to V_t as reference volume. Starting from the assumption reported in Section 5.2.4.4, it is possible to summarize the shape of the estimation relationship as function of the main parameters as in (111). Since in this case it may be difficult to represent separately governing equation $\mathcal{G}$ and estimation $\mathcal{F}$, the latter is directly included for clarity.

$$\mathcal{F} = f(GOP, SOP) = f(V, S_W, \rho_{material}, shape) \quad (111)$$

Where

$\rho_{material}$ is the density of the material in $[kg/m^3]$

The choice of the material (and then also the values of ρ and S_w) is directly related to the maximum working tank pressure, determined by the operating conditions, which determines also the thickness of the wall. Moreover, the required fluid volume is function of working pressure as well for a given fluid. Thus a more general representation of (111) can be proposed as in (112).

$$\mathcal{F}' = f(GOP, SOP) = f(p_t, fluid, shape) \quad (112)$$

Where

p_t is the tank pressure in [Pa]

It is clear that, for fixed mechanical characteristics of the material, a lighter one guarantees a lower mass per unit volume. The main parameters are reported in Table 27.

Table 27: List of parameters for tanks estimation relationships

Parameter	Type of parameter
Working tank pressure p_t	GOP - Input
Working fluid density ρ_{fluid}	GOP - Input
Material density $\rho_{material}$	GOP - Input
Material Young modulus E	GOP - Input
Material Poisson ratio ν	GOP - Input
Fluid volume V	GOP
Maximum allowable working stress S_w	GOP
Wall thickness t_w	GOP
Tank shape	SOP - Input

Tank shape has been taken as specific parameter (SOP) because of the different factors that shall be computed to characterize thickness, volume and mass, as described hereafter. The summary of the variable flowchart is shown in Fig. 177.

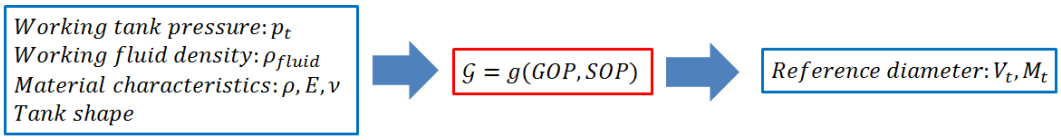

Fig. 177: Variables flowchart for input / output of estimation relationships for tanks

The main physical variables in output are then the design volume of the tank (not the volume of the required fluid which is known), which can be used to compute the mass following the assumptions on other parameters. The dimensions can be derived from information about tank shape. Spherical tanks represent the simple version of pressurized vessels. The design volume can be simply expressed as (113)

$$V_{t_S} = \frac{4\pi a^3}{3} \quad (113)$$

Where

a is the inner radius of the sphere $[m]$

The wall thickness for a spherical tank can then be determined as in (114).

$$t_{w_S} = \frac{p_t a}{2 S_w e_w} \quad (114)$$

Where

e_w is the weld efficiency which is function of the welding process and of the shape

It is straightforward to compute the internal wall surface as (115).

$$A_S = 4\pi a^2 \quad (115)$$

The tank mass is then function of the selected material as in (116).

$$M_S = \frac{4}{3}\pi \left[\left(a + t_{w_S} \right)^3 - a^3 \right] \rho_{material} \quad (116)$$

Cylindrical tanks are, as spherical ones, another simple kind of vessels used for different applications. Actually, pure cylinders are rare since tank ends shall be typically rounded to reduce pressure peaks over the wedges, but the estimations used for the cylinder remain valid for the central section. Dedicated estimations for spherical and ellipsoidal tank ends are included at the end of this paragraph to complete the formulation. The design volume can be expressed as in (117).

$$V_c = \pi a_C^2 l_C \quad (117)$$

Where

a_C is the inner radius of the cylinder base $[m]$
l_C is the length of the cylinder $[m]$

The wall thickness is provided by (118).

$$t_{w_C} = \frac{p_t a_C}{S_w e_w} \quad (118)$$

The internal wall surface area is in this case derived as in (119).

$$A_C = 2\pi a_C l_C \quad (119)$$

The tank mass (120) is then obtained with similar considerations reported in (116).

$$M_C = \pi \left[\left(a_C + t_{wC} \right)^2 - a_c^2 \right] l_C \rho_{material} \quad (120)$$

As already mentioned in this section, tank ends provide extra volume (and mass) to be carefully computed jointly with cylindrical section. The overall breakdown of the tank will be then composed by the different contributions. The typical tank ends arrangements are shown in Fig. 178 (Huzel & Huang, 1967). Two main points that determines the shape of the tank and related wall thicknesses are the knuckle, located at the intersection between the sphere and the cylinder, and the crown, which is the point on the longitudinal axis of the cylinder. The evaluation of the material stresses at these stations is fundamental to evaluate the minimum required wall thickness, with impact on the overall mass of the tank. For a spherical ends, the crown and the knuckle points have distance a_{e_S} from the origin of the sphere on longitudinal axis of the cylinder, since this is the actual radius of the sphere itself. In other words, the distance between the juncture and the crown is equal to the sphere radius. This allows also the tank end wall to be tangential to the cylinder at the juncture. Ellipsoidal tank ends have similar arrangement, even if an ellipse ratio shall be taken into account to represent the end surface shape. Thus, the distance between the origin point and the crown is different if compared to the distance between the origin and the knuckle.

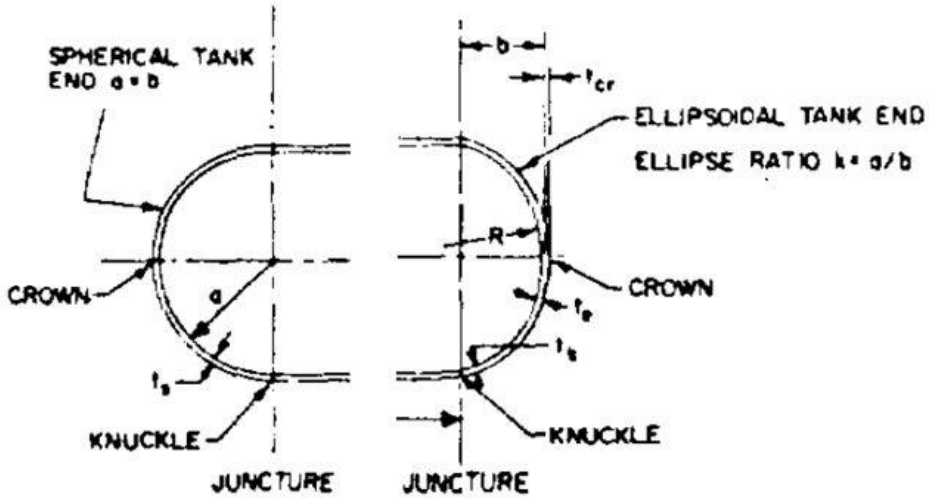

Fig. 178: Geometry of spherical and ellipsoidal tank ends (Huzel & Huang, 1967)

The volumes of the two types of tank ends can be computed as in (121) and (122) for sphere and ellipse respectively.

$$V_{e_S} = \frac{2\pi a_{e_S}^3}{3} \qquad (121)$$

$$V_{e_E} = \frac{2\pi a_{e_E}^2 b_{e_E}}{3} \qquad (122)$$

Where

a_{e_S} is the inner radius of the sphere $[m]$
a_{e_E} and b_{e_E} are the major and minor half diameters $[m]$

The thickness of the main aforementioned stations can be computed as in (123, 124) for the sphere and in (125, 126) for the ellipse.

$$t_{w_{KS}} = \frac{K p_t a_{e_S}}{S_w e_w} \qquad (123)$$

$$t_{w_{CRS}} = \frac{p_t a_{e_S}}{2 S_w e_w} \qquad (124)$$

$$t_{w_{KE}} = \frac{K p_t a_{e_E}}{S_w e_w} \qquad (125)$$

$$t_{w_{CRE}} = \frac{p_t k a_{e_E}}{2 S_w e_w} \qquad (126)$$

Where

$k = a_{e_E}/b_{e_E}$ is the ellipse ratio
K is a stress factor which is a function of ellipse ratio k and of the type of stress considered (membrane stress, combined stress etc…) as specified in (Huzel & Huang, 1967).

For simplicity, it is also possible to establish an equivalent wall thickness for both spherical and ellipsoidal tank ends as in (127) and (128).

$$t_{w_{eS}} = \frac{p_t a_{e_S}\left(K + \frac{1}{2}\right)}{2 S_w} \qquad (127)$$

$$t_{w_{eE}} = \frac{t_{w_{KE}} + t_{w_{CRE}}}{2} \qquad (128)$$

The wall surface areas are then computed as in (129) and (130) for both sphere and ellipse.

$$A_{e_S} = 2\pi a_{e_S}^2 \quad (129)$$

$$A_{e_E} = a_{e_E}^2 + \frac{\pi b_{e_E}^2 \ln\left(\frac{1+e}{1-e}\right)}{2e} \quad (130)$$

Where

$e = \sqrt{1 - \frac{1}{k^2}}$ is the eccentricity of the ellipse

Ultimately, it is possible to compute the mass of the tank ends, as in (131) and (131).

$$M_{e_S} = \frac{2}{3}\pi\left[\left(a_{e_S} + t_{w_{eS}}\right)^3 - a_{e_S}^3\right]\rho_{material} \quad (131)$$

$$M_{e_E} = \frac{\pi\left[\left(a_{e_E} + t_{w_{eE}}\right)^2 (b_{e_E} + t_{w_{e_E}}) - a_{e_E}^2 b_{e_E}\right] E' \rho_{material}}{3k} \quad (132)$$

Where

$E' = 2k + \frac{1}{\sqrt{k^2-1}} \ln \frac{k+\sqrt{k^2-1}}{k-\sqrt{k^2-1}}$ is the design factor.

Final breakdown can then be expressed as in (133), (134) and (135) for a cylindrical tank with spherical tank ends and as in (136), (137) and (138) for a cylindrical tank with ellipsoidal tank ends.

$$V_{C_{TOT_S}} = V_C + 2V_{e_S} \quad (133)$$

$$A_{C_{TOT_S}} = A_C + 2A_{e_S} \quad (134)$$

$$M_{C_{TOT_S}} = M_C + 2M_{e_S} \quad (135)$$

$$V_{C_{TOT_E}} = V_C + 2V_{e_E} \quad (136)$$

$$A_{C_{TOT_E}} = A_C + 2A_{e_E} \quad (137)$$

$$M_{C_{TOT_E}} = M_C + 2M_{e_E} \quad (138)$$

The volumes and surfaces here indicated correspond to the internal arrangement only.

Pipes. Together with tanks, pipes are another kind of simple passive component of a typical hydraulic system. Their main function consists in guaranteeing a continuous fluid flow within a prescribed path inside the system and among the different utilities. They are typically used to feed active components with the aim of reducing the pressure losses due to hydraulic friction and discontinuities like valves, junctions and turns. As for the tanks, the determination of the physical characteristics of the pipes is mainly related to the evaluation of the operating pressure. This is the result of the pressure levels at inlet and outlet of the pipe, which is mainly determined by computing the pressure loss within the duct. In fact, the pressure at the inlet shall usually be equal to the outlet pressure plus an additional pressure rise that is necessary to withstand the loss in the pipe. Additionally, mass flow is an important parameter to evaluate the diameter of the duct itself, not only to guarantee a reasonable fluid speed within the pipe, but also to avoid losses due to excessive friction against the walls. Conversely to what happens for the tank, the volume occupied by a pipe is not so important since, apart from the determination of its diameter, it depends essentially to the distance that the duct shall cover and from the path it shall follow. For the purpose of this analysis, since the distances between the different elements of the circuits are difficult to be determined, a specific mass in kg/m for a simple straight path is considered. Further analyses may be required to obtain a detailed result, especially considering vehicle integration issues. The main criteria to evaluate pipes mass estimation starts, as for the tanks, from the determination of the maximum allowable stress on the walls. In fact, a pipe is a pressure vessel which has the additional requirements of guaranteeing a proper fluid flow within its boundaries. Thus equations (139) and (140) can be defined, as for the tanks in (109) and (110).

$$S_{w_{p_1}} = \frac{F_y}{1.33} \quad (139)$$

$$S_{w_{p_2}} = \frac{F_u}{1.65} \quad (140)$$

Where the lower of the maximum allowable stresses $S_{w_{p_i}}$ is selected for sizing purposes. These relations allow defining the proper material to be used for the construction of the component. However, the selection of the material for pipes is also related to other physical characteristics which have impact on the pressure losses in operation. In fact, distributed pressure losses within a pipe are mainly determined by applying (141).

$$\Delta p = \frac{1}{2}\rho_{fluid} v^2 \, {l_p}/{d_p} \, \lambda \quad (141)$$

Where

$\frac{l_p}{d_p}$ is the length over diameter ratio of the pipe
v is fluid speed in $[m/s]$
λ is the friction factor

The friction factor λ is function of Reynolds number and of material roughness (Section 5.2.3.3). A rougher material will produce higher distributed pressure losses, thus requiring a higher inlet pressure to reach a fixed outlet pressure. For this reason, the operating pipe pressure p_p can be highly influenced by the selection of the material. As for tanks, it is not easy to distinguish between governing equations and estimation relationships, thus the general shape of an estimating function is directly presented in (142) and sketched in Fig. 179.

$$\mathcal{F} = f(GOP, SOP) = f\left(p_p, \dot{m}, \, fluid, pipe \; material\right) \quad (142)$$

As summary, the pressure level is influenced both by the pressure required by the components fed at the outlet of the pipe (i.e. by the pressure level which shall be maintained at outlet) and by the pressure drop produced by the fluid flowing at a certain speed in a pipe made by a specific material. Moreover, mass flow influences both the pressure levels and the drops.

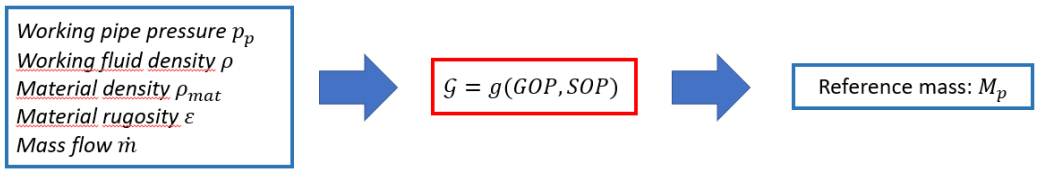

Fig. 179: Variables flowchart for input / output of estimation relationships for pipes

Particularly,

$$\lambda = f(Re, \varepsilon) \qquad (143)$$

where

ε is the absolute roughness of the pipe in $[m]$

This function may vary depending on the type of flow range (laminar, turbulent) and on other factors that are generally presented in the so-called Moody chart (Moody, 1944). Different formulations for the evaluation of λ are provided in literature. One of the most common relation is the so-called Colebrook-White formulation, which allows the computation of a generic fluid flow in a duct for both laminar and turbulent regime based on empirical results (Colebrook & White, 1937). The approximated relation defined in (62), which is explicit, is used (Haaland, 1983) as already reported in Section 5.2.3.3. As summary, the operating parameters included in Table 28 can then be considered.

Table 28: List of parameters for pipes estimation relationships

Parameter	**Type of parameter**
Working pipe pressure p_p	GOP - Input
Working fluid density ρ_{fluid}	GOP - Input
Material density $\rho_{material}$	GOP - Input
Mass flow $\dot{m}$	GOP - Input
Reynolds number Re	GOP
Maximum allowable working stress S_w	GOP
Wall thickness t_w	GOP
Material rugosity ε	SOP - Input
Pipe friction factor λ	SOP

The computation of component budgets for pipes starts from the evaluation of the wall thickness. This is computed with reference to the approach followed by cylindrical tanks. The pipe is represented, in this case, by a pressure vessel having pure cylindrical shape, whose thickness is derived as in (144). In this case, the welding efficiency (Huzel & Huang, 1967), present in (118), is here neglected.

$$t_{w_p} = \frac{p_p d_p}{2S_{w_p}} \quad (144)$$

Where

p_p is the pressure inside the pipe $[Pa]$

Since the length of the pipe may depend on various aspects, it may be useful to define a mass per unit kg as in (145).

$$M_p = \pi \left[\left(\frac{d_p}{2} + t_{w_p} \right)^2 - \frac{d_p^2}{4} \right] l_p \rho_{material} \quad (145)$$

Where

M_p is the specific mass of the pipe in $[kg/m]$

The overall (external) volume, considering a simple straight path is provided in (146).

$$V_p = \pi \left(\frac{d_p}{2} + t_{w_p} \right)^2 l_p \quad (146)$$

Heat exchangers. Heat exchangers are simple and effective solutions to control and manage thermal energy and related transfer in different situations. Being usually based upon conductive and convective heat exchange, they are adopted to balance temperature of compartments through direct contact and/or by means of driving fluids. The sizing of such components is mainly related to the selection of the architecture and to the identification of the thermal power that they shall manage in operation. Estimation of mass and volumes of the exchanger is then performed looking at these main aspects, by using semi-empirical formulations, as proposed, for example, in (Larson & Pranke, 1999). The main strategy adopted for the proposed study is then to evaluate firstly the thermal power managed by the

components, identifying proper governing equations, and then using the output of this first step to determine mass and volume, as consequence. In order to select the governing equations, the basic relations of fluid heat exchangers are used. Considering two fluids flowing within an exchanger at a certain temperature, it is possible to say that the thermal power balance is expressed by (147).

$$\dot{Q} = \dot{m}_c c_{p_c}(T_{co} - T_{ci}) = \dot{m}_h c_{p_h}(T_{hi} - T_{ho}) \quad (147)$$

Where

$\dot{m}_c$ and $\dot{m}_h$ are the mass flows of cold and hoot fluids respectively in $[kg/s]$
c_{p_c} and c_{p_h} are the specific heat at constant pressure of both fluids in $[J/kgK]$
T_{co} and T_{ho} are temperature of cold and hot fluids at exchanger outlet in $[K]$
T_{ci} and T_{hi} are temperatures of cold and hot fluids at exchanger inlet in $[K]$

Moreover, it is also possible to say that the thermal power $\dot{Q}$ can be also expressed as (148)

$$\dot{Q} = hS(\Delta T)_{LN} \quad (148)$$

Where

h is the convective heat exchanger coefficient in $[W/m^2K]$
S is the exchange surface

and

$$(\Delta T)_{LN} = \frac{\Delta T_1 - \Delta T_2}{\ln\left(\frac{\Delta T_1}{\Delta T_2}\right)} \quad (149)$$

is the so-called mean logarithmic temperature difference in $[K]$, for which

$$\Delta T_1 = T_{hi} - T_{ci} \quad (150)$$

$$\Delta T_2 = T_{ho} - T_{co} \quad (151)$$

From these relations it is easy to understand that, given the four limit temperatures, the thermal power can be evaluated for a specific mass flow. On the other hand, the same problem can be solved in a preliminary way by looking at (148), where it is necessary to specify h and S. In case fins heat exchangers are

considered, additional relations shall be introduced to specify limit temperatures and surfaces. In fact, the thermal power can be computed in this case as in (152).

$$\dot{Q} = hS\left(T_{ext} - T_f\right) \quad (152)$$

Where

T_{ext} is the temperature of the external fluid in $[K]$

and

$$T_f = \eta T_w \quad (153)$$

is the fin temperature [K] for which

η is the efficiency of the fin
T_w is the exchanger wall temperature in $[K]$

The efficiency is introduced to take into account that the conductivity of the fin is not infinite, thus its temperature is lower than the wall temperature of the exchanger (i.e. the thermal power which is expelled is lower than the ideal one because the temperature difference is lower). Moreover, the exchange surface is provided by (154), where rectangular fins are considered for simplicity.

$$S = S_e + S_f - S_i \quad (154)$$

Where

S_e is the surface of the exchanger without fins in $[m^2]$
S_f is the total surface of the fins in $[m^2]$
S_i is the interface surface (that shall be neglected since it is the base of the fin over the wall of the exchanger) in $[m^2]$

The governing equation of a general exchanger has the shape of (155) and is graphically represented as in Fig. 180.

$$\mathcal{G} = g(GOP) = g\left(\Delta T, \dot{m}, c_p\right) = g(\Delta T, h, S,) \quad (155)$$

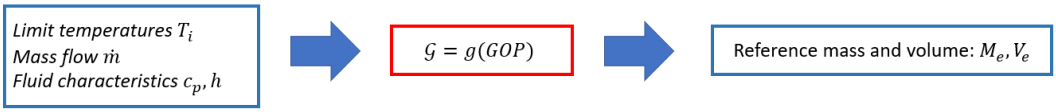

Fig. 180: Variables for input / output of estimation relationships for heat exchangers

The derivation of estimation relationships is then easy when considering semi-empirical models for the determination of mass and volume, since both estimations will be expressed as (156).

$$\mathcal{F} = f(GOP) = f(\dot{Q}) \quad (156)$$

Other dimensions can be computed basing on the exchange surface and volumes previously determined. The main operating parameter is then the thermal power, which can be computed by means of other variables, collected in Table 29.

Table 29: List of parameters for heat exchangers estimation relationships

Parameter	**Type of parameter**
Limit temperatures T_i	GOP - Input
Mass flow $\dot{m}_i$	GOP - Input
Specific heat c_{p_i}	GOP - Input
Convective heat exchanger coeff. h	GOP - Input
Exchanger surface S	GOP - Input
Thermal power $\dot{Q}$	GOP

Even if the evaluation of physical characteristics like mass and volume may be directly related to the thermal power managed by the exchanger, the estimation may be affected by component configuration and arrangement. In preliminary design, some semi-empirical models are usually adopted to derive very high-level estimations without going in details. For the purpose of this study, the assumptions of (Larson & Pranke, 1999) concerning the relationships for mass and volume estimations are used. For heat exchanger managing a thermal power greater than 5 kW, the following relationships apply for mass (157) and volume (158).

$$M = 17 + 0.25\dot{Q}_{kW} \quad (157)$$

$$V = 0.016 + 0.0012\dot{Q}_{kW} \quad (158)$$

Where

$\dot{Q}_{kW}$ is the thermal power expressed in $[kW]$

The extension of the exchanger can be evaluated knowing the volume and assuming a proper exchange surface. In this way, the component is fully characterized, even if with preliminary results. It shall be noticed that these estimations are not valid for exchangers constituted by cooling jackets or similar devices, since, in that case, they are directly embedded within the primary structure. This is similar to the integral tanks situation and, also in this example, the derived results shall be intended as an equivalent mass increase in case of adoption of dedicated exchangers having the same thermal loop capacity (i.e. capable of managing the same thermal power).

5.2.4.6 Select subsystems operating parameters

The selection of proper operating parameters to apply the models described within Section 5.2.4.5 to the physical characterization process of TEMS elements (Table 20) is here reported.

Turbopumps. Boundary conditions provided in (Balland, et al., 2015) are used to set the operating point of MR3 turbopump, as additional considerations are made to characterize the type of machine exploited (Table 30).

Table 30: Input and assumptions for MR3 turbopumps operating parameters

	Parameters	**Estimated Value for STRATOFLY MR3**	**Comments**
Input Parameters	Rotational speed N [rpm]	[10000 – 40000]	Considering a typical range of operations for turbopumps with LH2 working fluid.
	Flow rate ṁ[kg/s]	[0 - 100]	(Balland, et al., 2015)
	Fluid Density ρ [kg/m3]	70.8	Liquid Hydrogen (LH2)
	Pressure Rise Δp[N/m2]	$[75 \cdot 10^5]$	Performance analysis (Section 5.2.3)
	Efficiency [-]	0.7	Assumption considering currently available technologies

Design Assumptions	Turbopump type	Radial pump and axial turbine configuration	Considering the Balje and Cordier Diagrams
	Mechanical arrangement	Direct Driven	Depending on the speed variations between pump and turbine

Compressors and Turbines. Considering the TEMS architecture, the boil-off compressor and the expander reported in Fig. 54 (briefly sketched in Fig. 181) can be analysed following the proposed approach.

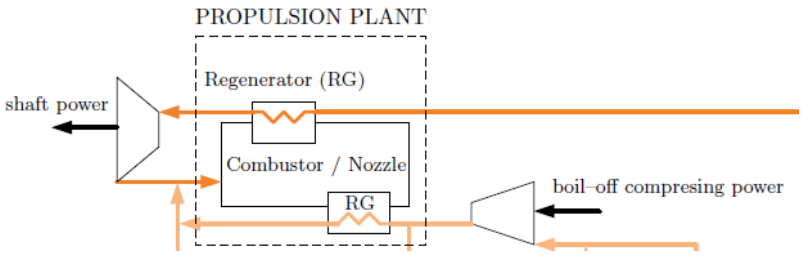

Fig. 181: Partial scheme of the TEMS (Balland, et al., 2015)

The compressor receives the hydrogen boil-off coming directly from the tanks as well as a dedicated boil-off flow, which is used to cool down the cabin. The two flows are mixed together before entering the compressor. On the other hand, the expander receives the liquid hydrogen, which is used as fuel for the power plant. The LH2 is also adopted as cooling fluid for the engines within a regenerator before entering the turbomachinery. After the expander outlet, the driving fluid is mixed with the boil-off coming from the compressor and with an additional flow, which is coming out from the air pack. The mixed flow is then injected within the combustion chamber. The analysis of the effects of the operating conditions specified during the design requires a sensitivity analysis of the main governing parameters. The reference conditions specified in (Balland, et al., 2015) for inlet/outlet of the two machines are summarized in Table 31.

Table 31: Selected values for operating parameters of boil-off compressor and LH2 expander

	Operating Parameter	**Inlet**	**Outlet**
l oil- off	Temperature [K]	270	950
	Pressure [bar]	1	60

	Mass flow [kg/s]	8	
	Rotational speed [rpm]	To be determined	
	Adiabatic efficiency	0.85	
	Number of stages	To be determined	
Expander	Temperature [K]	1300	1200
	Pressure [bar]	80	60
	Mass flow [kg/s]	100	
	Rotational speed [rpm]	To be determined	
	Adiabatic efficiency	0.85	
	Mechanical efficiency	0.98	
	Number of stages	3	

Compressor pressure ratio and turbine expansion ratio can be derived looking at inlet/outlet pressure.

$$\beta_C = \frac{p_{C\,out}}{p_{C\,in}} \quad (159)$$

$$\beta_T = \frac{p_{T\,in}}{p_{T\,out}} \quad (160)$$

The ratio between inlet and outlet pressure is quite different if comparing compressor and expander conditions. Because of these values, it may be necessary to consider two rotational speeds for compressor and expander, also because the driving fluid is not the same. Moreover, the allocation of specific stage pressure ratios may have influence on the number of stages. The selection of the values is made basing on the results coming from the sensitivity analysis reported hereafter. It is moreover interesting to focus on the value of expander inlet temperature and on the way through which it can be computed. Actually, between compressor and turbine, there is a source of thermal energy, which is injected within the cycle because of the heating of LH2 in the regenerator. Even if the cooling system of the propulsion plant is not yet fully characterized, it is possible to hypothesize that the thermal power exchanged through convection is represented by (161)

$$Pq = hS\left(T_{powerplant} - T_{LH2}\right) \quad (161)$$

Where

h is the convective heat exchange coefficient of the fluid $[W/m^2K]$
S is the interface surface $[m^2]$

$T_{powerplant}$ is the temperature at powerplant interface
T_{LH2} is the temperature of the fluid

However, for the purpose of this study, the reference value of 1300 K is selected, as advised by (Balland, et al., 2015). In order to evaluate the trend of the main physical characteristics of the machines, a sensitivity analysis is performed considering the assumptions listed in Table 31. Rotational speed of the machine is considered as free parameter in order to investigate its effect on the machine. Moreover, in order to draw the physical maps of the whole turbomachinery, a range of compressor pressure ratios is proposed. This allows understanding the effect of the compressor design points on the physical characteristics of the whole assembly. The turbine expansion ratio is quite low in this case study, so it has been kept as constant value. The diameter of the machine is used as parameter within the physical maps, since it influences the mass flow as well. Thus, with fixed free stream conditions, different maps have been represented for a set of machine diameters. Fig. 182 shows the map concerning the trend of the length as function of rotational speed and pressure ratio, whilst Fig. 183 and Fig. 184 reports similar views for mass and volume respectively. For the purpose of this analysis, diameter of 0.6, 0.9 and 1.2 m are shown.

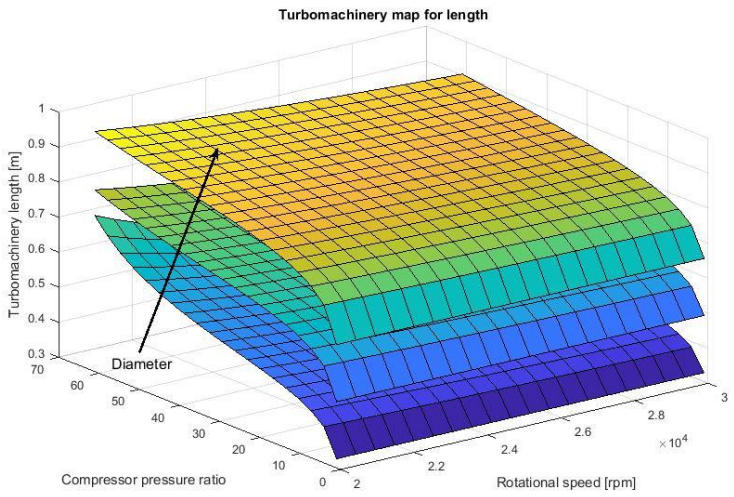

Fig. 182: Length of turbomachinery as function of compressor design point

The map in Fig. 182 shows an increase of turbomachinery assembly length with the compressor pressure ratio, whilst the raising of rotational speed produces a slight drop of axial dimension. Even if the effect of rotational speed appears less

important in this case, the increase of length with compressor pressure ratio is consistent, since this usually affects the number of stages. Moreover, the machine becomes longer as the diameter increase. This effect appears reasonable since the overall assembly increase its global dimensions with a larger diameter. It is also worth noticing that the effect of the diameter is not linear since, at low diameter high pressure ratio and low rotational speed, the machine increases its length much faster than in other design conditions. In turn, the map represented in Fig. 183 shows the mass trend as function of compressor pressure ratio and rotational speed. The diameter is here a clear representation of machine dimensions and, thus, a higher value brings a higher mass. Moreover, reducing the pressure ratio also produces a considerable lightening of the machine. The contribution of rotational speed is still less remarkable. For low diameters, high pressure ratio and low rotational speed a higher effect on mass increase can be noticed, as already mentioned for length (Fig. 182).

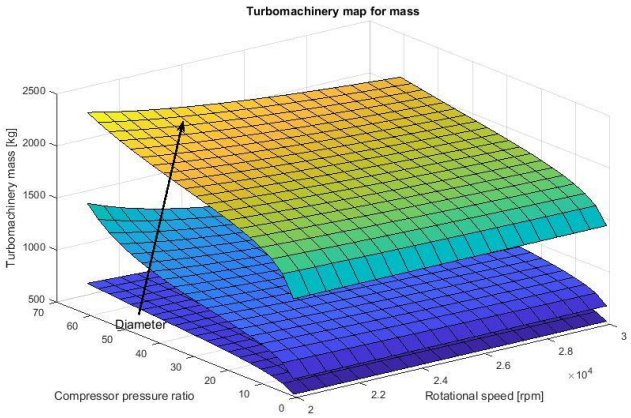

Fig. 183: Mass of turbomachinery as function of compressor design point

A similar result is plotted in Fig. 184 where the trend of volume as function of the same parameters is presented. As consequence of the trend obtained for the length and considering the diameters chosen for the analysis, the volume increase with increasing diameter and pressure ratio. The effect of rotational speed is less remarkable at fixed diameter.

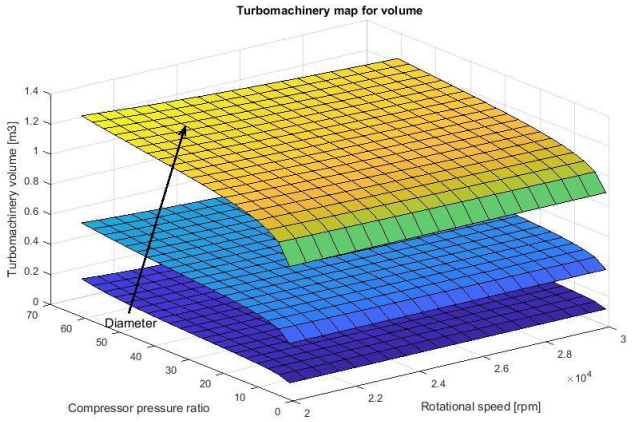

Fig. 184: Volume of turbomachinery as function of compressor design point

Additional trends can be identified looking at the relations between diameter, rotational speed and mass, as well as between number of stages and length. The effect of reference diameter on assembly mass can be directly assessed looking at the trends proposed in Fig. 185 and Fig. 186. In this case, compressor and turbine masses are shown with number of stages as additional parameter. Charts are shown for 20000 rpm.

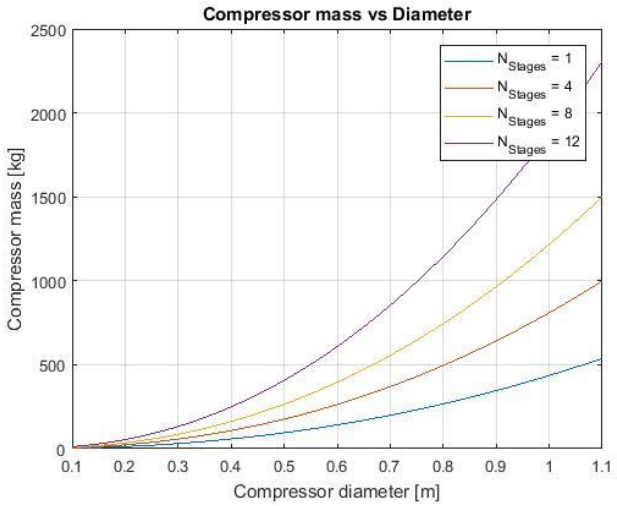

Fig. 185: Compressor mass as function of reference diameter

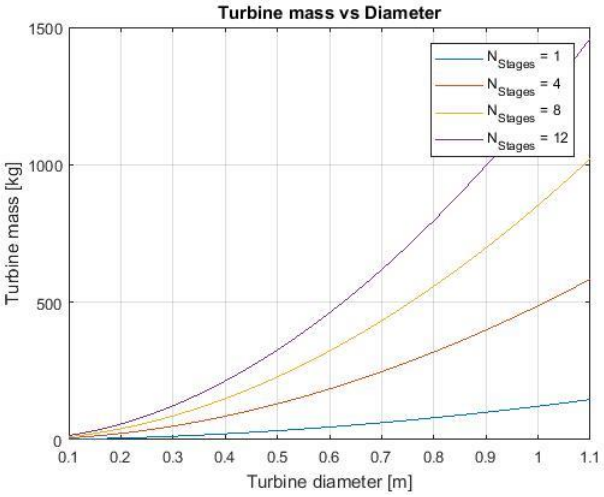

Fig. 186: Turbine mass as function of diameter

Comparing Fig. 185 and Fig. 186 it is possible to see how the effect of increasing diameter produces a mass increase which grows slower for the turbine than for the compressor. The effect of rotational speed is also important to evaluate mass trends. Fig. 187 and Fig. 188 shows these trends using as parameter the diameter of the machine.

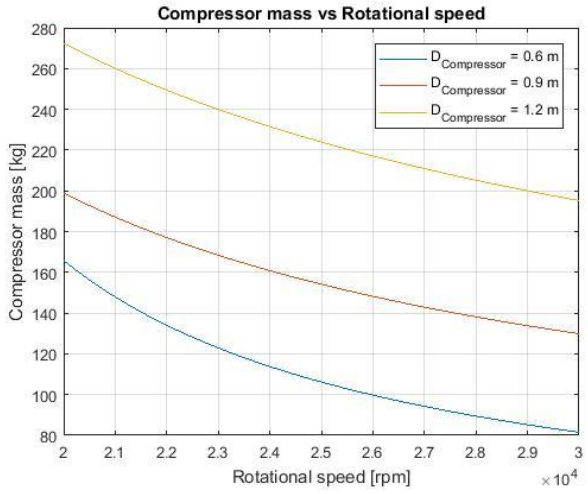

Fig. 187: Compressor mass as function of rotational speed

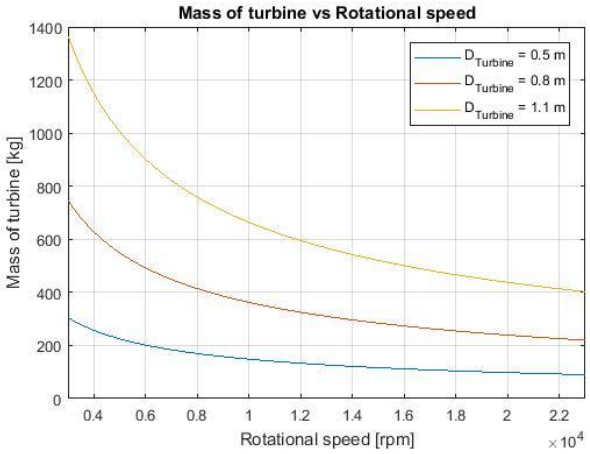

Fig. 188: Turbine mass as function of rotational speed

The increasing rotational speed produces a reduction of mass for both compressor and turbine. This reduction appears to have an asymptotic trend for turbine, whilst the theoretical mass of compressor does not reach a steady value. However, in both cases, it is reasonable to hypothesize that a minimum value, under which it is not possible to go for constructional reasons, shall be reached at a certain rotational speed. An additional aspect related to the determination of turbomachinery dimensions is the effect of number of stages on overall length. The relationships is quite simple to understand since a higher number of stages results in a longer machine. However, because of the contribution of the length to inlet mean diameter ratio (94), the relationships are different depending on the considered diameter (Fig. 189 and Fig. 190).

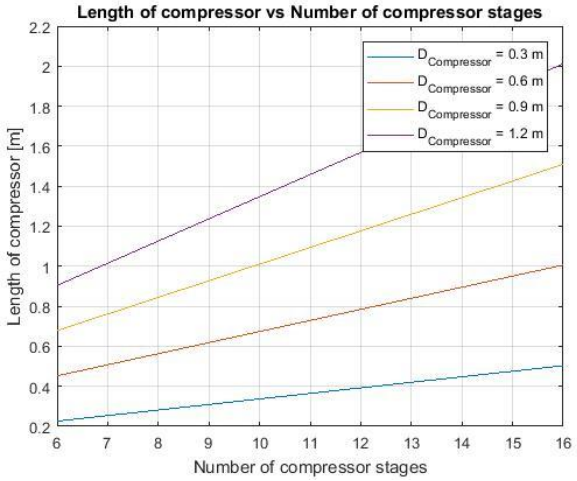

Fig. 189: Compressor length as function of number of stages

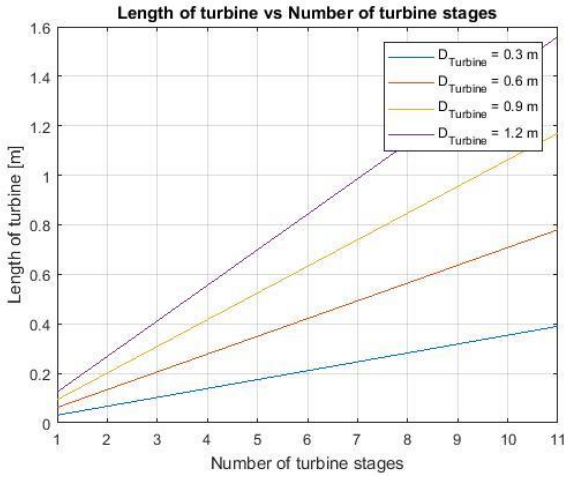

Fig. 190: Turbine length as function of number of stages

The effect is similar for both compressor and turbine, even if it is usual to have a lower number of stages for the latter and a higher one for the former.

Tanks. Since it is not useful to evaluate original tanks masses, being partially included within structural mass of the airframe, a parallel approach is here proposed in order to evaluate the hypothetical mass of equivalent rigid tanks having cylindrical shape with both spherical and ellipsoidal tank ends. An Aluminium alloy based material has been selected as reference material (characteristics in Table 32).

Table 32: Characteristics of reference tanks material

Parameter	Value
Ultimate tensile strength [MPa]	290
Young Modulus [GPa]	70
Density [kg/m3]	2700
Poisson ratio	0.33

A sensitivity analysis is performed in order to investigate the effect of tank working pressure, tank material density and tank volume on total component mass. The analysis is relatively agile for tanks since results can be grouped in three main charts, reported in this section. The main focus is dedicated to tank mass, since dimensions, surface and tank design volume are mainly related to the required fluid volume and integration with the vehicle. The considered tanks have cylindrical shape, with both spherical (indicated with dotted lines) and ellipsoidal ends (represented with solid lines). Tank ends have been computed considering that their volume is about 1% of the total volume. Fig. 191 shows the effect of tank operating pressure on its mass for three aluminium alloy vessels having different volumes.

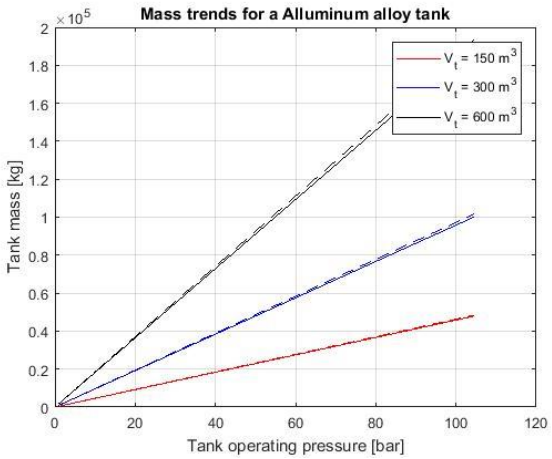

Fig. 191: Tank mass as function of working pressure

As it can be seen, it is reasonable that the mass of the tank is increasing linearly with the operating pressure. Moreover, it is interesting to see that spherical tank ends are slightly heavier than ellipsoidal ones for the same volume and pressure. Fig. 192 shows instead the effect of the ultimate strength of the material (taken as main variable to determine the maximum allowable stress of the tank, as for criteria (110)) on the mass of the tank, considering different densities. It is clear

that a higher ultimate tensile strength allows reducing the thickness of the tank wall, reducing the overall mass. Moreover, with equal ultimate strength characteristics, a lighter material produce an additional mass saving. As in Fig. 191, spherical tank ends cause an increase of mass even if maintaining constant the other variables.

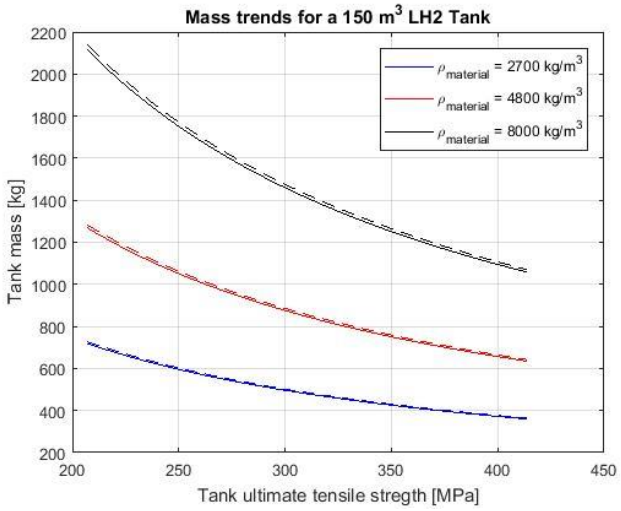

Fig. 192: Tank mass as function of ultimate tensile strength of the material

Fig. 193 represents the trend of tank mass as function of material density, being complementary to Fig. 192. The trend is in this case linear because of the effect of material density, at fixed ultimate strength.

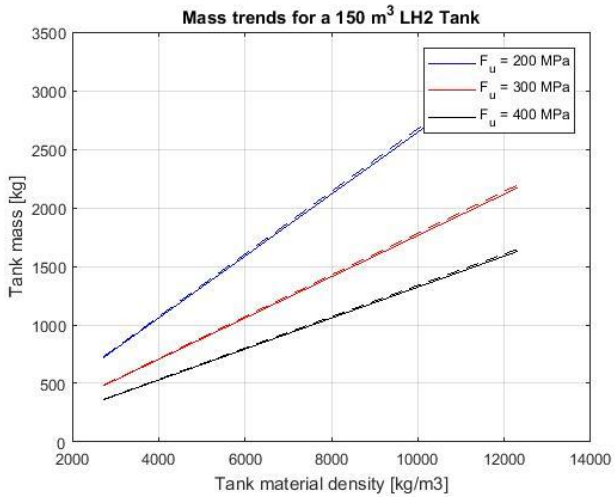

Fig. 193: Tank mass as function of material density

Pipes. The routings of the TEMS circuit of the STRATOFLY MR3 have still to be determined in detail, so a reference to specific coordinates for the installation of the different elements may be not appropriate. The results for the different parts of the circuit can be in any case determined following the input provided in (Balland, et al., 2015) concerning pressure levels and diameters (see Fig. 54 for TEMS schematic and pipes sections). Particularly, pressure levels indicated in Table 33 are referred to the pressure required at the end of the segment. The difference between the inlet and outer pressure is then the pressure drop due to pipes friction. All results reported in Section 5.2.4.7 are obtained considering aluminium alloy pipes, as already indicated for tanks in Table 32. The specific mass has been computed considering a minimum pipe wall thickness of 1 mm. This is necessary because, for low pressures, the computation of wall thickness may produce results which are not compatible with structural integrity (i.e. walls too thin to be realized). Notwithstanding the simplicity of the component, it is possible to make some considerations on pipe mass as function of some of the operating parameters defined in Table 28.

Table 33: Boundary conditions for TEMS pipes physical characterization

Circuit segment	**Pressure levels [MPa]**	**Mass flow [kg/s]**
From LH2 tank to pump	0.1	100
From pump to engine	8	100
From engine to expander	8	100
From LH2 tank to compressor	0.1	8
From compressor to expander	6	4.4
From compressor to air pack	6	3.6
From air pack to expander	0.075	3.6

Particularly, the influence of operating pipe pressure, mass flow and absolute roughness of pipe material on mass trends have been analysed. Fig. 194 shows the mass trend related to a pipe of 1 m length, supporting the maximum mass flow of 100 kg/s, as function of operating pressure, for different pipe radii.

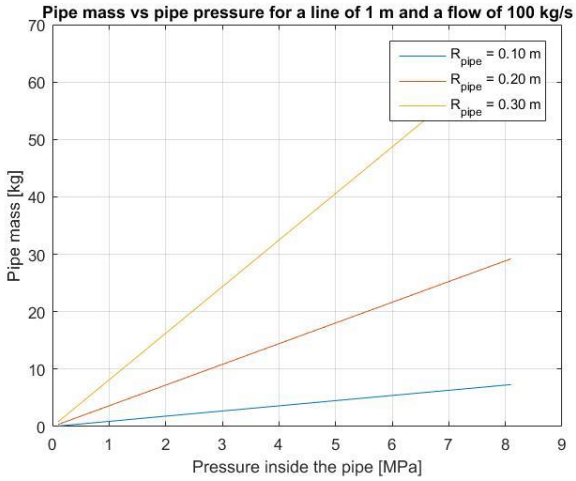

Fig. 194: Mass trend as function of operating pipe pressure

The influence of operating pressure is linear according to (144). The radius act as angular coefficient of the function, raising the mass as the pipe increases its dimensions. Fig. 195 shows the effect of mass flow for fixed diameter and pressure conditions. This allows appreciating the effect of distributed pressure drops for different lengths of the line.

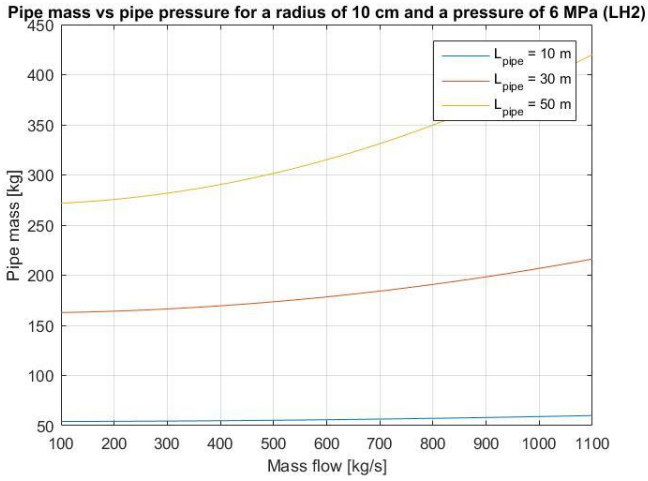

Fig. 195: Mass trend as function of mass flow

As it can be seen, the trend is strongly non-linear while increasing the length of the pipe. Moreover, it becomes to be important for very high circuit length. Ultimately, Fig. 196 presents the effect of material roughness on pipe mass for a fixed length and mass-flow.

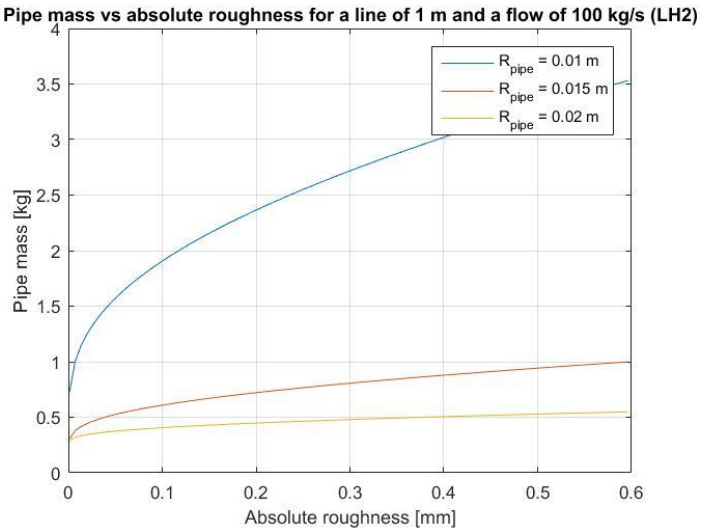

Fig. 196: Mass trend as function of pipe material roughness

It is possible to understand how the roughness of material has impact on pressure drops and, as consequence, on the higher inlet pressure required to balance them. This has a direct impact on pipe mass, even if it is remarkable only for very low diameters.

Heat exchangers. The TEMS circuit indicated in Fig. 54 has four main exchangers for cabin, power plant and air pack cooling. The exchanger for cabin cooling uses LH2 boil-off to cool down an air flow which is maintained between the LH2 tanks and the cabin walls in proper channels as indicated in Fig. 197 (Balland, et al., 2015).

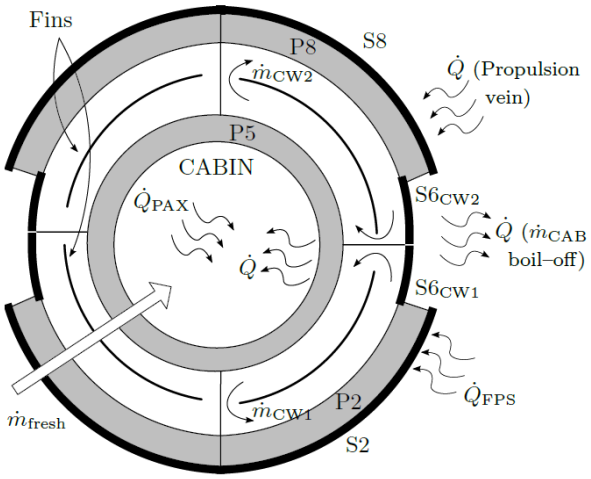

Fig. 197: Cabin cooling architecture (Balland, et al., 2015)

Boil-off is also used as main fluid for cooling the high-pressure and high-temperature air flow coming from the air pack, which is used for conditioning and pressurization of the vehicle. Moreover, the cooling of the power plant is performed through two regenerators using boil-off coming from the compressors shown in Fig. 54 and, on the other hand, by the liquid hydrogen pumped by the power plant feeding system. In order to perform the estimations, the assumptions listed in Table 34 are considered.

Table 34: Assumptions for MR3 heat exchangers characterization

Heat exchanger	**Inlet temperatures [K]**		**Outlet temperatures [K]**		**Mass flow (cooling fluid) [kg/s]**
	Hot fluid	**Cold fluid**	**Hot fluid**	**Cold fluid**	
Cabin exchanger	308	50	301	270	20
Air pack exchanger	3240	950	300	1200	3.6
Engine LH2 regenerator	1400	28	1000	1300	50
Engine boil-off regenerator	1400	950	1000	1200	4

The sensitivity analysis described in this section has been performed looking at the different exchangers of TEMS by considering the effect of mass flow, of

cooling fluid as well as of the temperatures difference to be managed and of the convection coefficient. This allows determining the variations of mass, volume, length and surface of the components. In general, as it is possible to see in the following figures, the increase of coolant flow produces a linear increase in mass, volume and exchange surface, whilst the length of the component reduces. Moreover, a higher ΔT causes a higher mass and volume of the component at fixed mass flow, producing at the same time a benefit in terms of length. Eventually, a higher convection heat transfer coefficient produces a lower exchange surface for a specific mass flow. Fig. 198 shows the analysis performed for cabin exchanger.

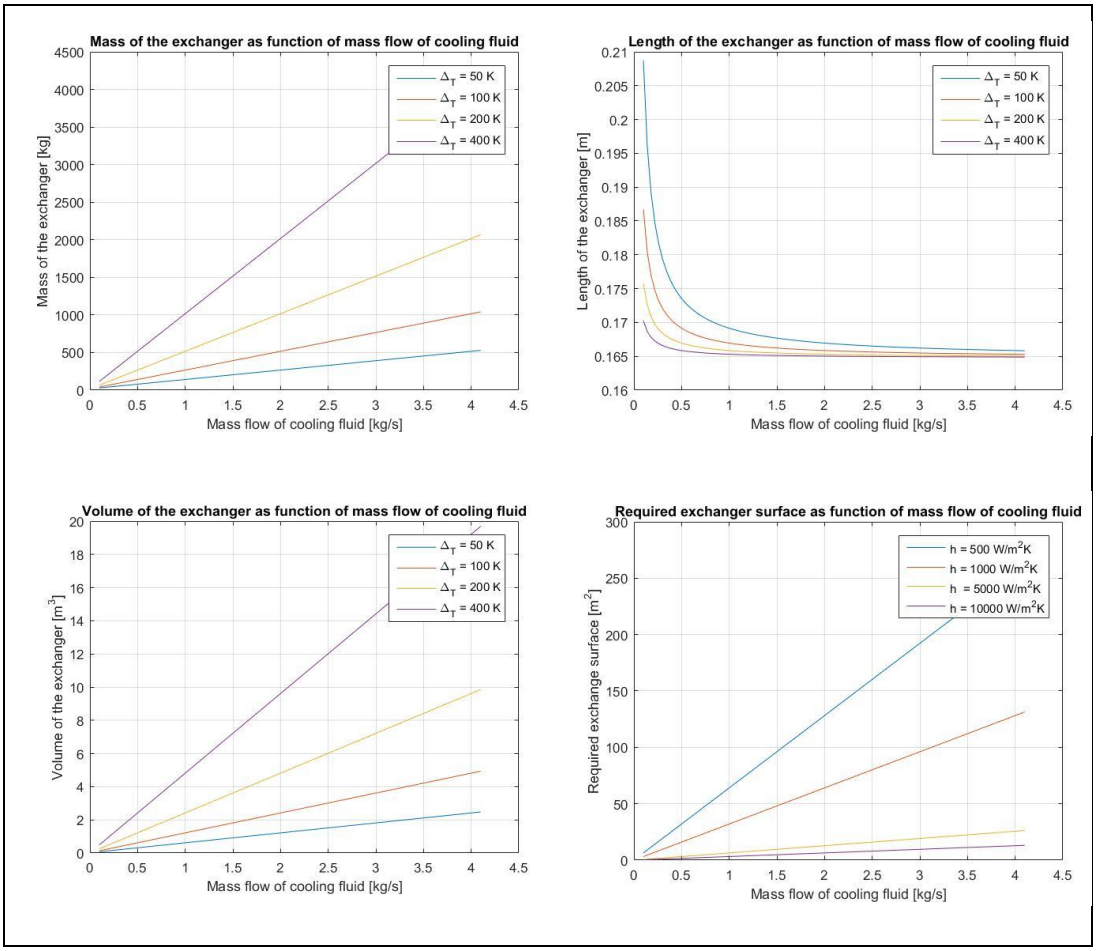

Fig. 198: Sensitivity analysis on cabin heat exchanger

Fig. 199 shows the sensitivity analysis for air pack exchanger.

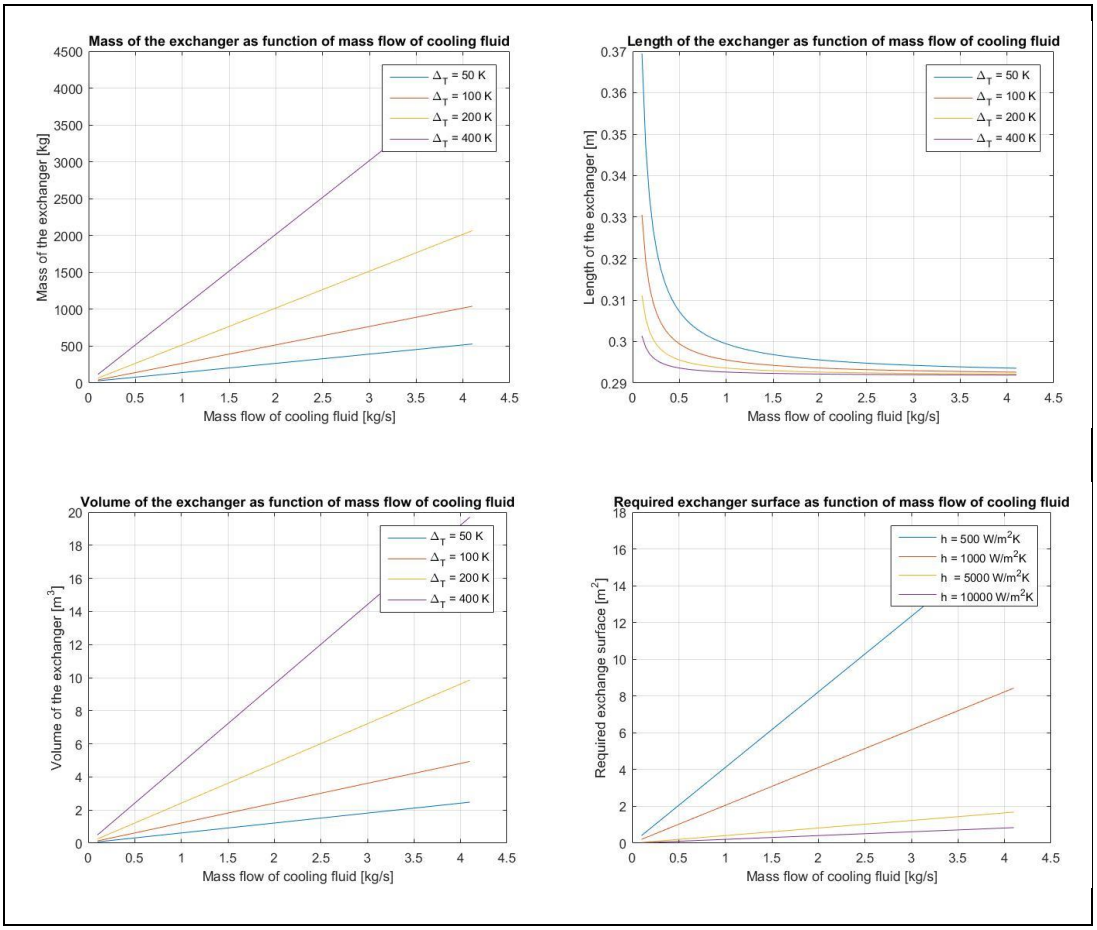

Fig. 199: Sensitivity analysis on air pack heat exchanger

Fig. 200 proposes the sensitivity analysis for hydrogen regenerator.

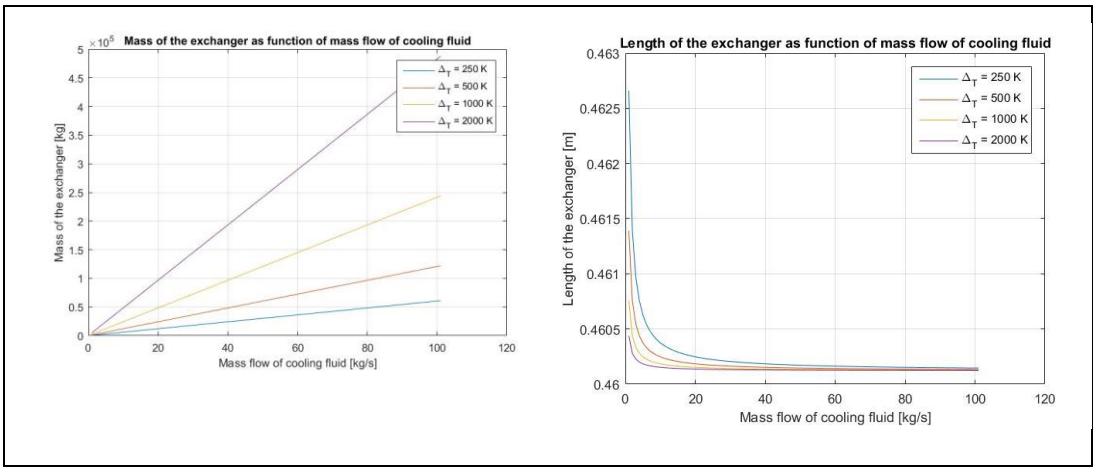

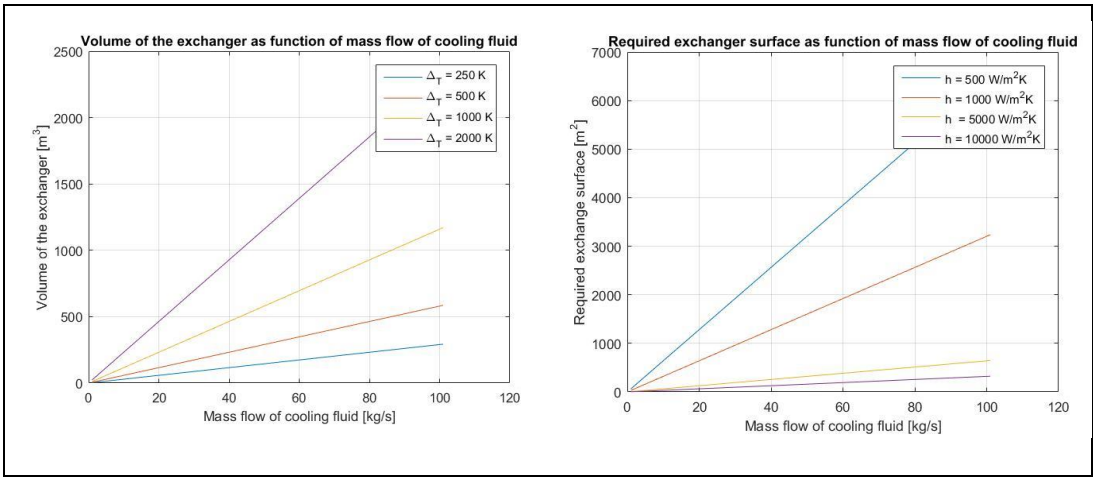

Fig. 200: Sensitivity analysis for hydrogen regenerator

Fig. 201 shows the sensitivity analysis for boil-off regenerator.

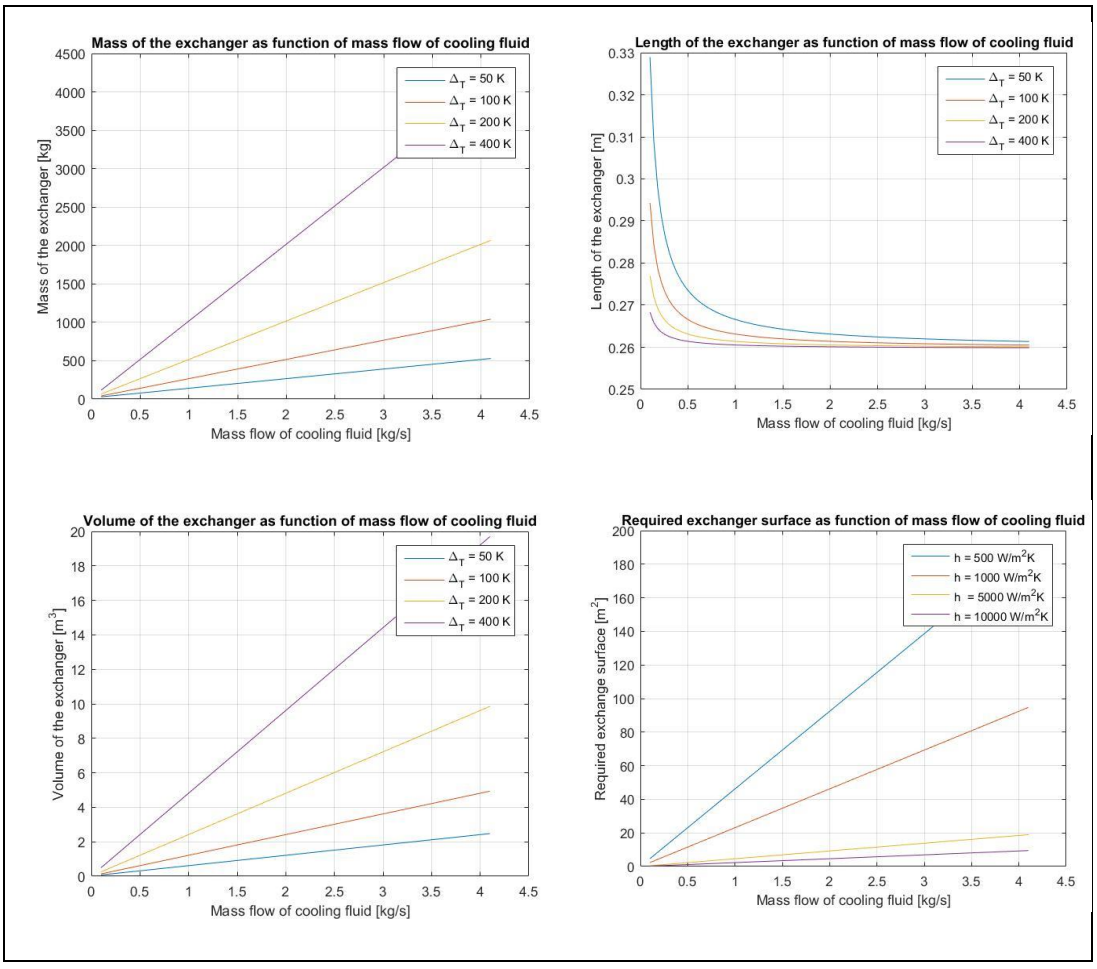

Fig. 201: Sensitivity analysis for boil-off regenerator

5.2.4.7 Compute subsystem breakdown (theoretical)

Turbopumps. With the hypotheses provided in (Balland, et al., 2015) and the physical models developed within Section 5.2.4.5, considering the operating conditions specified in Section 5.2.4.6, the results reported in Table 35 are obtained.

Table 35: STRATOFLY MR3 turbopump breakdowns

	Hypotheses			**Items**	**STRATOFLY MR3 estimated value**
	Input	**Value**	**Comment**		
Diameter	$k_{D/diff}$	1	Volute type diffuser	D_{TP}	0.549 m
	$k_{D/inlet}$	0	Frontal inlet		
	$k_{D/outlet}$	0	Not applicable		
	$k_{D/misc}$	0.01	Compact design		
Length	$k_{L/ind}$	2.5	Inducer	L_{TP}	0.873 m
	$k_{L/pb}$	0	-		
	$k_{L/out}$	1	Mean of the case-studies		
	$k_{L/other}$	2	Compact design		
Mass	I_N	0.6	Considering N=35000 rpm	M_{TP}	456 kg
	$I_{\dot{m}}$	1	Considering a flow rate of 100 kg/s		

Geometrical characteristics have been selected to obtain a baseline configuration with a single stage pump, featuring a frontal inlet equipped with an inducer and a volute diffuser, so to maximize the available pressure head. Results show that a single turbopump is similar to the High Pressure Fuel Turbo Pump (HPFTP) of the Space Shuttle Main Engine (SSME) (Sobin, 1974), for what concerns mass and dimensions.

Compressors and turbines. Considering the aforementioned analysis and the general input coming from (Balland, et al., 2015), reported in Table 31, a possible implementation for the boil-off compressor and the expander of MR3 TEMS system is here proposed. The application of the described methodology leads to the results collected in Table 36.

Table 36: STRATOFLY MR3 – output of compressor and turbine sizing

	Items	STRATOFLY MR3 estimated value
Diameter	$D_{Compressor}$	0.70 m
	$D_{Expander}$	0.50 m
Length	$L_{Compressor}$	0.47 m
	$L_{Expander}$	0.17 m
	L_{Total}	**0.64 m**
Mass	$M_{Compressor}$	168 kg
	$M_{Expander}$	97 kg
	$M_{Accessories\ \&\ Structure}$	80 kg
	M_{Total}	**345 kg**
Volume	$V_{Compressor}$	0.33 m^3
	$V_{Expander}$	0.08 m^3
	V_{Total}	**0.41 m^3**

The length and diameter values included in Table 36 for compressor and expander refer only to the single components, thus additional margins may be required to consider the case and mechanical fittings. Moreover, additional data concerning the design point have been obtained, following the exploitation of the proposed approach (Table 37) and the sensitivity analysis performed. It is particularly interesting to see that, with the proposed input and formulation, the resulting number of stages computed using (91) is about 5.

Table 37: Additional operating parameters for the case study

	Parameter	Value
Boil-off compressor	Rotational speed [rpm]	20000
	Number of stages	5
Expander	Rotational speed [rpm]	20000

As for turbopumps, the selection of proper redundancy strategies for the components of the system and/or the adoption of parallel/series architectures to guarantee the satisfaction of required performances may affect the mass and size of the gas generator assembly (Section 5.2.5). In this case, only a single unit has been considered so additional considerations concerning multiple components may be required for future assessments.

Tanks. The STRATOFLY MR3 vehicle has integral tanks. They have been grouped in 4 families (Fig. 202) (Viola & Fusaro, 2019) and, notably:

- Forward Fuselage Tank (FFT, blue);
- Centre Fuselage Tank (CFT, orange);
- Aft Fuselage Tank (AFT, grey);
- Wing Tanks (WT, yellow).

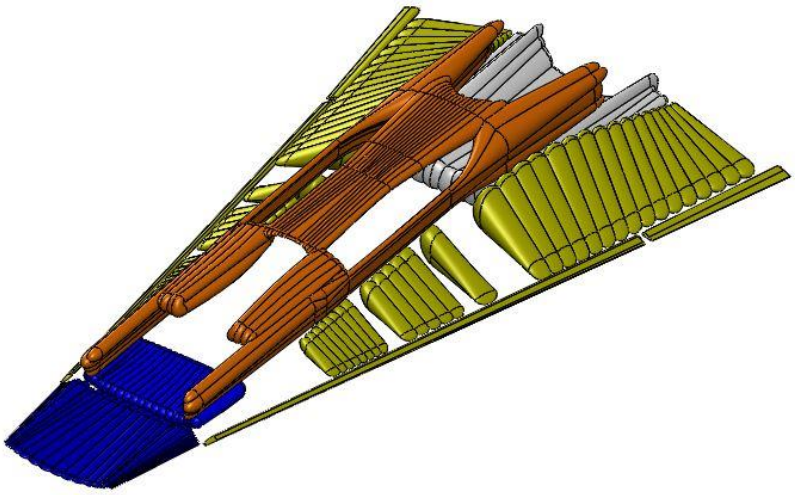

Fig. 202: STRATOFLY MR3 tanks architecture (Viola & Fusaro, 2019)

The reference volumes are reported in Table 38. According to the design of LAPCAT MR2.4, 186 tons of LH2 are required for the reference mission (around 2630 m^3). However, STRATOFLY MR3 vehicle may need 20 tons of additional LH2 if considering final powered descent and landing (bringing overall volume up to around 2900 m^3). The following (required) volume breakdown has been proposed concerning the vehicle allocation.

Table 38: Reference required volume breakdown

Tank	**Required tank volume [m^3]**
FFT	145
CFT	290
AFT	725
WTsx	870
WTdx	870
TOTAL	**2900**

Results reported in this section refer to the theoretical derivation process, as shown in Table 39, whilst margins are taken into account in Section 5.2.5.2. Working conditions have been kept constant and consistent with the study performed in (Balland, et al., 2015).

Table 39: Mass estimation for STRATOFLY MR3 in case of adoption of non-integral tanks

Tank	**Result considering spherical ends [kg]**	**Result considering ellipsoidal ends [kg]**
FFT	477	469
CFT	954	939
AFT	2352	2305
WTsx	2837	2803
WTdx	2837	2803
TOTAL	**9457**	**9319**

Present study does not take into account the mass required for insulation and thermal protection of the cryogenic fluid. It is reasonable to take the result of Table 39 as preliminary mass reduction index characterizing the design of actual MR3 vehicle if compared with an equal aircraft with non-integral tanks. However, the computation proposed in this report is simplifying the shape of the tank. Moreover, theoretical results consider very thin walls (around some millimetres)

to withstand the pressure levels specified by (Balland, et al., 2015), even if structural integrity may require wider shell. This may substantially increase the mass of the tanks.

Pipes. As already mentioned, for the purpose of the estimation of pipes breakdown of the case study, a specific mass per unit length is selected in $[kg/m]$. Results are shown in Table 40 for the different plant sections indicated in Fig. 54.

Table 40: Mass breakdown of the TEMS pipes

Circuit segment	**Diameter [m]**	**Specific Mass [kg/m]**
From LH2 tank to pump	0.10	0.85
From pump to engine	0.10	1.8
From engine to expander	0.92	152.7
From LH2 tank to compressor	0.46	3.9
From compressor to expander	0.13	2.3
From compressor to air pack	0.13	2.3
From air pack to expander	0.13	1.1

The high value of the third section of the circuit is due to the very high diameter hypothesized in (Balland, et al., 2015) for the worst condition and the highest pressure level. An average value of 2 $\frac{kg}{m}$ is thus reasonable for most of the pipes section, excluding the heat rejection assembly line. Again, as for tanks, these estimations take into account structural mass only. Detailed considerations on thermal insulation and on margins associated to temperature and conductivity of the material are reported in Section 5.2.5.2.

Heat exchangers. The results included in Table 41 have been obtained for the considered exchangers.

Table 41: Results for TEMS heat exchangers estimation

Heat exchanger	**Mass [kg]**	**Volume [m^3]**	**Exchange surface [m^2]**
Cabin exchanger	493	2.3	14.4
Air pack exchanger	2267	10.8	37
Engine LH2 regenerator	159017	763	1659
Engine boil-off regenerator	2517	12	46.2
Total*	**5277**	**25.1**	**97.6**

* Excluding hydrogen regenerator

The exchange surfaces have been computed according to (154). Knowing the surface and the volume, it is possible to assume a reference length for the exchanger as well. As it can be seen, the results are very high, especially in terms of mass. The estimation relationships described in Section 5.2.4.5 describe, in fact, the physical breakdowns of dedicated exchangers which are not integrated within structural assemblies, being characterized by a conventional architecture (fluid heat exchangers with parallel or counter flow configurations). It is then clear how the integration of such components within structural elements is fundamental to reduce the required mass.

Global results. Considering the assumptions and results listed in this section, the summary of Table 42 can be collected concerning TEMS mass breakdown. For pipes mass it is recommended to look at Table 40.

Table 42: Mass budget of TEMS

Component	**Mass [kg]**
LH2 Turbopump	456
Boil-off compressor	168
Boil-off expander	97 (177 considering accessories)
Heat Exchangers	5277
Total*	**6078**

* Excluding LH2 regenerator

Mass of gas generator accessories and structure has been allocated 1/3 on turbine and 2/3 on compressor. For the main parts of TEMS circuit pipes, the average value of 2 kg/m can be considered (this value is obtained neglecting the engine –

expander path contribution). Moreover, it would be necessary to consider an additional mass in case of utilization of non-integral tanks of at least 9319 kg. The mass allocated to heat exchangers can be also reduced depending on the level of integration of the devices with the airframe structure. As far as MR3 TEMS volume is concerned, Table 43 provides an overview of the contributions of the different items to the final breakdown

Table 43: Volume budget of TEMS

Component	**Volume [m^3]**
LH2 Turbopump	0.48
Boil-off compressor	0.33
Boil-off expander	0.08
Heat Exchangers	25.1
Total	**25.99**

Tanks total volume is about 2900 m^3, whilst pipes volume depends on the routings and mutual position of the different components.

5.2.5 Other aspects affecting the definition of subsystem breakdowns

5.2.5.1 Safety and reliability

Results computed in Section 5.2.4 are obtained considering only nominal scenarios and neglecting possible problems associated to dysfunctional behaviour (loss of functions during operation) and reliability of components responsible to guarantee the required capabilities. In fact, safety and reliability aspects are crucial in the aerospace domain, and, especially, for civil aviation, where safety critical systems shall be subjected to certification process before the entry-into-service. Particularly, considering the nature, category and application of STRATOFLY MR3 vehicle as well as its subsystems, it is reasonable to perform a short digression about the typical preliminary safety and reliability assessment performed at this design stage in civil aviation domain. A common best practice is proposed by (SAE, 1996), where a practical method to face the safety assessment of civil aircraft, as preparation of certification, is presented. The safety assessment process so defined (Fig. 203) follows the product lifecycle, and especially the

design phase, by proposing a set of different analyses to be performed at several hierarchical levels.

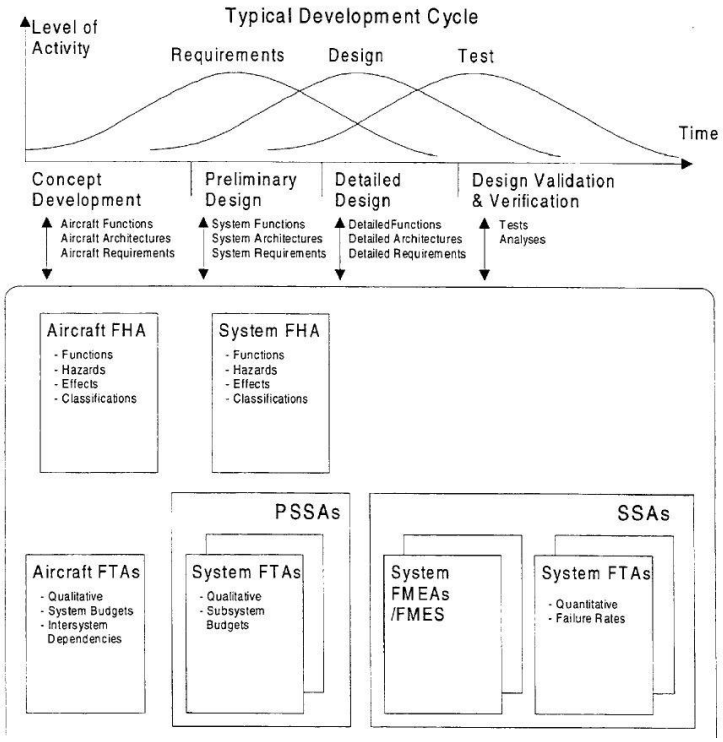

Fig. 203: Safety assessment process for civil aircraft defined in (SAE, 1996)

"A Functional Hazard Assessment (FHA) is conducted at the beginning of the aircraft/system development cycle. It should identify and classify the failure conditions associated with the aircraft functions and their combinations. These failure condition classifications establish the safety objectives" (SAE, 1996). The outcomes of the FHA are used to prepare and establish the Preliminary System Safety Assessment (PSSA). *"The PSSA is a systematic examination of the proposed system architecture to determine how failures can cause the functional hazards identified by the FHA. The objective of the PSSA is to establish the safety requirements of the system and to determine that the proposed architecture can reasonably be expected to meet the safety objectives identified by the FHA"* (SAE, 1996). This kind of assessment is performed at different levels while designing the subsystems. In fact, *"at lowest level, the PSSA determines the safety related design requirements of hardware and software. The PSSA usually takes the form of a Fault Tree Analysis (FTA)"* (SAE, 1996). Subsequently, the System Safety Assessment (SSA) *"is a systematic, comprehensive evaluation of the implemented*

system" (SAE, 1996). This means that the key aspect differentiating PSSA and SSA, other than the level of detail that can be used to perform the analyses, is that the former is focused on the qualitative description of the system, used to define safety objectives and to allocate safety levels on components, while the latter is clearly quantitative, being based on the prediction of the reliability levels associated to the selected architecture (implementation). From a designer point of view, the important effect of this kind of assessment mainly refers to the need of envisaging redundant configurations for critical components, thus raising the complexity of the system and, ultimately, increasing the breakdowns. This means that subsystems will be heavier and larger than expected, with unavoidable consequences on vehicle configuration and allocation strategy. For the purpose of this Dissertation, an example of application of a safety assessment methodology for trans-atmospheric and hypersonic transportation system, inspired by (SAE, 1996) and formalized in (Fusaro & Viola, 2017), is proposed, with special focus on TEMS. Notably, PSSA and SSA are discussed to show the impact on original subsystem layout, starting from subsystem level FHA. The aircraft level analysis (Babetto, 2018) is here neglected for conciseness needs. The PSSA process starts from and it is related to the functional analysis described in Section 5.2.1, at subsystem level. In fact, the FHA *"is defined as a systematic, comprehensive examination of functions to identify and classify failure conditions according to their severity"* (SAE, 1996). This means that the safety assessment shall start from the analysis of possible failure conditions affecting the on-design capabilities, as well as from the evaluation of the severity of the related effect. The FHA is thus the tool through which the *"qualitative analysis, where, starting from the top-level design activities, a safety assessment is performed following a top-down approach"* (Fusaro & Viola, 2017), can be tackled. Typically, safety objectives (probability of occurrence) are instantiated depending on the severity of the failure, as indicated in Fig. 204. FHA format is thus consisting of a table view that can be managed in different environments, where each function is associated to one or more failure conditions, characterized by a specific severity, also depending on mission phase. Starting from subsystem level and considering the main capability associated to TEMS, the following FHA (Table 44 and 45) can be derived.

Probability (Quantitative)		Per flight hour 1.0	1.0E-3	1.0E-5	1.0E-7	1.0E-9
Probability (Descriptive)	FAA	Probable		Improbable		Extremely Improbable
	JAA	Frequent	Reasonably Probable	Remote	Extremely Remote	Extremely Improbable
Failure Condition Severity Classification	FAA	Minor		Major	Severe Major	Catastrophic
	JAA	Minor		Major	Hazardous	Catastrophic
Failure Condition Effect	FAA & JAA	- slight reduction in safety margins - slight increase in crew workload - some inconvenience to occupants		- significant reduction in safety margins or functional capabilities - significant increase in crew workload or in conditions impairing crew efficiency - some discomfort to occupants	- large reduction in safety margins or functional capabilities - higher workload or physical distress such that the crew could not be relied upon to perform tasks accurately or completely - adverse effects upon occupants	- all failure conditions which prevent continued safe flight and landing
Development Assurance Level	ARP 4754	Level D		Level C	Level B	Level A

Fig. 204: Failure conditions severity and related probability (SAE, 1996)

Table 44: Functional Hazard Assessment at subsystem and assembly levels (Fusaro, et al., 2019)

FHA Subsystem Level		
Function	**Failure Condition**	**Severity**
SUF22000 – To provide thermal control	Loss of the capability to provide thermal control	A
FHA Assembly Level		
Function	**Failure Condition**	**Severity**
ASF1000 – To provide heat collection	Loss of the capability to provide heat collection	B
ASF2000 – To provide heat transportation	Loss of the capability to provide heat transportation	B
ASF3000 – To provide heat rejection	Loss of the capability to provide heat rejection	B

Table 45: Functional Hazard Assessment at equipment level (Fusaro, et al., 2019)

FHA Equipment Level		
Function	**Failure Condition**	**Severity**
EQF1000 – To collect heat from external skin	Loss of the capability to collect heat from external skin	C
EQF2000 – To collect heat from cabin	Loss of the capability to collect heat from cabin	C
EQF3000 – To collect heat from propulsion plant	Loss of the capability to collect heat from propulsion plant	C
EQF4000 – To collect heat from ECS	Loss of the capability to collect heat from ECS	D
EQF5000 – To transport heat from tanks to cabin collection equipment	Loss of the capability to transport heat from tanks to cabin collection equipment	C
EQF6000 – To transport heat from tanks to high pressure transport equipment	Loss of the capability to transport heat from tanks to high pressure transport equipment	C
EQF7000 – To transport heat from high pressure transport equipment to propulsion heat collection equipment	Loss of the capability to transport heat from high pressure transport equipment to propulsion heat collection equipment	C
EQF8000 – To transport heat from cabin to high pressure transport equipment	Loss of the capability to transport heat from cabin to high pressure transport equipment	C
EQF9000 – To transport heat from Propulsion plant to boil-off collection equipment.	Loss of the capability to transport heat from Propulsion plant to boil-off collection equipment.	D
EQF10000 – To transport heat from ECS to boil-off collection equipment.	Loss of the capability to transport heat from ECS to boil-off collection equipment.	D
EQF11000 – To transport heat from the compressor to the ECS.	Loss of the capability to transport heat from the compressor to the ECS.	C
EQF12000 – To assure an adequate pressure level in heat transportation assembly.	Loss of the capability to assure an adequate pressure level in heat transportation assembly.	C
EQF13000 – To mix heated flow with liquid propellant	Loss of the capability to mix heated flow with liquid propellant	C
EQF14000 – To inject heated flow and propellant in engine FCU	Loss of the capability to inject heated flow and propellant in engine FCU	C

In this case, only total loss of capabilities, in flight, are shown. As it can be seen, the FHA is consistent with the derivation of functionalities and subsequent FTA for the different levels strongly recalls the functional tree previously defined. The FTA *"is a deductive failure analysis which focuses on one particular undesired event and provides a method for determining causes of this even"* (SAE, 1996). In fact, each failure condition of the FHA is used to generate a proper FTA, where the top event is the condition itself. Fault trees are used to derive low level failure conditions, in accordance with the FHA, and to allocate the safety requirements on dysfunctional events. They used Boolean algebra and operators to translate into equations the structure they are representing. During the top-down qualitative approach, the probability of occurrence of the top event is distributed among low-level events, so to hypothesize their contribution as pre-condition to the main one. The failure condition at subsystem level thus allows sketching the first FTA, as shown in Fig. 205, where the hypothesis on failure rate allocation is proposed.

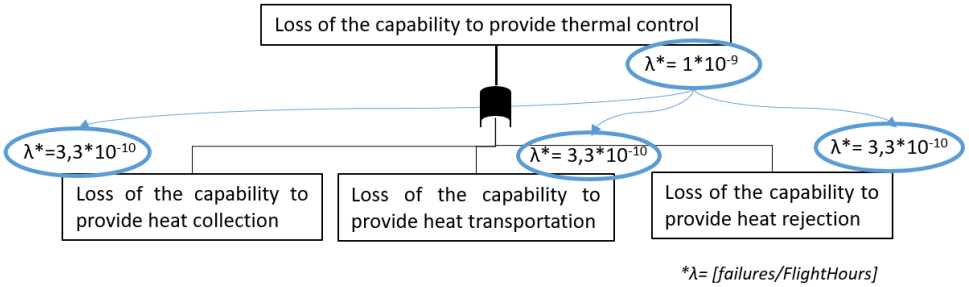

Fig. 205: FTA up to assembly level failure conditions (Fusaro, et al., 2019)

The subsystem level failure condition was categorized as a catastrophic event, being characterized by a consequent probability of occurrence corresponding to $1 \cdot 10^{-9} \frac{failure}{Flight\ Hours}$ or less. In order for the top event to happen, one of the low-level failure events shall occur. Particularly, it is sufficient that one of the events, at assembly level, takes place to produce the top one. Thus, severity of low-level events has been considered as homogeneous, equally distributing the probability of occurrence. Similarly, the FTA is detailed up to equipment level as shown in Fig. 206 and in accordance with the FHA reported in Table 45

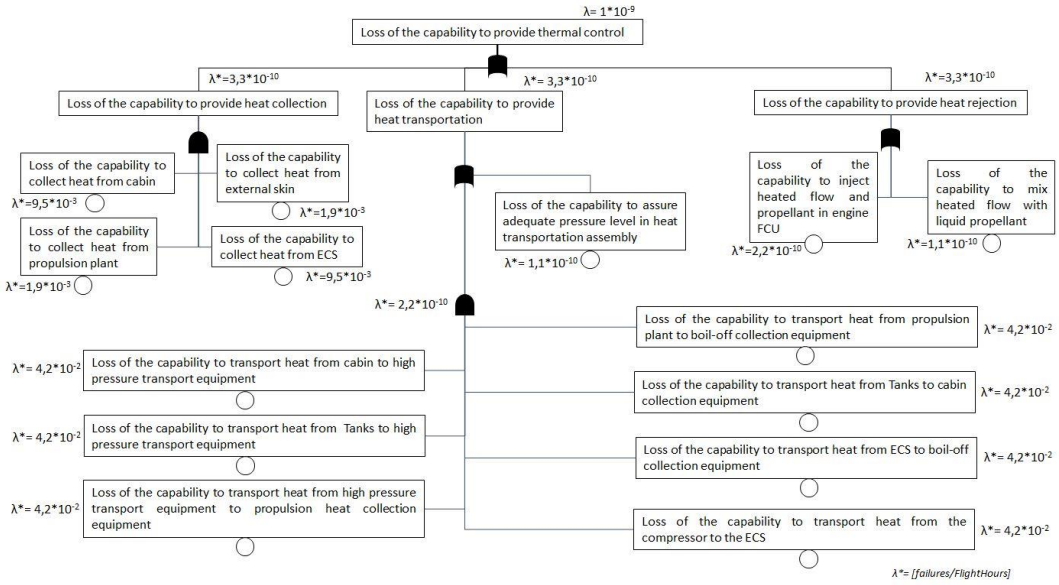

Fig. 206: FTA up to equipment level failure conditions

The allocation process on heat collection branch has been conceived to take into account the different heat fluxes coming from the sources listed in the functional breakdown. Particularly, the heat collection capability from external skin is considered to be five times more critical than the others, thus justifying the adoption of a more stringent requirement on probability occurrence. In this case, considering that assembly level failure refers to a total loss of heat collection capability, the low-level events shall occur simultaneously for the critical one to happen. For what concerns the heat transport branch, the capability of assuring an adequate pressure level within the plant is considered crucial, and more critical than the others. This is due to the fact that pressure inside the tanks is limited, and contribution from high-pressure devices is fundamental to guarantee a correct behaviour of the subsystem. Moreover, this capability is supposed to be performed by active components, rather than simple passive ones. In order to the total loss of heat transportation function to occur, either the capability of connecting the different elements of the plant or the nominal generation of suitable pressure levels shall fail. Considering the different transport capabilities, instead, a total loss shall happened to provide the final dysfunctional behaviour. Ultimately, looking at heat rejection branch, similar considerations related to active/passive functions have been applied to categorize the failure events. The loss of mixing capability is supposed to be more critical than the simple injection. One of these events is sufficient to provide the total loss of heat rejection

capability. Probabilities of occurrence for the different branches are in line with the objectives established within the FHA. The second part of the methodology consists of *"a quantitative analysis, where, starting from the results of the qualitative analysis, from the capabilities allocation on products and following a bottom-up approach, it is possible to retrace the way to derive the probability of the top-event related to the mission or to the system"* (Fusaro & Viola, 2017). In fact, once the safety requirements associated to functional capabilities are defined, it is necessary to verify whether the architecture hypothesized during the products allocation process meets the expectation as well as the safety objectives. Reliability thresholds for the different components can be derived upon statistical analysis or from data available in literature, so to rebuild the FTA from its basic elements. This allows computing the top event probability of occurrence that shall be subsequently compared with the result allocated within the qualitative approach. Resulting FTA is reported in Fig. 207, where each box represents a generic failure for the indicated element.

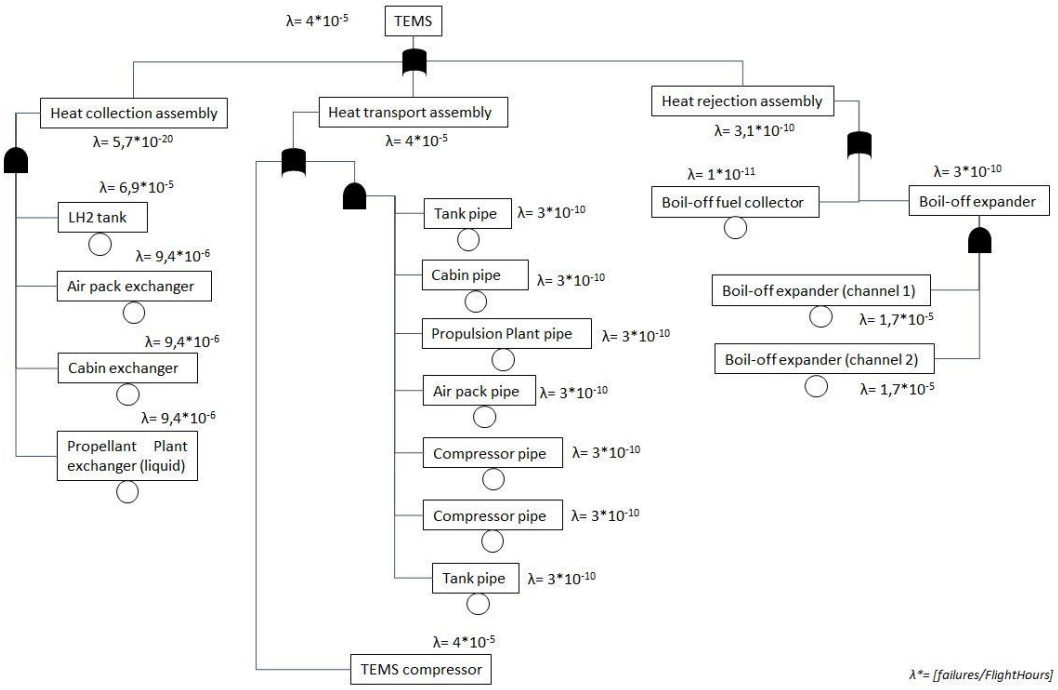

Fig. 207: Reliability prediction through bottom-up FTA

It is clear that, with the simple configuration shown in Fig. 54, the TEMS does not satisfy safety requirements, since it is characterized by $4 \cdot 10^{-5} \frac{failures}{FH}$. The most

critical element is the TEMS compressor that deeply influences the overall reliability of the subsystem, at least within the simplified architecture considered in the Dissertation. Even if a reasonable improvement in the technological level of the equipment can be envisaged considering the entry-into-service of the MR3 vehicle, allowing a reduction of the failure rate specified by (Jones, 2011) for turbomachinery, the gap to the requirements is considerably high. A suitable solution may include a parallel implementation of two, or more, compressors to increase the safety level of the subsystem. The FTA is thus modified as in Fig. 208, where a technological improvement is applied to the compressor. In this case, the safety objectives of $1 \cdot 10^{-9} \frac{failure}{FH}$ is met, since the TEMS is characterized by $4 \cdot 10^{-10} \frac{failure}{FH}$. Other equipment are already in line with the expectations, without the need of specifying additional redundancies.

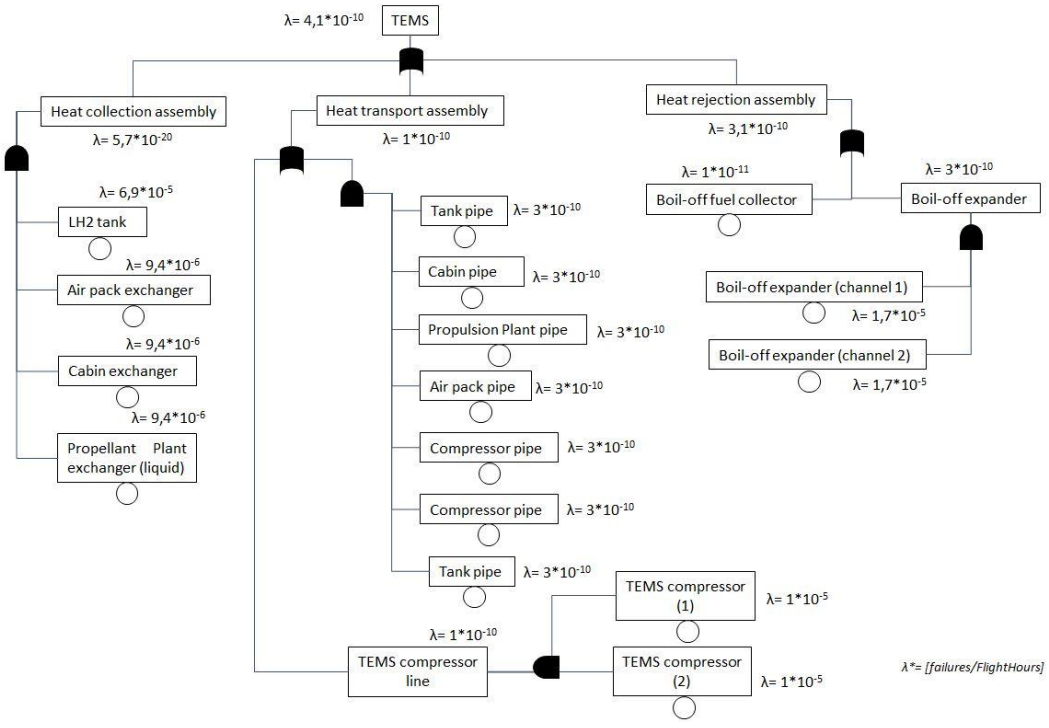

Fig. 208: Reliability prediction through bottom-up corrected FTA

With this short example, it is thus clear how the final breakdown of the subsystem, obtained looking merely at nominal scenarios and behaviour conditions may lead to underestimation of mass and volume, as well as dimensions on board. The calculation provided in this section is very preliminary

and has not the aim of being exhaustive, but it provides a clear outlook on the potential of the two stages approach, where qualitative and quantitative evaluations can be effectively combined to produce a first estimation of RAMS characteristics of a subsystem. As result of the overall process, safety and reliability requirements are listed in Sections 8.1.8 and 8.1.9. These are related to the safety objectives prescribed by FHA and decomposed within the FTA of the qualitative approach, in

Table 44 and in Fig. 206 respectively.

5.2.5.2 Margin policy

Mass properties and, in general, physical breakdown control is a critical aspect of aeronautical and space systems development. Different standards and best practices concerning mass control and allowances requirements are available in literature, as well as suggestions for the formulation of margin requirements for performance and physical characteristics. Depending on the engineering field and reference regulation or standard Agency, different requirements can be expressed. In this section, the standards used to perform physical breakdowns control in STRATOFLY are presented. The first one refers to the American National Standard ANSI/AIAA S-120A-2015 *"Mass Properties Control for Space Systems"* (ANSI/AIAA, 2015) and provides suggestions on how to perform mass control during the project, illustrating the process related to risk analysis and pointing out the main definitions related to the topic. The second document comes from the European Cooperation for Space Standardisation (ECSS) and it specifically refers to *"Margin philosophy for science assessment studies"* (ESA, 2012), being consistent with the relevant ECSS recommendations such as ECSS-E-ST-10-02C (Space engineering – Verification) (ECSS, 2009), ECSS-E-ST31C (Space engineering – Thermal control general requirements) (ECSS, 2008), ECSS-E-ST-50-05C (Space engineering – Radio frequency and modulation) (ECSS, 2011). Even if it is more convenient to look at the ECSS standards for the design of STRATOFLY vehicle, conceived as European endeavour, both recommendations are taken into account for the purpose of this study. First, they provide different views over the establishing of margins policy: the ANSI/AIAA standard is really focused on mass control whilst the ECSS best practices take into account different aspects related to dimensions, volume and performance. Secondly, they provide a convenient redundancy to mitigate the risk of mistakes in margins assignment, guaranteeing dissimilar approaches for computing

breakdowns allowances. In both cases, margins refer to the nominal configuration of the subsystems, thus neglecting RAMS aspects defined within Section 5.2.5.1.

ANSI/AIAA S-120A-2015 Standard. The standard is intended to provide acceptable mass properties requirements and guidance for the implementation of mass properties control plan, together with the SAWE RP A-3 (SAWE, 2015). It also defines "*terminology, and methods for the management, control, monitoring, determination, verification and documentation of mass properties during the design, development and operational phases of space systems"* (SAWE, 2015). The standard uses the mass definitions provided in Fig. 209, where:

- **Basic mass** indicates the dry mass derived from the latest baseline design;
- **Mass Growth Allowance (MGA)** is the predicted change to basic mass based on design maturity aiming at estimating the mass growth during product life-cycle because of in-scope design changes;
- **Predicted mass** is the sum of basic mass and MGA, defining the final mass at system delivery and operation;
- **Mass margin** is the difference between the allowable mass and predicted mass;
- **Allowable mass** is the limit against which mass margins are calculated.
- **Mass reserve** is the mass allowance defined by program management for potential out-of-scope changes or unforeseen impacts;
- **Mass limit** is the maximum mass that can satisfy mission performance requirements.

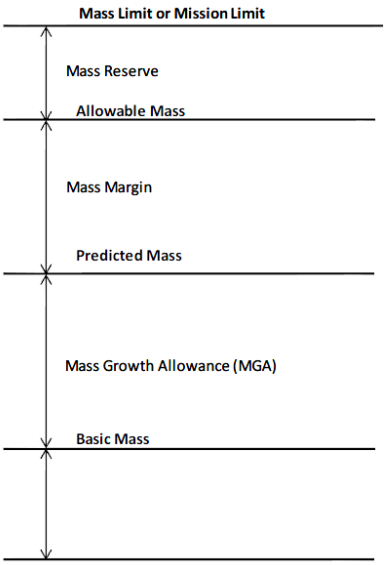

Fig. 209: Mass definitions according to ANSI/AIAA S-120A-2015 (ANSI/AIAA, 2015)

The overall mass estimation process starts with the identification of the basic mass of the product, derived from the (theoretical) mass estimation campaigns performed during the design process. It represents the ideal mass of the selected product, based on the available assumptions and performance. In order to derive the predicted mass, a suitable guideline is necessary to define proper MGA depending on the type of product considered and on the stage of the project. The standard suggests the values reported in Fig. 210. The additional mass margin is conceived to mitigate potential mass increases deriving from deviations from existing design that may exceed MGA allocations. These margins depend on the complexity and design maturity of the product and they are generally established depending on previous experience and data. The combination of MGA and mass margins allows determining the allowable mass, which is the real operating mass of the system under design (neglecting the mass reserve). The standard proposes the example reported in Fig. 210, where suitable combinations of MGA and mass margins depending on program phase are shown. Moreover, it provides also a possible risk matrix related to mass growth of a space system, categorized by specific grades (Fig. 211).

Maturity Code		Design Maturity (Basis for Mass Determination)	Percentage Mass Growth Allowance												
			Electrical/Electronic Components			Structure	Thermal Control	Propulsion	Batteries	Wire Harnesses	Solar Array	ECLSS, Crew Systems	Brackets, Clips and Hardware	Mechanisms	Instrumentation
			0-5 kg	5-15 kg	>15 kg										
E	1	**Estimated**	20-35	15-25	10-20	18-25	30-50	15-25	20-25	50-100	20-35	20-30	20-35	18-25	25-75
	2	**Layout**	15-30	10-20	5-15	10-20	15-30	10-20	10-20	15-45	10-20	10-20	10-25	10-20	20-30
C	3	**Preliminary Design**	8-20	3-15	3-12	4-15	8-15	5-15	5-15	10-25	5-15	5-15	8-15	5-15	10-25
	4	**Released Design**	5-10	2-10	2-10	2-6	3-8	2-7	3-7	3-10	3-5	3-8	3-8	3-4	3-5
A	5	**Existing Hardware**	1-5	1-3	1-3	1-3	1-3	1-3	1-3	1-5	1-3	1-4	1-5	1-3	1-3
	6	**Actual Mass**	Measured mass of specific flight hardware; no MGA; use appropriate measurement uncertainty.												
S	7	**CFE or Specification Value**	Typically, an NTE value is provided, and no MGA is applied.												

Expanded Definitions of Maturity Categories		
E1	**Estimated**	a. An approximation based on rough sketches, parametric analysis, or incomplete requirements b. A guess based on experience c. A value with unknown basis or pedigree
E2	**Layout**	a. A calculation or approximation based on conceptual designs (equivalent to layout drawings or models) prior to initial sizing b. Major modifications to existing hardware
C3	**Preliminary Design**	a. Calculations based on new design after initial sizing but prior to final structural, thermal or manufacturing analysis b. Minor modification of existing hardware
C4	**Released Design**	a. Calculations based on a design after final signoff and release for procurement or production b. Very minor modification of existing hardware
A5	**Existing Hardware**	a. Measured mass from another program, assuming that hardware will satisfy the requirements of the current program with no changes b. Values substituted based on empirical production variation of same or similar hardware or measured mass of qualification hardware c. Catalog values

Fig. 210: Mass Growth Allowance by design maturity (ANSI/AIAA, 2015)

Program Milestone	Recommended MGA (%)[1]	Recommended Mass Margin (%)[1]	MGA + Mass Margin (%)[2]	Grade
ATP	>15	>15	>30	Green
	9<MGA≤15	10<Mass Margin≤15	19<MGA + Mass Margin≤30	Yellow
	≤9	≤10	≤19	Red
PDR	>12	>9	>21	Green
	8<MGA≤12	5<Mass Margin≤9	13<MGA + Mass Margin≤21	Yellow
	≤8	≤5	≤13	Red
CDR	>7	>5	>12	Green
	4<MGA≤7	3<Mass Margin≤5	7<MGA + Mass Margin≤12	Yellow
	≤4	≤3	≤7	Red
Released Design	>3	>2	>5	Green
	2<MGA≤3	1<Mass Margin≤2	3<MGA + Mass Margin≤5	Yellow
	≤2	≤1	≤3	Red
Final	0	>1	>1	Green

Fig. 211: Mass risk assessment example (ANSI/AIAA, 2015)

As consequence, the example of mass trend versus time which, is characterized by the MGA and margins levels described in the risk matrix, is reported in Fig. 212.

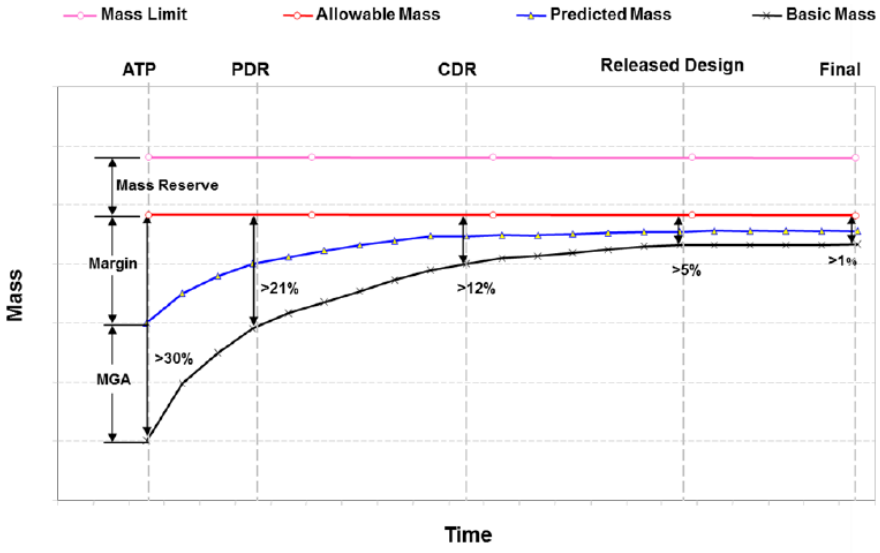

Fig. 212: Mass trend vs time (ANSI/AIAA, 2015)

As it can be seen, the MGA is reducing progressively when moving towards the final delivery of the product, usually getting closer to the basic mass. At the same time, the distance between the basic mass and the allowable mass reduces since the sum of MGA and mass margin gets smaller when approaching the delivery. The mass reserve is computed starting from the allowable mass and it is kept constant.

ECSS Margin philosophy for science assessment studies. The document aims at establishing a common margin philosophy in line with ECSS standards in the European context. It includes recommendations for mass, volume, delta-V, power, data processing, communication, thermal control and temperature margins. Moreover, a dedicated section is focused on the margin requirements for cryogenic systems. The recommendations are listed as requirements, being characterized by a standard syntax and a reference ID. For the purpose of this Dissertation, mass margins, volume margins and thermal control margins are considered. Particularly, the definition of mass margins is more detailed if compared to the approach proposed by ANSI/AIAA standard, including prescriptions for both different design maturity levels and hierarchical levels of product breakdown structure. Moreover, mass margins are prescribed for total dry

mass and maximum separated mass respectively, even if, for the purpose of this document, only total dry mass is considered. The definitions used in (ESA, 2012) to identify mass levels are based upon the following concepts:

- **Nominal dry mass at launch**, which is the system level mass of the product as computed during the design process;
- **Total dry mass at launch**, which is the nominal dry mass plus a specific mass margin.

Two approaches are proposed for subsystem and equipment level analysis. The first approach considers a mass margin of about 20% of the nominal dry mass at take-off for the subsystem level to compute the total dry mass. Moreover, the nominal dry mass at subsystem level shall include specific mass margin at equipment level, which depend on the type of equipment considered and on the ECSS category, as defined in Fig. 213.

Category	Description	Qualification programme
A	Off-the-shelf product without modifications and • subjected to a qualification test programme at least as severe as that imposed by the actual project specifications including environment and • produced by the same manufacturer or supplier and using the same tools and manufacturing processes and procedures	None
B	Off-the-shelf product without modifications. However: It has been subjected to a qualification test programme less severe or different to that imposed by the actual project specifications (including environment).	Delta qualification programme, decided on a case by case basis.
C	Off-the-shelf product with modifications. Modification includes changes to design, parts, materials, tools, processes, procedures, supplier, or manufacturer.	Delta or full qualification programme (including testing), decided on a case by case basis depending on the impact of the modification.
D	Newly designed and developed product.	Full qualification programme.

Fig. 213: ECSS equipment classes (ESA, 2012)

The equipment level margins shall be computed as follows:

- Off-the-shelf items (ECSS Category A/B): mass margin ≥ 5% of the equipment nominal dry mass
- Off-the-shelf items (ECSS Category C): mass margin ≥ 10% of the equipment nominal dry mass
- New designed/developed items (ECSS Category D): mass margin ≥ 20% of the equipment nominal dry mass

The mass margin at subsystem level is thus applied to a nominal dry mass which already accounts for margins at lower levels, guaranteeing an additional margin for allowances. An additional margin on harness mass is then prescribed directly, since a value of about 5% of the nominal dry mass (including equipment margins) is proposed as verification mean to compare the computed value with the actual one. Total propellant mass, i.e. the mass required to perform the mission, shall be computed starting from the total dry mass at take-off, since this one already accounts for margins.

Recommendations about volume margins are more qualitative than the prescriptions on mass margins. The standard basically proposes approaches to provide continuous volume control during the design phases, with more detailed statements about tank volumes. The means to provide volume control include but are not limited to trade-off and identification of figure of merit for volume growth, identification of critical equipment and allocation of extra volume to mitigate potential growth. The volume of the tanks shall be designed in order to contain the total propellant mass plus at least 10%.

A chapter dedicated to thermal control margins is included in (ESA, 2012), with the aim of providing quantitative indications about temperature and heat exchange capabilities margins, especially in case of cryogenic subsystems. Three main groups of margins are proposed. The first one is related to early design phases, thus containing high level prescriptions on thermal capabilities. The second group is instead related to performance uncertainties at lower level. The uncertainties are applied to specific components and they can be used to determine mass variations through sensitivity analysis. Ultimately, dedicated margins for cryogenic subsystems are listed. Qualification margins for coolers are also provided, but they are out of scope for this Dissertation. Particularly, the main requirements at high level are expressed for heat rejection capabilities. In fact, thermal control system shall provide 50% margin on heat rejection. This can be achieved through the following prescriptions:

- for radiators, $T_{Design} \leq \frac{T_{Required}}{\sqrt[4]{1.5}}$;
- for active coolers, 50% margins shall be available on the maximum cooling power.

Secondly, for other equipment, the following uncertainties shall apply:

- electrical dissipation +/- 30%;
- conductance of Kevlar, Composite or Plastic materials +/- 30%;
- conductance of Metallic Material (except Harness) +/- 15%;
- conductance of Harness +/- 30%;
- Multi-Layer Insulation (MLI) efficiency +/- 50%;
- contact resistance +/- 50%;
- if aging effects are identified +/- 10% shall be applied on the effect of the aging.

Uncertainties on Emissivity:

- high emissivity (>0.2) +/- 0.03;
- low emissivity (<0.2) +/- 0.02.

Uncertainties on Interface Temperatures:

- above 270K +/- 5K;
- between 80K and 270K +/- 3K;
- between 20K and 80K +/- 1K;
- between 10K and 20K +/- 0.5K.

Ultimately, in order to assure a robust design for cryogenic subsystems, the following requirements shall be met:

- passive cooling: +15% on radiator surfaces to be considered for accommodation;
- active cooling: the design of the cryogenic subsystem must demonstrate 15% margin on the available cooling power.

Application of ANSI/AIAA margins policy on TEMS design. The application of ANSI/AIAA standard for determining mass margins of TEMS is fairly straightforward since, considering the basic mass computed during the preliminary design, it is sufficient to look at the type of subsystem considered and at the design stage in order to select the consistent MGA. In this case, for a

thermal control subsystem at early design stages (category E of Fig. 210), the MGA is between 30 and 50%. Considering that multiple design loops have been already performed on TEMS (and thus an MGA plus mass margin increment should not exceed 50 % total) the value of 50% is selected to include both MGA and mass margin in order to derive the allowable mass of TEMS. With this approach, it is reasonable to estimate a predicted mass of about 30% higher than the basic mass reported in Table 42 and an allowable mass of about 20% higher of the predicted mass. The result brings the allowable mass of TEMS to

$$M_{TEMS_{allowable_{MAX}}} = 9117 \text{ kg}$$

(excluding tanks).

The total mass shall be computed accounting also for pipes, but the final value of pipes mass can be derived only when final physical paths will be established on the vehicle. The mass reserve is not taken into consideration for this study, since out-of-scope changes are not expected and no requirements have been established on this topic within program management.

Application of ECSS margins policy on TEMS design. The application of ECSS standard to the TEMS case study is more complex if compared to what previously reported, because different hierarchical levels of the TEMS breakdown shall be considered. In fact, both subsystem and equipment margins shall be analysed, as well as the impact of the performance uncertainties prescribed for thermal control subsystem. A sensitivity analysis is then performed at equipment level in order to identify the effect of performance uncertainties. The effect of these uncertainties on mass is evaluated and equipment level margins are applied to the new computed value of mass, determined by variations in operating conditions. If variation is not detected following the application of performance uncertainties, the equipment level mass margin is applied directly to the baseline mass, depending on equipment category. Eventually, system level mass margin is applied in order to obtain the total dry mass at launch/take-off. The overall process is qualitatively summarized in Fig. 214.

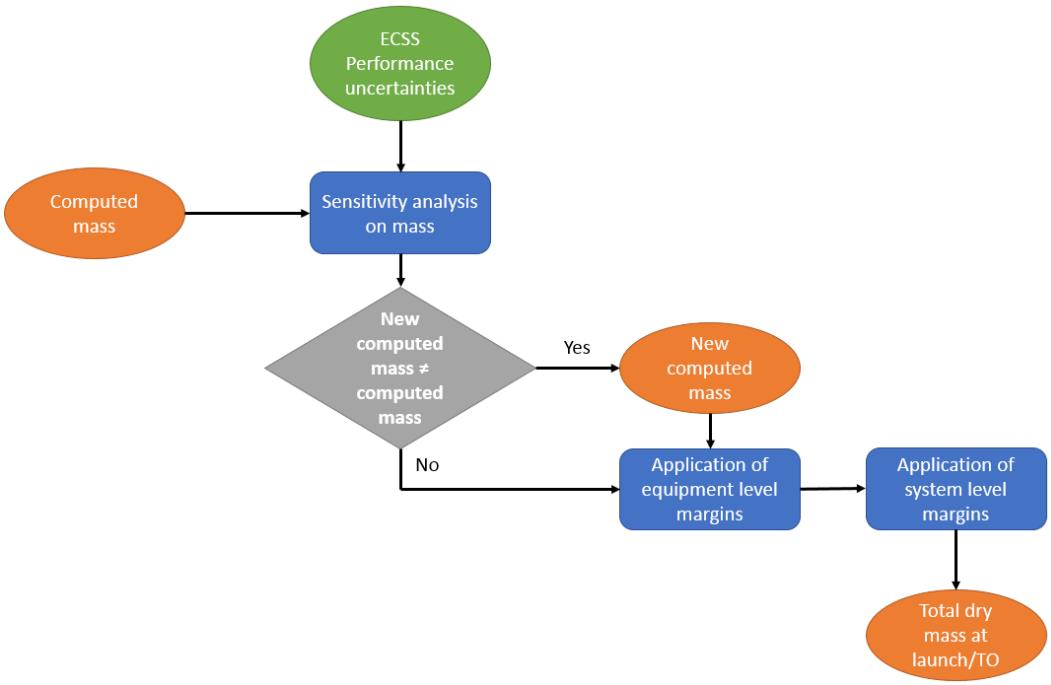

Fig. 214: Qualitative representation of mass margin approach following ECSS Standard

The ECSS performance uncertainties have been considered for the following components:

- LH2 Turbopump;
- boil-off compressor;
- LH2 expander;
- heat exchangers;
- pipes.

Following paragraphs present the result of the sensitivity analysis on the listed components, and report the results of the application of the general equipment level margin specified by ECSS depending on equipment type, starting from the new computed mass. However, considering the estimation relationships and hypotheses provided in Section 5.2.4.5, and detailed in (Fusaro, et al., 2019), the turbopump mass is not affected by temperature and conductance uncertainties. This means that, for this specific component, the general equipment level margin is directly applied, as specified by the lower branch of the diagram in Fig. 214. Ultimately, final results of the application of the margin policy suggested by ECSS are discussed and compared with the ANSI/AIAA approach.

As second components family, turbomachinery assembly is analysed. The baseline characteristics of compressor and expander are reported in Table 36 and 37. The uncertainties applied for this specific stage are related to interface temperatures at compressor and expander inlets. Looking at the baseline data (Balland, et al., 2015), the temperature uncertainties are defined as follows:

- $T_{compressor_{inlet}} = 270\ K\ \pm 3\ K$;
- $T_{expander_{inlet}} = 1300\ K\ \pm 5\ K$.

Variations of fluid properties with temperature are neglected. The sensitivity analysis shows a negligible impact of these uncertainties both on mass and volume breakdowns (<<1%), thus the general equipment margin is directly applied on the baseline mass.

The baseline breakdown of TEMS heat exchangers is reported in Table 41. The LH2 regenerator is not considered because the estimations provide very high mass and volume values. The considered uncertainties are related to inlet and outlet temperatures of "hot" and "cold" fluids of the exchangers and, notably:

Cabin exchanger

- $T_{hot_{inlet}} = 308\ K\ \pm 5K$;
- $T_{hot_{outlet}} = 301\ K\ \pm 5K$;
- $T_{cold_{inlet}} = 50\ K\ \pm 1K$;
- $T_{cold_{outlet}} = 270\ K\ \pm 3K$.

Engine boil-off exchanger

- $T_{hot_{inlet}} = 1400\ K\ \pm 5K$;
- $T_{hot_{outlet}} = 1000\ K\ \pm 5K$;
- $T_{cold_{inlet}} = 950\ K\ \pm 5K$;
- $T_{cold_{outlet}} = 1200\ K\ \pm 5K$.

Air pack exchanger

- $T_{hot_{inlet}} = 3240\ K\ \pm 5K$;
- $T_{hot_{outle}} = 300\ K\ \pm 5K$;
- $T_{cold_{inlet}} = 950\ K\ \pm 5K$;

- $T_{cold_{outlet}} = 1200\ K\ \pm 5K$.

Variations of fluid properties with temperature are neglected. Uncertainties on conductance are not present because the mass estimation does not take into account the effect of material conductivity. The results of the analysis are shown in Table 46.

Table 46: Mass and volume variations of TEMS exchangers

	Cabin exchanger	**Engine boil-off exchanger**	**Air pack exchanger**
Mass variation	± 2%	Negligible	Negligible
Volume variation	± 2%	Negligible	Negligible

Since cabin exchanger is the smallest one on board, the effect on total exchanger mass and volume is limited to an increase / reduction of 9.86 kg and 0.046 m3 respectively. New approximated mass and volume budgets for exchangers are then shown in Table 47.

Table 47: New mass breakdown of TEMS exchangers with uncertainties effect

Exchanger	**Mass [kg]**	**Volume [m3]**
Cabin exchanger	503	2.35
Engine boil-off exchanger	2517	12
Air pack exchanger	2267	10.8
Total	**5287**	**25.12**

Pipes represent one of the most impacting items for mass deviations at early design stages because of the uncertainties related to the paths that they will use to allow communication among TEMS equipment. Moreover, temperature and harness conductance uncertainties may have an important role in determining variations of mass. The specific mass of the different sections of TEMS circuits are reported in Table 40. The effect of temperature and material conductivity have been assessed separately to obtain the final result. However, the effect of temperature fluctuation in both fluid and pipe-compartment interface is negligible for all TEMS sections considering the uncertainties prescribed by ECSS. In general, the lower the temperature (of both fluid and pipe), the higher the effect of

uncertainty is on the breakdown, even if the result is always << 1% of the original mass. The effect of conductance has then been considered as unique source for mass deviations. Particularly, an uncertainty of about ± 30% has been adopted for material conductivity. The results of the sensitivity analysis are reported in Table 48 and Table 49 for an increase and decrease of conductivity respectively.

Table 48: Pipe mass variation with a 30% increased conductivity

Pipe section	**Mass increase (+30% conductivity)**
From LH2 tank to pump	+ 33.5 %
From pump to engine	Negligible < 1%
From engine to expander	+ 26.1 %
From LH2 tank to compressor	1 %
From compressor to expander	+ 13.1 %
From compressor to air-pack	+ 18 %
From air-pack to expander	+ 7.6 %
Total	**+ 25.8 %**

Table 49: Pipe mass variation with a 30% reduced conductivity

Pipe section	**Mass decrease (-30% conductivity)**
From LH2 tank to pump	- 24.8 %
From pump to engine	Negligible < -1%
From engine to expander	- 19.3 %
From LH2 tank to compressor	Negligible < - 1%
From compressor to expander	- 10 %
From compressor to air-pack	- 13.3 %
From air-pack to expander	- 5.6 %
Total	**- 19.1 %**

The example of pipe mass increase as function of conductivity variation is shown in Fig. 215 for the case of first pipe line of Table 48 - 49.

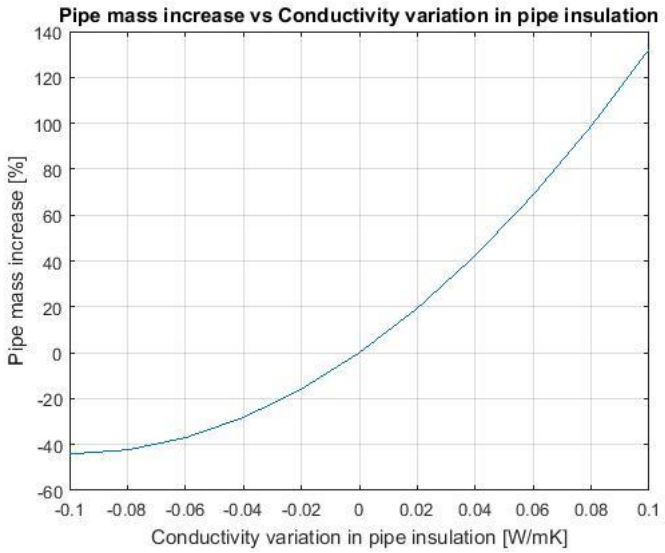

Fig. 215: Example of insulation conductivity variation influence on pipe mass

Two main effects of the fluctuation of material conductivity have been observed:

- the reduction of conductivity produces a reduction of mass which is lower (in module) if compared to the mass increase associated with the increase of conductivity of the same value;
- the ratio between mass reduction and increase associated with the same reduction and increase of conductivity (in module) is always around 0.73 – 0.76. This means that the reduction of a certain percentage of conductivity produces a reduction of mass which is always 73% - 76% of the mass increase produced by the increase of conductivity of the same value. This applies also to the total mass variation.

The new mass per unit length of the different pipes is then reported in Table 50.

Table 50: New mass breakdown for the pipes of TEMS with uncertainty effect

Circuit segment	**Specific Mass [kg/m]**
From LH2 tank to pump	***0.64 - 1.1***
From pump to engine	1.8
From engine to expander	***123.2 – 192.5***
From LH2 tank to compressor	3.9
From compressor to expander	***2.1 – 2.6***
From compressor to air-pack	***2 – 2.7***
From air-pack to expander	***1 – 1.2***

The new computed mass breakdown is used as basis to apply the equipment level margins prescribed by ECSS, as described in (ESA, 2012) and Fig. 213. For the purpose of this analysis, the following assumptions concerning equipment category are applied:

- LH2 Turbopump: newly designed product → Category D, margin 20 %;
- Boil-off compressor: off-the-shelf product with modifications → Category C, margin 10 %;
- LH2 Expander: newly designed product → Category D, margin 20 %;
- Heat exchangers: off-the-shelf-product with modifications → Category C, margin 10%;
- Pipes: off-the-shelf product without modifications → Category A, margin 5 %.

The final equipment level mass breakdown is reported in Table 51 and Table 52.

Table 51: New mass breakdown of TEMS components (excluding pipes) considering equipment level margins

Component	**Mass [kg]**
LH2 Turbopump	***547***
Boil-off compressor	***185***
Boil-off expander	***116 (212 considering accessories)***
Heat exchangers	***5816***
Total*	***6760***

* Excluding LH2 regenerator

Table 52: New mass breakdown for the pipes of TEMS considering equipment level margins

Circuit segment	**Specific Mass [kg/m]**
From LH2 tank to pump	***0.7 - 1.2***
From pump to engine	***1.9***
From engine to expander	***129.4 – 202***
From LH2 tank to compressor	***4.1***
From compressor to expander	***2.2 – 2.7***
From compressor to air-pack	***2.1 – 2.8***
From air-pack to expander	***1 – 1.3***

These new breakdowns will be used to compute the subsystem level dry mass, as previously described. The general indication of ECSS concerning subsystem level margins prescribes a value of 20 % to be applied to the nominal dry mass which already includes equipment level margins and uncertainties. The resulting value is then:

$$M_{TEMS_{total_{dry}}} = 8112 \text{ kg}$$

(excluding tanks).

As conclusion, the application of margin policies of both ANSI/AIAA and ECSS standards produces a mass increase for TEMS subsystem which is highly relevant and varies from 2034 kg (using ECSS) to 3039 kg (using ANSI/AIAA) with reference to the original 6078 kg. Pipes are not included in this total because detailed information about paths and routings is not available, even if the impact of uncertainties on total pipes mass seems to be very important to contribute to the total mass increase. In general, the ECSS standard is more detailed if compared to the ANSI/AIAA even if it suggests a mass increase of about 1 ton lower than the one predicted by the latter.

Currently, no requirements exist considering the mass budget allocation of subsystems on the MR3 vehicle. Thus, results obtained in previous sections of Chapter 5 represent cannot yet be verified directly, nor it is possible to express new requirements straight away (since obtained results are not requirement, but deterministic evaluation of theoretical equipment characteristics in a specific set of operating conditions). However, requirements related to volume allocation are

included in the specification (Section 8.1.3) and margin requirements are expressed following the ECSS approach (which results in line with the project context and scenario, even if less conservative), as specified in Section 8.1.10.

5.3 Mapping of proposed methodology on ECSS Phase A workflow

Similarly to what reported in Section 4.6, where a mapping between the proposed conceptual design methodology and the corresponding ECSS Phase 0 is proposed, a parallel between Phase A and preliminary design process described in previous sections is performed. The Phase A process flow, already shown in Fig. 60, is summarized in Table 53, where main tasks and work products are listed.

Table 53: ECSS Phase A tasks and associated input/output (ECSS, 2004)

ID	ECSS Task	Input	Output
1	*Kick-off Phase A*	-	Agreed Technical Assumptions
2	*Set-up appropriate SE organization plan for Phase A*	Business agreement	SEP
		Mission statement	
		Phase 0 output	
		SEP	
		Project management plan and management instructions	
3	*Consolidation of preliminary system functional specification*	Preliminary system functional specification	Consolidated issue of preliminary system functional specification
		Preliminary mission description document	
		Consolidated mission statement	
		Consolidated business agreement	Requirement justification file
		Space environment	
		Human factors for space systems	
4	*Consolidation of programmatic aspects*	Synthesis of programmatic aspects	Consolidated synthesis of programmatic aspects

ID	ECSS Task	Input	Output
		Consolidated mission statement	
		Consolidated business agreement	
		Project management plan and management instructions	
5	*System functional analysis*	System concept report	Functional architectures (logical solution representations)
		Consolidated issue of preliminary system functional specification	
		Preliminary mission description document	Function trees (ECSS-E-10 Part 17A Annex I)
6	*Technology identification*	Functional architecture	Preliminary technology matrix (ECSS-E-10 Part 17A Annex G)
		Database	
		COTS	
		Preferred parts list	
7	*Establishment and analysis of system implementation alternatives*	Functional architecture	Set of system implementation alternatives reports
		Preliminary technology matrix	Compliance matrices for the alternatives
		Preliminary system functional specification	Technical input to risk assessment
		Preliminary mission description document	Technical input to cost and schedule assessment
8	*System design trade-off (including cost, risk assessment, schedule)*	Preliminary system functional specification	Trade-off report
		Set of system implement alternatives	
		Compliance matrices for the alternatives	
		Consolidated synthesis of programmatic aspects	
		PA related to risk	

ID	ECSS Task	Input	Output
		assessment	
		Cost and schedule assessment	
		Trade-off instructions	
9	*Decision on the baseline design*	Trade-off report	Technical documents to support decision
10	*Establishment of system design baseline*	Management decision	System functional specification
		Trade-off report	Requirement justification file
		Preliminary system functional specification	Preliminary system baseline definition (ECSS-E-10 Part 17A Annexes H and L)
		Preliminary FMECA	Function tree
			Preliminary product tree (ECSS-M-40B Annex B)
			Mission description document
11	*Establishment of development and verification approach*	Programmatic and industrial policy information	SEP for next phases, including technology plan and models approach
			Preliminary system VP and AIT plan (ECSS-E-10 Part 2B Annex D and E)
			Input to project phasing and planning requirements document for next phases
12	*Establishment of the preliminary system technical specification*	Agreed system functional specification	Preliminary system technical specification (ECSS-E-10 Part &A Annex B)
			Requirements justification file
		Inputs from activities 10 and 11	Requirements traceability matrix
13	*Preliminary requirement review*	PRR review plan	Consolidated design and related document for approval
		PRR review data package	

As it can be seen, the quantity and variety of tasks is higher if compared to Phase 0, since the level of detail of the preliminary analysis is improved. Several analyses produce output like the updated functional specification and the product tree, provided by the LDE and described in Section 5.2.1 for the proposed methodology. Implementation aspects and technology assessment is studied within the physical and performance analysis, in cooperation with studies associated to safety and margin policies. Trade-off studies can be supported by numerical analysis, both from the point of view of the sizing and dynamic simulation. Inputs for cost assessment can be generated as well, as described in Chapter 6. Consolidated functional and technical specification, as well as requirements baseline are provided and integrated within the SEP, in order to be available for subsequent design phases. The Preliminary Requirements Review (PRR), in fact, is conceived to assess the design maturity at the end of Phase A, where a consolidated design is proposed and a suitable technical solution is selected to implement the required functionalities and performance. From this point of view, the methodology presented in this Dissertation appears consistent with the ECSS approach, being capable of supporting different tasks associated to design, sizing, safety and cost assessment.

6

Life Cycle Cost analysis for hypersonic vehicles

This chapter presents the life-cycle cost estimation process which allows determining and quantifying the economic effort required to develop, produce and operate hypersonic vehicles. Particularly, Section 6.1 provides a general description of the peculiarities of Life Cycle Costs estimation process in aeronautical and space domains, introducing those key elements that are used to derive the proposed cost model. In addition to that, it describes the life-cycle cost estimation models already available in literature and used as reference for the derivation of the new cost estimation relationships reported in Section 6.3. However, before moving to the ad-hoc developed model, Section 6.2 reports the formalization of the overall process following a SE approach. Then in Section 6.3, results of the application of the ad-hoc tailored cost model are provided for the STRATOFLY MR3 vehicle concept. The overall cost estimation process contains costs at both vehicle and subsystem levels, since cost estimation relationships for development and production can be derived for both aircraft and its on-board plants. Conversely, operating costs are more focused on aircraft deployment in service. Cost assessment is thus conceived as a multi-levels analysis, being an integral part of the conceptual design phase with some anticipations from preliminary design process. For this reason, the methodology is presented within a dedicated chapter, even if it has lots of implications on vehicle configuration.

6.1 Introduction

6.1.1 Life-Cycle Cost in aerospace industry: key concepts

Life-cycle cost analysis is a typical task of cost engineering which is usually performed during the early design stages of an aerospace product, or as preparatory step towards the development of a program. Notably, the life-cycle cost is defined as the financial resource required to develop, produce, operate and manage the disposal of a product during its entire life-cycle, from conceptual design to decommissioning. The cost prediction is particularly important for aerospace products, characterized by a long life-cycle, which is dominated by the operation phase that covers almost the 75% of the total cost (Asiedu & Gu, 1998). On the contrary, the design phase has a small impact on life-cycle cost (around 10%), even if the design choices taken during early design may allocate 65-85 % of the final concept of the product, fixing critical aspects associated to operation and influencing the viability of the whole future system (Roskam, 1985), as already reported in Section 2.3 (Fig. 29). In late 1980's cost engineering became an integral part of aircraft design process, since main industrial players started considering cost as a critical figure of merit to evaluate their engineering programs and to ultimately release on the market competitive products. (Roskam, 1985) qualitatively represented the magnitude of cost over time as in Fig. 216, where the impact of the contribution of operations phase can be highlighted.

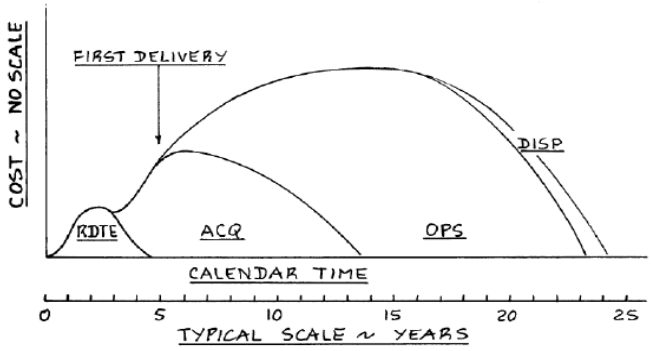

Fig. 216: Qualitative sketch of cost spending scheme for a general aircraft life-cycle (Roskam, 1985)

On the other hand, (Roskam, 1985) confirms once more the importance of the decision making process in development phase, whose impact on total cost

allocation is emphasized in Fig. 217, where the first life-cycle stage is expanded for clarity.

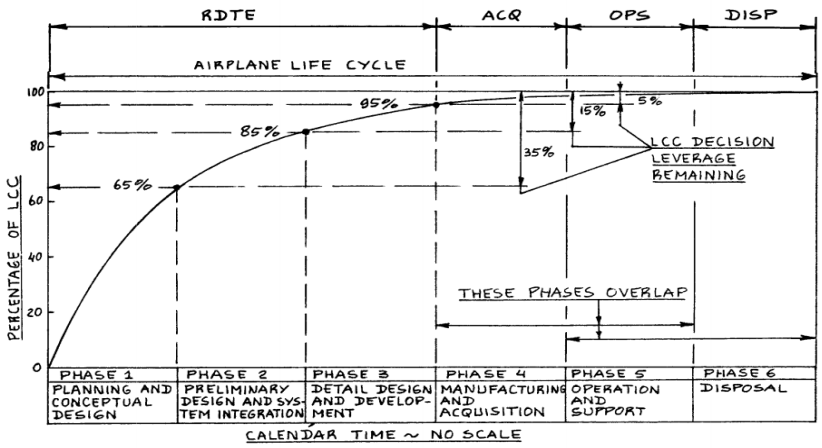

Fig. 217: Qualitative representation of total cost allocation process from (Roskam, 1985)

The subdivision of life-cycle phases suggested by (Roskam, 1985) is also helpful to identify the main cost categories usually adopted for this kind of assessment in the aerospace domain. In details:

- the costs associated to the development phase, also referred to as "Research Development Test and Evaluation" (RDTE) costs, cover the whole design phase, from conceptual study to detailed design;
- acquisition or production costs are associated to the manufacturing of the product;
- operating costs are related to the actual operation of the product when in service, and are typically subdivided in Direct Operating Costs (DOC) and Indirect Operating Costs (IOC). The first category of operating costs is directly affected by the quantity of in-service products (fleet), while the second one is a constant value which only depends on the type of product;
- ultimately, disposal costs represent the monetary resources required to decommission the product after the completion of operational life.

Life-cycle cost follows a similar breakdown also in space domain, where acquisition phase is usually referred to as procurement, and operating costs are generally defined as operating and maintenance (O&M) costs, as shown by (GAO, 2015) in Fig. 218.

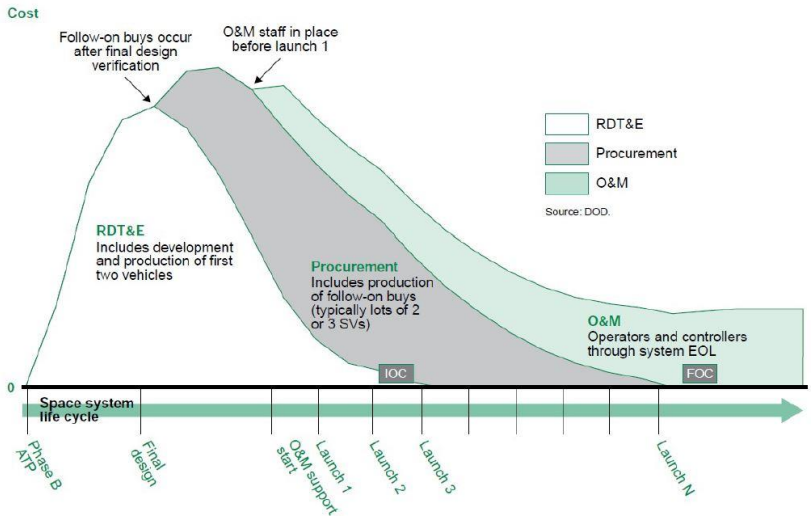

Fig. 218: Qualitative representation of cost breakdown for a general space system (GAO, 2015)

One of the main differences with aeronautical products is that a typical spacecraft rarely belongs to series, being rather a "one of a kind" system. This has a considerable impact on procurement and O&M costs. In case of launchers, the launch cost, often accounted separately within O&M expenses, is a key milestone to identify the competitiveness of a product, provided that the number of launches for a determined vehicle is very limited if compared to aircraft take-off and landing cycles.

Additionally, an alternative way to represent cost breakdown of aerospace products relies on the concepts of recurring and non-recurring costs. In fact, while recurring costs are defined as "*expenses incurred for each item produced or each service performed*" (GAO, 2015) , being clearly represented by production costs associated to *"manufacturing and testing, engineering support for production and spare parts procurement"* (Croce, 2017), non-recurring costs are labelled as "*the elements of development and investment costs that generally occur only once in a system's life cycle*" (GAO, 2015), i.e. *"design, analysis, development, qualification and verification activities"* (Croce, 2017). There is an interesting differences concerning the allocation of costs within the reference procurement costs breakdown when following the recurring/non-recurring scheme. In fact, even if the development costs are always considered as non-recurring expenses, production costs are split in both recurring and non-recurring categories. The former contribution indicates costs associated to the actual product manufacturing, while the latter item is referred to the procurement process of the production

plants and facilities, which are faced once in a life. Actually, there is an important difference to consider when evaluating fixed and variable contributions to production cost. In fact, independently from the way in which the variable cost associated to product manufacturing is represented, within acquisition or recurring cost scheme, one of the most important aspect to consider while performing the analysis is the learning curve effect. This is a peculiar aspect of costs which are associated to iterative processes, where experience of humans and machines about production procedures (and about the product itself) grows over time. Production process intrinsically becomes more effective while the number of produced units increase, since the production time lowers because of enhanced knowledge of the procedures as well as of the technology involved. A typical production cost trend, affected by a learning curve factor, which is a decreasing multiplier of the Theoretical First Unit (TFU) cost, can be depicted as in Fig. 219, where the residual production cost (in percentage) is function of the number of units built.

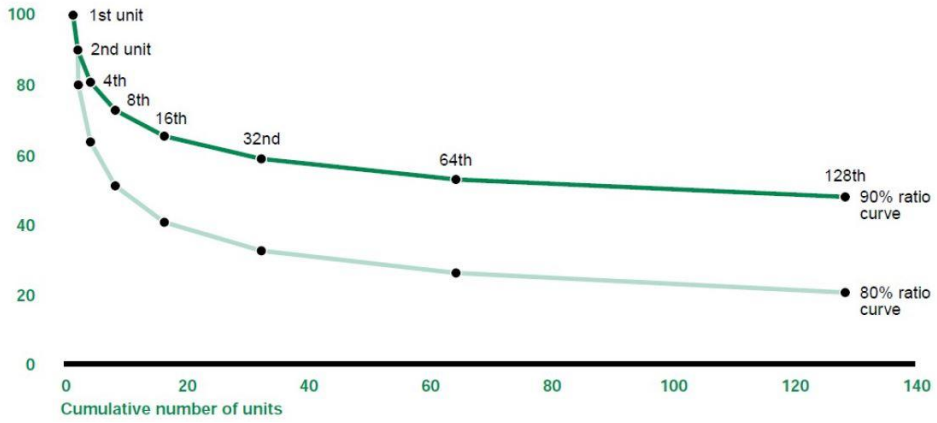

Fig. 219: Effect of learning factors on residual production cost as function of number of units produced (GAO, 2015)

As it can be seen, the cost reduction due to the learning process can be tuned depending on the impact of experience on production cost. The ratio of the curve is usually evaluated depending on the kind of production process (manual, semi-automated, fully automated etc…), as well as on past experience of the manufacturer and on the time frame in which this experience was acquired. In fact, one of the first lessons to learn when dealing with cost engineering is that numerical values, especially if associated to currencies, shall be evaluated with reference to a specific technical age and social context. This means that absolute monetary values do not exist on their own without a reference to a determined year. As consequence, it is a cost engineering best practice, for computation of all

kinds of costs, to indicate the year in/for which the estimation is performed/envisaged, so to establish a clear relative term of comparison. In order to provide a mean to scale cost values, it is very common to adopt the cost actualization approach based on the Cost Escalation Factor (CEF), which is a function of Consumer Price Index (CPI) of both the reference estimation year and the year for which actualization process is required. In fact, the CPI is defined as *"the cost of a bundle of goods and services purchased by a typical urban consumer compared to the cost of that bundle of goods and services in a base period"* (Vercella, 2017). This means that, moving from results proposed by an old estimation to a new one, it will be necessary to apply an actualization factor equal to (162), which is function of reference and target years (for the same currency). While moving from past to future estimations, the CEF is higher than 1, except in case of recession.

$$CEF = \frac{CPI_{target}}{CPI_{reference}} \qquad (162)$$

The adoption of specific factors, such as the learning curve and the CEF, is particularly important when trying to develop cost models.

Notably, three main approaches to cost engineering can be found in literature :

- analogy, which mainly uses cost data of past or similar programs to estimate the target program costs through the introduction of ad-hoc developed coefficients;
- engineering build-up, which is the recursive estimation process starting from bottom level of a Work Breakdown Structure (WBS) or PBS conceived to derive the top level cost as sum of the different elements;
- parametric approach, which is the engineering process of developing Cost Estimation Relationships (CERs) relating technical variables and characteristics of the product to its cost, using a statistical correlation.

For the purpose of the analysis performed in Section 6.3, concerning cost estimation of hypersonic transportation systems, with particular focus on STRATOFLY MR3 case study, the parametric cost analysis approach including RDTE, production and operating costs (both DOC and IOC) assessment is considered (disposal costs are neglected). Moreover, acquisition cost model is selected to account for production costs and 2017 is provided as reference year for the estimations. The proposed cost model makes benefit from existing parametric

cost models, available in literature for both aeronautical and space products, as briefly described in Section 6.1.2. For conciseness reasons, the complete set of CERs for (Roskam, 1990) are reported in Section 8.2, while in Section 6.1.2 a high-level view on the main characteristics of most important reference algorithms are discussed, with particular focus on the motivations for which they have been chosen as reference for the development of the new cost model for HST.

6.1.2 Parametric cost models for aerospace applications

6.1.2.1 Parametric cost models for development and production costs estimation

Roskam (Roskam, 1985)**.** This is certainly one of the most known model for airplanes costs estimation since late 1980's. The Part VIII of this work, focused on aircraft conceptual design, deals particularly with cost estimation methods for both military and commercial newly designed airplanes, focusing on development, acquisition, operating and disposal costs. In this section, development and acquisition cost models are assessed, while operating and disposal models are discussed in Section 6.1.2.2. For what concerns development cost, labelled as RDTE, the model was conceived to include seven non-recurring components or cost items defined within (163).

$$C_{rdte} = C_{aed} + C_{dst} + C_{fta} + C_{fto} + C_{tsf} + C_{pro} + C_{fin} \qquad (163)$$

Notably, the aircraft RDTE cost is made up of:

- C_{aed} airframe engineering and design cost;
- C_{dst} development support and testing cost;
- C_{fta} flight test airplane cost;
- C_{fto} flight test operations cost;
- C_{tsf} test and simulation facilities cost;
- C_{pro} profit margin;
- C_{fin} RDTE financing cost.

Detailed formulations for the different cost items are reported in Section 8.2.1.

The model to estimate manufacturing cost is quite similar to the one described for RDTE phase, even if this represent a recurring expense. This means that the

number of units built is important to estimate the actual acquisition cost of a single vehicle and, ultimately, its unit price. First of all, it is possible to define the manufacturing cost as sum of four main cost items (164).

$$C_{MAN} = C_{aed_m} + C_{apc_m} + C_{fto_m} + C_{fin_m} \qquad (164)$$

Notably:

- C_{aed_m} airframe engineering and design cost in early production phase;
- C_{apc} airplane production cost;
- C_{fto} flight test operations cost during production;
- C_{fin_m} financing cost for production phase.

Detailed formulations for the different cost items are reported in Sections 8.2.1 and 8.2.2.

The acquisition cost can thus be obtained following (165), where the manufacturing cost is increased by a certain profit margin.

$$C_{acq} = C_{MAN} + C_{pro_m} \qquad (165)$$

The Aircraft Estimated Price (AEP) can be obtained summing the remaining development cost to the total acquisition cost and dividing by the number of aircraft produced within the manufacturing phase, as in (166).

$$AEP_{average} = (C_{MAN} + C_{pro_m} + C_{rdte}) \frac{1}{N_m} \qquad (166)$$

It is possible to notice that this is an average price in $\left[\frac{\$}{unit}\right]$, since it is simply obtained considering overall program values for both costs and units. In order to obtain a true single unit price, it is necessary to isolate the contribution of cost items expressed in (166) for one aircraft only. Even if for profit and RDTE cost this value can be simply obtained dividing the results by the number of units (this actually depends also from the business plan of the manufacturer, which typically recovers the expenses on subsequent units, rather than on first ones, to reduce entry into service cost, so this assumptions may lead to overestimation of theoretical first unit price), this is not valid for manufacturing cost. In fact, the learning curve effect on manhours and related rate is highly important. In general,

the different cost items included in C_{MAN} can be related to the current number of units built, modifying (166) as (167).

$$AEP_i = C_{MAN_1} \cdot \Phi_i + \frac{C_{pro_m} + C_{rdte}}{N_m} \quad (167)$$

where AEP_i is the price of the i-th aircraft unit produced and

$$\Phi_i = i^{\frac{\log P}{\log 2}} \quad (168)$$

is the learning curve. For conventional aeronautical applications, the learning curve factor P is typically conceived to account for a 80% cost reduction every time the production doubles. This means that the exponent of "i" is equal to -0.322. All computed costs shall be actualized using proper CEF coefficient to obtain results with a specific year inflation, if reference year used in (Roskam, 1985) is not considered.

The model described by (Roskam, 1990) provides a detailed analysis on development and production costs estimation, assuring a high level of granularity for what concerns the types of cost items involved. Moreover, the way in which equations are arranged is perfectly in line with the parametric approach suggested for HST cost estimation in Section 6.3, since it allows assembling cost drivers through coefficient and exponents derived from statistical population. Some of the relationships between cost items and drivers suggested by (Roskam, 1990) is thus taken as reference for the definition of updated CERs for HST cost estimation, together with prescriptions provided by (Koelle, 2012), as described in the following section.

TRANSCOST (Koelle, 2012)**.** The TRANSCOST model for cost estimation of space transportation systems was published in its version 1.0 in 1971 by D. E. Koelle. It reaches the version 8.2 in 2012, collecting a database of US, European and Japanese space vehicles and engine projects for over 52 years (from 1960' to 2012). It includes CERs for the derivation of RDTE, production and operating cost estimations for different kinds of space transportation vehicles and advanced high speed aircraft, with related power plants. However, it is highly focused on expendable systems and it does not go in detail for what concerns the subsystems. Equations for estimation of re-usable vehicles and engines are thus not many, being integrally reported in this section.

The RDTE and production cost models are organized upon some core cost relationships, containing mathematical equations made up of main cost drivers, which are then enriched and tuned by the use of appropriate "factors" f_i (Table 54). For development costs, the core mathematical equation is generally as defined in (169), where for a general cost C the most usual cost driver is the reference mass M of the item

$$C = aM^x \qquad (169)$$

where

a is the system-specific constant value
x is the system-specific cost-to-mass sensitivity factor

The final CER is thus derived as composition of the core relationship and of the different factors (Table 54), where applicable, as in (170).

$$C_{final} = aM^x \prod_{i=1}^{n_{factors}} f_i \qquad (170)$$

Detailed description of the values assumed for these factors are reported in (Koelle, 2012). One of the most peculiar aspect of TRANSCOST model is that the unit of measure of the estimation is the Work Year (WYr) defined as *"the total company annual budget divided by the number of productive full-time people"* (Koelle, 2012). This is justified by the fact that cost estimations are generally influenced by inflation, currency fluctuations and conversions, as already stated in previous section. The Work Year can be then used independently from those aspects, and then converted in currency values depending on the needs of the user. The CERs described hereafter are then expressed in WYr.

The TRANSCOST development cost sub-model is aimed at evaluating RDTE (or non-recurring) costs focusing on the so-called "Most Probable/Realistic Development Cost". These are development costs including margin for unforeseeable technical problems and delay (potentially overestimating the real cost up to 15-20%).

Table 54. List of additional factors to TRANSCOST core CERs

Additional Factors to development core CERs	**Acronym**	**Type of CER**
Systems engineering / integration factor (Development)	f_0	RDTE
Development standard factor	f_1	RDTE
Technical quality factor	f_2	RDTE
Team experience factor	f_3	RDTE
Learning Curve factor	f_4	Production
Not defined	f_5	N/A
Deviation from optimal schedule	f_6	RDTE
Program organization factor	f_7	RDTE
Productivity of region	f_8	RDTE / Production
Impact of subcontractor	f_9	RDTE / Production
Reduction factor due to experience / cost engineering	f_{10}	RDTE
Reduction factor due to absence of government contracts	f_{11}	RDTE
Systems engineering / integration factor (Production)	$f_0{}'$	Production
Production cost improvements factor	$f_{10}{}'$	Production
Government contracts factor for production	$f_{11}{}'$	Production

An explicit format of the mathematical equation reported in (170) is shown in (171) for core RDTE formulation.

$$H = C f_1 f_2 f_3 f_8 f_9 f_{10} f_{11} \qquad (171)$$

where H is the cost of the item (vehicle or engine) in WYr and the coefficients may be present depending on the type of the item itself. The total system development cost, including integration, is derived by (172).

$$C_{TOT} = f_0 \sum_{i=1}^{N_{items}} H_i f_6 f_7 \qquad (172)$$

Due to the scope of the Dissertation and of the case study, in this section, only the core CERs related to air-breathing turbojet and ramjet engines as well as advanced

high-speed aircraft are described. The core CER for air-breathing turbojet development is shown in (173).

$$H_{ET} = 1380 M_{E_{dry}}^{0.295} f_1 f_3 \qquad (173)$$

where

$M_{E_{dry}}$ is the dry mass of the engine in $[kg]$

The core CER for air-breathing ramjet development is shown in (174).

$$H_{ER} = 355 M_{E_{dry}}^{0.295} f_1 f_3 \qquad (174)$$

where the cost drivers are defined similarly as in (173).

The core CER for advanced aircraft development is shown in (175).

$$H_{VA} = 2169 M_{OEW}^{0.262} f_1 f_2 f_3 f_8 f_{10} f_{11} \qquad (175)$$

where

$$f_2 = \mathcal{M}\text{^}0.15 \qquad (176)$$

and

$\mathcal{M}$ is the maximum design Mach number

The final core CER for an advanced high speed vehicle with air-breathing propulsion is then defined as in (177).

$$C_{TOT} = f_0 \left(H_{VA} + \sum_{i=1}^{N_{engines_{type}}} H_{Ei} f_6 f_7 \right) \qquad (177)$$

This is valid since this kind of vehicle may host both turbojet and ramjet engines, potentially requiring the combination of both development costs. Moreover

$$f_0 = 1.04^N \qquad (178)$$

$$f_7 = n^{0.2} \qquad (179)$$

where

N is the number of stages for the vehicle
n is the number of sub-contractors in the project

The TRANSCOST production cost sub-model deals with the recurring costs related to the production of engine(s) and airframe of the vehicle. Particularly, it focuses on the identification of proper CERs for the estimation of the Theoretical First Unit (TFU) cost. As already stated, this is particularly important since the overall production cost of a vehicle series, differently from what happens for RDTE costs, is highly affected by the number of vehicles produced. The sub-model proposes a set of equations similar to those presented for RDTE costs computation, being characterized by a core CER formulation (for both engines and airframes) enriched by specific factors depending on the considered item. The total production cost of a single unit is then derived by the combination of the contributions of engine and airframe cost. The final results are always expressed in WYr. The generic format of a core CER for the TRANSCOST production cost sub-model is shown in (180)

$$F = bM^y \quad (180)$$

where

b is the system-specific constant value (for production costs)
y is the system-specific cost-to-mass sensitivity factor (for production costs)

A wider expression, which takes into account also the number of units built and the effect of the learning curve, is reported in (181).

$$F_{tot} = \sum_{i=1}^{n} bM^y f_{4_i} \quad (181)$$

where

$$f_{4_i} = i^{\frac{\log P}{\log 2}} \quad (182)$$

is the cost reduction percentage of the i-th unit of the production run if compared to the TFU. It is important to highlight that expression (181) allows computing the total (core) production cost of a selected item and not the n-th value. In fact, the last unit cost can be derived as in (183).

$$F_{last} = bM^{y} f_{4_n} \qquad (183)$$

where

$$f_{4_n} = n^{\frac{\ln(p)}{\ln(2)}} \qquad (184)$$

By comparing (180), (181) and (183) it is easy to understand the difference between TFU, total production cost and last unit cost by evaluating the expression of the learning curve factor. The factor f_4 is only one of the factors used to tune the core production CERs of the TRANSCOST sub-model. In fact, a modified core CER F_i for production costs estimation can be expressed as in (185), where the i-th unit cost is represented.

$$F_i = bM^{y} f_{4_i} f_8 f_{10}{}' f_{11}{}' \qquad (185)$$

The total production cost of a vehicle is then the combination of both the engines and airframe production efforts as indicated in (186)

$$C_F = f_0{}'^{N} \left(\sum_{i=1}^{n} F_{A_i} + \sum_{j=1}^{n_E} F_{E_j} \right) f_9 \qquad (186)$$

where

n is the number of vehicles (i.e. number of airframes) built
n_E is the number of engines built
N is the number of vehicle stages
F_{A_i} is the i-th modified production core CER for the airframe
F_{E_i} is the j-th modified production core CER for the engine

It is worth noticing that the factor $f_0{}'$ is slightly different from f_0 (used within the development cost sub-model) and expressed in (187), since

$$f_0' = 1.03 \qquad (187)$$

As for development costs, some examples of production CERs are herein shown. In line with the scope of this Dissertation, the estimations refer again to air breathing engines and high speed aircraft respectively. The core CER for turbojet engines production is shown in (188):

$$F_{ET_j} = 2.29 M_{E_{dry}}^{0.545} f_{4_j} f_8 f_9 f'_{10} f'_{11} \qquad (188)$$

Ramjet production CERs are not available in TRANSCOST 8.2 because of lack of statistical data. The cost reported in (188) is the j-th engine cost where f_9 is directly allocated on core CER.

The core CER for the i-th high speed aircraft production is reported in (189). According to (Koelle, 2012) this is also valid for winged first stage vehicles.

$$F_{VF_i} = 0.357 M_{OEW}^{0.762} f_{4_i} f_8 f'_{10} f'_{11} \qquad (189)$$

The TRANSCOST approach is similar to the one described by (Roskam, 1985) even if the proposed CERs are defined in a simpler way. Because of the data laying behind the statistical correlations proposed by TRANSCOST, which are closer to the field of the case study, these CERs constitute the starting point for the definition of the proposed model (Section 6.3), even if some variables used by (Roskam, 1985) as cost drivers are added to improve the TRANSCOST formulation. Operating costs are also included within TRANSCOST model, but the domain of application appears too far from the considered case study. For this reason, they are not considered as reference model, being substituted in Section 6.1.2.2 by a more consistent methodology proposed by (Repic, et al., 1973).

6.1.2.2 Parametric cost models for operating costs estimation

Roskam (Roskam, 1985)**.** As anticipated in Section 6.1.2.1, the model provided in (Roskam, 1985) includes dedicated CERs for the computation of operating costs, as herein briefly described. First of all, the Total Operating Cost (TOC) of a single aircraft is defined as the sum of DOC and IOC expressed in $\left[\frac{\$}{nm}\right]$ as indicated in (190).

$$TOC = \sum_{i=1}^{n_{DOC}} DOC_i + \sum_{j=1}^{n_{IOC}} IOC_j \qquad (190)$$

It is easy to understand that both DOC and IOC are made up of different cost items, as summarized hereafter. The DOC breakdown can be identified as in (191).

$$DOC = DOC_{flt} + DOC_{maint} + DOC_{depr} + DOC_{lnr} + DOC_{fin} \qquad (191)$$

Notably:

- DOC_{flt} direct operating cost associated to the flight;
- DOC_{maint} direct operating cost associated to maintenance;
- DOC_{depr} direct operating cost associated to depreciation
- DOC_{lnr} direct operating cost associated to landing and navigation fees;
- DOC_{fin} direct operating cost for operations financing.

Detailed formulations for the different cost items are reported in Section 8.2.3.

For what concerns the IOC, (Roskam, 1985) uses a simple ratio to compute indirect costs as function of DOC, following (192)

$$IOC = f_{IOC} \cdot DOC \quad (192)$$

where f_{IOC} is a fraction of DOC through which IOC are estimated, whose detailed formulation is here omitted. For the model specified in (Roskam, 1985), IOC include:

- IOC_{pax} evaluating the cost associated to passenger services, meals, insurance and cost of cabin attendants;
- IOC_{sta} which is the cost for maintaining ground equipment;
- IOC_{ascf} evaluating the cost for airplane and traffic servicing;
- IOC_{pse} evaluating the cost for promotion, sales and entertainment;
- IOC_{gaa} which is the cost for general and administrative expenses.

As described in this section, operating costs are expressed as $[\frac{\$}{nm}]$ even if, with simple modification to the expressions, it is also possible to use $\left[\frac{\$}{bh}\right]$, i.e. dollars (or other currencies) per block hours. This is used most frequently than the flight hour as reference, because of the extra time considered by block hour, which is always producing an additional cost for operators (Section 8.2.3).

The DOC model proposed by (Roskam, 1990) is used as reference for the selection of typical operating cost items, usually already adopted also for the development of other models as shown in the following section. However, the approach for IOC estimation provided in (Roskam, 1990) is not considered for the model proposed in Section 6.3, since the direct correlation of IOC with DOC may

lead to wrong results when evaluating TOC, especially in case DOC are considerably higher than those expected for conventional airliners.

NASA (Repic, et al., 1973)**.** The approach provided in (Roskam, 1985) is applicable to conventional aircraft. However, around ten years earlier, (Repic, et al., 1973) defined a specific DOC estimation model for high speed transportation systems, starting from the analysis of data and methods proposed Air Transport Association of America (ATA, 1967). This approach produced interesting CERs for some DOC cost items as herein described. The cost breakdown of the derived DOC is similar to the one described by (Roskam, 1985), even if only some of the items are computed. All DOC items are expressed in $\left[\frac{\$}{ton \cdot statute\ mile}\right]$. Because of the similarity with CERs described in Section 6.3, the model provided by (Repic, et al., 1973) is entirely provided in this section.

The cost associated to fuel is provided by (193)

$$DOC_f = \frac{1460 \cdot C_f \cdot \frac{W_{f_T}}{W_{GTO}} \cdot (1 - K_R)}{LF \cdot \frac{W_{PL}}{W_{GTO}} \cdot R_T} \qquad (193)$$

where

C_f is the fuel cost per unit mass in $\left[\frac{\$}{kg}\right]$
W_{f_T} is the weight of fuel in $[kg]$
W_{GTO} is gross take-off weight in $[kg]$
K_R is reserve fuel fraction
LF is aircraft load factor (ratio of average payload carried to normal maximum capability)
W_{PL} is weight of payload in $[kg]$
R_T is operational range in $[km]$

The flight crew cost is computed as in (194)

$$DOC_{crew} = \frac{320}{0.725 \cdot LF \cdot W_{PL} \cdot M \cdot \frac{V_{bl}}{V_{Cr}}} \qquad (194)$$

where

M is the cruise mach number

V_{Cr} is cruise velocity in $\left[\frac{km}{h}\right]$

The insurance cost can be expressed as in (195)

$$DOC_{insurance} = \frac{IR \cdot \frac{C_{HST}}{W_{GTO}}}{0.725 \cdot LF \cdot \frac{W_{PL}}{W_{GTO}} \cdot M \cdot \left(\frac{V_{bl}}{V_{Cr}} \cdot U\right)} \quad (195)$$

where

IR is the annual insurance rate in percentage
C_{HST} is the cost of HST aircraft in [$]
U is aircraft utilization in $\left[\frac{hr}{year}\right]$

The depreciation cost can be computed as in (196)

$$DOC_{depreciation} = \frac{1.1 \cdot \frac{C_{HST}}{W_{GTO}} + 0.3 \cdot \left(\frac{C_{TJ}}{W_{GTO}} + \frac{C_{RJ}}{W_{GTO}}\right)}{0.725 \cdot LF \cdot \frac{W_{PL}}{W_{GTO}} \cdot M \cdot \frac{V_{bl}}{V_{Cr}} \cdot U \cdot L_d} \quad (196)$$

where

C_{TJ} is turbojet engine set cost per aircraft in [$]
C_{RJ} is ramjet engine set cost per aircraft in [$]
L_d is depreciation life of aircraft in years

Maintenance cost is split in different contributions, which take into account both labour and material, as for the previous (Roskam, 1985) model, with specific CERs depending on engine types. The maintenance labour and material cost for airframe are provided in (197) and (198) respectively

$$DOC_{M_{AF_L}} = \frac{(3.22 + 1.93 \cdot t_F) \cdot \left(0.05 \cdot \left(\frac{W_{AF}}{W_{GTO}} + \frac{W_{AV}}{W_{GTO}}\right) + 0.009\right) \cdot M^{\frac{1}{2}} \cdot r_L}{LF \cdot \frac{W_{PL}}{W_{GTO}} \cdot R_T} \quad (197)$$

$$DOC_{M_{AF_M}} = \frac{(4.52 \cdot t_F + 9.04) \cdot \left(\frac{C_{HST}}{W_{GTO}} - \frac{C_{TJ}}{W_{GTO}} - \frac{C_{RJ}}{W_{GTO}}\right)}{LF \cdot \frac{W_{PL}}{W_{GTO}} \cdot R_T \cdot 10^3} \quad (198)$$

where

t_F is flight time in hours
W_{AF} is airframe weight in $[kg]$
W_{AV} is avionic system weight in $[kg]$
r_L is average maintenance labor rate in $\left[\frac{\$}{manhour}\right]$

The maintenance costs for turbojet are provided in (199) and (200) respectively for labour and material

$$DOC_{M_{TJ_L}} = \frac{\left(\frac{T}{W}\right)_{GTO} \cdot (1 + 0.3 \cdot t_F) \cdot \left(\frac{8.6}{T_{TJ}/10^3} + 0.087\right) \cdot r_L \cdot K_{LTJ}}{LF \cdot \frac{W_{PL}}{W_{GTO}} \cdot R_T} \quad (199)$$

$$DOC_{M_{TJ_M}} = \frac{\frac{C_{TJ}}{W_{GTO}} \cdot (0.011 \cdot t_F + 0.029) \cdot K_{MTJ}}{LF \cdot \frac{W_{PL}}{W_{GTO}} \cdot R_T} \quad (200)$$

where

$\frac{T}{W_{GTO}}$ is the thrust to weight ratio considering W_{GTO}
T_{TJ} is turbojet sea level thrust per engine in $[N]$
K_{LTJ} is a labor correction factor to take into account the complexity of HST if compared to conventional aircraft
K_{MTJ} is a material correction factor to take into account the complexity of HST if compared to conventional aircraft

Ultimately, the labour and material cost associated to ramjet maintenance are reported in (201) and (202) respectively.

$$DOC_{M_{RJ_L}} = \frac{(1 + t_F) \cdot \left(\frac{0.876 \cdot N_{RJ} \cdot \frac{L}{D}}{\frac{W_{GTO}}{10^3}}\right) \cdot r_L \cdot K_{LRJ}}{\frac{L}{D} \cdot LF \cdot \frac{W_{PL}}{W_{GTO}} \cdot R_T} \quad (201)$$

$$DOC_{M_{RJ_M}} = \frac{\frac{C_{RJ}}{W_{GTO}} \cdot (0.036 \cdot t_F + 0.029) \cdot K_{MRJ}}{LF \cdot \frac{W_{PL}}{W_{GTO}} \cdot R_T} \quad (202)$$

where

$\frac{L}{D}$ is the aerodynamic efficiency of the aircraft
N_{RJ} is the number of ramjet modules per aircraft
K_{LRJ} is a labor correction factor to take into account the complexity of HST if compared to conventional aircraft
K_{MRJ} is a material correction factor to take into account the complexity of HST if compared to conventional aircraft

The model proposed by (Repic, et al., 1973) is considered as main reference for the estimation of DOC for HST systems. However, it does not take into account costs associated to fees, so an additional formulation shall be added to the equations set. Moreover, IOC are not computed and, for this reason, in order to be able to define a more consistent IOC estimation model (if compared to (Roskam, 1985)), the references reported in the following section are considered.

ICAO (ICAO, 2017) **and IATA** (Ferjan, 2013)**.** Generally, it is quite difficult to find in literature an affordable method for IOC assessment for civil aircraft. It is principally due to the consistent lack of IOC data and to the fact that indirect operating cost is strictly related to the specific airline. Moreover, it considerably varies between major airlines, low-cost carriers, regional airlines, and so forth. Difficulty increases when hypersonic vehicles are treated, taking into account that they consist of a complex mixture of aircraft and space vehicle. However, the similarities between hypersonic point-to-point transportation and conventional aeronautics in terms of provided services, required ground infrastructures and personnel, lead to the consideration that hypersonic vehicles will be probably characterized by IOC similar to present large subsonic commercial aircraft. In account of this, the available IOC data provided by ICAO (ICAO, 2017) and (Ferjan, 2013), have been exploited to provide IOC estimations for hypersonic cruisers, as described in Section 6.3. Notably, Table 55 introduces and defines the IOC items treated in this work as defined by ICAO (ICAO, 2017).

Table 55: IOC items definition from (ICAO, 2017)

IOC Item	Definition
Aircraft Servicing Costs	Handling of the aircraft on the ground, including landing fees
Traffic Servicing Costs	Processing passengers, baggage and cargo at airports
Passenger Servicing Costs	Meals, flight attendants, and in-flight services
Reservations and Sales Costs	Airline reservations and ticket offices, travel agency commissions
Other Indirect and System Overhead Costs	Advertising and publicity expense, general and administrative expense
Airport Charges and Air Navigation Charges	Landing fees, pollutant emissions charges, and air navigation charges.

A high-level derivation strategy of these IOC items is also suggested as in Table 56, where the main cost drivers involved are shown according to (ICAO, 2017).

Table 56: Average values for IOC items according to (ICAO, 2017)

IOC Item	High-level estimation (average values)
Aircraft Servicing Costs	$800 per Aircraft Departure
Traffic Servicing Costs	$15 per Enplaned Passenger
Passenger Servicing Costs	$0.015 per RPM
Reservations and Sales Costs	14% of Total Airline Revenue
Other Indirect and System Overhead Costs	13% of Total Operating Expense, including: Advertising and Publicity (2% of TOC) General and Administrative (6% of TOC) System Overhead (5% of TOC)

Looking at the way IOC items are defined and quantified it is possible to notice that:

- Aircraft Servicing Costs usually represent a fixed amount per aircraft departure (this value is probably slightly influenced by the aircraft dimensions);
- Traffic Servicing Costs are calculated per enplaned passenger; therefore, they are function of the load factor;
- Passenger Servicing Costs are given per Revenue Passenger Mile (RPM);
- Reservations and Sales Costs is a fraction of the total airline revenue;

- Other Indirect and System Overhead Costs are expressed as a percentage of total operating cost (TOC, given by the sum of DOC and IOC). They include advertising and publicity and general and administrative expenses.

An alternative approach to estimate IOC is provided by (Ferjan, 2013), where different cost items are identified as indicated in Table 57, together with related values (average). The costs provided in Table 57 are given per Available Seat Kilometre (ASK).

Table 57: Average data for IOC items specified in (Ferjan, 2013)

IOC items	$ per ASK (average values)
General and Administrative	0.0072
Reservation, Ticketing, Sales and Promotion	0.0076
Station and Ground	0.0092
Airport Charges and Air Navigation Charges	0.0083
Passenger Service and Cabin Attendants	0.0079

It is thus interesting to compare the IOC items of the two references to understand the differences through which costs are computed. A direct comparison is provided in Table 58. The comparison is not aimed at evaluating the difference concerning quantitative values, which cannot be discussed directly because of the different actualization. However, looking at the cost items, it appears that (ICAO, 2017) and (Ferjan, 2013) data are complementary. Thus, the exploitation of data from the two sources allows covering all the major IOC cost items, even if a proper actualization factor shall be applied to overcome currency problems. Section 6.3 describes in detail how the IOC model for HST is derived, starting from the assumptions just described.

Table 58: Comparison of IOC items

Cost Item	IATA (2013)	ICAO (2017)
General and Administrative	0.0072 $ per ASK	Included into *Other Indirect and System Overhead Costs*
Reservation, Ticketing, Sales and Promotion	0.0076 $ per ASK	14% of Total Airline Revenue
Station and Ground	0.0092 $ per ASK	Included into *Other Indirect and System Overhead Costs*
Airport Charges and Air Navigation Charges	0.0083 $ per ASK	Included into *Other Indirect and System Overhead Costs*
Passenger Service and Cabin Attendants	0.0079 $ per ASK	$0.015 per RPM
Aircraft Servicing Costs	-	$800 per Aircraft Departure
Traffic Servicing Costs	-	$15 per Enplaned Passenger
Advertising and Publicity	Included into *Reservation, Ticketing, Sales and Promotion*	Included into *Other Indirect and System Overhead Costs*
Airport Charges and Air Navigation Charges	0.0083 $ per ASK	Not specified

6.2 Description of high-level Life Cycle Cost estimation process

From a high-level perspective, the parametric cost estimation process for high-speed vehicles is similar to the one applied for conventional systems belonging to aeronautical and space domains. This means that the general approach can be divided in four main activities, as depicted in Fig. 220.

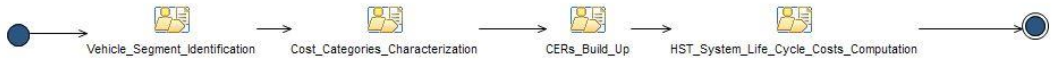

Fig. 220: Reference process for life-cycle cost estimation of high-speed transportation systems

The first activity is related to the identification of a set of reference vehicles and associated performance that can be used as basis to build a cost database. As part of this first activity, the review of suitable reference cost models is generally useful to verify, at first, whether the existing Cost Estimation Relationships (CERs) can be updated or modified to take into account peculiar aspects of high-speed flight, starting from conventional analyses. This means that, on one side, it is important to identify the main parameters characteristic of the family of hypersonic vehicles, and to properly populate the database. Indeed, the availability of cost data of reference vehicles is a noticeable help when building a cost model, since parametric cost estimation is undoubtedly based on available information. On the other hand, it is crucial to carefully look at existing methodologies to verify the limits of applicability of already available models and in case, to develop new ones.

Once the reference vehicles and cost models are known, it is possible to hypothesize suitable cost categories to be characterized. Cost categories are typically defined depending on the considered engineering domain. Maintaining consistency with existing models coming from the same field of analysis is crucial not only for standardization purposes, but also to allow a direct comparison between two or more approaches, easing the understanding of common points and differences. As specified in Section 6.1, a conventional cost breakdown proposed within the aeronautical domain exploits a list made up of development (also known as Research, Development, Test and Evaluation – RDTE), production and operating costs (both Direct Operating Costs – DOC, and Indirect Operating Costs – IOC). Each category is furthermore made up of different cost items, as already stated in Section 6.1 and detailed in Section 6.3. The identification of cost categories is also important when looking at the CERs themselves and at their structure. In fact, the third activity of the proposed process is associated to the definition of proper cost drivers as fundamental bricks for the cost equations. Identification of cost drivers is one of the most important activity of cost engineering, since the quality of estimation relies on the effectiveness of the correlation between cost (for a specific cost category and item) and drivers. This is the most challenging aspect of cost engineering when dealing with innovative models, since the lack of cost data associated to the reference vehicles population may preclude the possibility of identify straightforward the contribution of drivers to the final cost, as well as their mutual relationships.

The architecture of the CERs shall then be derived following an iterative process, not shown in Fig. 220, through which the combination of drivers is

carefully explored comparing provisional cost estimation results with existing data, derived from the first activity of the process. In this stage, the experience of the designer, as well as its knowledge of the system of interest, is crucial to guarantee a positive outcome of the analysis. Once CERs are successfully defined, the cost estimation process can be applied to the case study. This final activity requires a preliminary validation campaigns of cost equations on existing, or at least known, examples in order to evaluate discrepancies and approximation of the values. A sensitivity analysis can be also required in case the contribution of the different drivers to the final result is not sufficiently clear. The output obtained from the updated cost models can then be used as first means of verification for the viability of vehicle concept during development and production phases, as well as sustainability assessment when looking at operational aspects. Moreover, a proper business plan can be developed starting from cost assumptions derived from the LCC estimation, producing hypotheses on service and product prices. Formalized cost data can then be stored as cost requirements within a proper RDB and associated to physical and performance characteristics of the vehicle. Particularly, the cost estimation process can be performed at different design levels in order to obtain cost data for both vehicle and subsystems. In fact, as already mentioned, the level of granularity of costs computation depends on cost categories and items, whose scope can be very different. Operating costs are in fact more focused on aircraft level analysis, even if the impact of technologies adopted for the design of selected on-board subsystems can be non-negligible on the final product lifecycle, as explained in Section 6.3. On the other hand, a detailed cost breakdown during development and production phases helps designers controlling cost escalation in early design stages, allocating resources on specific areas of interest. For this reason, the process shown in Fig. 220 for aircraft level cost estimation can be re-applied at lower levels, focusing on specific assemblies and subsystems, at least for development and production costs assessment. This is exactly the way in which cost estimation for STRATOFLY MR3 vehicle is proposed in Section 6.3, where development and production costs are proposed for the vehicle, its main assemblies, such as airframe and propulsion plant, as well as for some of most critical subsystems, while a higher level is devoted to operating costs analysis.

6.3 Discussion on LCC estimation for STRATOFLY MR3

6.3.1 Introduction

In this section, the definition of a proper cost model for the LCC estimation of hypersonic vehicles is proposed, with particular focus on MR3 case study. Particularly development, production and operating cost CERs are presented in Sections 6.3.2, 6.3.3 and 6.3.4 respectively. In each of these sections, dedicated paragraphs for both general model definition and MR3 costs computation are included. Operating CERs are furthermore divided in DOC and IOC related items, as described in Section 6.1.2.2. The vehicles considered for the formulation of the statistical trends of development and production cost estimations are included in Table 59, with their main characteristics. These vehicles will serve as additional database to improve TRANSCOST formulations.

Table 59: Reference vehicles used for the development of TRANSCOST modified CERs

Vehicle	OEW [kg]	Engine	(One) Engine thrust [kN]	(One) Engine dry mass [kg]	Updated vehicle TFU [2017 M€]
X-15	6620	XLR-11 (rocket)	27	95	93.1
Concorde	78700	Olympus 593 (TJ with AB)	155	3175	620.4
SR-71	30600	PW J58 (TJ/RJ with AB)	151	2700	317
XB-70	93000	GEYJ93 (TJ with AB)	114	2300	651.4
Spaceliner Orbiter	140000	SLME (rocket)	2050	3375	517.1
LAPCAT A2	200000	Scimitar	300	10200	1340.6
LAPCAT MR2	200000	ATR+DMR	250 + 5000	4000 + 1400	N/A

As it can be seen, the statistical population is quite poor, considering that only few vehicles have reached the operational stage, and for most of those which have never left the development stage only partial data are available in literature. The driving choice for the selection of these candidates was then the availability of

complete set of data, in order not to affect the solution obtained from the statistical regression. The obtained model shall, however, be considered as provisional, since a more reliable estimation can be formulated only when the statistical population will reach a higher number of elements.

6.3.2 Development cost estimation model

6.3.2.1 Definition of development CERs

The development CERs definition approach is based on the identification of proper equations from the analysis of cost trends obtained looking at statistical regressions applied to a population of vehicles belonging to the same category. In particular, cost drivers are properly identified and selected depending on the correlation with cost. The result is a set of equations which have a shape that is similar to the one proposed by (Koelle, 2012), even if the main drivers may be different from the pure mass. The original formulation of CERs proposed in (Koelle, 2012) is thus assessed with reference to the set of vehicles reported in Table 59 (since some of them were not included in the original model) to verify whether the general validity of the results is still applicable or not. In case updates are needed, new cost drivers or modification to the coefficients are proposed. CERs are provided for vehicle and power plant, as in (Koelle, 2012), but ad-hoc built equations are developed for critical subsystems of such as TPS, TEMS and propellant subsystem. Evaluation of development cost is thus subdivided following a PBS-oriented approach, where missing items are evaluated following literature suggestions on cost allocation (Beltramo, et al., 1979), or exploiting commercial software for cost estimation like the Price True Planning® platform, as described in (Fusaro, et al., 2018). The reference PBS is shown in Fig. 230, Section 6.3.2.2 for MR3 case study. In order to keep consistency with (Koelle, 2012) core CERs are formulated to provide the results in [WYr], even if the charts representing the cost trends are in 2017 [M€]. For the sake of clarity, only core CERs are shown, whilst factor coefficients proposed by (Koelle, 2012) are kept for complete formulation, unless otherwise specified, to obtain the final results reported in the charts.

Advanced aircraft development cost (RDTE). The TRANSCOST CER for the estimation of development costs of high-speed vehicles (175) is tested on the aircraft list provided in Table 59, keeping also the original dataset. This test is done to verify whether the estimation is still valid when considering innovative hypersonic aircraft concepts, like the A2, the MR2 or even the Spaceliner Orbiter

(Sippel, et al., 2015). From the analysis of the results applying (175) it is possible to obtain the results depicted in Fig. 221 and Fig. 222, where the core CER is also reported.

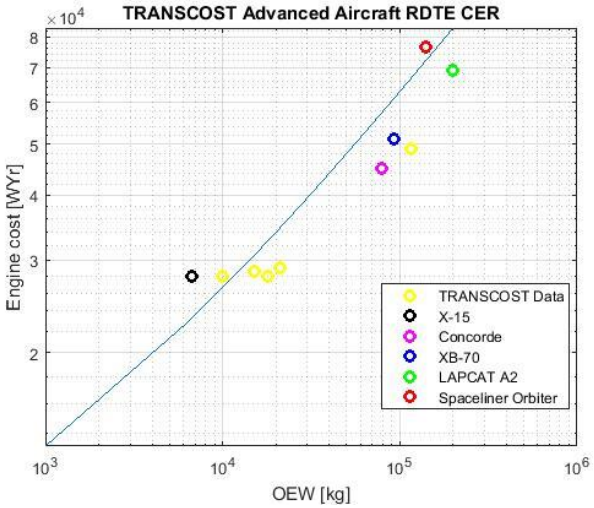

Fig. 221: Logarithmic chart for advanced aircraft development cost trend

It is interesting to note the effect of design Mach number on the correlation. Particularly, it is nice to see how the CER correctly interpolates the dataset while the Mach number increases. Both 2D and 3D trends appear to be in line with real data, also considering new concepts. Looking closer to the 3D results and analysing the 2D parametric views it appears that the correlation between estimation and data are good even if an error still remains. The CER provided in (Koelle, 2012) appears in any case still valid, and can be used for HST development cost estimation.

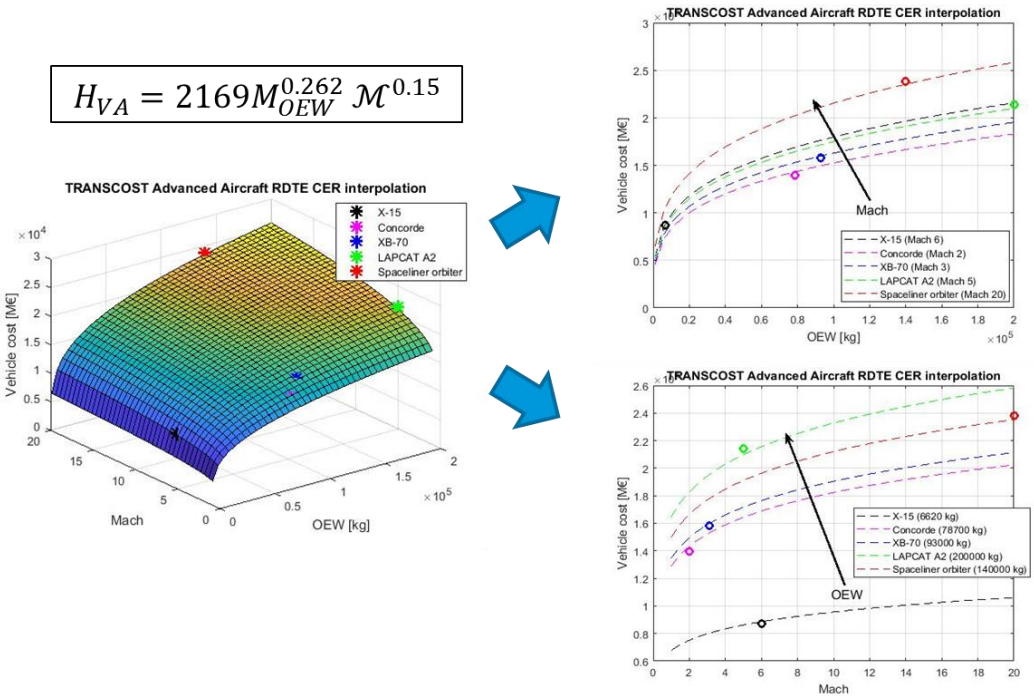

Fig. 222: Summary of advanced aircraft development CER trends

Turbojet engine development cost (RDTE). The TRANSCOST development CER related to air breathing engines is only dependent on dry mass (173). This may lead to bad correlations at high flight speed. A modified relationship is presented in (203).

$$H'_{ET} = \left(232.4 M_{E_{dry}}^{0.509} + 1.12v\right) f_1 f_3 \qquad (203)$$

where v is the cruise speed in $\left[\frac{m}{s}\right]$.

The situation is clarified in Fig. 223 and Fig. 224, where it is possible to see how the new trend better suits the innovative propulsive configurations, even if a wider displacement with the original formulation can be denoted at low engine dry mass (which is in any case out of scope for the boundaries of the analysis). In the 3D view reported in Fig. 224 it is possible to see how the contribution of flight speed positively affects the estimation. Moreover, since the new correlation (203) provides better results starting from 1000 kg of dry mass, considering that lower masses are very rare for turbojets in hypersonic applications, this trend is selected for the updated cost model.

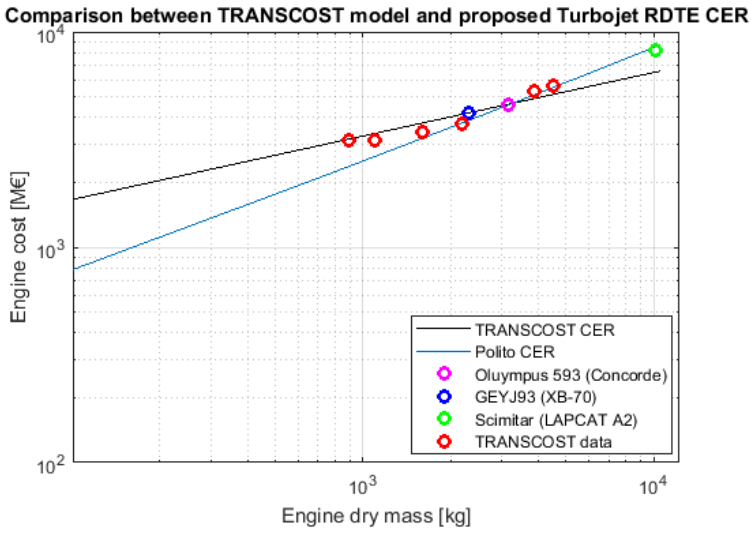

Fig. 223: Comparison between logarithmic trend of development cost for turbojet using TRANSCOST and updated model

The new CER proves also a good correlation between flight speed and engine dry mass parameters.

$$H'_{ET} = \left(232.4 M_{E_{dry}}^{0.509} + 1.12v\right)$$

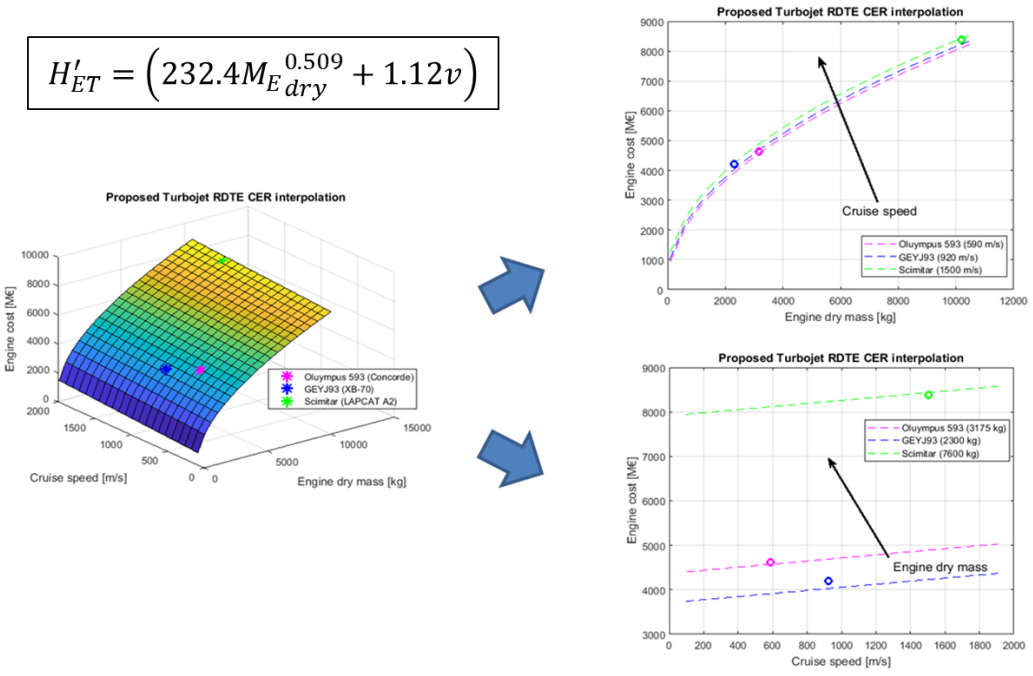

Fig. 224: Summary of turbojet engine development CER trends

Ramjet engine development cost (RDTE). Ramjet development cost formulation (174) appears instead acceptable looking at the available data, as reported in Fig. 225. The position of the DMR of the MR2 seems reasonable considering the estimated cost for the Sanger ramjet (Koelle & Kuczera, 1989).

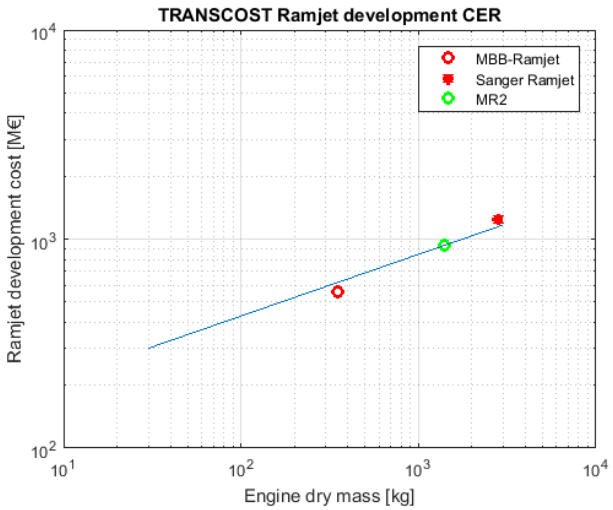

Fig. 225: Logarithmic trend of development cost for ramjet using TRANSCOST model

The equation reported in (174) is very simple, being function of engine dry mass only. It is difficult to further validate the CER, since the number of operational ramjet for which a declared cost value is available is quite low. However, the relationship is used within the proposed model, since alternatives correlations are not known found in literature.

Combined cycle engine development cost (RDTE). It is difficult to evaluate more specific power plant solution which exploits, for example, combined cycle engines like turboramjets, and innovative propulsion concepts, as the Scimitar (Jivraj, et al., 2007). An average solution relies on the evaluation of the cost by exploiting a mixed formulation reported in (204).

$$H_{CCE} = C_{complexity}(k_{TJ}H'_{ET} + k_{RJ}H_{ER})f_1 f_3 \qquad (204)$$

where

k_{TJ} and k_{RJ} are the turbojet and ramjet configuration coefficients used to represent the characteristics of the engine (i.e. if it is closer either to a turbojet or to a ramjet), ranging from 0 to 1 (e.g. $k_{TJ} = 0.6$, $k_{RJ} = 0.4$)

$C_{complexity}$ is a multiplication factor used to compare the considered design to a an existing one (i.e. it can be exploited as escalation or reduction cost factor depending on the global configuration of the considered engine)

H'_{ET} and H_{ER} represent cost of turbojet and ramjet with updated and original formulations respectively.

Fig. 226 shows the trend of equation (204) if compared to (203) and (174) with a $C_{complexity} = 1$ and an equal contribution (0.5) of turbojet and ramjet configurations. The dotted blue line in Fig. 226 shows how (203) could be expressed if using the original TRANSCOST formulation for turbojet development cost (H_{ET} instead of H'_{ET}). Looking at the cost evolution of the three solid lines, the adoption of the new turbojet formulation (204) seems better representing the average trend, being selected for the proposed cost model.

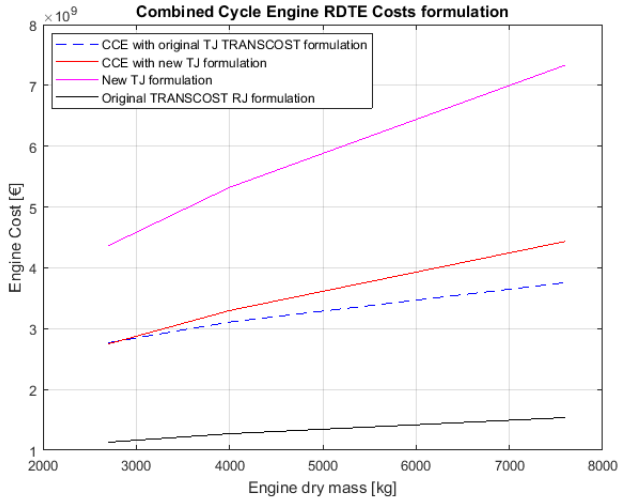

Fig. 226: Comparison with simple and combined cycle engine RDTE cost formulations

Propellant subsystem development cost (RDTE). Apart from power plant, other critical on-board subsystems costs were described using dedicated CERs inspired by the TRANSCOST approach. The CER for fuel/propellant system development is proposed in (205). The equation is based on aircraft OEW. The application of power plant dry mass as additional driver allows also scaling the cost of the system depending on the size and complexity of the propulsive architecture.

$$S_{Fuel_{dev}} = \left(0.1 M_{OEW}^{0.68} + 0.49 {M_E}_{dry}^{0.51}\right) f_1 f_3 \qquad (205)$$

The trend derived applying (205) is reported in Fig. 227. As it can be seen the main contribution is due to the OEW since it represents the size of the vehicle, even if the dry mass of the power plant allows tuning the final result.

$$S_{Fuel_{dev}} = \left(0.1M_{OEW}^{0.68} + 0.49M_{E_{dry}}^{0.51}\right)$$

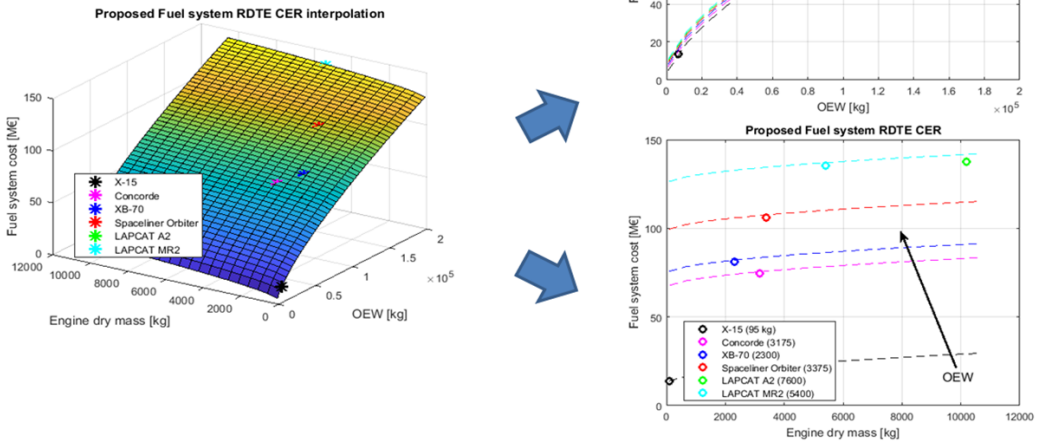

Fig. 227: Summary of propellant subsystem development CER trends

Thermal Protection Subsystem (TPS) development cost (RDTE). A similar approach can be applied to derive the CER related to TPS development (206)

$$S_{TPS_{dev}} = (0.56M_{OEW}^{0.59} + 1.8q^{0.51})f_1 f_3 \qquad (206)$$

where q is the reference heat flux for the considered vehicle in $\left[\frac{W}{m^2}\right]$ as reported in literature. The resulting trend is reported in Fig. 228. The contributions of the two cost drivers are in this case more balanced than in the fuel/propellant system CER, even if the heat flux is now the main parameter. This is reasonable considering the nature of the system under design.

$$S_{TPS_{dev}} = \left(0.56M_{OEW}^{0.59} + 1.8q^{0.51}\right)$$

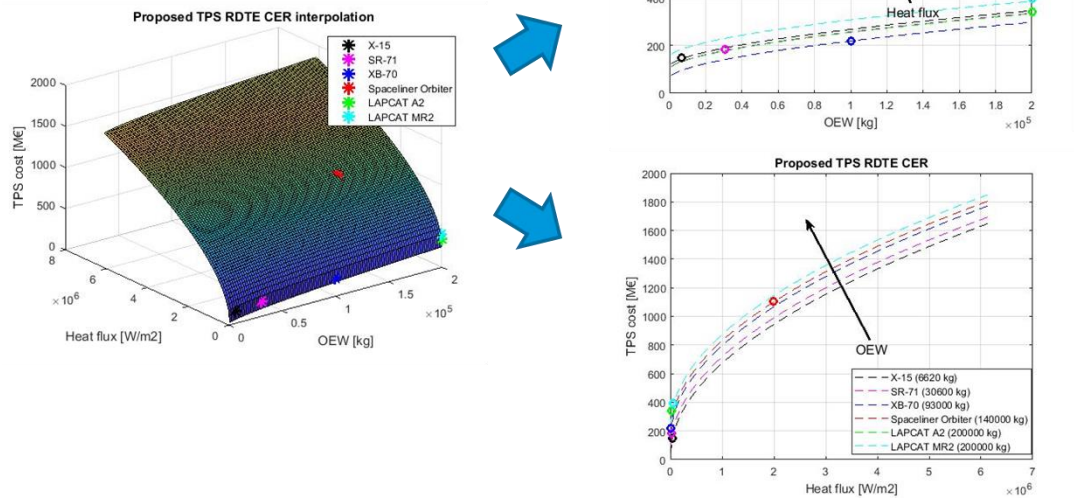

Fig. 228: Summary of TPS development CER trends

TEMS development cost (RDTE). The TEMS is instead a very peculiar system which has been hypothesized on LAPCAT MR2 (and subsequent STRATOFLY MR3) only. In order to sketch a possible trend, the application of TEMS to A2 is simulated as well. The final cost is computed basing on some of the main operating parameters of the system under design and, notably, generated power as well as boil-off flow rate (together with the OEW, as always). The final CER is reported in (207)

$$S_{TEMS_{dev}} = \left(5.73M_{OEW}^{0.26} + 0.8P^{0.17} + 0.53\dot{m}_{BO_{LH2}}^{0.19}\right)f_1 f_3 \qquad (207)$$

where

P is the power generated in [W]
$\dot{m}_{BO_{LH2}}$ is the boil-off flow rate (hydrogen is hypothesized) in $\left[\frac{kg}{s}\right]$

The resulting trend is depicted in Fig. 229. In this case, since the number of data points is too low to fix a specific surface, the trend is hypothesized looking at the variations resulting from the application of TEMS case study to both vehicles. Result shall be interpreted as very preliminary, considering that non-negligible

fluctuations may affect the final RDTE costs because of the lack of vehicles within the statistical population.

$$S_{TEMS_{dev}} = \left(5.73 M_{OEW}^{0.26} + 0.8 P^{0.17} + 0.53 \dot{m}_{BO_{LH2}}^{0.19}\right)$$

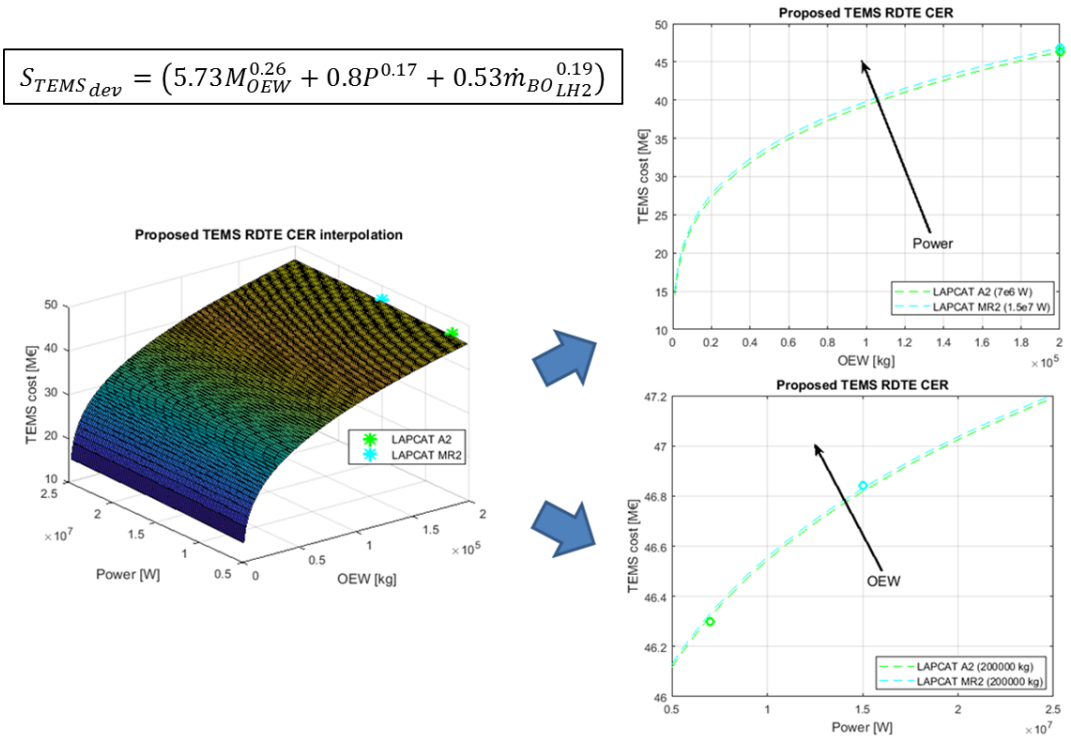

Fig. 229: Summary of TEMS development CER trends

6.3.2.2 Application of development CERs to MR3 case study

The CERs described in Section 6.3.2.1 have been applied to MR3 case study to derive the RDTE cost using a PBS-oriented approach. The reference PBS is reported in Fig. 230, where the hierarchy levels are also shown. The subsystem level is chosen as the lowest one that can be estimated with the existing model. As anticipated in Section 6.3.2.1, the remaining subsystems costs are evaluated following an allocation process based on existing literature. In this way, the cost breakdown may vary depending on the configuration of the vehicle and on the kind of sub-systems or, in general, items hosted on-board.

Target PBS	
Vehicle	Vehicle Level
Integration	Assembly Level
Structure and Mechanisms	System Level
Movable Surfaces	Subsystem Level
Landing Gear	Subsystem Level
On-Board Systems	System Level
Powerplant	Subsystem Level
APU System	Subsystem Level
Hydraulic System	Subsystem Level
Fuel System	Subsystem Level
ECS	Subsystem Level
Ice Protection System	Subsystem Level
Fire Protection System	Subsystem Level
Flight Control System	Subsystem Level
Avionic System	Subsystem Level
Electrical Power System	Subsystem Level
VEMS	Subsystem Level
TPS	Subsystem Level
Water System	Subsystem Level
Oxygen System	Subsystem Level
Lights	Subsystem Level
Furnishing and Interior	System Level

Fig. 230: Reference PBS used for MR3 case study

The results for MR3 case study are reported in Table 60 and summarized in Fig. 231, where the pie chart depicting the percentage allocation of cost on the PBS is reported (only cost item with an impact on the overall RDTE cost >1% are shown). The development cost of MR3 is thus around 24.5 B€ with around 7.2 B€ dedicated to power plant, considering an all-electric aircraft architecture (no hydraulic subsystem). Results shown in Table 60 are rounded.

Table 60: Cost breakdown for STRATOFLY MR3

Cost items	STRATOFLY MR3 estimation [€] 2017
Total Structure	€ 10.472.000.000
Total Movable Surfaces	€ 100.850.000
Total Landing Gear	€ 87.403.000
Total Structure and Mechanisms	**€ 10.660.253.000**
Total ATR engines	€ 5.525.000.000
Total DMR engines	€ 1.675.500.000
Total APU	€ 84.042.000
Total Hydraulic System	-
Total Fuel System	€ 114.460.000
Total Environmental Control System	€ 352.980.000
Total Ice Protection System	€ 117.660.000
Total Fire Protection System	€ 126.060.000
Total Flight Control System	€ 487.440.000
Total Avionic System	€ 164.720.000
Total Electrical Power System	€ 504.250.000
Total TEMS	€ 40.116.000
Total Thermal Protection System	€ 331.070.000
Total Water System	€ 100.850.000
Total Oxygen System	€ 100.850.000
Total Lights	€ 50.425.000
Total On-board Systems	**€ 9.775.423.000**
Total Furnishing and Interior	**€ 58.829.000**
Total Vehicle Integration	**€ 4.000.400.000**
TOTAL	**€ 24.454.000.000**

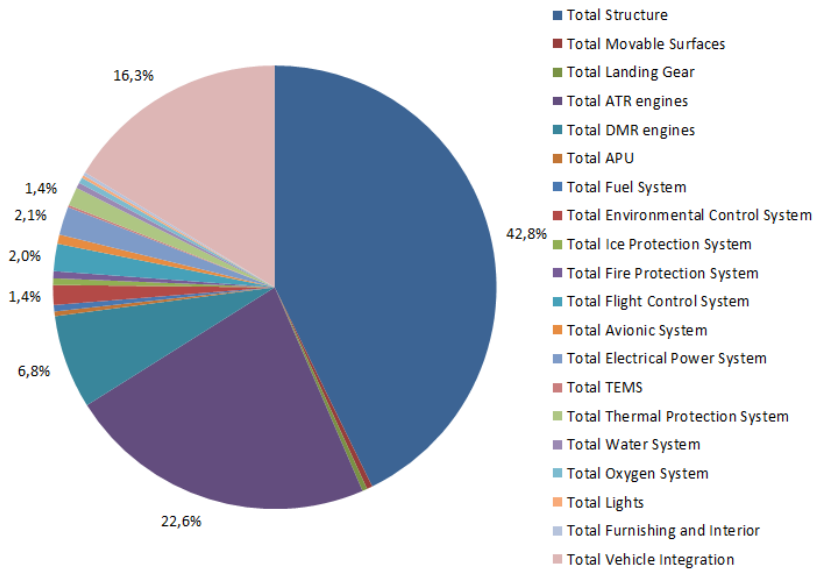

Fig. 231: Summary of PBS development cost allocation for MR3 vehicle

6.3.3 Production cost estimation model

6.3.3.1 Definition of production CERs

The definition process of production CERs follows what already applied for RDTE costs. Original TRANSCOST formulations (Koelle, 2012) are considered and analyse to verify their validity with respect to HST systems cost, and updated if necessary. All production CERs displayed in this section refer to the Theoretical First Unit (TFU), i.e. to the cost associated to the first unit built during the manufacturing phase (series production). A proper learning curve (Section 6.1.2.1) is applied to show the cost reduction trend as function of number of units built. The computed costs are related to recurring costs only.

Advanced aircraft production cost (TFU). The CER for the estimation of vehicle production cost reported in (189) is based on the OEW only for the advanced high speed aircraft category, following (Koelle, 2012) assumptions. However, since the speed ranges for this category may vary a lot, a better correlation may introduce flight speed within the equation. The formulation in (208) is then proposed.

$$F'_{VF} = \left(0.34 M_{T_{OEW}}^{1.75} + 7.06 v_k^{0.4}\right) f'_{10} \qquad (208)$$

where

$M_{T_{OEW}}$ is the Operating Empty Weight in [ton]
v_k is the cruise speed in $\left[\frac{km}{h}\right]$

The results are shown in Fig. 232, where (189) and (208) are compared. TRANSCOST CER tends to overestimate TFU cost if compared to the proposed trend within the considered range. Moreover, the increase of flight speed produces a higher cost escalation for higher OEW since the new formulation is not linear within the bi-logarithmic graph. With the original trend, instead, this effect is not captured.

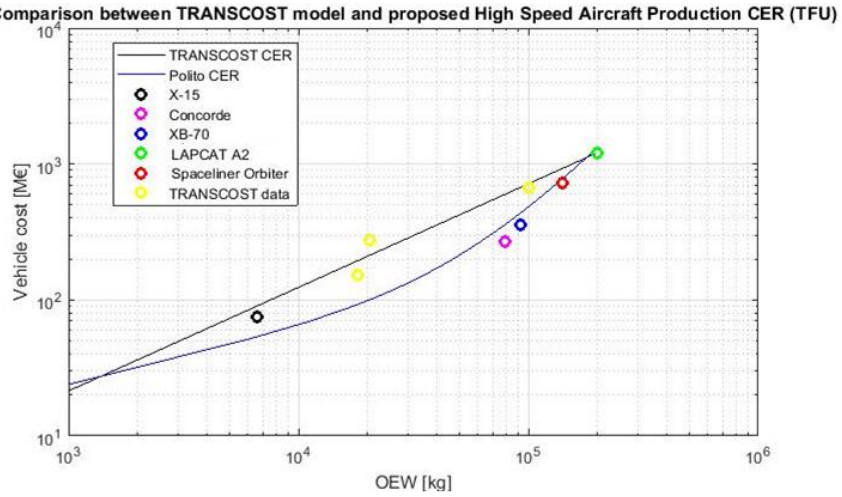

Fig. 232: Logarithmic trends of TRANSCOST and new model for advanced aircraft production cost estimation

The trend appears more in line with innovative vehicle concepts so it is selected for the proposed cost model. Looking closer to the parametric analysis of (208) it is possible to understand the global trend in 3D and 2D views, as reported in Fig. 233. As it can be seen, the effect of OEW is still dominant, even if the cruise speed has a non-negligible impact of the final result.

$$F'_{VF} = \left(0.34 M_{T_{OEW}}^{1.75} + 7.06 v_k^{0.4}\right)$$

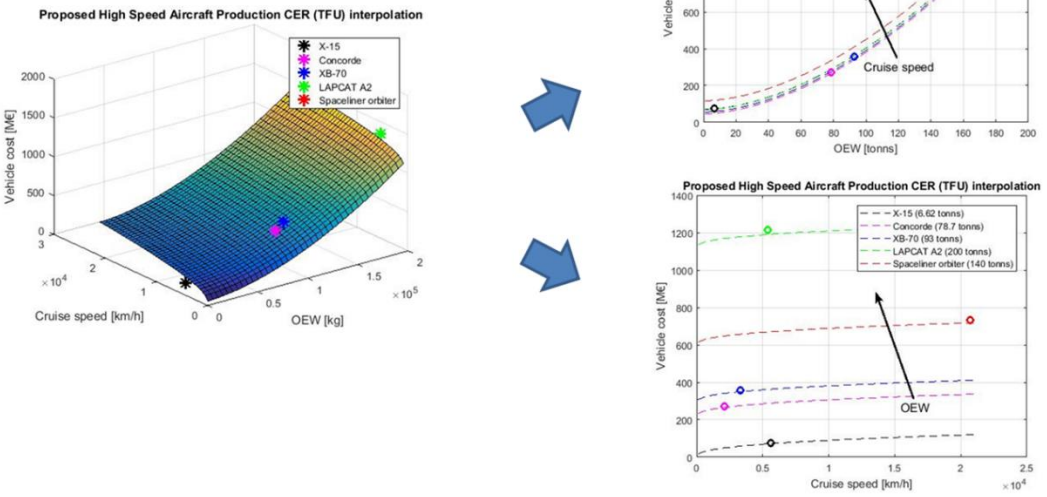

Fig. 233: Summary of advanced aircraft production CER trends

Turbojet engine production cost (TFU). A similar correction is applied to turbojet production CER, which in TRANSCOST is expressed as function of engine dry mass only (188). The proposed CER can be found in (209), where the flight speed is included in [m/s] (this is the higher speed value in turbojet operation range for the selected vehicle).

$$F'_{ET} = 2.29 M_{E_{dry}}^{0.530} + 0.50 v^{0.60} \qquad (209)$$

Fig. 234 shows the difference between the original formulation and the new one. The effect of speed correction, together with a slightly modified regression coefficients, brings a higher cost evaluation with a final trend which is similar to what proposed by TRANSCOST. However, the new estimation appears more in line with advanced propulsion concepts related to air breathing solutions for high speed aircraft, as it is possible to see from the regression. Thus, equation (209) is taken as reference for this kind of engines within the proposed model.

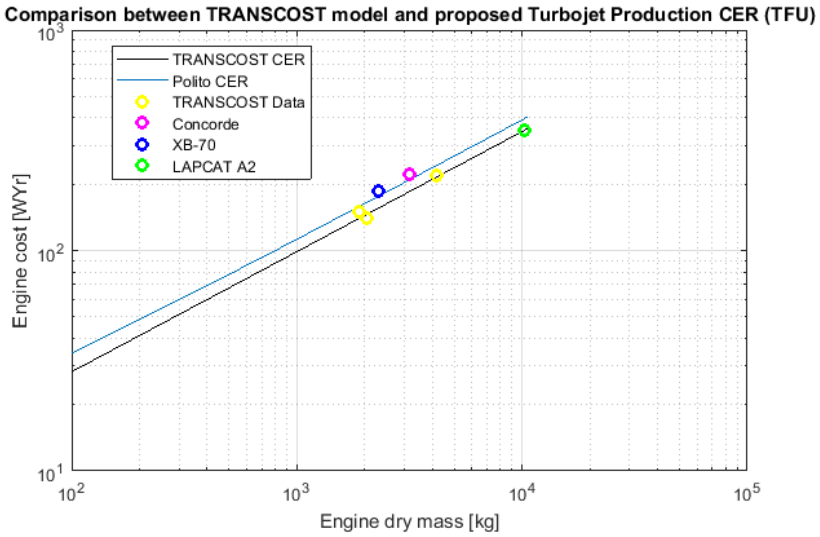

Fig. 234: Logarithmic trends of TRANSCOST and proposed model for turbojet production cost estimation

Detailed trends can be found in Fig. 235.

$$F'_{ET} = 2.29 M_{E_{dry}}^{0.530} + 0.50 v^{0.60}$$

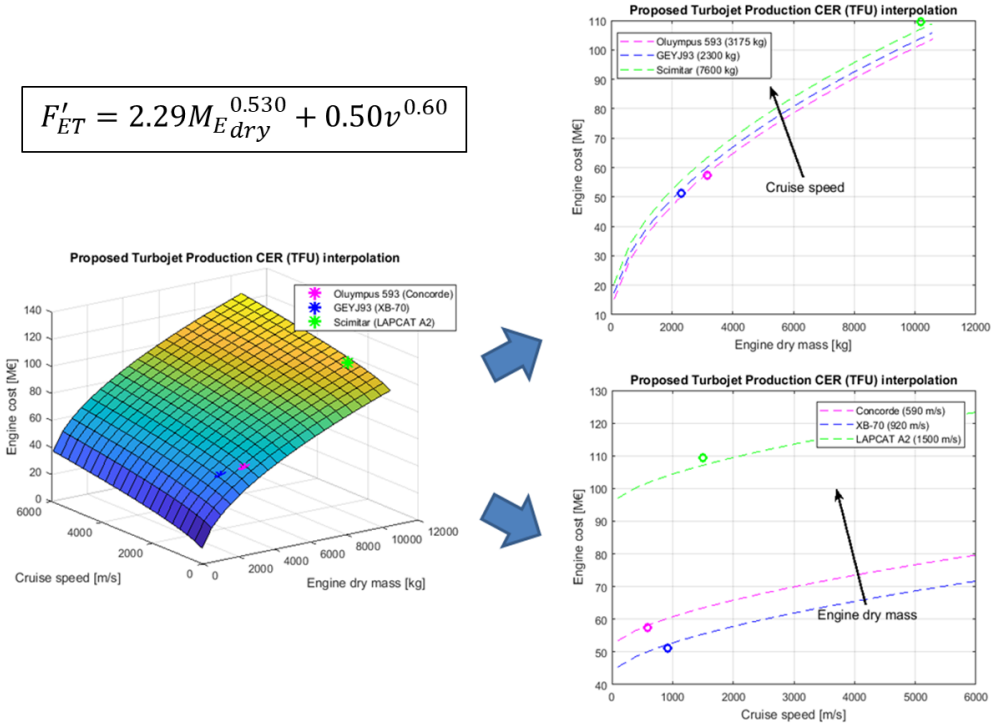

Fig. 235: Summary of turbojet engine production CER trends

From the 2D trends of Fig. 235 it appears clear how the contribution of the correction through flight speed within the CER is important for the overall cost estimation. The effect of both cost drivers is, in fact, more balanced if compared to the vehicle production cost estimation (Fig. 233).

Ramjet engine production cost (TFU). No equation for ramjet production cost estimation is provided in (Koelle, 2012) due to lack of data. However, since a CER exists for the development costs, it is mandatory to formulate a relationship to be included within the proposed model. A reasonable approach relies on the evaluation of the thrust generated by the engine. Looking at the data available in literature it is possible to sum up the simple CER reported in (210)

$$F_{ER} = 5.63T^{0.35} \qquad (210)$$

where T is the ramjet thrust in $[kN]$.

The trend generated by (210) is shown in Fig. 236.

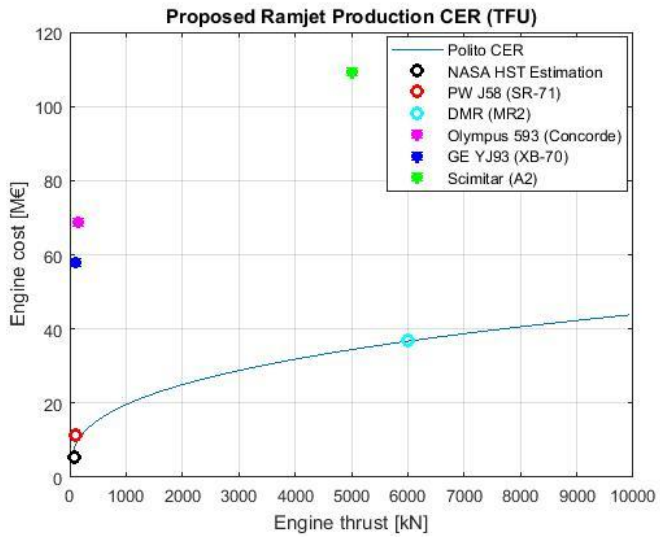

Fig. 236: Proposed ramjet engine production CER

A small number of points is currently available in the database. However, the evaluation of DMR cost for the MR2 vehicle, using commercial software for cost estimation as Price True Planning®, allows proposing an additional data point which is in line with the proposed trend (cyan dot in Fig. 236). Moreover, looking at the distribution of some turbojet engines having thrusts within a similar range (purple, blue and green dots), a similar law can be hypothesized, at least

considering its shape, even if with higher cost, confirming that this trend can be promising. The higher cost of turbojet is expected because of the increased complexity of the engine if compared to a ramjet, which has a lower number of components.

Combined cycle engines production cost (TFU). For hybrid engines, having characteristics that are typical of both turbojet and ramjet, or which may work in different configurations depending on the flight regime, a mixed formulation is proposed, as already done for development costs in (204). The equation reported in (211) is then derived

$$F_{CCE} = C_{complexity}(k_{TJ}F'_{ET} + k_{RJ}F_{ER}) \quad (211)$$

where, as in (204)

k_{TJ} and k_{RJ} are the turbojet and ramjet configuration coefficients used to represent the characteristics of the engine (i.e. if it is closer either to a turbojet or to a ramjet), ranging from 0 to 1 (e.g. $k_{TJ} = 0.6$, $k_{RJ} = 0.4$)

$C_{complexity}$ is a multiplication factor used to compare the considered design to a an existing one (i.e. it can be exploited as escalation or reduction cost factor depending on the global configuration of the considered engine).

Propellant subsystem production cost (TFU). The approach followed to determine production costs of sub-systems is similar to the one described for development costs. The CER for propellant subsystem production is shown in equation (212). As it can be seen, the cost drivers populating the equation are the same of (205), i.e. OEW and power plant dry mass, even if with different regression parameters.

$$S_{Fuel_{prod}} = 0.48M_{OEW}^{0.38} + 0.5{M_E}_{dry}^{0.39} \quad (212)$$

The results coming from this CER can be represented as in Fig. 237.

$$S_{Fuel_{prod}} = 0.48M_{OEW}^{0.38} + 0.5M_{E\,dry}^{0.39}$$

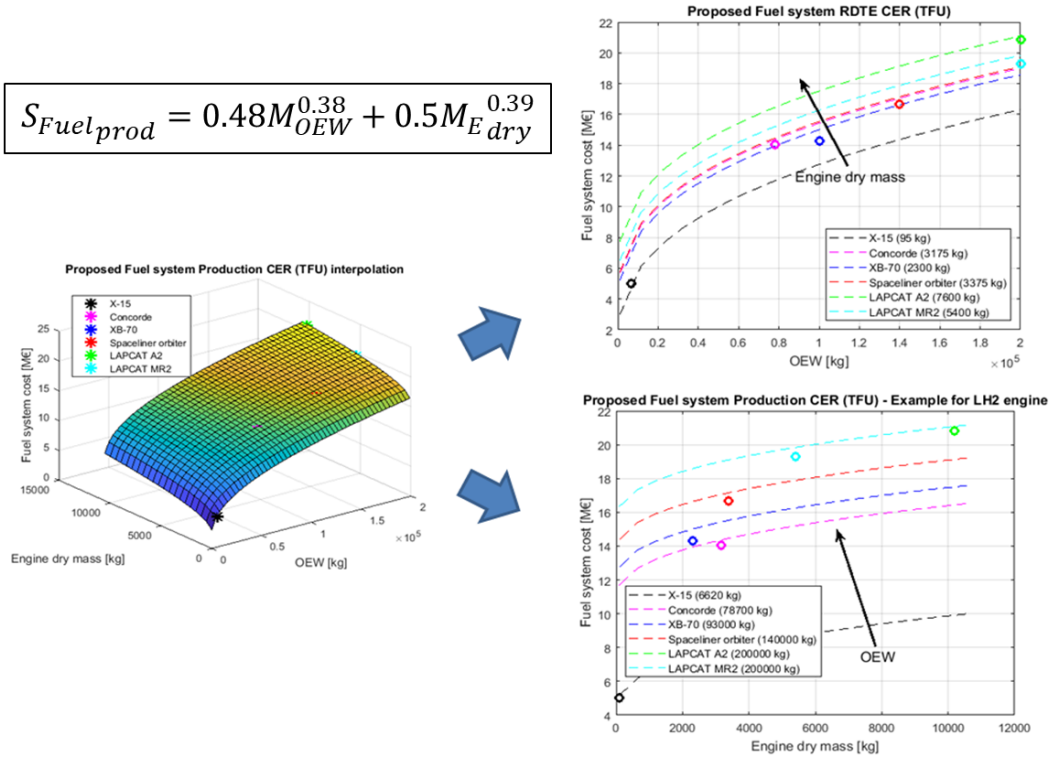

Fig. 237: Summary of propellant production CER trends

As it can be seen, the effect of both drivers is similar and both contributions are almost equally necessary to produce the desired result.

Thermal Protection Subsystem (TPS) production cost (TFU). The CER related to production cost of TPS is presented in equation (213). It uses three cost drivers since it includes also the heat load Q together with heat flux q and OEW, already defined within development cost CER equation (206). This is due to the fact that, even if the heat flux is the main parameter used to select the type of material (and also of TPS), having a high effect on production cost, the heat load can be used to specify the amount of material (thickness) to be manufactured, with subsequent contribution to the final expense.

$$S_{TPS_{prod}} = 0.51M_{OEW}^{0.19} + 3.41q^{0.12} + 0.68Q^{0.11} \qquad (213)$$

Particularly

q is the heat flux in $\left[\frac{W}{m^2}\right]$

Q is the heat load in $\left[\frac{J}{m^2}\right]$

Adding the heat load as cost drivers allows taking into account the reduction of the material of the TPS when considering high speed (and, thus, a lower exposure time), balancing the production cost which may be too high if basing on the pure heat flux. The resulting trend can be observed in Fig. 238.

$$S_{TPS_{prod}} = 0.51M_{OEW}^{0.19} + 3.41q^{0.12} + 0.68Q^{0.11}$$

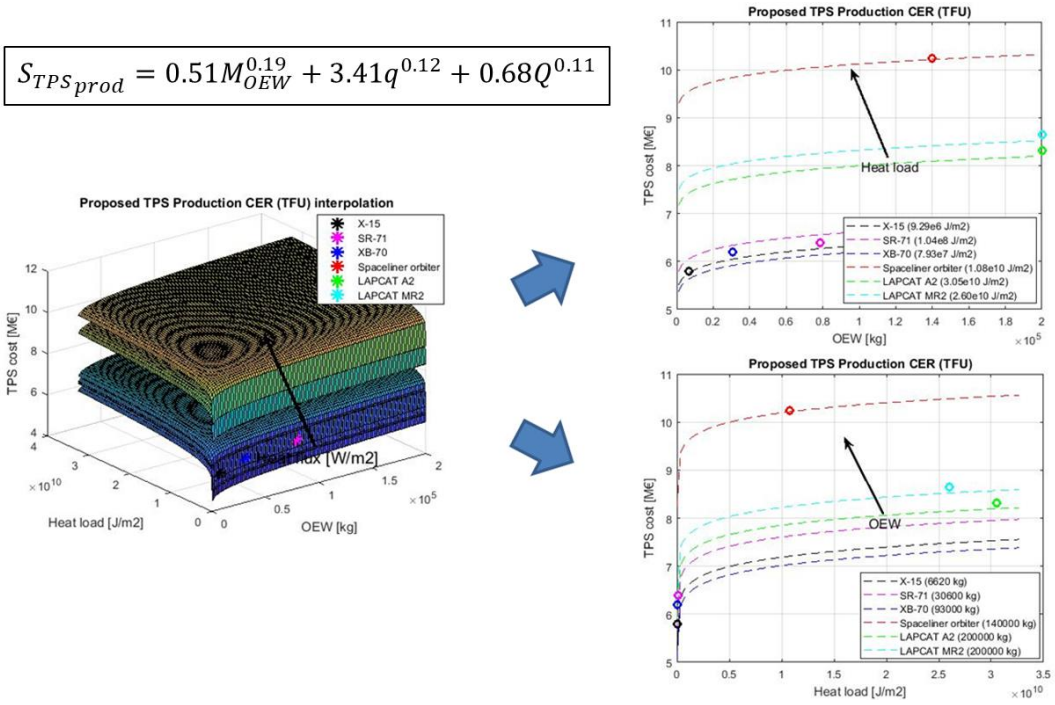

Fig. 238: Summary of TPS production CER trends

The 2D trends are shown for OEW and heat load, while the 3D surface shows the effect of heat flux.

TEMS production cost (TFU). The evaluation of TEMS production cost is performed with the same cost drivers already adopted to compute development costs, as the CER reported in (214) shows. Notably, OEW, power generated by TEMS, in [W], and boil-off flow rate, in $\left[\frac{kg}{s}\right]$, are used as main drivers.

$$S_{TEMS_{prod}} = 5.41M_{OEW}^{0.23} + 0.79P^{0.15} + 0.52\dot{m}_{BO_{LH2}}^{0.19} \quad (214)$$

The resulting trend is shown in Fig. 239.

$$S_{TEMS_{prod}} = 5.41 M_{OEW}^{0.23} + 0.79 P^{0.15} + 0.52 \dot{m}_{BO_{LH2}}^{0.19}$$

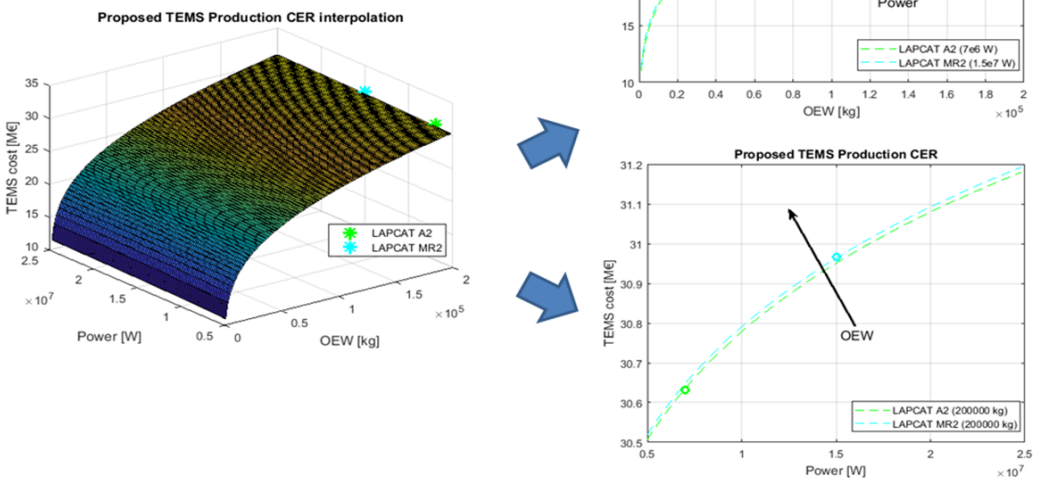

Fig. 239: Summary of TEMS production CER trends

As for the results obtained considering TEMS development costs (Fig. 229), the main effect is produced by OEW, which is the driver affecting the scalability of the equation since it identifies the size of the aircraft under design. The effect of power is lower even if it is useful to tune the final result. The boil-off flow rate has instead a reduced impact on the overall computed cost.

6.3.3.2 Application of production CERs to MR3 case study

Proposed CERs described in Section 6.3.3.1 are used to compute production costs of MR3 vehicle. The same assumptions reported in Section 6.3.2.2 are applied for production costs of additional on-board systems. This means that the allocation percentages from literature are assumed for more conventional sub-systems hosted on-board. The production cost breakdown for TFU is shown in Table 61, and a summary of cost allocation is provided in Fig. 240 (only cost item with an impact on the overall RDTE cost >1% are shown).

Table 61: Production cost breakdown (TFU) for STRATOFLY MR3

Costs items	**STRATOFLY MR3 estimation [€] 2017 (TFU)**
Total Structure	€ 657.960.000
Total Movable Surfaces	€ 3.549.500
Total Landing Gear	€ 5.367.600
Total Structure and Mechanisms	**€ 666.877.100**
Total ATR engines	€ 421.920.000
Total DMR engines	€ 34.339.000
Total APU	€ 11.255.000
Total Hydraulic System	-
Total Fuel System	€ 18.746.000
Total Environmental Control System	€ 16.449.000
Total Ice Protection System	€ 2.770.300
Total Fire Protection System	€ 3.030.100
Total Flight Control System	€ 25.972.000
Total Avionic System	€ 9.523.100
Total Electrical Power System	€ 186.130.000
Total TEMS	€ 31.959.000
Total Thermal Protection System	€ 8.500.200
Total Water System	€ 1.385.200
Total Oxygen System	€ 1.731.500
Total Lights	€ 1.298.600
Total On-board Systems	**€ 775.009.000**
Total Furnishing and Interior	**€ 519.440**
Total Vehicle Integration	**€ 25.106.000**
TOTAL	**€ 1.467.511.540**

The production cost of first MR3 unit is thus around 1470 M€, with about 456 M€ dedicated to power plant, considering an all-electric aircraft architecture (no hydraulic subsystem). Results shown in Table 61 are rounded.

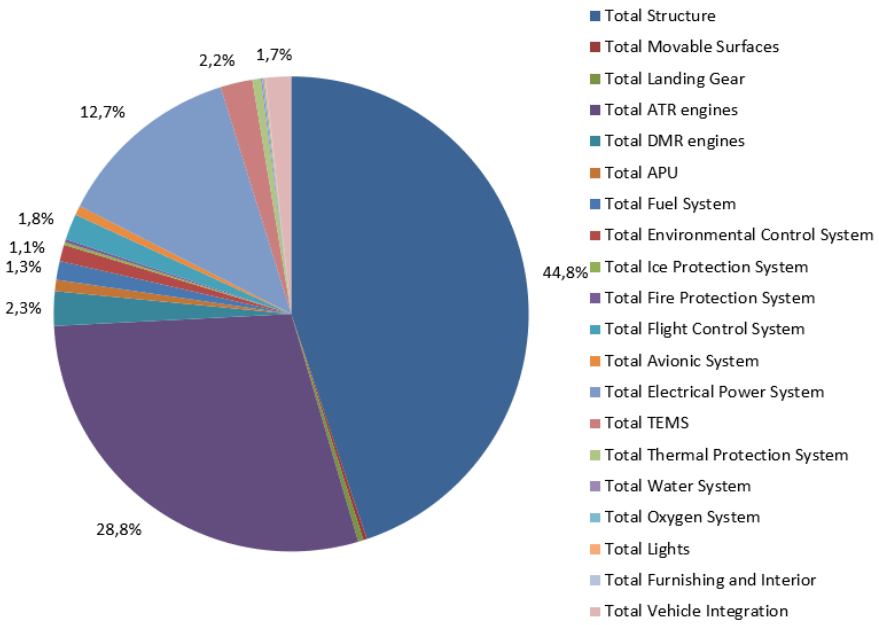

Fig. 240: Summary of PBS production cost allocation (TFU) for MR3 vehicle

Of course, the learning curve effect has a considerable impact on units production cost. The hypothesized trend for overall vehicle production cost, considering a homogeneous 83% learning curve over the breakdown for all subsystems, except power plant, is shown Fig. 241. Actually, low-speed propulsion plant (ATR) has a learning curve which is much faster than the one adopted for all other subsystems since for each vehicle six engines are produced.

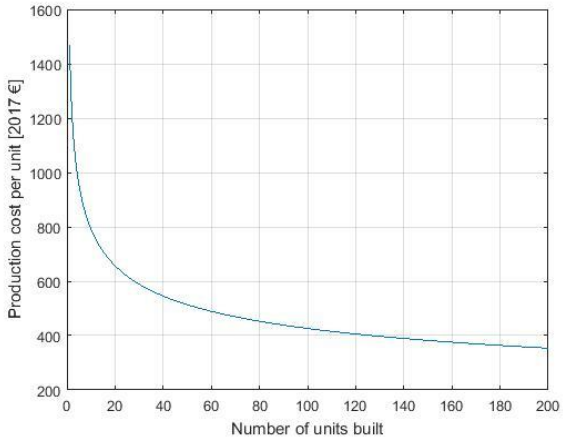

Fig. 241: Production cost reduction due to learning curve effect

Last vehicle cost (200^{th}) can be estimated around 354 M€. Moreover, considering this production series, the total production cost reaches around 182.4 B€, with an average cost for each unit of about 912 M€.

6.3.4 Operating cost estimation model

6.3.4.1 Definition of operating CERs

DOC. As already mentioned, in Section 6.1.2.2 the DOC for an HST vehicle are determined exploiting a modified version of the equations developed by the Air Transport Association of America (ATA, 1967) (obtaining the "NASA-Modified ATA CERs"). The version of the ATA method considered within (Repic, et al., 1973) provides DOC for turboprop, turbojet subsonic aircraft, and supersonic aircraft. These equations have been revised in order to evaluate the DOC associated to HST concepts. The NASA-Modified ATA CERs are applicable in a hypersonic Mach range from 5 to 12, without any specifications on the type of payload to be hosted. The applicability beyond the indicated Mach range should be carefully verified. For lower Mach number the method can be applied introducing proper coefficients, while for higher values, different models, probably closer to space domain, should be investigated. The costs resulting from the NASA-Modified ATA CERs are expressed per ton-mile, where the term "mile" refers to "statute mile". In this work, all the CERs have been re-expressed in ton-nautical miles. Moreover, considering that costs are expressed in US$, a proper exchange rate from US$ to € shall be introduced. The cost breakdown adopted for DOC computation is the same used by (Repic, et al., 1973), as reported in Fig. 242.

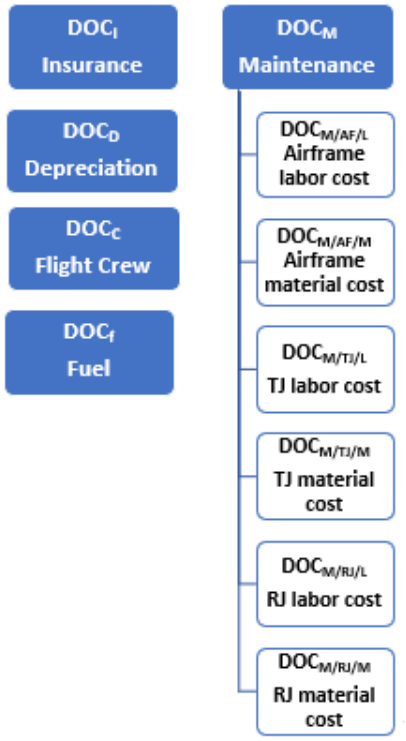

Fig. 242: DOC breakdown used within the proposed methodology

An important feature of the NASA-Modified ATA CERs is that fuel type does not explicitly appear in the equations. Thus, considering that fuel cost represents the biggest part of DOC for a hypersonic vehicle, a proper formulation of the fuel price has been derived and the related CERs updated. The fuel cost per flight is determined by multiplying the quantity of fuel used per flight by the fuel price per unit mass, taking into account the impact of fuel reserves. Introducing the following conversion factor from Cost per Flight to Cost per ton-mile the equation reported in (215) (in Imperial Units) can be obtained

$$\frac{Fuel\ Cost}{ton-mile} = \frac{2000 \cdot \mathrm{C_{f,lb}} \left(\frac{m_{\mathrm{fT}}}{m_{\mathrm{GTO}}}\right)(1-\mathrm{K_R})}{(\mathrm{LF})\left(\frac{m_{\mathrm{PL}}}{m_{\mathrm{GTO}}}\right)\mathrm{R_{T,m}}} \quad (215)$$

where all mass variables are in $[lb]$ and fuel price is in $\left[\frac{\$}{lb}\right]$. The fuel cost per ton-mile in SI units can be obtained from (215) exploiting the conversions reported in (216) and (217)

$$C_{f,lb} = C_f \cdot 0.453 \quad (216)$$

$$R_{T,m} = \frac{R_T}{1.852} \qquad (217)$$

where C_f is the fuel price per unit mass in [kg] and R_T is the range in [km]. Substituting the expressions of $C_{f,lb}$ and $R_{T,m}$ in (215), the following expression reported in (218) for $\mathrm{DOC_{Fuel}}$ in SI units $\left[\frac{\$}{ton-mile}\right]$ can be derived.

$$\mathrm{DOC_{Fuel}} = \frac{1677.78\ \mathrm{C_f}\left(\frac{m_{\mathrm{f}_T}}{m_{\mathrm{GTO}}}\right)(1-\mathrm{K_R})}{(\mathrm{LF})\left(\frac{\mathrm{m_{PL}}}{m_{\mathrm{GTO}}}\right)\mathrm{R_T}} \qquad (218)$$

The shape of (218) is similar to (193). However, apart from conversion and regression factors, other aspects have been taken into account. Firstly, the fuel reserve fraction has been further subdivided in order to take into account possible additional reserve fuel fraction for boil-off ($\mathrm{K_B}$). Moreover, the estimation of propellant cost per unit mass is based on a review of existing cost models which have been adapted to proper represent the operating scenario of STRATOFLY MR3 vehicle. Notably, liquid hydrogen cost is mainly affected by three aspects:

- Geographical context in which the LH2 is produced. There is a clear difference between USA and EU scenarios, mainly due to the cost of the energy. As stated in TRANSCOST (Koelle, 2012), the LH2 produced in Europe can be twice as expensive as in USA due to different costs of the electrical energy.
- Daily production rate. The amount of LH2 produced per day, is strongly affecting the LH2 costs and this is clearly stated in different references (Koelle, 2012), (IEA, 2006).
- Production process. In order to assess LH2 cost per kg to be used for a LH2 hypersonic vehicle operating costs estimation, it is important to notice that the final product cost is given by the sum of all the costs incurred during the phases of the production process. Indeed, LH2 production process is constituted by two steps:
  - the gaseous hydrogen extraction (in this case, the production by means of electrolysis has been considered);
  - the subsequent liquefaction.

Details concerning the complete model used for propellant price estimation is included in (Vercella, et al., 2018), and here omitted for conciseness. The results these estimations are reported in Table 62, where it is possible to understand the

impact of production scenario, area of production and impact of liquefaction cost on the overall price per unit mass. Currency is 2017 $.

Table 62: LH2 price assessment as function of production rate for both EU and USA facilities

		Europe			**USA**			
SCENARIO	ton/ day per plant	Elect. $/kg	Liq. $/kg	**Tot $/kg**	Elect. $/kg	Liq. $/kg	**Tot $/kg**	% Liq. Cost
Today Small Plant	2.29	9.83	2.75	**12.58**	5.20	1.38	**6.58**	100%
Today Large Plant	10	5.98	2.33	**8.32**	3.70	1.17	**4.86**	85%
Future Continuous	50	3.48	1.35	**4.83**	2.89	0.68	**3.57**	49%
Future Off-peak	200	2.18	0.92	**3.10**	2.31	0.46	**2.77**	33%

A qualitative chart depicting cost reduction trend as function of production rate is shown in Fig. 243, where data from (Koelle, 2012), labelled as "TC", and proposed estimations are reported. In order to compare the results, currency is expressed, in this case, as 2013 $.

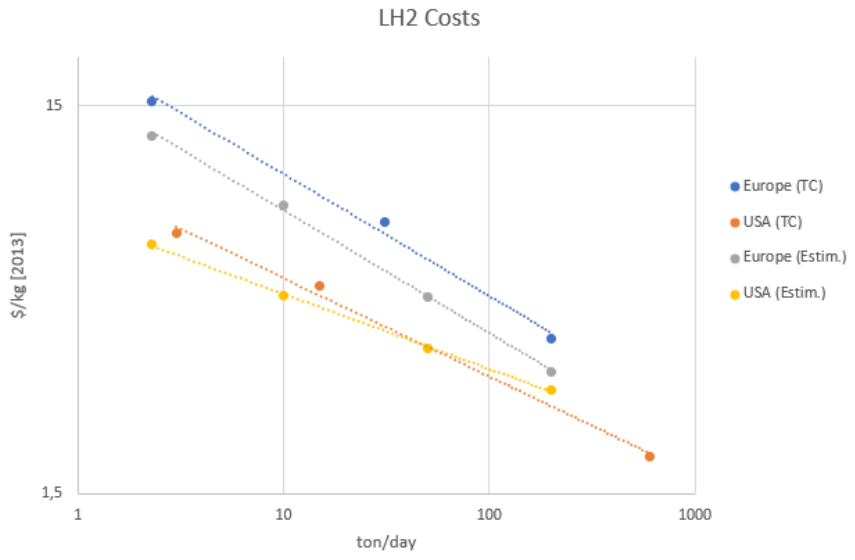

Fig. 243: Comparison of between TRANSCOST and proposed model for LH2 production

Moving to crew cost, it is assumed that an HST has a 2-members crew like large subsonic jets. Cabin crew costs are not included into DOC but are modelled within IOC as "Passenger Service Cost". The derived crew cost per ton-mile in SI units is expressed in (219), where the differences with (194) are due to the

increase of cruise altitude (which has an impact on block time and speed) to take into account future vehicle concepts.

$$\mathrm{DOC_C} = \frac{\frac{320}{m_{GTO}}}{0.63(\mathrm{LF})\left(\frac{\mathrm{m_{PL}}}{m_{GTO}}\right)\mathrm{M}\left(\frac{\mathrm{V_B}}{\mathrm{V_{CR}}}\right)} \qquad (219)$$

Insurance cost is given by the product of the annual insurance rate and the acquisition cost of the aircraft (obtaining an annual cost). The insurance cost per ton-mile in SI units is reported in (220).

$$\mathrm{DOC_I} = \frac{(\mathrm{IR})\left(\frac{\mathrm{C_{HST}}}{m_{\mathrm{GTO}}}\right)}{0.63(\mathrm{LF})\left(\frac{m_{\mathrm{PL}}}{m_{\mathrm{GTO}}}\right)\mathrm{M}\left(\frac{\mathrm{V_B}}{\mathrm{V_{CR}}}\right)\mathrm{U}} \qquad (220)$$

where differences with (195) are due to the application of the same correction of (219) concerning cruise altitude and C_{HST} is the acquisition cost of the aircraft in 2017 €.

With a similar approach, the CER for depreciation is derived starting from (Repic, et al., 1973), as reported in (221).

$$DOC_D = \frac{1.1\left(\frac{C_{HST}}{m_{GTO}}\right) + 0.3\left(\frac{C_{TJ}}{m_{GTO}} + \frac{C_{RJ}}{m_{GTO}}\right)}{0.63\ (\mathrm{LF})\left(\frac{\mathrm{m_{PL}}}{\mathrm{m_{GTO}}}\right)\mathrm{M}\left(\frac{\mathrm{V_B}}{\mathrm{V_{CR}}}\right)\mathrm{U}\,\mathrm{L_d}} \qquad (221)$$

Maintenance cost is derived, as stated by (Repic, et al., 1973), as sum of contributions associated to both labour and material cost for airframe, turbojet and ramjet maintenance tasks. Updated formulations considering DOC sub items are here reported. The term related to labour contribution to airframe maintenance is reported in (222).

$$\mathrm{DOC_{M/AF/L}} = \frac{(3.70 + 2.18\,\mathrm{t_f})\left[\frac{0.05}{1000}\left(\frac{\mathrm{m_{AF}}}{\mathrm{m_{GTO}}} + \frac{\mathrm{m_{AV}}}{\mathrm{m_{GTO}}}\right) + \left(\frac{3}{m_{GTO}} - \frac{315}{\left(\frac{2(m_{AF}+m_{AV})}{1000} + 120\right)m_{GTO}}\right)\right]\mathrm{M}^{\frac{1}{2}}(\mathrm{r_L})}{(\mathrm{LF})\left(\frac{m_{\mathrm{PL}}}{\mathrm{m_{GTO}}}\right)\frac{\mathrm{R_T}}{1000}} \qquad (222)$$

The formulation has been adapted to take into account updates to the ATA model concerning maintenance data and to use SI units. Differences with (196) are thus evident when looking at numerator and regression coefficients, even if the main CER architecture keeps its original meaning. Particularly, contribution of manhours per flight cycle is included along with manhour per flight hour.

Airframe material cost associated to maintenance was not subjected to substantial update apart from actualization. The CER reported in (223) is thus derived by applying conversion factors from imperial to SI units considering the actualized equation.

$$\mathrm{DOC_{M/AF/M}} = \frac{(5.22 \cdot \mathrm{t_f} + 10.57)\left(\frac{\mathrm{C_{HST}}}{\mathrm{m_{GTO}}} - \frac{\mathrm{C_{TJ}}}{\mathrm{m_{GTO}}} - \frac{\mathrm{C_{RJ}}}{\mathrm{m_{GTO}}}\right)}{(\mathrm{LF})\left(\frac{\mathrm{m_{PL}}}{\mathrm{m_{GTO}}}\right)\mathrm{R_T} \cdot 10^3} \quad (223)$$

Similar considerations apply also for turbojet and ramjet DOC maintenance sub-items as reported in (224 – 227)

$$\mathrm{DOC_{M/TJ/L}} = \frac{\left(\frac{\mathrm{T}}{\mathrm{W}}\right)_{\mathrm{GTO}}\left(1 + k'_{TJ} \cdot \mathrm{t_F}\right)\left(\frac{9.91}{\mathrm{T_{TJ}}/10^3} + 0.1\right)\mathrm{r_L}\,\mathrm{K_{LTJ}}}{(\mathrm{LF})\left(\frac{\mathrm{m_{PL}}}{\mathrm{m_{GTO}}}\right)\mathrm{R_T}} \quad (224)$$

$$\mathrm{DOC_{M/TJ/M}} = \frac{\left(\frac{\mathrm{C_{TJ}}}{\mathrm{m_{GTO}}}\right)\left(0.034 \cdot k'_{TJ} \cdot \mathrm{t_F} + 0.042\right)\mathrm{K_{MTJ}}}{(\mathrm{LF})\left(\frac{\mathrm{m_{PL}}}{\mathrm{m_{GTO}}}\right)\mathrm{R_T}} \quad (225)$$

$$\mathrm{DOC_{M/RJ/L}} = \frac{\left(1 + k'_{RJ} \cdot \mathrm{t_F}\right)\left(\frac{1.01\,\mathrm{N_{RJ}}\left(\frac{\mathrm{L}}{\mathrm{D}}\right)}{\mathrm{m_{GTO}}/\,10^3} + 0.1\right)\mathrm{r_L}\,\mathrm{K_{LRJ}}}{\left(\frac{\mathrm{L}}{\mathrm{D}}\right)(\mathrm{LF})\left(\frac{m_{\mathrm{PL}}}{\mathrm{m_{GTO}}}\right)\mathrm{R_T}} \quad (226)$$

$$\mathrm{DOC_{M/RJ/M}} = \frac{\left(\frac{\mathrm{C_{RJ}}}{\mathrm{m_{GTO}}}\right)\left(0.034 \cdot k'_{RJ} \cdot \mathrm{t_F} + 0.042\right)\mathrm{K_{MRJ}}}{(\mathrm{LF})\left(\frac{\mathrm{m_{PL}}}{\mathrm{m_{GTO}}}\right)\mathrm{R_T}} \quad (227)$$

where proper coefficients k'_{TJ} and k'_{RJ} are introduced to take into account time of operation of turbojet and ramjet engines during the reference mission. In this way, the model may support DOC estimation for coupled propulsion plant of advanced HST.

As final remark, it is interesting to evaluate the evolution of DOC with major operating parameters. As already discussed in Section 6.1, DOC items are

function of the usage of the fleet. As consequence, there is also a considerable relation with the so-called launch rate (or take-off rate), being defined as the number of flights per year. As a matter of fact, the overall DOC for a specific vehicle can be split as proposed in (228)

$$DOC = DOC_{fix} + DOC_{var} \quad (228)$$

where

DOC_{fix} is the part of DOC which is constant with Launch Rate (LR)
DOC_{var} is the part of DOC which varies with LR

Typically, fuel and crew cost does not vary with launch rate, whilst maintenance depreciation and insurance cost are usually function of the LR. (Koelle, 2012) proposed a power law to describe DOC reduction due to LR, as reported in (229)

$$CpF = K_T \cdot LR^{\alpha} \quad (229)$$

where

$K_T = 58.344$ is a constant factor derived from statistical analysis performed in (Koelle, 2012)

$\alpha = -0.341$ is the parameter which represents the evolution of the cost per flight (CpF) as function of LR, for the vehicle population reported in (Koelle, 2012)

This particular model was applied to LAPCAT vehicle series to adapt the coefficients of the power law, since several data concerning fleet size and business plan were available, especially for LAPCAT A2. The equation reported in (230) was thus derived

$$DOC_{LAPCAT} = K_{LAPCAT} \cdot LR^{\alpha} \quad (230)$$

where K_{LAPCAT} is a coefficient dedicated to LAPCAT case study. The resulting trend is depicted in Fig. 244, where 2006 € are used to match data..

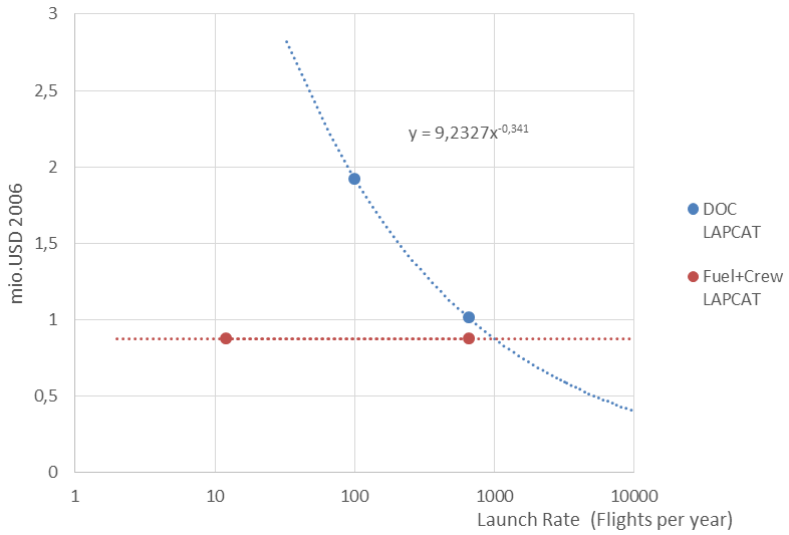

Fig. 244: Effect of launch rate on DOC for LAPCAT vehicle series

As it can be seen, very low LR cause a considerable escalation of overall DOC, whilst there is an optimum point, at medium-high LR, where variable DOC equals fixed DOC contribution. After this point, variable DOC become lower than fix DOC, even if the LR becomes unfeasible. It is thus possible, for every vehicle in service, to identify the optimum point where the two contribution to DOC equals each other. This can be selected as reference point for fleet planning purposes. The equation reported in (230) is used as reference within the proposed model.

IOC. As discussed in Section 6.1.2.2, the definition of a proper cost model for IOC is difficult since this kind of costs usually depends upon the organization of the airline which operates the vehicles. Table 58 of Section 6.1.2.2 provides a comparison between two reference IOC models suggested by (ICAO, 2017) and (Ferjan, 2013). The proposed model makes benefit of most promising equations proposed by these references, looking at the way they are derived, trying to identify the most suitable algorithms for HST application. The result of this selection process is reported in Table 63, where the list of applicable CERs is provided, together with the related reference.

Table 63: Selected IOC CERs

Cost Item	Formula	Source
General and Administrative	0.0072 $ per ASK	IATA
Reservation, Ticketing, Sales and Promotion	0.0076 $ per ASK	IATA
Station and Ground	0.0092 $ per ASK	IATA
Airport Charges and Air Navigation Charges	0.0083 $ per ASK	IATA
Passenger Service and Cabin Attendants	0.015 $ per RPM	ICAO
Aircraft Servicing Costs	800 $ per Flight	ICAO
Traffic Servicing Costs	15 $ per Enplaned Passenger	ICAO

In particular:

- General and Administrative costs shall be calculated following (Ferjan, 2013), considering that in (ICAO, 2017) this IOC item is included into Other Indirect and System Overhead Costs and expressed as a percentage of TOC, which is unknown. Analogous considerations apply to the item Station and Ground;
- Reservation, Ticketing, Sales and Promotion expenses shall be determined following (Ferjan, 2013). This formulation shall be preferred considering that, in (ICAO, 2017), this item is split into Advertising and Publicity and Reservations and Sales Costs. The former is presented as a percentage of TOC and the latter as a percentage of airline revenue, which could be unknown;
- Airport Charges and Air navigation charges shall be calculated according to (Ferjan, 2013), taking into account that (ICAO, 2017) does not provide specific guidelines for this IOC item;
- Passenger Service and Cabin Attendants cost can be calculated either following (Ferjan, 2013) or (ICAO, 2017). It has been verified that the two formulations provide similar results. In account of this, the (ICAO, 2017) CER has been finally selected considering that it is more recent with respect to (Ferjan, 2013);
- Aircraft and Traffic Servicing Costs shall be evaluated following (ICAO, 2017) because no specific data are available from (Ferjan, 2013).

6.3.4.2 Application of operating CERs to MR3 case study

DOC. The DOC model proposed in Section 6.3.4.1 is used to compute costs associated to operation of MR3 vehicle. The data included in are used together with general aircraft performance introduced in previous sections.

Table 64: Operating parameters used to evaluate MR3 DOC

Input	**Definition**	**Value**
M	Cruise Mach	8
RT	Operational Range, [km]	18700
RB	Block Distance, [km]	20000
tF	Flight Time, [h]	2.8
tB	Block Time, [h]	3.05
VB	Block Speed, [m/s]	1145.47
zcr	Cruise Altitude, [km]	25.4
Vcr	Cruise Speed, [m/s]	2360.56
L/D	Lift-to-drag Ratio	6.5
kTJ	TJ engine time of operation	20% of tF
kRJ	RJ engine time of operation	52% of tF

Times of operation for engines are selected considering that:

- The turbojet component is in operation for almost 20% of flight time;
- The ramjet component is in operation for almost 52% of flight time;
- during the remaining flight time there is engine switch off.

Table 65 shows the results of DOC evaluation (expressed in 2017 €) for the STRATOFLY MR3 vehicle. These results, for both EU and USA LH2 production scenarios, are graphically depicted in Fig. 245.

Table 65: DOC breakdown for MR3 vehicle

Cost Item	Cost, [€/flight], FY2017, LH2 produced in Europe	Cost, [€/flight], FY2017, LH2 produced in the USA
DOCF	626881	463347
DOCC	4849	4849
DOCI	10433	10433
DOCD	64088	64088
DOCM/AF/L	2856	2856
DOCM/AF/M	4488	4488
DOCM/TJ/L	1227	1227
DOCM/TJ/M	10191	10191
DOCM/RJ/L	1091	1091
DOCM/RJ/M	2044	2044
DOCM	21897	21897
Total DOC	**750045**	**586511**

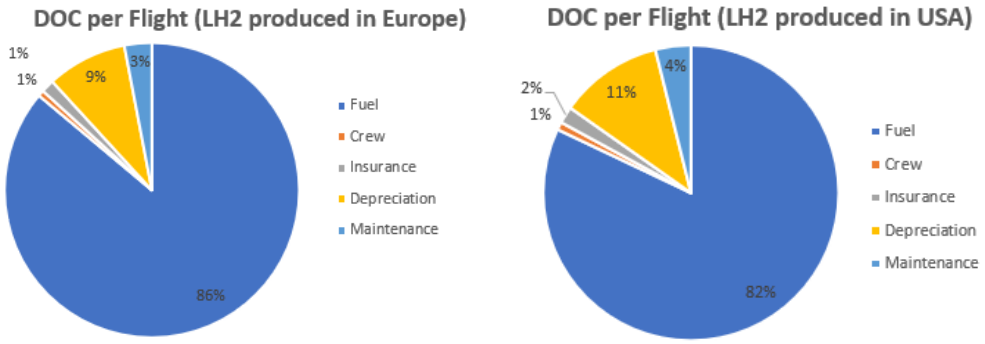

Fig. 245: DOC per flight for MR3 vehicle considering two LH2 production scenarios

As it can be seen, most of the DOC is allocated on propellant, and the difference between EU and USA production scenarios is non negligible. DOC are computed considering the optimum LR of about 657 flights per year.

IOC. Similarly to what already done for DOC, the proposed cost model for IOC is used to perform the estimation of indirect aspects on MR3 case study. The input reported in Table 66 are used as starting point of the analysis.

Table 66: Operating parameters used to evaluate MR3 IOC

Input	**Value**
Range	20000 km
Number of seats	300
LF	75%
Enplaned passengers per flight	225

Table 67 shows the results of the application of the IOC relationships for the MR3 vehicle. Results are furthermore graphically depicted in Fig. 246.

Table 67: IOC breakdown for MR3 vehicle

IOC Item	**Value, [€/Flight], FY2017**
Station and Ground	52088
Traffic Service	3185
Reservation and Sales	39578
Passenger Service	43029
General and Administrative	40764
Aircraft Servicing	755
Airport Charges and Air Navigation Charges	46992
Total	**226391**

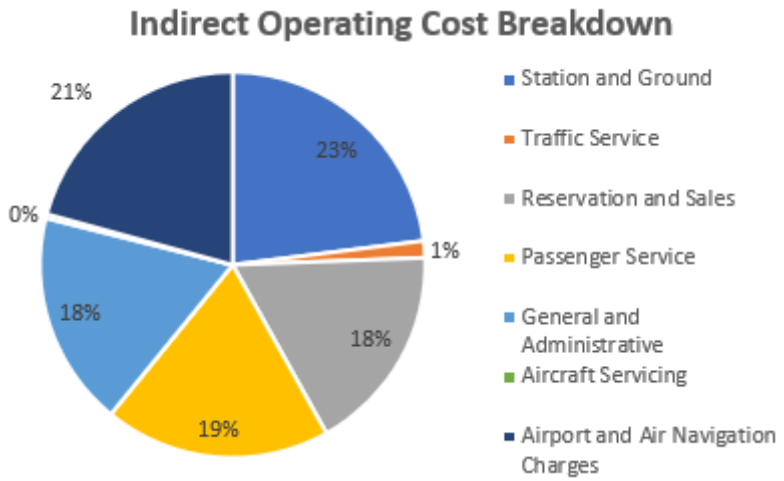

Fig. 246: IOC per flight for MR3 vehicle

As it can be seen, most of the items are balanced within the IOC breakdown, even if contributions of traffic service and aircraft service are negligible.

TOC. The resulting Total Operating Cost (TOC) for the STRATOFLY vehicle can be derived combining the results of DOC and IOC per flight. This is the actual value that can be used by airliners to establish ticket price and to plan routes and fleet management. The TOC is reported in Table 68, where results of previous analyses are used to account for DOC and IOC. Overall cost allocation is ultimately shown in Fig. 247.

Table 68: TOC breakdown for MR3 vehicle

OC Category	EU Scenario, [€/Flight], FY2017	US Scenario, [€/Flight], FY2017
DOC	750045	586511
IOC	226391	226391
Total	**976436**	**812902**

Independently from the LH2 production scenario, the cost per flight is around three times the typical cost faced by an airline to operate a long haul flight with a conventional aircraft. Most of the difference is due to the cost of propellant itself, which is an order of magnitude higher if compared to kerosene, looking at the results provided in Section 6.3.4.1.

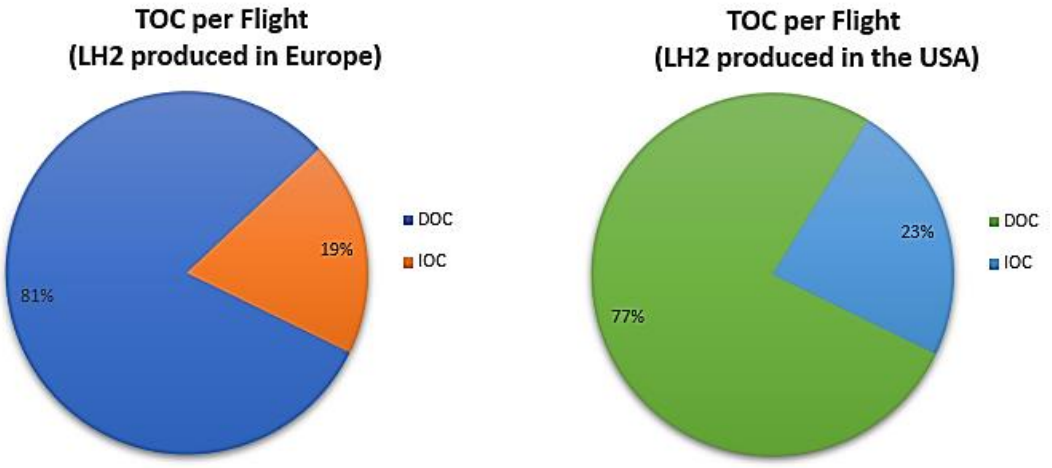

Fig. 247: TOC for MR3 vehicle considering both EU and US LH2 production scenarios

7

Conclusions and future perspectives

This Dissertation proposed a new methodology for conceptual and preliminary design of Hypersonic Transportation Systems (HST). The overall methodology has been presented and formalized through the Systems and Software Engineering Meta-model (SPEM), whilst the overall process has been applied to validate the conceptual design of the STRATOFLY MR3 hypersonic cruiser, as well as to the preliminary design of its Thermal and Energy Management Subsystem (TEMS).

In details, after an in-depth analysis of all high-speed aircraft developed or simply sketched during the history of aviation and space travels, special attention has been devoted the conceptual design process including mission statement analysis, functional and interface analyses, vehicle matching analysis as well as feasibility analysis. In particular, within the Dissertation, a few specific topics have been analysed in details, such as the formalization of the elicitation of mission objectives and requirements, the identification of proper high-level performance indexes, such as required Thrust-to-Weight ratio (T/W) and Wing Loading during the different flight phases, as well as the vehicle size assessment in terms of wing surface and internal available volume. In this context, the innovative Multiple Matching Chart (MMC) approach has been proposed to face the conceptual design of hypersonic vehicles, for which a conventional approach can be unsuitable to support the matching analysis. Moreover, an integrated

preliminary design methodology has been proposed, starting from the formalization of functional and interface analyses at subsystem level, and encompassing the development of ad-hoc parametric models to allow a physical characterization of each subsystem on the basis of their expected operating conditions. In accomplishing this task, special attention has been devoted to the development of estimation relationships for innovative and complex subsystems, such as the Thermal and Energy Management Subsystem, as well as to the estimation of design margins and reliability aspects. Ultimately, a preliminary Life Cycle Cost (LCC) assessment has been proposed and applied to the MR3 case study to provide a first estimation of the development, production and operating costs.

The main result shown within the Dissertation is, without any doubts, the successful definition and formalization of the conceived methodology for conceptual and preliminary design of HST. Moreover, the results of the application of the methodology to the STRATOFLY MR3 case study demonstrated that the updated configuration is still feasible with respect to the previous one, belonging to LAPCAT II Project, even if some of the requirements have to be traded. Particularly, the updated MR3 concept resulted not to be perfectly in line with the need of reaching the lift-over-drag ratio (L/D) of about 6.5 in hypersonic cruise (limited to 6.12) and the Thrust-to-Weight ratio (T/W) of 0.311 (limited to around 0.3) in hypersonic regime. The reduced L/D does not hamper the fulfilment of the prescribed range of about 18700 km. However, detailed analyses shall be performed to verify the possibility of modifying and/or updating the high-speed engine architecture to meet the T/W requirement in hypersonic regime. Moreover, additional vehicle characteristics (required), such as internal volume, planform and wing surface, respectively 8600 m^3, 2360 m^2 and 1117 m^2 have been derived, confirming requirements associated to the allocation of on-board subsystems and to the generation of proper lift at low speed. Re-formulation of mission profile may furthermore justify the need of taking into account 20 additional tons of liquid hydrogen, as propellant, to consider re-ignition of low-speed engines for approach and landing, with a total Maximum Take-Off Weight (MTOW) of about 420 tons. Moreover, cost assessment allowed identifying development, production and operating costs for the aforementioned aircraft, respectively around 24494 M€, 1470 M€ (first unit), 977 k€/flight. Results concerning the sizing of Thermal and Energy Management Subsystem (TEMS), obtained following the preliminary design process defined within the methodology, have been derived as well. The overall mass of the

subsystem was estimated around 6078 kg, with hypotheses on 25 – 50 % mass increase depending on the margin policy used. Redundancies have been proved to be also crucial to meet safety requirements, preventing catastrophic failures. The TEMS shall be capable of managing, together with the Thermal Protection Subsystem (TPS), peak surface temperatures of about 2000 K as well as average surface temperatures of 1000 K, and thermal flux of about 1 MW/m^2 in the most critical regions. A boil-off flow rate of about 5 – 10 kg/s is produced within LH2 tanks as result of the aerodynamic and internal heating, being sufficient for the vehicle cooling purposes (requiring 3.5 kg/s).

While the proposed methodology, for both conceptual and preliminary design stages, demonstrated to be generally applicable to several HST case studies, because of the way in which it has been conceived, in all its activities and tasks described within this Dissertation, the results obtained for the STRATOFLY MR3 vehicle shall be interpreted with caution. Current stage of proposed methods and models is in fact preliminary for this kind of high-speed applications, being based on assumptions and data that make benefit of past experience and statistical population which are considerably reduced, if compared to the conventional field of aeronautics. Numerical results are thus obtained looking at nominal design scenario, where deterministic rules allow deriving finite and specific aircraft and subsystems characteristics. A wider margin policy shall be applied to take into account fluctuations during the design stage in presence of uncertainties. The evolution of the technological level concerning the items which have been characterized during the work represents a further aspect potentially affecting the results, especially when dealing with performance and physical features of the considered products. Moreover, specific data belonging to domains like cost engineering and risk and reliability assessment are deeply influenced by non-negligible variations that are difficult to predict in early stages of design. Quantitative values shall then be considered as the outcomes of the first loop iteration of a wider development process of both the enabling technologies and their integration, required for this aircraft segment to exist. The envisaged timeframe for the entry-into-service of these vehicles introduces another tricky element to evaluate, since estimation of performance and physical characteristics may be overestimated considering today's knowledge. The proposed design process is in fact conceived to provide a basic model-set, coupling different aspects typically affecting high-level design, which can be further detailed or updated.

Main future works may deal with the development of new conceptual and preliminary design algorithms, specifically dedicated to the definition of advanced aircraft and/or power plant configurations, to the formalization of new methodologies for physical characterization both at aircraft and subsystem levels, as well as to the development of updated algorithms for cost and reliability estimation in presence of breakthrough technologies. The overall content of this Dissertation shall thus be considered as a mandatory step paving the way towards the development of updated methodologies for HST systems design, which is nowadays a challenging and equally fascinating engineering field, candidate to play a major role for the future of aviation.

8

Annexes

This chapter collects appendices and annexes referenced within the Dissertation chapters.

8.1 STRATOFLY Requirements Specification

8.1.1 Mission Requirements

Table 69: STRATOFLY Mission Requirements

Derived from	ID	Mission Requirements
PO1	MR_1000	The flight time of civil passenger flights over long haul and antipodal routes shall be shortened of at least one order of magnitude with respect to the current state-of-the-art for civil aviation.
PO2	MR_2000	The transportation system shall be able to transfer at least 300 civil passengers.
PO3	MR_3000	The transportation system shall be able to flight along long haul and antipodal routes.
PO4	MR_4000	The design of the transportation system shall be based on the refinement of the LAPCAT MR2.4 waverider configuration previously investigated in Europe.
PO5	MR_5000	The transportation system shall be able to reach at least Mach 8.
PO6	MR_6000	The transportation system shall be able to fly in the stratosphere.
PO7	MR_7000	The overall System of Systems shall be compatible with the future CNS/ ATM scenario.
PO8	MR_8000	The impact on existing on-ground infrastructures shall be minimized.
PO9	MR_9000	The economic viability of the solution shall be thoroughly assessed.
PO10	MR_10000	The compliance with environmental compatibility regulations shall be guaranteed.
PO11	MR_11000	The compliance with safety requirements shall be guaranteed.
PO12	MR_24000	Human factor issues shall be in depth analysed.
PO13	MR_25000	Flight Ticket cost shall be kept down.
PO14	MR_26000	Life Cycle Cost shall be kept down.

8.1.2 Programmatic Requirements

Table 70: STRATOFLY Programmatic Requirements

Derived From	ID	Programmatic Requirements
SO3	ProgR_1000	TRL 6 shall be reached by 2030-2035.
SO10	ProgR_2000	STRATOFLY project (The preliminary design of LAPCAT MR2.4 and its mission) shall be completed in 30 months.
SO10	ProgR_3000	The cost of STRATOFLY project shall not exceed 4 million euros.
SO1	ProgR_4000	STRATOFLY project shall aim at extending the European industrial leadership.
SO2	ProgR_5000	STRATOFLY project shall foster the development of breakthrough innovative technologies with TRL not higher than 3.
SO4	ProgR_6000	STRATOFLY project shall investigate and suggest breakthrough innovative concepts.
SO5	ProgR_7000	STRATOFLY project shall evaluate innovative airframe concepts.
SO6	ProgR_8000	STRATOFLY project shall investigate innovative propulsion concepts.
SO7	ProgR_9000	STRATOFLY project shall investigate innovative on-board systems and equipment.
SO8	ProgR_10000	STRATOFLY project shall tackle systems and subsystems integration issues envisaging innovative design methodologies.
SO9	ProgR_11000	STRATOFLY project shall foster the development of advanced numerical and experimental methods for concept validation purposes.
SO13	ProgR_12000	STRATOFLY project shall enhance the development and validation of enabling technologies for future reusable space transportation systems.
SO14	ProgR_13000	STRATOFLY project shall enhance the development and validation of innovative strategies for integrated logistic support to comply with civil aviation standard operations.
SO11	ProgR_14000	STRATOFLY project shall foster the dissemination of the results.
SO12	ProgR_15000	STRATOFLY project shall plan a broad exploitation of the results.

8.1.3 Configuration Requirements

Table 71: Mission level configuration requirement for STRATOFLY case study

Derived from	ID	Configuration Requirements @ Top Level
LAPCAT MR2.4	CR_ML1000	STRATOFLY System Of Systems consists of a Ground and a Flight Segment

Table 72: Segment level configuration requirements for STRATOFLY case study

Derived from	ID	Configuration Requirements @ Segment Level
LAPCAT MR2.4	CR_SegL1000	STRATOFGLY Ground Segment consists of at least two airports (with related infrastructures and personnel) and TBD Ground Stations
LAPCAT MR2.4	CR_SegL2000	STRATOFLY Flight Segment coincides with the hypersonic vehicle

Table 73: System level configuration requirements for STRATOFLY case study

Derived from	ID	Configuration Requirements @ System Level
LAPCAT MR2.4	CR_SysL1000	STRATOFLY vehicle consists of the following subsystems: - Structure - Wing - Fuselage - Empennages - Propulsion Subsystem - Propellant Subsystem - Hydraulic Subsystem - Auxiliary Power Unit - Flight Control Subsystem - Landing Gear - Environmental Control and Life Support Subsystem - Fire Protection Subsystem - Thermal Protection Subsystem - Thermal and Energy Management Subsystem - Electrical Power Subsystem
LAPCAT MR2.4	CR_SysL2000	STRATOFLY vehicle shall exploit a waverider configuration

LAPCAT MR2.4	CR_SysL3000	STRATOFLY vehicle shall be based on LAPCAT MR2.4 design
LAPCAT MR2.4	CR_SysL4000	The STRATOFLY vehicle shall be characterized by a cabin volume of at least 1400 m^3
LAPCAT MR2.4	CR_SysL5000	The STRATOFLY vehicle shall be characterized by a wingspan of 41 m
LAPCAT MR2.4	CR_SysL6000	The STRATOFLY vehicle shall be characterized by an overall length of 94 m
LAPCAT MR2.4	CR_SysL7000	The STRATOFLY vehicle shall be characterized by a MTOW of 400000 kg
Matching Analysis	CR_SysL8000	The STRATOFLY vehicle shall be characterized by a wing loading of about 358 $\frac{kg}{m^2}$
Matching Analysis	CR_SysL9000	The STRATOFLY vehicle shall be characterized by a wing surface of about 1117 m^2
Feasibility Analysis	CR_SysL10000	The STRATOFLY vehicle shall be characterized by a Kuchemann parameter of at least 0.09
Feasibility Analysis	CR_SysL11000	The STRATOFLY vehicle shall be able to host an internal volume of at least 8600 m^3
LAPCAT MR2.4	CR_SysL12000	The STRATOFLY vehicle shall be able to host an internal volume for propellant of at least 2900 m^3 in nominal conditions

Table 74: Subsystem level configuration requirements for STRATOFLY case study

Derived from	**ID**	**Configuration Requirements @ Subsystem Level**
LAPCAT MR2.4	CR_SubSys1000	The airframe (wing, fuselage, empennages) of STRATOFLY MR3 shall be based on the airframe of LAPCAT MR2.4 vehicle
LAPCAT MR2.4	CR_SubSys2000	The Propulsion subsystem of STRATOFLY MR3 shall be based on the Propulsion subsystem of LAPCAT MR2.4 vehicle
LAPCAT MR2.4	CR_SubSys3000	The Propellant subsystem of STRATOFLY MR3 shall be based on the Propellant subsystem of LAPCAT MR2.4 vehicle
LAPCAT MR2.4	CR_SubSys4000	The FCS of STRATOFLY MR3 shall be based on the FCS of LAPCAT MR2.4 vehicle
LAPCAT MR2.4	CR_SubSys5000	The Landing Gear of STRATOFLY MR3 shall be based on the Landing Gear of LAPCAT MR2.4 vehicle
LAPCAT MR2.4	CR_SubSys6000	The TPS of STRATOFLY MR3 shall be based on the TPS of LAPCAT MR2.4 vehicle

LAPCAT MR2.4	CR_SubSys7000	The TEMS of STRATOFLY MR3 shall be based on the TEMS LAPCAT MR2.4 vehicle

8.1.4 Functional Requirements

Table 75: Top and segment level functional requirements for STRATOFLY case study

ID	Functional Requirements @ Top Level
FR@SoSL_1000	The mission shall allow reducing flight time over long haul and antipodal routes for routine civil passengers service.
ID	**Functional Requirements @ Segment Level**
FR@SegL_1000	The Ground Segment shall provide vehicle support.
FR@SegL_2000	The Flight Segment shall enable high speed high altitude transportation.

Table 76: System level functional requirements for STRATOFLY case study

ID	Functional Requirements @ System Level
FR@SysL_1000	The airport infrastructures and personnel shall support on-ground operations.
FR@SysL_2000	The ground stations shall support in-flight operations from ground.
FR@SysL_3000	The vehicle shall transport civil passengers flying at hypersonic speed in the stratosphere.

Table 77: Subsystem level functional requirements for STRATOFLY case study

ID	Functional Requirements @ Subsystem Level
FR@SubSysL_1000	The vehicle structure shall withstand structural loads.
FR@SubSysL_2000	The wing shall generate lift over the whole flight envelope.
FR@SubSysL_3000	The wing shall maximize aerodynamic efficiency.
FR@SubSysL_4000	The wing shall guarantee safe emergency splashdown.
FR@SubSysL_5000	The fuselage shall accommodate civil passengers.
FR@SubSysL_6000	The fuselage shall accommodate crew members.
FR@SubSysL_7000	The fuselage shall host other on-board subsystems.
FR@SubSysL_8000	The fuselage shall provide sufficient arm for empennages.
FR@SubSysL_9000	The wing and empennages shall guarantee static stability.
FR@SubSysL_10000	The propulsion subsystem shall generate thrust allowing hypersonic flight.
FR@SubSysL_11000	The hydraulic subsystem shall provide hydraulic power.
FR@SubSysL_12000	The Thermal and Energy Management Subsystem (TEMS)

ID	Functional Requirements @ Subsystem Level
	shall provide electrical power.
FR@SubSysL_13000	The Auxiliary Power Unit (APU) shall provide auxiliary power.
FR@SubSysL_14000	The propellant subsystem shall manage propellant on board.
FR@SubSysL_15000	The Environmental Control and Life Support Subsystem (ECLSS) shall guarantee survivability of passengers.
FR@SubSysL_16000	The Flight Control Subsystem (FCS) shall control the vehicle.
FR@SubSysL_17000	The Landing Gear (LG) shall support the vehicle when on ground.
FR@SubSysL_17500	The Landing Gear (LG) shall guarantee a safe landing.
FR@SubSysL_19000	The Fire Protection Subsystem (FPS) shall guarantee fire protection.
FR@SubSysL_20000	The Thermal Protection Subsystem (TPS) shall guarantee thermal protection.
FR@SubSysL_21000	The Avionic Subsystem shall guarantee vehicle management capabilities.
FR@SubSysL_22000	The Thermal and Energy Management Subsystem (TEMS) shall provide thermal control.

Table 78: Assembly level functional requirements for TEMS subsystem

ID	Functional Requirements @ Assembly Level
FR@AL_1000	The heat collection assembly of TEMS shall provide heat collection capabilities.
FR@AL_2000	The heat transport assembly of TEMS shall provide heat transport capabilities.
FR@AL_3000	The heat rejection assembly of TEMS shall provide heat rejection capabilities.

Table 79: Equipment level functional requirements for different TEMS assemblies

ID	Functional Requirements @ Equipment Level
FR@EL_1000	LH2 tanks shall be able to collect heat coming from external skin.
FR@EL_2000	The cabin exchanger(s) shall be able to collect heat coming from

ID	Functional Requirements @ Equipment Level
	passenger cabin.
FR@EL_3000	The propulsion plant heat exchanger(s) shall be able to collect heat from propulsion plant.
FR@EL_4000	The ECS heat exchanger(s) shall be able to collect heat from the Air Pack.
FR@EL_5000	Tank pipes shall be able to transport heat from tanks to cabin collection equipment.
FR@EL_6000	Tank pipes shall be able to transport heat from tanks to high pressure transport equipment.
FR@EL_7000	Compressor pipes shall be able to transport heat from high pressure transport equipment to propulsion heat collection equipment.
FR@EL_8000	Cabin pipes shall be able to transport heat from cabin to high pressure transport equipment.
FR@EL_9000	Propulsion plant pipes shall be able to transport heat from Propulsion plant to boil-off collection equipment.
FR@EL_10000	Air Pack pipes shall be able to transport heat from ECS to boil-off collection equipment.
FR@EL_11000	The compressor pipe shall be able to transport heat from the compressor to the ECS.
FR@EL_12000	TEMS compressor shall be able to assure an adequate pressure level in heat transportation assembly.
FR@EL_13000	The boil-off expander shall be able to mix heated flow with liquid propellant.
FR@EL_14000	The boil-off fuel collector shall be able to inject heated flow and propellant in engine FCU.

8.1.5 Mission Concept Requirements

Table 80: Top level mission concept requirements for STRATOFLY case study

Derived from	ID	Mission concept requirements @ Top Level
Lifecycle analysis (UCD)	OP_ML1000	The STRATOFLY HST product shall have a lifecycle characterized by the following phases: - Conceptual design and development - Production - Operation - Disposal

Table 81: Segment level mission concept requirements for STRATOFLY case study

Derived from	ID	Mission concept requirements @ Segment Level
Use cases analysis (UCD)	OP_SegL1000	The Operations of STRATOFLY HST shall include the following phases: - Ground Phase - Flight Phase
Use cases analysis (UCD)	OP_SegL2000	The Ground Segment of STRATOFLY HST shall be involved in ground operations
Use cases analysis (UCD)	OP_SegL3000	The Ground Segment of STRATOFLY HST shall be involved in flight operations
Use cases analysis (UCD)	OP_SegL4000	The Flight Segment of STRATOFLY HST shall be involved in ground operations
Use cases analysis (UCD)	OP_SegL5000	The Flight Segment of STRATOFLY HST shall be involved in flight operations

Table 82: System level mission concept requirements for STRATOFLY case study

Derived from	ID	Mission concept requirements @ System Level
Use cases analysis (UCD)	OP_SysL1000	The Ground Operations of STRATOFLY vehicle shall include the following phases: - Parking - Gate holding - Taxi
Use cases analysis (UCD)	OP_SysL2000	The airport infrastructure shall be involved in parking operations
Use cases analysis (UCD)	OP_SysL3000	The airport infrastructure shall be involved in gate operations
Use cases analysis (UCD)	OP_SysL4000	The airport infrastructure shall be involved in taxi operations
Use cases analysis (UCD)	OP_SysL5000	The vehicle shall be involved in all ground operations
Timing analysis (SD)	OP_SysL6000	The vehicle shall be able to communicate with airport infrastructure to ask for gate while on parking

Timing analysis (SD)	OP_SysL7000	The vehicle shall wait until gate data is provided before proceeding to gate
Timing analysis (SD)	OP_SysL8000	The vehicle shall remain at gate no longer than 45 minutes
Timing analysis (SD)	OP_SysL9000	The vehicle shall be able to communicate with ground station to request mission data while on gate
Timing analysis (SD)	OP_SysL10000	The vehicle shall allow servicing while at gate
Timing analysis (SD)	OP_SysL11000	The vehicle shall allow refuelling while at gate
Timing analysis (SD)	OP_SysL12000	The vehicle shall allow passengers boarding while at gate
Timing analysis (SD)	OP_SysL13000	The vehicle shall be able to communicate with airport infrastructure to request push-back and engine start procedures
Timing analysis (SD)	OP_SysL14000	The vehicle shall be able to perform taxi-out phase in 15 minutes
Use cases analysis (UCD)	OP_SysL15000	The Flight Operations of STRATOFLY vehicle shall include the following phases: - Take-off - Subsonic Climb - Subsonic Cruise - Supersonic Climb - Supersonic Cruise - Hypersonic Climb - Hypersonic Cruise - Descent - Approach - Landing
Use cases analysis (UCD)	OP_SysL16000	The airport infrastructure shall be involved in take-off operations
Use cases analysis (UCD)	OP_SysL17000	The airport infrastructure shall be involved in landing operations
Use cases	OP_SysL18000	The ground stations shall be involved in climb

analysis (UCD)		(subsonic, supersonic, hypersonic) operations
Use cases analysis (UCD)	OP_SysL19000	The ground stations shall be involved in cruise (subsonic, supersonic, hypersonic) operations
Use cases analysis (UCD)	OP_SysL20000	The ground stations shall be involved in descent operations
Use cases analysis (UCD)	OP_SysL21000	The ground stations shall be involved in approach operations
Use cases analysis (UCD)	OP_SysL22000	The vehicle shall be involved in all flight operations
Timing analysis (SD)	OP_SysL23000	The vehicle shall be able to communicate with airport infrastructure to request take-off clearance
Timing analysis (SD)	OP_SysL24000	The vehicle shall complete the take-off phase in 5 minutes
Timing analysis (SD)	OP_SysL25000	The vehicle shall complete the second segment phase after take-off in 2 minutes
Timing analysis (SD)	OP_SysL26000	The vehicle shall complete the subsonic climb phase in 5 minutes
Timing analysis (SD)	OP_SysL27000	The vehicle shall be able to operate in subsonic regime at a cruise altitude of about 12000 m
Timing analysis (SD)	OP_SysL28000	The vehicle shall be able to operate in subsonic regime at Mach 0.8
Timing analysis (SD)	OP_SysL29000	The vehicle shall complete the subsonic cruise phase in 20 minutes
Timing analysis (SD)	OP_SysL30000	The vehicle shall complete the supersonic climb phase in 7 minutes
Timing analysis (SD)	OP_SysL31000	The vehicle shall be able to operate in supersonic regime at a cruise altitude of about 24000 m
Timing analysis	OP_SysL32000	The vehicle shall be able to operate in supersonic regime at Mach 4

(SD)		
Timing analysis (SD)	OP_SysL33000	The vehicle shall complete the supersonic cruise phase in 2 minutes
Timing analysis (SD)	OP_SysL34000	The vehicle shall complete the hypersonic climb phase in 10 minutes
Timing analysis (SD)	OP_SysL35000	The vehicle shall be able to start the DMR engine at Mach 4.5
Timing analysis (SD)	OP_SysL36000	The vehicle shall be able to switch-off ATR engine at Mach 4.5
Timing analysis (SD)	OP_SysL37000	The vehicle shall be able to operate in hypersonic regime at a cruise altitude of about 33000 m
Timing analysis (SD)	OP_SysL38000	The vehicle shall complete the supersonic cruise phase in 97 minutes
Timing analysis (SD)	OP_SysL39000	The vehicle shall complete the descent phase in 35 minutes
Timing analysis (SD)	OP_SysL40000	The vehicle shall be able to switch-off DMR engine in descent phase
Timing analysis (SD)	OP_SysL41000	The vehicle shall be able to re-start at least 1 ATR engine during approach in subsonic regime
Timing analysis (SD)	OP_SysL42000	The vehicle shall complete the approach phase in 5 minutes
Timing analysis (SD)	OP_SysL43000	The vehicle shall be able to communicate with airport infrastructure to request landing clearance
Timing analysis (SD)	OP_SysL44000	The vehicle shall complete the landing phase in 1 minute
Timing analysis (SD)	OP_SysL45000	The vehicle shall be able to communicate with ground station to request/provide mission data during the whole set of flight phases

8.1.6 Performance Requirements

Table 83: High-level performance requirements for STRATOFLY case study

Derived From	ID	High-Level Performance requirements
MR1000 / FR@ML_1000	Per_HL1000	The flight time of civil passengers flights over long haul and antipodal routes shall not exceed 4 hours
MR2000	Per_HL2000	The transportation system shall be able to transfer at least 300 civil passengers for a total mass of 33000 kg including 80 + 30 kg per passenger
MR2000	Per_HL3000	The vehicle shall be able to host a cabin with a volume of at least 1400 m3
MR3000	Per_HL4000	The transportation system shall be able to flight along long haul and antipodal routes with a range of at least 18700 km
MR3000	Per_HL12000	The vehicle shall be characterized by an aerodynamic efficiency of about 6.5 in hypersonic cruise
MR5000	Per_HL5000	The vehicle shall reach Mach 8 in hypersonic cruise
MR6000	Per_HL6000	The transportation system shall have a ceiling altitude of at least 33000 m
MR8000	Per_HL7000	The vehicle shall be able to perform take-off and landing from prepared runways having a total length of no more than 4 km
MR10000	Per_HL8000	The vehicle noise levels shall comply with the ICAO Annex 16 Vol. 1 Part II Chapter 4 requirements
MR11000	Per_HL9000	The transportation system shall meet the safety requirements expressed within the CS-25 regulation
MR10000	Per_HL10000	The vehicle shall fly at subsonic speed within an area of 400 km around the departure and arrival airports
MR24000	Per_HL11000	The vehicle shall guarantee in-flight axial acceleration levels of no more than 0.3 g

Table 84: System level performance requirements for STRATOFLY case study

Derived from	ID	System-Level Performance requirements
Matching Analysis	Per_SysL1000	The STRATOFLY vehicle shall be characterized by a thrust-to-weight ratio of about 0.732 in subsonic regime
Matching Analysis	Per_SysL2000	The STRATOFLY vehicle shall be characterized by a thrust-to-weight ratio of about 0.660 in supersonic regime
Matching Analysis	Per_SysL3000	The STRATOFLY vehicle shall be characterized by a thrust-to-weight ratio of about 0.312 in hypersonic regime

Table 85: Subsystem level performance requirements for STRATOFLY case study

Derived From	ID	Low-Level Performance requirements
FR@SubSysL_1000	Per_SubSys1100	The vehicle structure shall be able to withstand 2.5 load factor manoeuvre
FR@SubSysL_1000	Per_SubSys1200	The vehicle structure shall be able to withstand a 100kPa internal pressurization
FR@SubSysL_2000	Per_SubSys2100	The vehicle structure shall be able to withstand a lift distribution of 200 kg/m2 on the wing and of 130 kg/m2 on the body
FR@SubSysL_5000	Per_SubSys5100	The fuselage shall include 300 passengers seats for a total mass of 10500 kg (35 kg each)
FR@SubSysL_5000	Per_SubSys5200	The fuselage shall host passengers supplies for a total mass of 4500 kg (15 kg for each passenger)
FR@SubSysL_5000	Per_SubSys5300	The fuselage shall include galleys and toilets for a total mass of 2000 kg
FR@SubSysL_5000	Per_SubSys5400	The fuselage shall include 4 doors for passengers boarding and egression for a total mass

		of 2000 kg
FR@SubSysL_6000	Per_SubSys6100	The fuselage shall host the flight deck for a total mass of 2000 kg
FR@SubSysL_5000	Per_SubSys5500	The fuselage shall host the internal cabin structure for a total mass of 5000 kg
FR@SubSysL_6000	Per_SubSys6200	The fuselage shall host the flight crew (pilots and flight attendants) with a total mass of 1040 kg (80 kg each)
FR@SubSysL_12000	Per_SubSys12100	The TEMS shall be able to generate at least 50 MW for compressor operation
FR@SubSysL_12000	Per_SubSys12200	The TEMS shall be able to generate at least 10 MW for propellant subsystem operation
FR@SubSysL_12000	Per_SubSys12300	The TEMS shall be able to generate at least 50 MW of secondary power for other on-board subsystems
FR@SubSysL_14000	Per_SubSys14100	The propellant subsystem shall host 200000 kg of LH2
FR@SubSysL_14000	Per_SubSys14200	The propellant subsystem shall be able to feed the engines with a mass flow of at least $4.5\frac{m^3}{s}$
FR@SubSysL_14000	Per_SubSys14300	The propellant subsystem shall be able to provide a minimum volumetric flow of LH2 at a pressure of at least 61 bar when engines are operating
FR@SubSysL_14000	Per_SubSys14400	The propellant subsystem shall be able to provide a maximum volumetric flow of LH2 at a pressure of at least 75 bar when engines are operating
FR@SubSysL_15000	Per_SubSys15000	The ECLSS shall be able to provide 3.6 kg/s of fresh air at 298K and 75 kPa
FR@SubSysL_20000	Per_SubSys20100	The TPS shall be able to manage an average

		temperature of 1000 K on the vehicle pressure side of the forward fuselage
FR@SubSysL_20000	Per_SubSys20200	The TPS shall be able to manage an average temperature of 930 K on the vehicle pressure side of the wing
FR@SubSysL_20000	Per_SubSys20300	The TPS shall be able to manage an average temperature of 890 K on the vehicle pressure side of the centre fuselage
FR@SubSysL_20000	Per_SubSys20400	The TPS shall be able to manage an average temperature of 810 K on the vehicle pressure side of the aft fuselage
FR@SubSysL_20000	Per_SubSys20500	The TPS shall be able to manage a heat load of about 5 GJ on forward fuselage compartments
FR@SubSysL_20000	Per_SubSys20600	The TPS shall be able to manage a heat load of about 9.5 GJ on wing compartments
FR@SubSysL_20000	Per_SubSys20700	The TPS shall be able to manage a heat load of about 1.5 GJ on centre fuselage compartments
FR@SubSysL_20000	Per_SubSys20800	The TPS shall be able to manage a heat load of about 6.5 GJ on aft fuselage compartments
FR@SubSysL_20000	Per_SubSys20900	The TPS shall withstand an average heat flux of 30 kW/m2
FR@SubSysL_22000	Per_SubSys22100	The TEMS shall be able to provide a boil-off mass flow of about 3.5 kg/s all along the mission
FR@SubSysL_22000	Per_SubSys22200	The TEMS shall be able to provide an overall boil-off mass of about 52 tons during the mission

FR@SubSysL_22000	Per_SubSys22300	The TEMS shall be able to manage an incoming heat flow of about 30 $\frac{kW}{m^2}$ on forward fuselage compartments
FR@SubSysL_22000	Per_SubSys22400	The TEMS shall be able to manage an incoming heat flow of about 23 $\frac{kW}{m^2}$ on wing compartments
FR@SubSysL_22000	Per_SubSys22500	The TEMS shall be able to manage an incoming heat flow of about 16 $\frac{kW}{m^2}$ on centre fuselage compartments
FR@SubSysL_22000	Per_SubSys22600	The TEMS shall be able to manage an incoming heat flow of about 14 $\frac{kW}{m^2}$ on aft fuselage compartments

8.1.7 Interface Requirements

Table 86: Interface requirements at segment level for STRATOFLY case study

ID	Interface Requirements @ Segment Level
IR@SegL_1000	The Ground Segment shall be able to send data to the Flight Segment.
IR@SegL_2000	The Ground Segment shall be able to provide electrical power to Flight Segment.
IR@SegL_3000	The Ground Segment shall be able to provide propellant to the Flight Segment.
IR@SegL_4000	The Ground Segment shall be able to receive data from the Flight Segment.
IR@SegL_5000	The Ground Segment shall be able to retrieve propellant from Flight Segment.
IR@SegL_6000	The Flight Segment shall be able to provide data to the Ground Segment.
IR@SegL_7000	The Flight Segment shall be able to receive electrical power from Ground Segment.
IR@SegL_8000	The Flight Segment shall be able to receive propellant from the Ground Segment.
IR@SegL_9000	The Flight Segment shall be able to receive data from the Ground Segment.
IR@SegL_10000	The Flight Segment shall be able to discharge propellant to the

ID	Interface Requirements @ Segment Level
	Ground Segment.

Table 87: Interface requirements at system level for STRATOFLY case study

ID	Interface Requirements @ System Level
IR@SysL_1000	The Airport shall be able to provide electrical power to the STRATOFLY vehicle.
IR@SysL_2000	The Airport shall be able to provide propellant to the STRATOFLY vehicle.
IR@SysL_3000	The Airport shall be able to retrieve the propellant from the STRATOFLY vehicle.
IR@SysL_4000	The Ground Station shall be able to send data to the STRATOFLY vehicle.
IR@SysL_5000	The Ground Station shall be able to receive data from the STRATOFLY vehicle.
IR@SysL_6000	The STRATOFLY vehicle shall be able to send data to the Ground Station.
IR@SysL_7000	The STRATOFLY vehicle shall be able to discharge the propellant to the Airport.
IR@SysL_8000	The STRATOFLY vehicle shall be able to receive data from the Ground Station.
IR@SysL_9000	The STRATOFLY vehicle shall be able to receive electrical power from the Airport.
IR@SysL_10000	The STRATOFLY vehicle shall be able to receive propellant from the Airport.

Table 88: Interface requirements at subsystem level for STRATOFLY case study

ID	Interface Requirements @ Subsystem Level
IR@SubSysL_1000	The Structure shall provide physical support to the Wing.
IR@SubSysL_2000	The Structure shall provide physical support to the Fuselage.
IR@SubSysL_3000	The Structure shall provide physical support to the Empennages.
IR@SubSysL_4000	The Structure shall provide physical support to the Propulsion Subsystem.
IR@SubSysL_5000	The Structure shall provide physical support to the Hydraulic Subsystem.
IR@SubSysL_6000	The Structure shall provide physical support to the Auxiliary Power Unit.

ID	Interface Requirements @ Subsystem Level
IR@SubSysL_7000	The Structure shall provide physical support to the Propellant Subsystem.
IR@SubSysL_8000	The Structure shall provide physical support to the Flight Control Subsystem.
IR@SubSysL_9000	The Structure shall provide physical support to the Landing Gear.
IR@SubSysL_10000	The Structure shall provide physical support to the ECLSS.
IR@SubSysL_11000	The Structure shall provide physical support to the Fire Protection Subsystem.
IR@SubSysL_12000	The Structure shall provide physical support to the Avionic Subsystem.
IR@SubSysL_13000	The Structure shall provide physical support to the TEMS.
IR@SubSysL_14000	The Structure shall provide physical support to the Electrical Power Subsystem.
IR@SubSysL_15000	The Structure shall provide physical support to the Thermal Protection Subsystem.
IR@SubSysL_16000	The Wing shall be hosted on the Fuselage.
IR@SubSysL_17000	The Wing shall be physically supported by the Structure.
IR@SubSysL_18000	The Wing shall host the Propellant Subsystem.
IR@SubSysL_19000	The Wing shall host the Flight Control Subsystem.
IR@SubSysL_20000	The Wing shall host the Thermal Protection Subsystem.
IR@SubSysL_21000	The Wing shall host the TEMS.
IR@SubSysL_22000	The Wing shall provide heat to the Propellant Subsystem
IR@SubSysL_23000	The Fuselage shall be physically supported by the structure.
IR@SubSysL_24000	The Fuselage shall host the Wing.
IR@SubSysL_25000	The Fuselage shall host the Empennages.
IR@SubSysL_26000	The Fuselage shall host the Propulsion Subsystem.
IR@SubSysL_27000	The Fuselage shall host the Hydraulic Subsystem.
IR@SubSysL_28000	The Fuselage shall host the Auxiliary Power Unit.
IR@SubSysL_29000	The Fuselage shall host the Propellant Subsystem.
IR@SubSysL_30000	The Fuselage shall host the Landing Gear.
IR@SubSysL_31000	The Fuselage shall host the ECLSS.
IR@SubSysL_32000	The Fuselage shall host the Fire Protection Subsystem.
IR@SubSysL_33000	The Fuselage shall host the Thermal Protection Subsystem.
IR@SubSysL_34000	The Fuselage shall host the Avionic Subsystem.
IR@SubSysL_35000	The Fuselage shall host the TEMS.
IR@SubSysL_36000	The Fuselage shall host the Electrical Power Subsystem.
IR@SubSysL_37000	The Fuselage shall host the Flight Control Subsystem.

ID	Interface Requirements @ Subsystem Level
IR@SubSysL_38000	The Fuselage shall receive air from the ECLSS.
IR@SubSysL_39000	The Fuselage shall be able to provide heat to the TEMS.
IR@SubSysL_40000	The Fuselage shall be able to provide heat to the Propellant Subsystem.
IR@SubSysL_41000	The Fuselage shall be able to provide heat to the ECLSS.
IR@SubSysL_42000	The Fuselage shall be able to receive heat from the ECLSS.
IR@SubSysL_43000	The Empennages shall be physically supported by the Structure.
IR@SubSysL_44000	The Empennages shall be hosted on the Fuselage.
IR@SubSysL_45000	The Empennages shall host the Thermal Protection Subsystem.
IR@SubSysL_46000	The Empennages shall host the Flight Control Subsystem.
IR@SubSysL_47000	The Propulsion Subsystem shall be physically supported by the Structure.
IR@SubSysL_48000	The Propulsion Subsystem shall be hosted in the Fuselage.
IR@SubSysL_49000	The Propulsion Subsystem shall receive propellant from the Propellant Subsystem.
IR@SubSysL_50000	The Propulsion Subsystem shall be able to send data to the Avionic Subsystem.
IR@SubSysL_51000	The Propulsion Subsystem shall be able to receive data from the Avionic Subsystem.
IR@SubSysL_52000	The Propulsion Subsystem shall be able to receive boil-off from TEMS.
IR@SubSysL_52001	The Propulsion Subsystem shall be able to receive propellant from the TEMS.
IR@SubSysL_53000	The Propulsion Subsystem shall be mechanically interfaced with the Electrical Power Subsystem in order to transfer mechanical power.
IR@SubSysL_54000	The Propulsion Subsystem shall be able to provide heat to the TEMS.
IR@SubSysL_55000	The Propulsion Subsystem shall receive the heat rejected in the fuel mixture by the TEMS.
IR@SubSysL_55001	The Propulsion Subsystem shall be able to receive electrical power during ignition/re-ignition.
IR@SubSysL_56000	The Hydraulic Subsystem shall be physically supported by the structure.
IR@SubSysL_57000	The Hydraulic Subsystem shall be hosted on the Fuselage.
IR@SubSysL_58000	The APU shall be physically supported by the structure.
IR@SubSysL_59000	The APU shall be hosted on the Fuselage.
IR@SubSysL_60000	The APU shall be able to send data to the Avionic

ID	Interface Requirements @ Subsystem Level
	Subsystem.
IR@SubSysL_61000	The APU shall be able to receive data from the Avionic Subsystem.
IR@SubSysL_62000	The APU shall be mechanically interfaced with the Electrical Power Subsystem in order to transfer mechanical power.
IR@SubSysL_63000	The APU shall provide heat to the TEMS.
IR@SubSysL_64000	The APU shall receive propellant from the Propellant Subsystem.
IR@SubSysL_64001	The APU shall be able to receive electrical power during ignition.
IR@SubSysL_65000	The Propellant Subsystem shall be physically supported by the Structure.
IR@SubSysL_66000	The Propellant Subsystem shall be hosted on the Fuselage.
IR@SubSysL_67000	The Propellant Subsystem shall be hosted on the Wing.
IR@SubSysL_68000	The Propellant Subsystem shall be able to provide propellant to the Propulsion Subsystem.
IR@SubSysL_69000	The Propellant Subsystem shall be able to send propellant to the TEMS.
IR@SubSysL_70000	The Propellant Subsystem shall receive electrical power from the Electrical Power Subsystem.
IR@SubSysL_71000	The Propellant Subsystem shall receive propellant from the Airport.
IR@SubSysL_72000	The Propellant Subsystem shall be able to discharge propellant to the Airport.
IR@SubSysL_73000	The Propellant Subsystem shall be able to send data to the Avionic Subsystem.
IR@SubSysL_74000	The Propellant Subsystem shall be able to receive data from the Avionic Subsystem.
IR@SubSysL_75000	The Propellant Subsystem shall be able to receive heat from the Fuselage.
IR@SubSysL_75001	The Propellant Subsystem shall receive heat from the Wing.
IR@SubSysL_76000	The Propellant Subsystem shall provide propellant to the APU.
IR@SubSysL_76001	The Propellant Subsystem shall provide boil-off to the TEMS.
IR@SubSysL_77000	The Flight Control Subsystem shall be physically supported by the Structure.
IR@SubSysL_78000	The Flight Control Subsystem shall be hosted on the Wing.

ID	Interface Requirements @ Subsystem Level
IR@SubSysL_79000	The Flight Control Subsystem shall be hosted on the Empennages.
IR@SubSysL_80000	The Flight Control Subsystem shall be able to send data to the Avionic Subsystem.
IR@SubSysL_81000	The Flight Control Subsystem shall be able to receive data from the Avionic Subsystem.
IR@SubSysL_82000	The Flight Control Subsystem shall receive electrical power from the Electrical Power Subsystem.
IR@SubSysL_83000	The Landing Gear shall be physically supported by the Structure.
IR@SubSysL_84000	The Landing Gear shall be hosted in the Fuselage.
IR@SubSysL_85000	The Landing Gear shall be able to send data to the Avionic Subsystem.
IR@SubSysL_86000	The Landing Gear shall be able to receive data from the Avionic Subsystem.
IR@SubSysL_87000	The Landing Gear shall receive electrical power from the Electrical Power Subsystem.
IR@SubSysL_88000	The ECLSS shall be physically supported by the Structure.
IR@SubSysL_89000	The ECLSS shall be hosted in the Fuselage.
IR@SubSysL_90000	The ECLSS shall provide air to the Fuselage.
IR@SubSysL_91000	The ECLSS shall be able to send data to the Avionic Subsystem.
IR@SubSysL_92000	The ECLSS shall be able to receive data from the Avionic Subsystem.
IR@SubSysL_93000	The ECLSS shall receive electrical power from the Electrical Power Subsystem.
IR@SubSysL_94000	The ECLSS shall be able to provide heat to the TEMS.
IR@SubSysL_95000	The ECLSS shall be able to receive heat from the Fuselage.
IR@SubSysL_96000	The ECLSS shall be able to provide heat to the Fuselage.
IR@SubSysL_97000	The Fire Protection Subsystem shall be physically supported by the Structure.
IR@SubSysL_98000	The Fire Protection Subsystem shall be hosted on the Fuselage.
IR@SubSysL_99000	The Thermal Protection Subsystem shall be physically supported by the Structure.
IR@SubSysL_100000	The Thermal Protection Subsystem shall be hosted on the Fuselage.
IR@SubSysL_101000	The Thermal Protection Subsystem shall be hosted on the Wing.
IR@SubSysL_102000	The Thermal Protection Subsystem shall be hosted on the

ID	Interface Requirements @ Subsystem Level
	Empennages.
IR@SubSysL_103000	The Avionic Subsystem shall be hosted on the Fuselage.
IR@SubSysL_104000	The Avionic Subsystem shall be physically supported by the Structure.
IR@SubSysL_105000	The Avionic Subsystem shall be able to send data to the Propulsion Subsystem.
IR@SubSysL_106000	The Avionic Subsystem shall be able to receive data from the Propulsion Subsystem.
IR@SubSysL_107000	The Avionic Subsystem shall be able to send data to the Hydraulic Subsystem.
IR@SubSysL_108000	The Avionic Subsystem shall be able to receive data from the Hydraulic Subsystem.
IR@SubSysL_109000	The Avionic Subsystem shall be able to send data to the Auxiliary Power Unit.
IR@SubSysL_110000	The Avionic Subsystem shall be able to receive data from the Auxiliary Power Unit.
IR@SubSysL_111000	The Avionic Subsystem shall be able to send data to the Propellant Subsystem.
IR@SubSysL_112000	The Avionic Subsystem shall be able to receive data from the Propellant Subsystem.
IR@SubSysL_113000	The Avionic Subsystem shall be able to send data to the Flight Control Subsystem.
IR@SubSysL_114000	The Avionic Subsystem shall be able to receive data from the Flight Control Subsystem.
IR@SubSysL_115000	The Avionic Subsystem shall be able to send data to the Landing Gear.
IR@SubSysL_116000	The Avionic Subsystem shall be able to receive data from the Landing Gear.
IR@SubSysL_117000	The Avionic Subsystem shall be able to send data to the ECLSS.
IR@SubSysL_118000	The Avionic Subsystem shall be able to receive data from the ECLSS.
IR@SubSysL_119000	The Avionic Subsystem shall be able to send data to the TEMS.
IR@SubSysL_120000	The Avionic Subsystem shall be able to receive data from the TEMS.
IR@SubSysL_121000	The Avionic Subsystem shall be able to send data to the Electrical Power Subsystem.
IR@SubSysL_122000	The Avionic Subsystem shall be able to receive data from the Electrical Power Subsystem.
IR@SubSysL_123000	The Avionic Subsystem shall receive electrical power from the Electrical Power Subsystem.

ID	Interface Requirements @ Subsystem Level
IR@SubSysL_124000	The Avionic Subsystem shall be able to send data to the Ground Station Subsystem.
IR@SubSysL_125000	The Avionic Subsystem shall be able to receive data from the Ground Station Subsystem.
IR@SubSysL_126000	The Avionic Subsystem shall provide heat to the TEMS.
IR@SubSysL_127000	The TEMS shall be physically supported by the Structure.
IR@SubSysL_128000	The TEMS shall be hosted on the Fuselage.
IR@SubSysL_129000	The TEMS shall receive heat from the Fuselage.
IR@SubSysL_130000	The TEMS shall be hosted on the Wing.
IR@SubSysL_131000	The TEMS shall receive heat from the Propulsion Subsystem.
IR@SubSysL_132000	The TEMS shall reject heat in the fuel mixture of Propulsion Subsystem.
IR@SubSysL_133000	The TEMS shall provide boil-off to the Propulsion Subsystem.
IR@SubSysL_134000	The TEMS shall receive propellant from the Propellant Subsystem.
IR@SubSysL_134001	The TEMS shall receive boil-off from the Propellant Subsystem.
IR@SubSysL_135000	The TEMS shall receive heat from the ECLSS.
IR@SubSysL_136000	The TEMS shall be mechanically interfaced with the Electrical Power Subsystem in order to transfer mechanical power.
IR@SubSysL_137000	The TEMS shall be able to send data to the Avionic Subsystem.
IR@SubSysL_138000	The TEMS shall be able to receive data from the Avionic Subsystem.
IR@SubSysL_139000	The TEMS shall receive heat from the APU.
IR@SubSysL_140000	The TEMS shall receive heat from the Avionic Subsystem.
IR@SubSysL_141000	The TEMS shall receive heat from the Electrical Power Subsystem.
IR@SubSysL_142000	The TEMS shall be able to provide propellant to the Propulsion Subsystem.
IR@SubSysL_143000	The Electrical Power Subsystem shall be physically supported by the Structure.
IR@SubSysL_144000	The Electrical Power Subsystem shall be hosted on the Fuselage.
IR@SubSysL_145000	The Electrical Power Subsystem shall be interfaced with the APU to receive mechanical power.
IR@SubSysL_146000	The Electrical Power Subsystem shall provide electrical power to the APU for ignition.

ID	Interface Requirements @ Subsystem Level
IR@SubSysL_147000	The Electrical Power Subsystem shall be interfaced with the Propulsion Subsystem to receive mechanical power.
IR@SubSysL_148000	The Electrical Power Subsystem shall provide electrical power to the Propulsion Subsystem for ignition.
IR@SubSysL_149000	The Electrical Power Subsystem shall provide electrical power to the Propellant Subsystem.
IR@SubSysL_150000	The Electrical Power Subsystem shall provide electrical power to the Flight Control Subsystem.
IR@SubSysL_151000	The Electrical Power Subsystem shall provide electrical power to the Landing Gear.
IR@SubSysL_152000	The Electrical Power Subsystem shall provide electrical power to the ECLSS.
IR@SubSysL_153000	The Electrical Power Subsystem shall provide electrical power to the Avionic Subsystem.
IR@SubSysL_154000	The Electrical Power Subsystem shall be able to send data to the Avionic Subsystem.
IR@SubSysL_155000	The Electrical Power Subsystem shall be able to receive data from the Avionic Subsystem.
IR@SubSysL_156000	The Electrical Power Subsystem shall receive electrical power from Airport GPU.
IR@SubSysL_157000	The Electrical Power Subsystem shall be interfaced with the TEMS to receive mechanical power.
IR@SubSysL_158000	The Electrical Power Subsystem shall be able to provide heat to the TEMS.

Table 89: Assembly level interface requirements for TEMS subsystem

ID	Interface Requirements @ Assembly Level
IR@AL_1000	The Heat Collection Assembly of TEMS shall be hosted in the Fuselage.
IR@AL_2000	The Heat Collection Assembly of TEMS shall be hosted in the Wing.
IR@AL_3000	The Heat Collection Assembly of TEMS shall be physically supported by the Structure.
IR@AL_4000	The Heat Collection Assembly of TEMS shall receive propellant from the Propellant Subsystem.
IR@AL_5000	The Heat Collection Assembly of TEMS shall receive heat from the Propulsion Subsystem.
IR@AL_6000	The Heat Collection Assembly of TEMS shall receive heat from

ID	Interface Requirements @ Assembly Level
	the APU.
IR@AL_7000	The Heat Collection Assembly of TEMS shall receive heat from the ECLSS.
IR@AL_8000	The Heat Collection Assembly of TEMS shall receive heat from the Avionic Subsystem.
IR@AL_9000	The Heat Collection Assembly of TEMS shall receive heat from the Electrical Power Subsystem.
IR@AL_10000	The Heat Collection Assembly of TEMS shall receive heat from the Fuselage.
IR@AL_11000	The Heat Collection Assembly of TEMS shall provide boil-off to the Heat Transport Assembly.
IR@AL_12000	The Heat Collection Assembly of TEMS shall receive boil-off from the Heat Transport Assembly.
IR@AL_13000	The Heat Collection Assembly of TEMS shall provide propellant to the Heat Rejection Assembly.
IR@AL_14000	The Heat Collection Assembly of TEMS shall provide heat to the Heat Transport Assembly.
IR@AL_15000	The Heat Collection Assembly of TEMS shall provide heat to Heat Rejection Assembly.
IR@AL_16000	The Heat Transport Assembly of TEMS shall be physically supported by the Structure.
IR@AL_17000	The Heat Transport Assembly of TEMS shall be hosted in the Fuselage.
IR@AL_18000	The Heat Transport Assembly of TEMS shall be hosted in the Wing.
IR@AL_19000	The Heat Transport Assembly of TEMS shall receive boil-off from the Propellant Subsystem.
IR@AL_20000	The Heat Transport Assembly of TEMS shall be able to send data to the Avionic Subsystem.
IR@AL_21000	The Heat Transport Assembly of TEMS shall be able to receive data from the Avionic Subsystem.
IR@AL_22000	The Heat Transport Assembly of TEMS shall provide boil-off to the Heat Collection Assembly.
IR@AL_23000	The Heat Transport Assembly of TEMS shall receive boil-off from the Heat Collection Assembly.
IR@AL_24000	The Heat Transport Assembly of TEMS shall receive heat from the Heat Collection Assembly.
IR@AL_25000	The Heat Transport Assembly of TEMS shall provide boil-off to the Heat Rejection Assembly.
IR@AL_26000	The Heat Transport Assembly of TEMS shall provide heat to the

ID	Interface Requirements @ Assembly Level
	Heat Rejection Assembly.
IR@AL_27000	The Heat Rejection Assembly shall be physically supported by the Structure.
IR@AL_28000	The Heat Rejection Assembly shall be hosted in the Fuselage.
IR@AL_29000	The Heat Rejection Assembly shall be hosted in the Wing.
IR@AL_30000	The Heat Rejection Assembly shall provide boil-off to the Propulsion Subsystem.
IR@AL_31000	The Heat Rejection Assembly shall provide propellant to the Propulsion Subsystem.
IR@AL_32000	The Heat Rejection Assembly shall be able to send data to the Avionics Subsystem.
IR@AL_33000	The Heat Rejection Assembly shall be able to receive data from the Avionic Subsystem.
IR@AL_34000	The Heat Rejection Assembly of TEMS shall reject heat in the fuel mixture of Propulsion Subsystem.
IR@AL_35000	The Heat Rejection Assembly shall receive propellant from the Heat Collection Assembly.
IR@AL_36000	The Heat Rejection Assembly shall receive boil-off from the Heat Transport Assembly.
IR@AL_37000	The Heat Rejection Assembly of TEMS shall receive heat from the Heat Transport Assembly.
IR@AL_38000	The Heat Rejection Assembly of TEMS shall receive heat from Heat Collection Assembly.
IR@AL_39000	The Heat Rejection Assembly of TEMS shall be interfaced with the EPS in order to transfer mechanical power.

Table 90: Equipment level interface requirements for different TEMS assemblies

ID	Interface Requirements @ Equipment Level
IR@EL_1000	The Cabin Exchanger shall provide boil-off to the Tank pipe.
IR@EL_2000	The Cabin Exchanger shall receive boil-off from the Cabin pipe.
IR@EL_3000	The Cabin Exchanger shall spread heat through the Cabin pipe.
IR@EL_4000	The Cabin Exchanger shall receive heat from the Fuselage.
IR@EL_5000	The Cabin Exchanger shall receive heat from the Avionic Subsystem.
IR@EL_6000	The Cabin Exchanger shall receive heat from the Electrical Power Subsystem.
IR@EL_6001	The Cabin Exchanger shall be physically supported by Structure

ID	Interface Requirements @ Equipment Level
	Equipment.
IR@EL_7000	The Propulsion Plant Liquid Exchanger shall provide fuel to the Expander.
IR@EL_8000	The Propulsion Plant Liquid Exchanger shall receive fuel from the Pump (delivery) pipe.
IR@EL_9000	The Propulsion Plant Liquid Exchanger shall provide heat to the Expander.
IR@EL_10000	The Propulsion Plant Liquid Exchanger shall receive heat from the APU.
IR@EL_11000	The Propulsion Plant Liquid Exchanger shall receive heat from the Propulsion Subsystem.
IR@EL_11001	The Propulsion Plant Liquid Exchanger shall be physically supported by Structure Equipment.
IR@EL_12000	The Propulsion Plant Vapour Exchanger shall provide boil-off to the Rejection pipe.
IR@EL_13000	The Propulsion Plant Vapour Exchanger shall receive boil-off from Compressor pipe.
IR@EL_14000	The Propulsion Plant Vapour Exchanger shall spread heat through the Rejection pipe.
IR@EL_15000	The Propulsion Plant Vapour Exchanger shall receive heat from the Propulsion Plant.
IR@EL_16000	The Air Pack Exchanger shall provide boil-off to the Rejection Pipe.
IR@EL_17000	The Air Pack Exchanger shall receive boil-off from the Compressor Pipe.
IR@EL_18000	The Air Pack Exchanger shall spread heat through the Boil-Off Collector.
IR@EL_19000	The Air Pack Exchanger shall receive heat from the ECLSS.
IR@EL_19001	The Air Pack Exchanger shall be physically supported by Structure Equipment.
IR@EL_20000	The Tank pipe shall provide boil-off to the Cabin Exchanger.
IR@EL_21000	The Tank pipe shall provide boil-off to the Compressor.
IR@EL_22000	The Tank pipe shall receive boil-off from the Propellant Subsystem.
IR@EL_23000	The Cabin pipe shall spread heat through the Compressor.
IR@EL_24000	The Cabin pipe shall receive heat from the Cabin Exchanger.
IR@EL_25000	The Cabin pipe shall receive boil-off from the Cabin Exchanger.
IR@EL_26000	The Compressor shall provide boil-off to the Compressor pipe.
IR@EL_27000	The Compressor shall receive boil-off from the Tank pipe.
IR@EL_28000	The Compressor shall spread heat through the Propulsion pipe.

ID	Interface Requirements @ Equipment Level
IR@EL_29000	The Compressor shall spread heat through the Compressor pipe.
IR@EL_30000	The Compressor shall receive heat from the Cabin pipe.
IR@EL_31000	The Propulsion Plant pipe shall provide boil-off to the Boil-Off Collector.
IR@EL_32000	The Propulsion Plant pipe shall receive boil-off from the Propulsion Plant Vapour Exchanger.
IR@EL_33000	The Propulsion Plant pipe shall spread heat through the Boil-Off Collector.
IR@EL_34000	The Propulsion Plant pipe shall receive heat from the Compressor.
IR@EL_35000	The Compressor pipe shall provide boil-off to the Propulsion Plant Vapour Exchanger.
IR@EL_36000	The Compressor pipe shall receive boil-off from the Compressor.
IR@EL_37000	The Compressor pipe shall spread heat through the Air Pack pipe.
IR@EL_38000	The Compressor pipe shall receive heat from the Compressor.
IR@EL_39000	The Air Pack pipe shall provide boil-off to the Boil-Off Collector.
IR@EL_40000	The Air Pack pipe shall receive boil-off from the Air Pack Exchanger.
IR@EL_41000	The Air Pack pipe shall spread heat through the Boil-Off Collector.
IR@EL_42000	The Air Pack pipe shall receive heat from the Compressor pipe.
IR@EL_43000	The Boil-Off Expander shall provide fuel to the Boil-Off Collector.
IR@EL_44000	The Boil-Off Expander shall receive fuel from the Propulsion Plant Liquid Exchanger.
IR@EL_45000	The Boil-Off Expander shall provide mechanical power to the Electrical Power Subsystem.
IR@EL_46000	The Boil-Off Expander shall spread heat through the Boil-Off Collector.
IR@EL_47000	The Boil-Off Expander shall receive heat from the Propulsion Plant Liquid Exchanger.
IR@EL_48000	The Boil-Off Collector shall provide fuel to the Propulsion Plant.
IR@EL_49000	The Boil-Off Collector shall receive fuel from the Boil-Off Expander.
IR@EL_50000	The Boil-Off Collector shall provide boil-off to the Propulsion Subsystem.
IR@EL_51000	The Boil-Off Collector shall receive boil-off from the Propulsion pipe.

ID	Interface Requirements @ Equipment Level
IR@EL_52000	The Boil-Off Collector shall receive boil-off from the Air Pack pipe.
IR@EL_53000	The Boil-Off Collector shall spread heat through the Propulsion Subsystem.
IR@EL_54000	The Boil-Off Collector shall receive heat from the Propulsion Plant Liquid Exchanger.
IR@EL_55000	The Boil-Off Collector shall receive heat from the Air Pack pipe.
IR@EL_56000	The Boil-Off Collector shall receive heat from the Boil-Off Expander.

8.1.8 Safety Requirements

Table 91: Subsystem level safety requirements for the thermal control case study

ID	Safety requirements @ Subsystem Level
SASub1000	The probability of total loss of thermal control capability shall be less than $1 \cdot 10^{-9} \frac{failures}{FH}$

Table 92: Assembly level safety requirements for thermal control case study

ID	Safety requirements @ Assembly Level
SAAsy1000	The probability of total loss of heat collection capability shall be less than $3{,}3 \cdot 10^{-10} \frac{failures}{FH}$
SAAsy2000	The probability of total loss of heat transport capability shall be less than $3{,}3 \cdot 10^{-10} \frac{failures}{FH}$
SAAsy3000	The probability of total loss of heat rejection capability shall be less than $3{,}3 \cdot 10^{-10} \frac{failures}{FH}$

Table 93: Equipment level safety requirements for thermal control case study

ID	Safety requirements @ Equipment Level
SAEq1000	The probability of total loss of heat collection capability from external skin shall be less than $1{,}9 \cdot 10^{-3} \frac{failures}{FH}$
SAEq2000	The probability of total loss of heat collection capability from cabin shall be less than $9{,}5 \cdot 10^{-3} \frac{failures}{FH}$
SAEq3000	The probability of total loss of heat collection capability from propulsion plant shall be less than $1{,}9 \cdot 10^{-3} \frac{failures}{FH}$
SAEq4000	The probability of total loss of heat collection capability from ECS shall be less than $9{,}5 \cdot 10^{-3} \frac{failures}{FH}$
SAEq5000	The probability of total loss of heat transport capability from tanks to cabin collection equipment shall be less than $4{,}2 \cdot 10^{-2} \frac{failures}{FH}$
SAEq6000	The probability of total loss of heat transport capability from tanks to high pressure transport equipment shall be less than $4{,}2 \cdot 10^{-2} \frac{failures}{FH}$
SAEq7000	The probability of total loss of heat transport capability from high pressure transport equipment to propulsion heat collection shall be less than $4{,}2 \cdot 10^{-2} \frac{failures}{FH}$
SAEq8000	The probability of total loss of heat transport capability from cabin to high pressure transport equipment shall be less than $4{,}2 \cdot 10^{-2} \frac{failures}{FH}$
SAEq9000	The probability of total loss of heat transport capability from propulsion plant to boil-off collection equipment shall be less than $4{,}2 \cdot 10^{-2} \frac{failures}{FH}$
SAEq10000	The probability of total loss of heat transport capability from ECS to boil-off collection equipment shall be less than $4{,}2 \cdot 10^{-2} \frac{failures}{FH}$
SAEq11000	The probability of total loss of heat transport capability from compressor to ECS shall be less than $4{,}2 \cdot 10^{-2} \frac{failures}{FH}$
SAEq12000	The probability of total loss of pressure generation capability in heat transportation assembly shall be less than $1{,}1 \cdot 10^{-10} \frac{failures}{FH}$
SAEq13000	The probability of total loss of heat rejection capability associated to heated flow mixing with propellant shall be less than $1{,}1 \cdot 10^{-10} \frac{failures}{FH}$

SAEq14000	The probability of total loss of heat rejection capability through injection of propellant in FCU shall be less than $2{,}2 \cdot 10^{-10} \frac{failures}{FH}$

8.1.9 Reliability Requirements

Table 94: Subsystem level reliability requirements for TEMS case study

ID	Reliability requirements @ Subsystem Level
RRSub1000	The TEMS shall have a failure rate lower than $4{,}1 \cdot 10^{-10} \frac{failures}{FH}$

Table 95: Assembly level reliability requirements for TEMS case study

ID	Reliability requirements @ Assembly Level
RRAsy1000	The TEMS heat collection assembly shall have a failure rate lower than $5{,}7 \cdot 10^{-20} \frac{failures}{FH}$
RRAsy2000	The TEMS heat transport assembly shall have a failure rate lower than $1 \cdot 10^{-10} \frac{failures}{FH}$
RRAsy3000	The TEMS heat rejection assembly shall have a failure rate lower than $3{,}1 \cdot 10^{-10} \frac{failures}{FH}$

Table 96: Equipment level reliability requirements for different TEMS assemblies

ID	Reliability requirements @ Equipment Level
RREq1000	The LH2 tanks shall have a failure rate lower than $6{,}9 \cdot 10^{-5} \frac{failures}{FH}$
RREq2000	The air pack exchanger shall have a failure rate lower than $9{,}4 \cdot 10^{-6} \frac{failures}{FH}$
RREq3000	The cabin exchanger shall have a failure rate lower than $9{,}4 \cdot 10^{-6} \frac{failures}{FH}$

RREq4000	The propulsion plant liquid exchanger shall have a failure rate lower than $9{,}4 \cdot 10^{-6}\ \frac{failures}{FH}$
RREq5000	The tank pipe shall have a failure rate lower than $3 \cdot 10^{-10}\ \frac{failures}{FH}$
RREq6000	The cabin pipe shall have a failure rate lower than $3 \cdot 10^{-10}\ \frac{failures}{FH}$
RREq7000	The propulsion plant pipe shall have a failure rate lower than $3 \cdot 10^{-10}\ \frac{failures}{FH}$
RREq8000	The air pack pipe shall have a failure rate lower than $3 \cdot 10^{-10}\ \frac{failures}{FH}$
RREq9000	The compressor pipe shall have a failure rate lower than $3 \cdot 10^{-10}\ \frac{failures}{FH}$
RREq10000	The TEMS compressor shall have a failure rate lower than $1 \cdot 10^{-5}\ \frac{failures}{FH}$
RREq11000	The boil-off expander shall have a failure rate lower than $1{,}7 \cdot 10^{-5}\ \frac{failures}{FH}$
RREq12000	The boil-off fuel collector shall have a failure rate lower than $1 \cdot 10^{-11}\ \frac{failures}{FH}$

8.1.10 Margin Requirements

Table 97: Margin requirements for STRATOFLY MR3 vehicle

ID	Margin requirements
RMar1000	Total dry mass of the vehicle at take-off shall include 20% margin of the nominal computed dry mass (already including considerations coming from RMar2000 and RMar4000)
RMar2000	Total mass of equipment shall be computed considering ECSS low-level margin philosophy (ESA, 2012)
RMar3000	Total mass of harness shall be computed considering 5% margin of the nominal harness mass
RMar4000	TEMS subsystem and equipment mass shall be computed considering uncertainties policy specified by (ESA, 2012)
RMar5000	Total tanks volume shall be designed to consider 10% margin of the volume required to host the total propellant mass.

8.2 Roskam cost model for aeronautical application (Roskam, 1990)

8.2.1 Aircraft development cost estimation

The aircraft development cost model proposed by (Roskam, 1990) includes the following cost items, as indicated in Section 6.1.2.1 (163):

- C_{aed} airframe engineering and design cost;
- C_{dst} development support and testing cost;
- C_{fta} flight test airplane cost;
- C_{fto} flight test operations cost;
- C_{tsf} test and simulation facilities cost;
- C_{pro} profit margin;
- C_{fin} RDTE financing cost.

Particularly, the first one is associated to airframe engineering and design cost, defined by the CER reported in (231).

$$C_{aed} = MHR_{aed} \cdot R_e \qquad (231)$$

Where

$$MHR_{aed} = 0.0396 \cdot W_{ampr}^{0.791} \cdot V_{Max}^{1.526} \cdot N_{rdte}^{0.183} \cdot F_{diff} \cdot F_{cad} \qquad (232)$$

are the total engineering manhours required to complete conceptual, preliminary and detailed design, considering that

$$W_{ampr} = 1.25 \cdot 10^{(0.1936+0.8645 \cdot \log_{10}(MTOW))} \qquad (233)$$

is the mass (in kg) associated to the Aeronautical Manufacturers Planning Report, and

V_{Max} is the design speed in $[kt]$
N_{rdte} is the number of airplanes built in RDTE phase
F_{diff} is a judgment factor to take into account program difficulty
F_{cad} is a judgment factor to take into account company experience with CAD
R_e is the engineering manhour rate in $\left[\frac{\$}{h}\right]$

The second cost item for RDTE cost determination is associated to development support and testing, as specified in (234).

$$C_{dst} = 0.008325 \cdot W_{ampr}^{0.873} \cdot V_{Max}^{1.89} \cdot N_{rdte}^{0.346} \cdot F_{diff} \qquad (234)$$

Moreover, flight test airplanes cost is considered in (235)

$$C_{fta} = C_{ea} + C_{man_r} + C_{mat} + C_{tool} + C_{qc} \qquad (235)$$

where

$$C_{ea} = (N_{rdte} - N_{st}) \cdot (C_e \cdot N_e + C_{avionic}) \qquad (236)$$

is the cost associated to avionics and engines acquisition,

$$C_{man_r} = MHR_{man} \cdot R_m \qquad (237)$$

is the production cost for test vehicle, expressed similarly to (232), but with different manhours rates and coefficients (Roskam, 1985),

$$C_{mat} = 37.632 \cdot F_{mat} \cdot W_{ampr}^{0.689} \cdot V_{Max}^{0.624} \cdot N_{rdte}^{0.792} \qquad (238)$$

is the material cost for the flight test vehicle,

$$C_{tool} = MHR_{tool} \cdot R_t \qquad (239)$$

is the tooling cost for test vehicle, expressed similarly to (232), but with different manhours rates and coefficients (Roskam, 1985), and

$$C_{qc} = 0.13 \cdot C_{man} \qquad (240)$$

is the quality control cost for flight test aircraft, considering that

N_{st} is the number of airframes built for static tests
C_e is the engine unit cost in [$]
N_e is the number of engines per aircraft
$C_{avionic}$ is the avionic system cost in [$]
MHR_{man} is the amount of manufacturing manhours
R_{man} is the manufacturing manhour rate in $\left[\frac{\$}{h}\right]$
F_{mat} is a judgement factor to account for differing materials cost
MHR_{tool} is the amount of manhours for tooling

R_t is the tooling manhour rate in $\left[\frac{\$}{h}\right]$

The flight test operations cost is included within C_{rdte} as fourth item. Even if this is related to operations, it is included within RDTE estimation since it is a direct consequence of the use of a test vehicle within the development activities. It is defined as in (241).

$$C_{fto} = 0.001244 \cdot W_{ampr}^{1.16} \cdot V_{Max}^{1.371} \cdot (N_{rdte} - N_{st})^{1.281} \cdot F_{diff} \cdot F_{obs} \qquad (241)$$

where

F_{obs} is a judgement factor accounting for the number of observables characteristics during flight test.

The fifth cost item is associated to test and simulation facilities as indicated in (242)

$$C_{tsf} = F_{tsf} \cdot C_{rdte} \qquad (242)$$

where

F_{tsf} is a judgement factor to account for number and complexity of simulation facilities required.

This item is basically a percentage of total RDTE cost, so the procedure shall be iterated to obtain a final converged value. Ultimately, a profit margin C_{pro} and an extra cost due to RDTE phase financing are included to obtain the final development cost value, as sixth and seventh cost items. They are defined similarly to (242) with different judgement factors.

8.2.2 Aircraft production cost estimation

The aircraft production cost model proposed by (Roskam, 1990) includes the following cost items, as indicated in Section 6.1.2.1 (164):

- C_{aed_m} airframe engineering and design cost in early production phase;
- C_{apc} airplane production cost;
- C_{fto} flight test operations cost during production;
- C_{fin_m} financing cost for production phase.

The first item represents the cost associated to airframe engineering and design in early production phase as in (243)

$$C_{aed_m} = MHR_{aed_m} \cdot R_{e_m} \quad (243)$$

where

$$MHR_{aed_m} = \left(0.0396 \cdot W_{ampr}^{0.791} \cdot V_{Max}^{1.526} \cdot N_m^{0.183} \cdot F_{diff} \cdot F_{cad}\right) - MHR_{aed} \quad (244)$$

is the amount of manhours spent for production (obtained as the total program manhours minus those allocated on development stage)

and

$N_{program}$ is the total number of vehicles built (prototypes + serie aircraft)
R_{e_m} is the mahours rate in the manufacturing phase in $\left[\frac{\$}{h}\right]$
The second item of (164) is related to airplane production cost, which is dependent on the category of the selected aircraft). It is defined as in (245)

$$C_{apc_m} = C_{e+a} + C_{int} + C_{man_m} + C_{mat_m} + C_{tool_m} + C_{qc_m} \quad (245)$$

where

$$C_{e+a} = \left(C_{e_m} N_e + C_{p_m} N_p + C_{avionic_m}\right) N_m \quad (246)$$

is the cost associated to engines and avionic equipment as paid to vendors,

$$C_{int} = F_{int} \cdot N_{pax} \cdot N_m \quad (247)$$

is the interior cost component,

$$C_{man_m} = \left(28.984 \cdot W_{ampr}^{0.740} \cdot V_{Max}^{0.543} \cdot N_{program}^{0.524} \cdot F_{diff}\right) R_{m_m} - C_{man} \quad (248)$$

is the manufacturing cost in the production phase obtained from the total manufacturing program cost (which includes also the manufacturing of prototypes in RDTE phase),

$$C_{mat_m} = 37.632 \cdot F_{mat} \cdot W_{ampr}^{0.689} \cdot V_{Max}^{0.624} \cdot N_{program}^{0.792} - C_{mat} \quad (249)$$

is the material cost in the production phase obtained from the total material program cost (which includes also the material necessary to build prototypes in RDTE phase),

$$C_{tool_m} = MHR_{tool_{program}} \cdot R_{t_m} - C_{tool} \quad (250)$$

is the tooling cost for produced series aircraft, derived from total program production (which includes prototypes), expressed similarly to (239) but with different manhours rates (Roskam, 1985), neglecting RDTE cost phase,

$$C_{qc_m} = 0.13 \cdot C_{man_m} \quad (251)$$

is the quality control cost in production expressed as percentage of manufacturing cost, and

C_{e_m} is the cost per engine during manufacturing phase in [$]
N_e is the number of engines per airplane
C_{p_m} is the cost per propeller (if applicable) during the manufacturing phase in [$]
N_p is the number of propellers per airplane (if applicable)
$C_{avionic_m}$ is the cost of avionic equipment per airplane in [$]
N_m is the number of aircraft built in the manufacturing phase
$N_{program}$ is the number of aircraft built within the entire program (including prototypes)
N_{pax} is the number of passengers per airplane
F_{int} is the interior cost factor expressed in $\left[\frac{\$}{pax}\right]$
R_{m_m} is the manhour rate in manufacturing phase in $\left[\frac{\$}{h}\right]$
$MHR_{tool_{program}}$ is the amount of manhours to produce tools over the entire program in [$]
R_{t_m} is the mahour rate for tooling production in [$]

The third item of (164) is associated to flight tests operations during production, defined as in (252).

$$C_{fto_m} = N_m \cdot C_{\frac{ops}{hr}} \cdot t_{pft} \cdot F_{ftoh} \quad (252)$$

where

$C_{\frac{ops}{hr}}$ is the airplane operating cost per hour as computed from estimations reported in Section 6.1.2.2 in $\left[\frac{\$}{h}\right]$

t_{pft} is the number of flight test hours
F_{ftoh} is the overhead factor associated to production flight test activities

Ultimately, the cost associated to finance the manufacturing phase is included as final item to include a certain percentage on final manufacturing cost.

8.2.3 Aircraft direct operating costs estimation

The aircraft DOC model proposed by (Roskam, 1990) includes the following cost items, as indicated in Section 6.1.2.2:

- DOC_{flt} direct operating cost associated to the flight;
- DOC_{maint} direct operating cost associated to maintenance;
- DOC_{depr} direct operating cost associated to depreciation
- DOC_{lnr} direct operating cost associated to landing and navigation fees;
- DOC_{fin} direct operating cost for operations financing.

The DOC_{flt} represents the direct operating cost associated to the flight, and can be further decomposed as in (253)

$$DOC_{flt} = C_{crew} + C_{pol} + C_{ins} \quad (253)$$

where

$$C_{crew} = \sum_{k=1}^{n_{crew}} n_{C_k} \left(\frac{1+K_k}{V_{bl}}\right) \cdot \left(\frac{SAL_k}{AH_k}\right) + \frac{TEF_k}{V_{bl}} \quad (254)$$

is the cockpit crew cost per nautical mile (where cost may be different depending on the role),

$$C_{pol} = \left(\frac{W_{F_{bl}}}{R_{bl}}\right) \cdot \left(\frac{FP}{FD}\right) + \left(\frac{W_{ol_{bl}}}{R_{bl}}\right) \cdot \left(\frac{OLP}{OD}\right) \quad (255)$$

is the fuel and oil cost per nautical mile,

$$C_{ins} = f_{ins_{hull}} \cdot \frac{AMP}{U_{ann_{bl}} \cdot V_{bl}} \quad (256)$$

is the insurance cost per nautical mile and

n_{c_k} is the k-th number of cockpit crew members
K_k is a factor accounting for vacation pay, cost of training, crew insurance etc…
SAL_k is the annual salary of the crew member in [$]
AH_k is the number of flight hours per year for each crew member
TEF_k is the travel expense factor associated to each type of crew member
$W_{F_{bl}}$ is the block fuel used in $[lb]$
FP is fuel price in $\left[\frac{\$}{gal}\right]$
FD is fuel density in $\left[\frac{lb}{gal}\right]$
$W_{ol_{bl}}$ is the weight of oil and lubricants used in $[lb]$
OLP is the oil price in $\left[\frac{\$}{gal}\right]$
OD is the oil density in $\left[\frac{lb}{gal}\right]$
$f_{ins_{hull}}$ is the annual hull insurance rate in $\left[\frac{\$}{\$/_{airplane\ year}}\right]$
AMP is the aircraft market price in [$]
$U_{ann_{bl}}$ is the annual block hour utilization.

Moreover,

$$V_{bl} = \frac{R_{bl}}{t_{bl}} \qquad (257)$$

is the airplane block speed in $\left[\frac{nm}{h}\right]$ defined as the ratio between the block hour distance R_{bl} and the block time t_{bl}. This is an important concept in cost estimation for the aeronautical domain, since the operating costs is usually referred to the true operating distance in nautical miles (taking into account the distance flown plus the distance covered on ground) and to the actual "engines on" time in hours. Particularly, the block time is defined as in (258)

$$t_{bl} = t_{gm} + t_{cl} + t_{cr} + t_{de} \qquad (258)$$

where

t_{gm} is the time spent in ground manoeuvres and phases, such as pushback, taxi, take-off and landing run
t_{cl} is the tiem required for climb and acceleration to cruise speed
t_{cr} is the time spent in cruise
t_{de} is the time spent for the descent phase

The DOC_{maint} represents the cost associated to maintenance, which can be split in the contributions represented in (259)

$$DOC_{maint} = C_{lab_{ap}} + C_{lab_{eng}} + C_{mat_{ap}} + C_{mat_{eng}} + C_{amb} \quad (259)$$

where

$$C_{lab_{ap}} = 1.03 \cdot MHR_{map_{bl}} \cdot \frac{R_{l_{ap}}}{V_{bl}} \quad (260)$$

is the maintenance labour cost per nautical mile of airframe and systems,

$$C_{mat_{ap}} = 1.03 \cdot \frac{C_{mat_{apblhr}}}{V_{bl}} \quad (261)$$

is the cost of maintenance materials for airframe and systems other than engines, per nautical mile,

$$C_{lab_{eng}} = 1.03 \cdot 1.3 \cdot N_e \cdot MHR_{meng_{bl}} \cdot \frac{R_{l_{eng}}}{V_{bl}} \quad (262)$$

is the maintenance labour cost per nautical miles of engines,

$$C_{mat_{eng}} = 1.03 \cdot 1.3 \cdot N_e \cdot \frac{C_{mat_{engblhr}}}{V_{bl}} \quad (263)$$

is the cost of maintenance materials for engines per nautical mile,

$$C_{amb} = 1.03 \cdot \frac{f_{amb_{lab}} \cdot \left(MHR_{map_{bl}} \cdot R_{l_{ap}} + N_e \cdot MHR_{eng_{bl}} \cdot R_{l_{eng}}\right) + f_{amb_{mat}} \cdot \left(C_{mat_{apblhr}} + N_e \cdot C_{mat_{engblhr}}\right)}{V_{bl}} \quad (264)$$

is the cost of applied maintenance burden per nautical mile and

$MHR_{map_{bl}}$ is the number of airframe and systems maintenance man hours needed per block hour
$R_{l_{ap}}$ is the airplane maintenance labour rate per manhour in $\left[\frac{\$}{hr}\right]$
$MHR_{meng_{bl}}$ is the number of engine maintenance hours needed per block hour per engine
$R_{l_{eng}}$ is the engine maintenance labour rate per manhour in $\left[\frac{\$}{hr}\right]$

$C_{mat_{apblhr}}$ is the airframe and systems maintenance material cost per airplane block hour
$C_{mat_{engblhr}}$ is the engine maintenance material cost per airplane block hour
$f_{amb_{lab}}$ and $f_{amb_{mat}}$ are overhead distribution factors for labor and material costs.

The cost item associated to depreciation can be broken down in the contributions shown in (265)

$$DOC_{depr} = C_{dap} + C_{deng} + C_{dprp} + C_{dav} + C_{dapsp} + C_{dengsp} \quad (265)$$

where

$$C_{dap} = \frac{F_{dap}(AEP - N_e \cdot EP - N_p \cdot PP - ASP)}{DP_{ap} \cdot U_{ann_{bl}} \cdot V_{bl}} \quad (266)$$

is the cost of airframe depreciation per nautical mile,

$$C_{deng} = \frac{F_{deng} \cdot N_e \cdot EP}{DP_{eng} \cdot U_{ann_{bl}} \cdot V_{bl}} \quad (267)$$

is the engine depreciation per nautical mile

$$C_{dprp} = \frac{F_{deng} \cdot N_e \cdot EP}{DP_{eng} \cdot U_{ann_{bl}} \cdot V_{bl}} \quad (268)$$

is the propellers depreciation per nautical mile (if applicable),

$$C_{dav} = \frac{F_{dav} \cdot ASP}{DP_{av} \cdot U_{ann_{bl}} \cdot V_{bl}} \quad (269)$$

is the avionic system depreciation per nautical mile,

$$C_{dapsp} = \frac{F_{dapsp} \cdot F_{apsp} \cdot (AEP - N_e \cdot EP)}{DP_{apsp} \cdot U_{ann_{bl}} \cdot V_{bl}} \quad (270)$$

is the depreciation of airplane spare parts per nautical mile,

$$C_{dengsp} = \frac{F_{dengsp} \cdot F_{engsp} \cdot N_e \cdot EP \cdot ESPPF}{DP_{engsp} \cdot U_{ann_{bl}} \cdot V_{bl}} \quad (271)$$

is the depreciation of engine spare parts per nautical mile and

F_{dap} is airframe depreciation factor
AEP is aircraft estimated price in [$]
EP is the engine price (per engine) in [$]
PP is the propeller price per propeller in [$]
ASP is the avionic system price per airplane in [$]
DP_{ap} is the airplane depreciation period
F_{deng} is the engine depreciation factor
DP_{eng} is the engine depreciation period
F_{dprp} is propeller depreciation factor
DP_{prp} is propeller depreciation period
F_{dav} is avionic system depreciation factor
DP_{av} is the avionic system depreciation period
F_{dapsp} is the airplane spare parts depreciation factor
F_{apsp} is the airplane spare parts factor
$DP_{apsp}$is the airplane spare parts depreciation period
F_{dengsp} is the engine spare parts depreciation factor
F_{engsp} is the engine spare parts factor
$ESPPF$ is the engine spare parts price factor
DP_{engsp} is the depreciation period for engine spare parts.

The cost item for navigation fees and other taxes, defined as in (272)

$$DOC_{lnr} = C_{lf} + C_{nf} + C_{rt} \quad (272)$$

where

$$C_{lf} = \frac{0.002(W_{TO})}{V_{bl} \cdot t_{bl}} \quad (273)$$

is the cost associated to landing fees per mile,

$$C_{nf} = \frac{0.036 + 4 \cdot 10^{-8}(W_{TO})}{V_{bl} \cdot t_{bl}} \quad (274)$$

is the cost associated to navigation fee charged per airplane per flight,

$$C_{rt} = \left(0.001 + 10^{-8}(W_{TO})\right) \cdot DOC \quad (275)$$

is the cost of registry taxes per nautical mile and

W_{TO} is airplane take-off weight in $[lb]$

Ultimately, the cost associated to financing is generally estimated as 7% of the total DOC.

8.3 STRATOFLY MR3 vehicle drawing

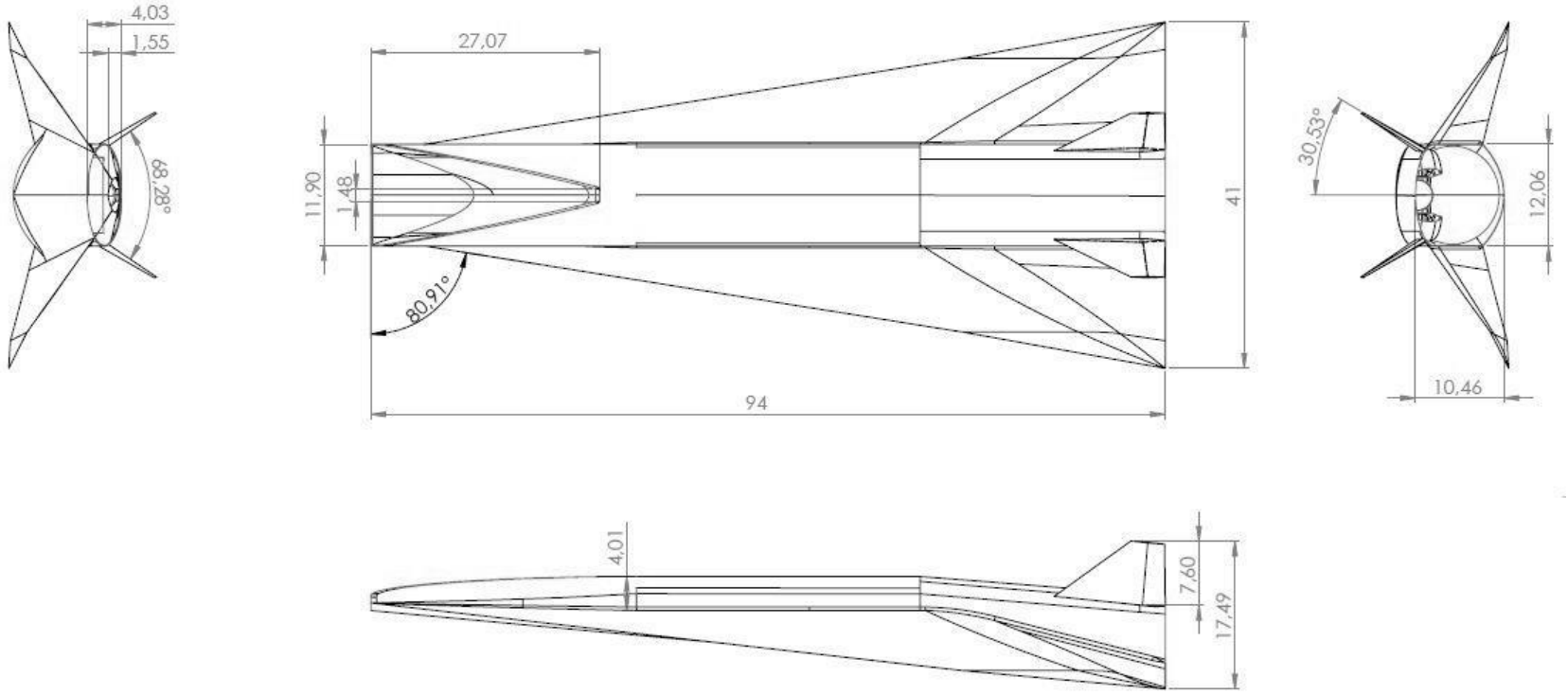

Fig. 248: Basic dimensions of STRATOFLY MR3 (meters)

References

Varvill , R. & Bond, A., 2006. *Cost analysis of Configuration A2 vehicle and Scimitar engine.*

AEA, 1989. *Short-medium range aircraft – AEA requirements.*

Alexander, C. C., Grimwood, J. M. & Swenson, L. S., 1966. *This New Ocean: a History of Project Mercury.* Washington D.C. (USA): NASA.

Anderson, J. D., 2006. *Hypersonic and High Temperature Gas Dynamics.* Second Edition ed. Reston VA (USA): American Institute of Aeronautics and Astronautics.

Anderson, J. D., 2007. *Fundamentals of Aerodynamics.* New York (NY) USA: McGraw-Hill.

Andro, J.-Y., Scigliano, R., Kallenbach, A. & Steelant, J., 2018. *Thermal Management of the HEXAFLY-INT Hypersonic Glider.* Moscow (RU), CEAS.

Anon., n.d. *Aircraft Maintenance Services Hourly Rate.* [Online] Available at: http://www.payscale.com/research/US/Industry=Aircraft_Maintenance_Services/Hourly_Rate

Anon., n.d. *Measuring Worth.* [Online] Available at: https://www.measuringworth.com

Anon., n.d. *MIT Global Airline Industry Program.* [Online] Available at: http://web.mit.edu/airlinedata/www/default.html

ANSI/AIAA, 2015. *S-120A-2015 Mass properties control for space systems.* Washington DC (USA): ANSI/AIAA.

ANSI/EIA, 1998. *EIA-632: Processes for engineering a System.* s.l.:Electronic Industries Alliance.

Asiedu, Y. & Gu, P., 1998. Product Life Cycle Cost Analysis: State of the art review. *International Journal of Production Research,* 36(1), pp. 883-908.

ATA, 1967. *Standard method of estimating comparative direct operating costs of turbine powered transport.*

Babetto, L., 2018. *Reliability and Safety Assessment of a Thermal Control System of a Hypersonic Transportation Vehicle.* Torino (IT): Politecnico di Torino, http://webthesis.biblio.polito.it/6855/1/tesi.pdf Accessed October 2019.

Bachelor, G., Brusa, E., Ferretto, D. & Mitschke, A., 2019. Model-Based Design of Complex Aeronautical Systems Through Digital Twin and Thread Concepts. *IEEE Systems Journal,* 13(3).

Bader, P., 2019. *Preliminary design of a thermal and energy management subsystem for hypersonic vehicle concepts.* Torino (IT): Politecnico di Torino.

Balland, S., Fernandez Villace, V. & Steelant, J., 2015. *Thermal and Energy Management for Hypersonic Cruise Vehicle - Cycle Analysis.* Glasgow, Scotland (UK), AIAA.

Bartolotta, P., McNeils, N. & Shafer, D., 2003. *High Speed Turbines: Development of a Turbine Accelerator (RTA) for Space Access.* Reston, VA USA: AIAA.

Beltramo, N., Anderson, J. L. & Morris, M. A., 1979. *Application of parametric weight and cost estimating relationships to future transport aircraft.* New York (USA): Society of Allied Weight Engineers Inc..

Bertalanffy, L. v., 1972. General Systems theory. *The Academy of Management Journal,* 15(4), pp. pp 407-426.

Berteau, D. J., 2016. *Operating and Support Cost Management Guidebook.* Washington D.C. (USA): US Department of Defence.

Bilstein, R. E., 2003. *Testing aircraft, exploring space: an illustrated history of NACA and NASA.* Baltimore MD (USA): Johns Hopkins Univ. Press.

Bizer, C., Heath, T. & Berners-Lee, T., 2009. Linked Data - The Story so Far. *International Journal on Semantic Web and Information Systems,* 5(3).

Blanvillain, E., 2014. *A holistic approach to hypersonic aircraft design: ZEHST.* St. Petersburg (RU), ICAS.

Blanvillain, E. & Gallic, G., 2015. *HIKARI: Paving the way towards high speed air transport.* Glasgow (UK), American Institute of Aeronautics and Astronautics.

Blochwitz, T., et al., 2011. *The Functional Mockup Interface for tool independent exchange of simulation models.* Dresden (DE), Linkoping University Electronic Press.

Bocciarelli, P., et al., 2017. *A BPMN extension for modeling Cyber-Physical-Production-Systems in the context of Industry 4.0.* Lamezia Terme (IT), IEEE, pp. pp 599-604.

Bond, A., 2007. Turbine-Based Combined Cycles, advances on propulsion technology for high-speed aircraft. *RTO-AVT-VKI Lecture series.*

Bosak, J. & Bray, T., 1999. *XML and the Second-Generation Web.* s.l.:Scientific American.

Bowcutt, K. G., 2001. Multidisciplinary optimization of airbreathing hypersonic vehicles. *Journal of Propulsion and Power,* 17(6), pp. 1184 - 1190.

Brown, M. T., 2004. A picture is worth a thousand words: energy systems language and simulation. *Ecological Modelling,* 178(1-2), pp. pp 83-100.

Brusa, E., Calà, A. & Ferretto, D., 2018. *Systems Engineering and Its Application to Industrial Product Development.* Cham, Switzerland: Springer International Publishing AG.

Budin, G., 2005. *Ontology-driven translation management.* Berlin (DE): Mouton de Gruyter.

Byko, M., 2004. SpaceShipOne, the Ansari X Prize and the materials of the civilian space race. *Journal of the Minerals, Metals and Materials Society,* pp. pp. 24-28.

Calà, A., Ryashentseva, D. & Luder, A., 2016. *Modeling approach for a flexible manufacturing control system.* Berlin (DE), IEEE.

Campbell, W. E. & Farquhar, J., 1974. *Centrifugal Pumps for Rocket Engines.* Springfield, VA (USA): NERVA Rocket Operations.

Cardella, U., Decker, L. & Klein, H., n.d. Economically viable large-scale hydrogen liquefaction.

Chavagnac, C., 2014. *The HIKARI project and safety (of flight).* Toronto (CA), IAF.

Chudoba, B. et al., 2012. *Solution-Space Screening of a Hypersonic Endurance Demonstrator.* Hampton, VA (USA): NASA.

Clements, P., 1996. *Clements, Paul C. "A survey of architecture description languages.* s.l., IEEE.

Cockrell, C. E., Huebner, L. D. & Finley, D. B., 1996. *Aerodynamic Characteristics of Two Waverider-Derived Hypersonic Cruise Configurations.* Hampton, VA, USA: NASA.

Colebrook, C. F. & White, C. M., 1937. Experiments with fluid friction in roughened pipes. *Proceedings of the Royal Society of London,* 161(906), pp. 367-381.

Corda, S. & Anderson, J. O. H. N., 1988. *Viscous optimized hypersonic waveriders designed from axisymmetric flow fields.* Reno, NV (USA), AIAA.

Croce, F., 2017. *Development of a new Life Cycle Cost model for innovative regional aircraft.* Turin (IT): Politecnico di Torino.

Curran, E. T. & Murthy, S. N., 2001. *Scramjet Propulsion.* I ed. Reston VA (USA): AIAA.

Decker, L., December 2013. The Latest Developments and Outlook for Hydrogen Liquefaction Technology.

Dick, E., 2015. *Fundamentals of Turbomachines.* New York (USA): Springer.

Ding, F., et al., 2018. An overview of waverider design concept in airframe/inlet integration methodology for air-breathing hypersonic vehicles. *Acta Astronautica.*

Ding, F., Liu, J., Shen, C. B. & Huang, W., 2015. *Simplified osculating cone method for design of a waverider.* Montreal, CA, ASME.

Dixon, M., 2006. *The maintenance costs of aging aircraft : insights from commercial aviation.*

Domack, C. S. et al., 1990. *Concept Development of a Mach 4 High-Speed Civil Transport,* Washington DC: NASA.

Dove, R., 2012. *Agile Systems and Processes: Necessary and Sufficient Fundamental Architecture (Agile 101).* s.l.:INCOSE.

Dujarric, C., 1999. Possible future European launchers - A process of Convergence. *ESA Bulletin 97*, February.

EASA, 2019. *CS-25 Certification Specifications and Acceptable Means of Compliance for Large Aeroplanes.* Cologne (DE): EASA.

ECSS, 2004. *Space engineering - Systems Engineering Part 1: Requirements and process.* Noordwijk (NL): ESA.

ECSS, 2008. *ECSS-E-ST-31C Space engineering - Thermal Control general requirements.* Noordwijk (NL): ESA.

ECSS, 2009. *ECSS-E-ST-10-02C Space Engineering - Verification.* Noordwijk (NL): ESA.

ECSS, 2011. *ECSS-E-ST-50-05C Rev2 Space engineering - Radio frequency and modulation.* Noordwijk (NL): ESA.

Ekvall, J. C. R. J. E. a. W. G. G., 1982. Methodology for Evaluating Weight Savings from Basic Material Properties. In: A. S. f. T. a. Materials, ed. *Design of Fatigue and Fracture Resistant Structures.* s.l.:P. R. Abelkis and C. M. Hudson, Eds.,, pp. 328-341.

Epple, P., Durst, F. & Delgado, A., 2010. A theoretical derivation of the Cordier diagram for turbomachines.. *Proceedings of the IMechE Part C: Journal of Mechanical Engineering Science,* Volume 225, pp. 354 - 368.

ESA, 2012. *Margin philosophy for science assessment studies.* Noordwijk (NL): SRE-PA & D-TEC ESA.

ESA, n.d. [Online] Available at: http://www.esa.int/Our_Activities/Space_Engineering_Technology/LAPCAT_II

European Commission - High Level Group on Aviation Research, 2011. *Flightpath 2050 - Europe's Vision for Aviation.* Luxemburg: EU.

FAA (Federal Aviation Administration), n.d. *Economic Values for FAA Investment & Regulatory Decisions Guide - Section 4.* [Online] Available at: https://www.faa.gov/regulations_policies/policy_guidance/benefit_cost/media/econ-value-section-4-op-costs.pdf

FAA, 2019. *FAR 25 - Airworthiness standards: transport category airplanes.* Washington DC; USA: FAA.

Falempin, F., Bouchez, M. & Perillat, V., 2009. *LAPCAT-II: Axisymmetric Concept for a Mach 8 Cruiser – Preliminary Design and Performance Assessment.* Bremen (DE), AIAA.

Falempin, F., Scherrer, D. & Rostand, P., 1998. *French Hypersonic Propulsion Program PREPHA. Results, Lessons and Perspectives.* Norfolk VA (USA), American Institute of Aeronautics and Astronautics (AIAA).

Favaloro, N. et al., 2015. *Design analysis of the high-speed experimental flight test vehicle HEXAFLY International.* Glasgow (UK), American Institute for Aeronautics and Astronautics, p. p. 3607.

Ferjan, K., 2013. *IATA Airline Operational Cost Task Force.* Geneva (CH): IATA.

Fernandez Villace, V. & Steelant, J., 2015. *The thermal paradox of hypersonic cruisers.* Glasgow (UK), AIAA.

Fioriti, M., 2014. Adaptable conceptual aircraft design model. *Advances in aircraft and spacecraft science,* 1(1), pp. pp 43-67.

Forsberg, K., Mooz, H. & Cotterman, H., 2005. *Visualizing Project Management.* 3rd edition ed. Hoboken NJ, USA: John Wiley & Sons Inc..

Friedenthal, S., Moore, A. & Steiner, R., 2012. *A Practical Guide to SysML: The Systems Modeling Language.* 2nd Edition ed. New York, USA: Morgan Kaufmann Publishers, Inc..

Fusaro, R., 2016. *Comparative analysis of new configuration of aircraft aimed at competitivenes, environmental compatibility and safety.* Torino (IT): Politecnico di Torino.

Fusaro, R. et al., 2018. *Life-Cycle Cost estimation methodology for hypersonic transportation systems.* Belo Horizonte (BR), ICAS.

Fusaro, R., Ferretto, D. & Viola, N., 2016. *Model-Based Object-oriented Systems Engineering methodology for the conceptual design of hypersonic transportation system.* Edimburgh (UK), IEEE.

Fusaro, R., Ferretto, D. & Viola, N., 2017. *MBSE approach to support and formalize mission alternatives generation and selection processes for hypersonic and suborbital transportation systems.* Vienna, A, IEEE.

Fusaro, R. et al., 2019. A methodology for preliminary sizing of a Thermal and Energy Management System for a hypersonic vehicle. *The Aeronautical Journal,* 123(1267).

Fusaro, R. & Viola, N., 2017. Preliminary reliability and safety assessment methodology for trans-atmospheric transportation systems. *Aircraft Engineering and Aerospace Technology,* 90(4), pp. 639-651.

Fusaro, R., Viola, N., Babetto, L. & Ferretto, D., 2019. *MBSE methodology to support a safety and reliability assessment of the thermal and energy management subsystem of the STRATOFLY vehicle.* Los Angeles, CA (USA), IAASS.

GAO, 2015. *Cost estimating and assessment guide: best practices for developing and managing capital program costs.* Washington DC (USA): GAO.

Goehlich, R. A. e. a., 2013. Pilots for space tourism. *Space Policy ,* Volume 29.2 , pp. 144-153..

Gopalaswami, R., 2010. Critical Factors In Conceptual Design And Techno-Economics Of Reusable Spaceplanes. *Journal of the British Interplanetary Society,* 63(11), p. 395.

Gregory, J., Berthoud, L., Tryfonas, T. & Pezzavento, A., 2019. *Early Validation of the Data Handling Unit of a Spacecraft Using MBSE.* Big Sky, MT USA, IEEE.

Haaland, S. E., 1983. Simple and explicit formulas for the friction factor in turbulent flow. *Journal of Fluids Engineering,* 105(1), pp. 89-90.

Hall, A. D., 1962. *A methodology for systems engineering.* s.l.:van Nostrand.

Hall, R. & Shayler, D., 2001. *The rocket men: Vostok & Voskhod, the first Soviet manned spaceflights.* London UK: Springer.

Hamilton, M. H. & Hackler, W. R., 2008. *Universal Systems Language: Lessons Learned from Apollo.* s.l.:Hamilton Technologies Inc..

Hank, J., Murphy, J. & Mutzman, R., 2012. *The X-51A Scramjet Engine Flight Demonstration Program.* Dayton OH (USA), American Institute for Aeronautics and Astronautics.

Harris, F. D., 2005. *An economic eodel of U.S. airline operating expenses,* s.l.: s.n.

Hendrickx, B. & Vis, B., 2007. *Energiya-Buran: The Soviet Space Shuttle.* Chichester UK: Springer-Praxis.

HEXAFLY Int, 2017. *HEXAFLY International Periodic Report II.* s.l.:HEXAFLY Int.

Hirschel, E. H., 2005. *Basics of Aerothermodynamics.* Berlin (DE): Springer.

Hirschel, E. H. & Weiland, C., 2009. *Selected aerothermodynamic design problems of hypersonic flight vehicles.* Berlin (DE): Springer Science & Business Media.

Huzel, D. K. & Huang, D. H., 1967. *Design of Liquid Propellant Rocket Engines.* Washington DC (USA): Rocketdyne Division North America Aviation Inc..

ICAO, 2017. *Airline Operating Costs and Productivity.* Tehran (IRAN): ICAO.

IEA, 2006. *Hydrogen production and storage - R&D Priorities and Gaps.* Paris (FR): International Energy Agency.

IEEE, 1998. *Standard for Application and Management of the Systems Engineering Process.*

INCOSE, 2007. *INCOSE Systems Engineering Vision 2020.* San Diego, CA, USA: INCOSE.

INCOSE, 2015. *Systems Engineering Handbook - A guide for system life cycle process and activities.* Fourth Edition ed. San Diego, CA, USA: Wiley.

Ingenito, A., Gulli, S. & Bruno, C., 2009. *Preliminary Sizing of Hypersonic Airbreathing Airliner.* Okinawa, ISTS.

International Air Transport Association (IATA), 2013. *Labor Rate and Productivity Calculations for Commercial Aircraft Maintenance.*

International Energy Agency, 2006. *Hydrogen Production and Storage - R&D Priorities and Gaps.*

Interstellar. 2014. [Film] Directed by Christopher Nolan. USA: Syncopy Films.

ISO, 2015. *ISO 15288: Systems and Software engineering - System life cycle processes.* Geneva, Switzerland: ISO/IEC/IEEE.

Ispir, A. C., Saracoglu, B. & Goncalves, P., 2019. *Assessment of Combustion Models for thermodynamic modeling of the engines for hypersonic propulsion.* Monopoli (IT), ESA.

Jenkins, D. R., Landis, T. & Miller, J., 2003. *American X-Vehicles: An Inventory - X-1 to X-50.* Monograph in Aerospace History No.31 - Centennial of Flight ed. Washington DC, USA: National Aeronautics and Space Administration (NASA).

Jenkinson, L. R., Simpkinq, P. & Rhodes, D., 1999. *Civil Jet Aircraft Design.* London (UK): Arnold.

Jivraj, F., Bond, A., Varvill, R. & Paniagua, G., 2007. *The scimitar precooled Mach 5 engine.* Abingdon (UK): REL.

Jones, T. L., 2011. *Handbook of Reliability Prediction Procedures for Mechanical Equipment.* West Bethesda MD, USA: NSWC.

Keady, G., 1998. Colebrook-White formula for pipe flows. *Journal of Hydraulic Engineering,* 124(1), pp. 96 - 97.

Kennedy, G. P., 1984. *Vengeance Weapon 2: The V-2 Guided Missile.* Washington D.C. (USA): Smithsonian Institution Press.

Koelle, D. E., 2012. *Handbook of Cost Engineering and Design of Space Transportation Systems: TransCost 8.2 Model Description.* s.l.:TCS.

Koelle, D. E. & Kuczera, H., 1989. Sanger II, an advanced launcher system for Europe. *Acta Astronautica,* 19(1), pp. 63-72.

Krein, A. & Williams, G., 2012. *Flightpath 2050: Europe's vision for aeronautics. Innovation for Sustainable Aviation in a Global Environment..* Madrid (ES), IOS Press.

Krempus, D., 2017. *Evaluation of the Aero-propulsive Performance of a Hypersonic Aircraft during the acceleration phase.* Stuttgart (DE): University of Stuttgart.

Kuchemann, D., 2012. *The Aerodynamic Design of Aircraft.* Reston VA (USA): American Institute for Aeronautics and Astronautics (AIAA).

Labanca, A., Feugeas, J. & Miranda, P., 2006. *Economic Analysis of CO2-free Hydrogen Production from Natural Gas by Plasma Pyrolysis.*

Laney, M., 2015. *German rocketeers in the heart of dixie: Making sense of the nazi pasrt during the civil rights era.* New Heaven CT (USA): Yale University Press.

Langener, T., Erb, S. & Steelant, J., 2014. *Trajectory simulation and optimization of the LAPCAT MR2 hypersonic cruiser concept.* St. Petersburg (RU), ICAS.

Larson, J. W. & Pranke, L. K., 1999. *Human Spaceflight: mission analysis and design.* New York (USA): McGraw-Hill.

Larson, W. J., Henry, G. N. & Humble, R. W., 1995. *Space propulsion analysis and design.* New York (USA): McGraw-Hill.

Liebeck, R. H. et al., 1995. *Advanced subsonic airplane design and economic studies.*

Loftin, L. K., 1980. *Subsonic Aircraft: Evolution and the Matching of Size to Performance.* Hampton, VA (USA): NASA.

Lombardi, M., 2007. *The Jet that started a revolution.* Renton VA (USA): The Boeing Company.

Longo, J., Sippel, M. & Carrier, G., 2009. *Concept Study for a Mach 6 Transport Aircraft.* Orlando FL, USA, AIAA.

Mahulikar, S. P., 2005. Theoretical aerothermal concepts for configuration design of hypersonic vehicles. *Aerospace Science and Technology,* 9(8), pp. 681-685.

Marini, M. & Roncioni, P., 2019. *STRATOFLY MR3 Aero-Propulsive Database.* Bruxelles (BE): EC-H2020 769246.

Martin, J. N., 1996. *Systems Engineering Guidebook: A process for Developing Systems and Products.* Boca Raton, FL, USA: CRC Press.

Merriam Webster, 2002. *Dictionary.* s.l.:Merriam Webster.

Mesa, V., 2014. *Environmentally Friendly Hydrogen Production Study.*

Messerschmid, E. & Bertrand, R., 1999. *Space Stations: system and utilization.* 1st ed. Berlin (DE): Springer-Verlag.

Mihara, S. K., 2003. *A Current Summary of RLV Activities in the US.* s.l., AIP, pp. pp. 263-268.

Moody, L. F., 1944. Friction factors for pipe flow. *Transactions of the ASME,* 66(8), pp. 671-684.

Murray, N., 2011. *Waverider design using a generalised flare flowfield.* Bruges (BE), ESA.

NASA, 1968. *X-15. Extending the frontiers of flight.* Washington D.C. (USA): National Aeronautics and Space Administration (NASA).

NASA, 2007. *NASA Systems Engineering Handbook.* Washington DC, USA: NASA.

Nichele, F., 2016. *Methodologies for the analysis of space systems: supporting the decision making in the early design phases.* Torino (IT): Politecnico di Torino.

Nista, L., 2019. *Development of a robust solver to model the flow inside the engines for high speed propulsion.* Brussels (BE): VKI.

Object Management Group - OMG, 2007. *OMG Systems Modeling Language (OMG SysML™) - Version 1.0.* Needham, MA, USA: OMG.

Object Management Group - OMG, 2008. *Software & Systems Process Engineering Meta-Model Specification.* Needham, MA: OMG.

Object Management Group - OMG, 2018. *OMG Systems Modeling Language (OMG SysML™) - Version 1.6.* Needham, MA, USA: OMG.

Object Management Group, 2002. *Software & Systems Process Engineering - Version 1.0.* Needham, MA, USA: OMG.

Object Management Group, 2012. *Service oriented architecture Modeling Language (SoaML) Specification.* Needham, MA, USA: OMG.

Object Management Group, 2017. *OMG Unified Modeling Language (OMG UML).* Needham, MA, USA: OMG.

Oppenheim, B. W., 2011. *Lean for Systems Engineering with Lean Enablers for Systems Engineering.* Hoboken, NJ, USA: John Wiley & Sons Inc..

Oxford English, 1989. *Oxford English Dictionary.* London (UK): Simpson JA & Weiner ESC.

Parkinson, R. C., 1990. *A total system approach towards the design of future cost-effective launch systems.* San Diego CA (USA), IAA.

Petersen, R. H. & Waters, M. H., 1972. *Hypersonic Transports - Econimics and Environmental Effects.*

Rangwala, A. S., 2005. *Turbo-Machinery Dynamics: design and operations.* I ed. New York (USA): McGraw-Hill.

Raymer, D. P., 1995. *Aircraft design: a conceptual approach.* Reston VA, USA: American Institute of Aeronautics and Astronautics.

Raymer, D. P., 2012. *Aircraft Design: a conceptual approach.* 5th ed. Reston VA, USA: American Institute of Aeronautics and Astronautics.

Raymer, D. P. & Burnside Clapp, M., 2012. Pioneer Rocketplane Conceptual Design Study. *Journal of Aircraft,* 39(3), pp. pp. 507-511.

Reaction Engines Ltd, 2006. *Cost analysis of Configuration A2 vehicle and Scimitar engine.*

Repic, E. M., Olson, G. A. & Milliken, R. J., 1973. *A methodology for hypersonic transport technology planning.* Downey CA (USA): NASA.

Roskam, J., 1985. *Airplane Design.* Ottawa (CAN): Roskam Aviation and Engineering Corp..

SAE, 1996. *Guidelines and methods for conducting the safety assessment process on civil airborne systems and equipment.* Warrendale, PA (USA): SAE.

SAE, 2010. *Guidelines for Development of Civil Aircraft and Systems.* Warrendale, PA, USA: SAE.

Sagerser, D., Lieblein, S. & Krebs, R. P., 1971. *Empirical expressions for estimating length and weight of axial-flow components of VTOL powerplants.* Cleveland OH (USA): NASA.

Saunders, D. J., 1979. *A method of calculating the weight and dimensions of a turbopump for rocket propellants.* Farnborough (UK): Royal Aircraft Establishment.

SAWE, 2015. *Recommended Practice A-3, Mass properties control for space systems.* Long Beach (CA) USA: SAWE.

Schweikart, L., 1998. *The Quest for the Orbital Jet: The National Aero-Space Plane Program (1983-1995).* Washington D.C. (USA): Air Force Historical Studies Office.

Serre, L. & Falempin, F., 2013. *Promethee-the French military hypersonic propulsion program.* Norfolk, VA, USA, AIAA.

Sippel, M., et al., 2015. *SpaceLiner Technical Progress and Mission Definition.* Glasgow (UK), American Institute for Aeronautics and Astronautics.

Sippel, M., Klevanski, J. & Steelant, J., 2005. *Comparative Study on Options for High-Speed Intercontinental Passenger Transports: Air-breathing vs Rocket-Propelled.* Fukuoka, JP, IAF.

Sippel, M., Stappert, S. & Koch, A., 2018. *Assessment of multiple mission reusable launch vehicles.* Bremen (DE), IAF.

Sobin, A. J., 1974. *Turbopump Systems for Liquid Rocket Engines.* Washington DC (USA): NASA.

Steelant , J., Fernandez Villace, V., Dalenbring, M. & Wang, G. S., 2015. *The Thermal and Structural Paradox for Hypersonic Cruisers.* Noordwijk (NL), ESA.

Steelant, J., 2008. *Achievements obtained for sustained hypersonic flight within the LAPCAT project.* Dayton OH (USA), American Institute for Aeronautics and Astronautics.

Steelant, J., 2008. *ATLLAS: Aero-Thermal Loaded Material Investigations for High-Speed Vehicles.* Dayton, OH USA, AIAA.

Steelant, j., 2008. *LAPCAT Long-Term Advanced Propulsion Concepts and Technologies SPECIFIC TARGETED RESEARCH PROJECT.*

Steelant, J., 2008. LAPCAT: High-Speed Propulsion Technology. *Educational Notes RTO-EN-AVT,* 150(12), pp. pp 12-1 12-38.

Steelant, J., 2009. *Achievements obtained on aero-thermal loaded materials for high-speed atmospheric vehicles within ATLLAS.* Bremen (DE), American Institute for Aeronautics and Astronautics, p. p. 7225.

Steelant, J., 2010. Hypersonic Technology Developments with EU Co-Funded Projects. *NATO RTO-EN-AVT,* Issue 185, pp. 15-1 15-68.

Steelant, J., 2014. *High Speed Experimental Fly Vehicles - Final Report.* Noordwijk (NED): ESA.

Steelant, J., et al., 2015. *Achievements Obtained for Sustained Hypersonic Flight within the LAPCAT II Project.* Glasgow (UK), American Institute for Aeronautics and Astronautics.

Steelant, J. et al., 2008. *LAPCAT Long-Term Advanced Propulsion Concepts and Technologies Final Activity Report.*

Steelant, J. et al., 2017. *Achievements obtained within ATLLAS II on Aero-Thermal Loaded Material Investigations for High-Speed Vehicles.* Xiamen (CN), AIAA.

Steelant, J. & Fernandez Villace, V., 2015. *The thermal paradox of hypersonic cruisers.* Glasgow, Scotland (UK), AIAA.

Steelant, J. & Langener, T., 2014. *The LAPCAT MR2 hypersonic cruiser concept.* St. Petersburg (RU), ICAS.

Steelant, J. & van Duijn, M., 2011. *Structural analysis of the LAPCAT MR2 waverider based vehicle.* San Francisco, CA, USA, AIAA.

Steelant, J. et al., 2015. *Achievements Obtained for Sustained Hypersonic Flight within the LAPCAT-II Project.* Glasgow (UK), AIAA.

Steelant, J., Villace, V. & Kallenbach, A., 2018. *Flight Testing Designs in HEXAFLY-INT for High-Speed Transportation.* Moscow (RU), CEAS.

Stesina, F., 2014. *Design and verification of Guidance, Navigation and Control systems for space applications.* Torino (IT): Politecnico di Torino.

The Boeing Company, 2016. *Frontiers.* Chicago IL (USA): Boeing.

Torenbeek, E., 1976. *Synthesis of subsonic airplane design.* Rotterdam (NED): Delft University Press.

Tumino, G. & Yves, G., 2006. IXV: the Intermediate eXperimental Vehicle - Europe among the world players in atmospheric re-entry. *ESA Bulletin 128*, pp. pp. 62-67.

Vagliano, I. et al., 2017. *Tool Integration in the Aerospace Domain: A case study.* Torino, IEEE.

Van Bodegraven, G., 1990. *Van BodegrCommercial aircraft DOC methods.*

Van den Abeelen, L., 2016. *Spaceplane HERMES: Europe's Dream of Independent Manned Spaceflight.* Cham (CH): Springer.

Varvill, R. & Bond, A., 2004. The Skylon spaceplane. *Journal of the British Interplanetary Society,* Volume 57, pp. pp. 22-32.

Vellaramkalayil, J., Langener, T. & Steelant, J., 2013. *LAPCAT II Project Deliverable 6.4.3: RANS based supersonic combustor scaling modeling.* Noordwijk (NL): ESA.

Vercella, V., 2017. *Development and implementation of a cost model for aircraft operating costs evaluation.* Turin (IT): Politecnico di Torino.

Vercella, V. et al., 2018. *Towards future LH2 productive scenarios: economic assessment and environmental effects on hypersonic transportation systems.* Moscow (RU), CEAS.

Villace, V. F. & Steelant, J., 2015. *The Thermal Paradox of Hypersonic Cruisers.* Glasgow.

Viola, N. & Fusaro, R., 2019. *STRATOFLY MR3 vehicle configuration.* Roma (IT), Springer.

Viola, N. et al., 2019. *Main Challenges and Goals of the H2020 STRATOFLY Project.* Monopoli (IT), ESA.

Virgin Galactic, 2016. *SpaceShip Two: An introductory guide for payload users.* Mojave CA (USA): Virgin Group.

Walden, D. D. et al., 2015. *INCOSE Systems Engineering Handbook - A guide for System Life Cycle Processes and Activities.* Fourth Edition ed. San Diego CA, USA: Wiley.

Weihs, H., Longo, J. & Turner, J., 2008. *The Sharp Edge Flight Experiment SHEFEX II, a mission overview and status.* Dayton, OH, USA, AIAA.

Weiland, C., 2014. *Aerodynamic Data of Space Vehicles.* London UK: Springer Science & Business Media.

Wertz, J. R. & Larson, W. J., 2005. *Space Mission Analysis and Design.* Third Edition ed. Boston, MA USA: Kluwer Academic Publishers.

Williamson, R., 1999. *Developing the Space Shuttle.* Washington D.C. (USA): National Aeronautics and Space Administration (NASA).

Yanagihara, M. et al., 2001. *HOPE-X high speed flight demonstration program phase II.* Kyoto (JP), American Institute for Aeronautics and Astronautics (AIAA).

Young, T. M., 2007. Aircraft design innovation: creating an environment for creativity. *Proc. IMechE Part G: Aerospace Engineering,* Volume 221, pp. pp. 165 - 174.

Zagainov, G. & Plokhikh, V., 1991. *USSR aerospace plane program.* Orlando FL (USA), American Institute for Aeronautics and Astronautics (AIAA).